Magneto-optical Analysis of Magnetic Microstructures*

R. Schäfer,

Leibniz Inst. for Solid State and Materials Research (IFW) Dresden, Germany

*Review of Magnetic Domains, studied (mostly) by Kerr microscopy

What are magnetic domains ?

What are magnetic domains ?

(100) iron whisker

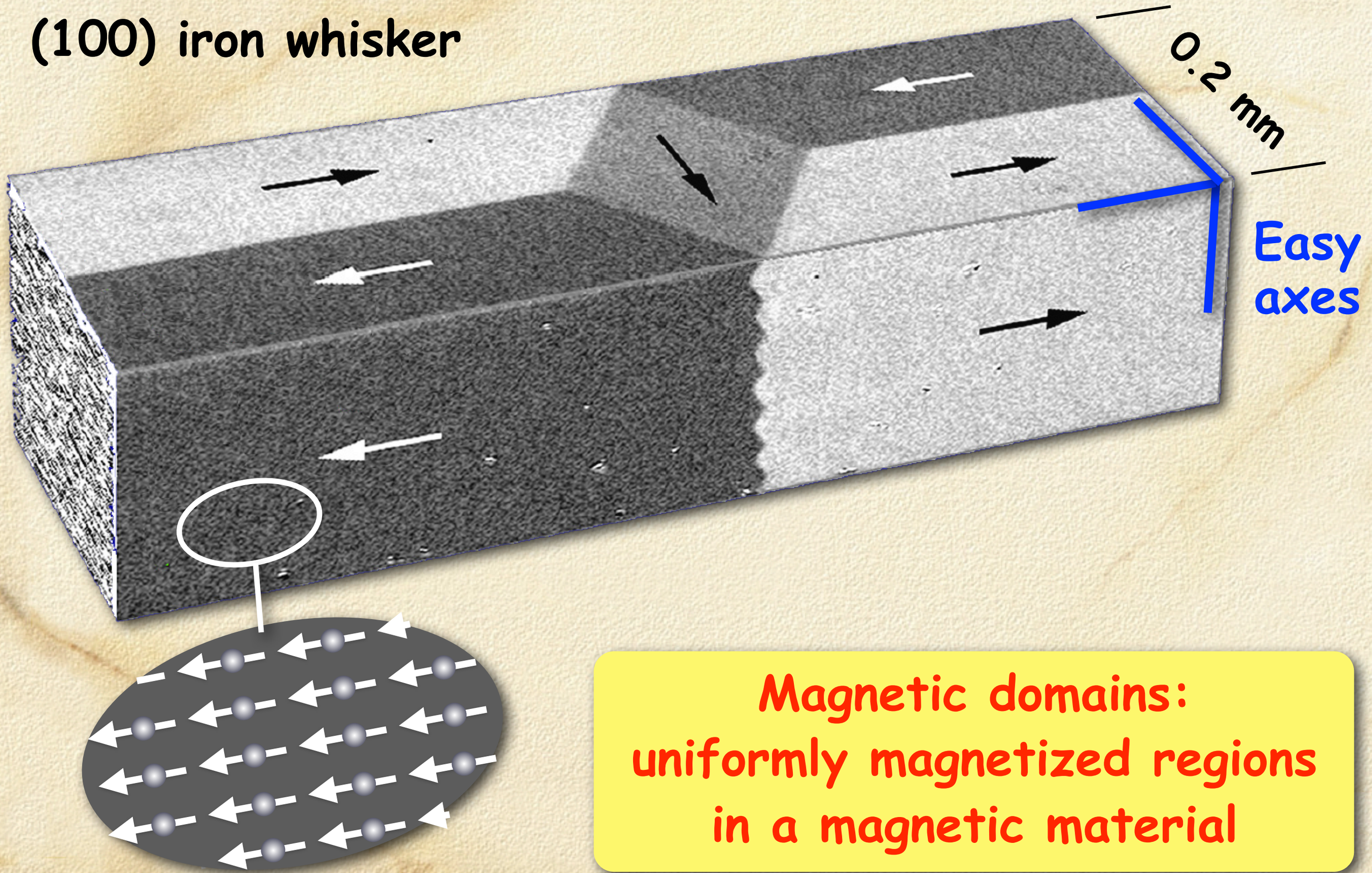

Magnetic domains:
uniformly magnetized regions
in a magnetic material

What are magnetic domains?

FeN film

NiFe film

NiFe film

FeSi sheet

Co crystal

metalic glass

Fe film

NiFe

FeSi sheet

Garnet film

FeSi sheet

Magnetic domains:
can be more or less complex,
depending on circumstances

What are magnetic domains?

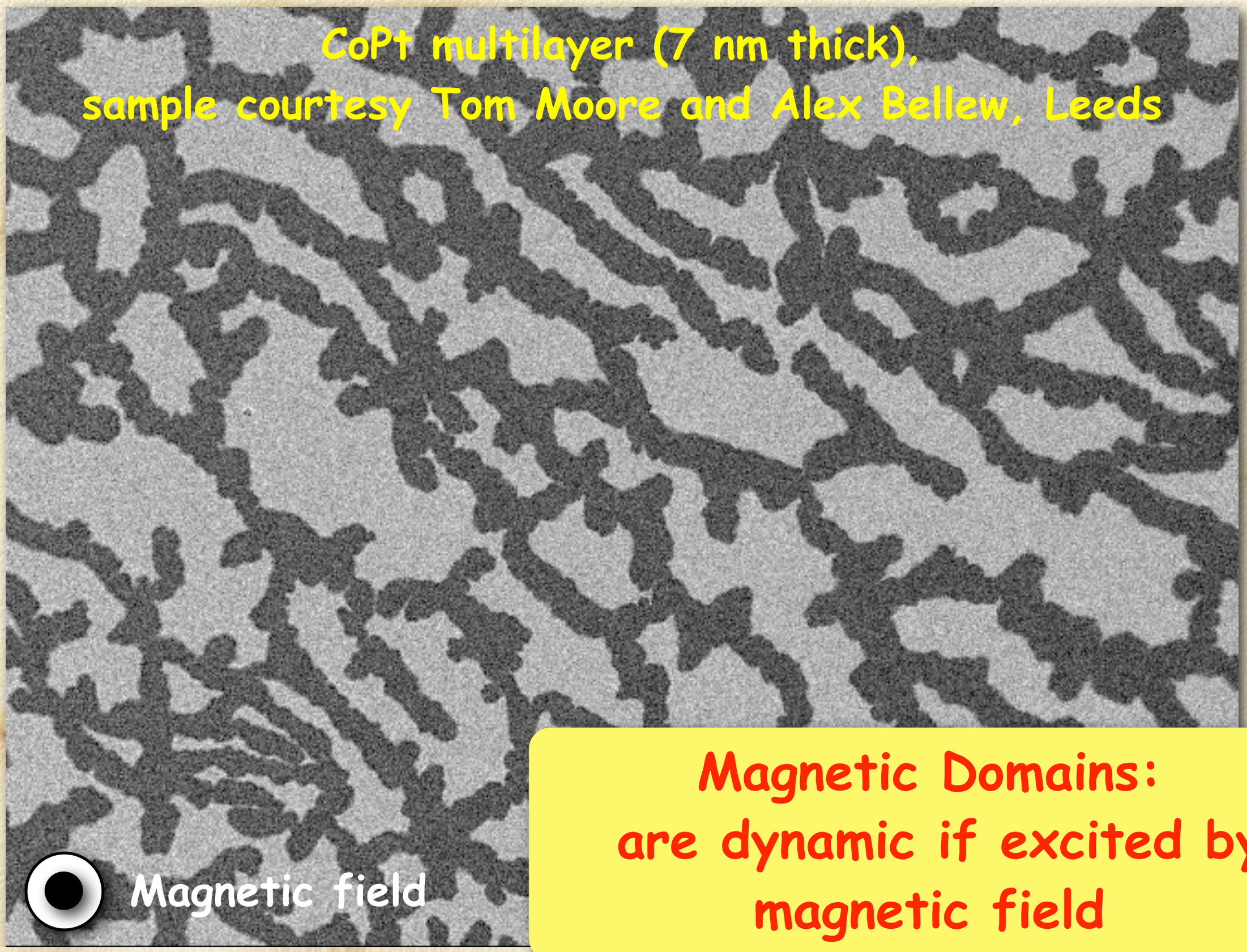

Magnetic Domains:
are dynamic if excited by magnetic field

What are magnetic domains?

Pulse-field excitation

Quasistatic excitation

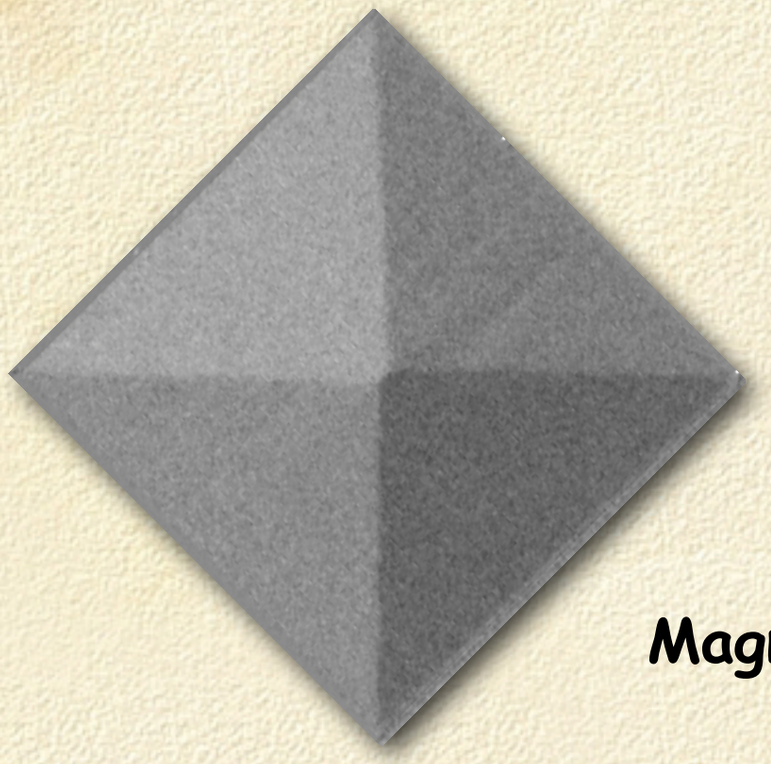

Permalloy (NiFe) film

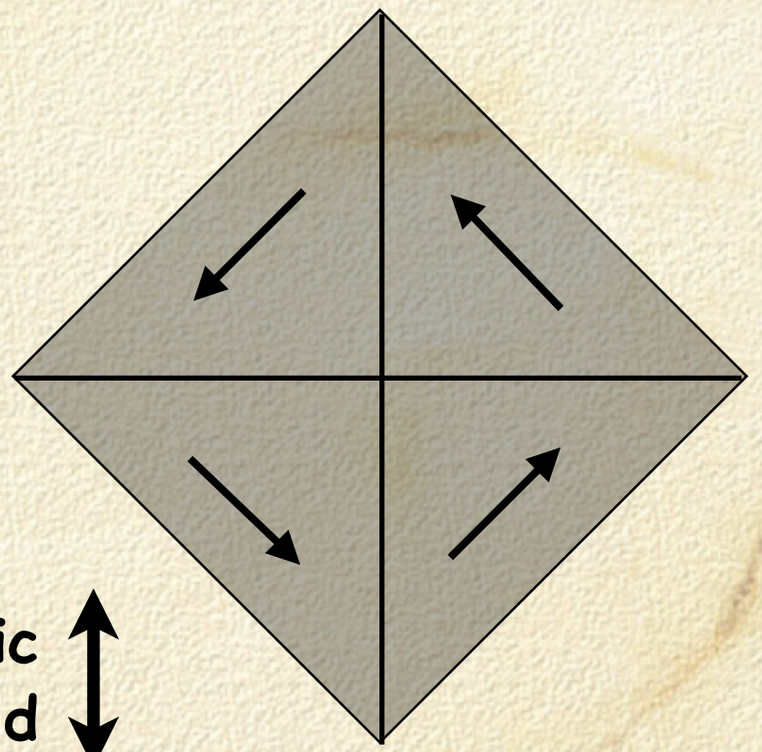

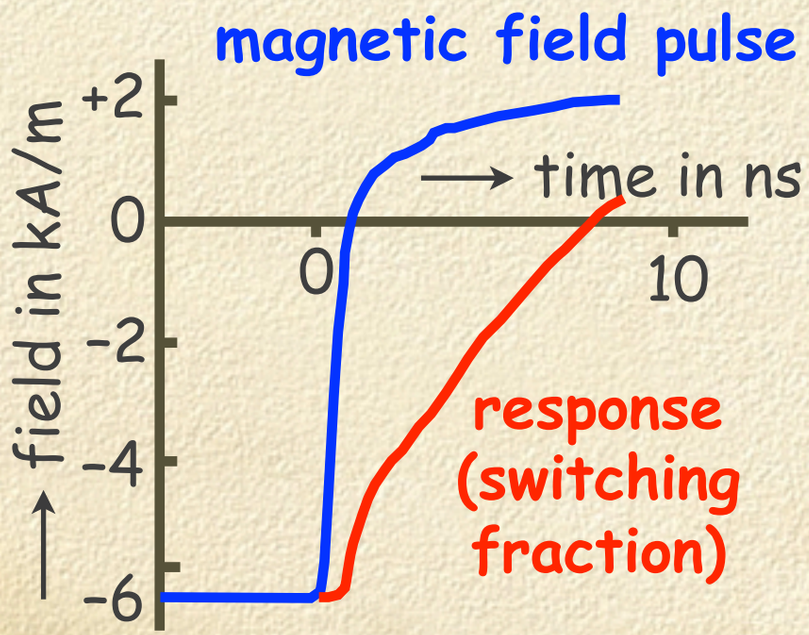

D. Chumakov et al.,
PRB 71, 014410 (2005)

Domain dynamics depends on excitation speed

Magneto-optical Kerr microscopy

Kerr effect

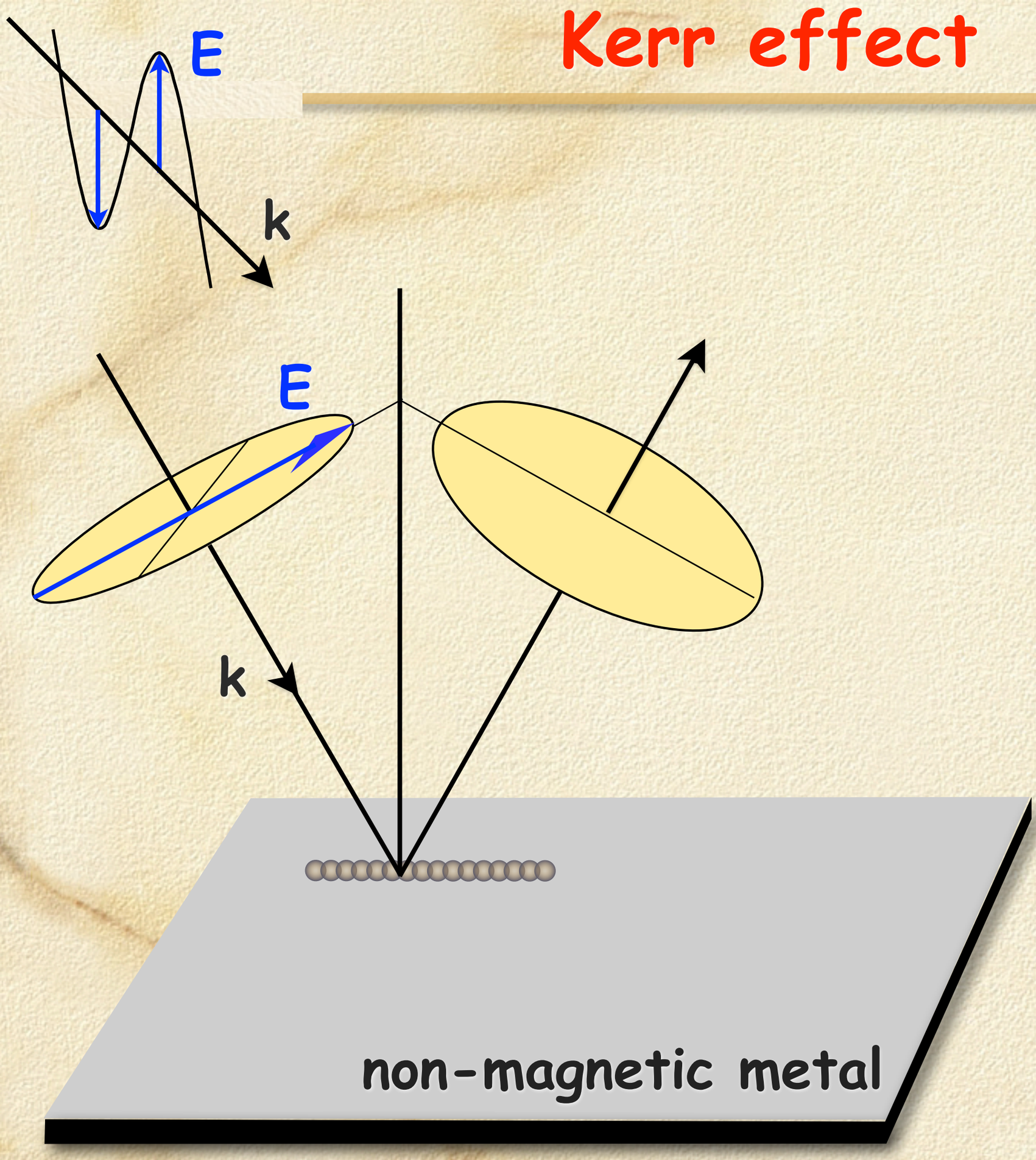

Kerr effect

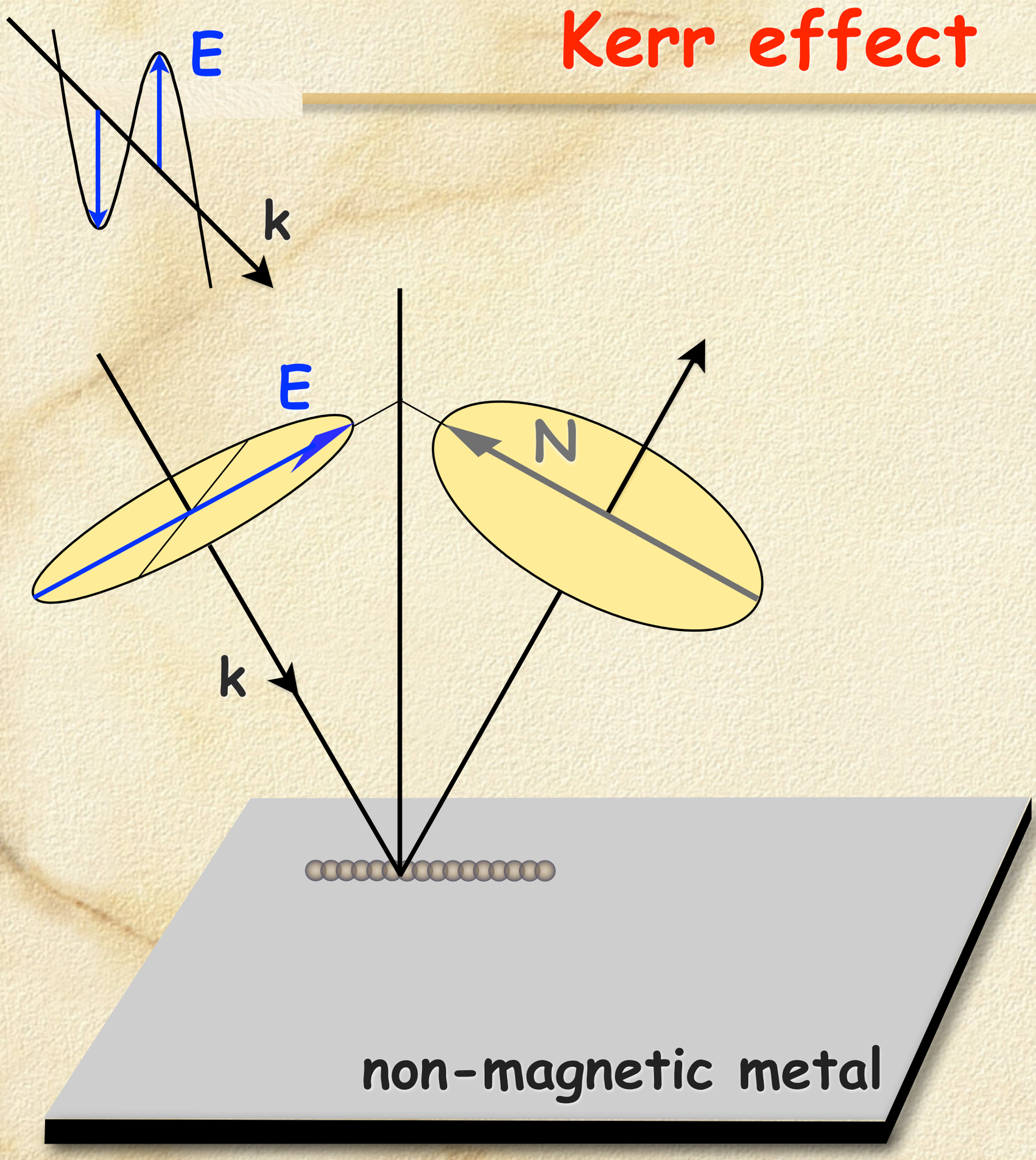

Kerr effect

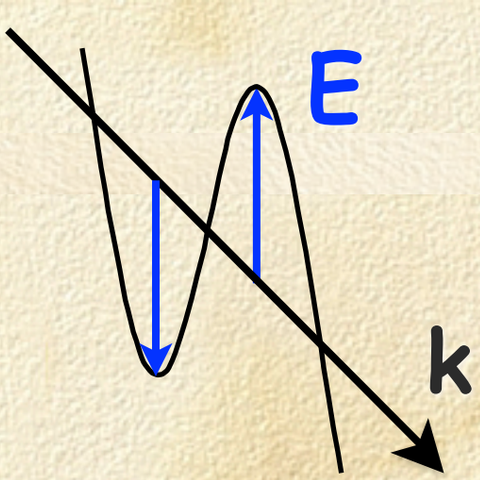

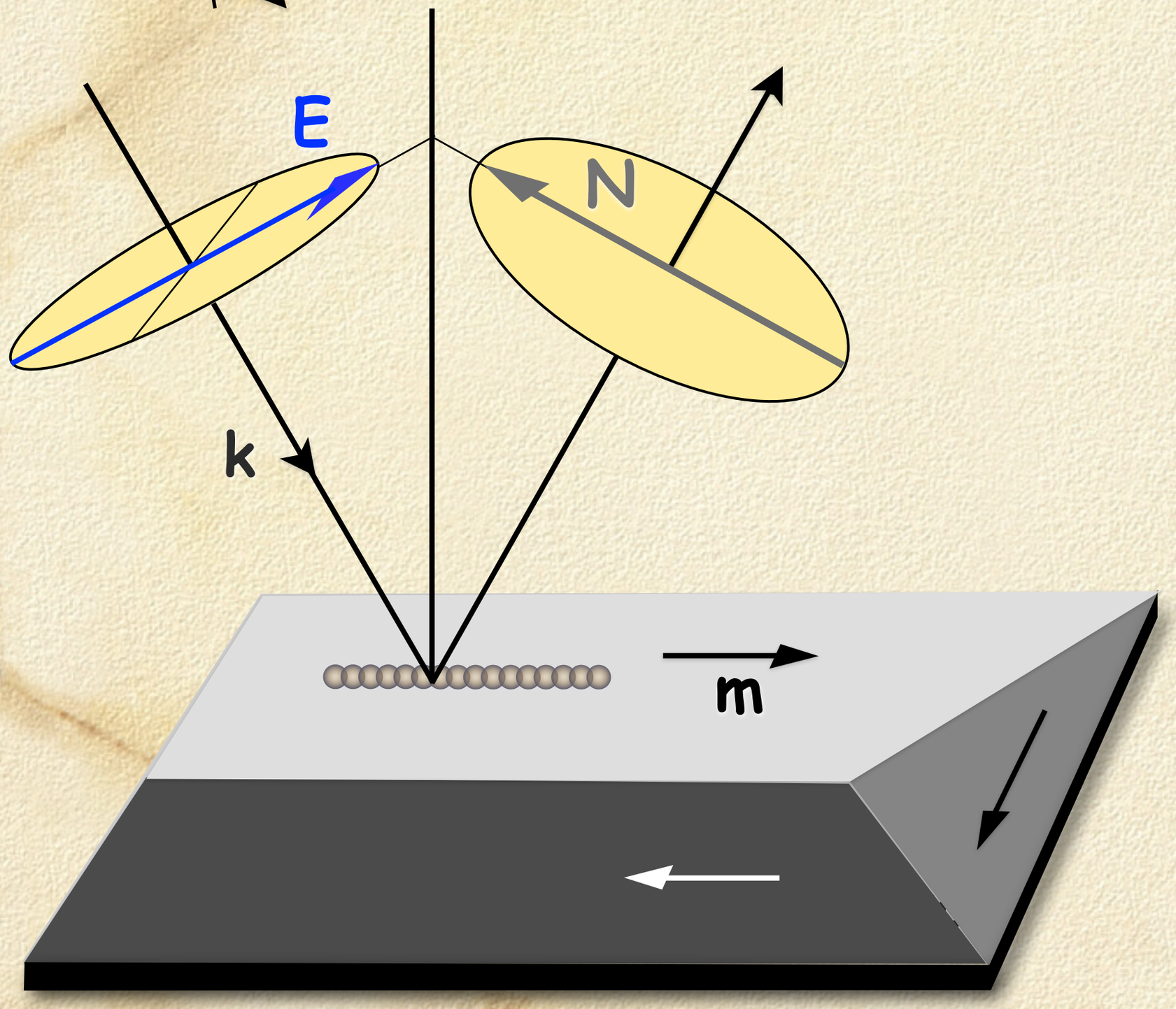

Kerr effect

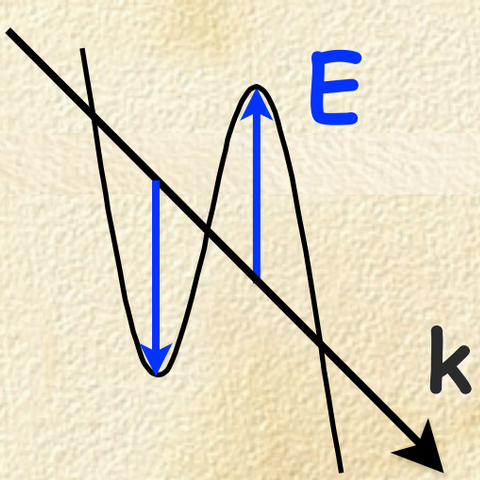

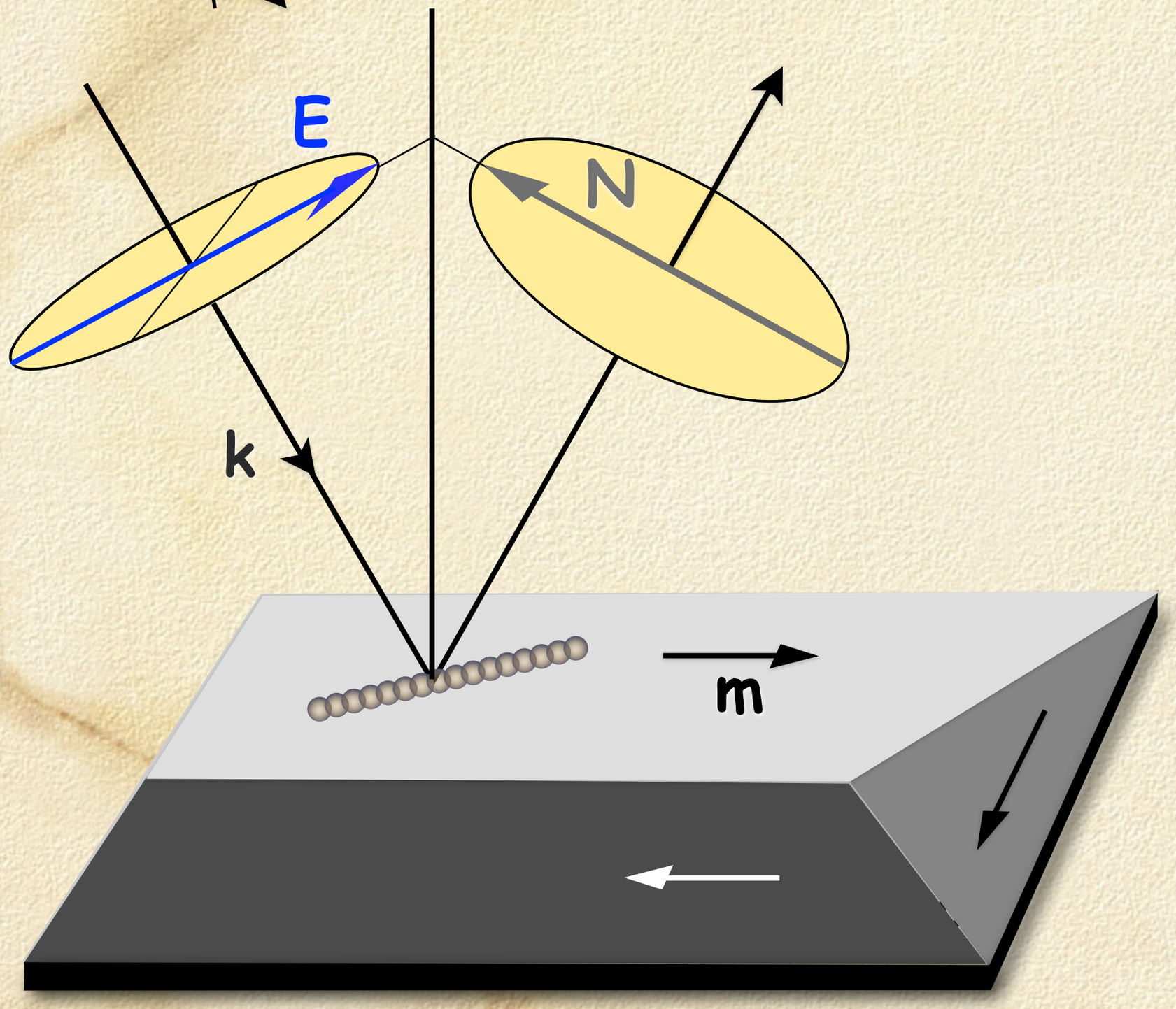

Kerr effect

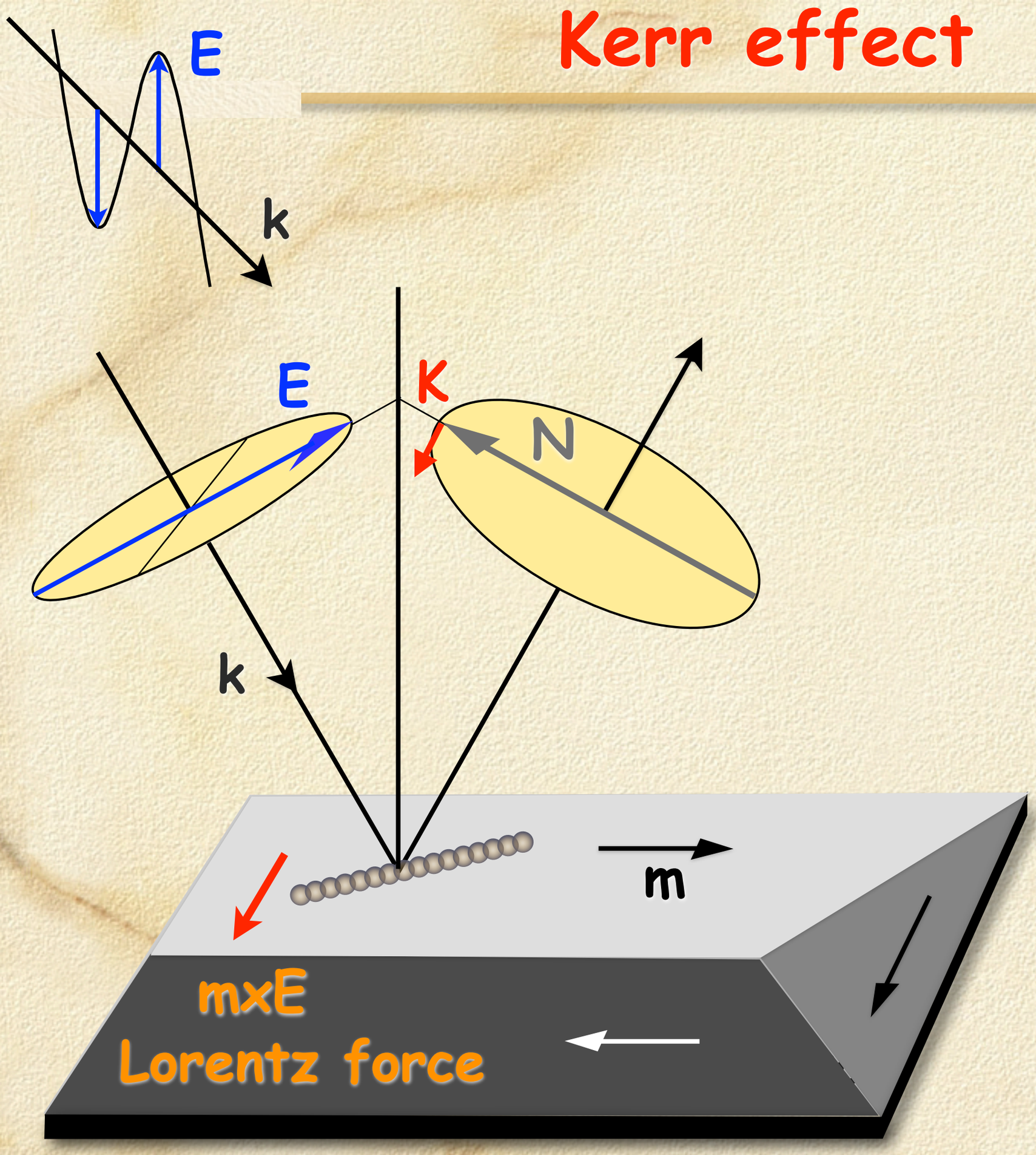

Kerr effect

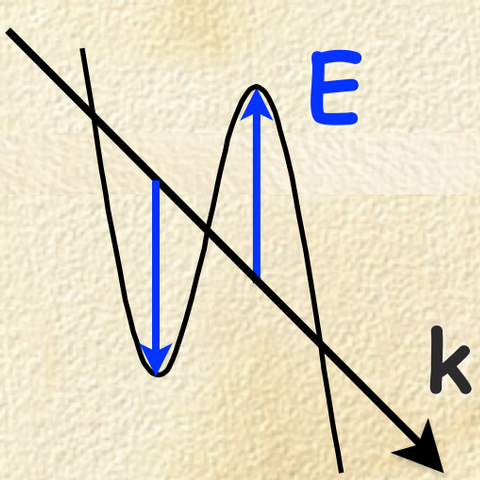

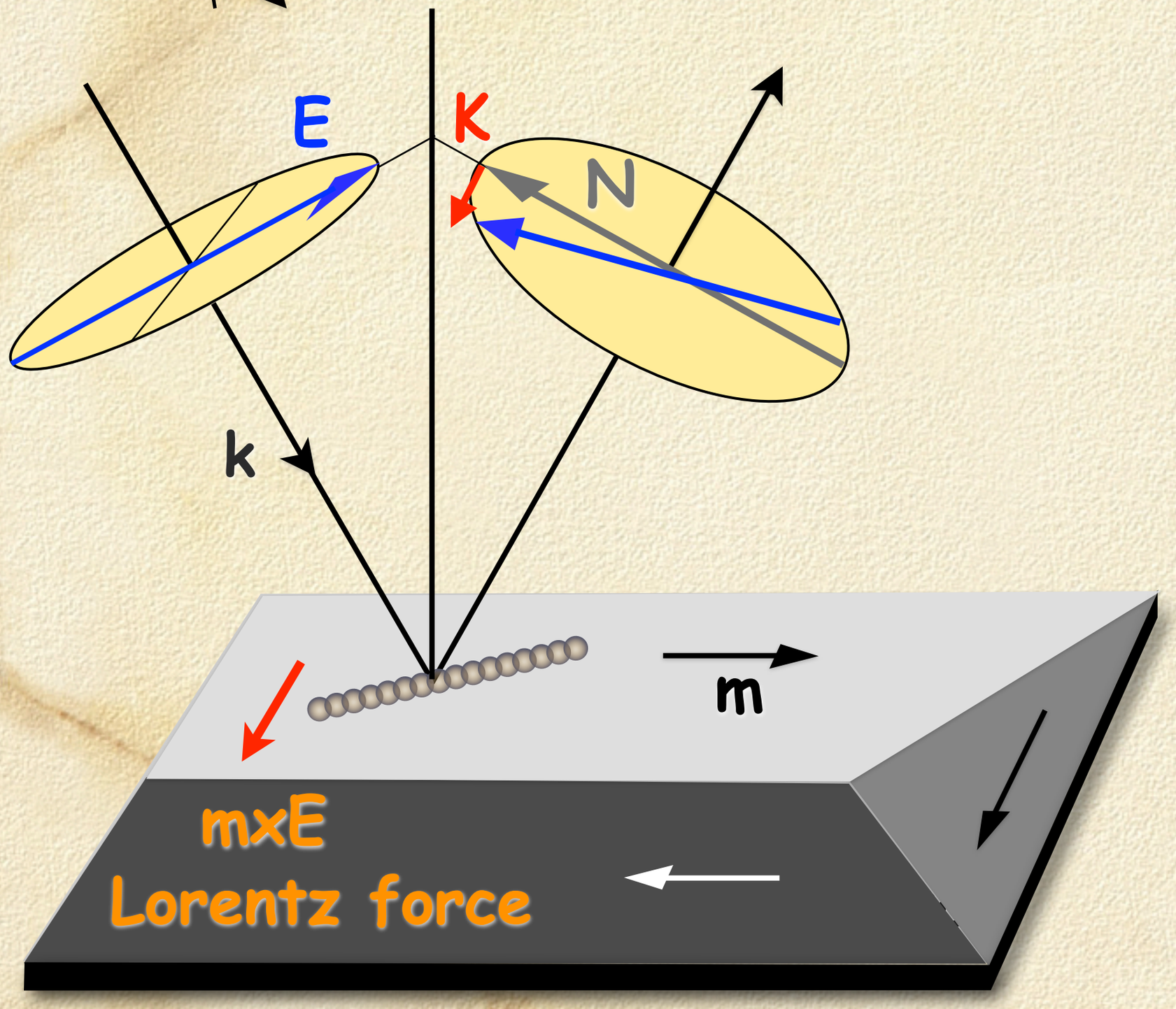

Kerr effect

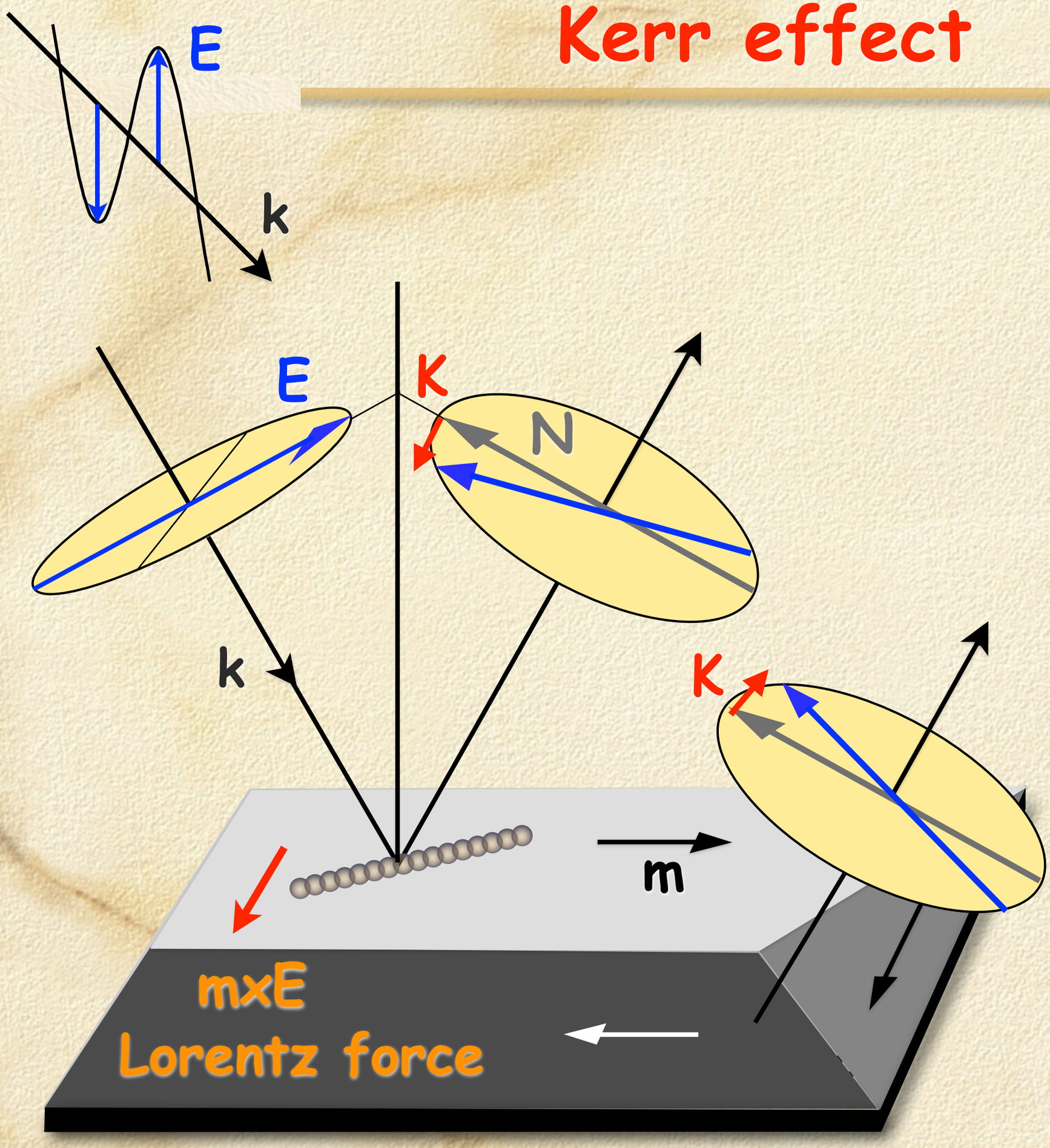

E

k

E

K

N

k

K

m

mxE
Lorentz force

-K

+K

N

polarizer

analyser

Kerr rotation
= K/N

Kerr microscope

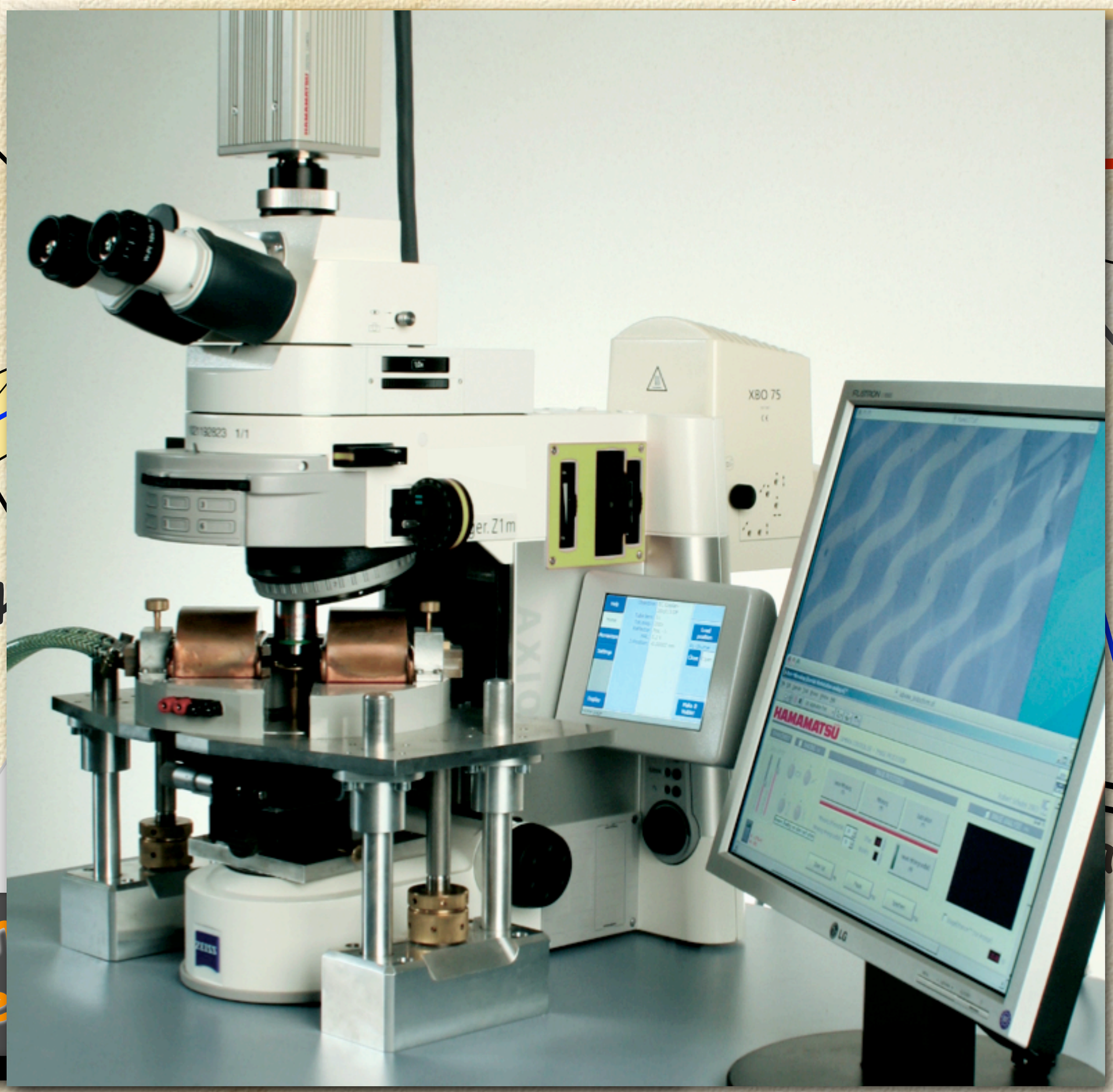

E

+K

lyser

rotation
K/N

Kerr microscope

Digital contrast enhancement (difference image technique)

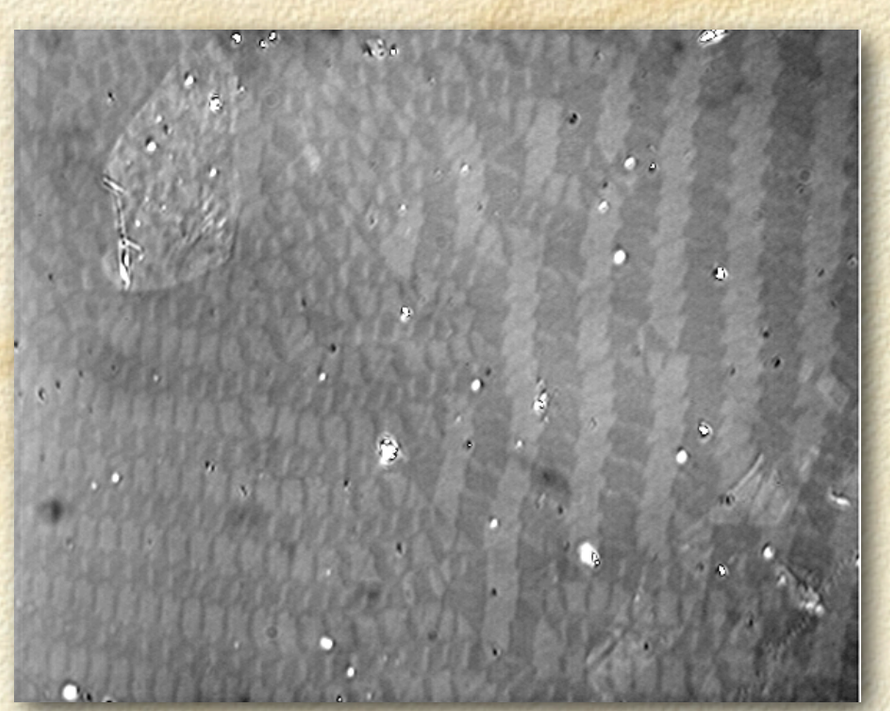

Original image

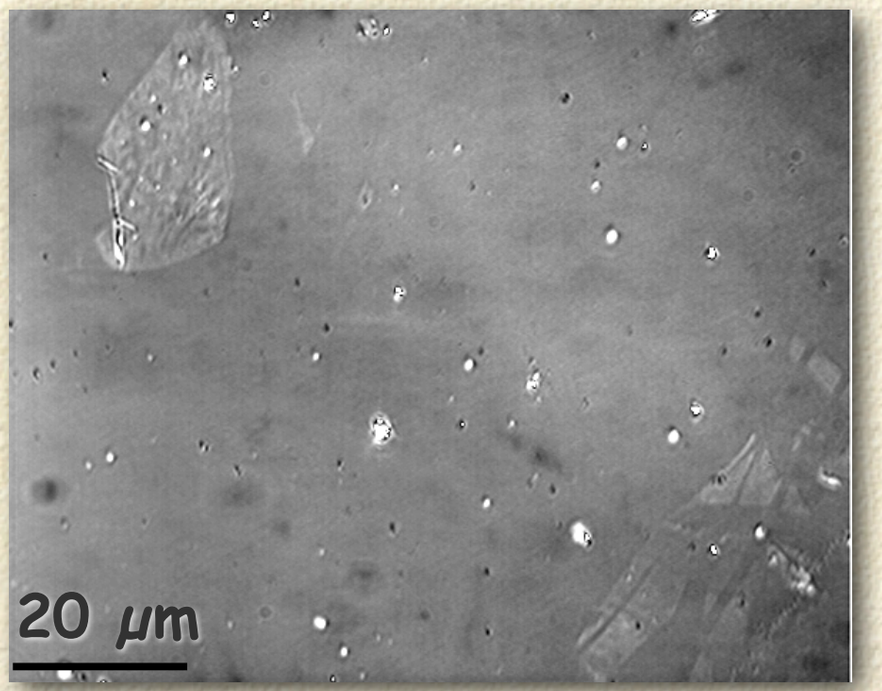

Reference image

amorphous ribbon

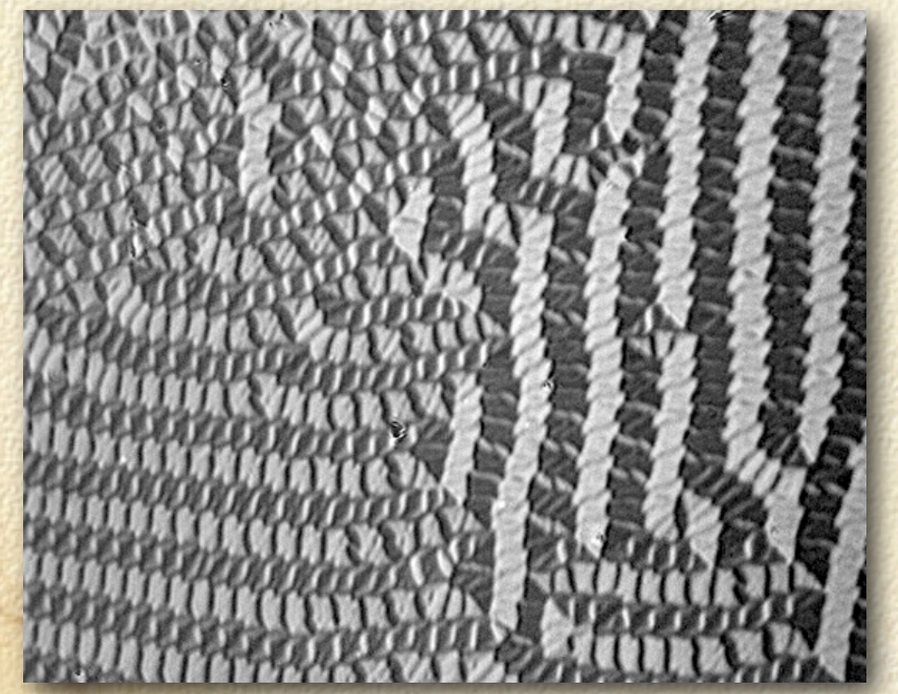

Difference image

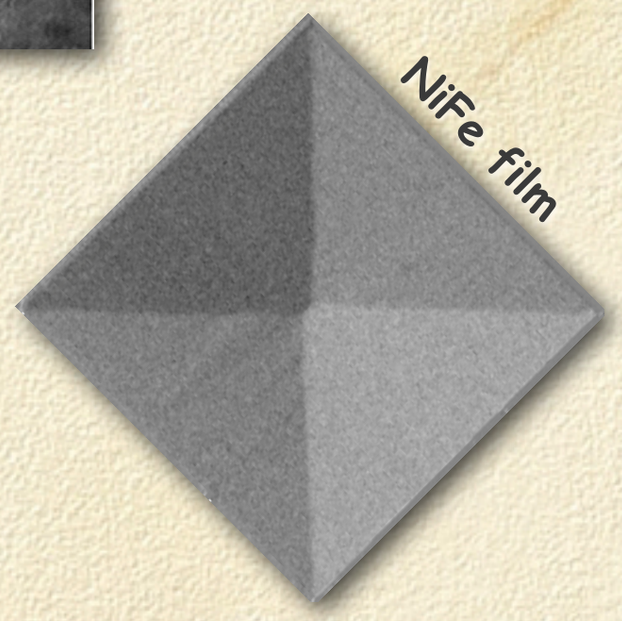

Important: Difference Imaging in real time !

Comparison of Domain Obervation Techniques

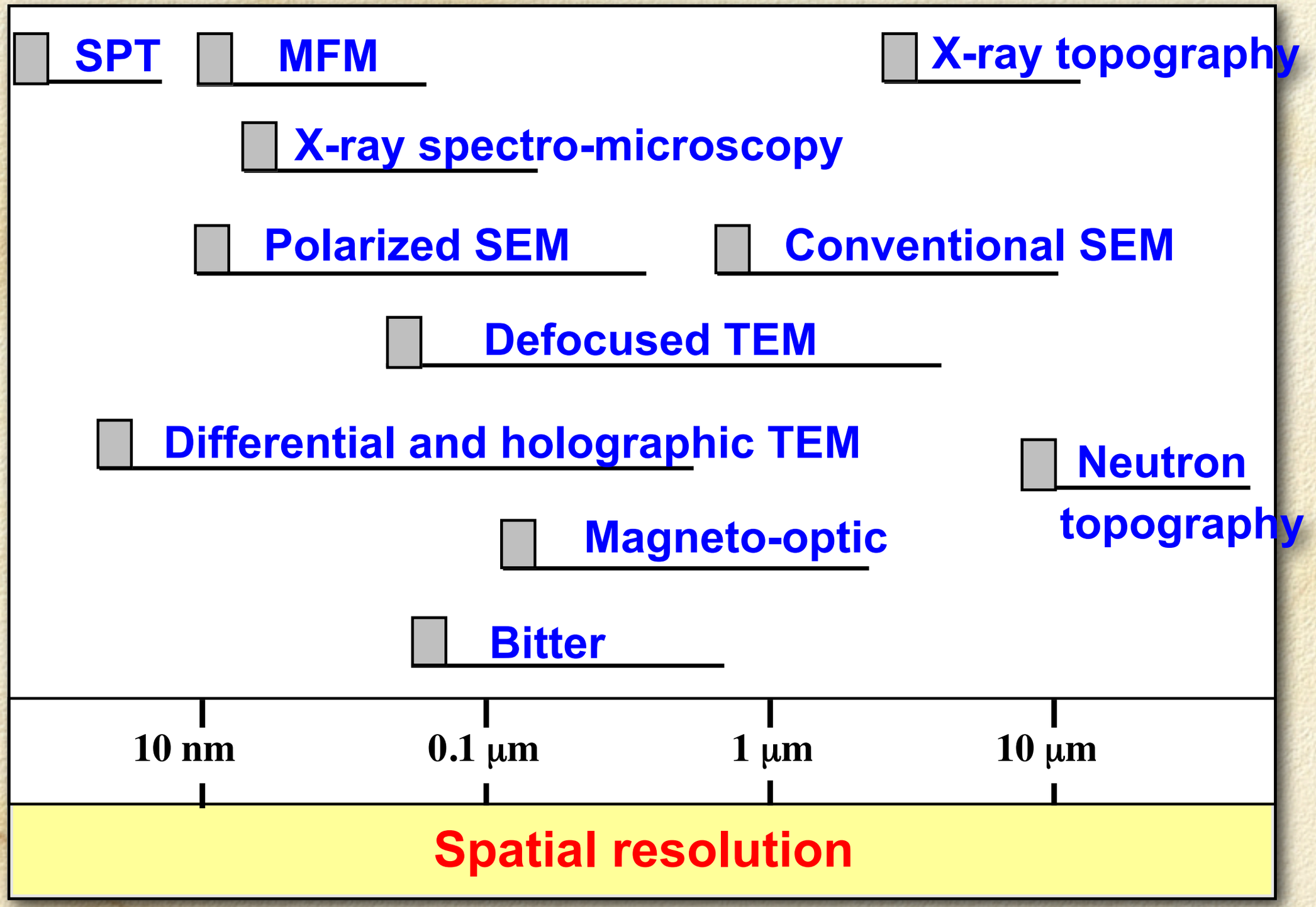

MFM: Magnetic Force Microscopy
SPT: Spin-Polarized Tunneling
SEM: Scanning (reflection) Electron Microscopy
TEM: Transmission Electron Microscopy

Comparison of Domain Obervation Techniques

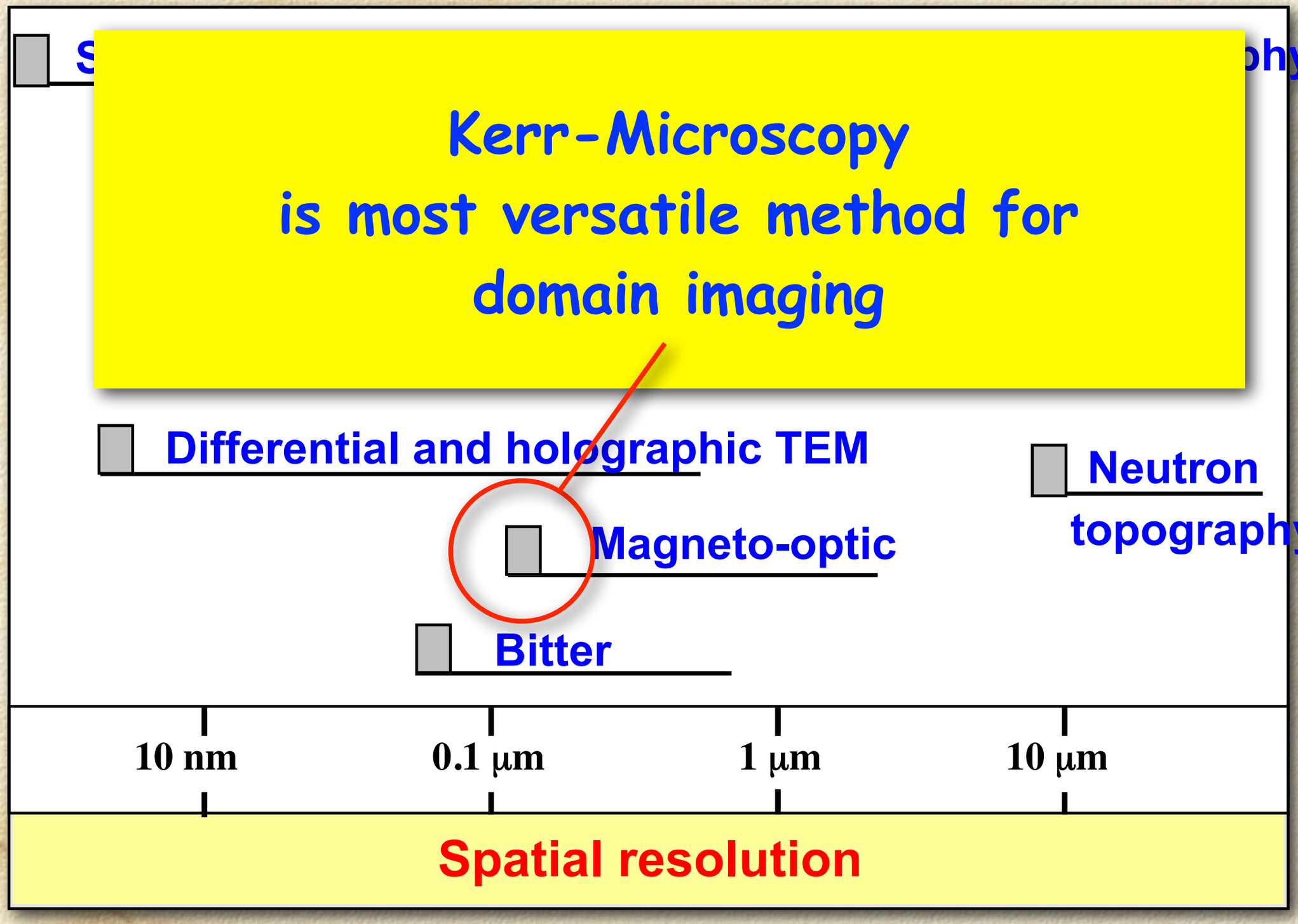

MFM: Magnetic Force Microscopy
SPT: Spin-Polarized Tunneling
SEM: Scanning (reflection) Electron Microscopy
TEM: Transmission Electron Microscopy

Why magnetic microstructure analysis?

M(H) loop and domains

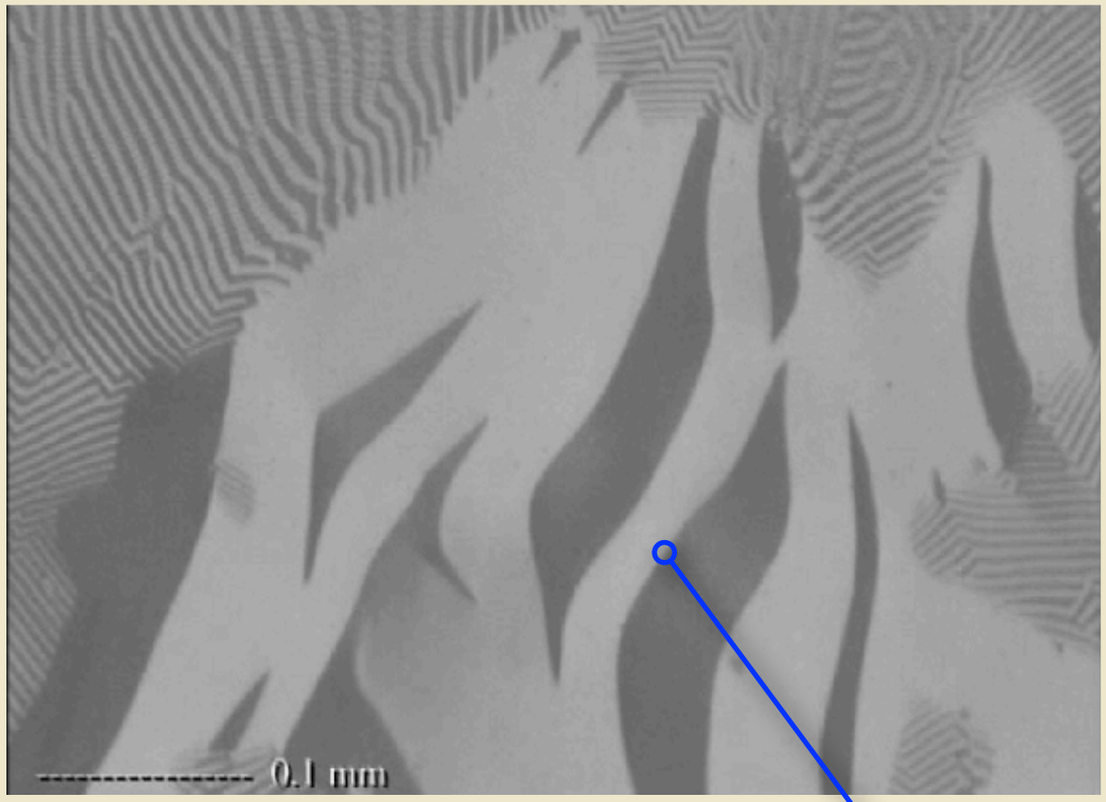

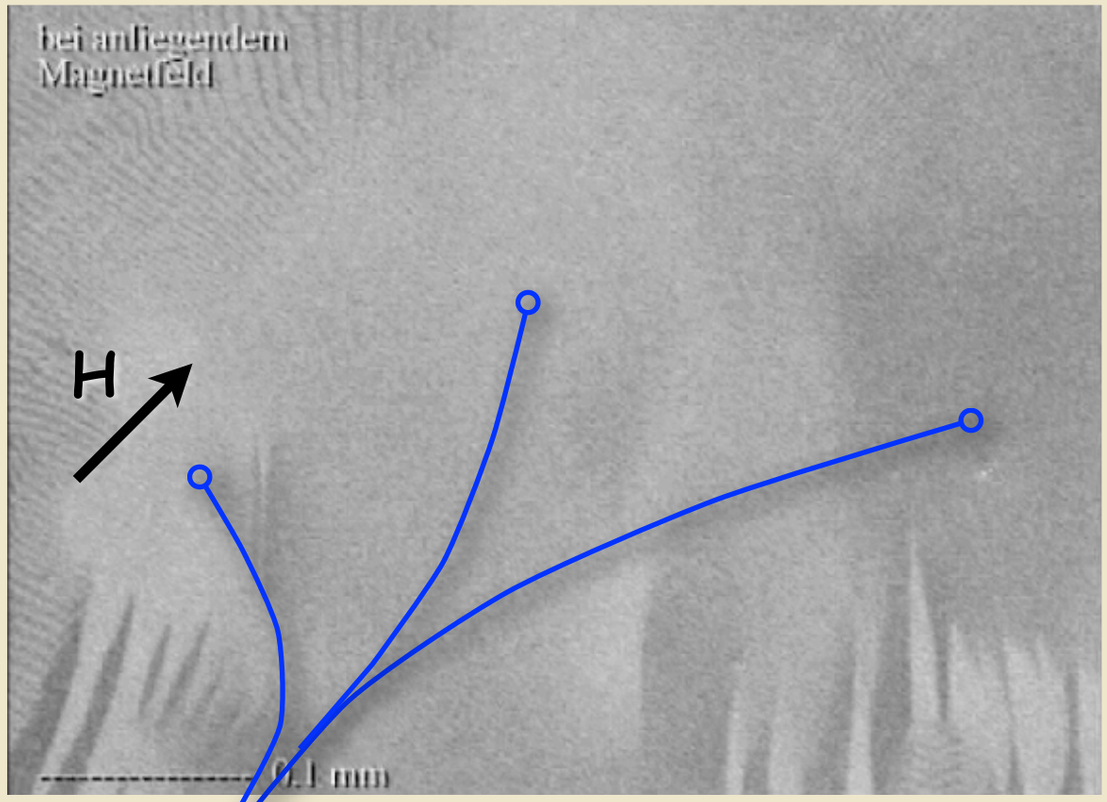

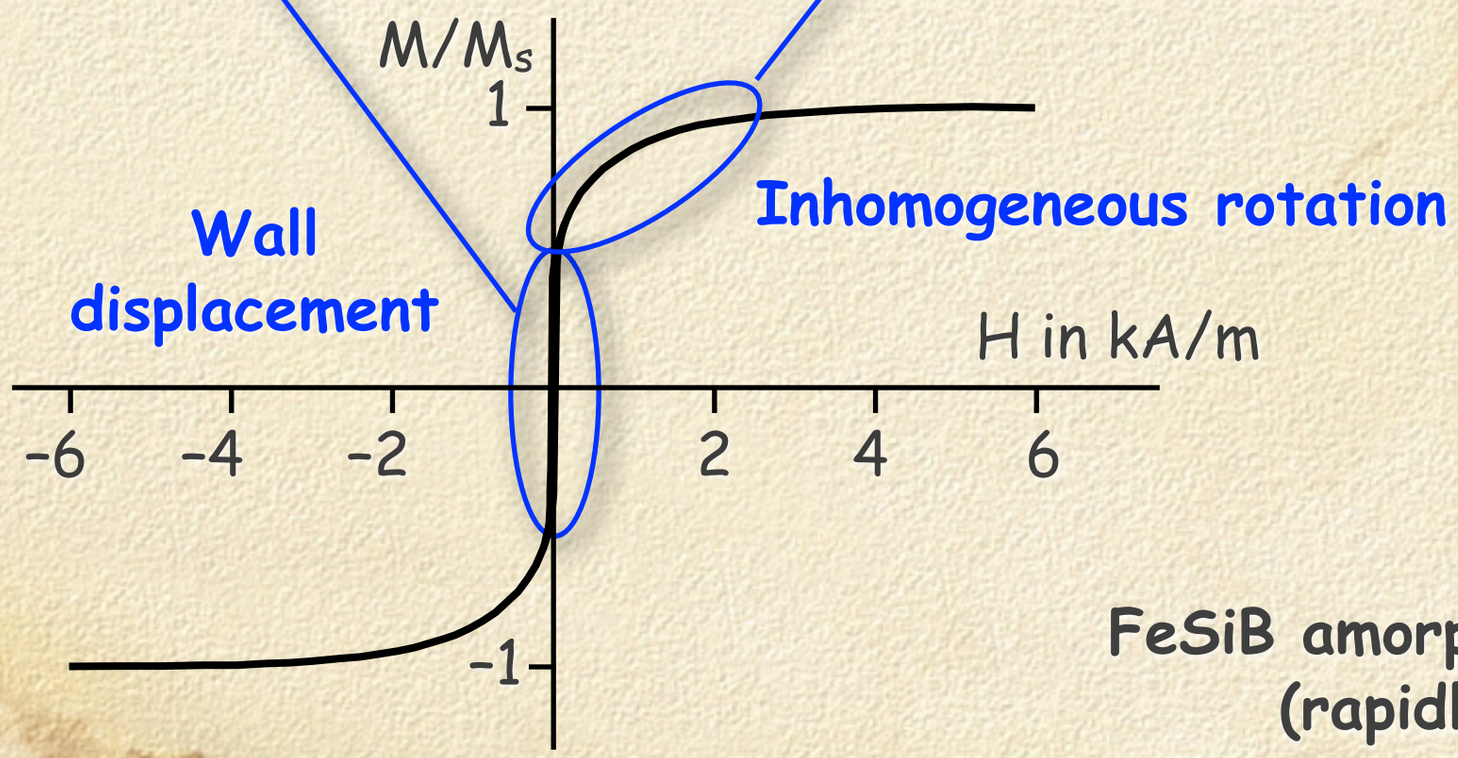

FeSiB amorphous ribbon
(rapidly quenched)

M(H) loop and domains

Permalloy (NiFe) film
207 nm thick

57 μm

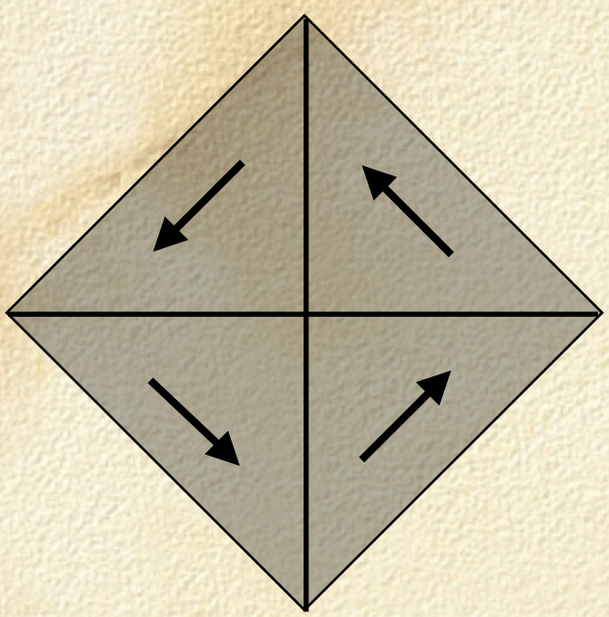

Magnetic field H

Concertina

$H = H_K$

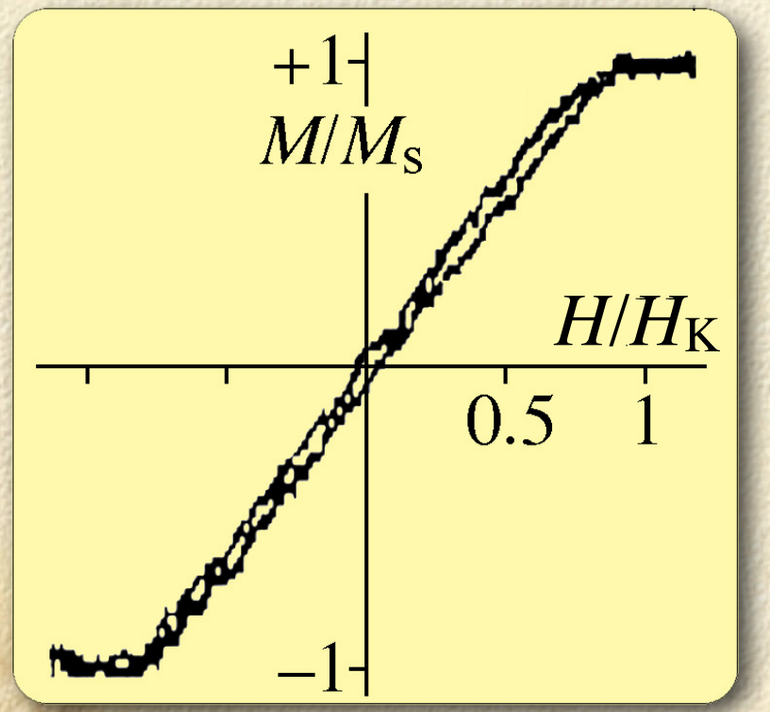

$H > H_K$

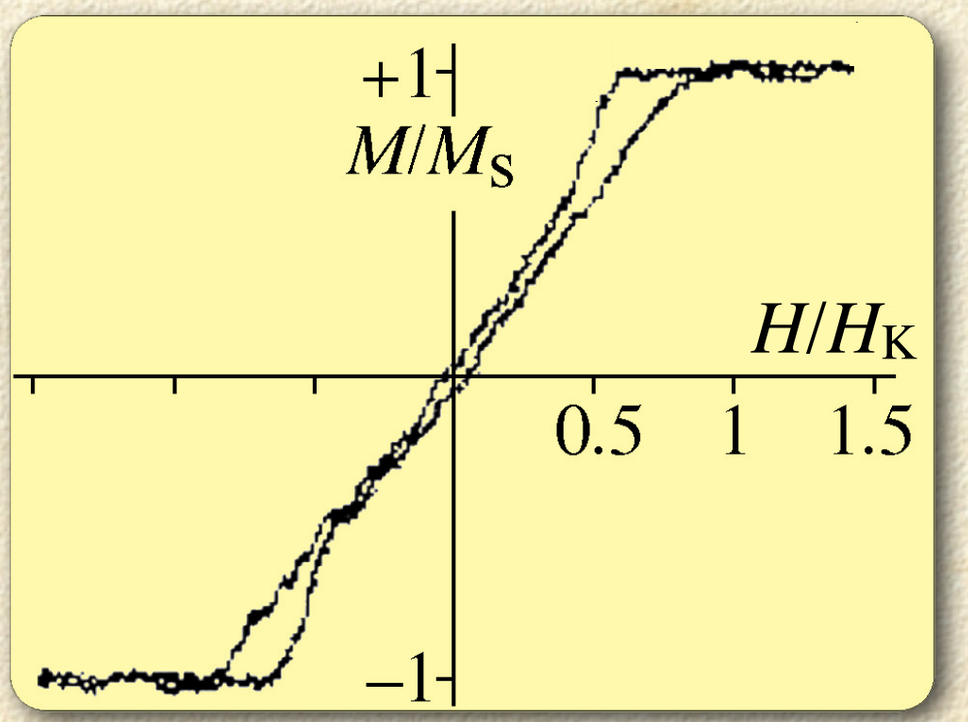

M(H) loop and domains

Permalloy (NiFe) film
207 nm thick

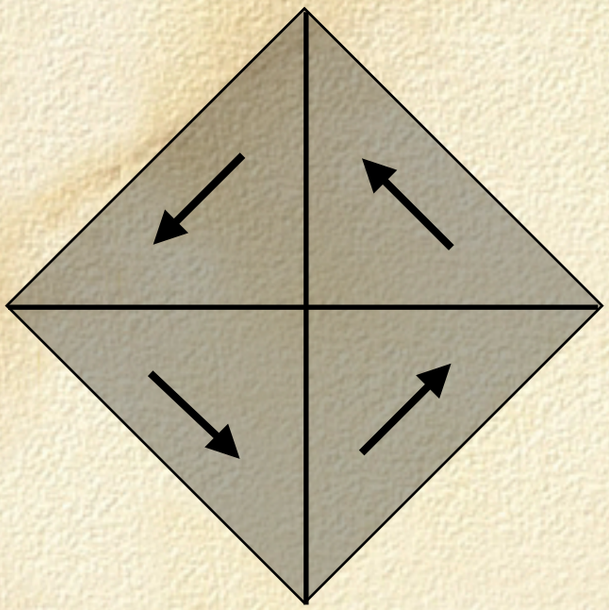

Magnetic field H

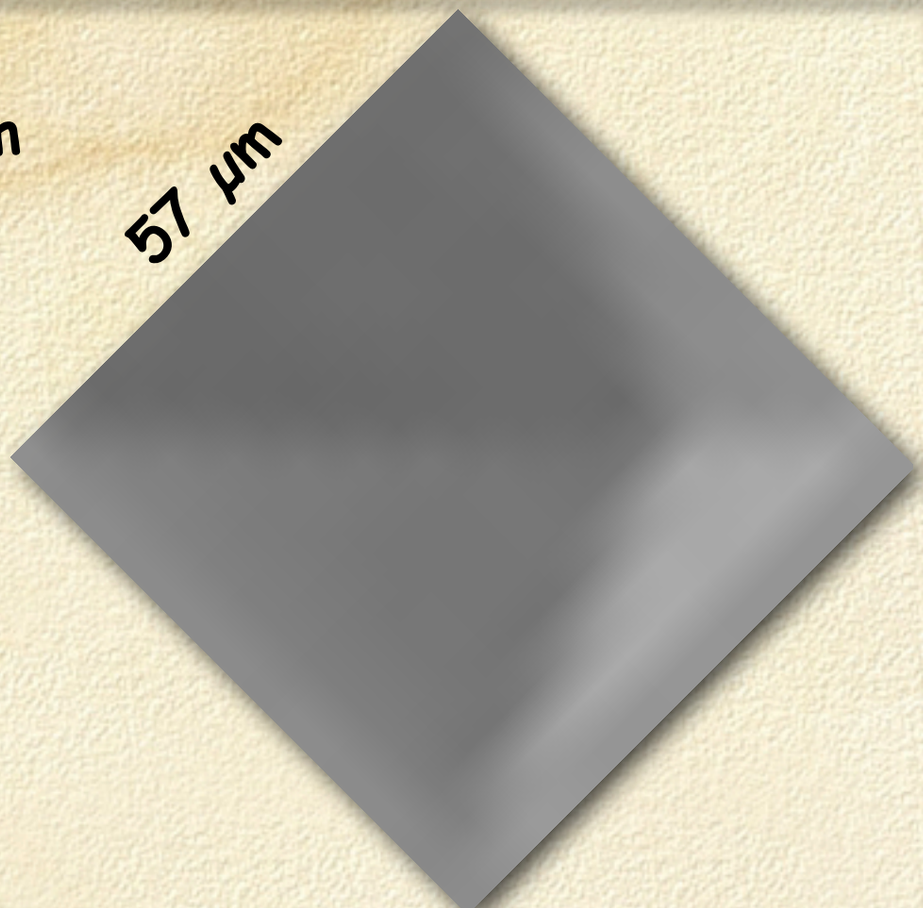

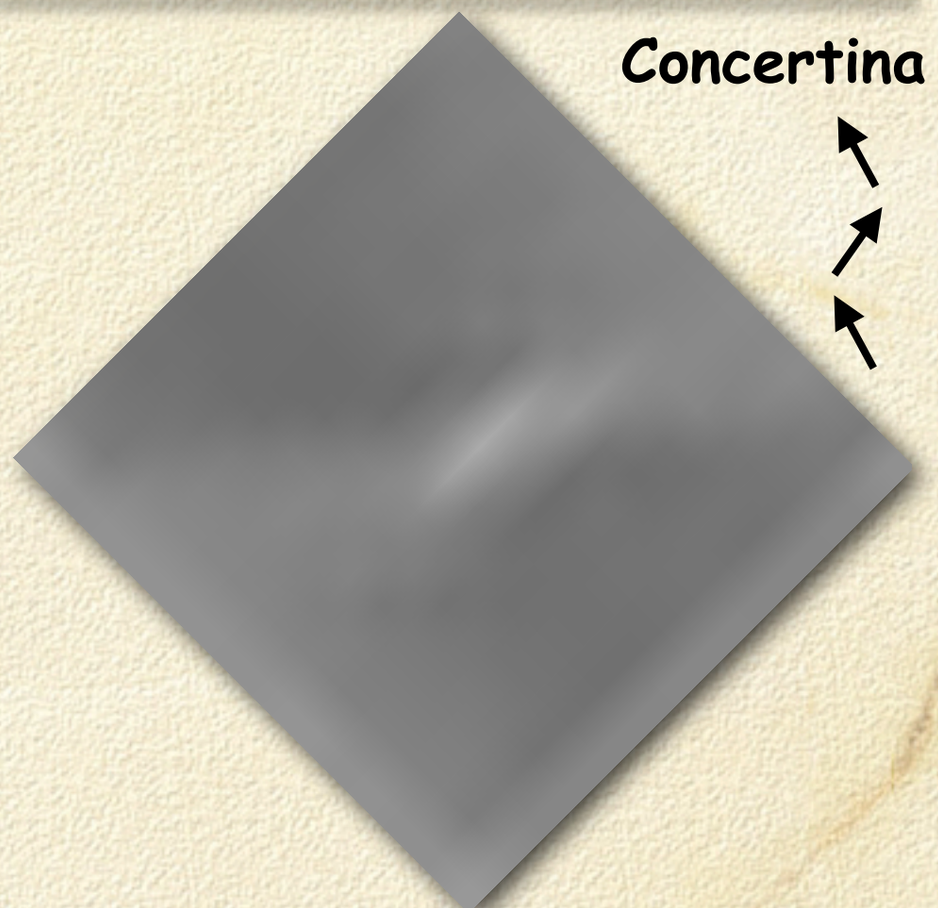

$H = H_K$

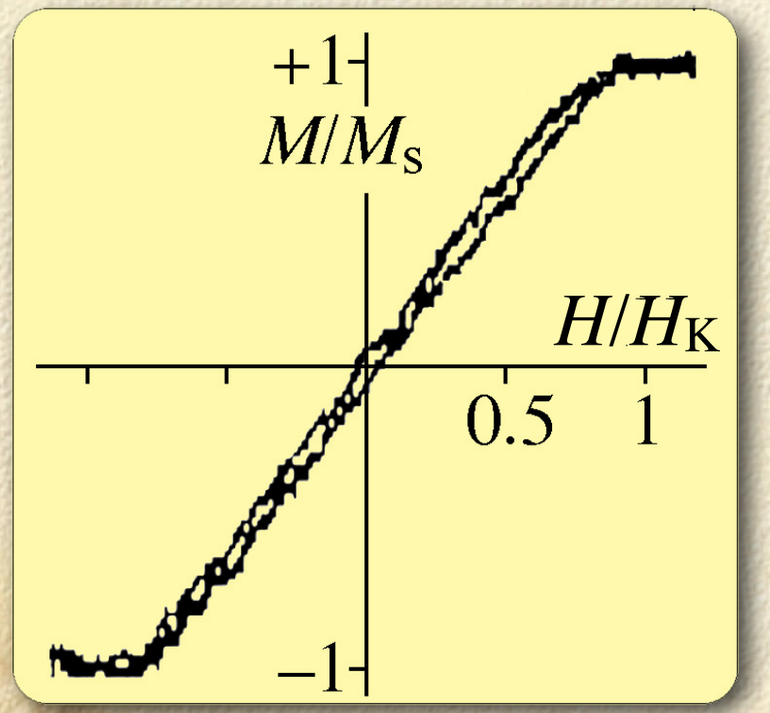

$H > H_K$

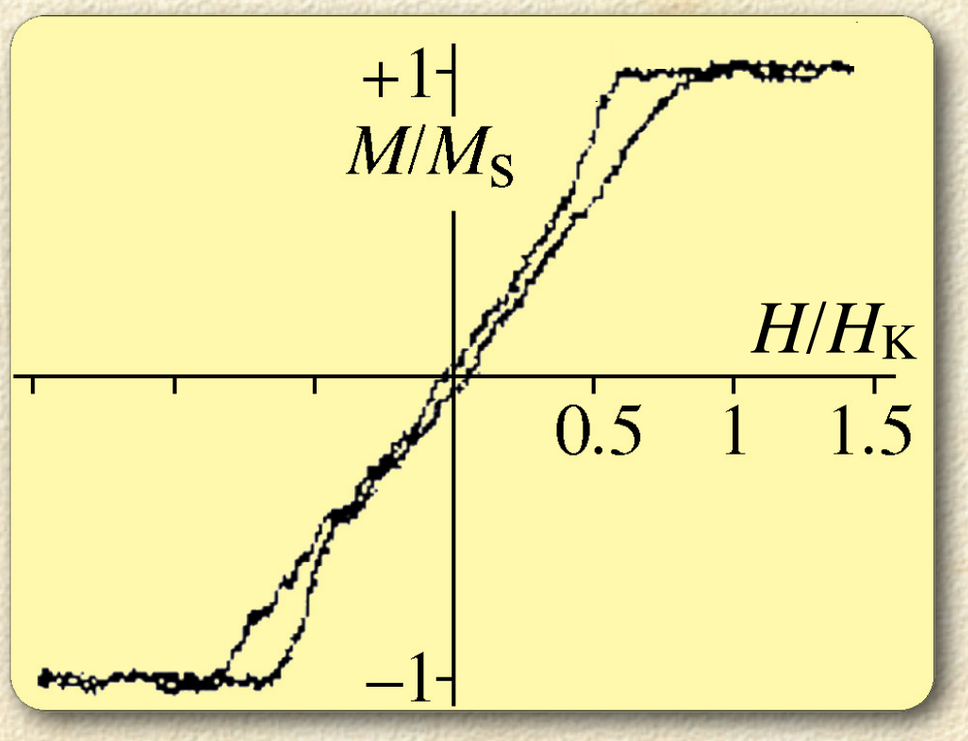

M(H) loop and domains

Permalloy (NiFe) film
207 nm thick

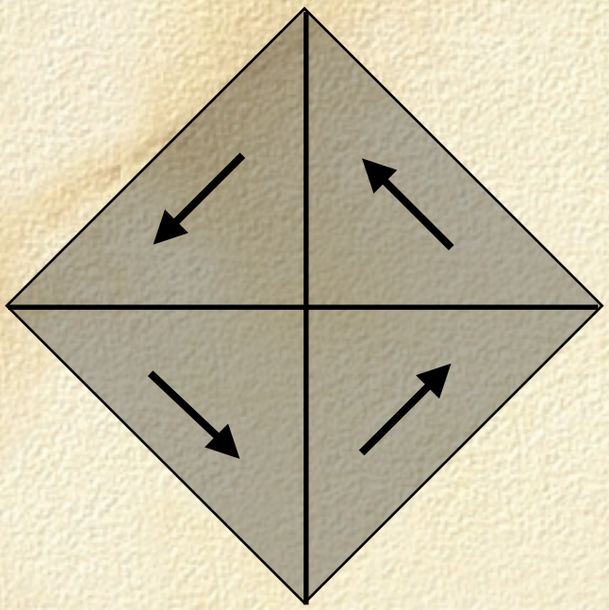

Magnetic field H

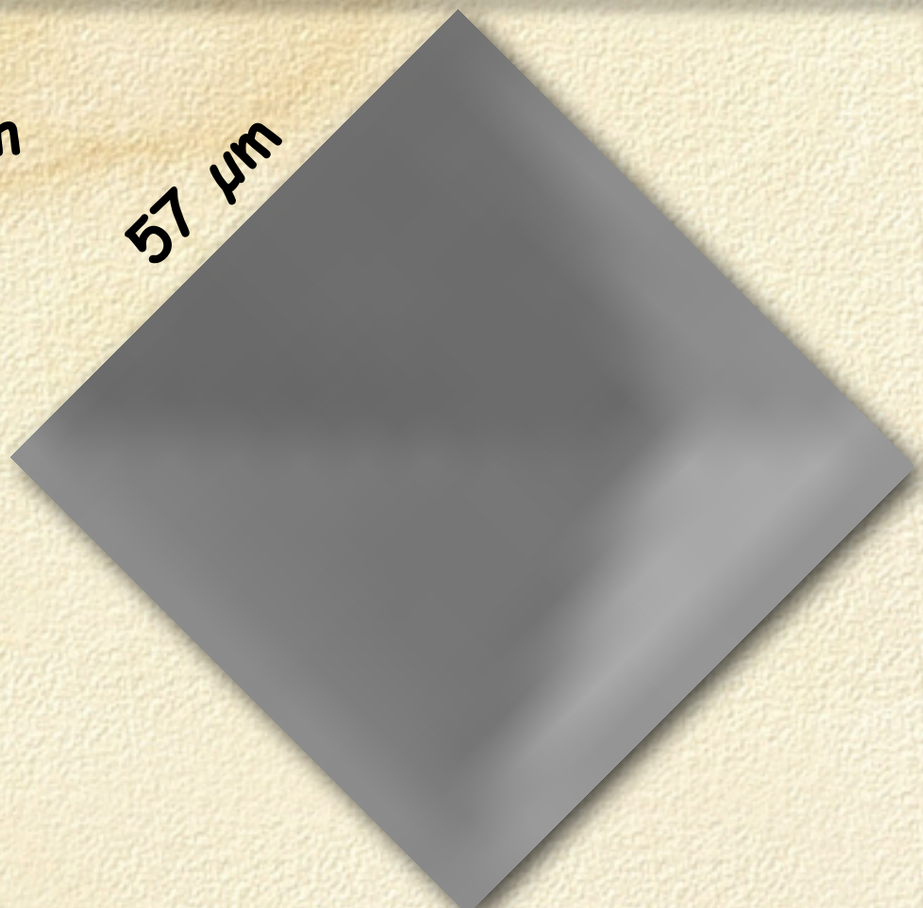

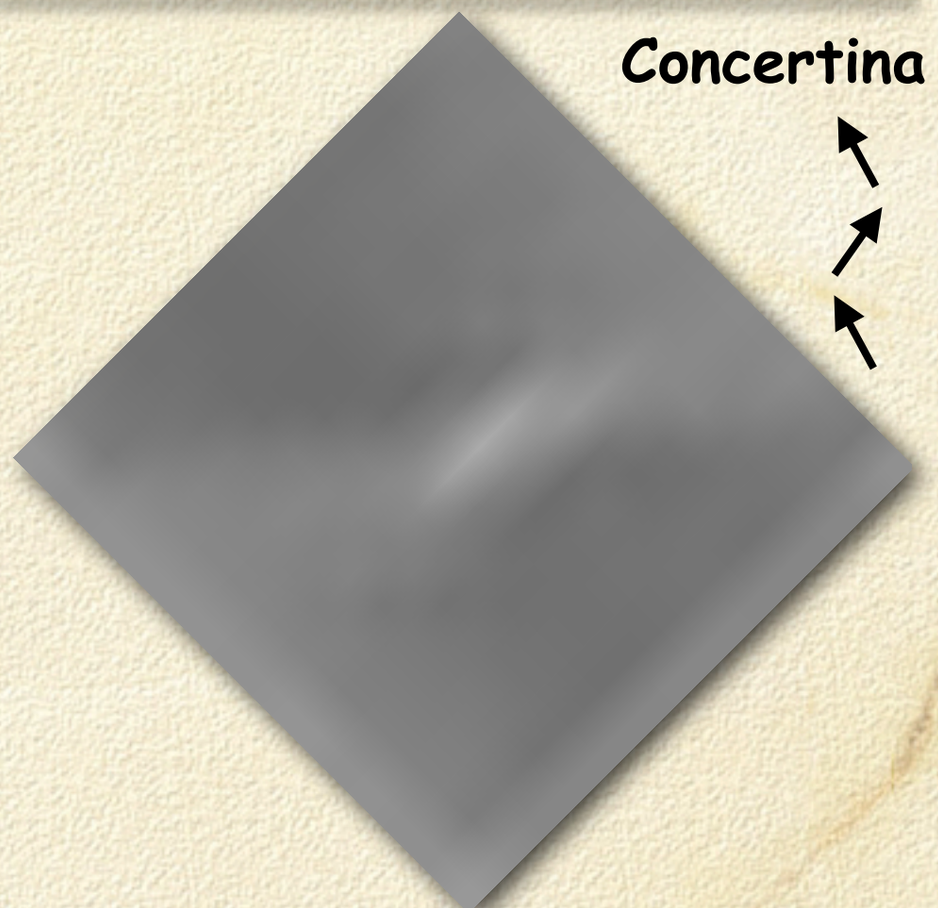

$H = H_K$

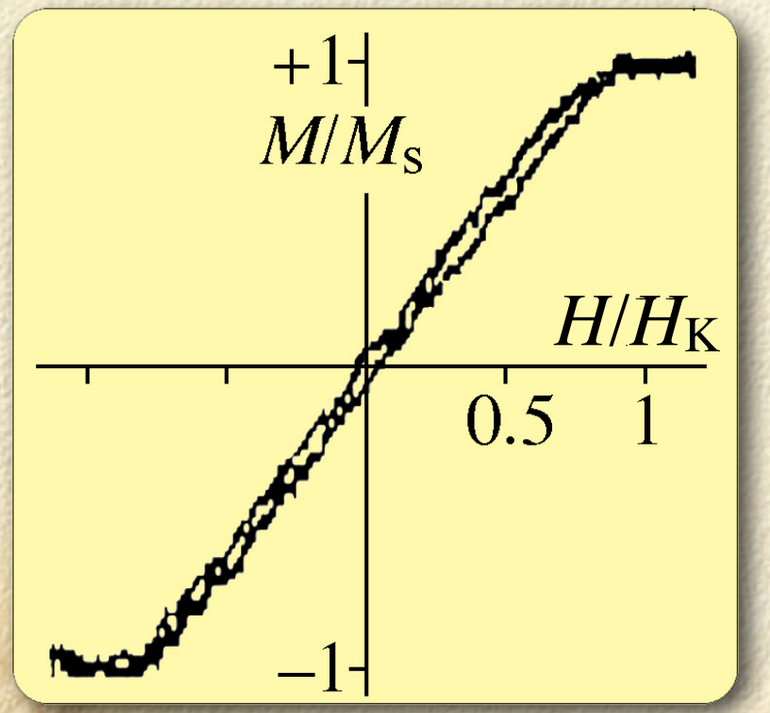

$H > H_K$

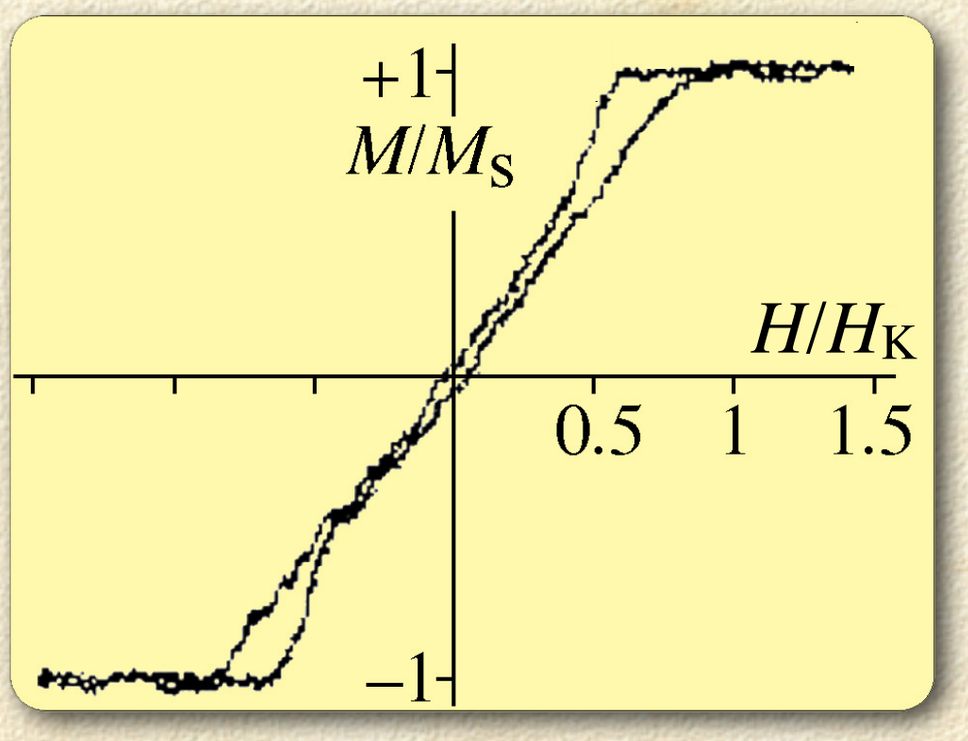

M(H) loop and domains

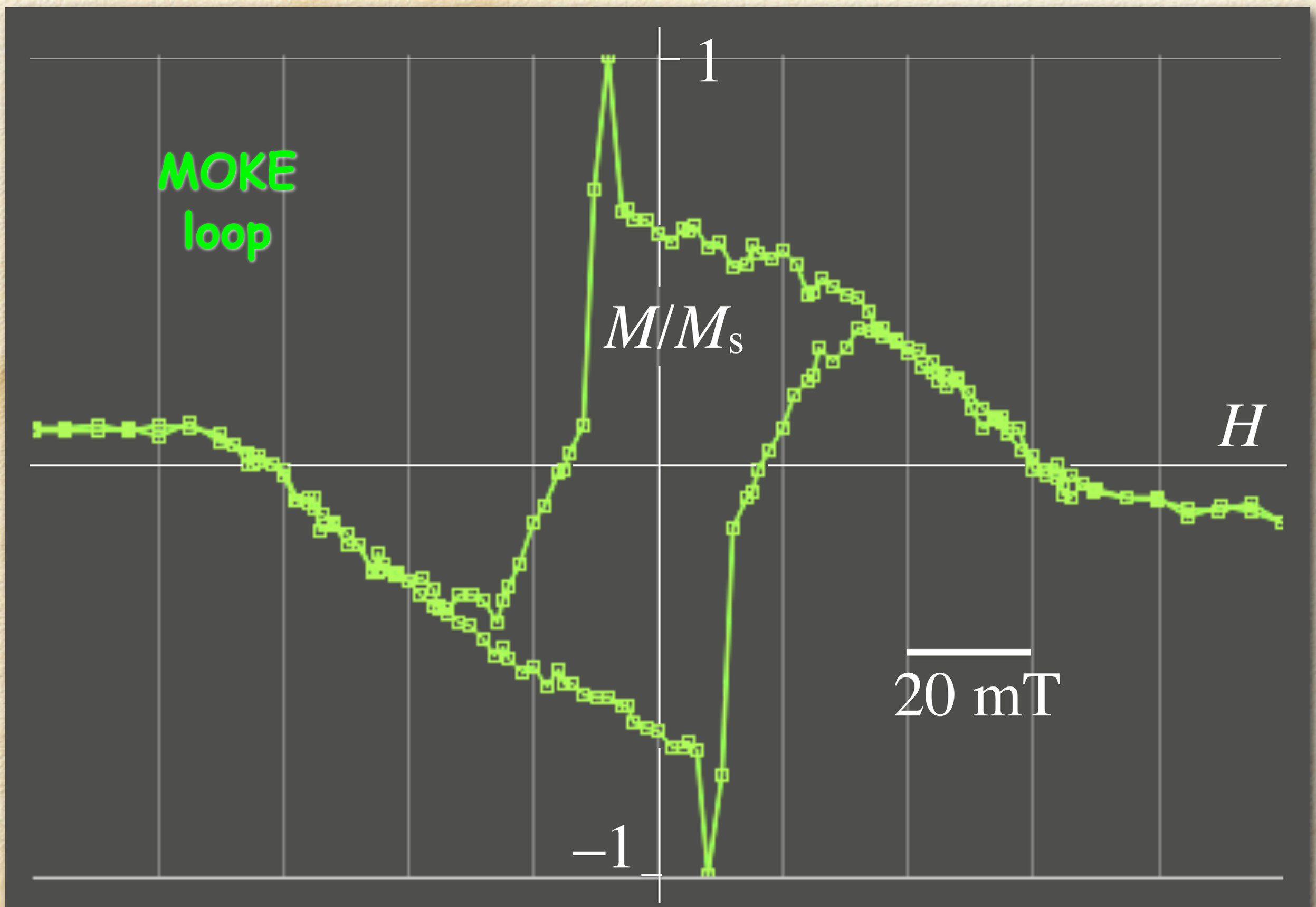

M(H) loop and domains

$Co_{27}Sm_{73}$ amorphous film (thickness 200 nm)

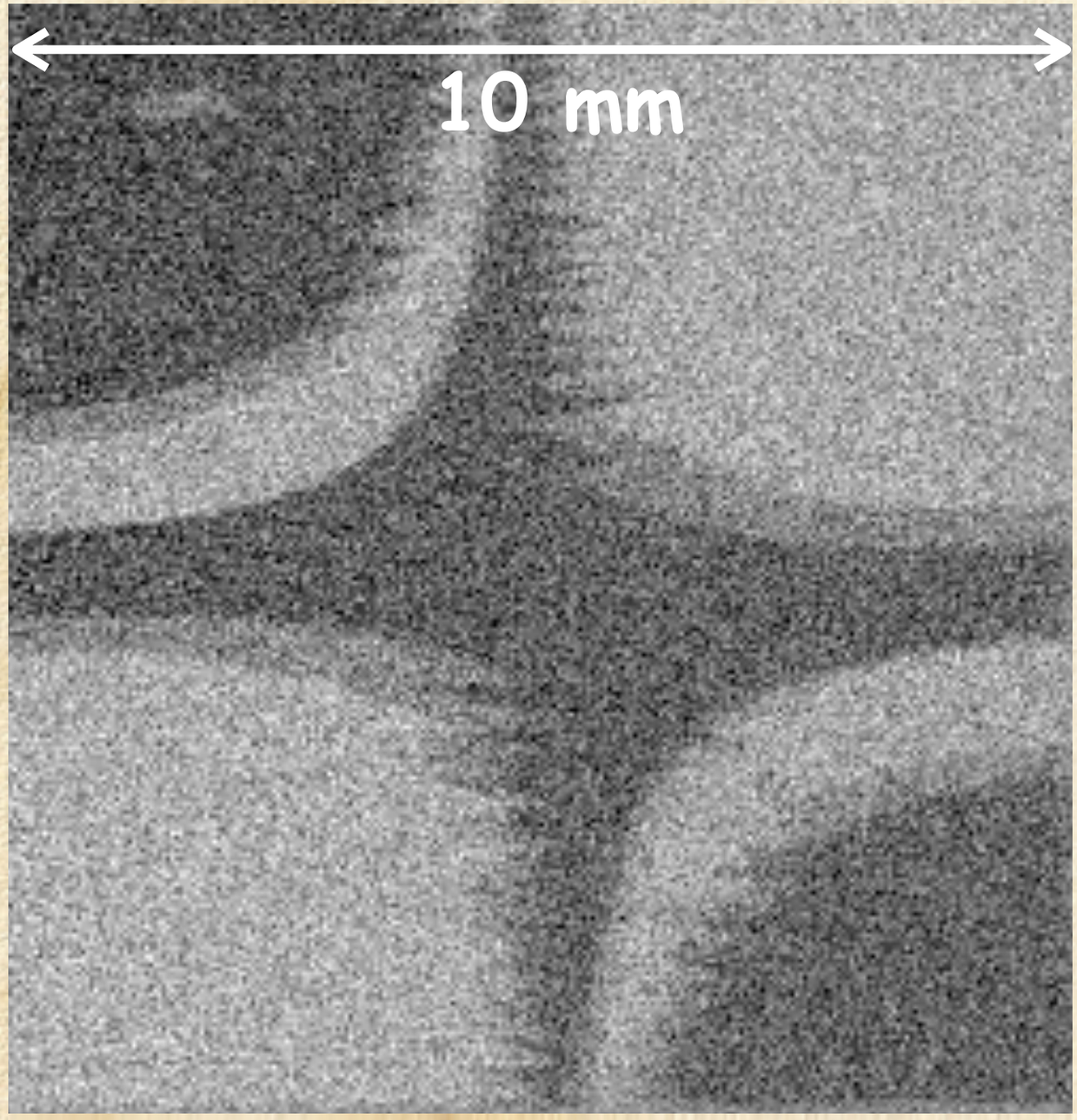

Sample: F. Magnus and B. Hjörvarsson, Uppsala University (unpublished)

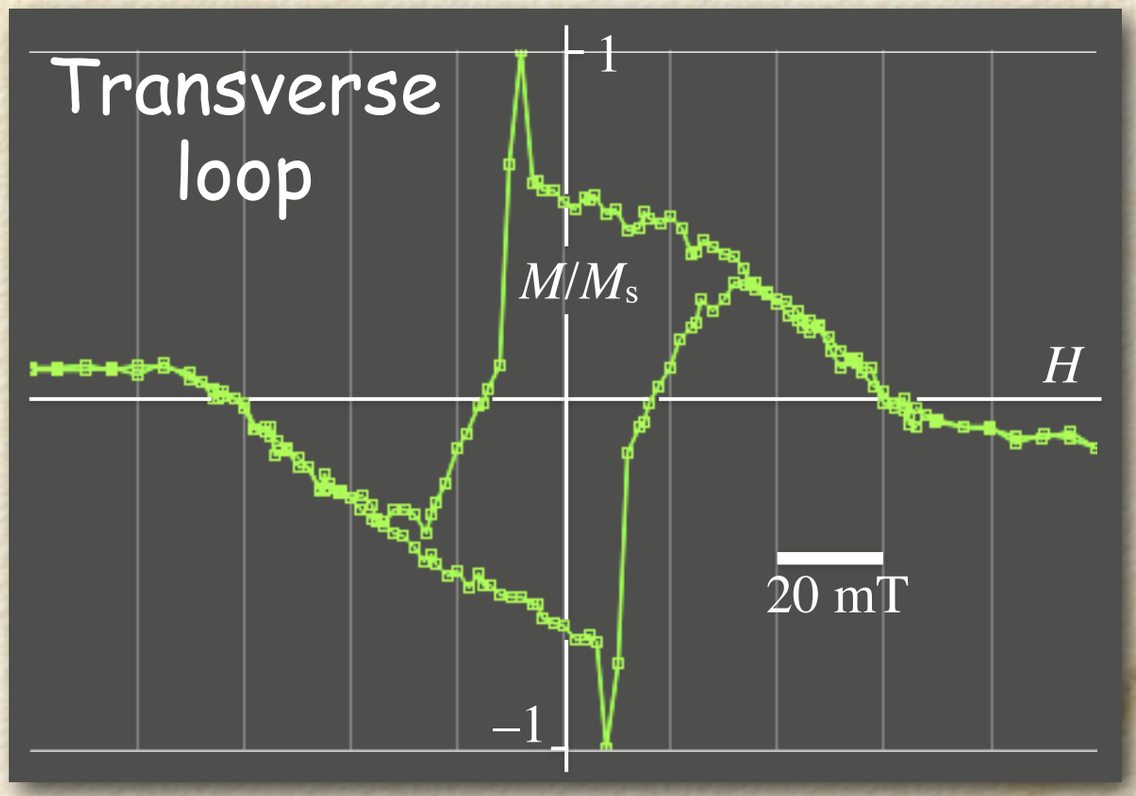

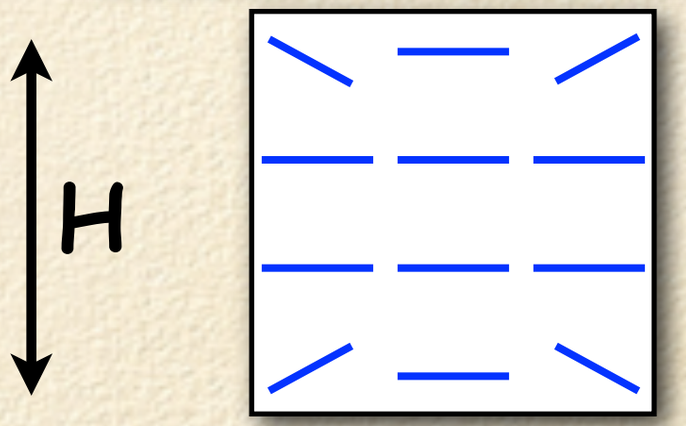

Anisotropy

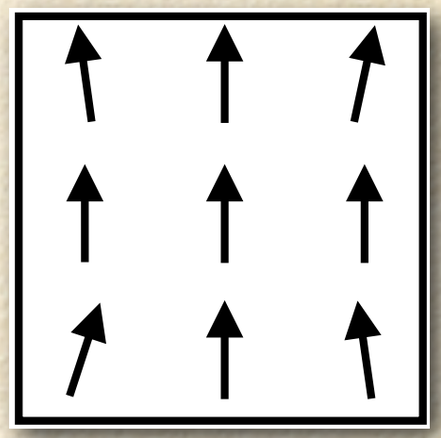

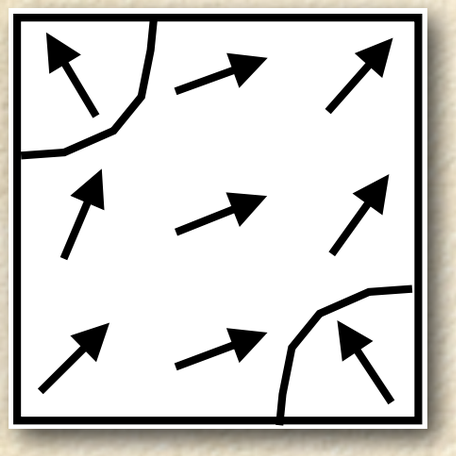

M(H) loop and domains

Reversal of $Ni_{81}Fe_{19}$ (30 nm) / NiO (30 nm)

Exchange bias

Pinning direction

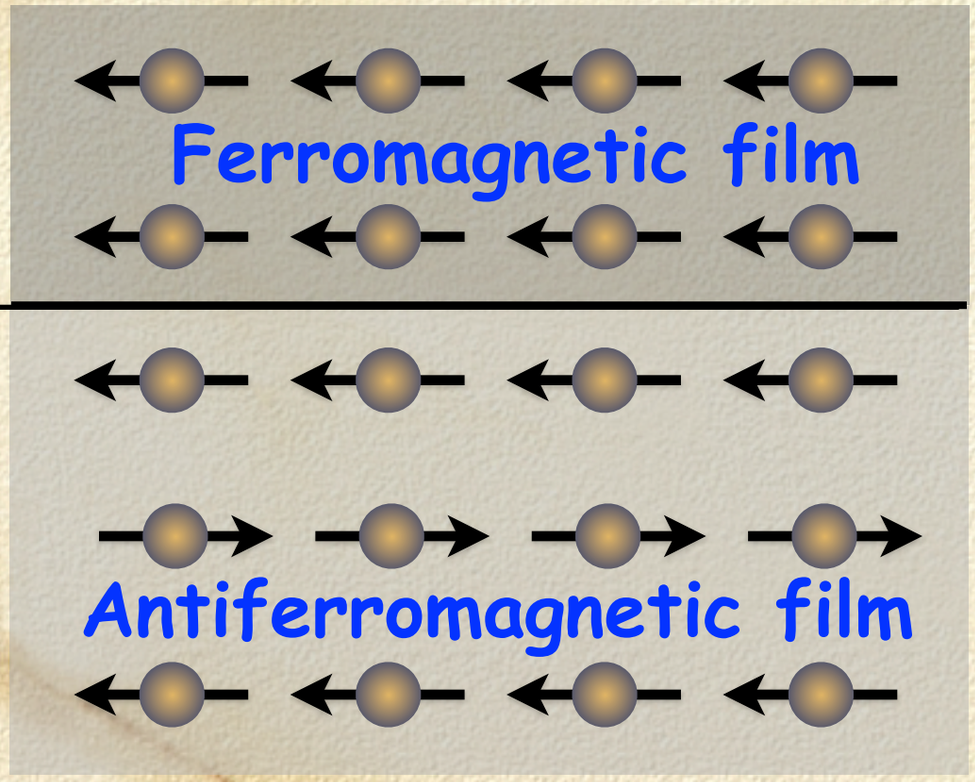

Unidirectional anisotropy

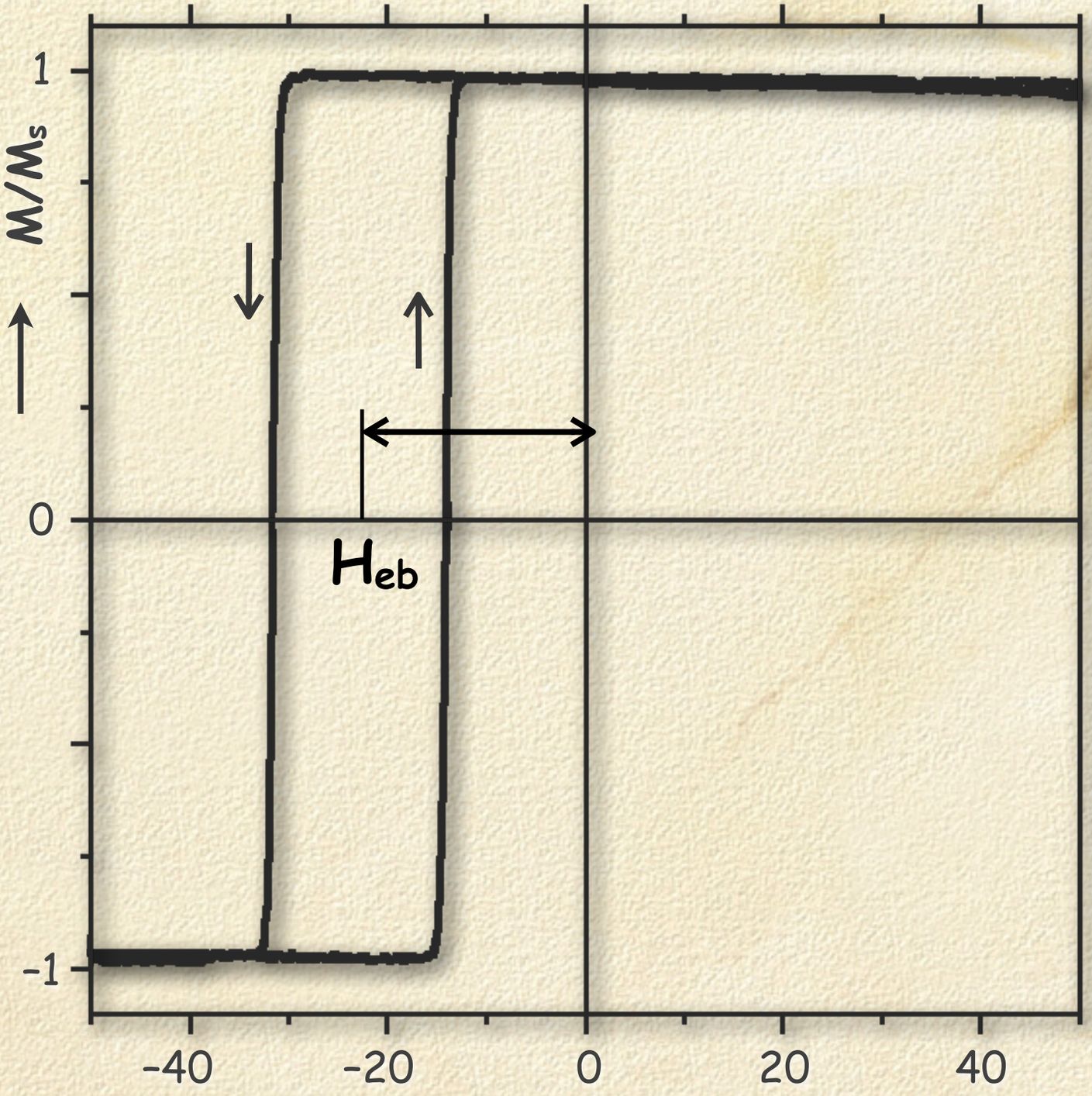

J. McCord and R.S., New J. Phys. 11, 83016 (2009)

M(H) loop and domains

Reversal of $Ni_{81}Fe_{19}$ (30 nm) / NiO (30 nm)

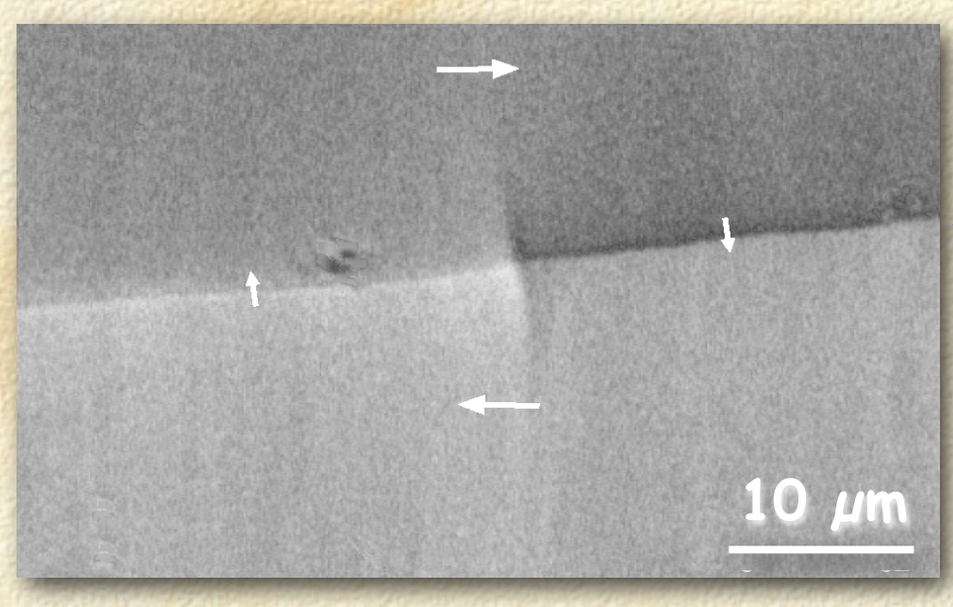

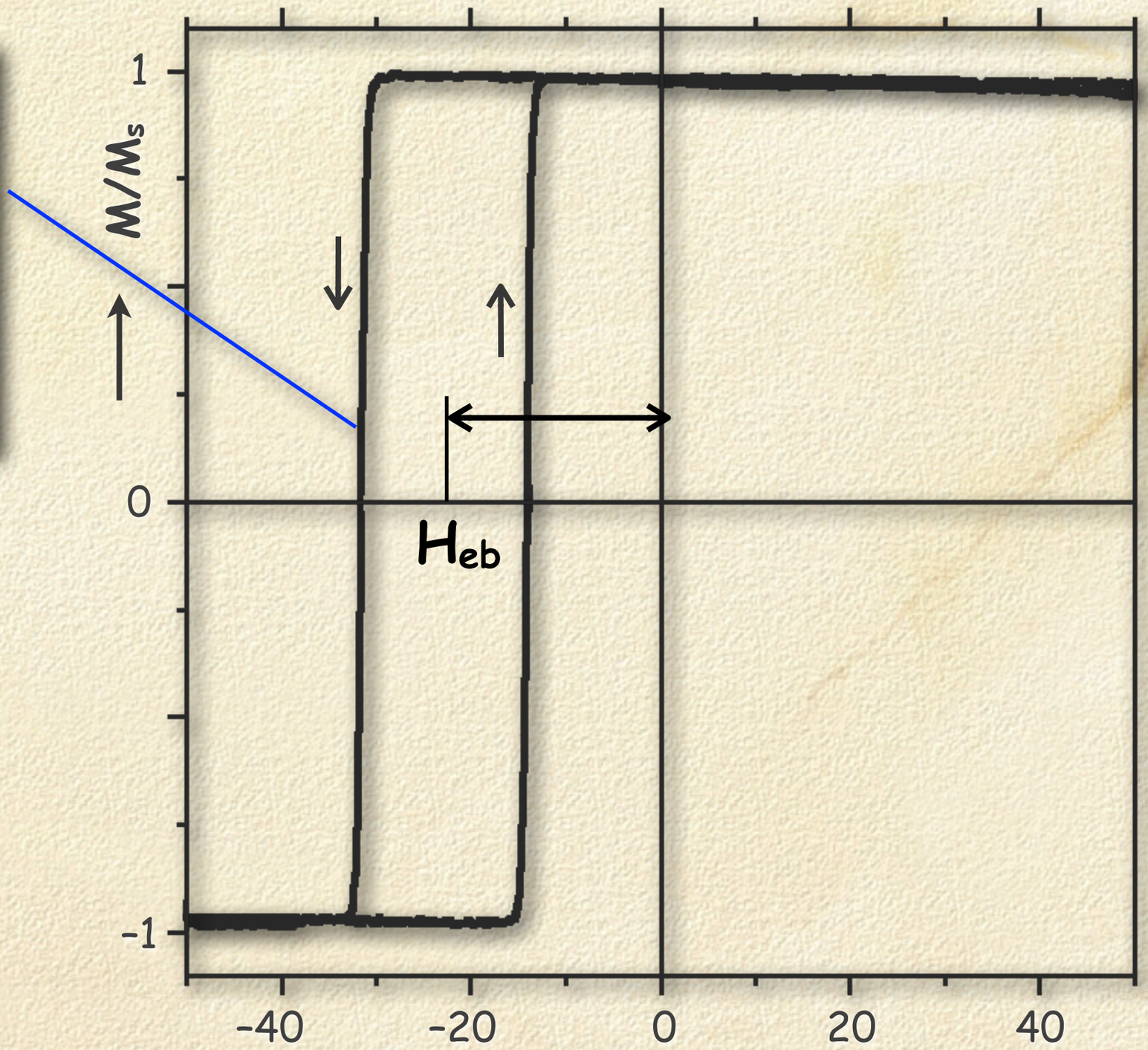

J. McCord and R.S., New J. Phys. 11, 83016 (2009)

M(H) loop and domains

Reversal of $Ni_{81}Fe_{19}$ (30 nm) / NiO (30 nm)

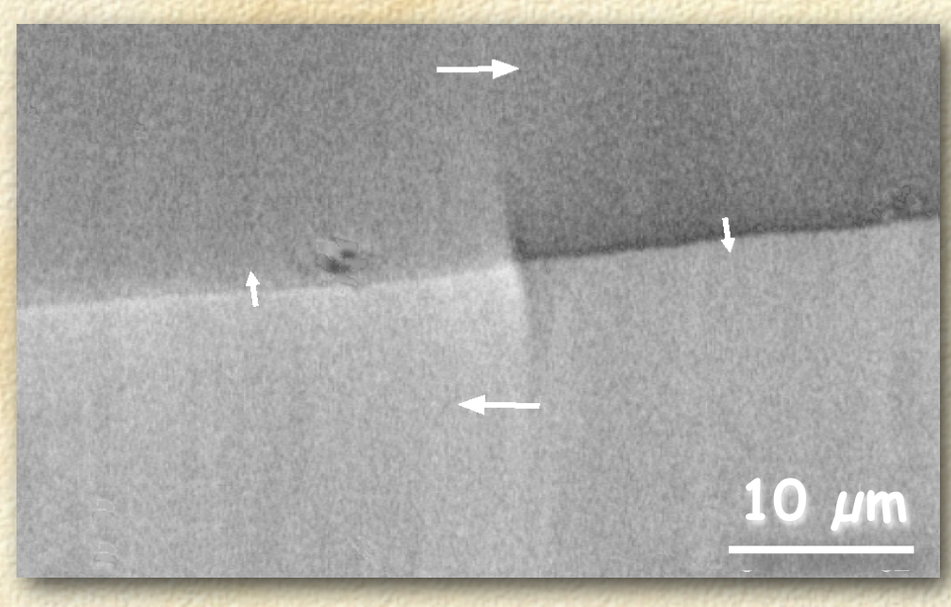

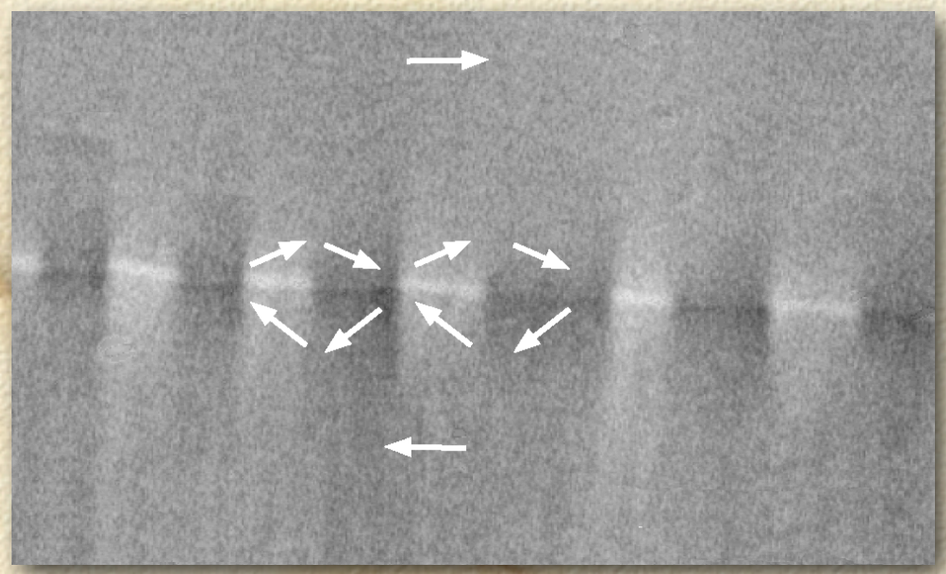

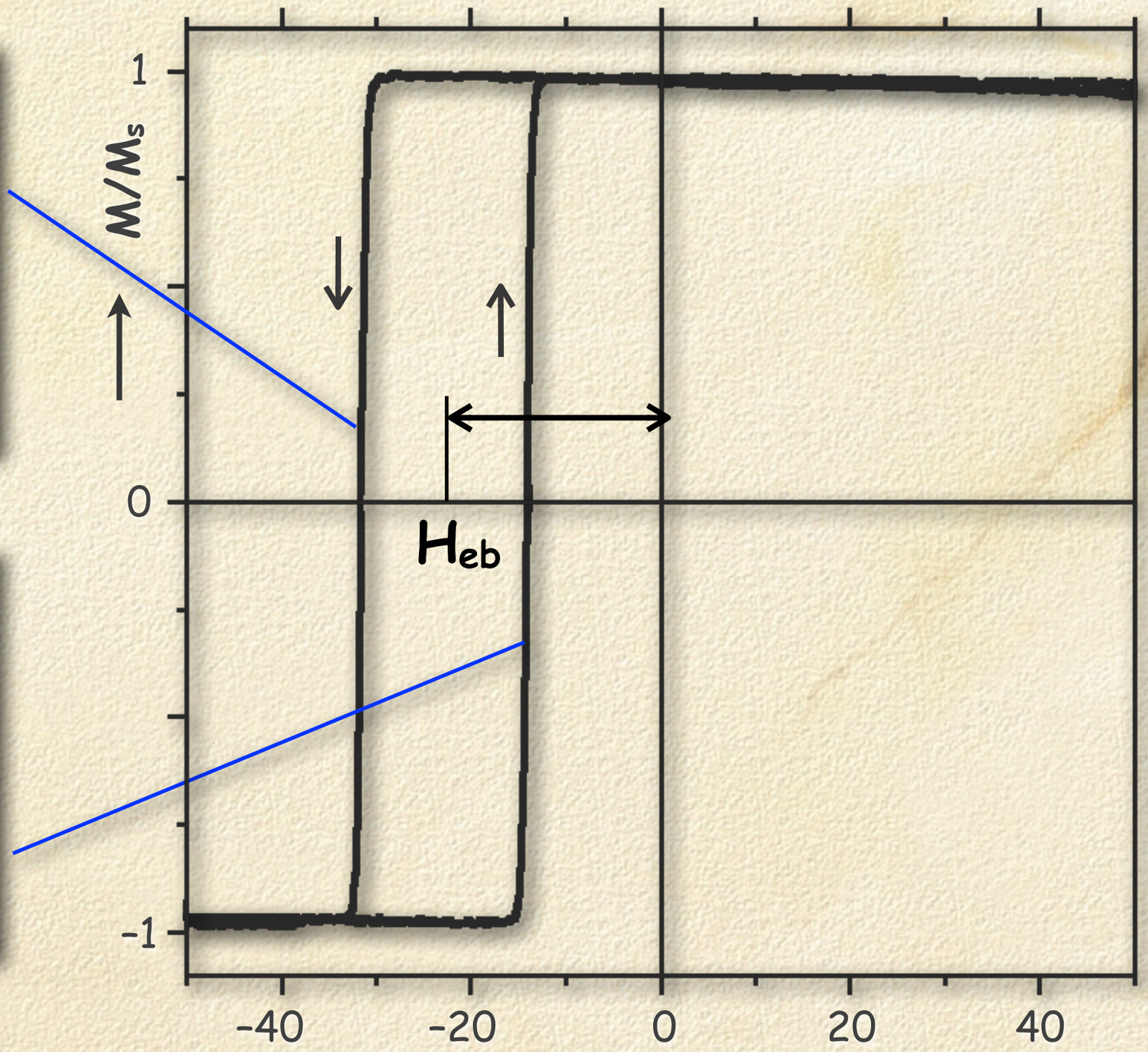

J. McCord and R.S., New J. Phys. 11, 83016 (2009)

M(H) loop and domains

M(H) loop and domains

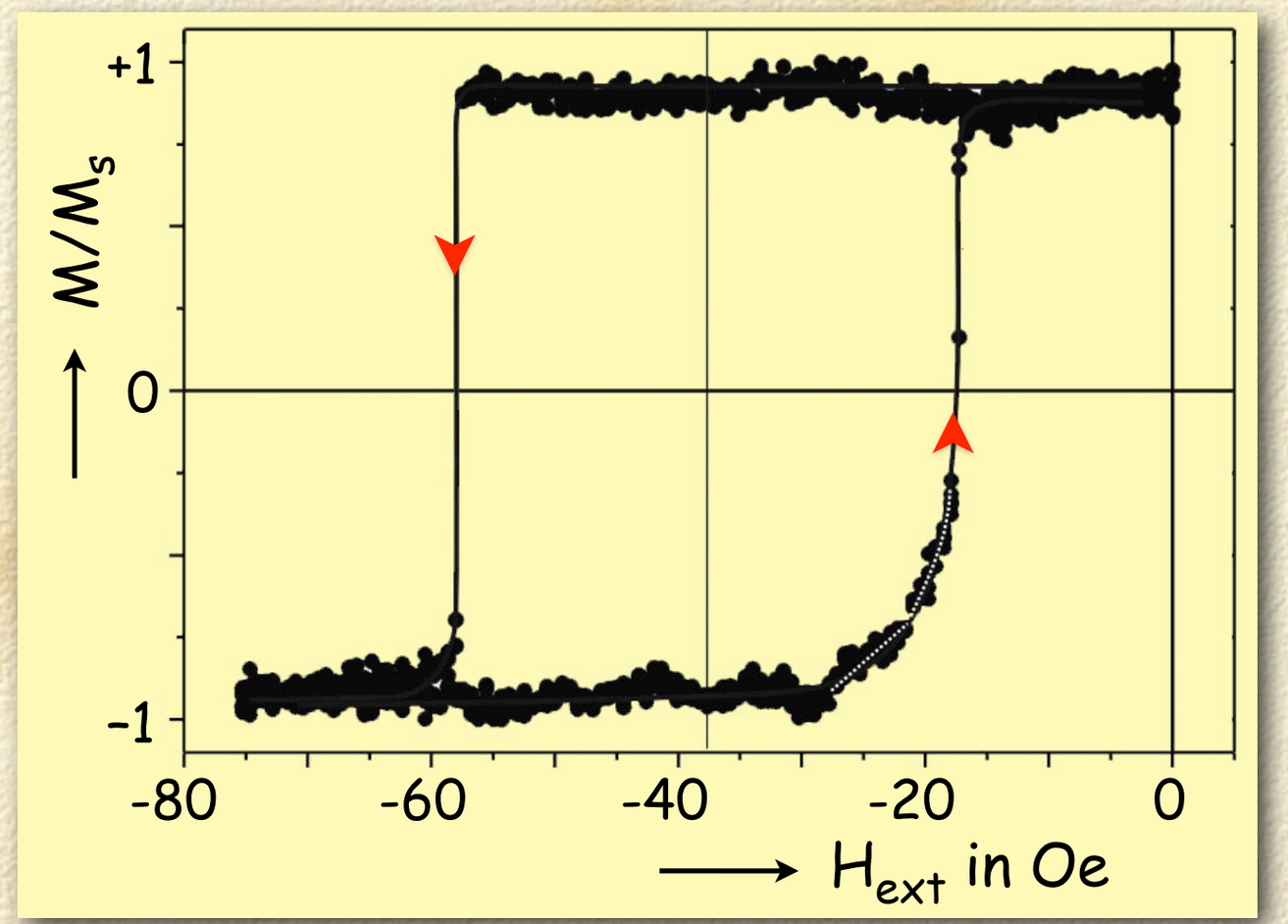

$Co_{90}Fe_{10}$ (20 nm)
$Ir_{23}Mn_{77}$ (10 nm)

J. McCord, R.S., R. Mattheis, K.-U. Barholz:
J. Appl. Phys. 93, 5491 (2003)

M(H) loop and domains

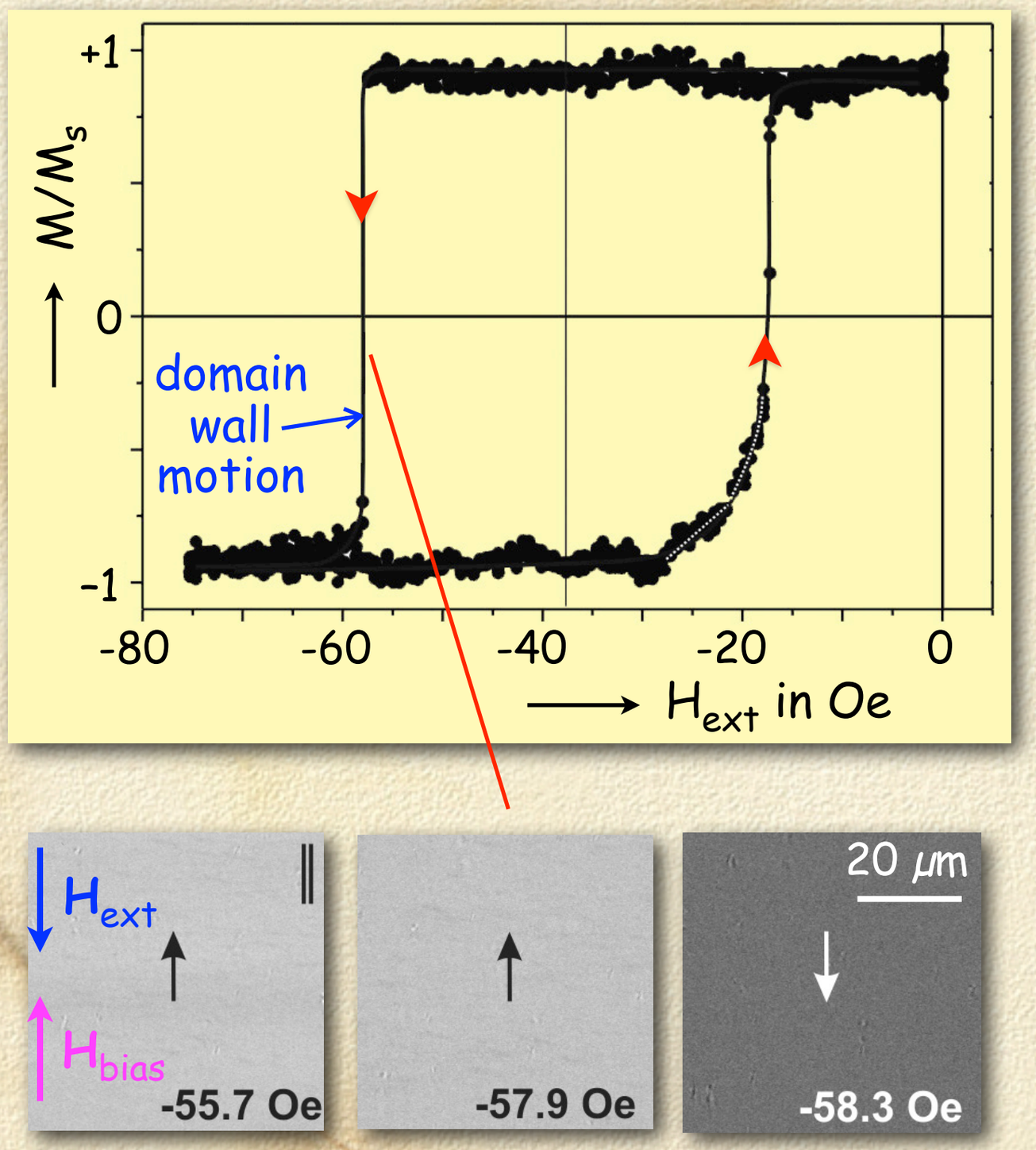

$Co_{90}Fe_{10}$ (20 nm)

$Ir_{23}Mn_{77}$ (10 nm)

J. McCord, R.S., R. Mattheis, K.-U. Barholz:
J. Appl. Phys. 93, 5491 (2003)

M(H) loop and domains

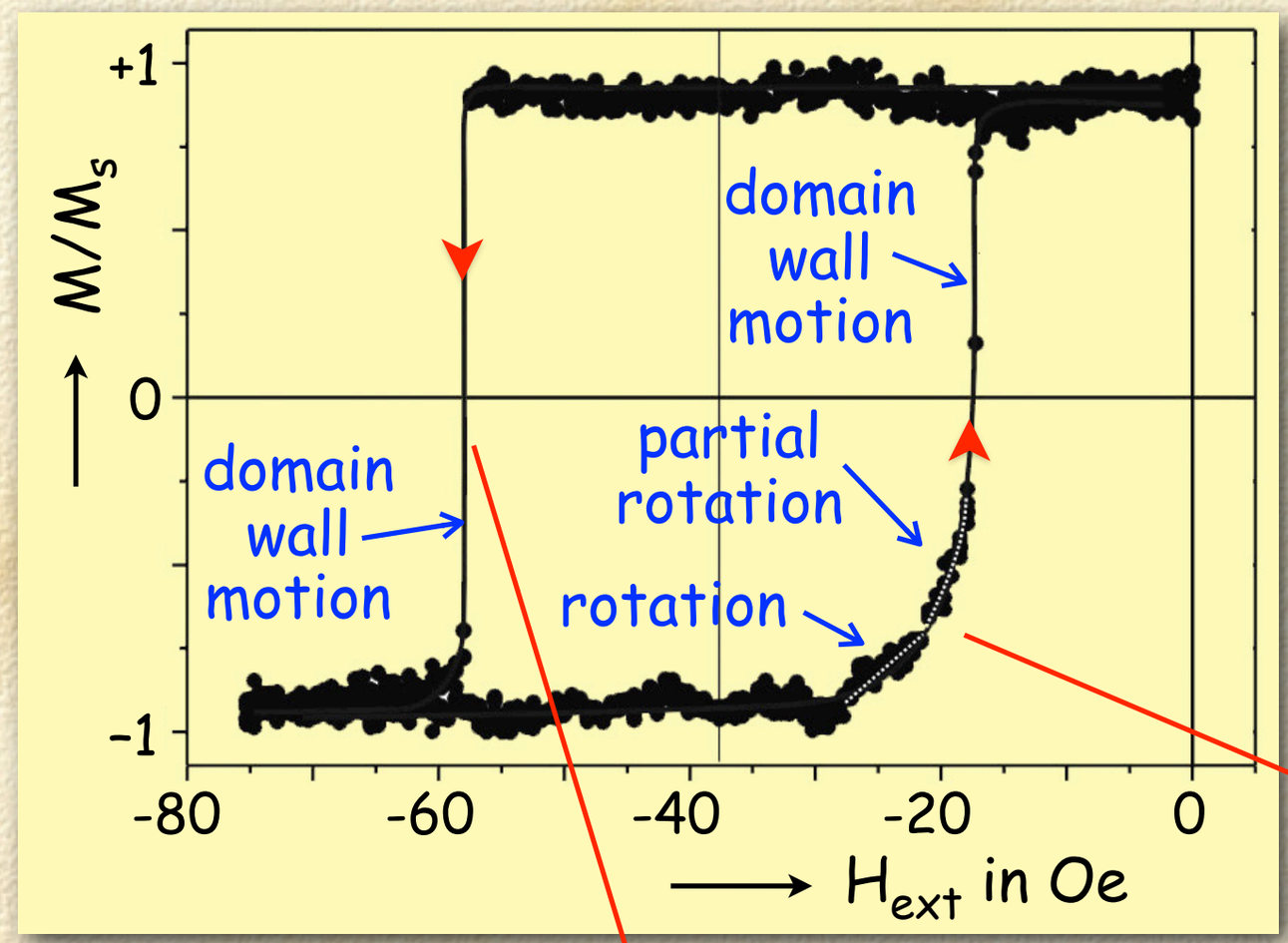

$Co_{90}Fe_{10}$ (20 nm)

$Ir_{23}Mn_{77}$ (10 nm)

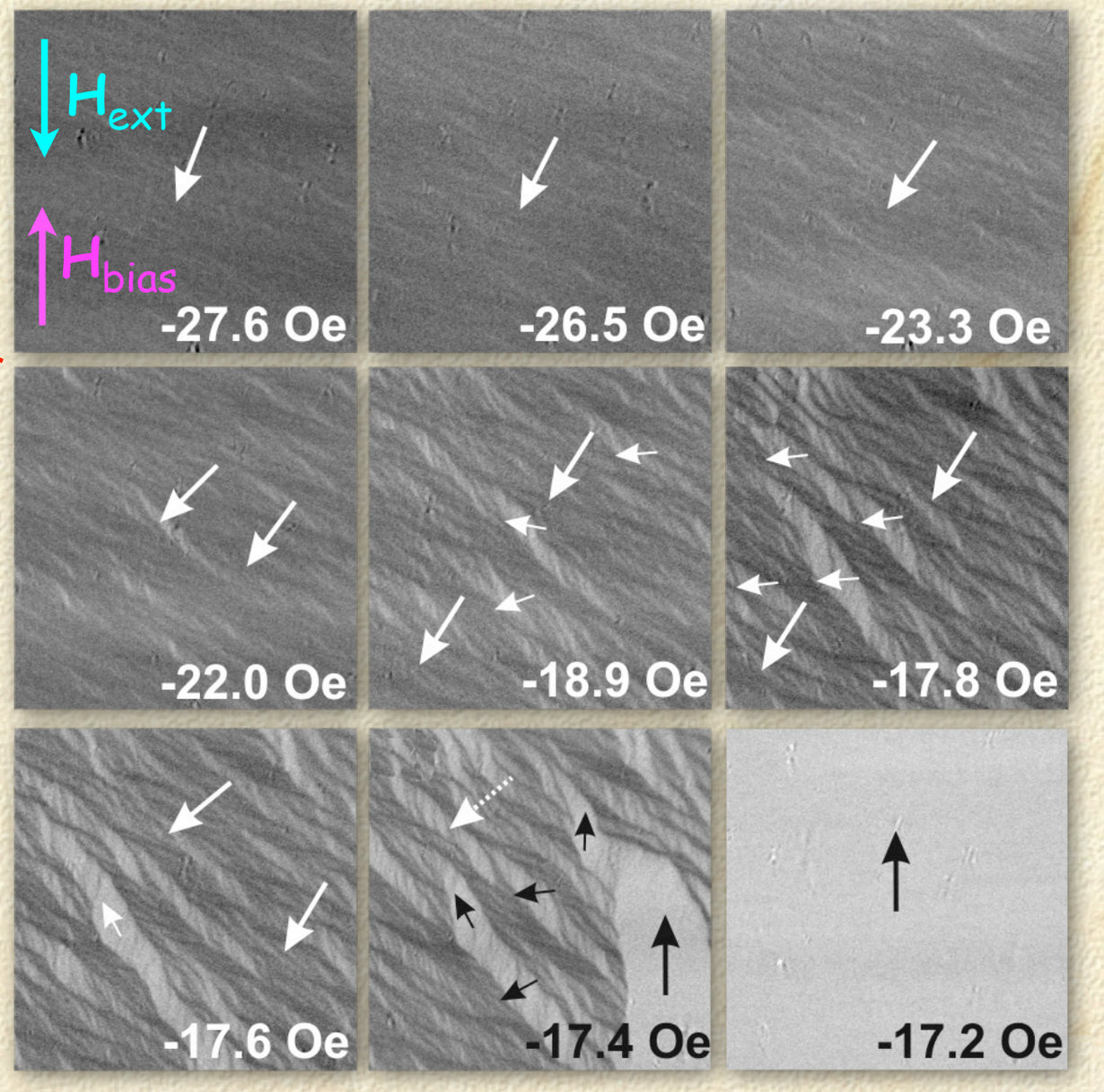

J. McCord, R.S., R. Mattheis, K.-U. Barholz:
J. Appl. Phys. 93, 5491 (2003)

indication of strong anisotropy dispersion

Oscillatory coupling in multilayers

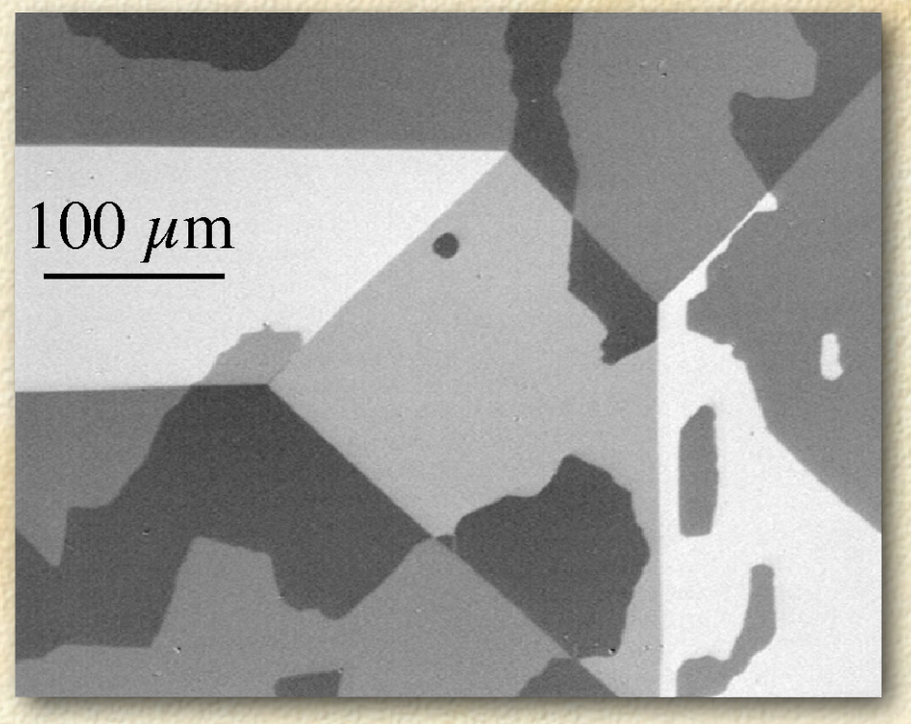

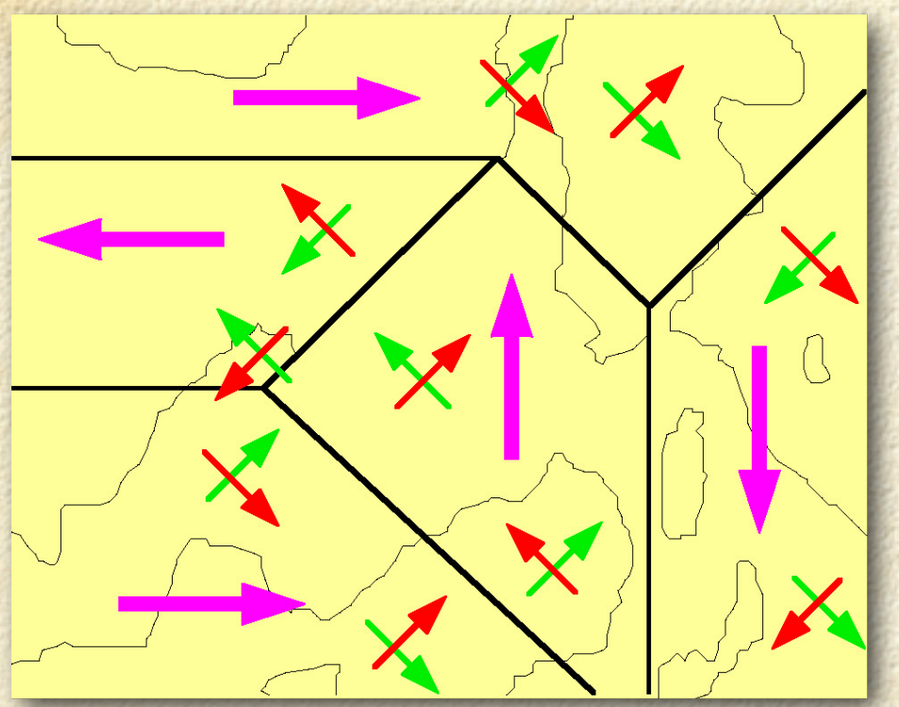

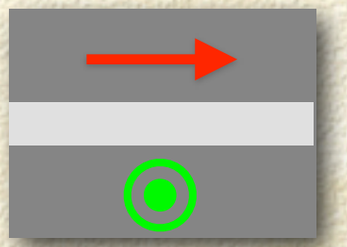

Fe (30 nm)
Cr (1.6 nm)
Fe (30 nm)

M. Rührig, RS, et al., Phys. Stat. Sol. 125 (1991)

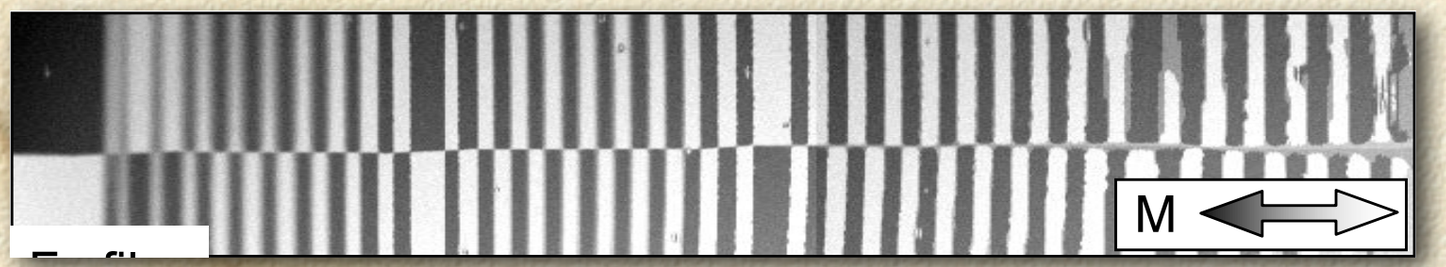

Images by SEMPA,
courtesy J. Unguris, NIST

J. Unguris, R. Celotta, D. Pierce, PRL 67 (1991)

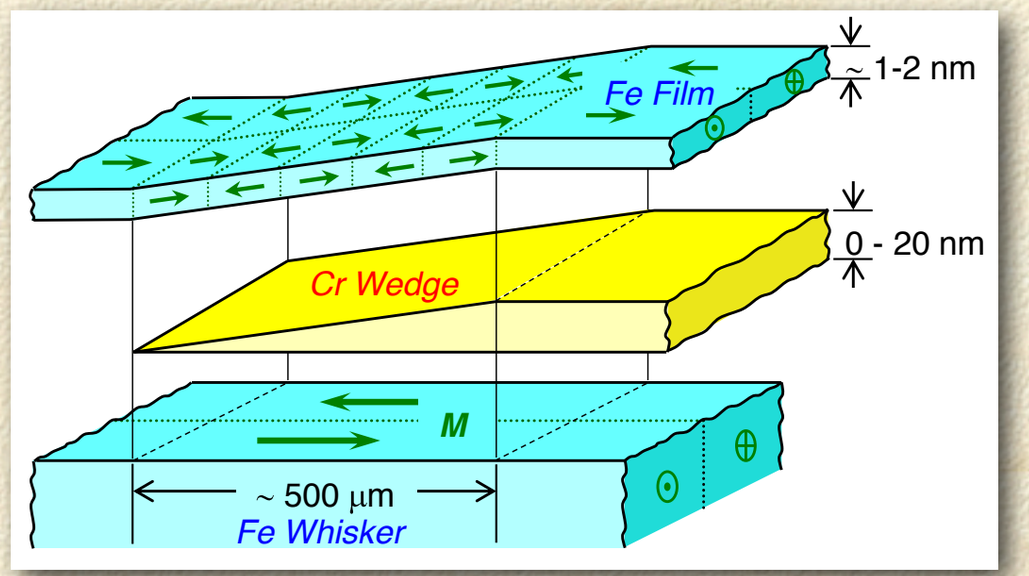

Domain Shift Register Devices

Bubble Memory

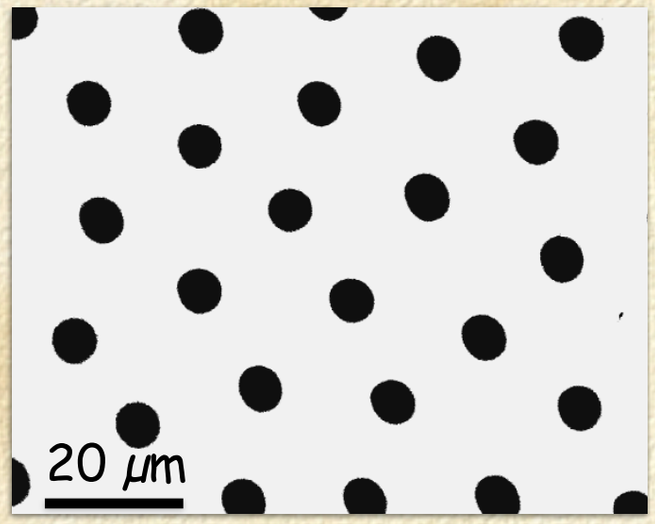

Bubble domains

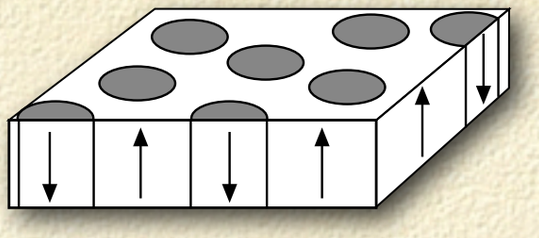

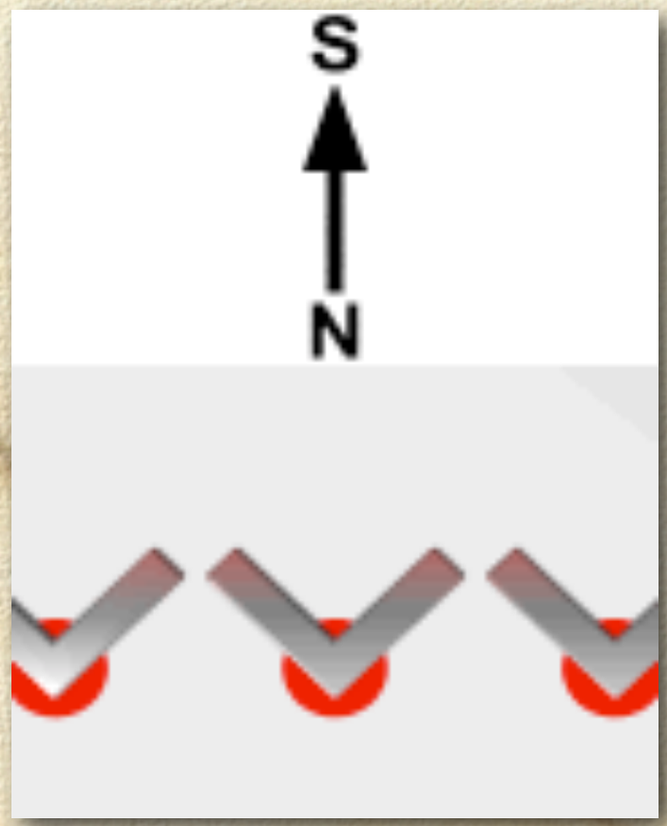

http://commons.wikimedia.org/wiki/How_bubble_memory_works

Race Track Memory

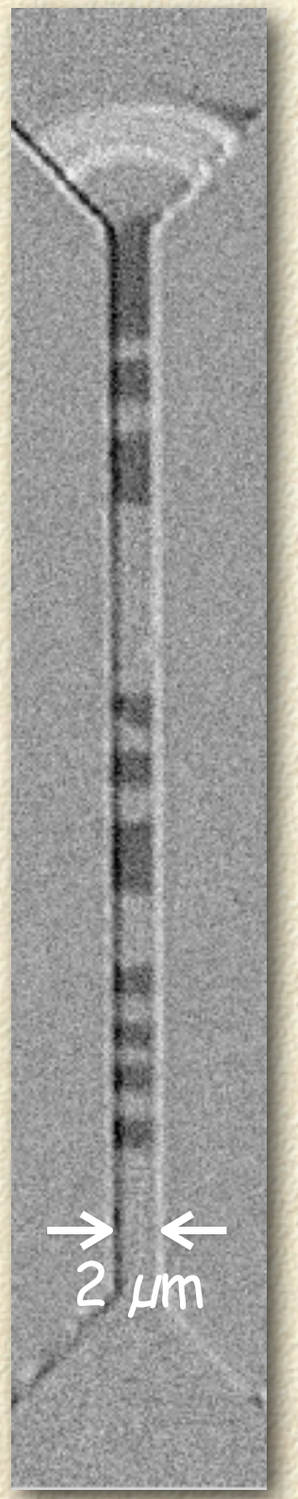

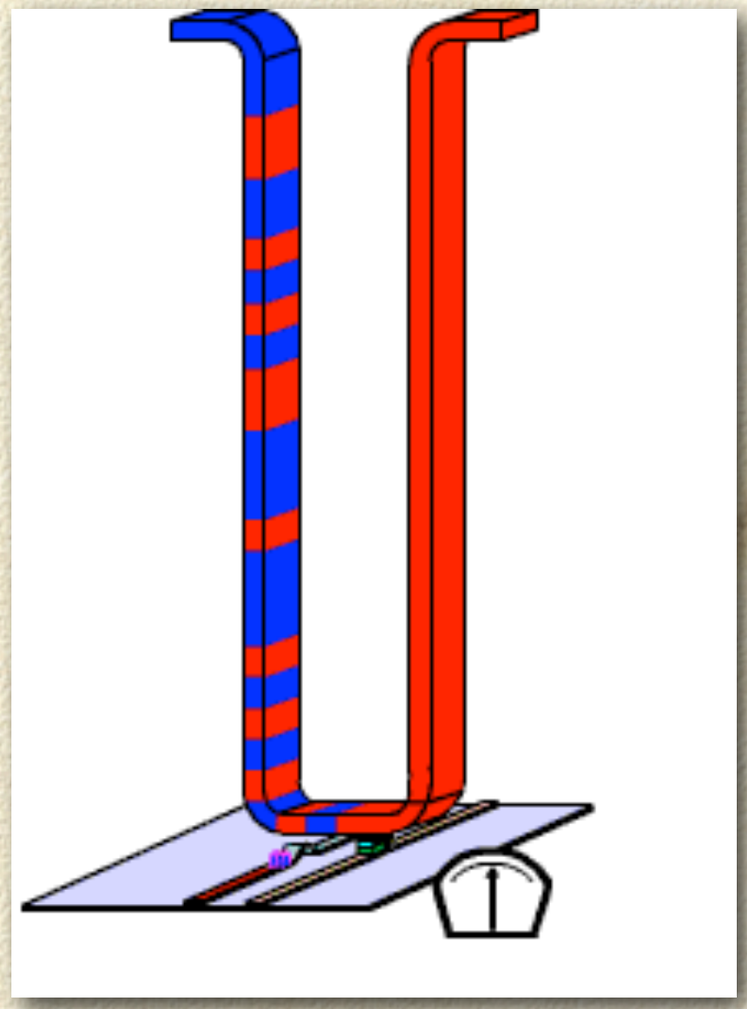

Kerr-movie of Co/Ni PMA multilayer

courtesy
S. Parkin, IBM

Grain-oriented FeSi transformer material

Loss control by domain control in transformer steel

Without artificial domain refinement

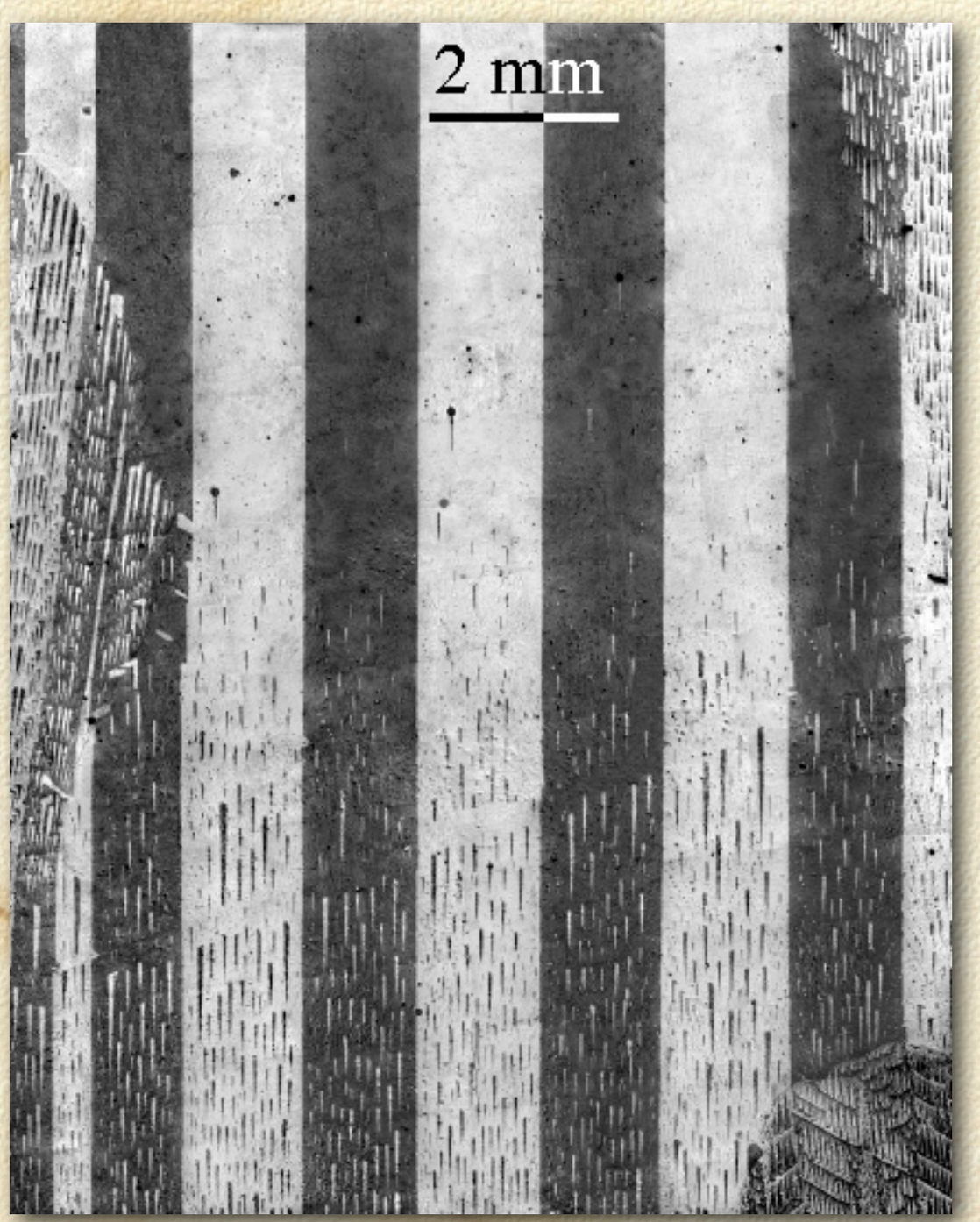

After laser scribing

Magneto-acoustic Article Surveillance

semihard metall
(on-/off-switch)

amorphous ribon
(Sensor)

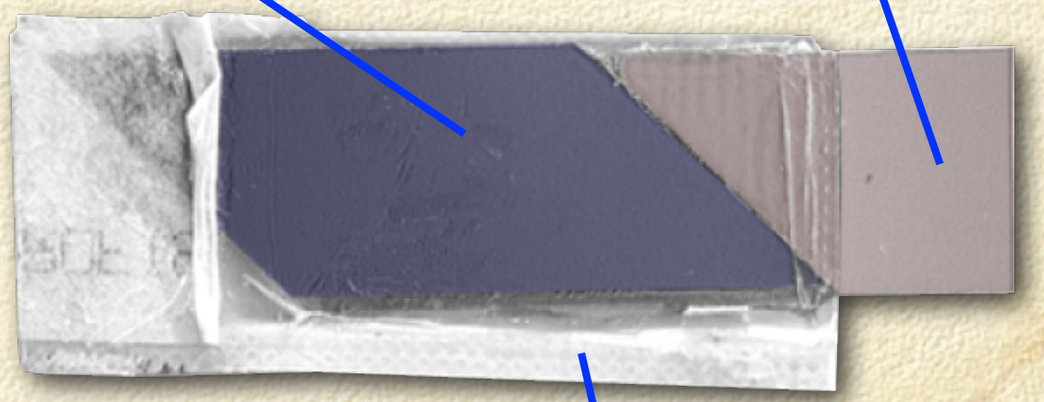

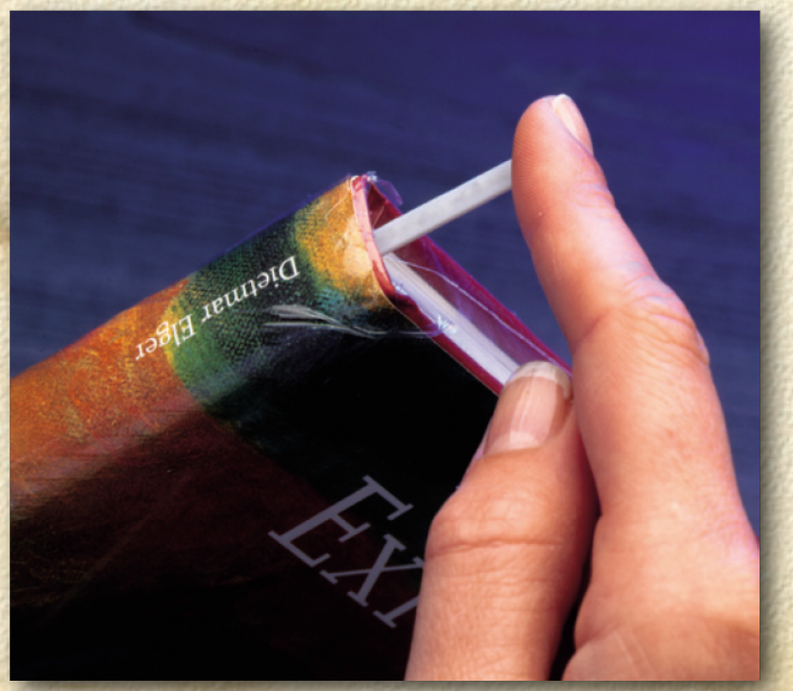

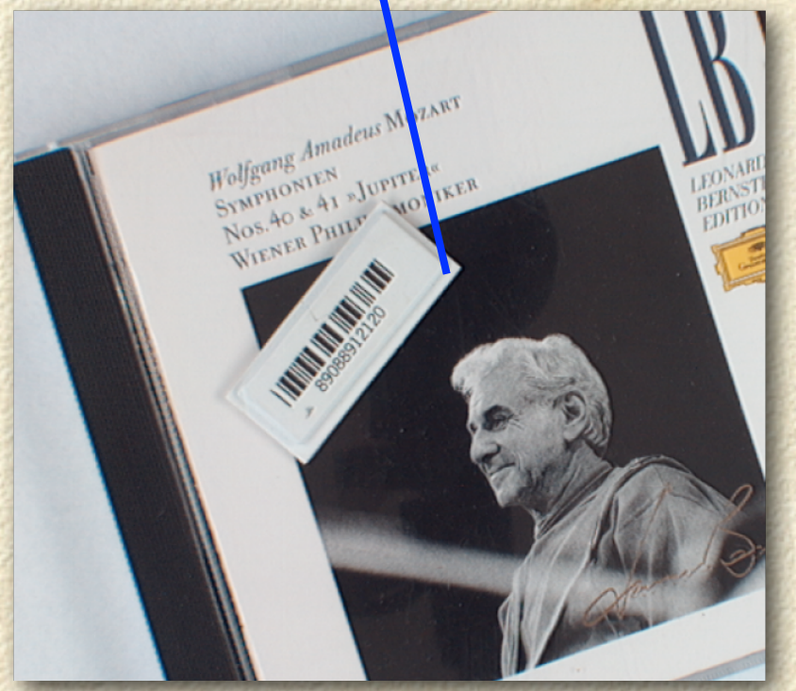

Magneto-acoustic Article Surveillance

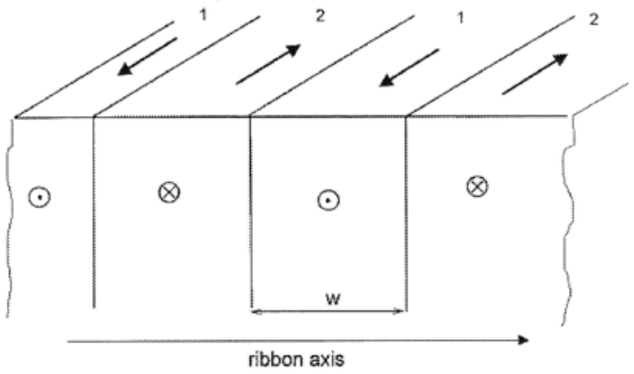

Fig. 1a (Prior Art)

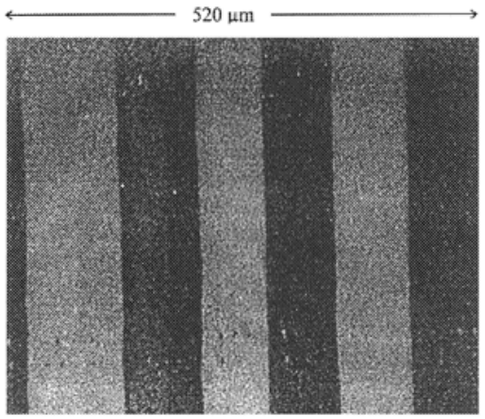

Fig. 1b (Prior Art)

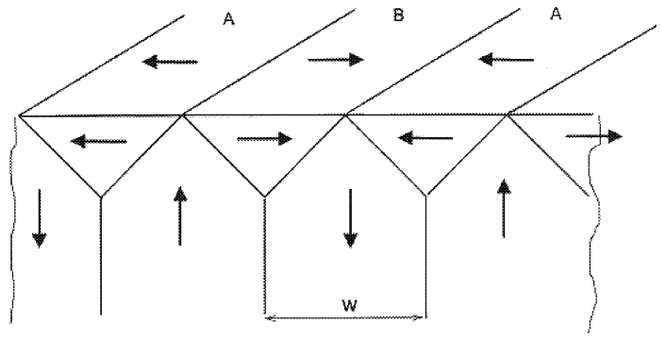

Fig. 2a (Prior Art)

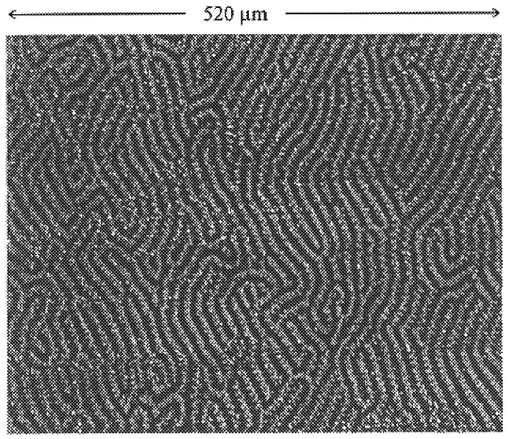

Fig. 2b

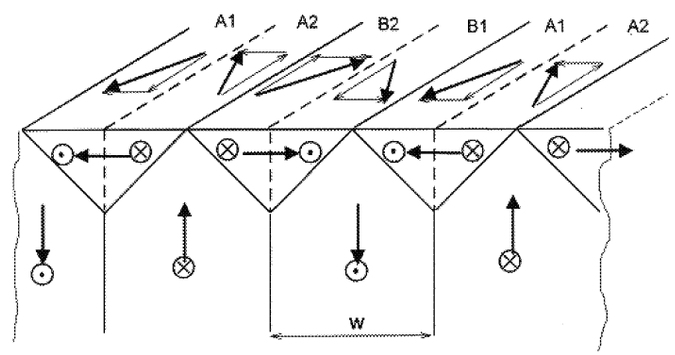

Fig. 8a

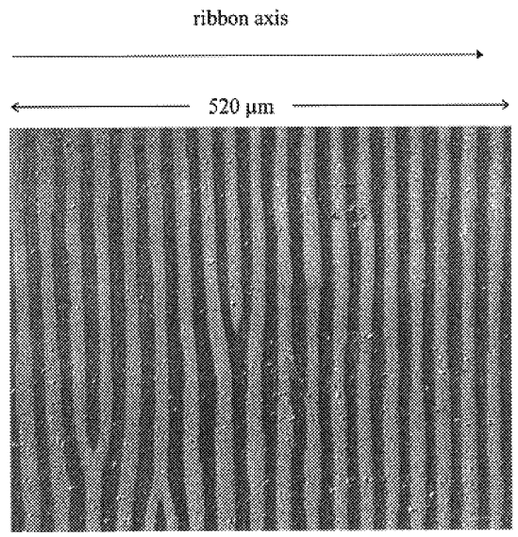

Fig. 8b

United States Patent [19]

Herzer

[54] **METHOD OF ANNEALING AMORPHOUS RIBBONS AND MARKER FOR ELECTRONIC ARTICLE SURVEILLANCE**

[75] Inventor: **Giselher Herzer**, Bruchkoebel, Germany

[73] Assignee: **Vacuumschmelze GmbH**, Hanau, Germany

Origin of Magnetic Domains and Domain Classification

Origin of magnetic domains

Origin of magnetic domains

Landau and Lifshitz (1935):

Domains are formed to minimize total energy

Origin of magnetic domains

Landau and Lifshitz (1935):

Domains are formed to minimize total energy

Exchange energy

$e_A = 0$

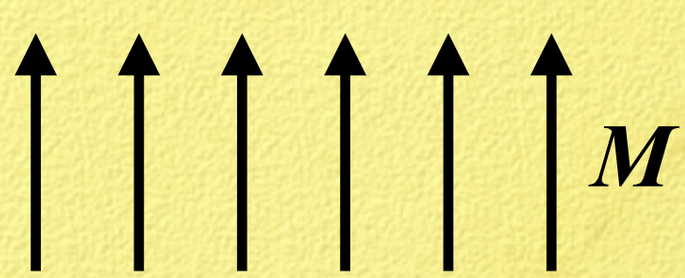

$e_A > 0$

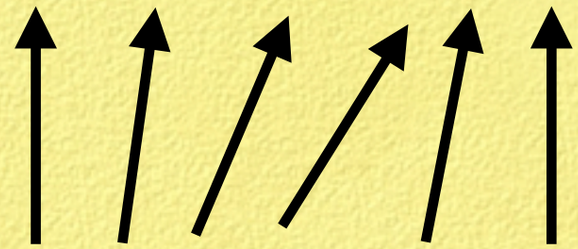

Origin of magnetic domains

Landau and Lifshitz (1935):

Domains are formed to minimize total energy

Exchange energy

$e_A = 0$

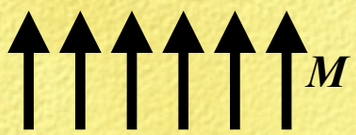

$e_A > 0$

Anisotropy energy

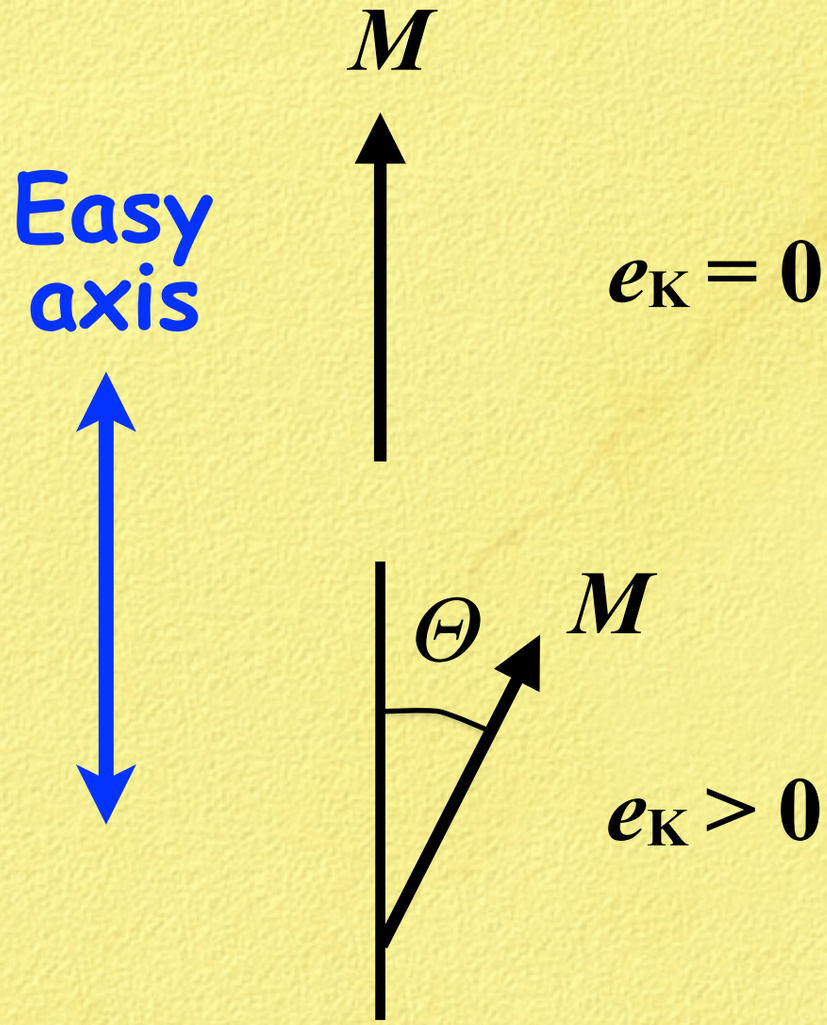

Origin of magnetic domains

Landau and Lifshitz (1935):

Domains are formed to minimize total energy

Exchange energy

$e_A = 0$

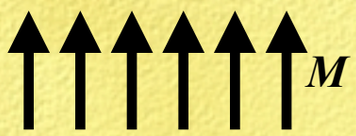

$e_A > 0$

Anisotropy energy

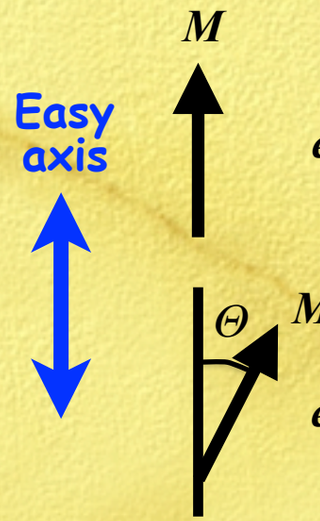

Stray field energy

$$\operatorname{div} \boldsymbol{H}_d = -\operatorname{div} \boldsymbol{M}$$

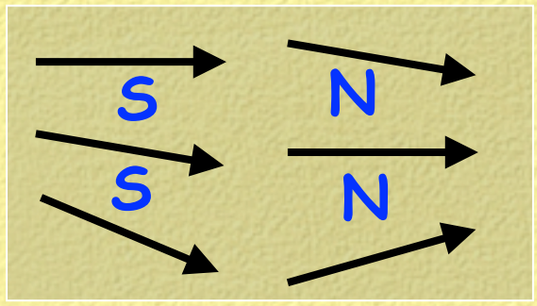

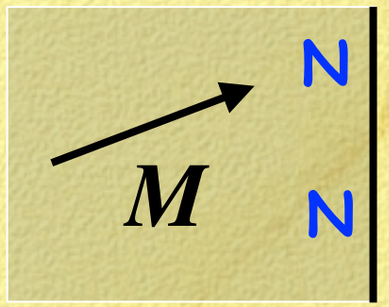

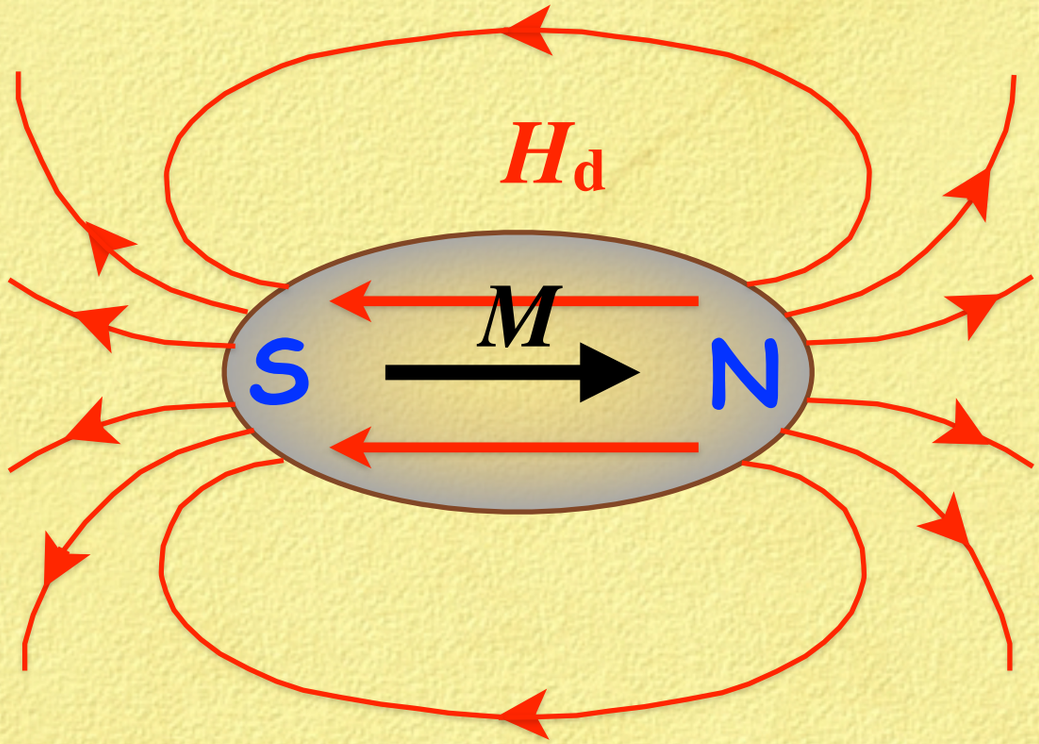

Origin of magnetic domains

Landau and Lifshitz (1935):

Domains are formed to minimize total energy

Exchange energy

$e_A = 0$

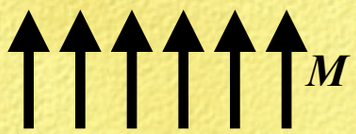

$e_A > 0$

Stray field energy

$$\text{div}\, \boldsymbol{H}_d = -\,\text{div}\, \boldsymbol{M}$$

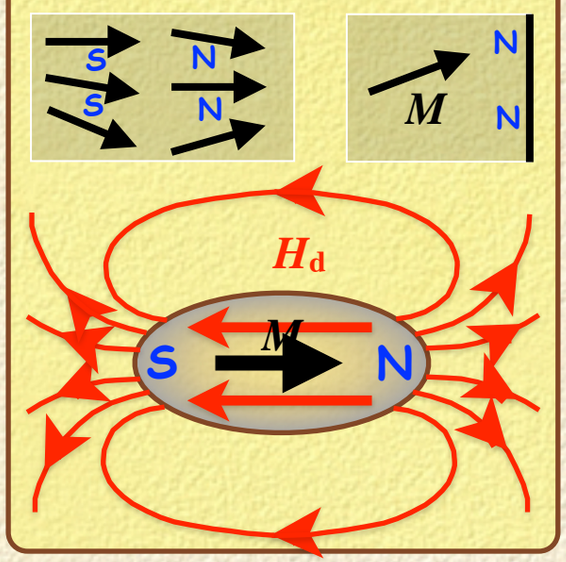

Anisotropy energy

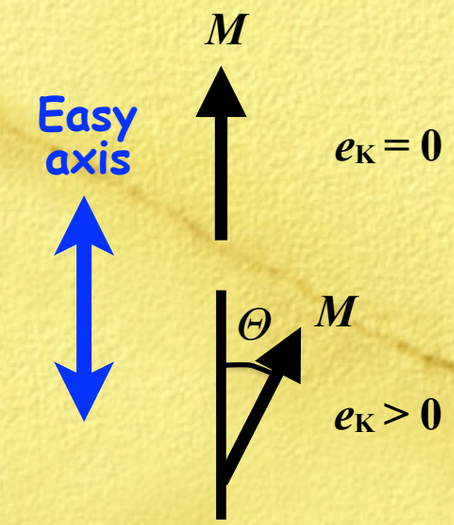

External field energy

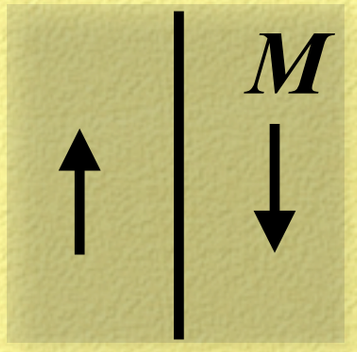

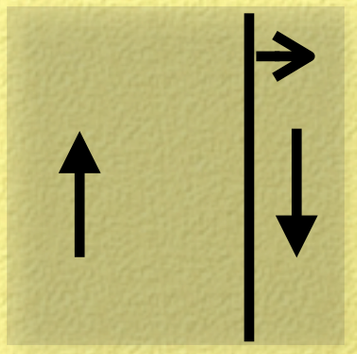

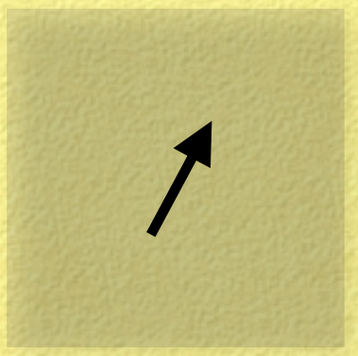

Origin of magnetic domains

Landau and Lifshitz (1935):

Domains are formed to minimize total energy

Exchange energy

$e_A = 0$

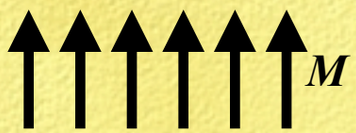

$e_A > 0$

Stray field energy

$$\operatorname{div} \boldsymbol{H}_d = -\operatorname{div} \boldsymbol{M}$$

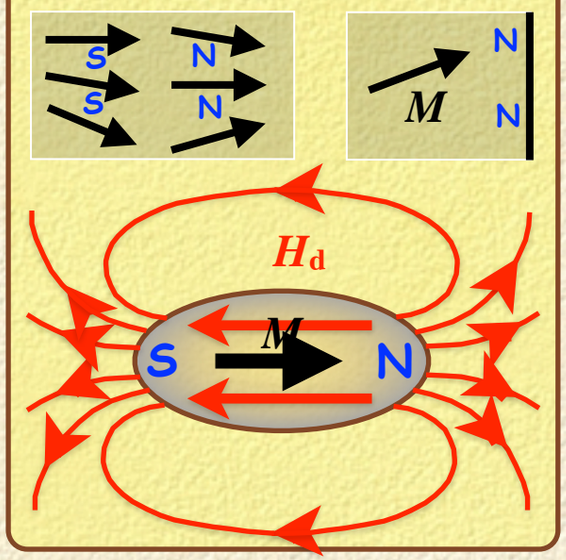

Magnetostrictive self energy

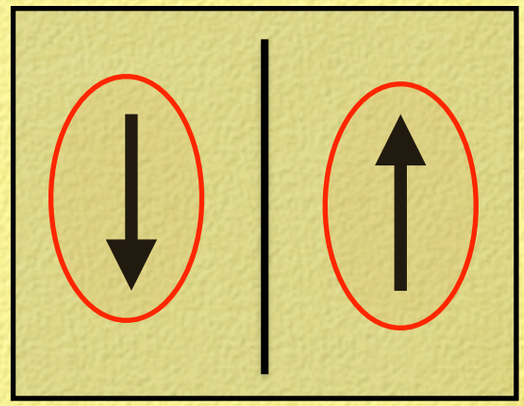

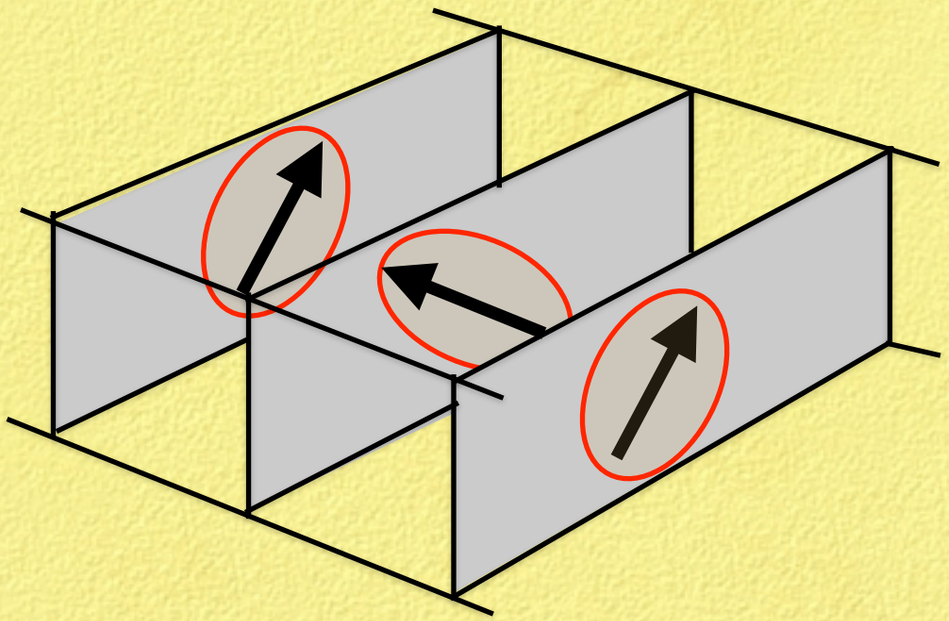

Anisotropy energy

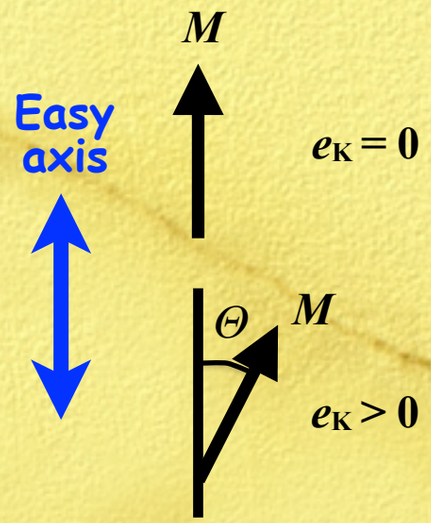

External field energy

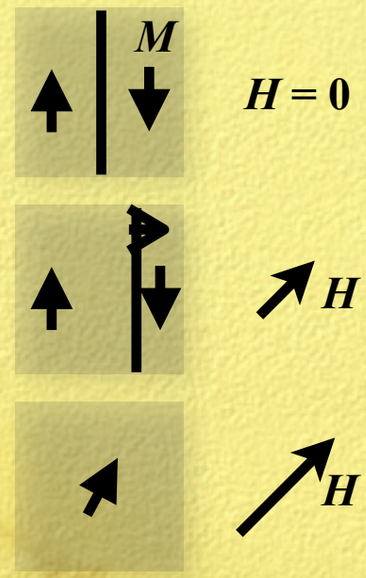

Origin of magnetic domains

Landau and Lifshitz (1935):

Domains are formed to minimize total energy

Exchange energy

$e_A = 0$

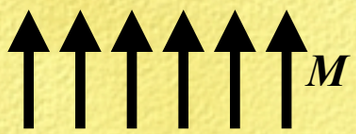

$e_A > 0$

Stray field energy

$$\operatorname{div} \boldsymbol{H}_d = -\operatorname{div} \boldsymbol{M}$$

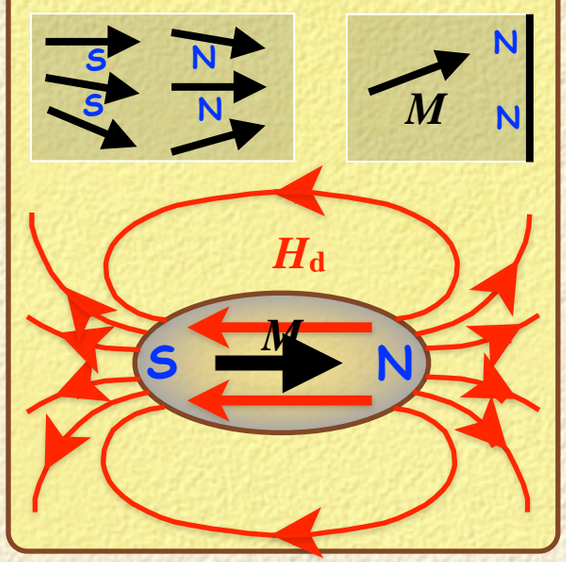

Magnetostrictive self-

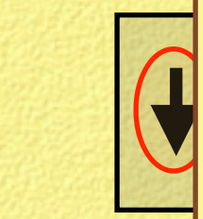

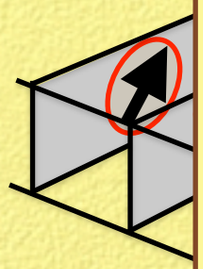

External stress energy

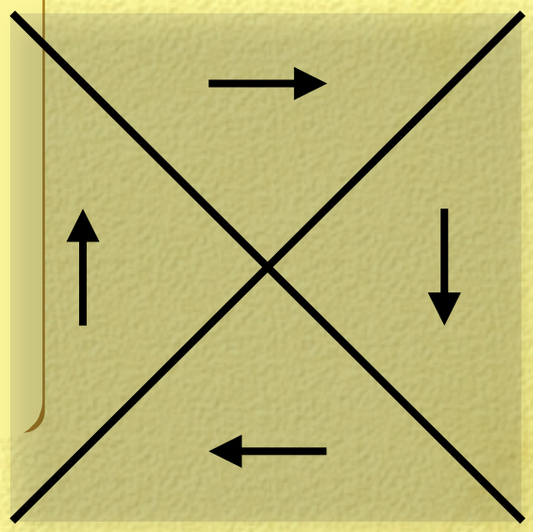

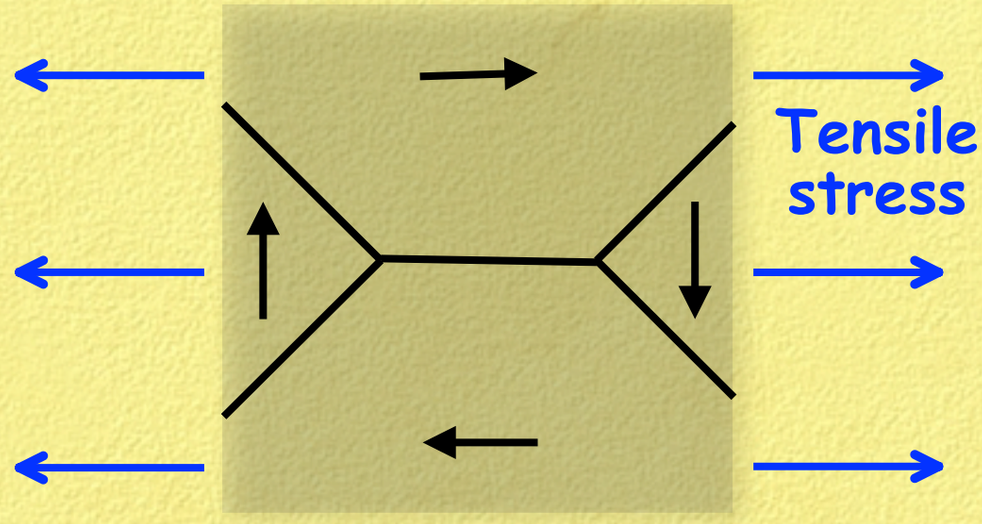

Anisotropy energy

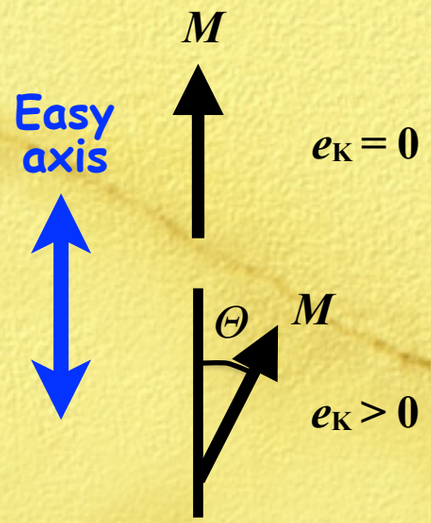

External field energy

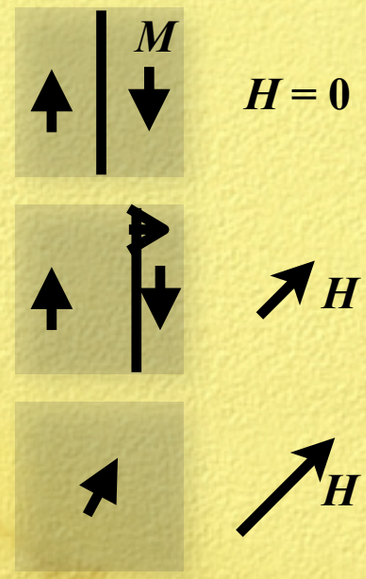

Origin of magnetic domains

Landau and Lifshitz (1935):

Domains are formed to minimize total energy

Exchange energy

$e_A = 0$

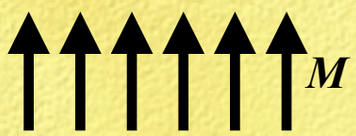

$e_A > 0$

Stray field energy

$$\operatorname{div} \boldsymbol{H}_d = -\operatorname{div} \boldsymbol{M}$$

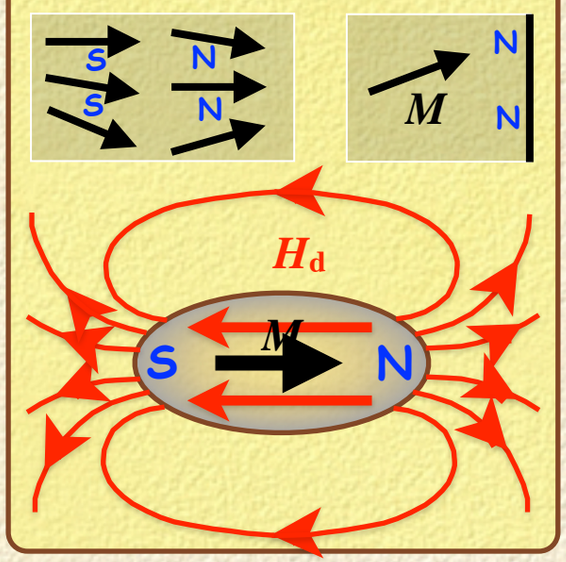

Magnetostrictive self energy

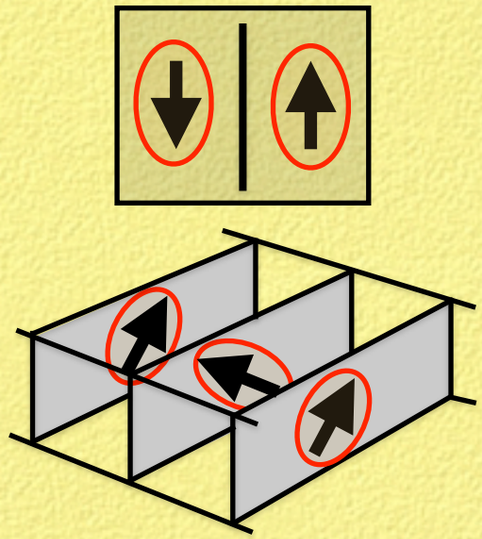

External stress energy

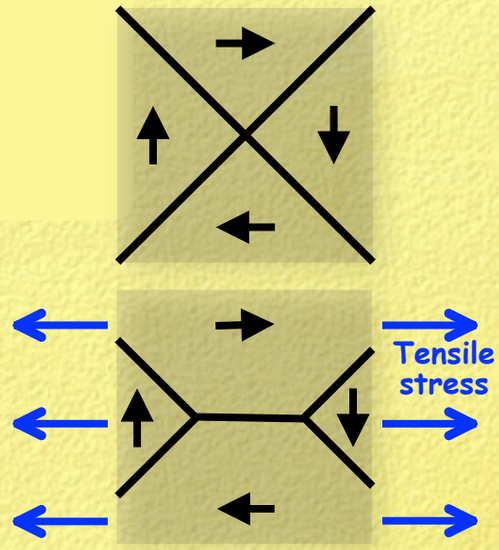

Anisotropy energy

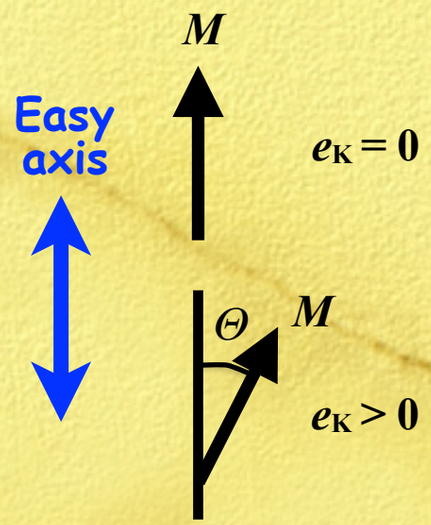

External field energy

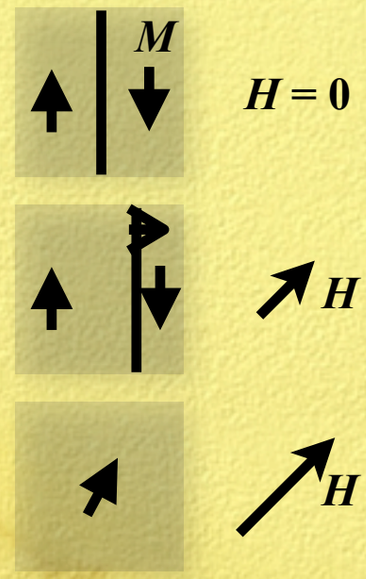

Origin of magnetic domains

Landau and Lifshitz (1935):

Domains are formed to minimize total energy

Exchange energy

$e_A = 0$

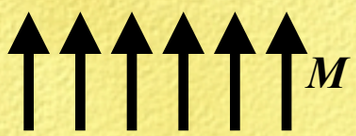

$e_A > 0$

Stray field energy

$$\operatorname{div} \boldsymbol{H}_d = -\operatorname{div} \boldsymbol{M}$$

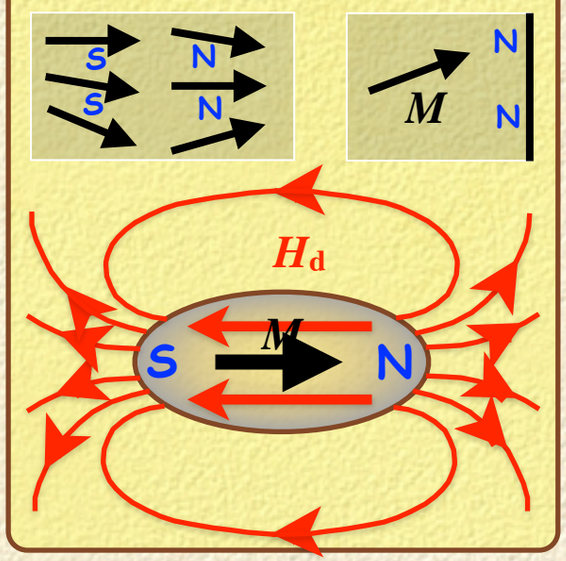

Magnetostrictive self energy

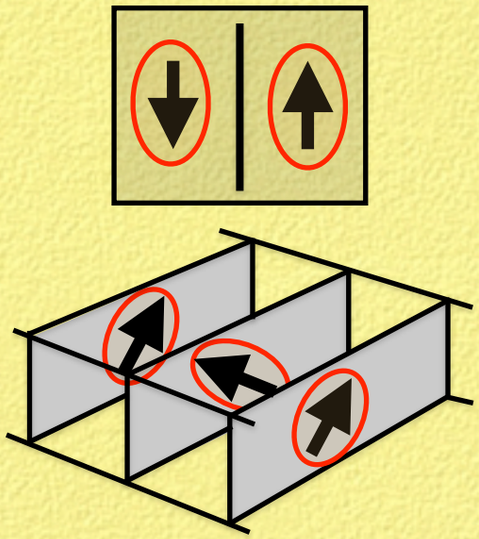

External stress energy

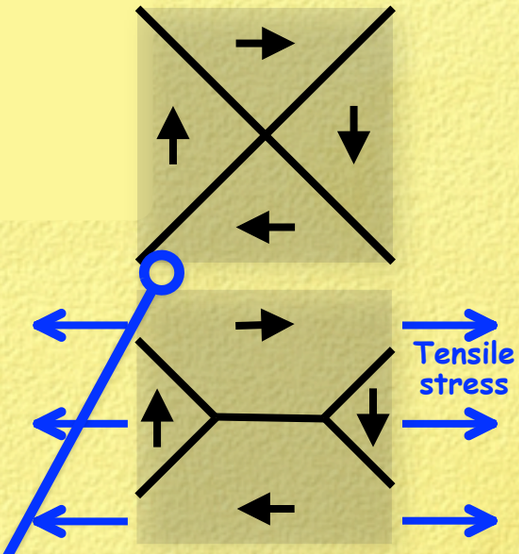

Anisotropy energy

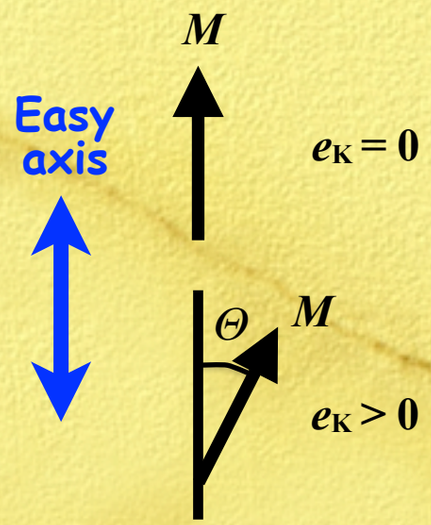

External field energy

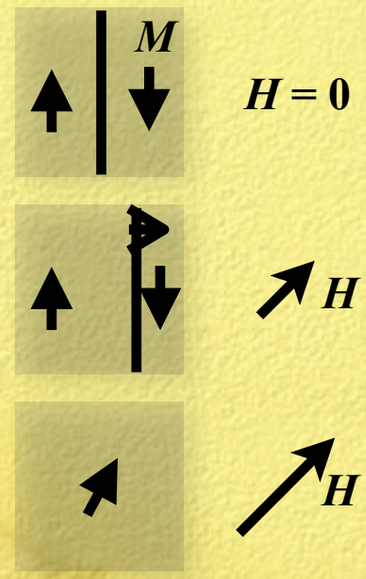

Can create dominating anisotropy when magnetocrystalline anisotropy is lacking (stress-induced anisotropy)

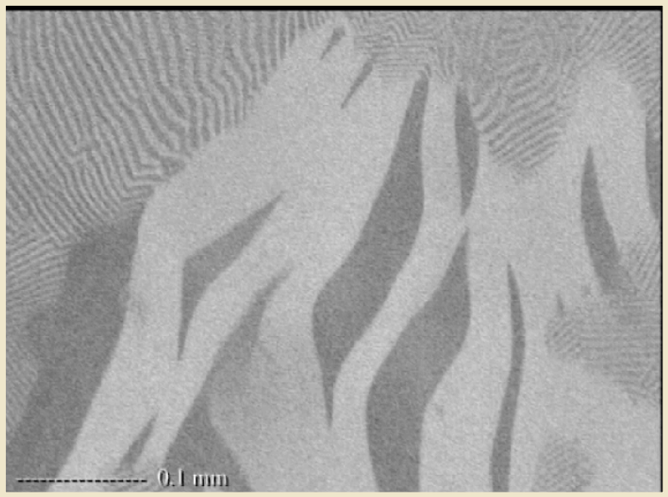

Origin of magnetic domains

Landau and Lifshitz (1935):

Domains are formed to minimize total energy

Exchange energy

$e_A = 0$

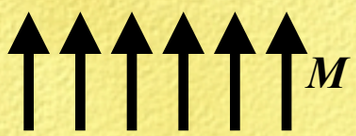

$e_A > 0$

Stray field energy

$$\operatorname{div} \boldsymbol{H}_d = -\operatorname{div} \boldsymbol{M}$$

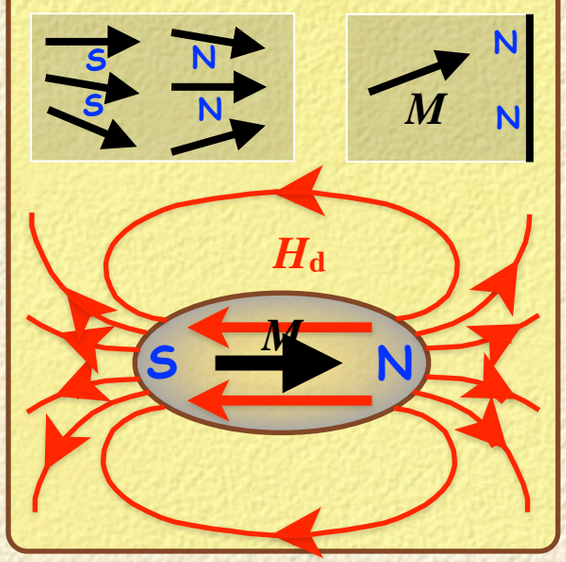

Magnetostrictive self energy

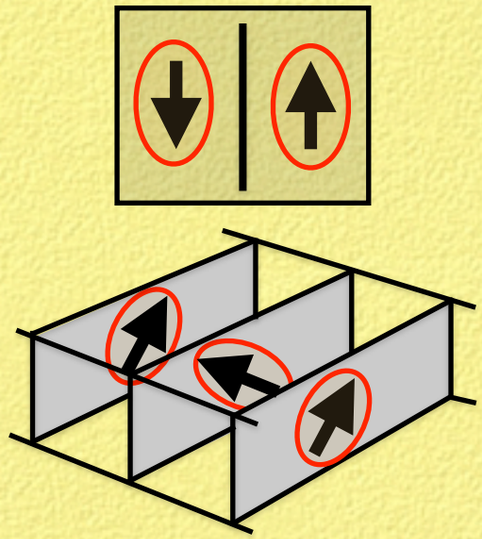

External stress energy

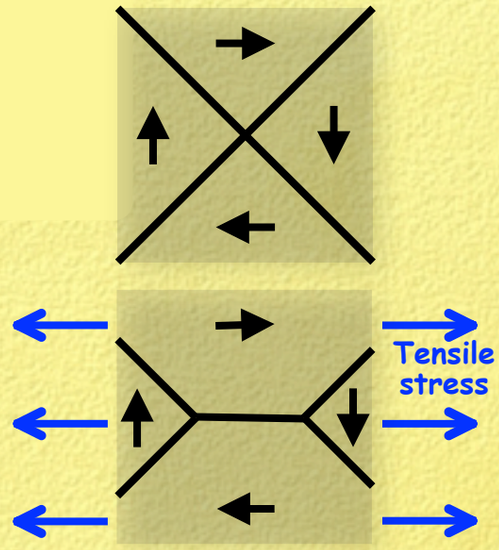

Anisotropy energy

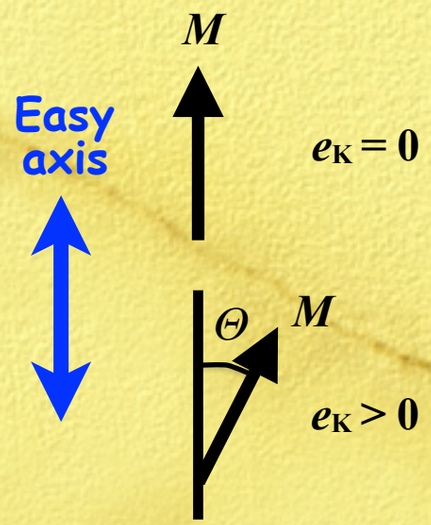

External field energy

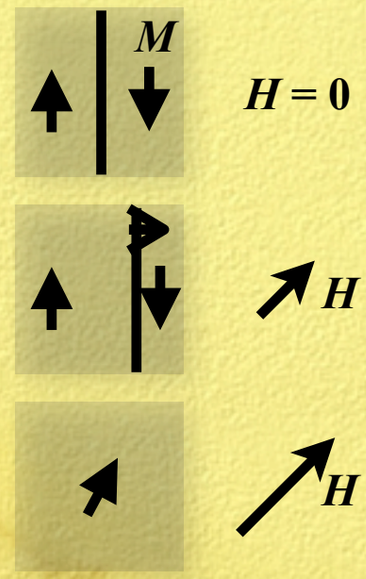

Origin of magnetic domains

Landau and Lifshitz (1935):

Domains are formed to minimize total energy

Exchange energy

$e_A = 0$

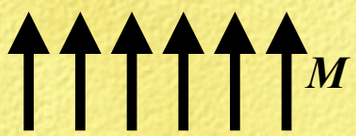

$e_A > 0$

Stray field energy

$$\operatorname{div} \boldsymbol{H}_d = -\operatorname{div} \boldsymbol{M}$$

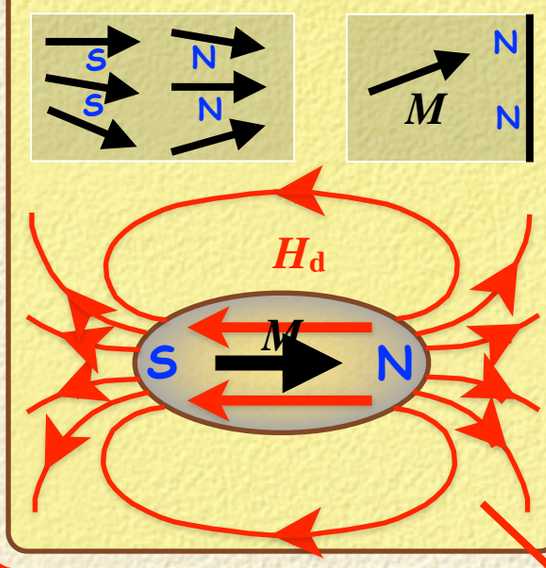

Magnetostrictive self energy

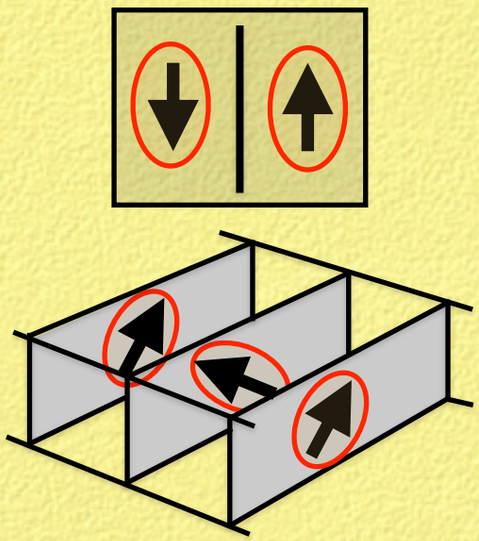

External stress energy

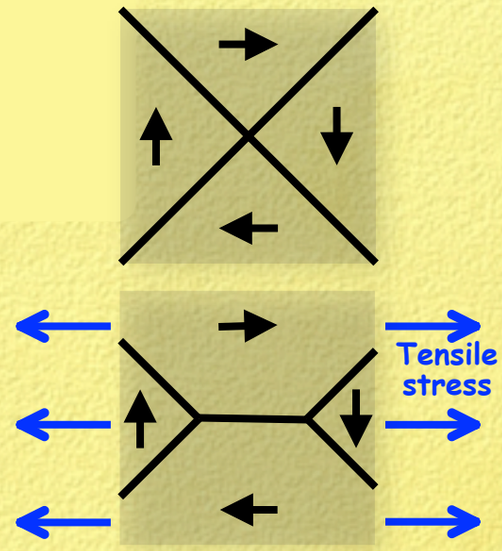

Anisotropy energy

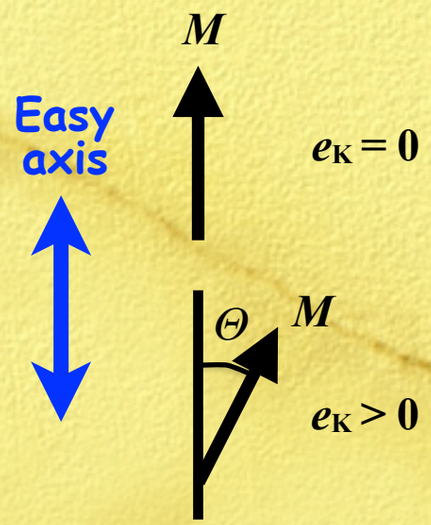

External field energy

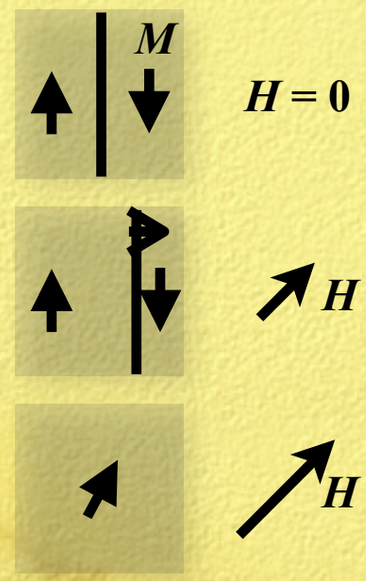

$$E_s = -\tfrac{1}{2}\mu_0 \int_{\text{Sample-volume}} \boldsymbol{H}_d \boldsymbol{M}\, dV$$

With $\boldsymbol{H}_d = -N\boldsymbol{M}$:

$$E_s = \tfrac{1}{2}\mu_0 N M^2 V$$

$$(0 < N < 1)$$

Origin of magnetic domains

$Ni_{80}Fe_{20}$ film (240 nm thick)

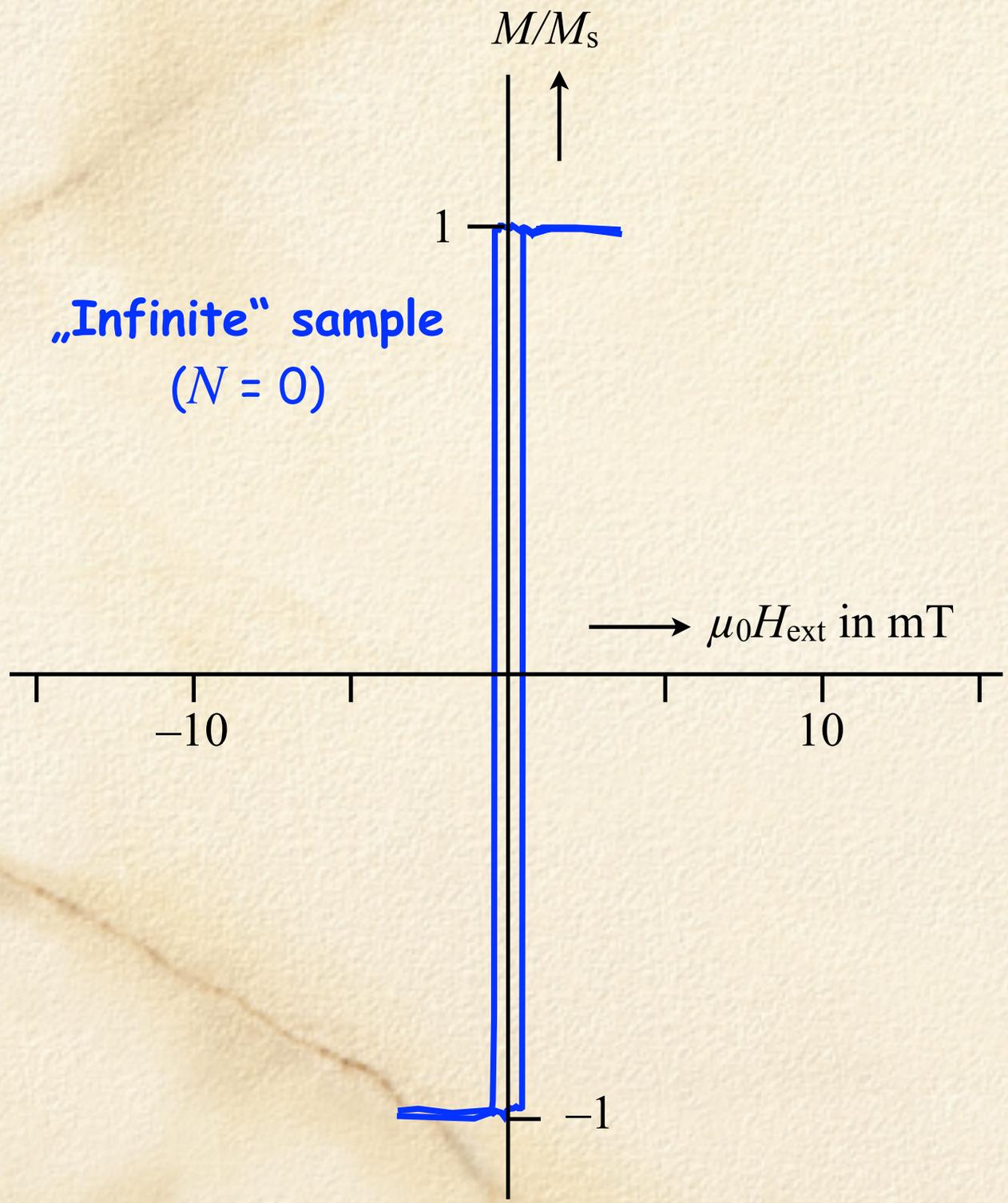

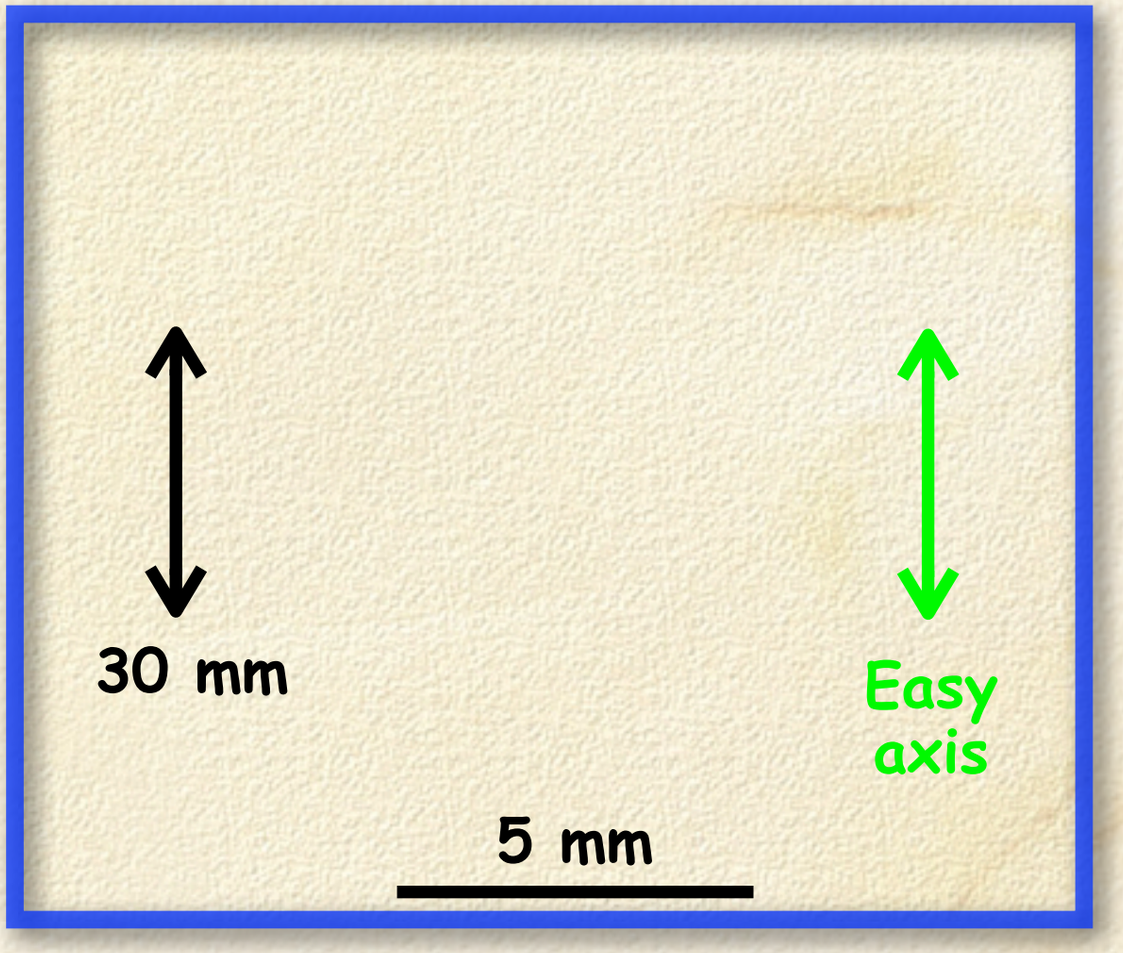

Origin of magnetic domains

$Ni_{80}Fe_{20}$ film (240 nm thick)

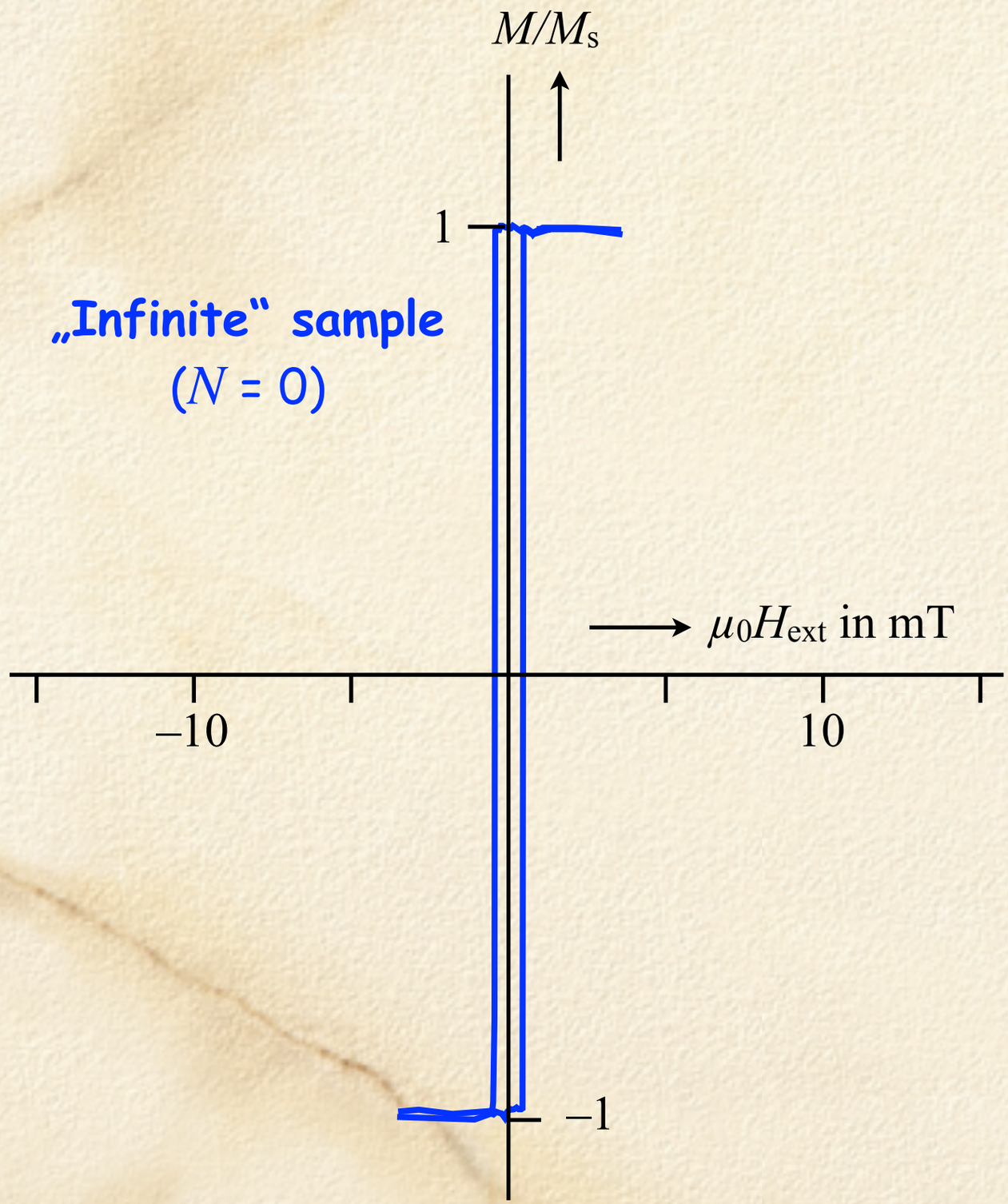

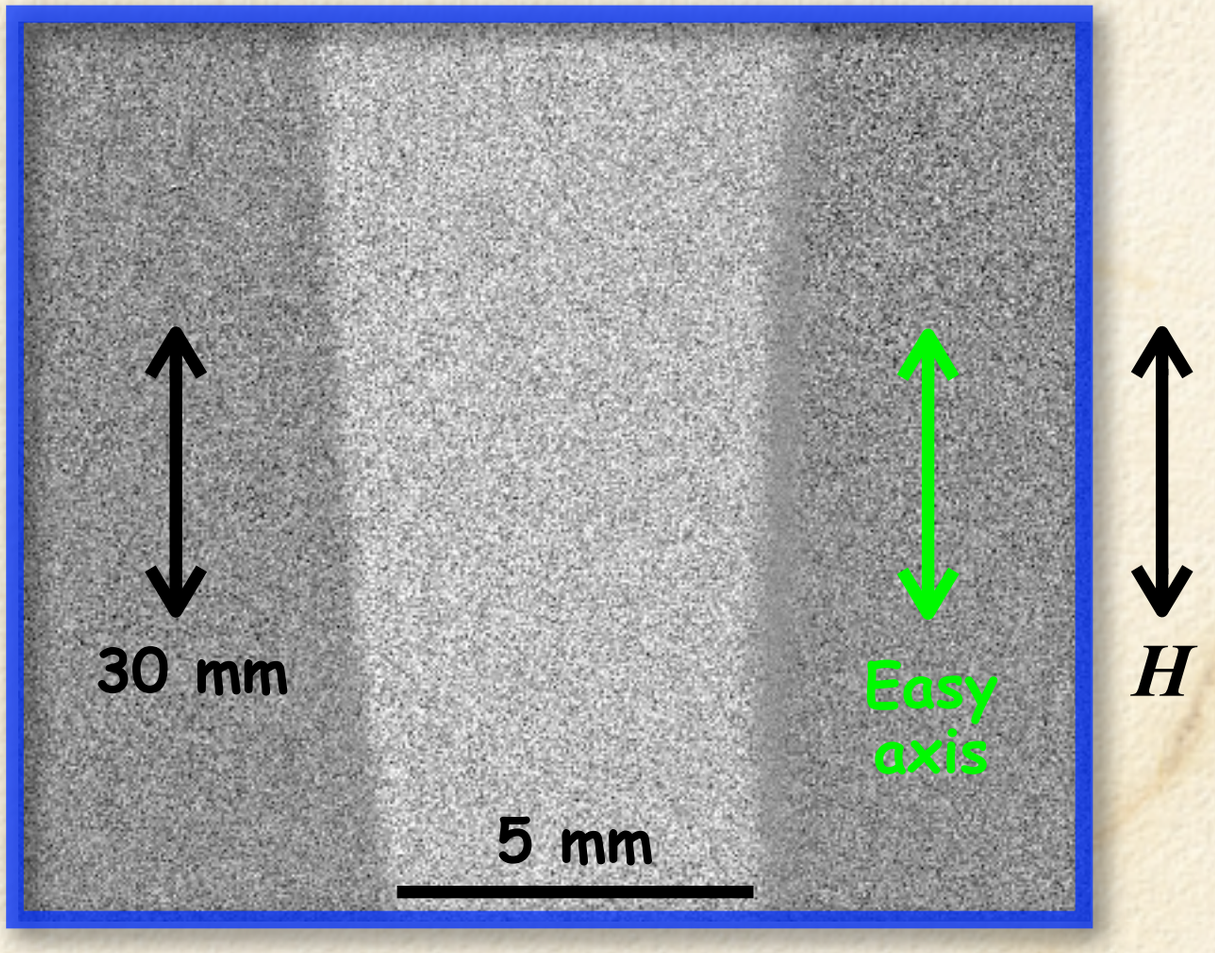

Origin of magnetic domains

$Ni_{80}Fe_{20}$ film (240 nm thick)

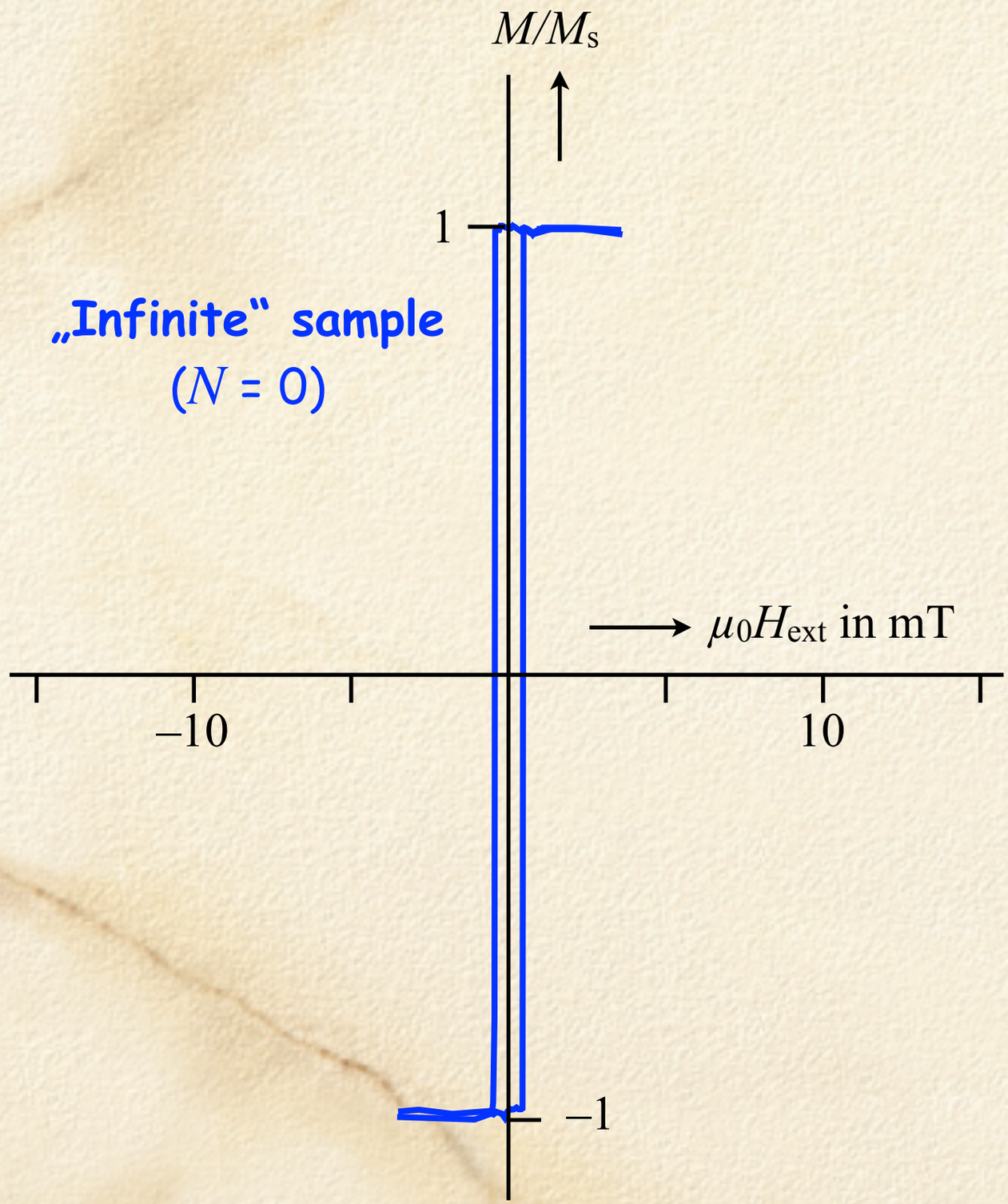

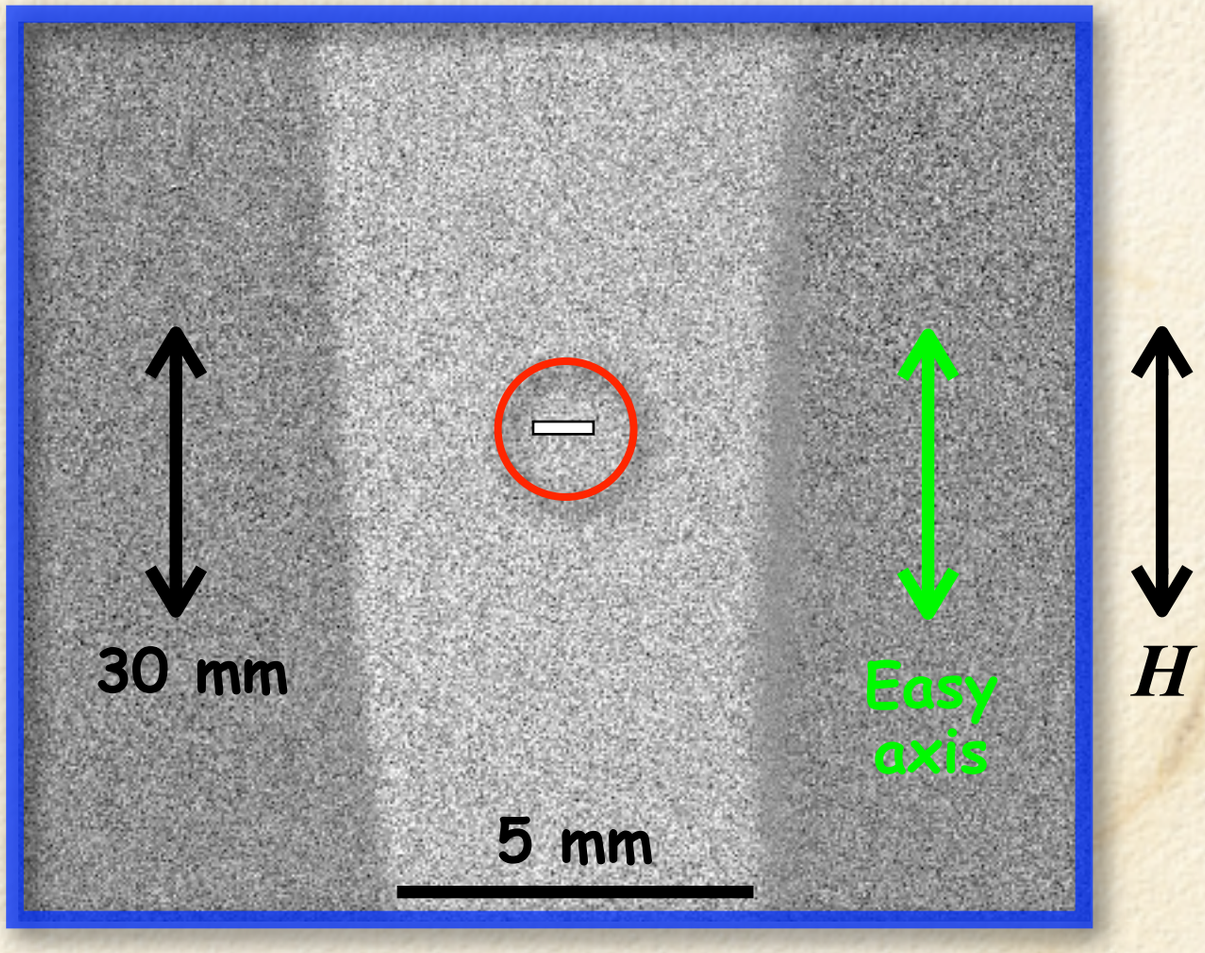

Origin of magnetic domains

$Ni_{80}Fe_{20}$ film (240 nm thick)

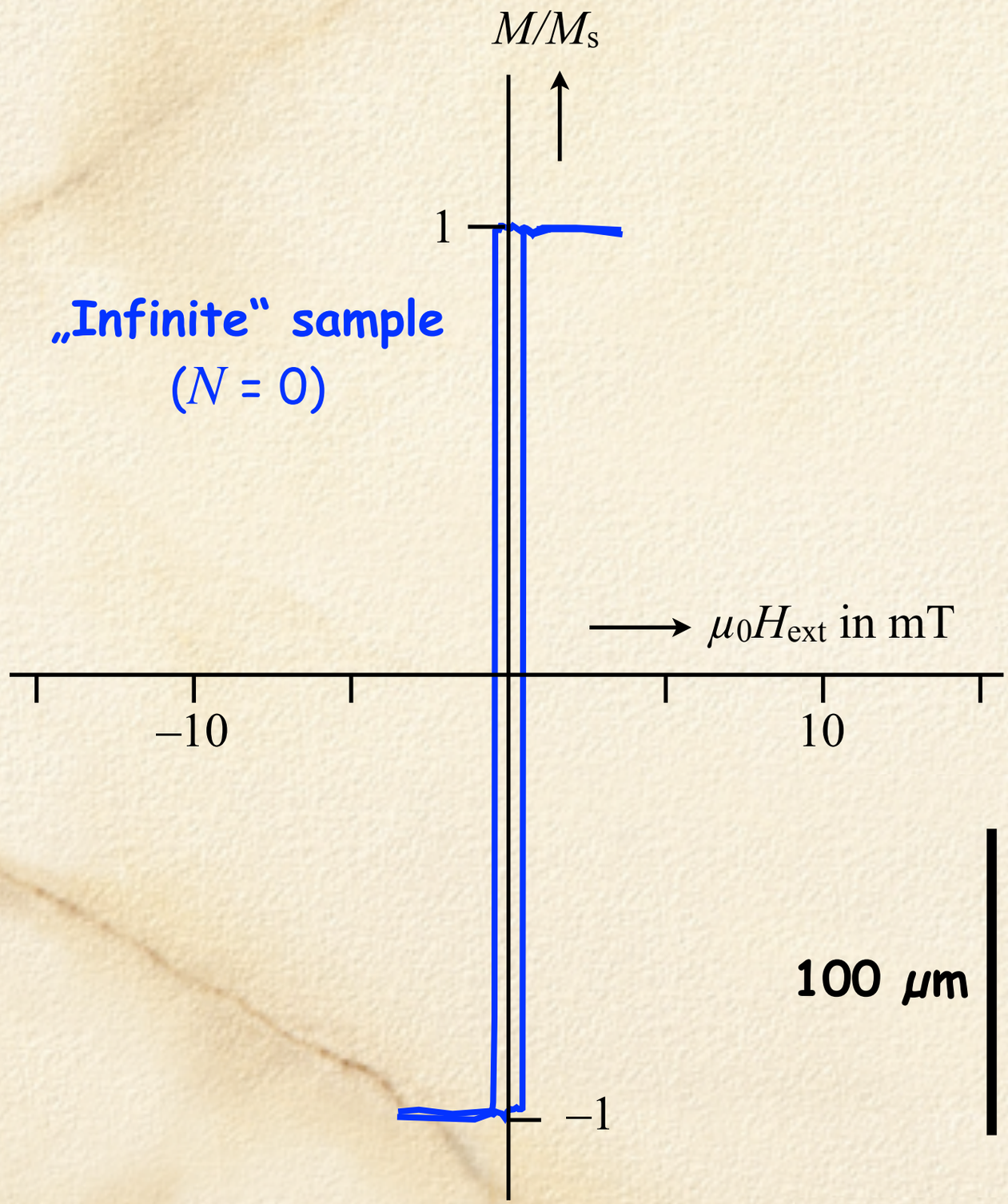

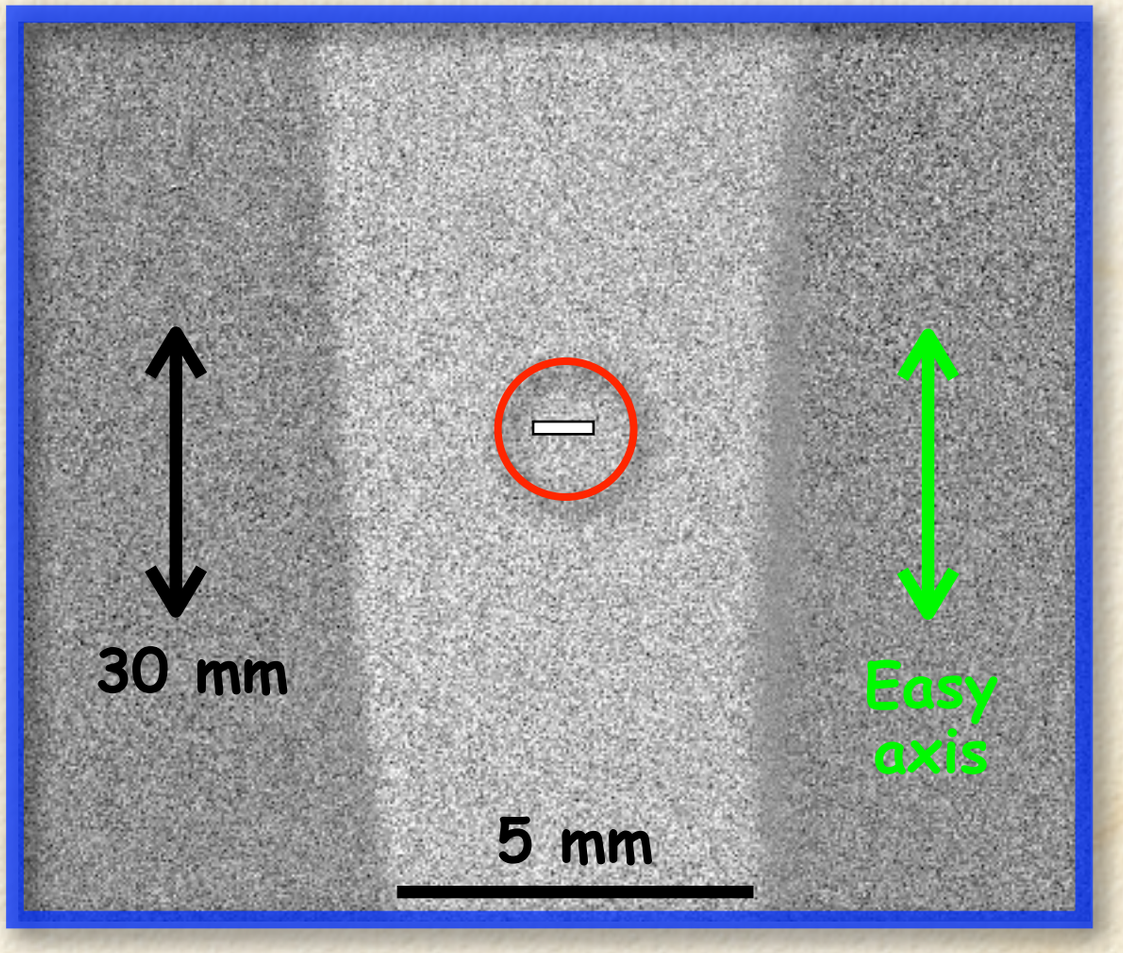

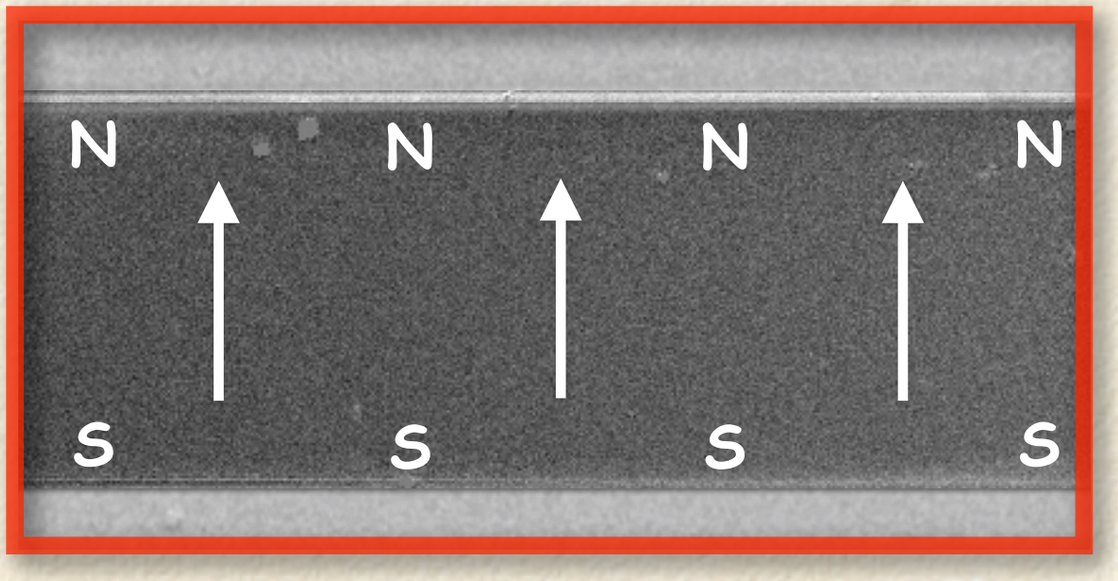

Origin of magnetic domains

$Ni_{80}Fe_{20}$ film (240 nm thick)

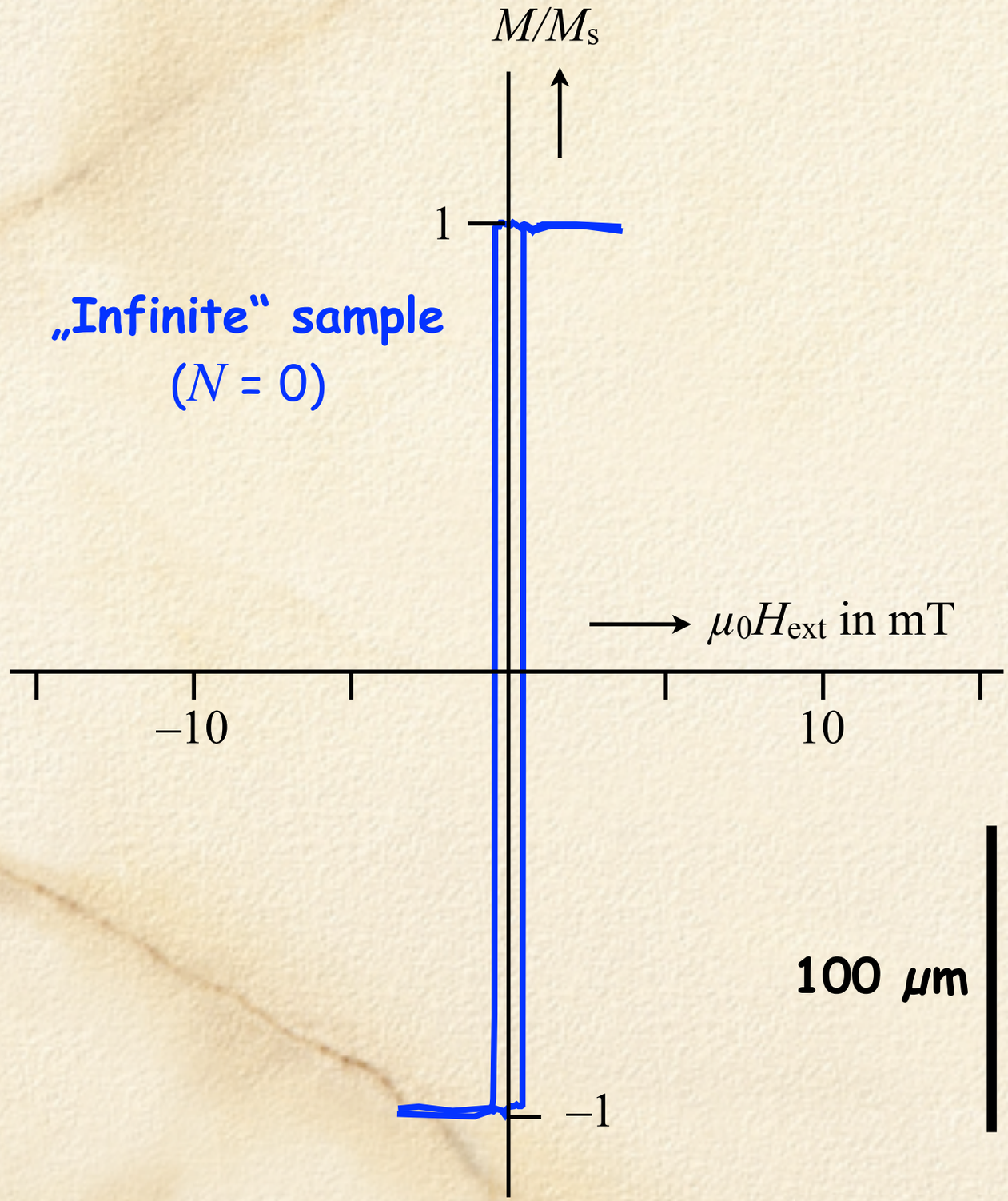

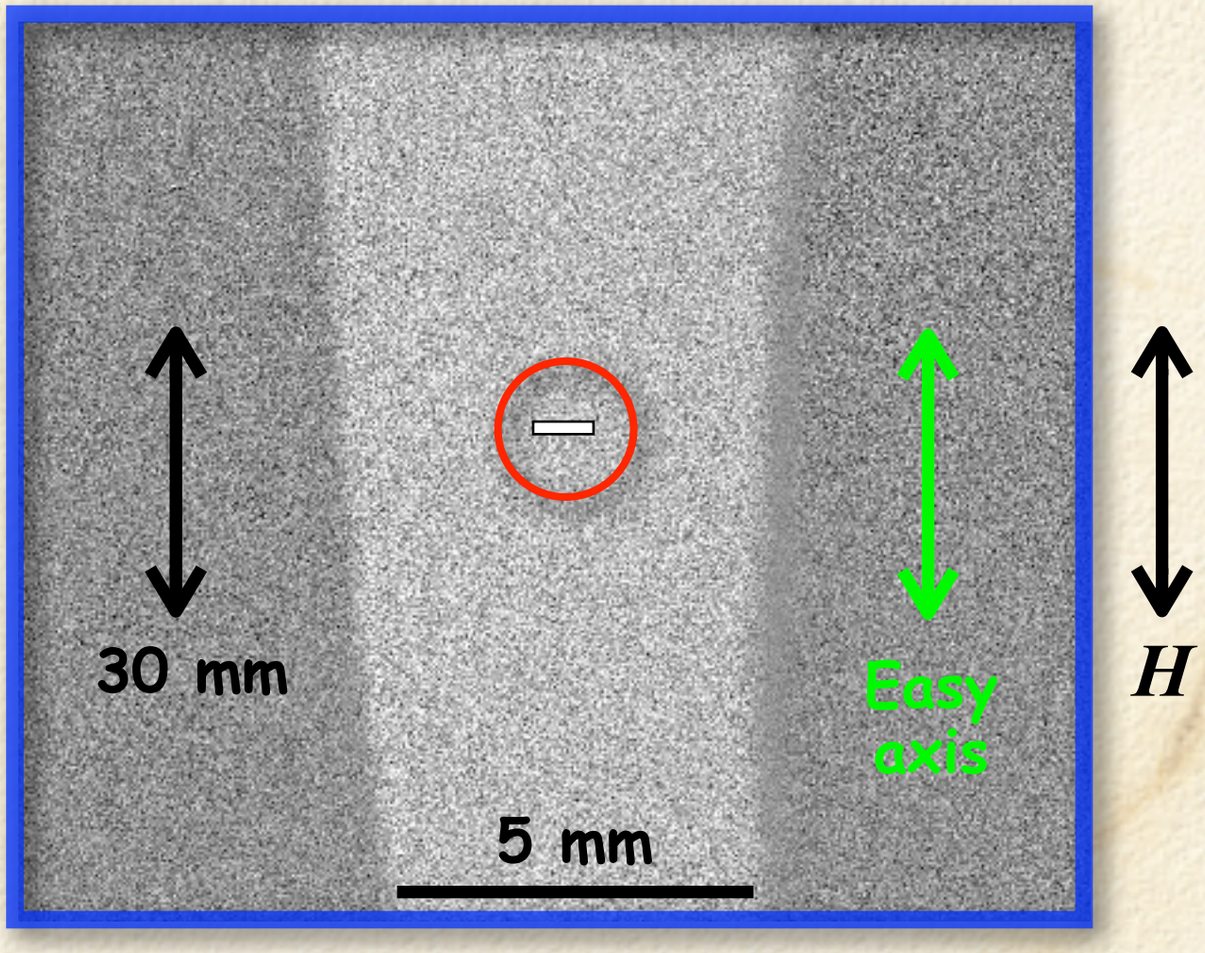

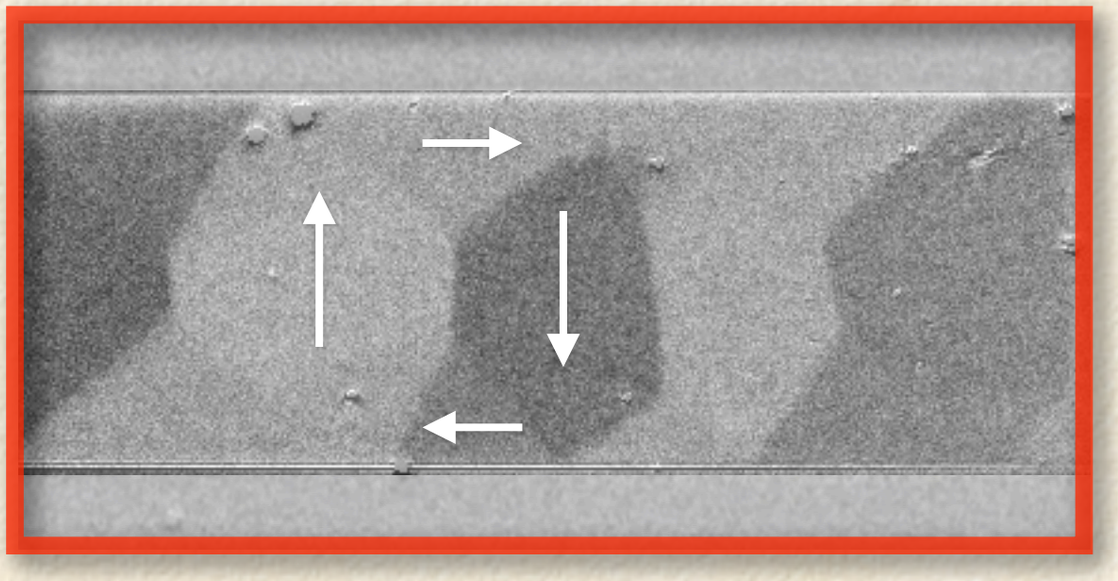

Origin of magnetic domains

$Ni_{80}Fe_{20}$ film (240 nm thick)

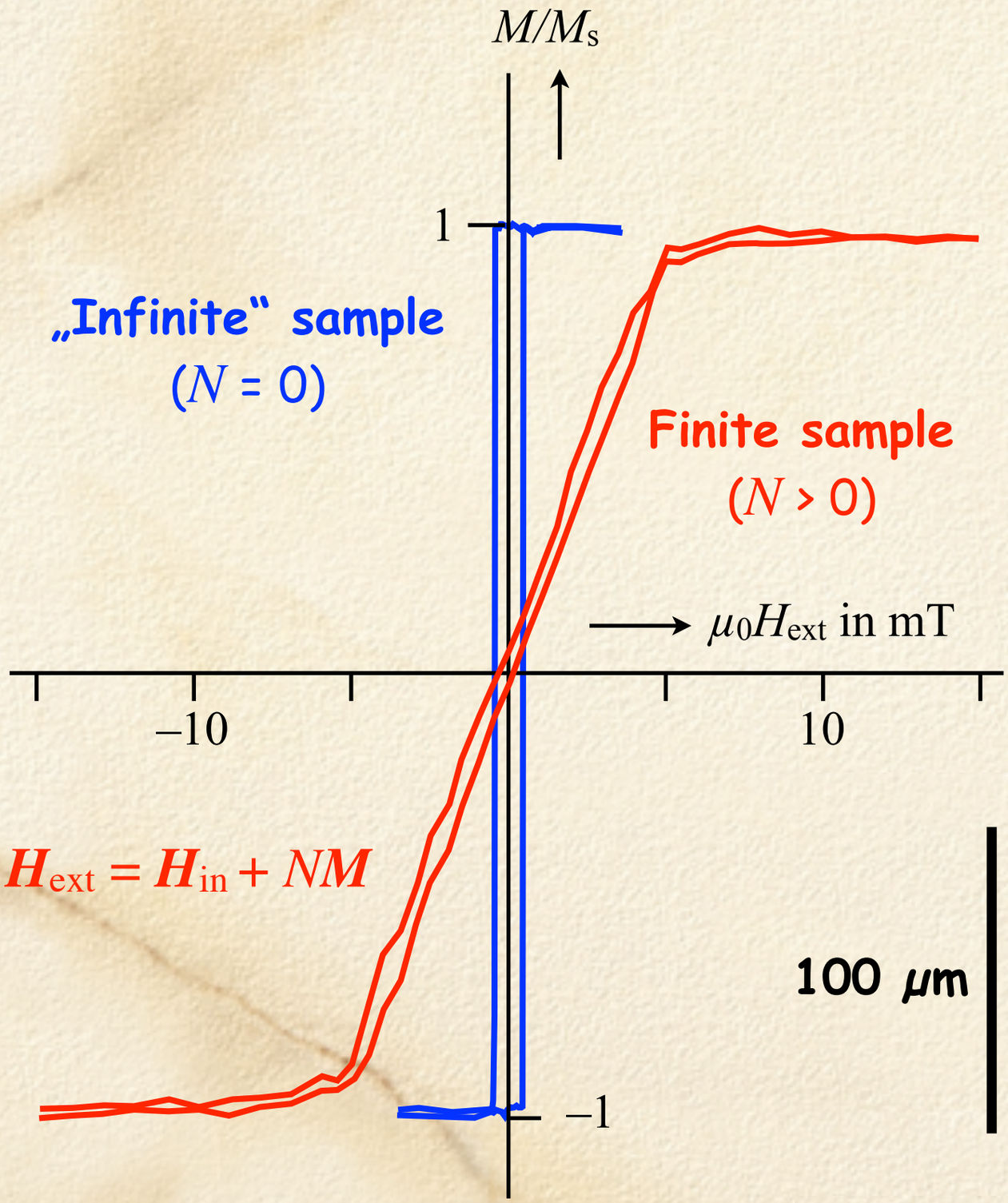

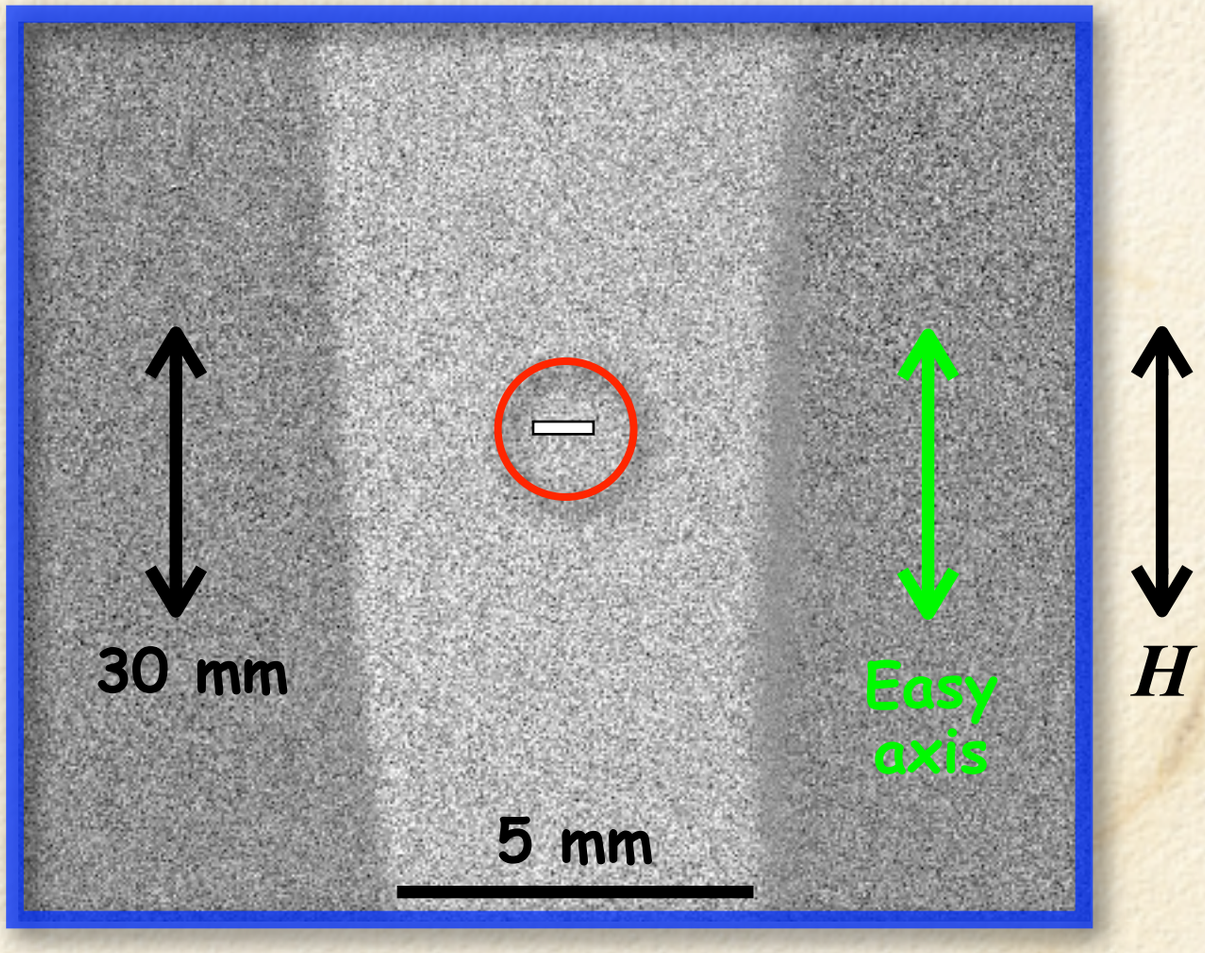

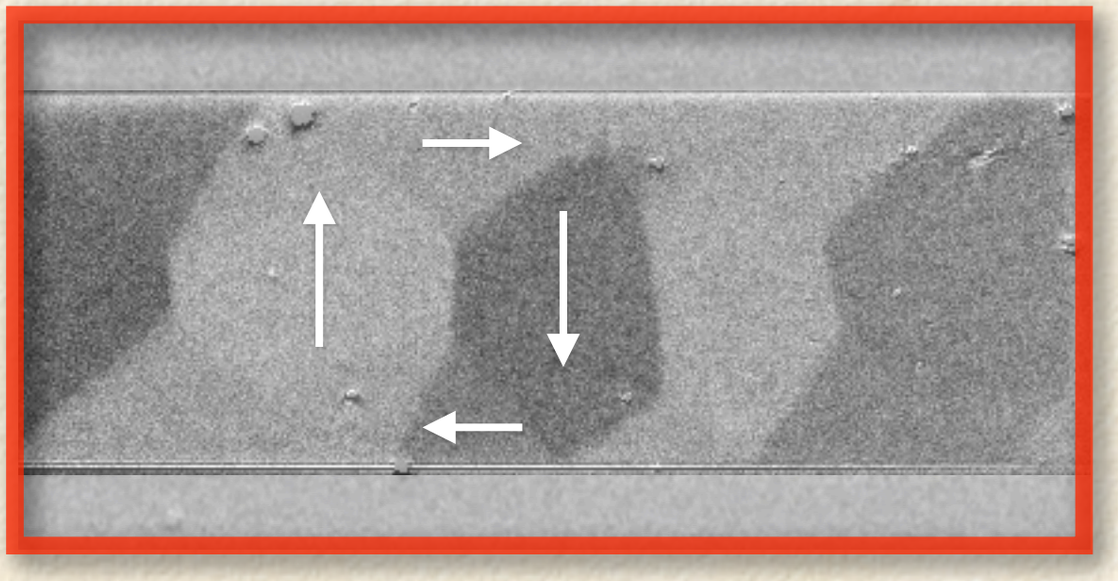

Origin of magnetic domains

$Ni_{80}Fe_{20}$ film (240 nm thick)

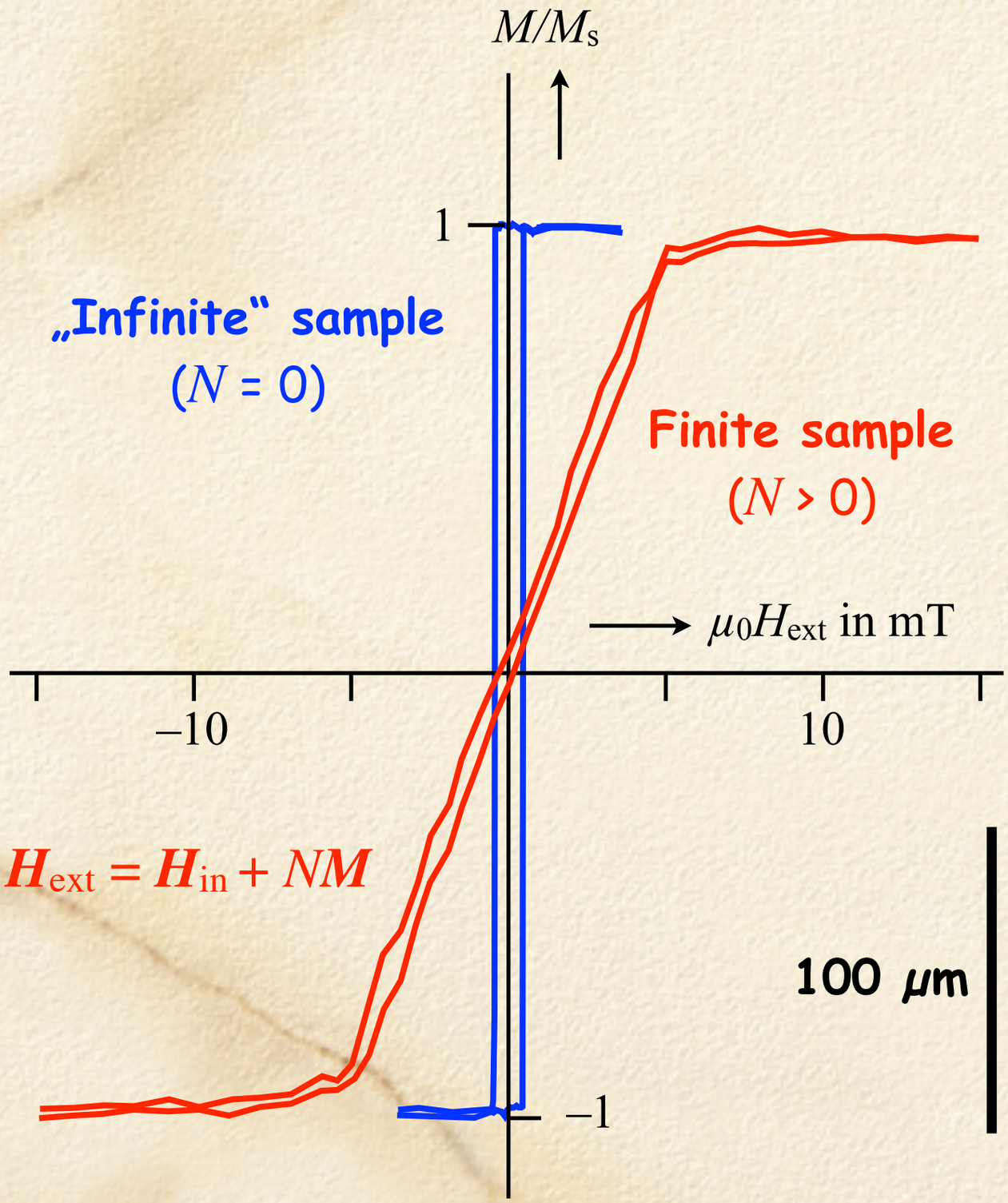

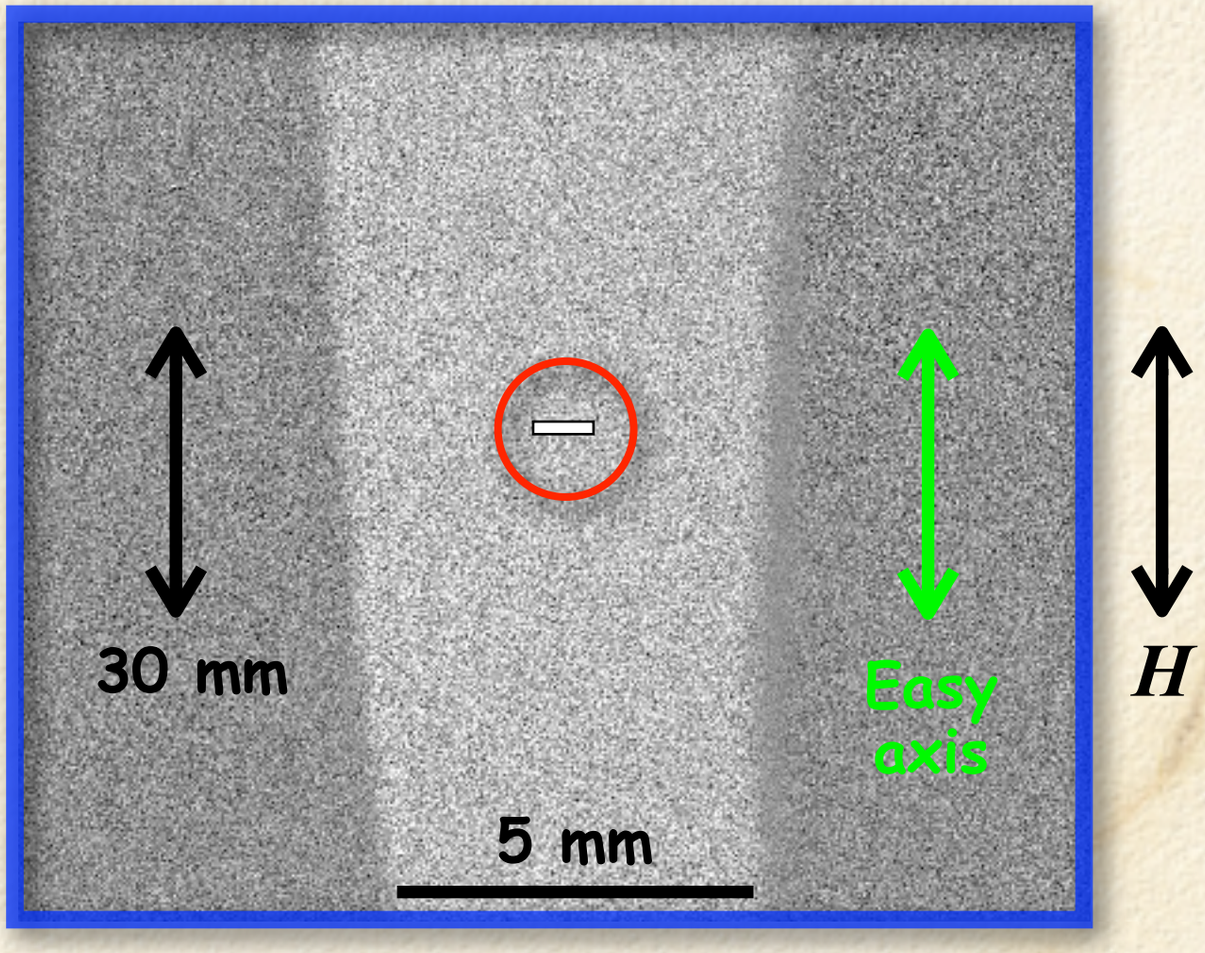

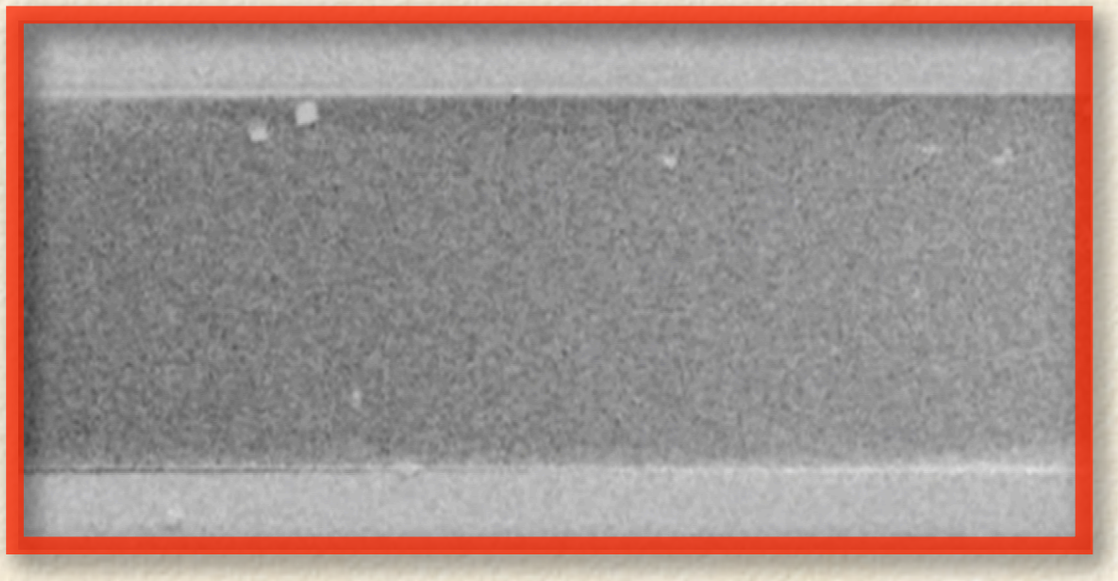

Origin of magnetic domains

$Ni_{80}Fe_{20}$ film (240 nm thick)

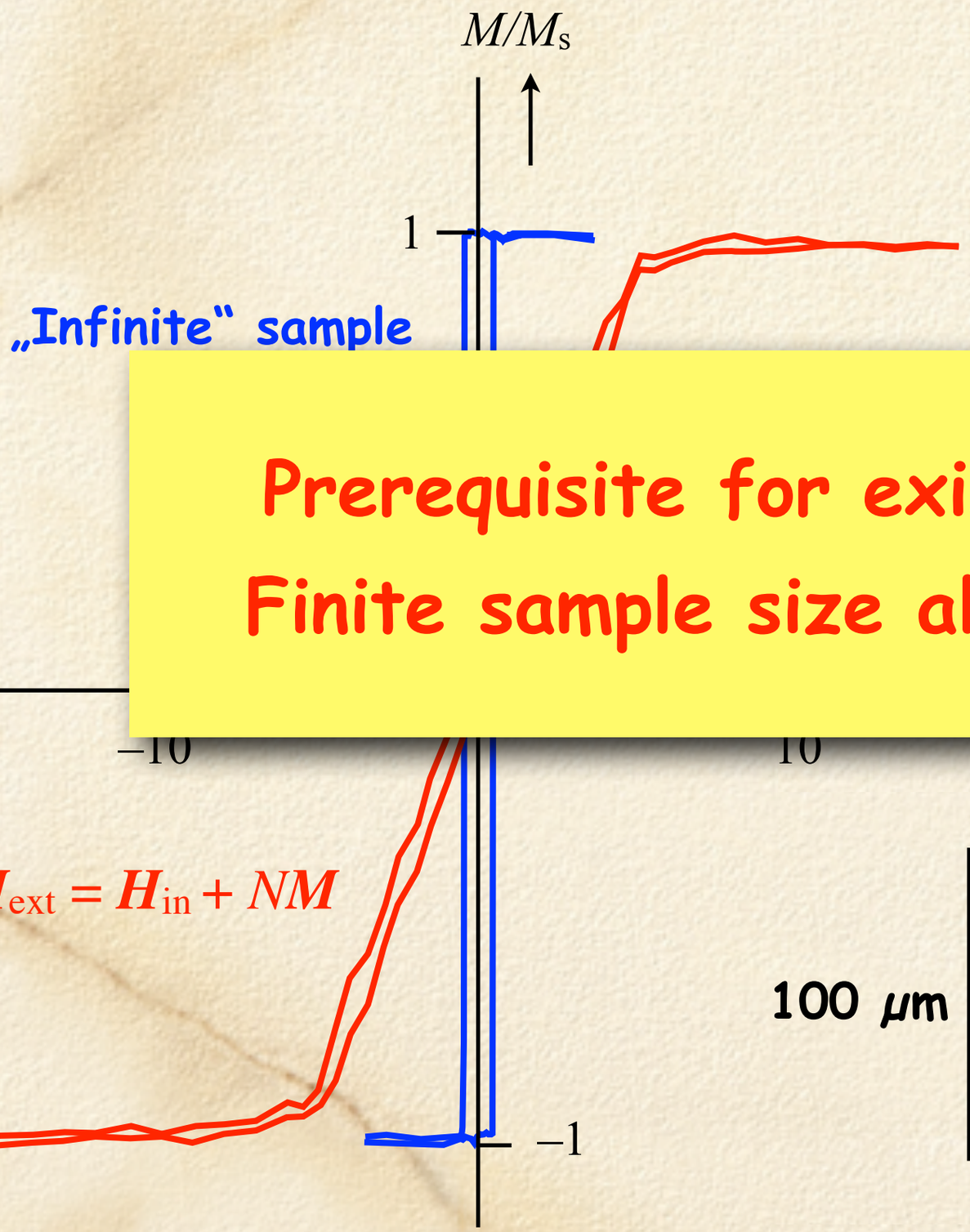

„Infinite" sample

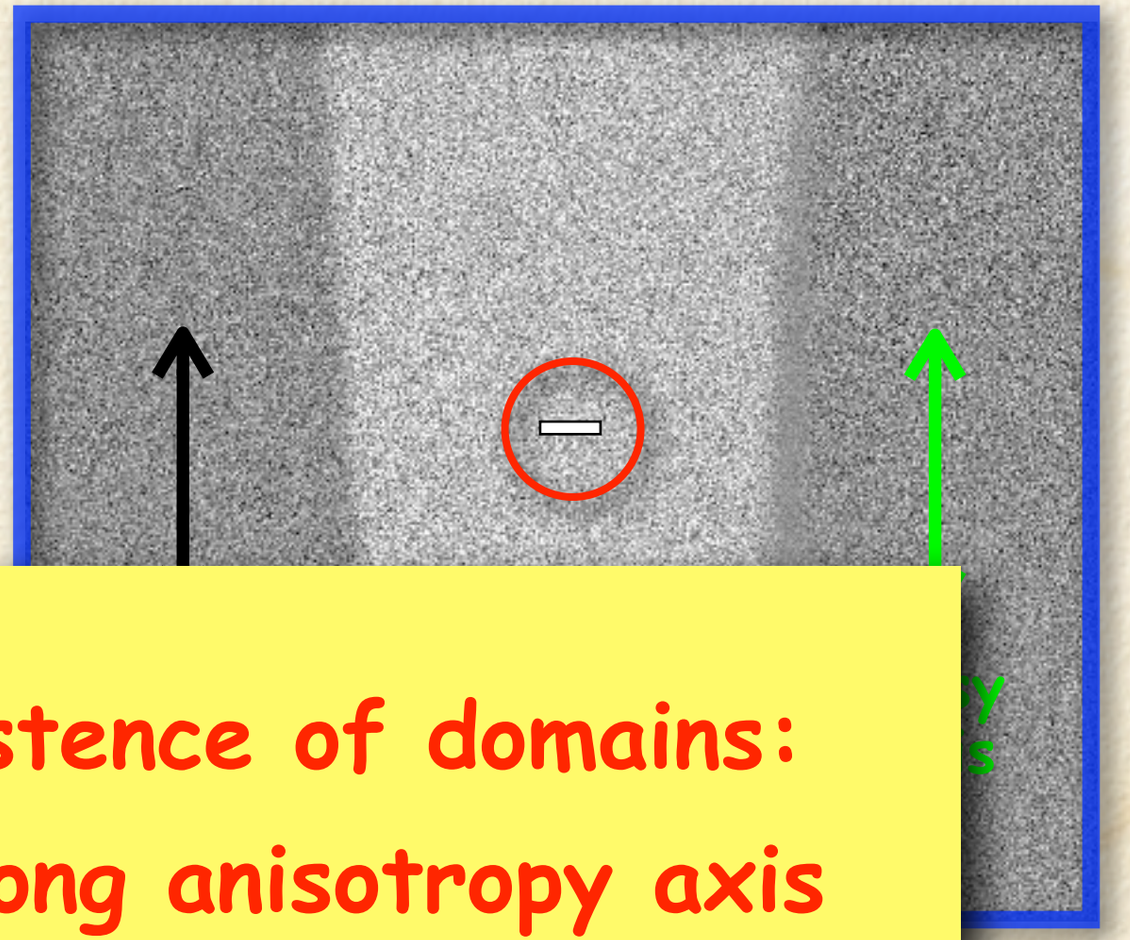

Prerequisite for existence of domains:

Finite sample size along anisotropy axis

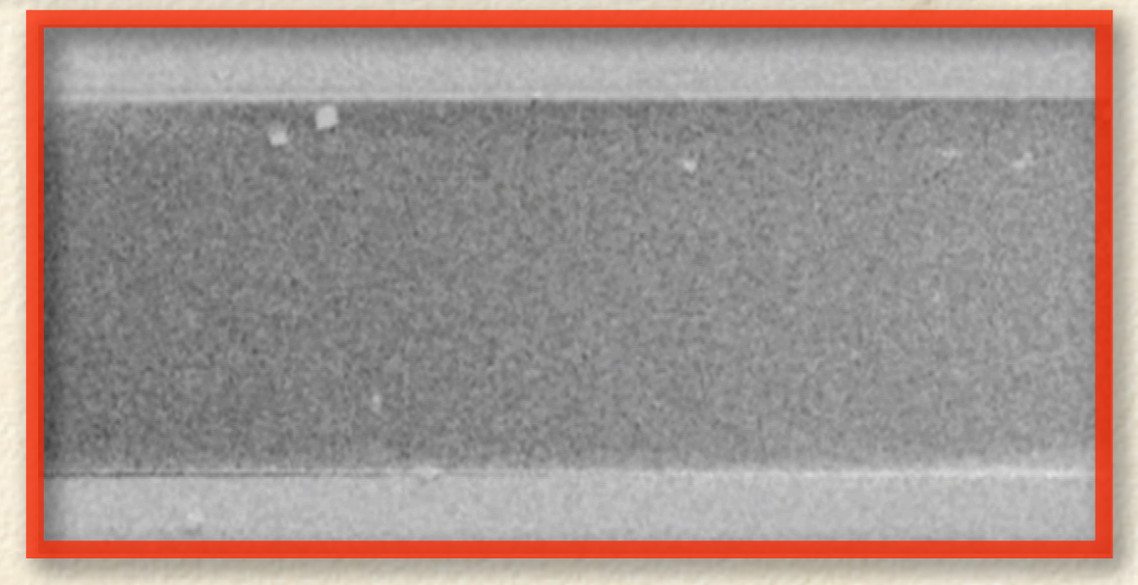

Magnetic Energies

Exchange energy

$e_A = 0$

$e_A > 0$

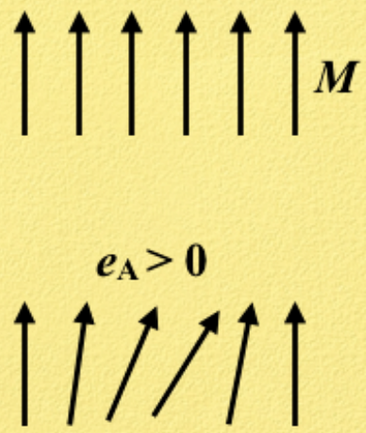

Stray field energy

$$\operatorname{div} \boldsymbol{H}_d = -\operatorname{div} \boldsymbol{M}$$

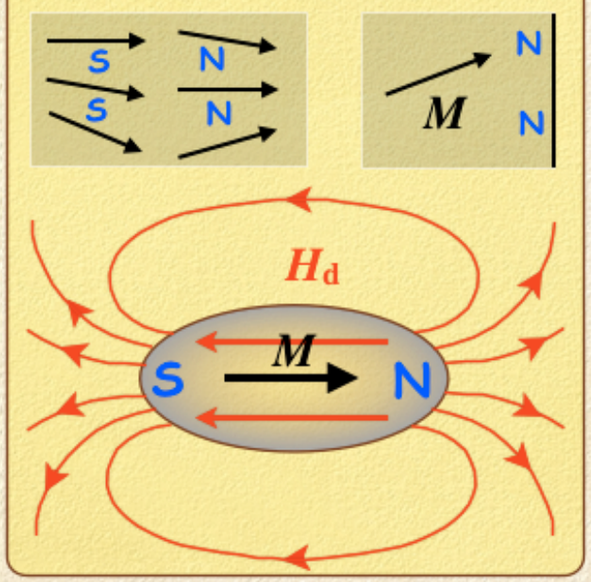

Magnetostrictive self energy

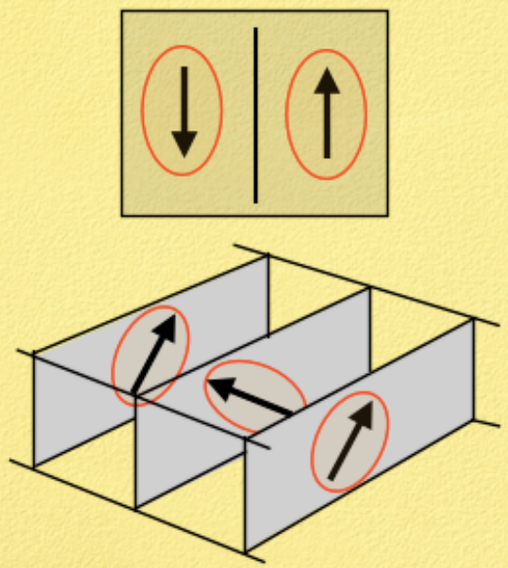

External stress energy

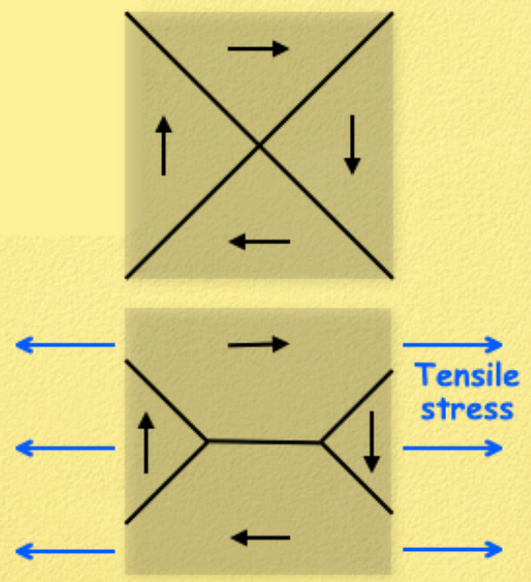

Anisotropy energy

Easy axis

$e_K = 0$

$e_K > 0$

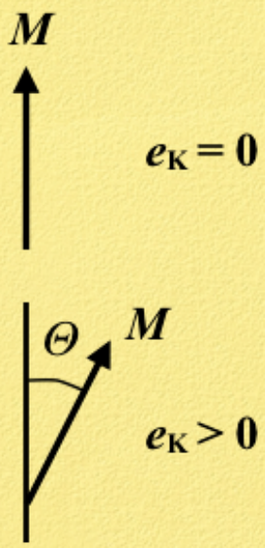

External field energy

$H = 0$

H

H

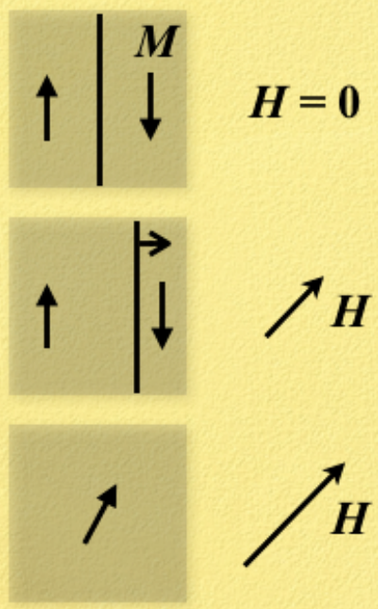

Magnetic Energies

Exchange energy

$e_A = 0$

$e_A > 0$

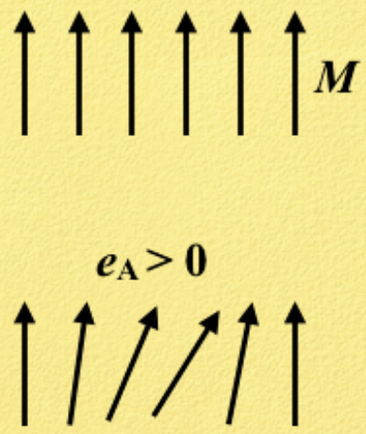

Stray field energy

$$\text{div}\, \boldsymbol{H}_d = -\,\text{div}\, \boldsymbol{M}$$

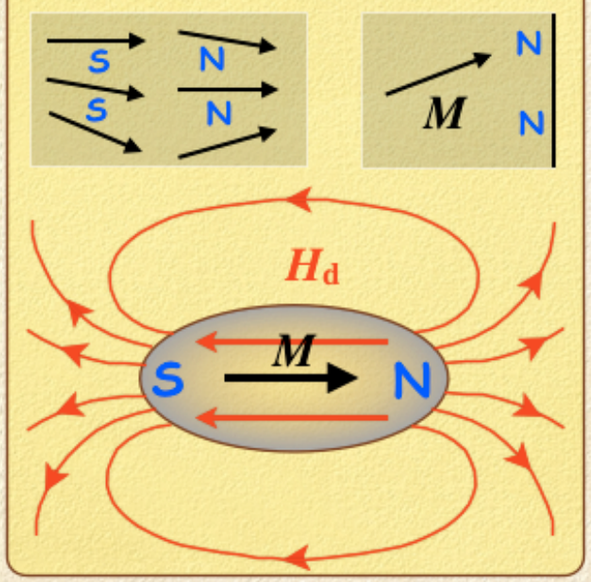

Magnetostrictive self energy

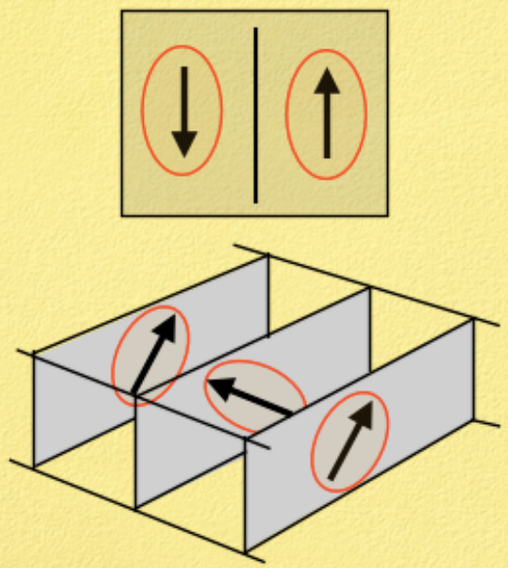

External stress energy

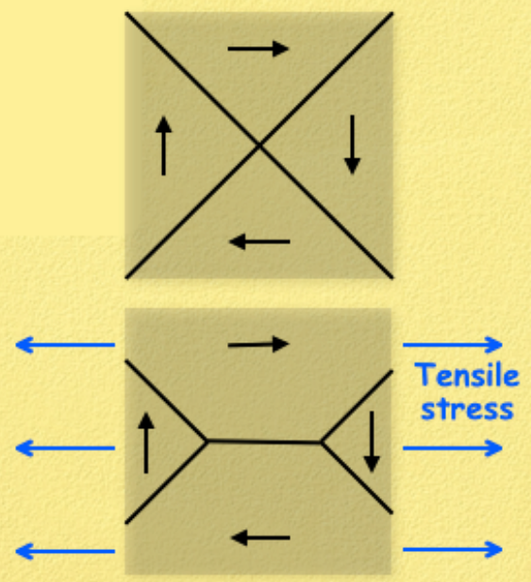

Anisotropy energy

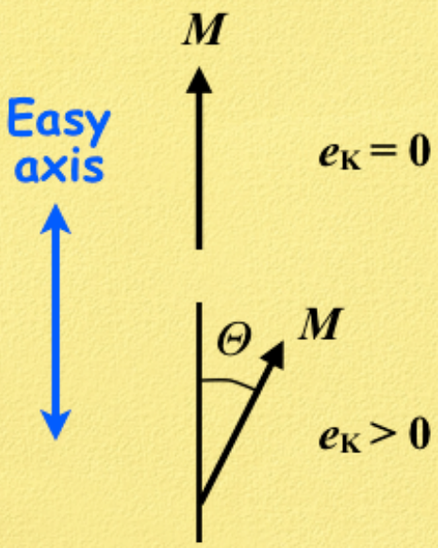

External field energy

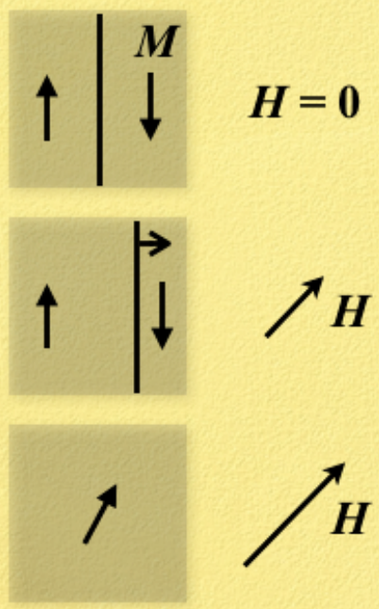

Domain character: determined by interplay of energies

Transformer sheet

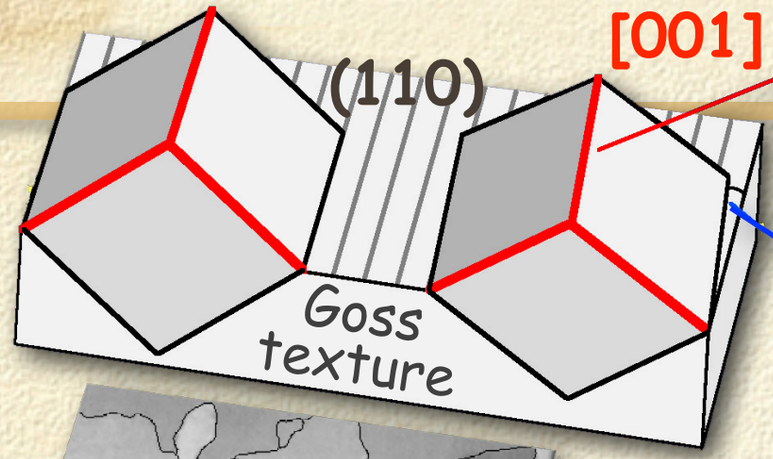

0.1 mm

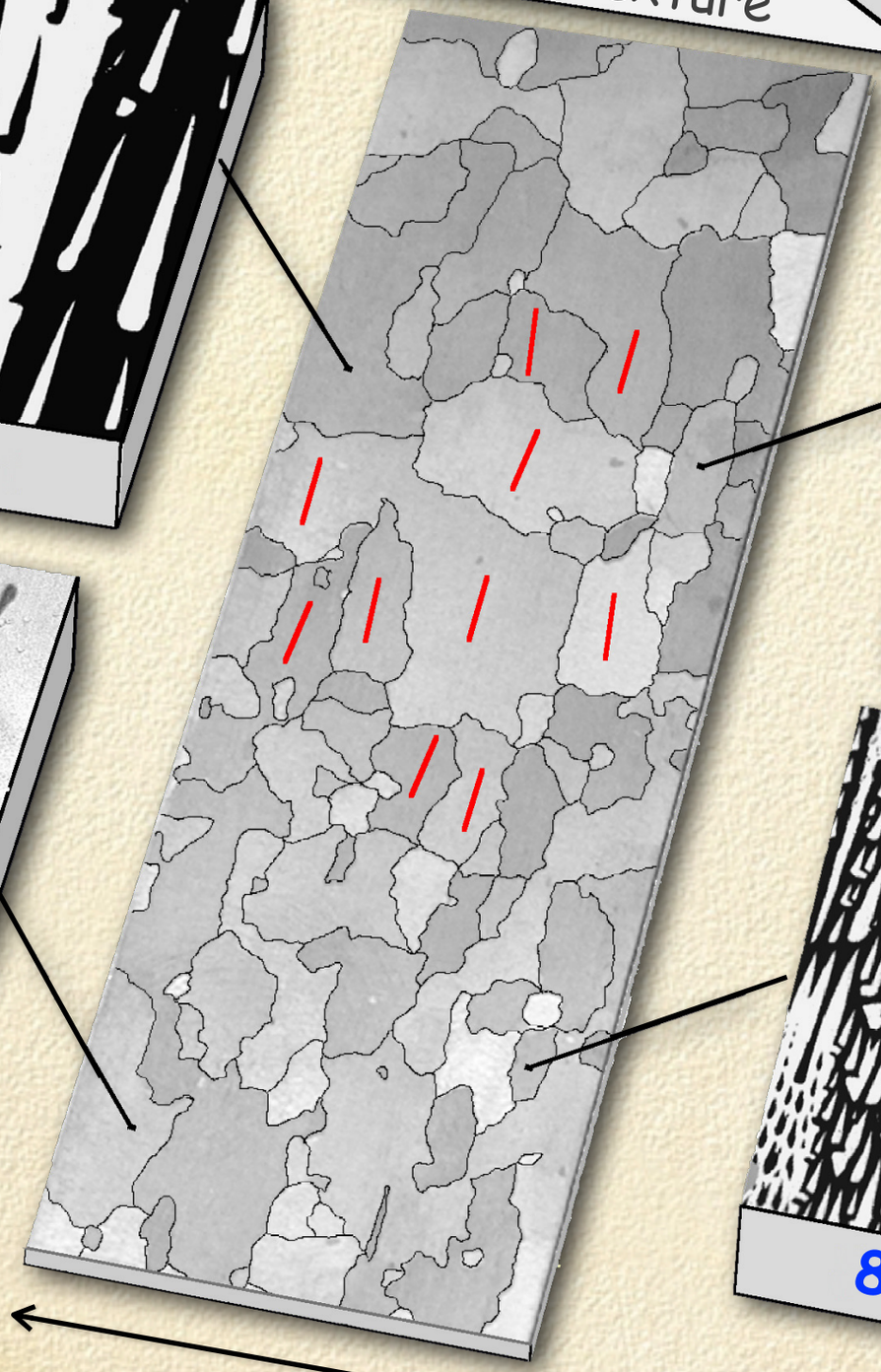

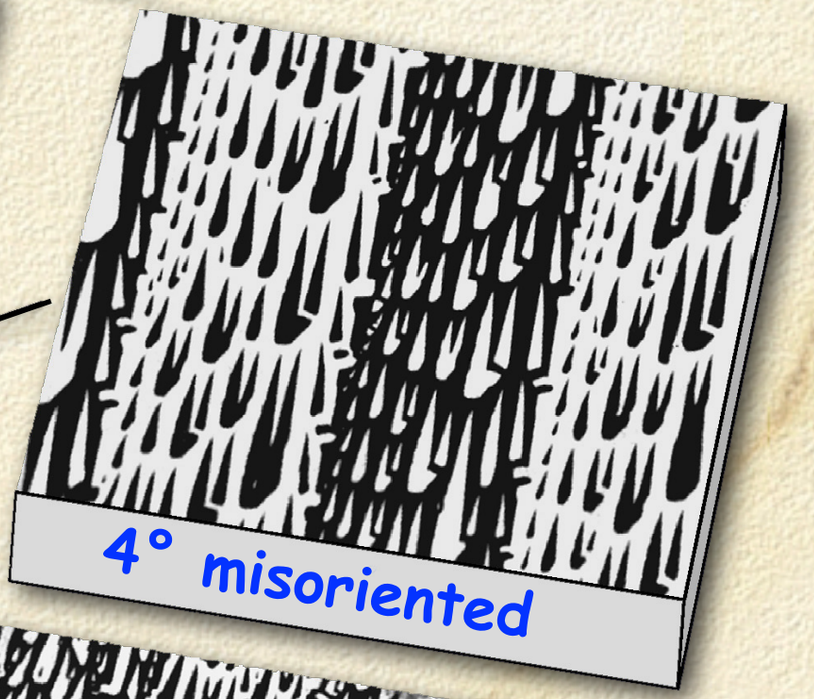

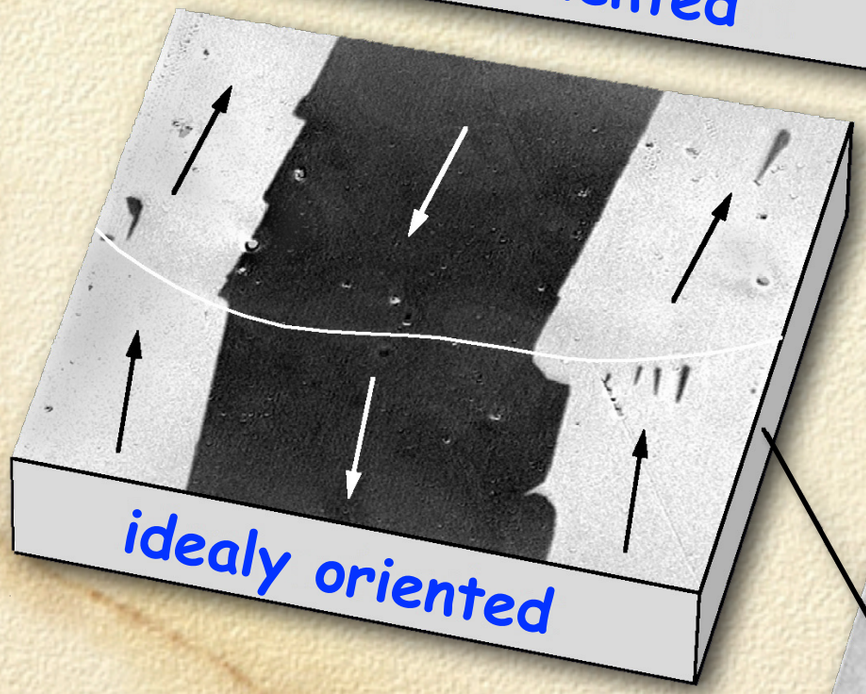

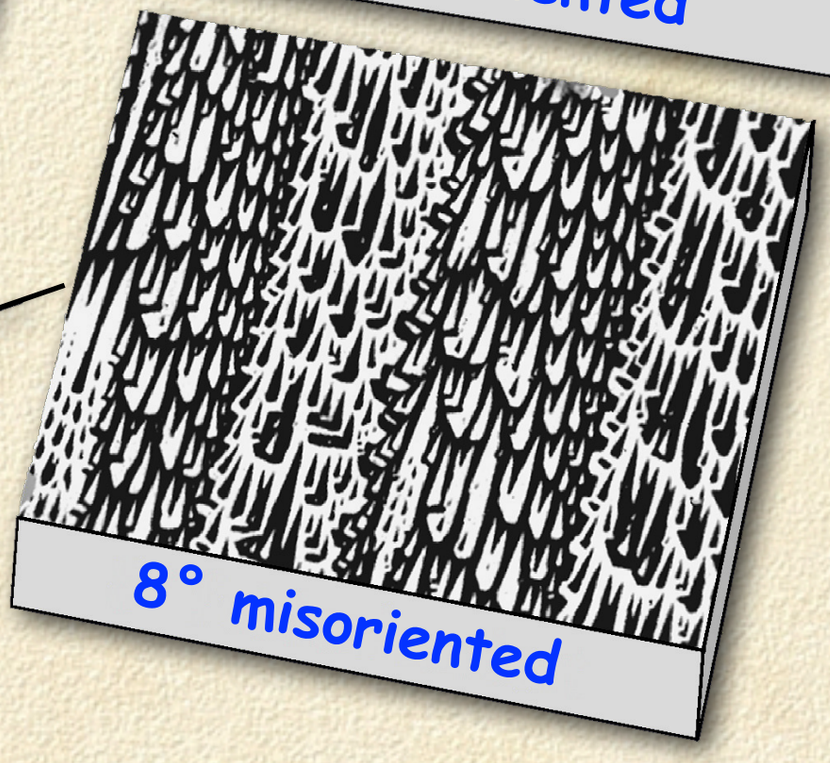

30 mm

Transformer sheet

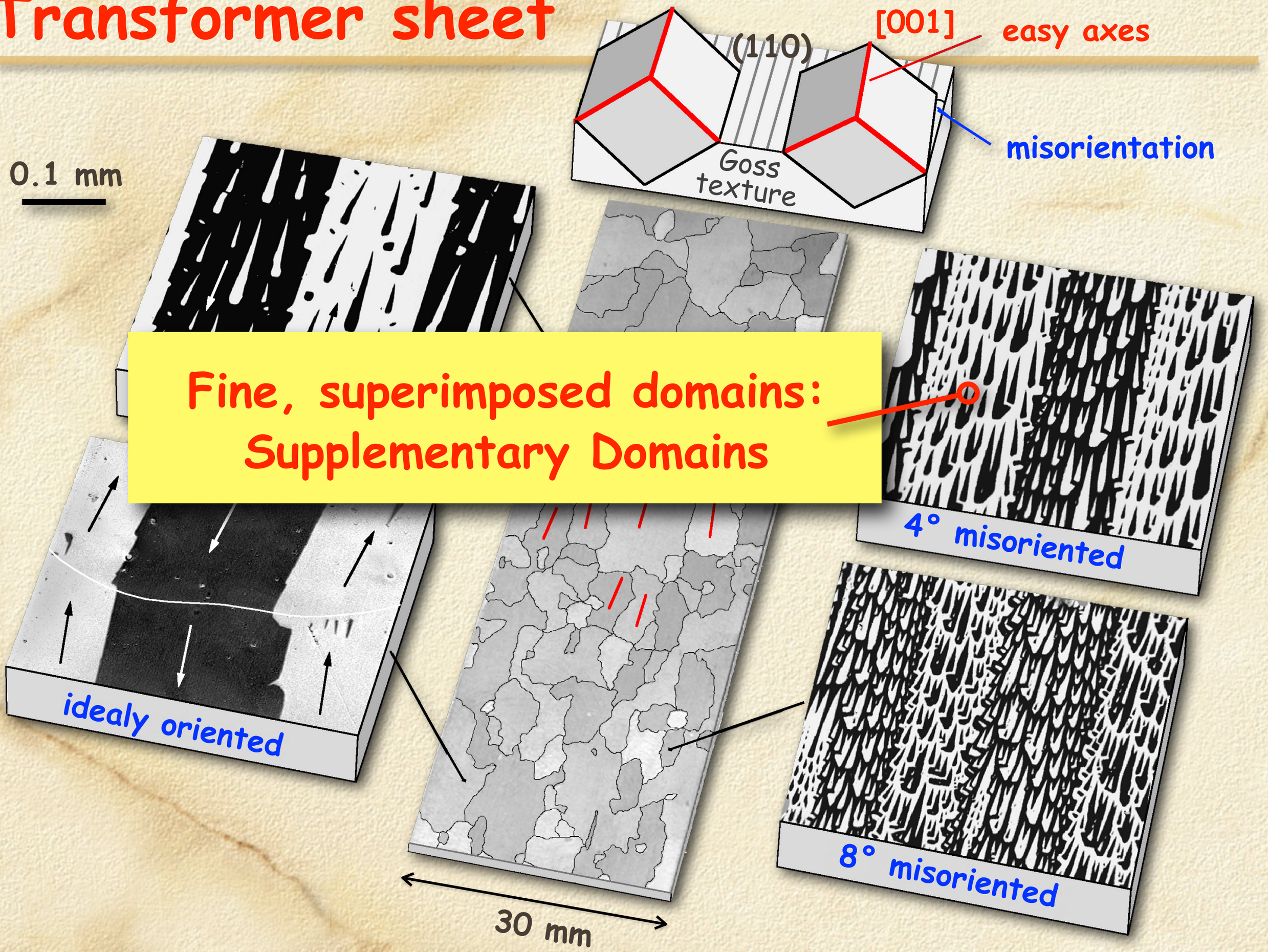

Grain-oriented FeSi transformer material

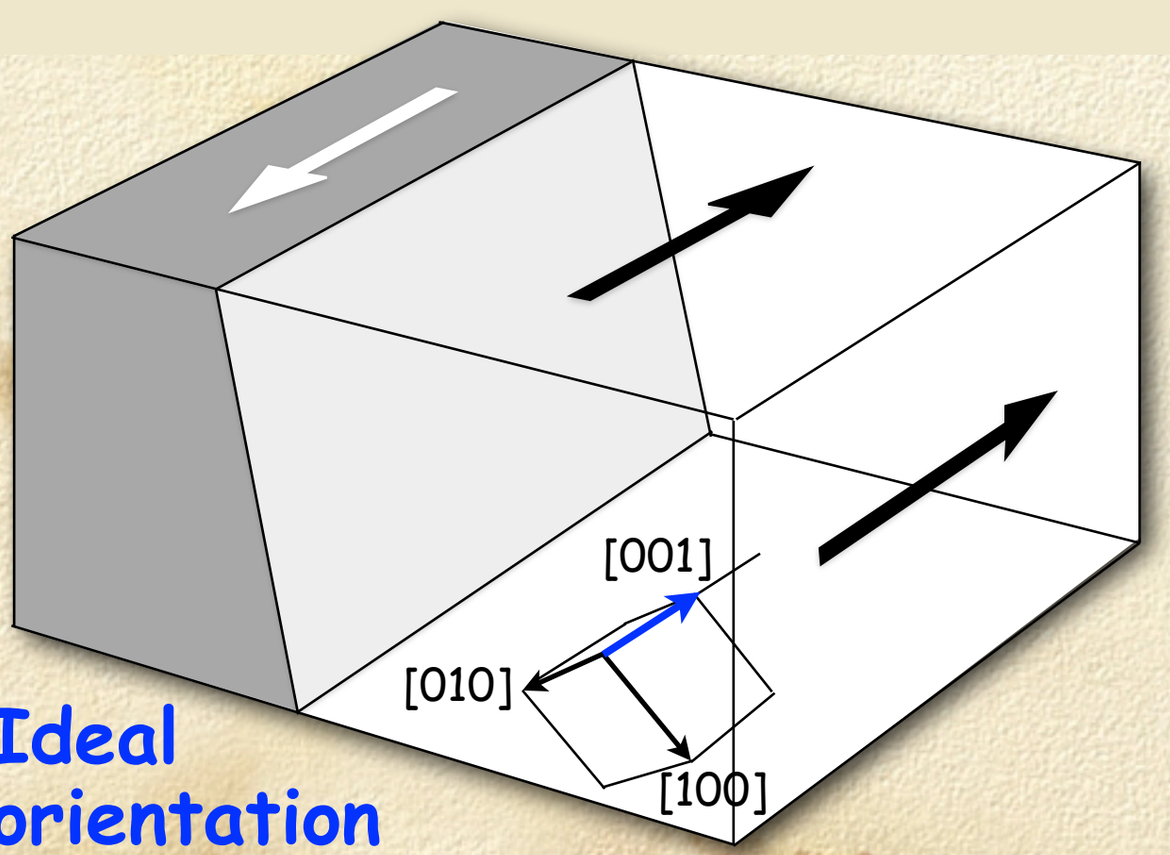

Ideal orientation

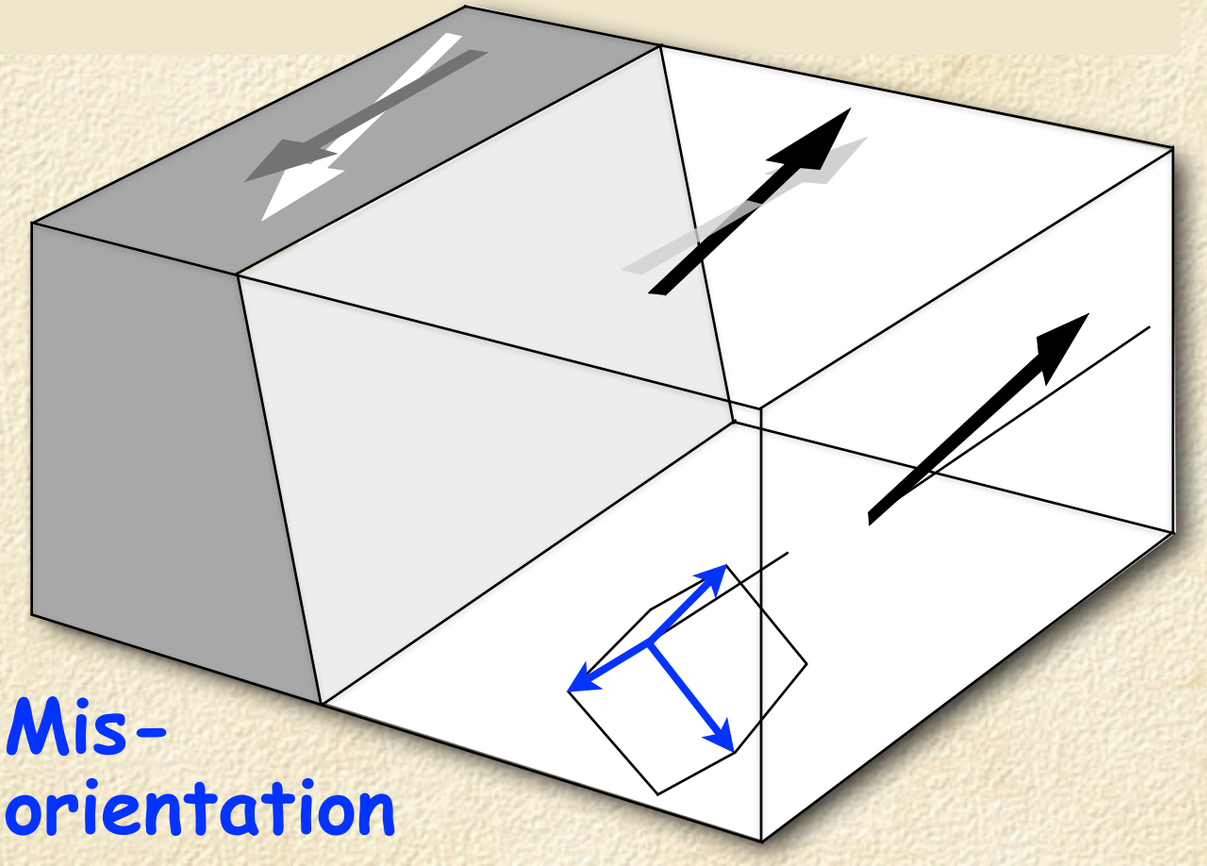

Mis-orientation

Grain-oriented FeSi transformer material

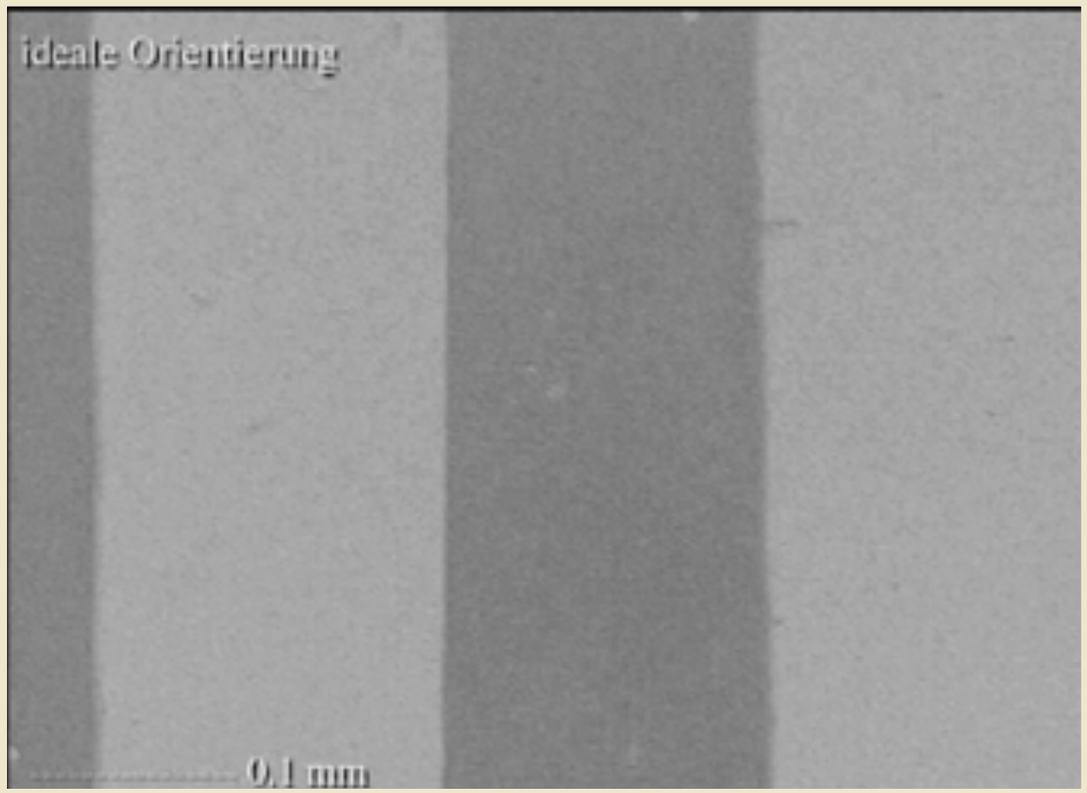

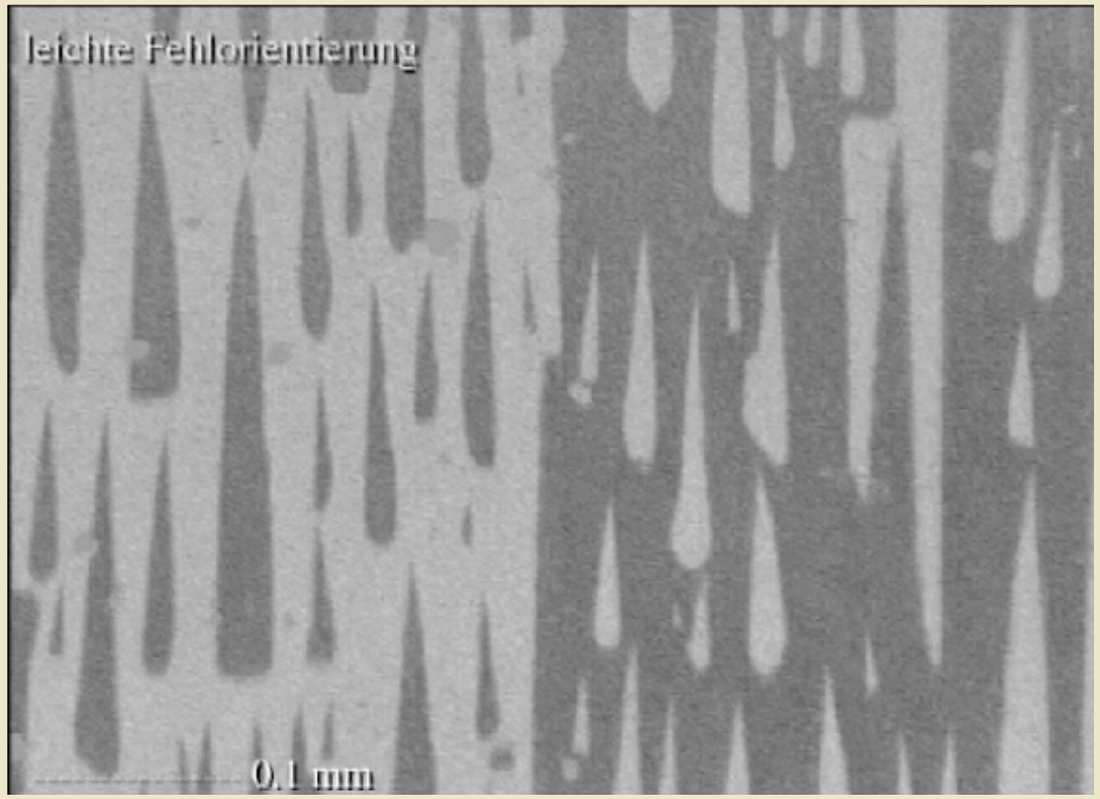

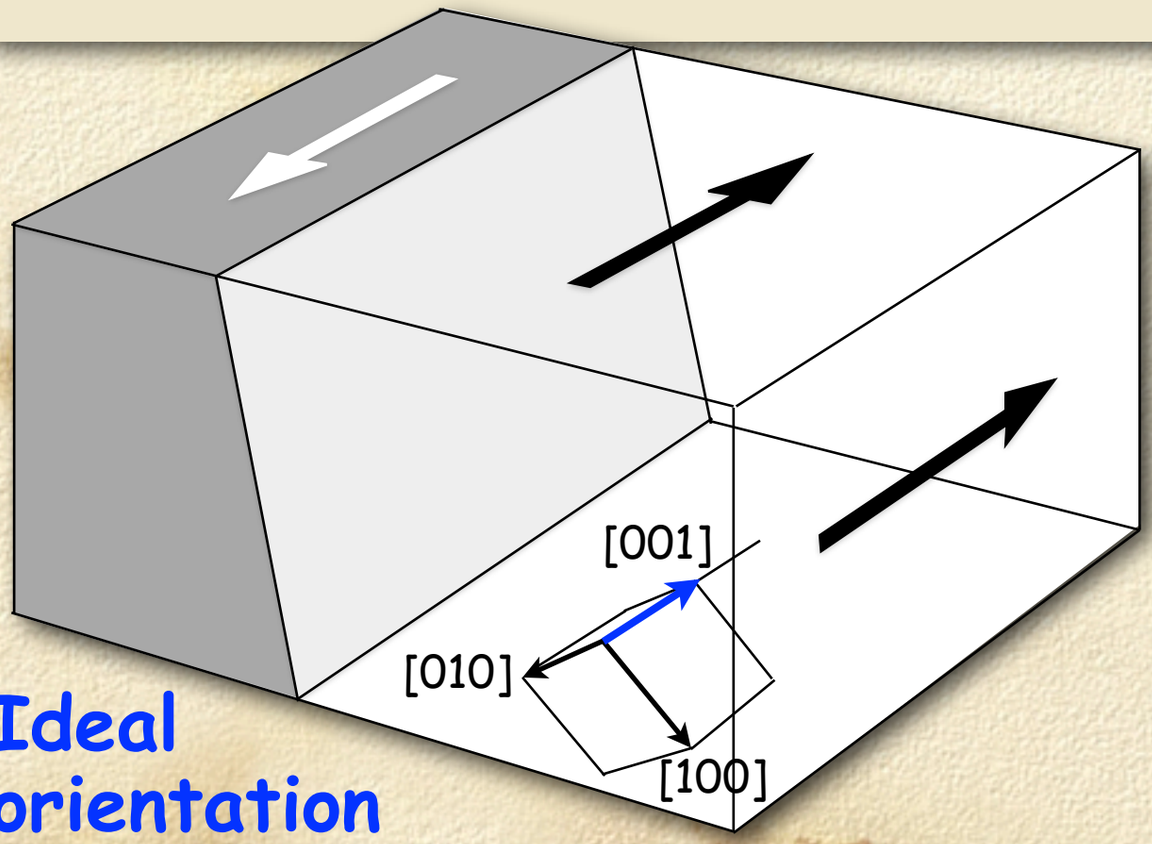

Ideal orientation

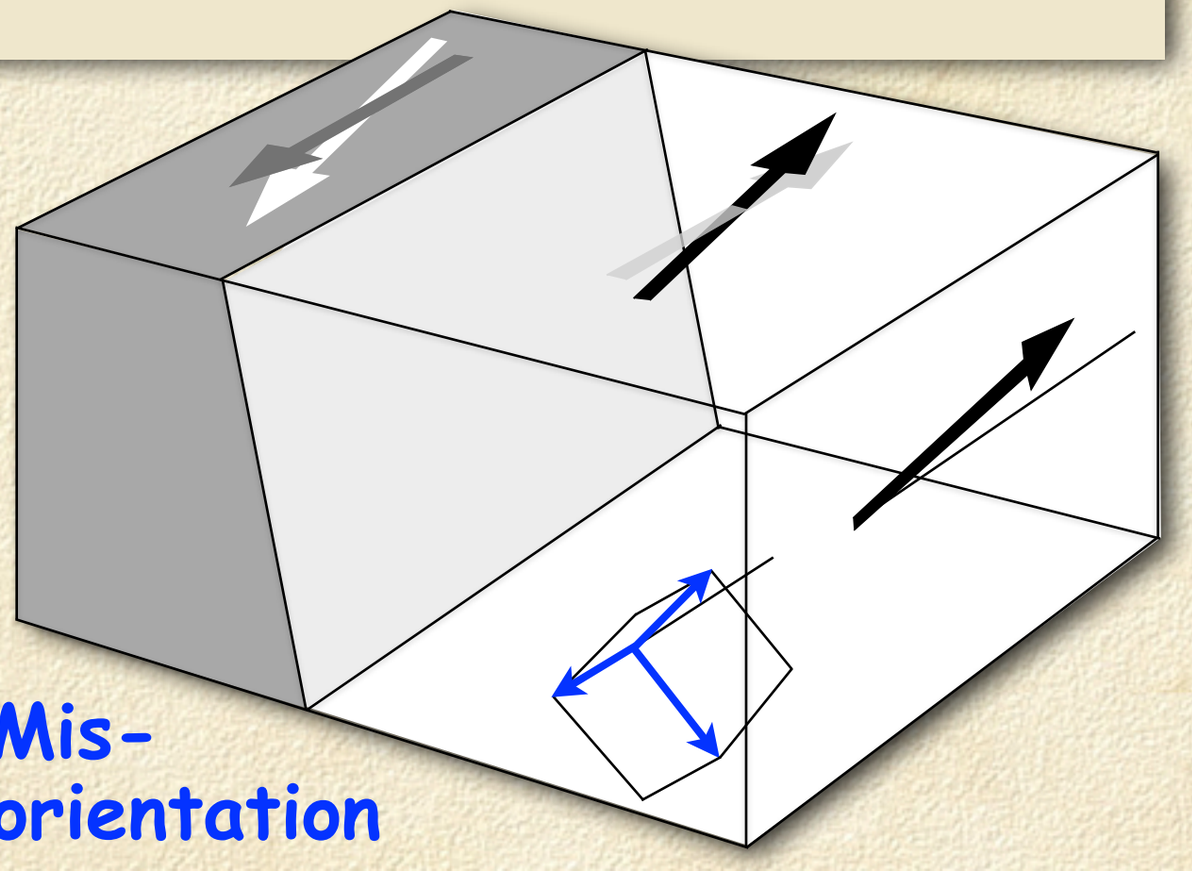

Mis-orientation

Grain-oriented FeSi transformer material

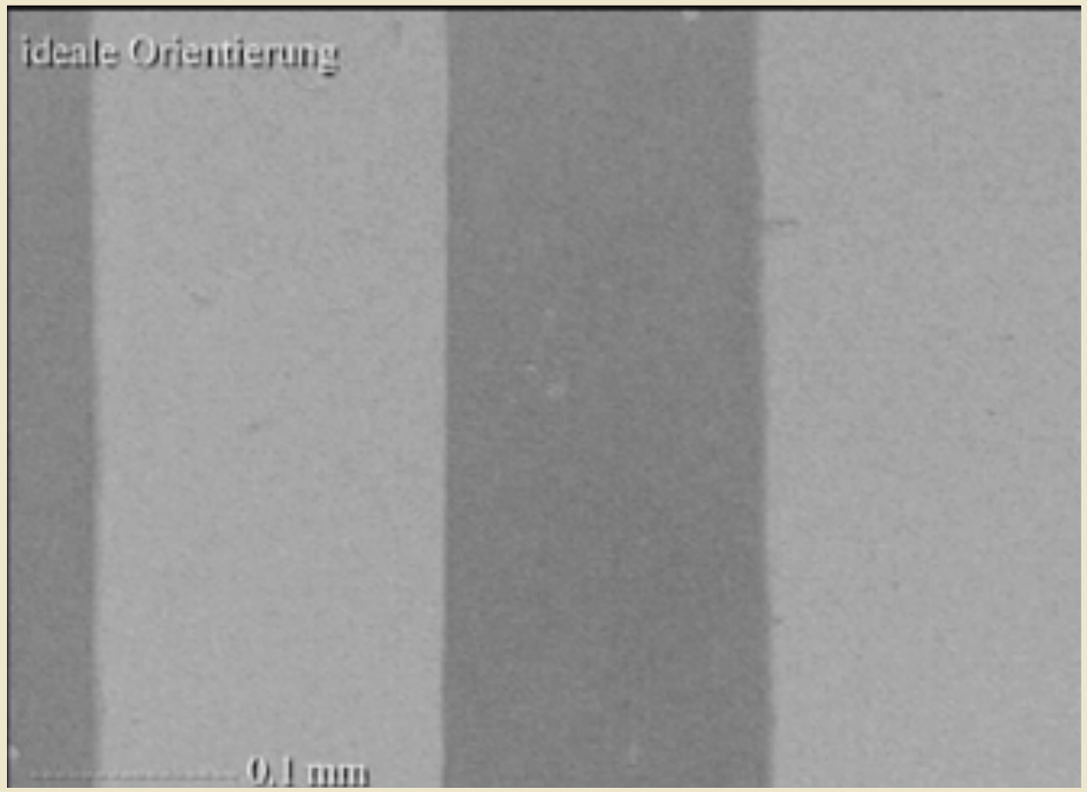

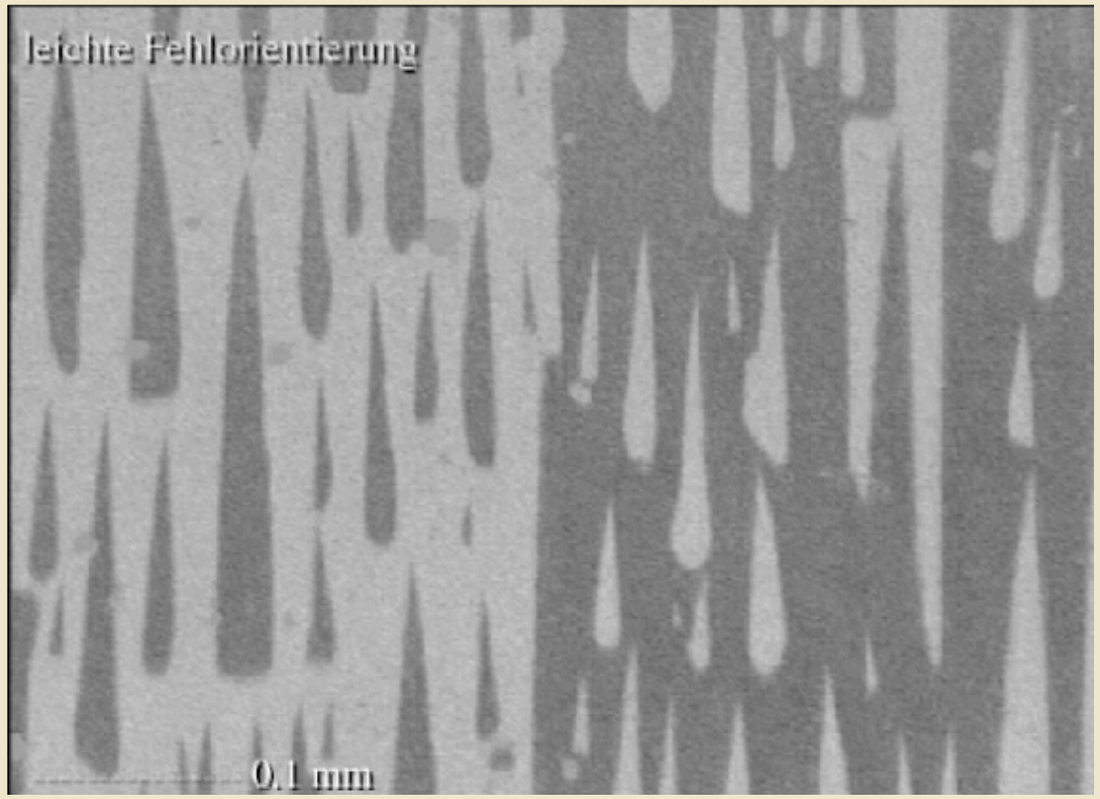

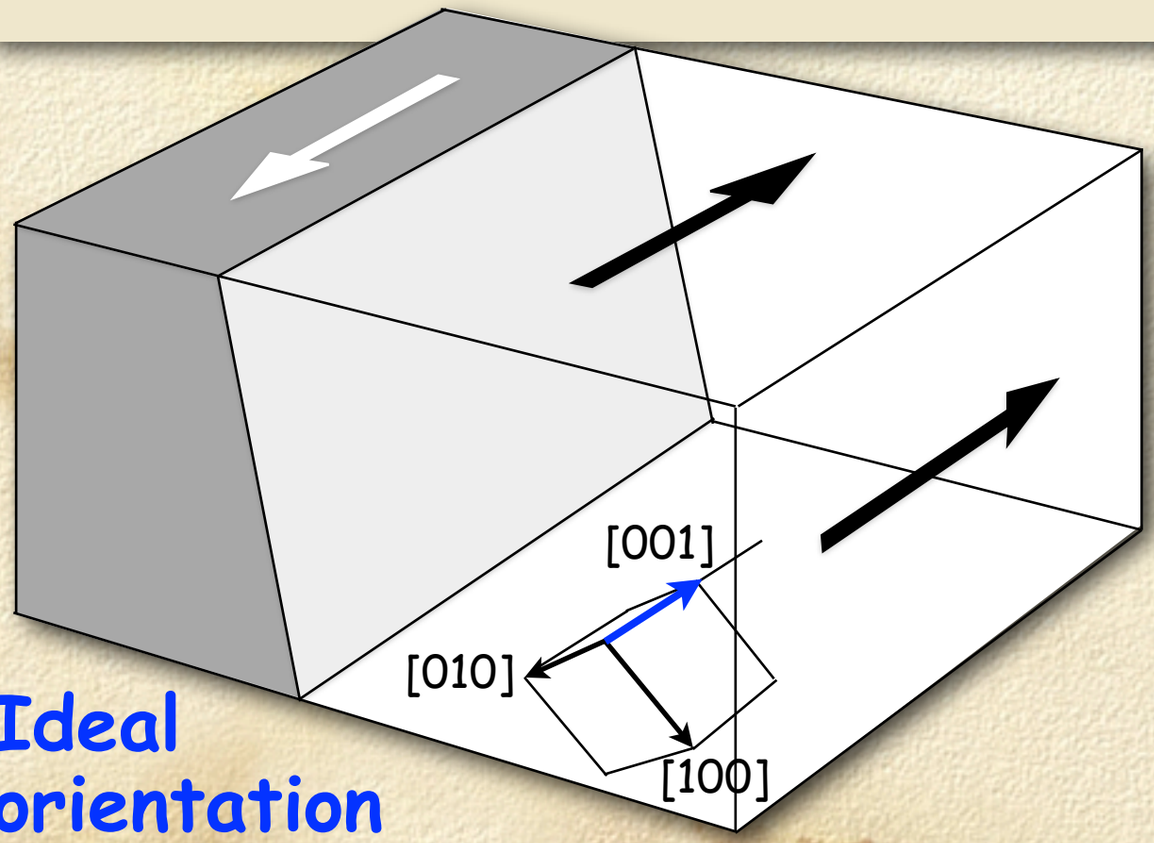

Ideal orientation

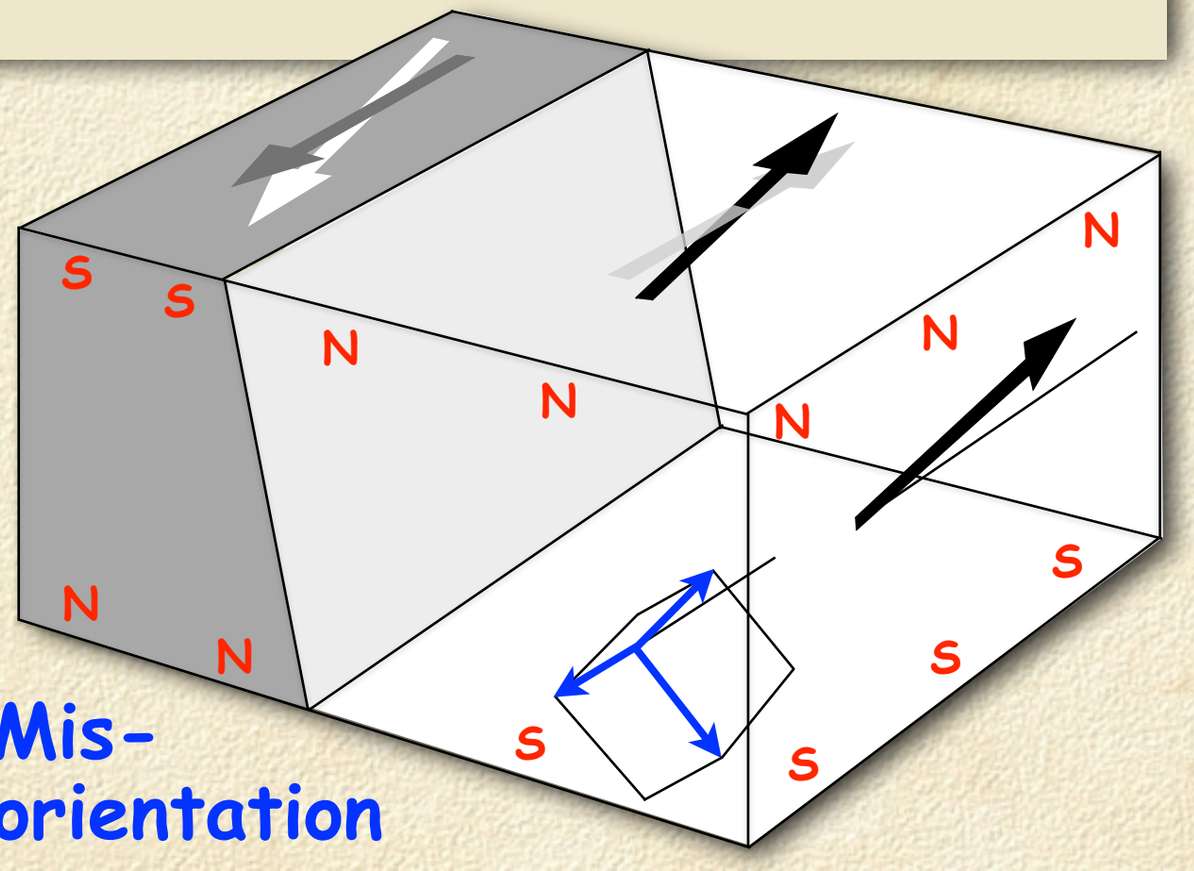

Mis-orientation

Grain-oriented FeSi transformer material

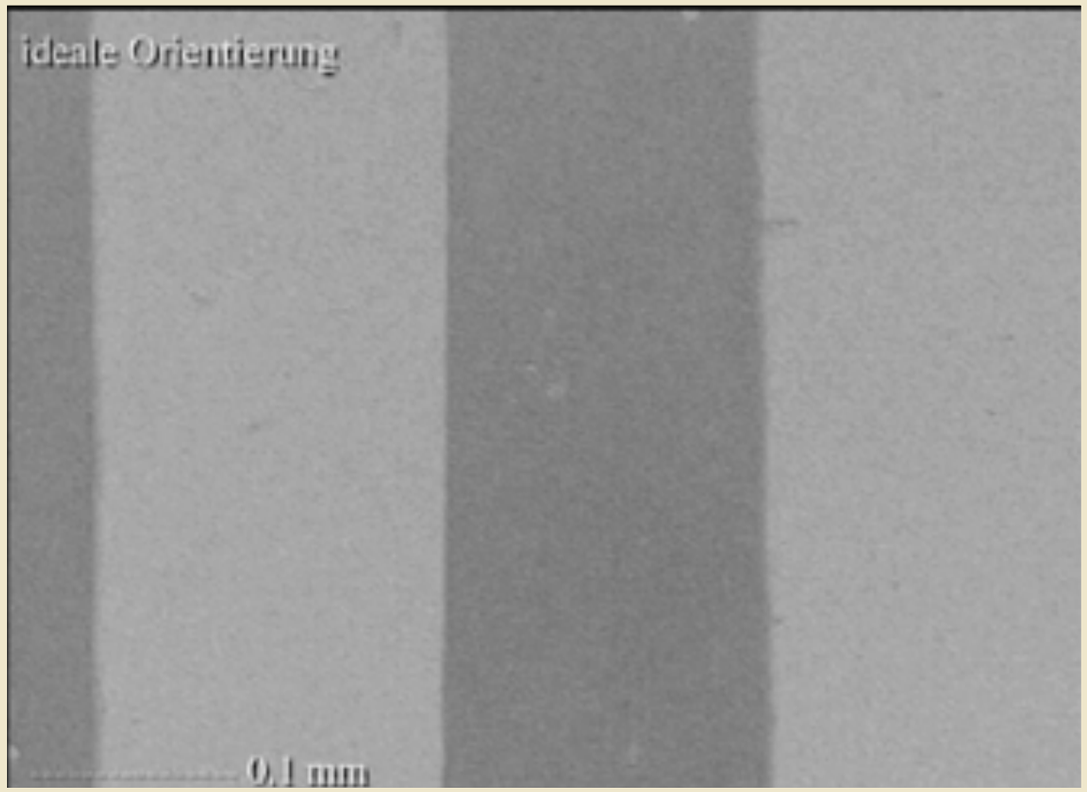

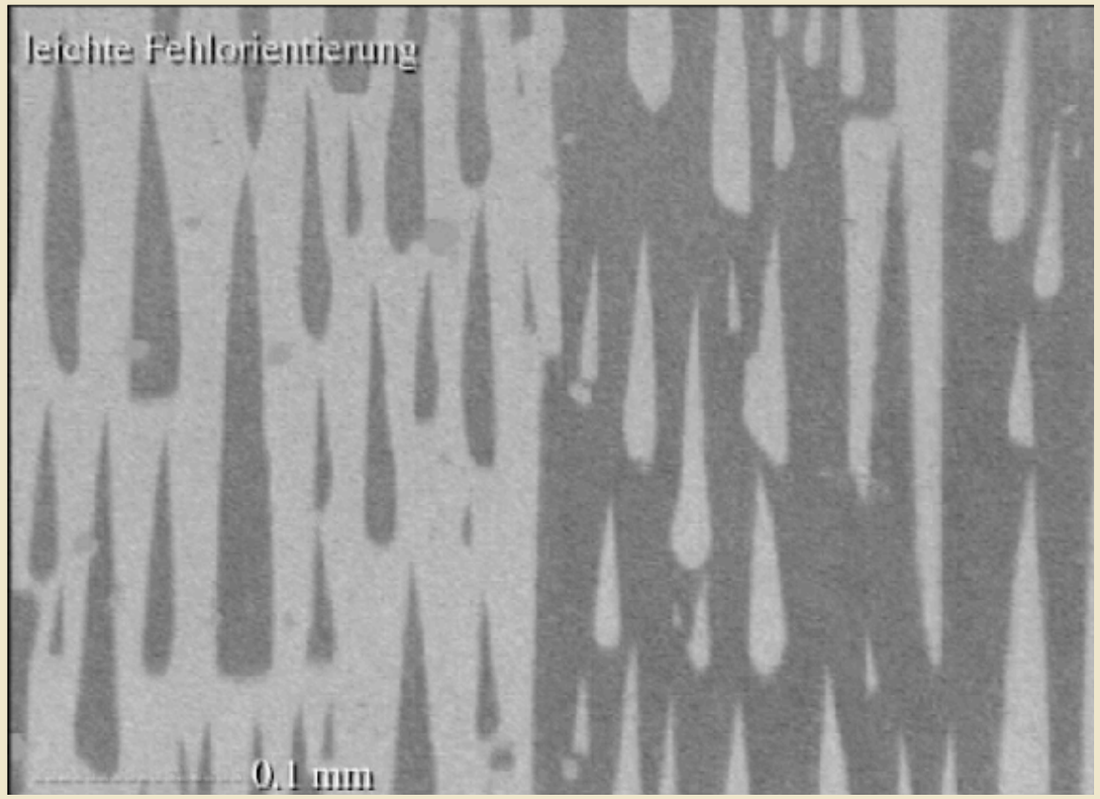

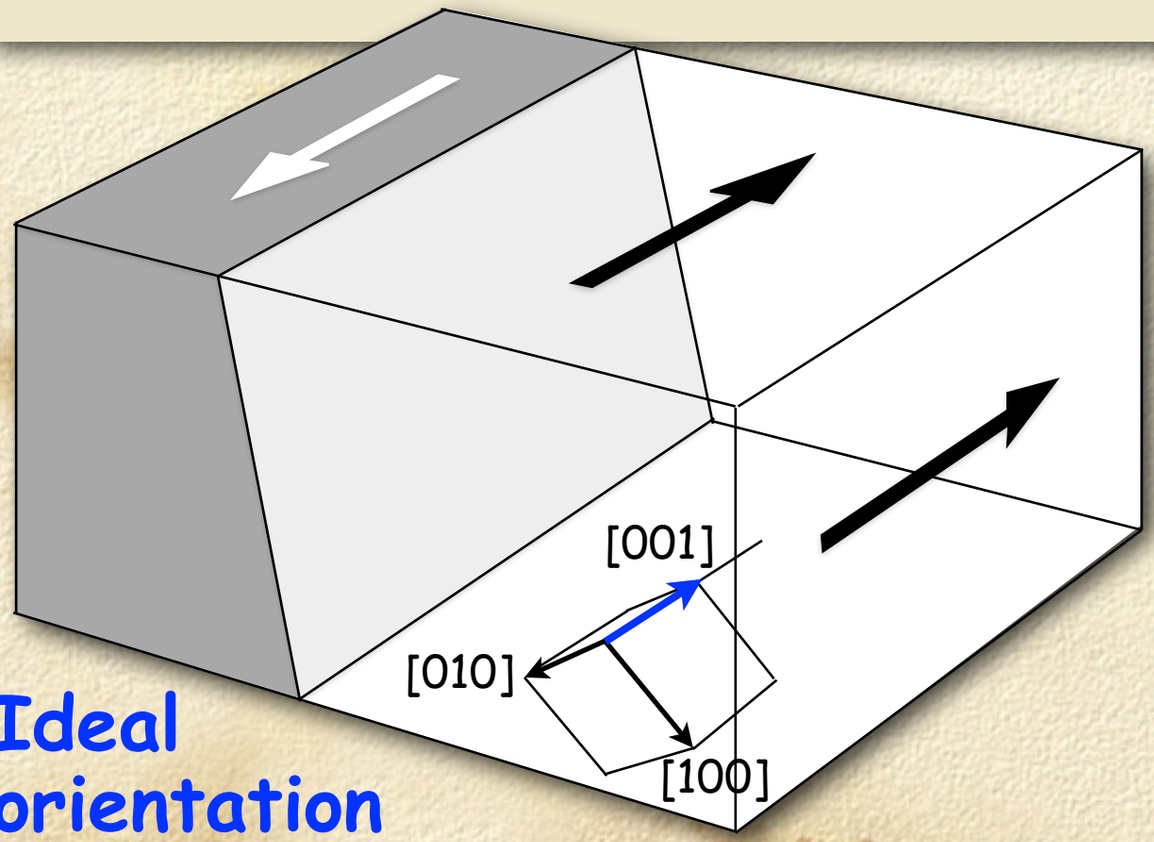

Ideal orientation

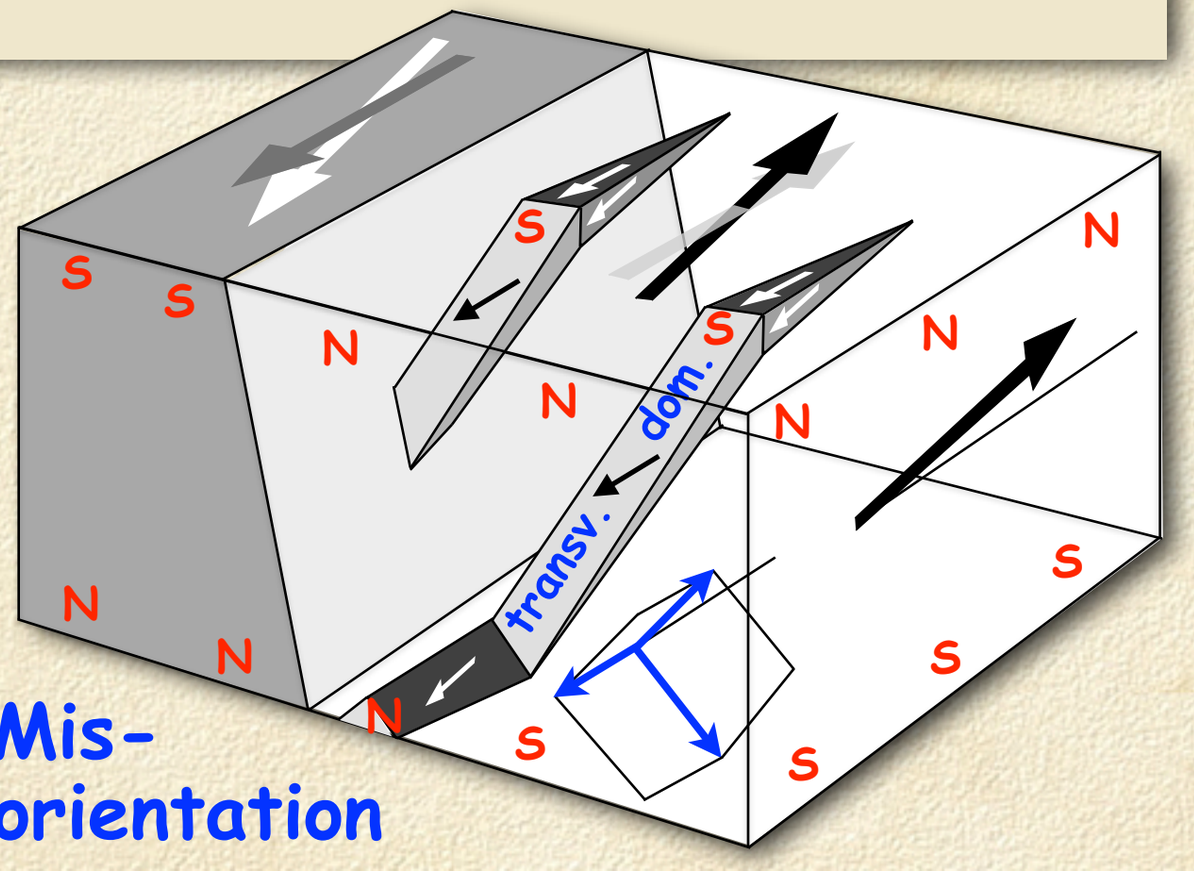

Mis-orientation

Grain-oriented FeSi transformer material

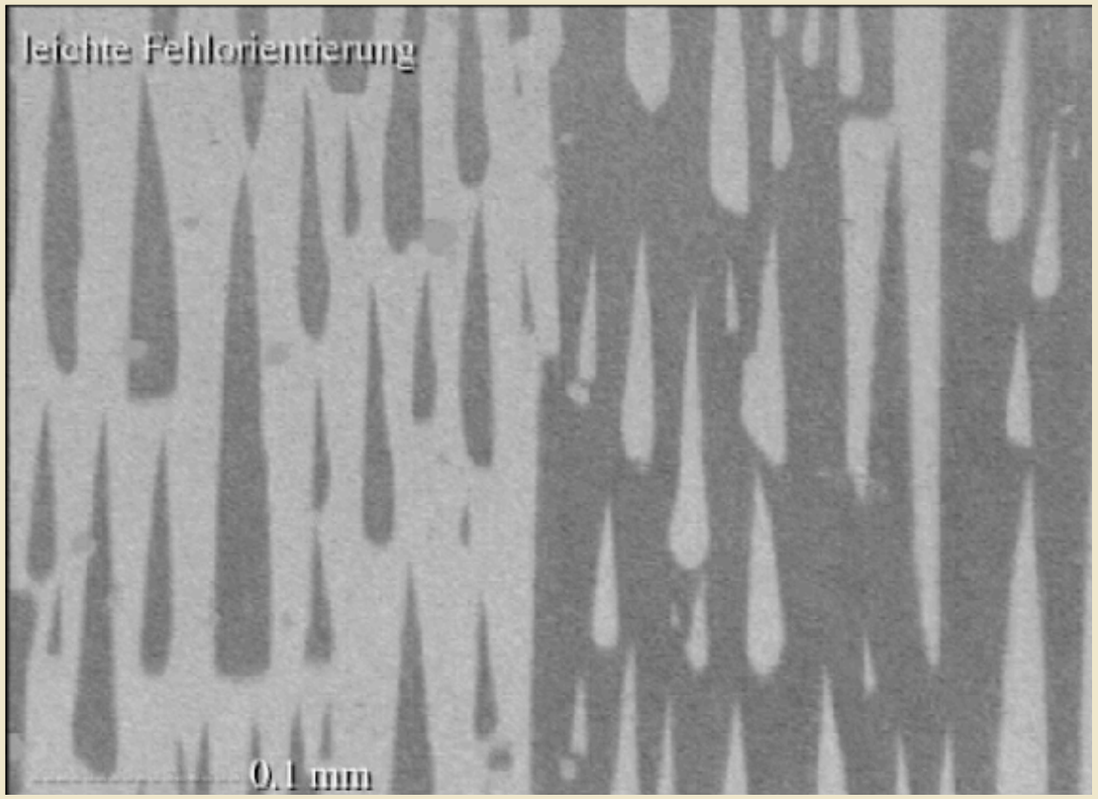

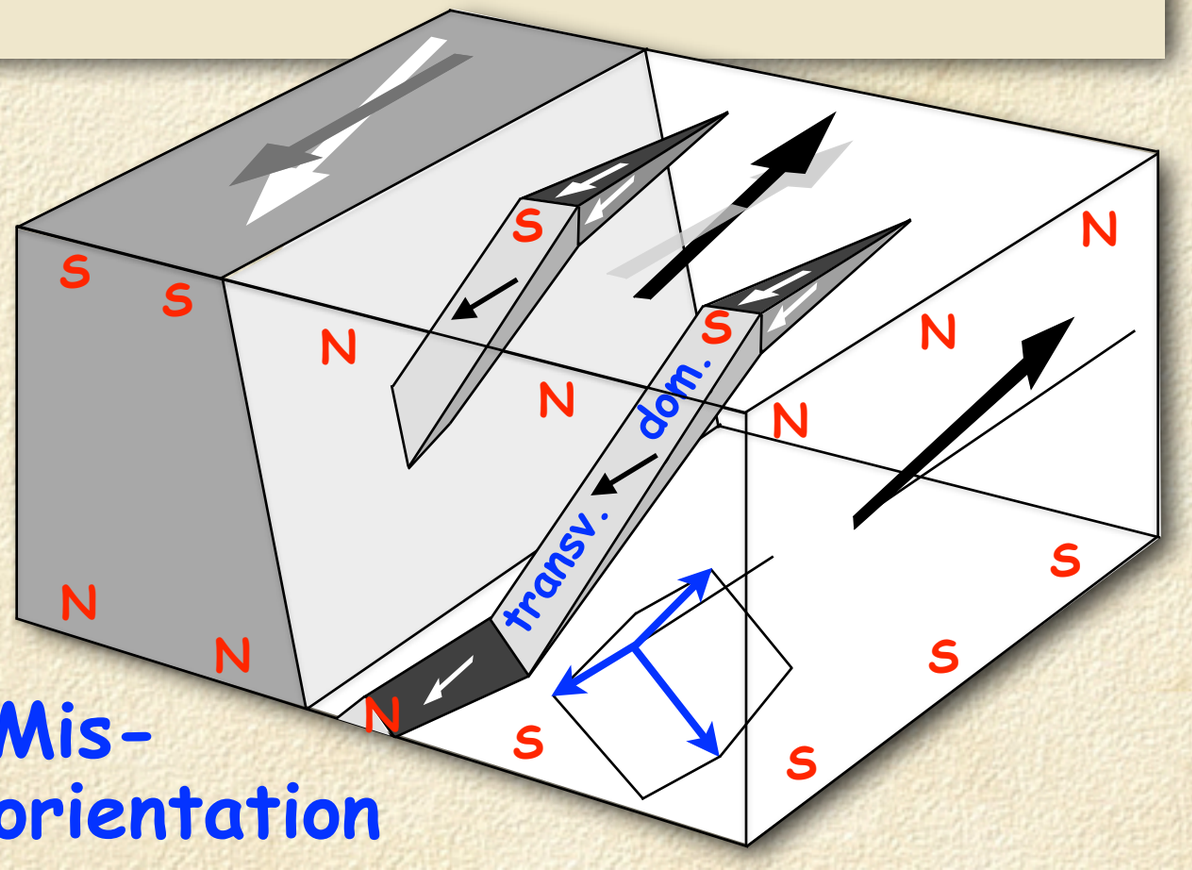

Mis-orientation

Grain-oriented FeSi transformer material

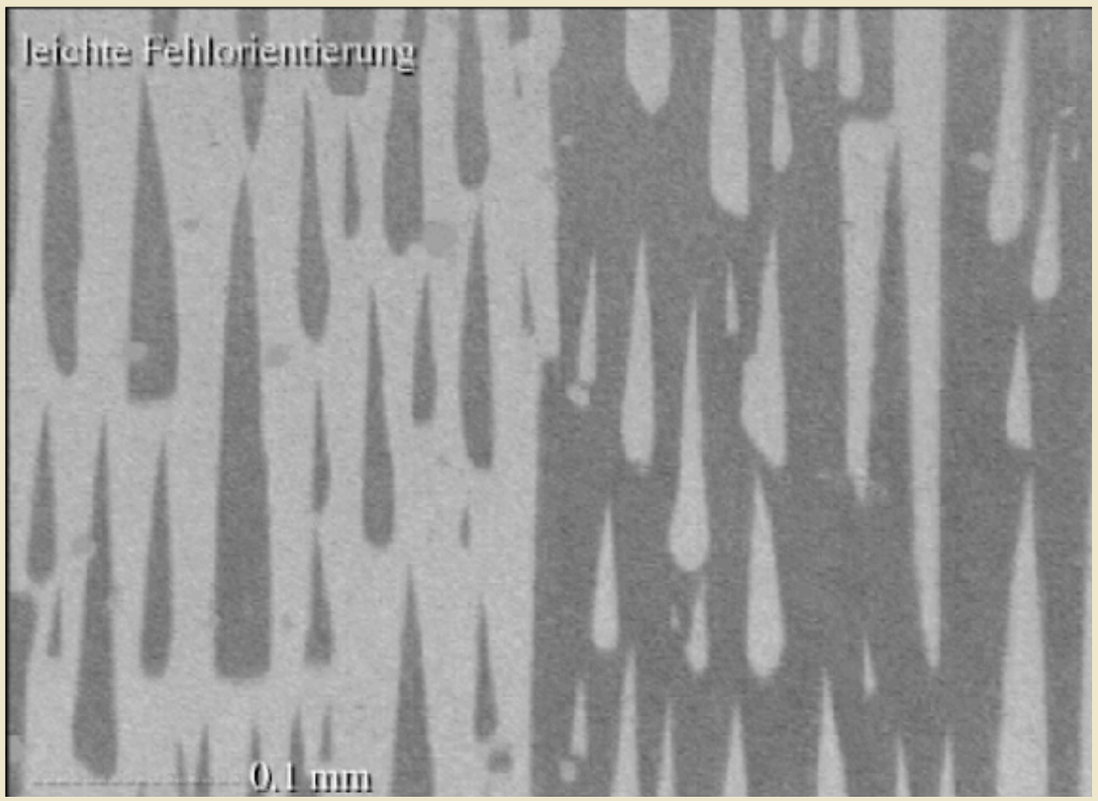

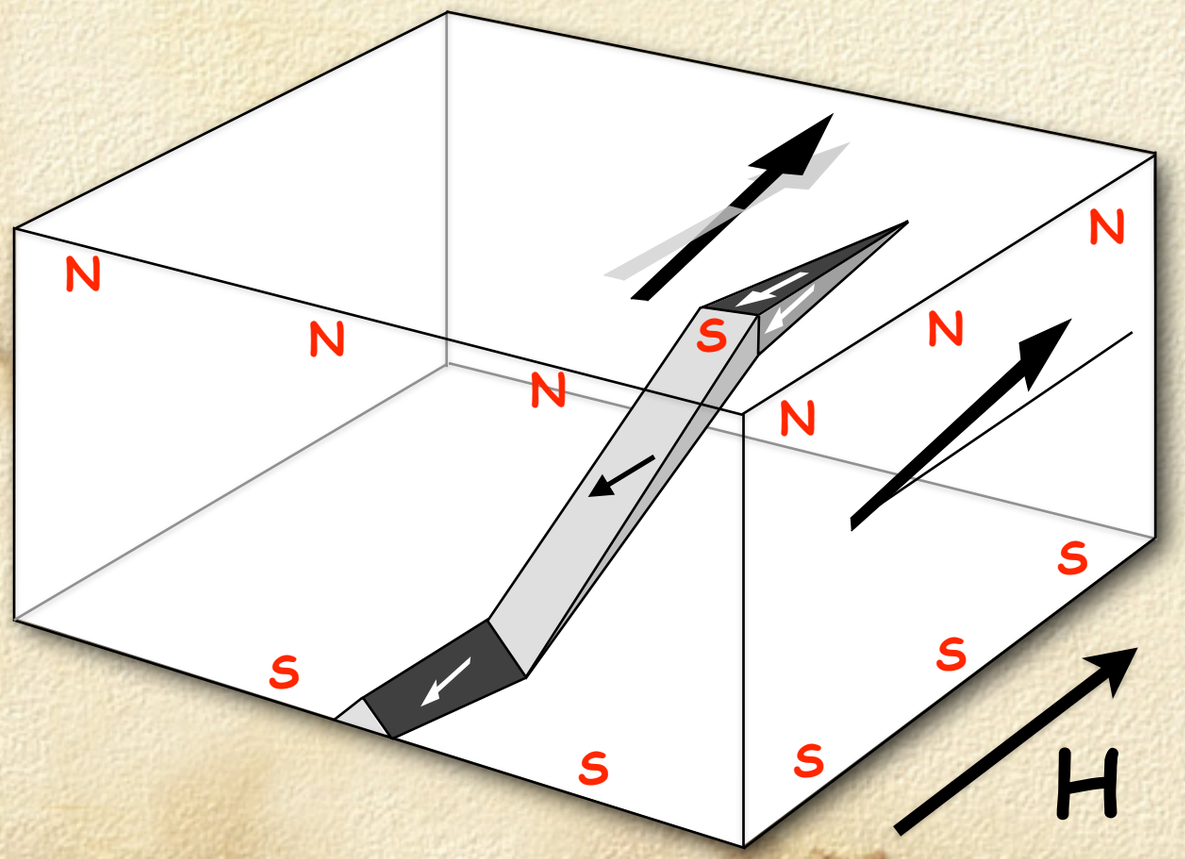

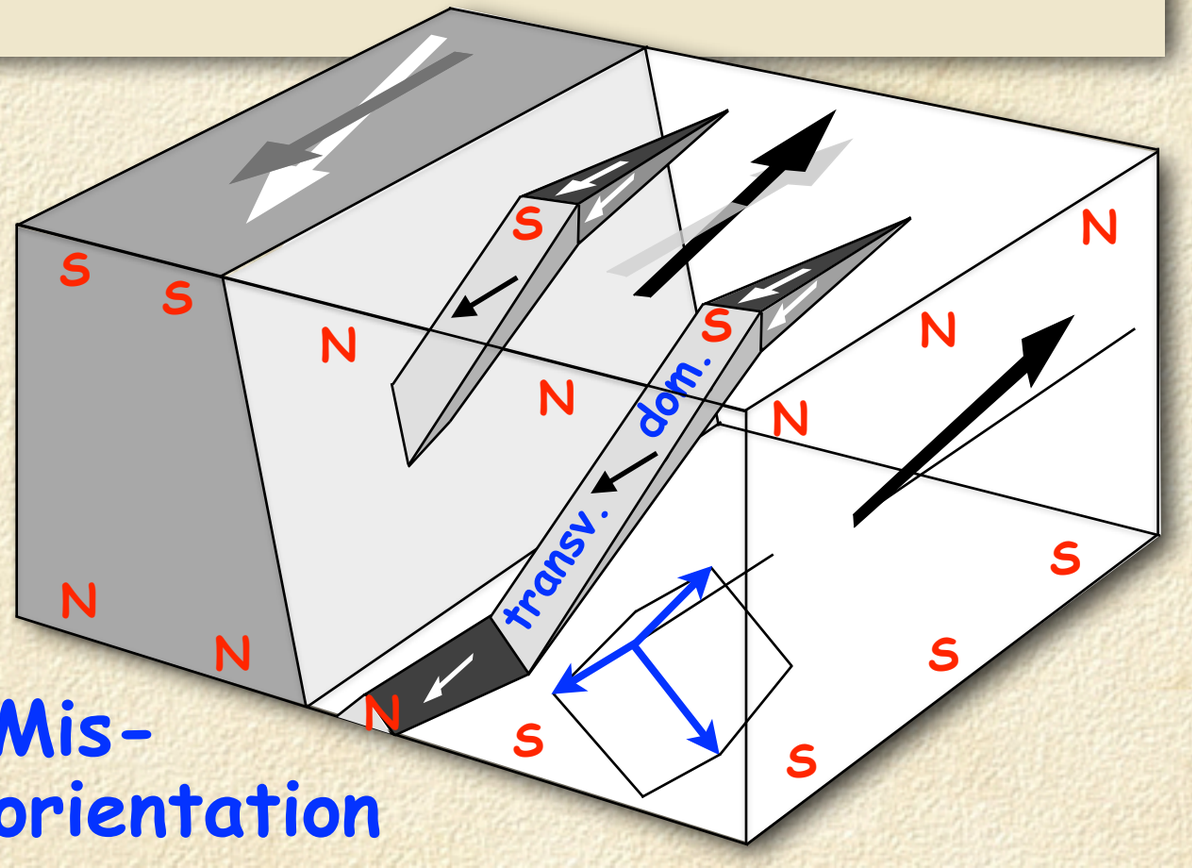

Mis-orientation

Grain-oriented FeSi transformer material

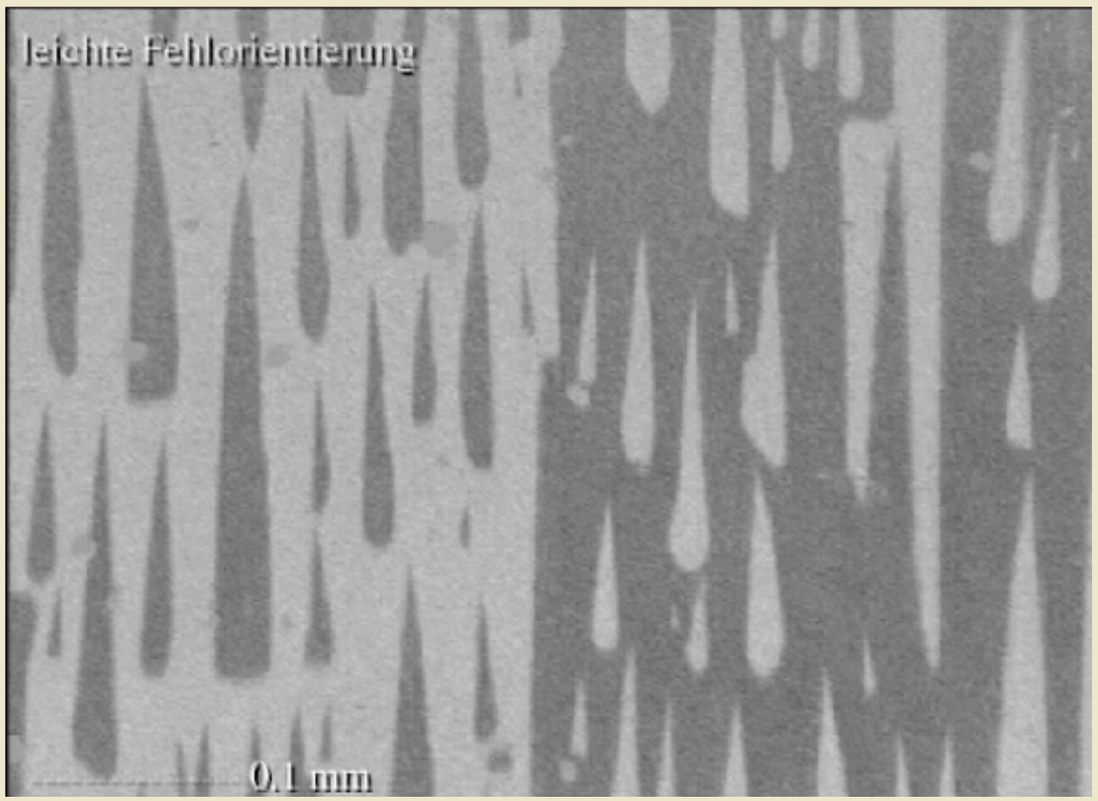

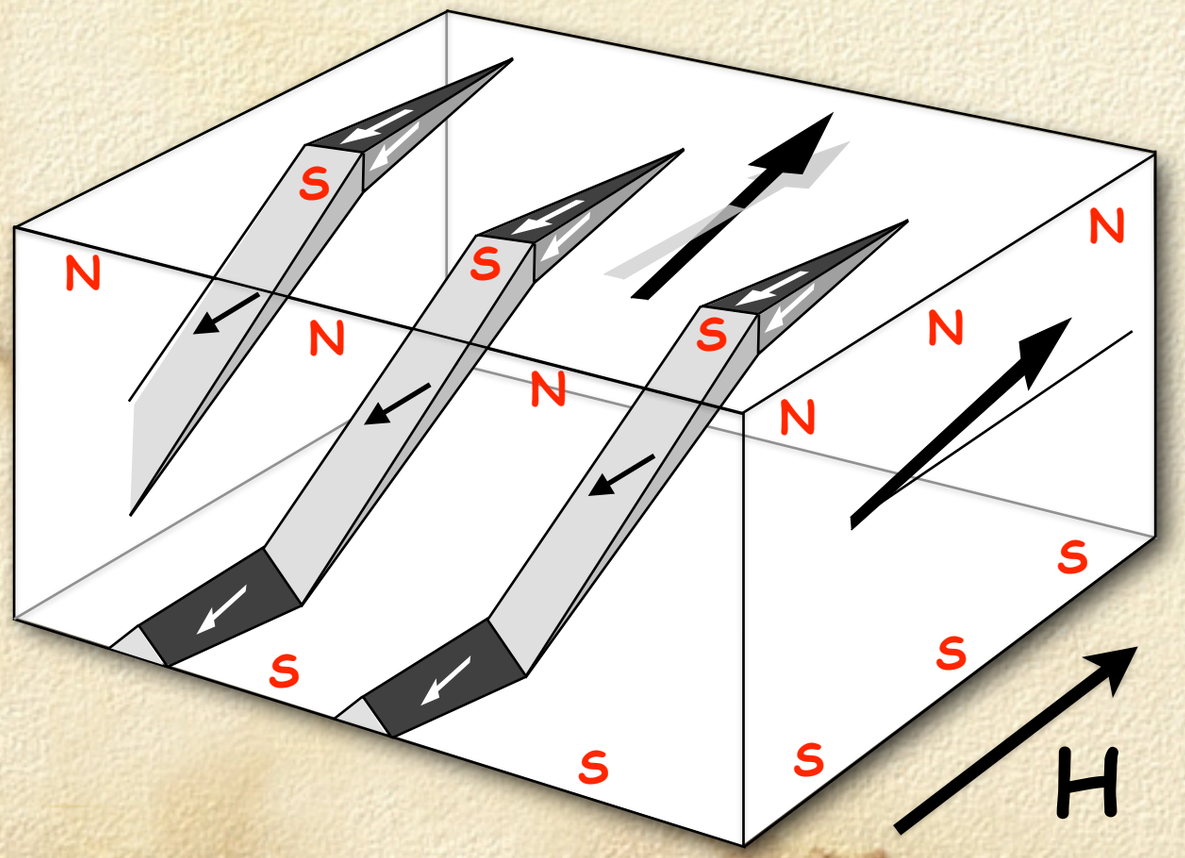

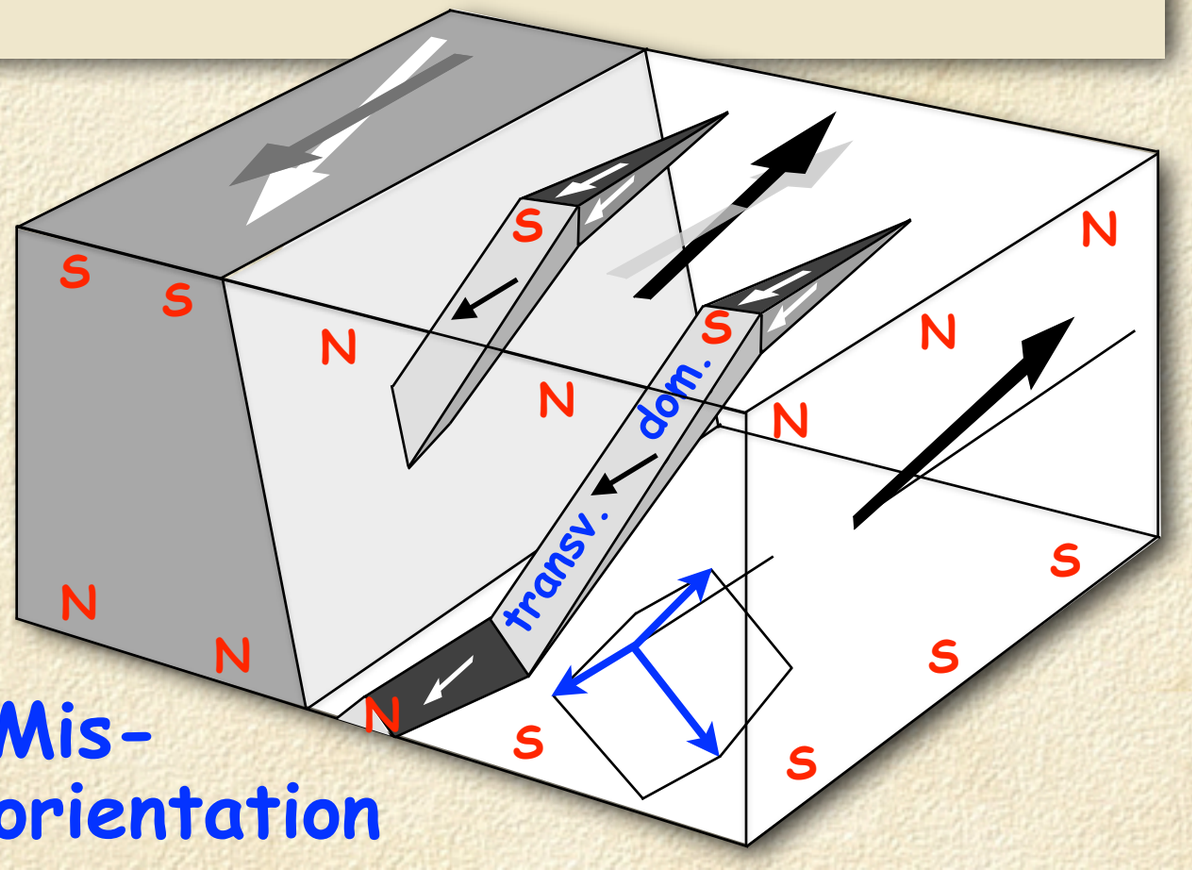

Grain-oriented FeSi transformer material

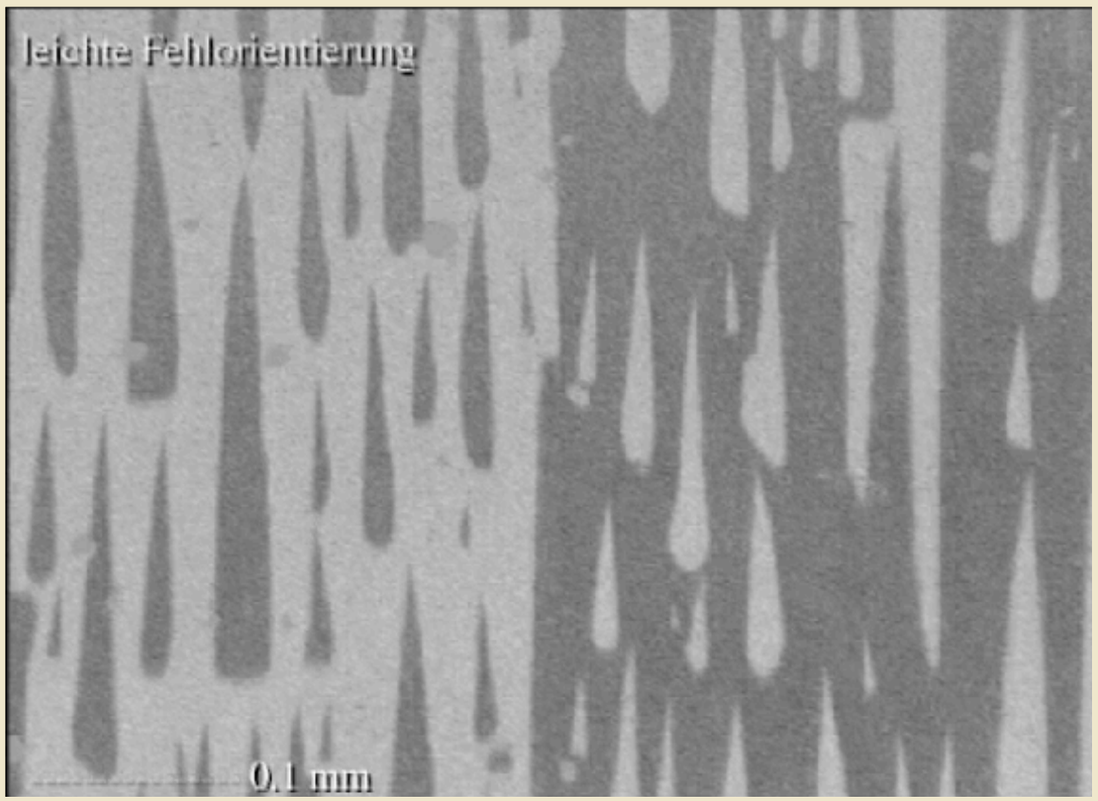

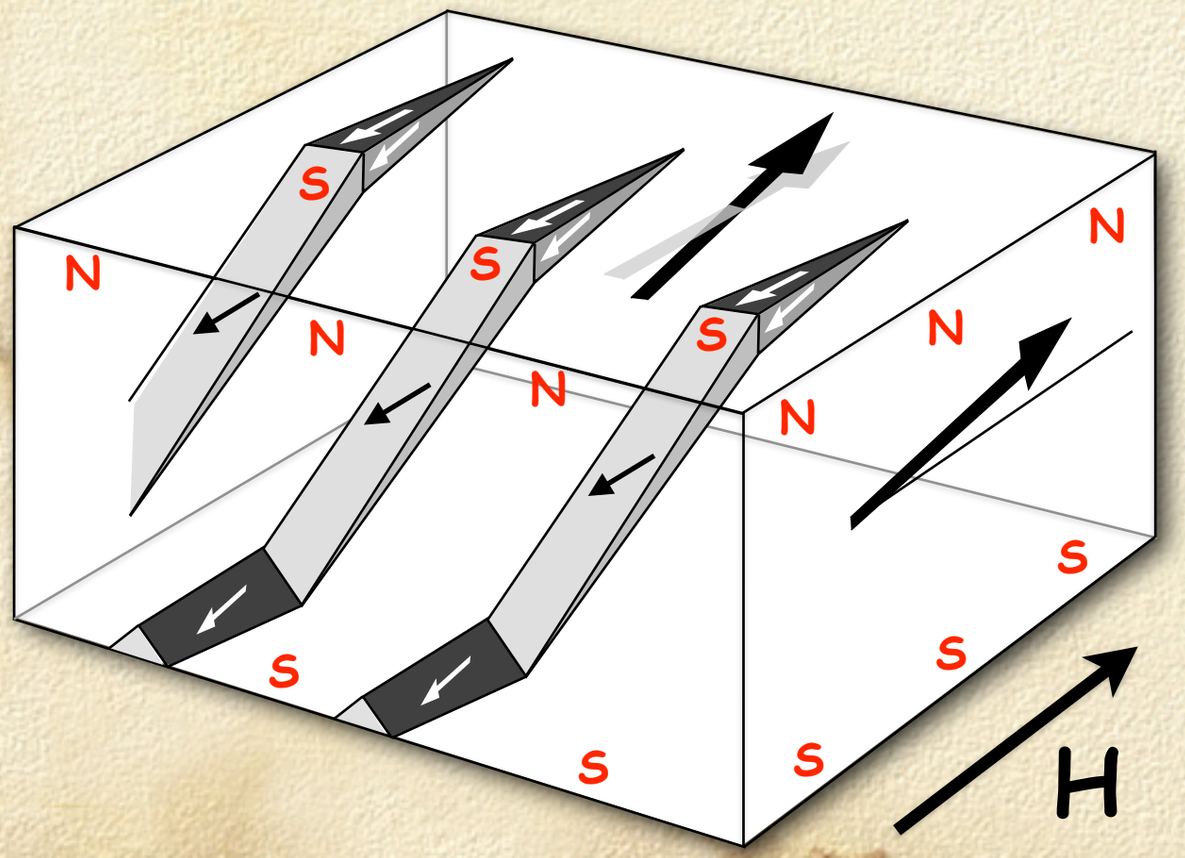

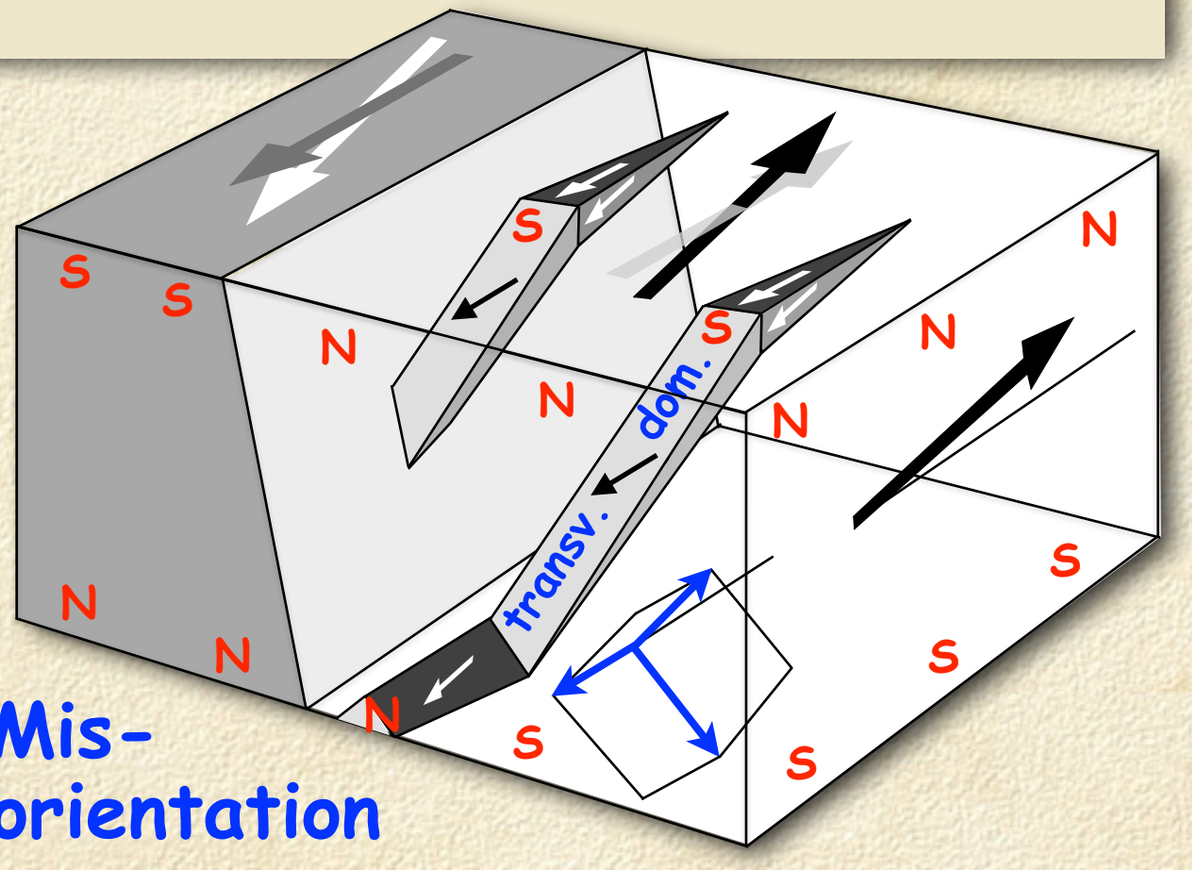

Grain-oriented FeSi transformer material

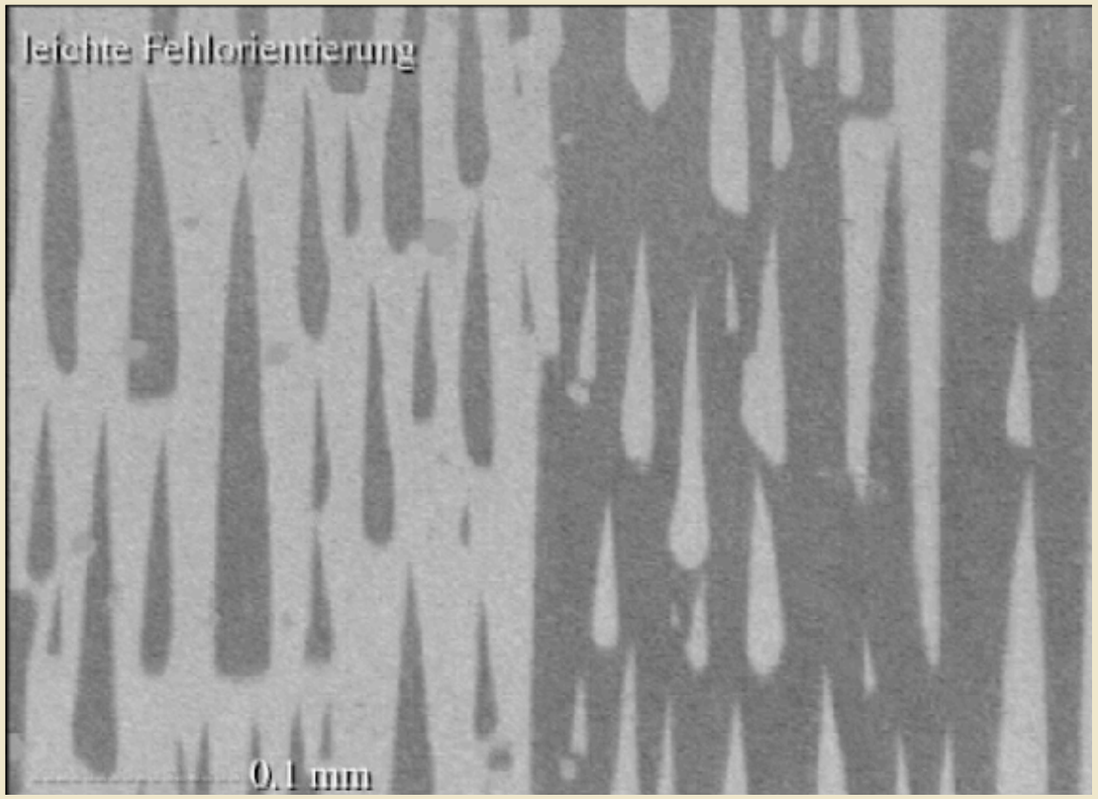

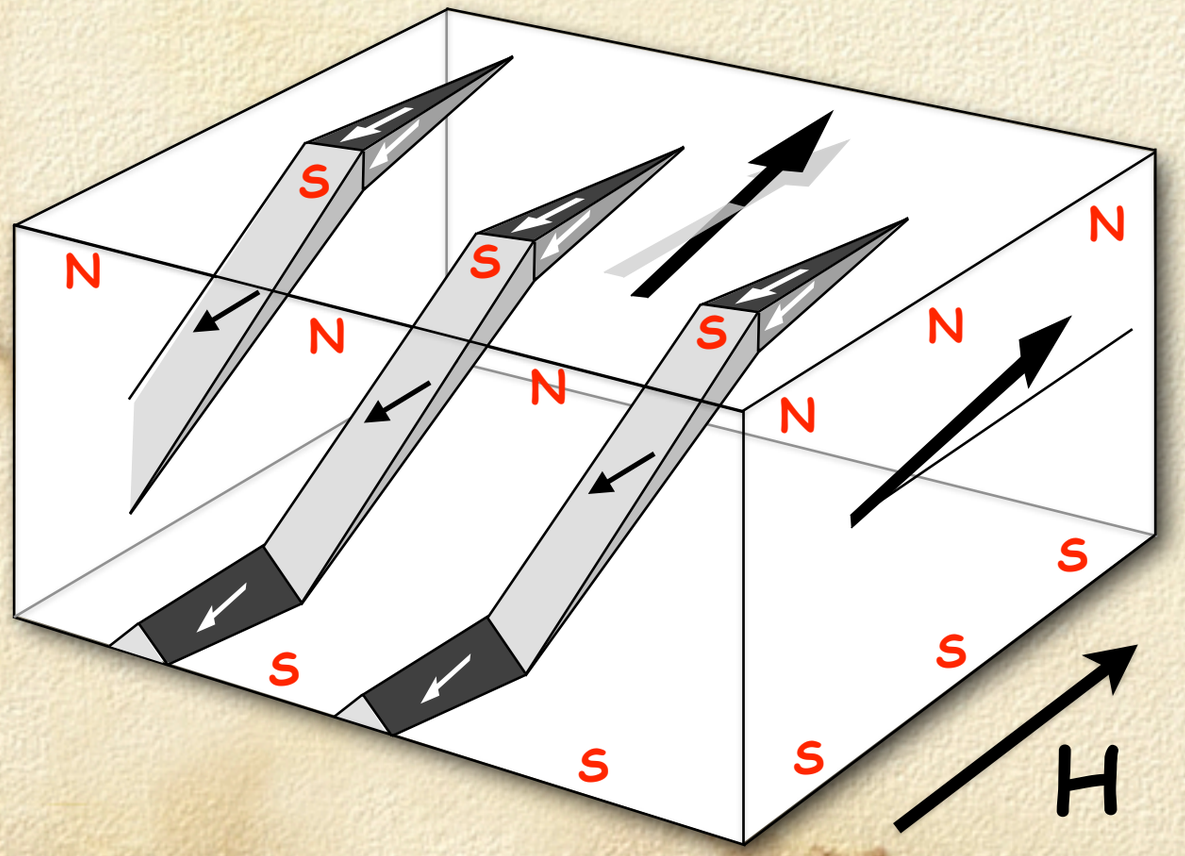

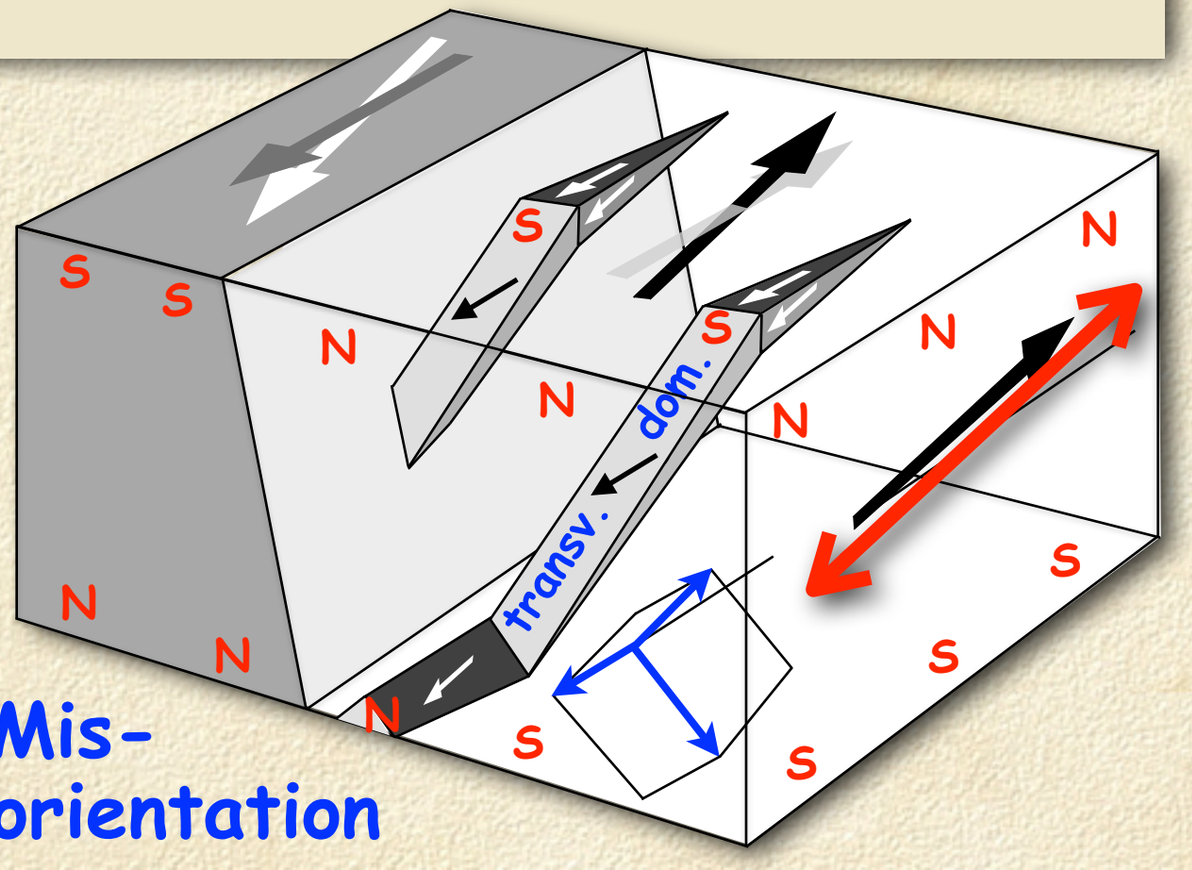

Grain-oriented FeSi transformer material

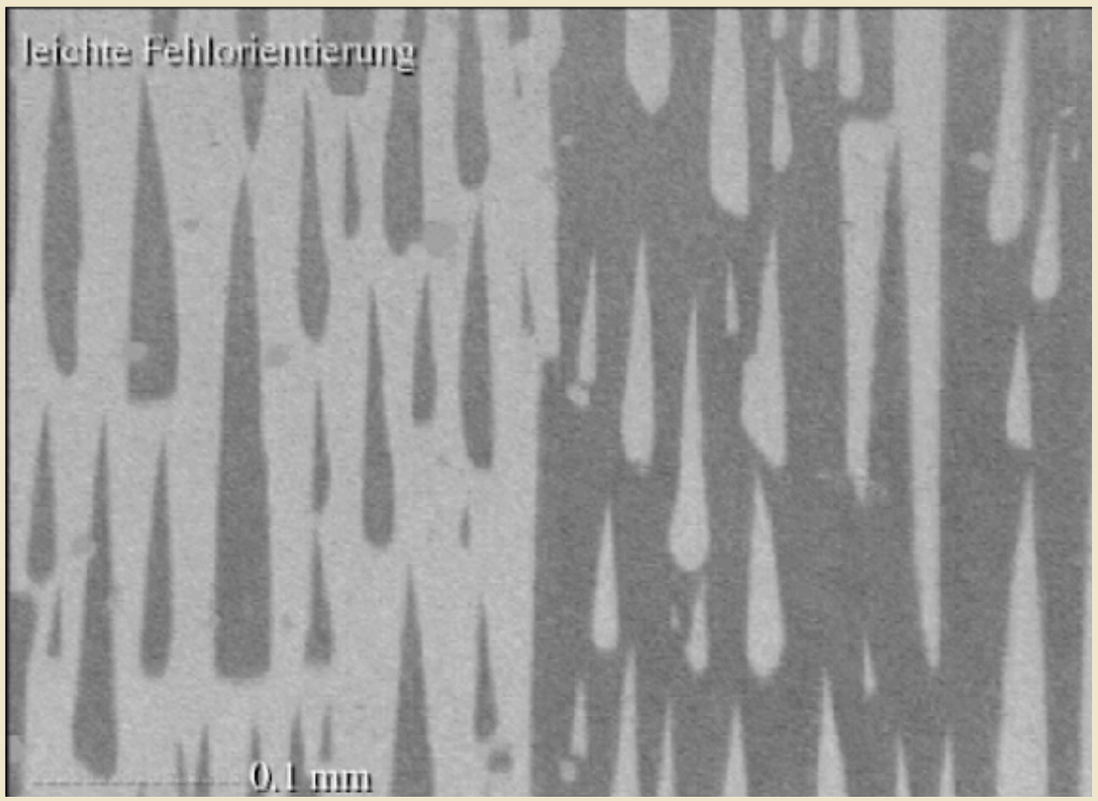

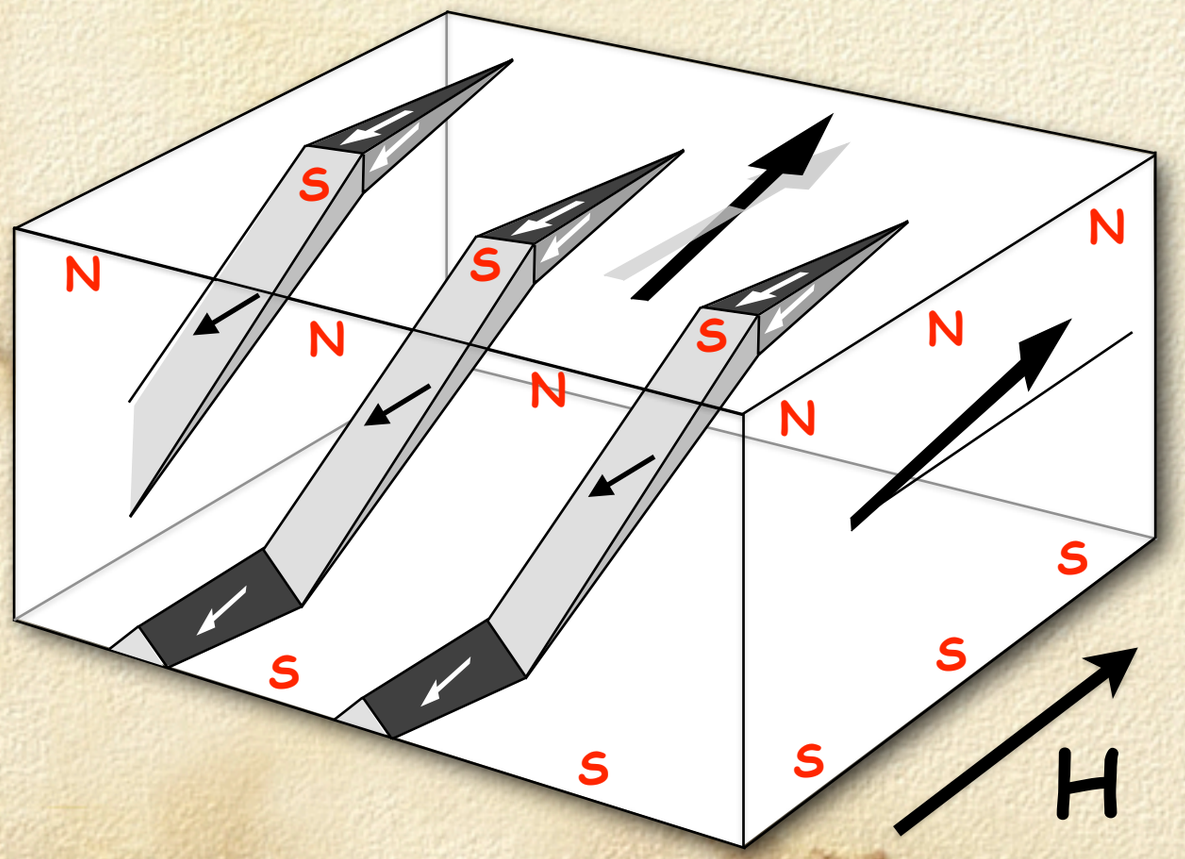

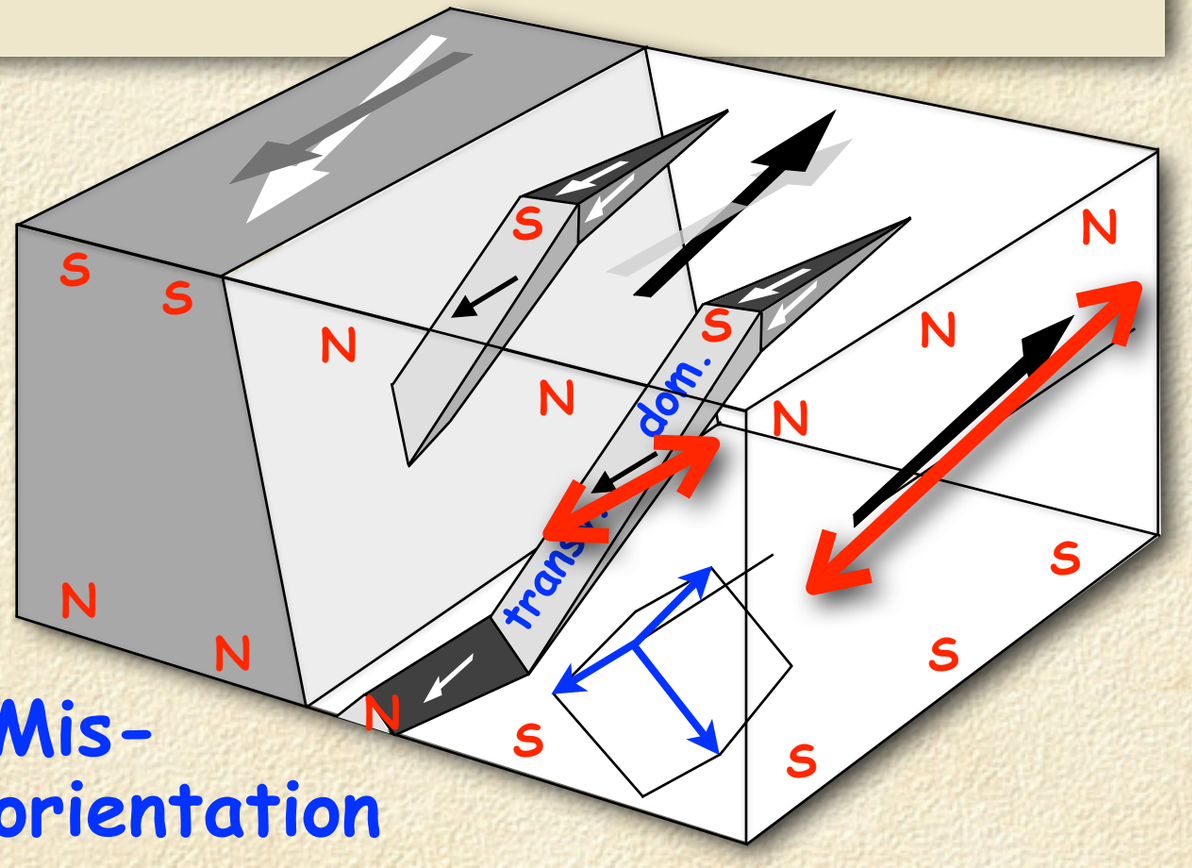

Mis-
orientation

Grain-oriented FeSi transformer material

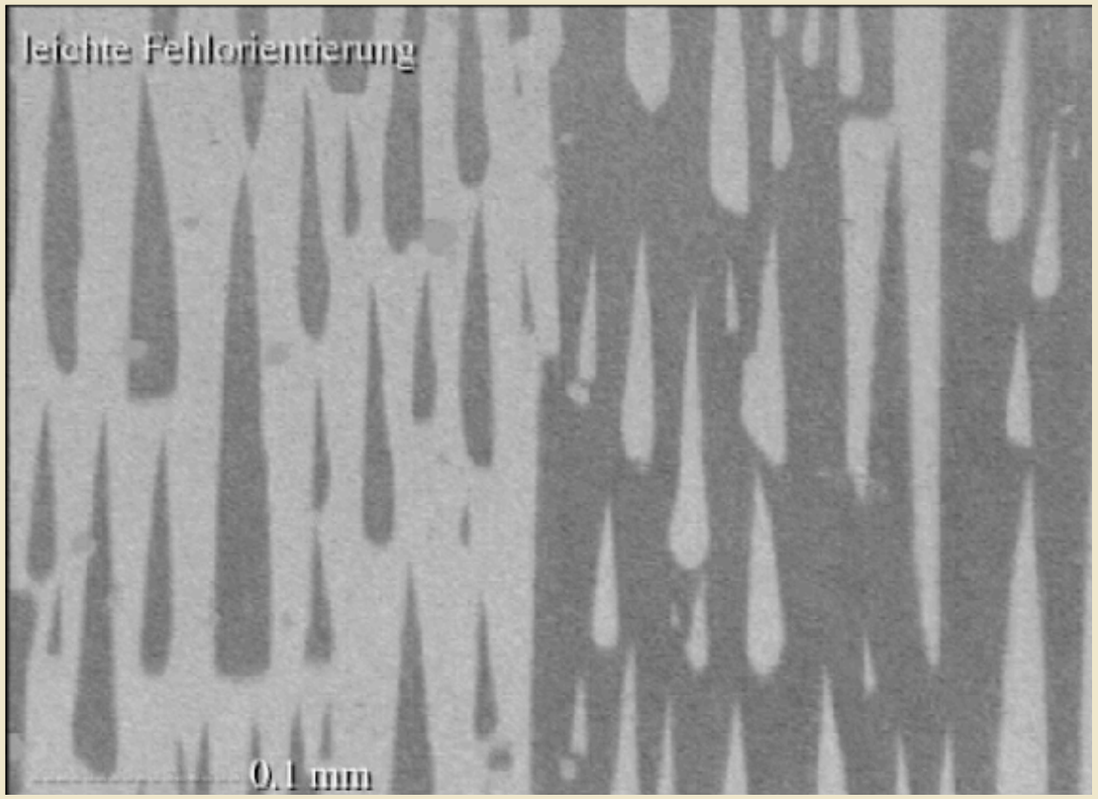

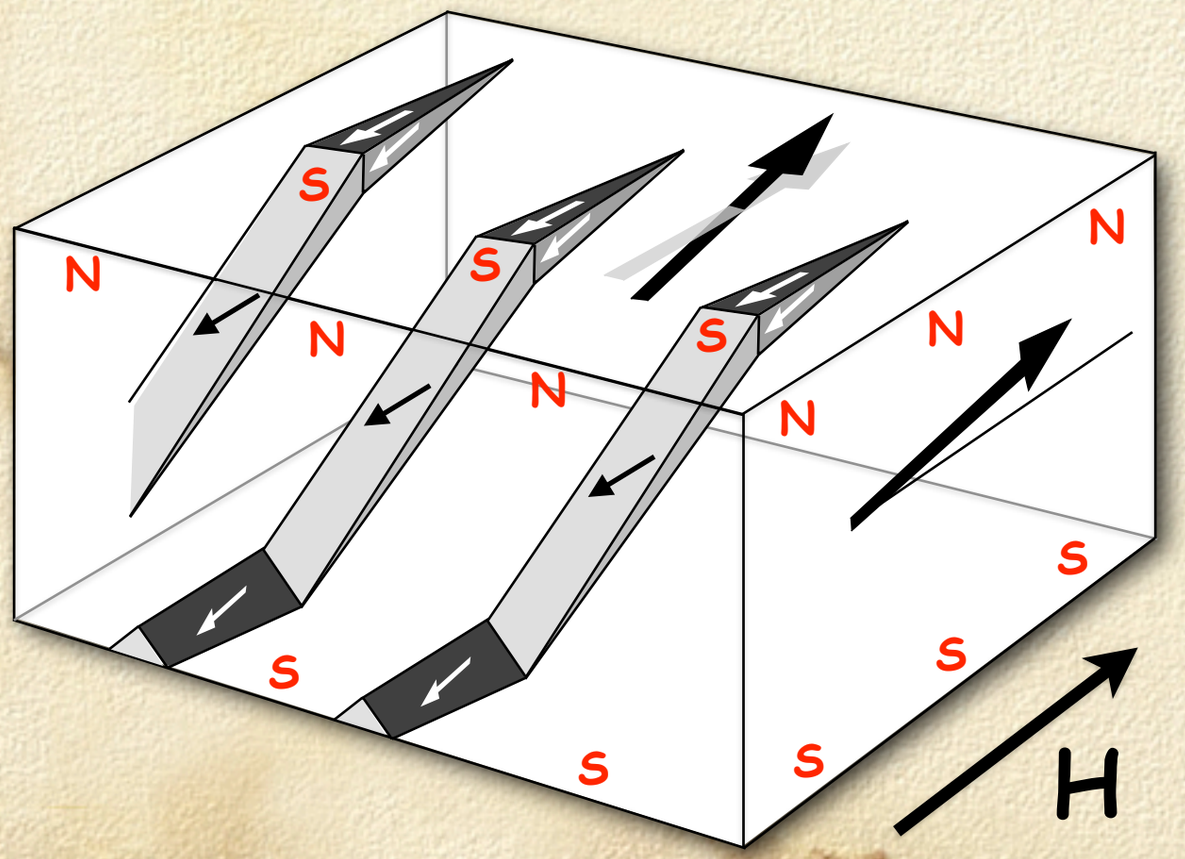

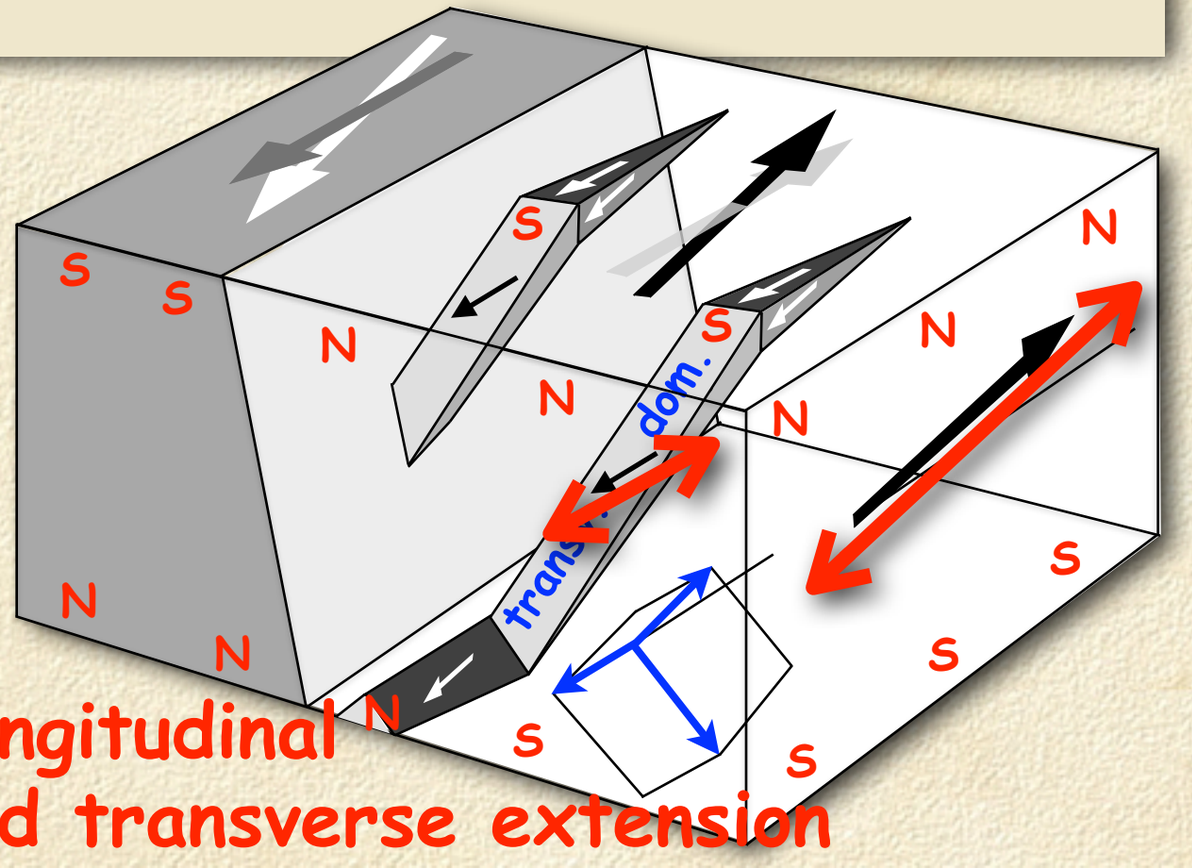

Longitudinal and transverse extension

Grain-oriented FeSi transformer material

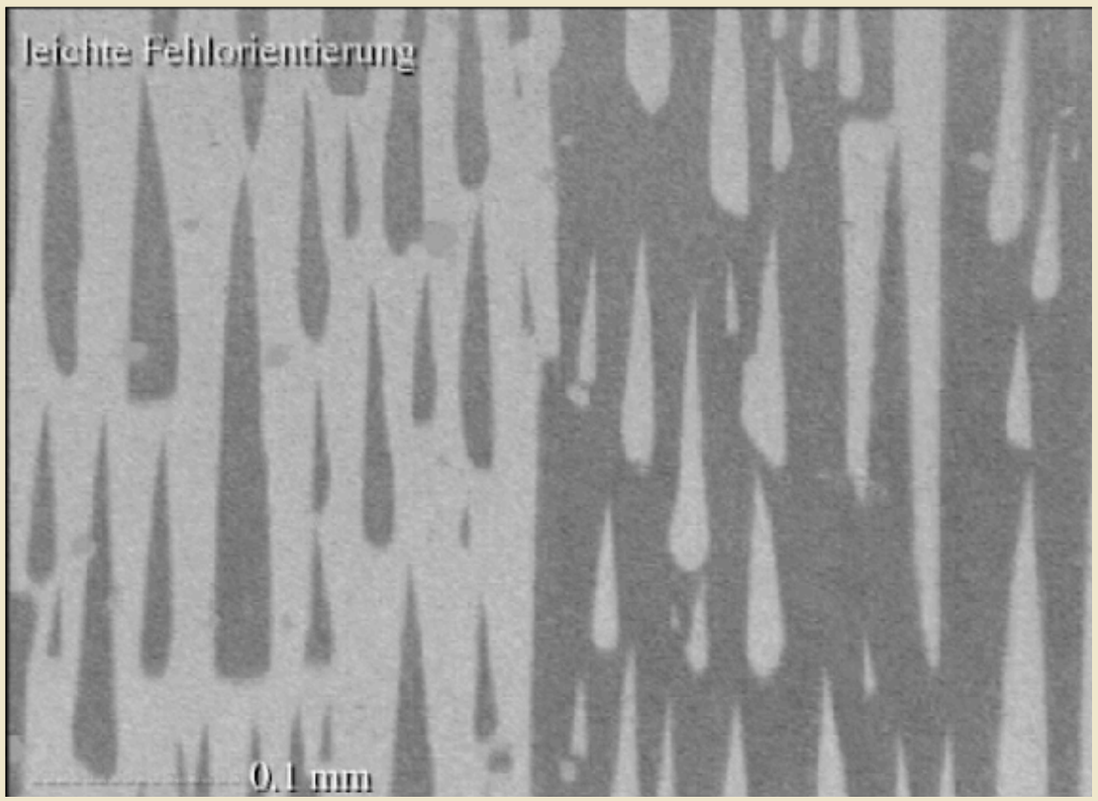

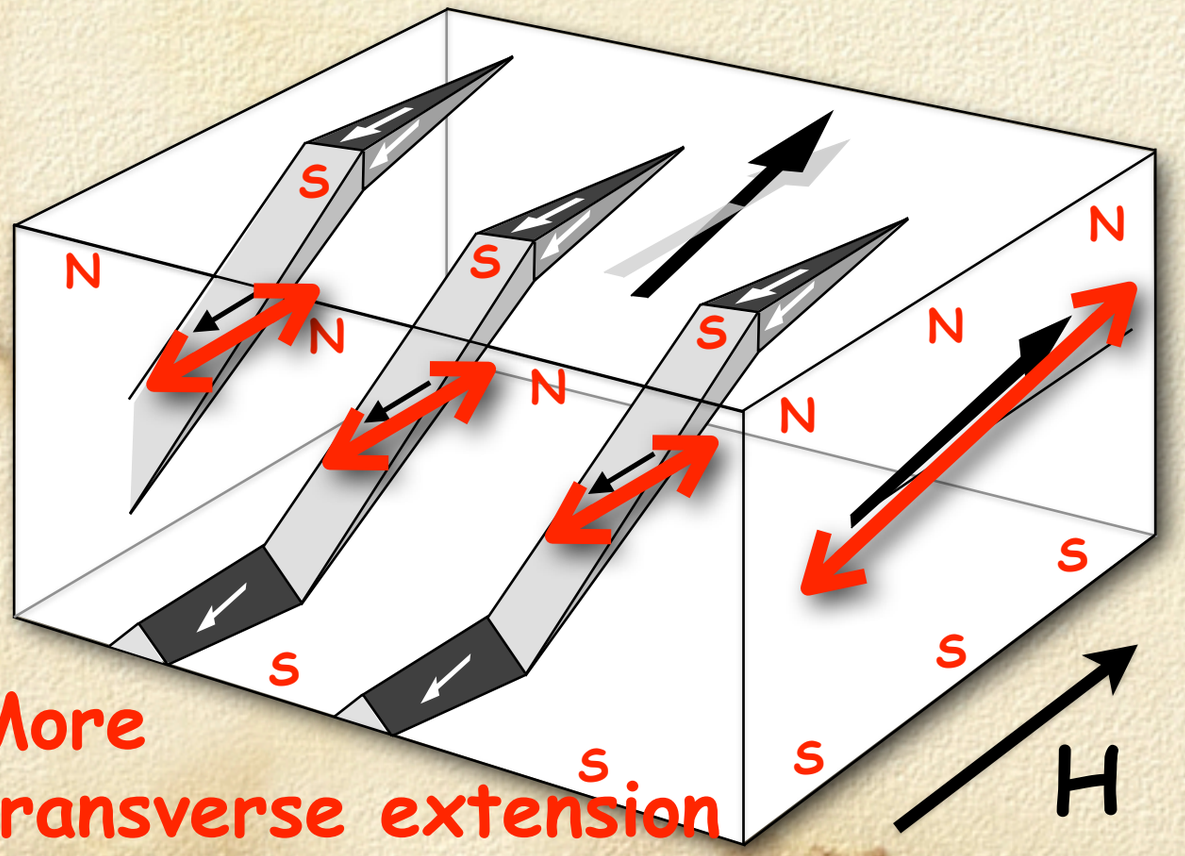

More transverse extension

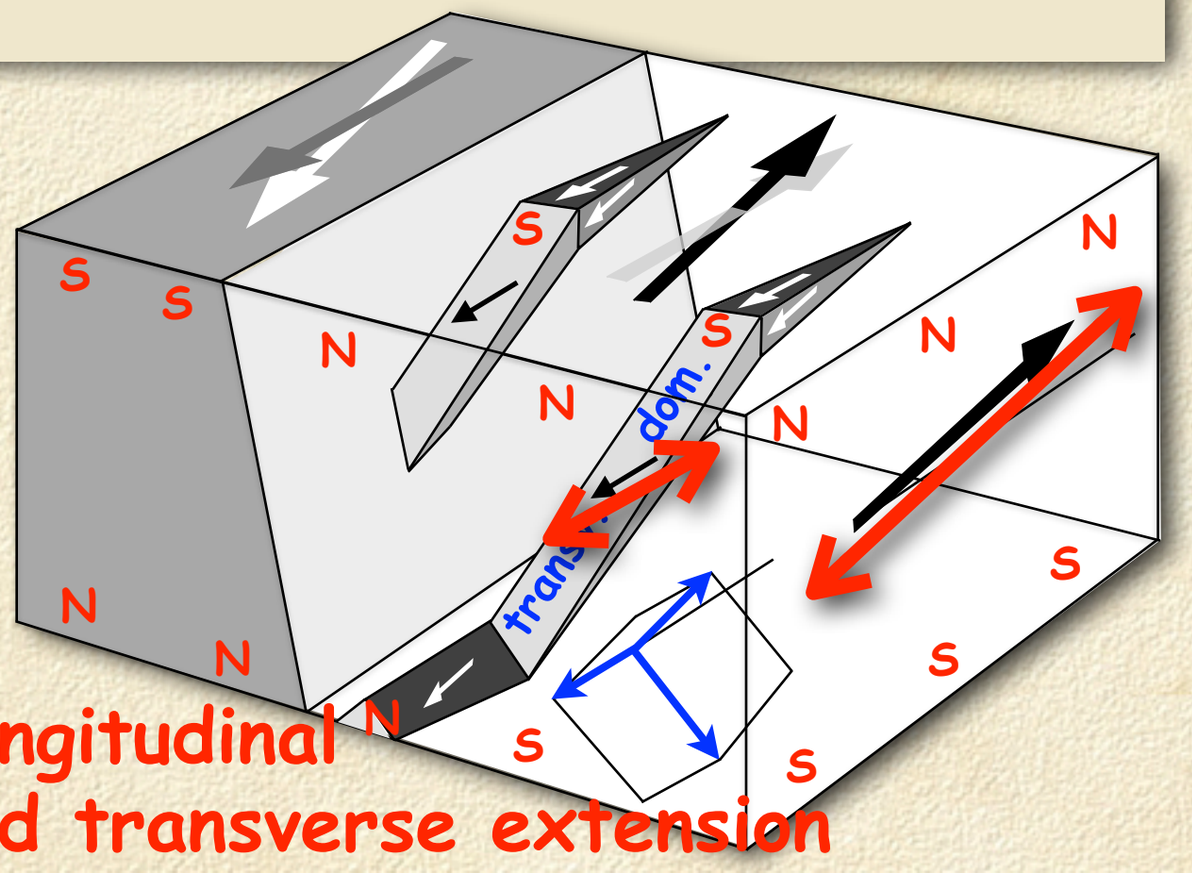

Longitudinal and transverse extension

Grain-oriented FeSi transformer material

Tension and compression in rhythm of magnetic field

The sheet vibrates (= transformer noise)

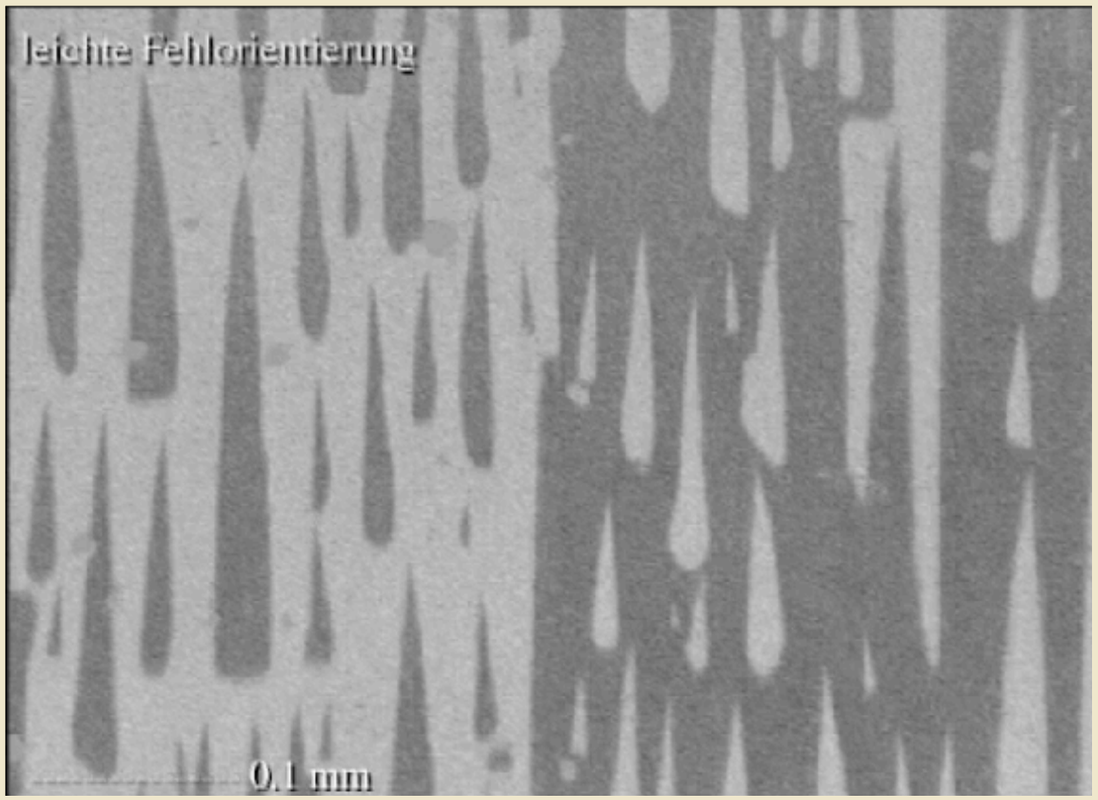

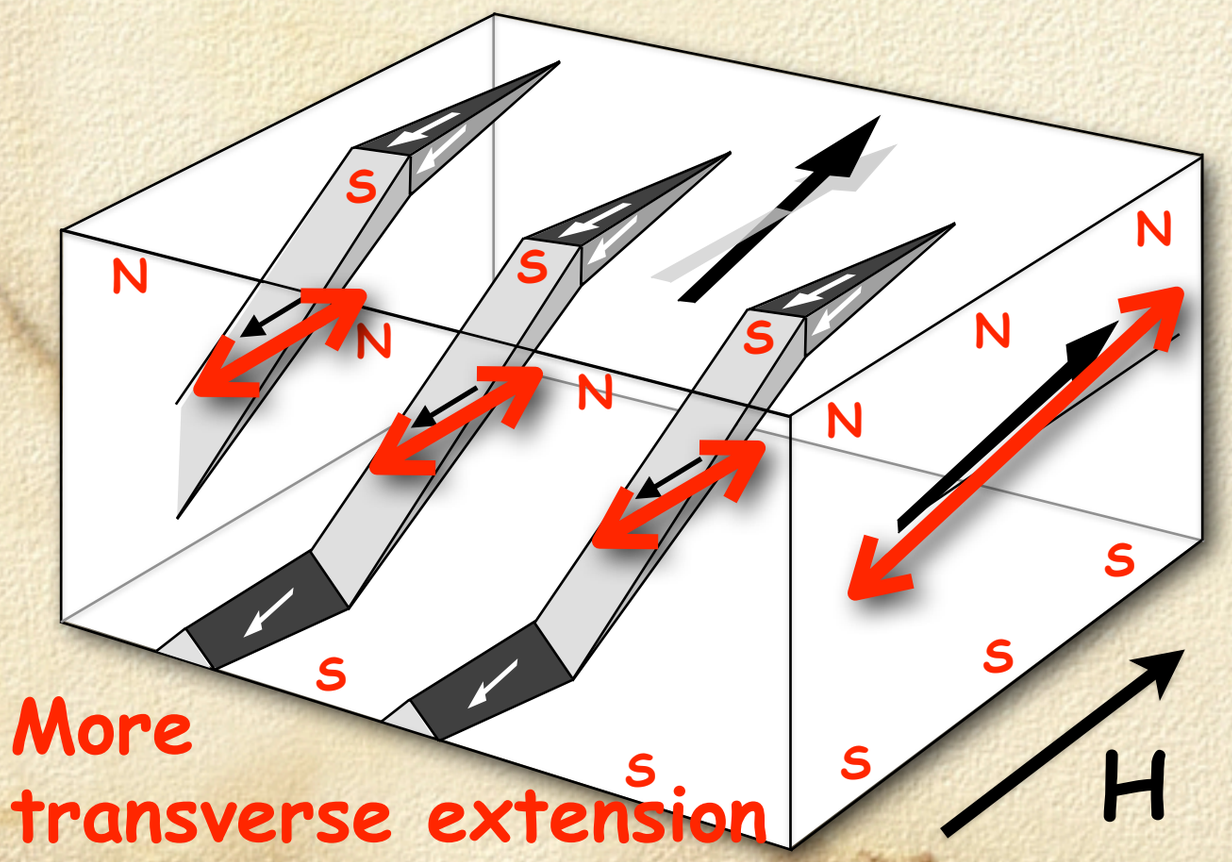

More transverse extension

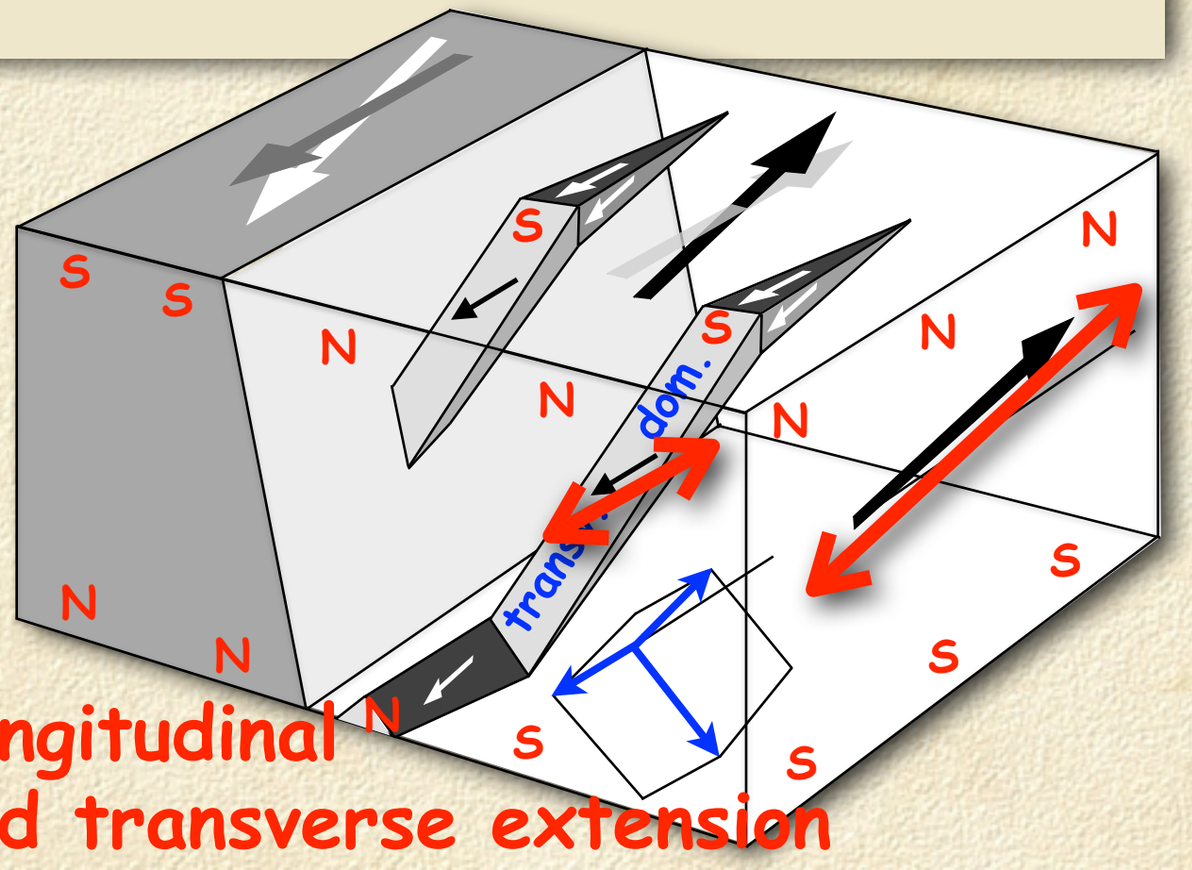

Longitudinal and transverse extension

Grain-oriented FeSi transformer material

With tensile stress

Without tensile stress

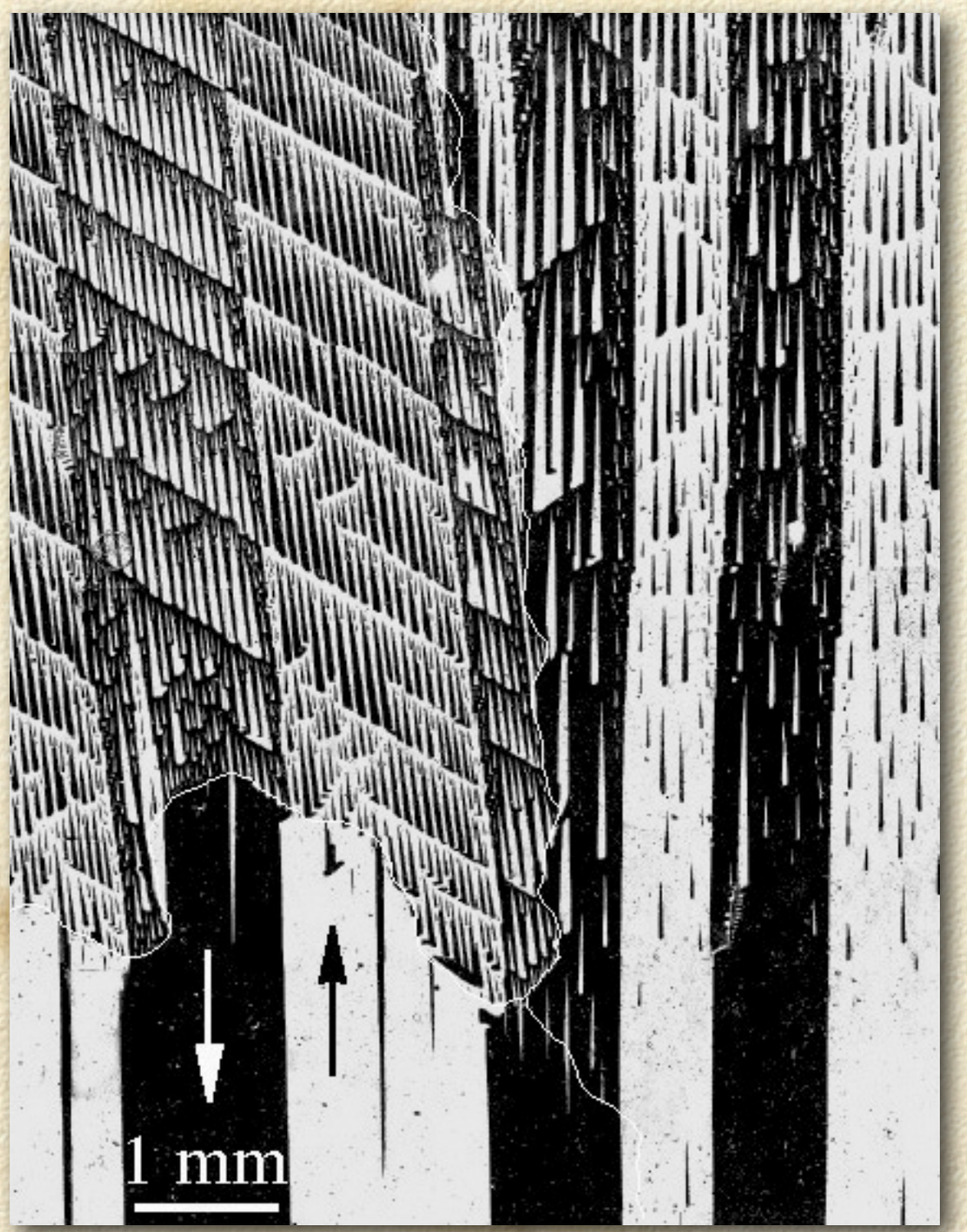

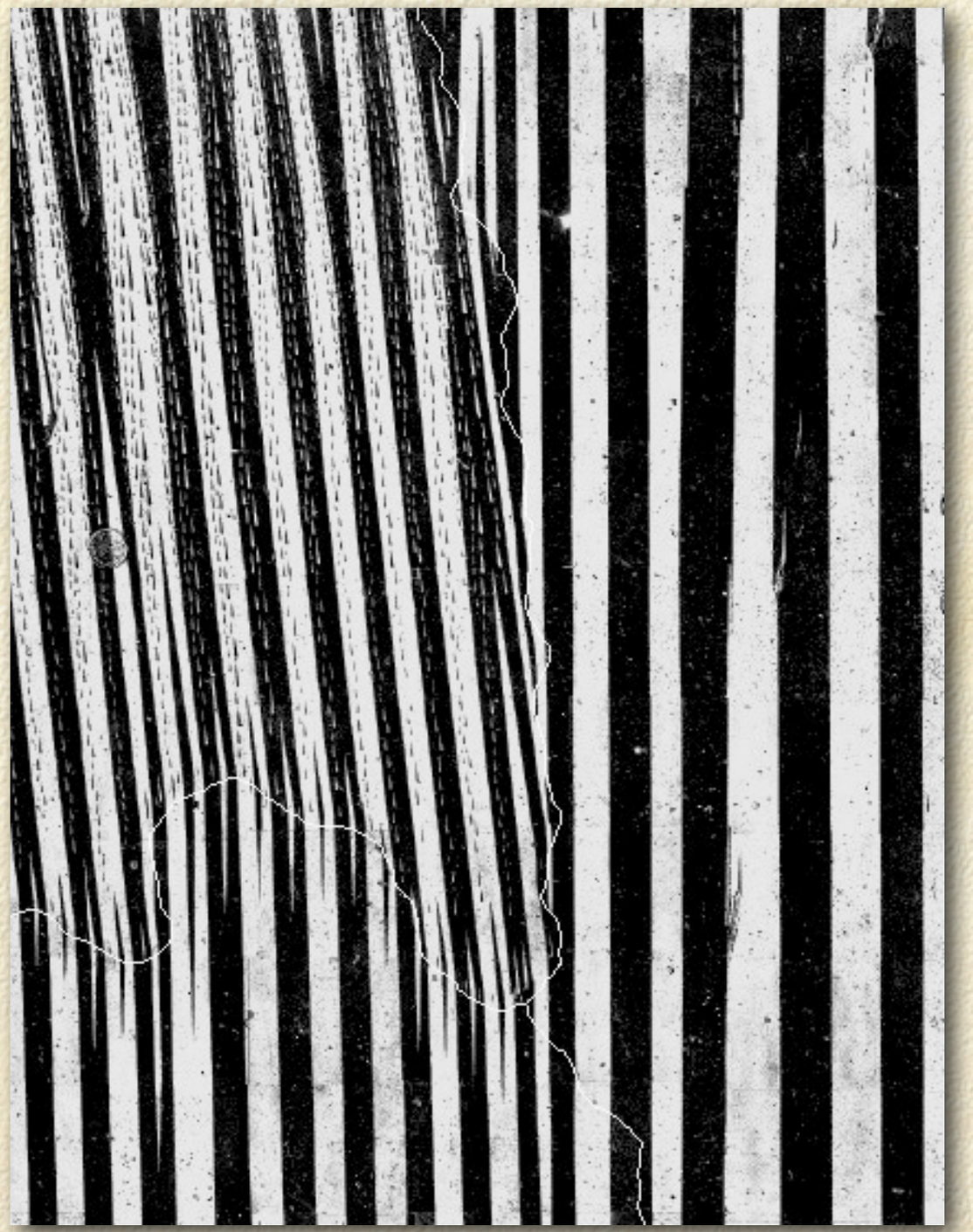

Tensile stress

Grain-oriented FeSi transformer material

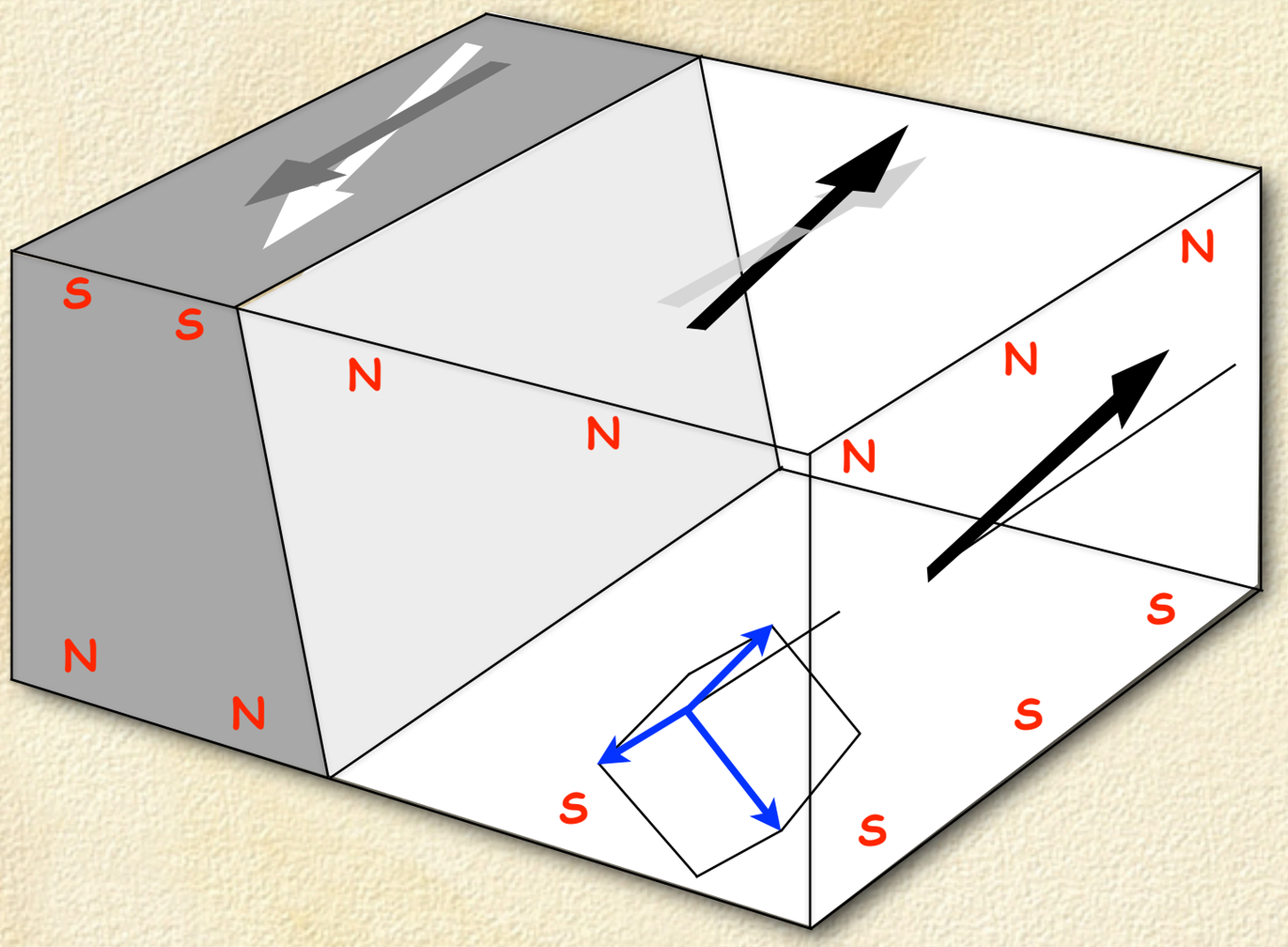

Grain-oriented FeSi transformer material

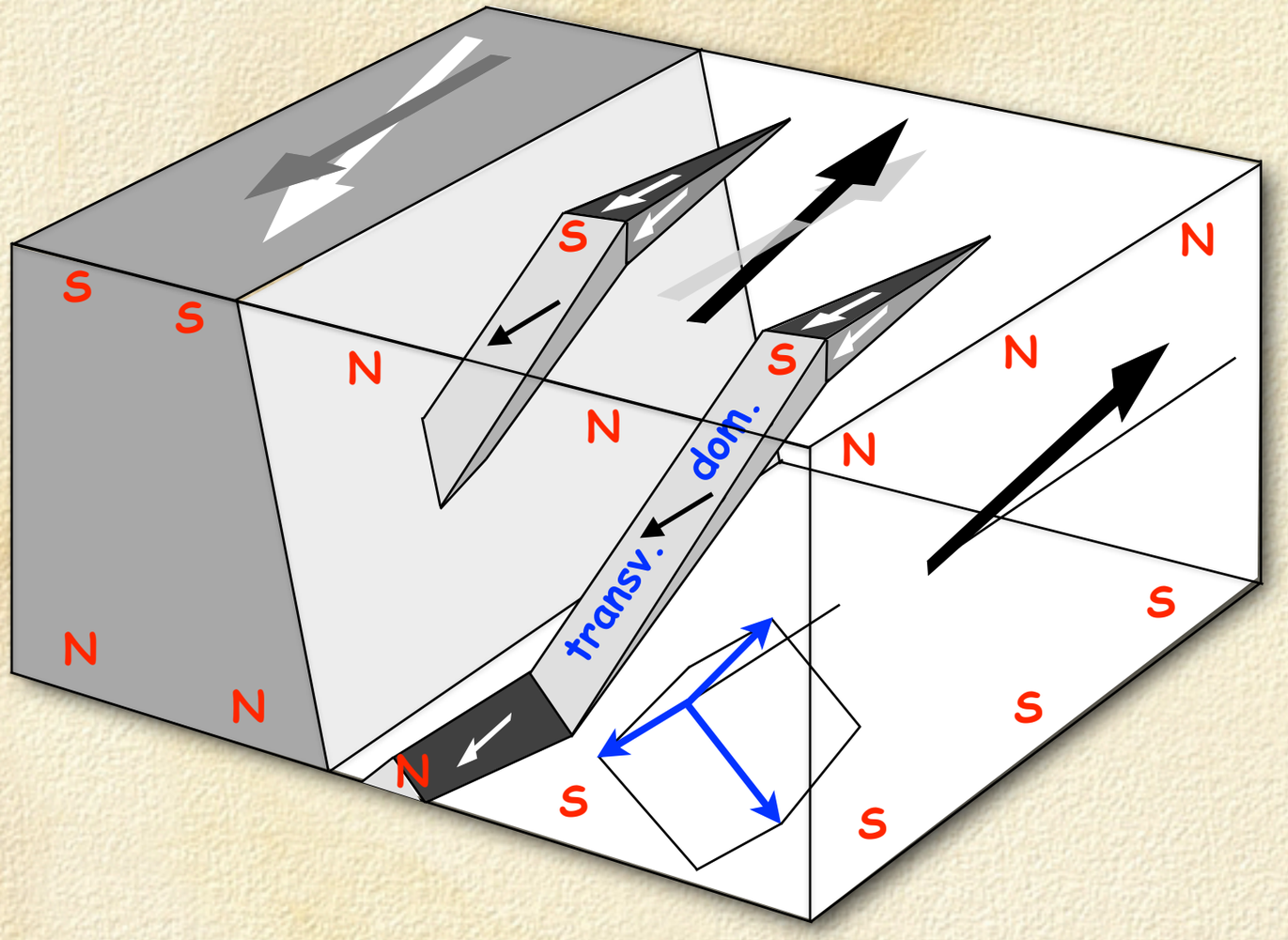

Grain-oriented FeSi transformer material

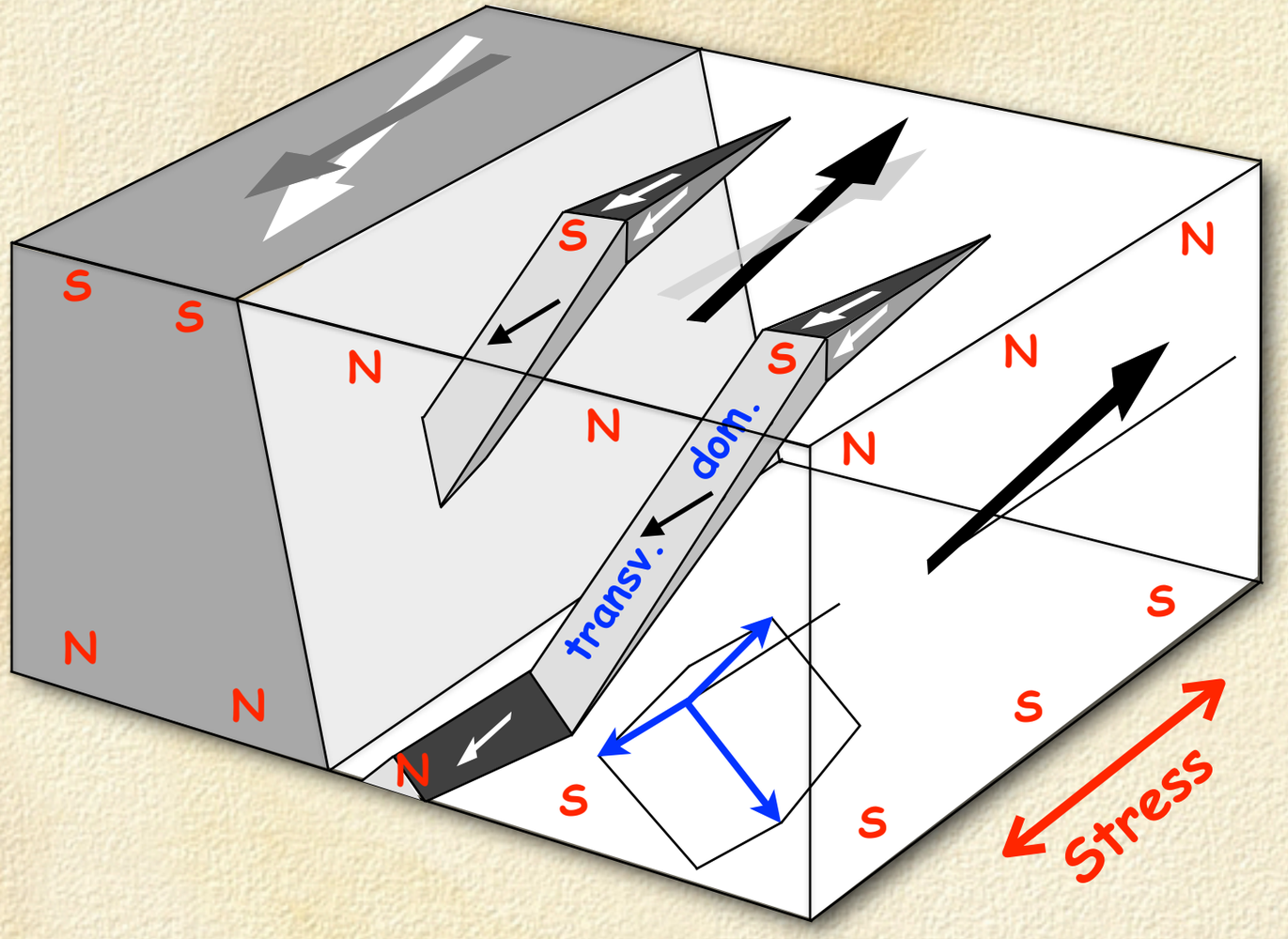

Grain-oriented FeSi transformer material

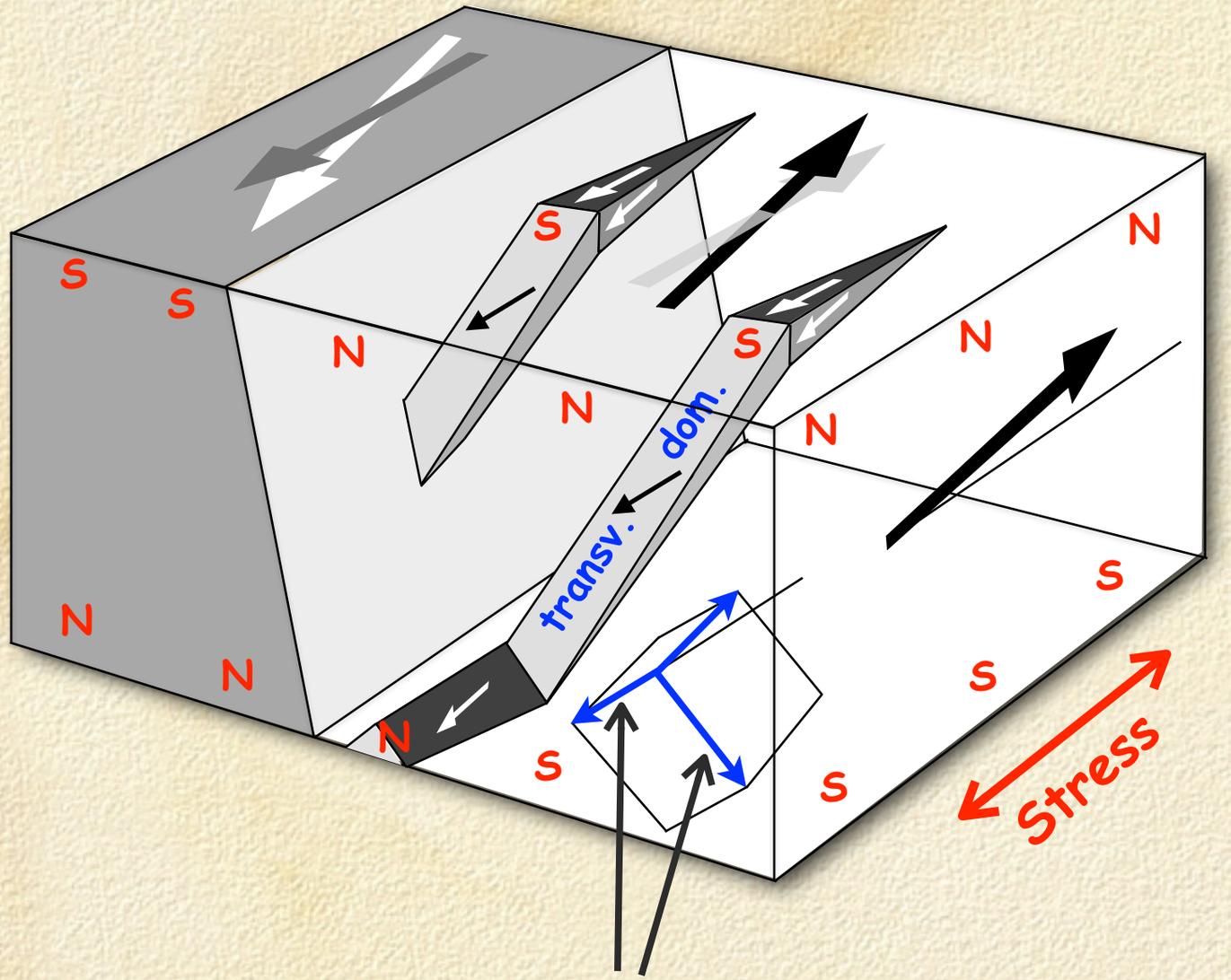

transverse easy axes
disfavored

Grain-oriented FeSi transformer material

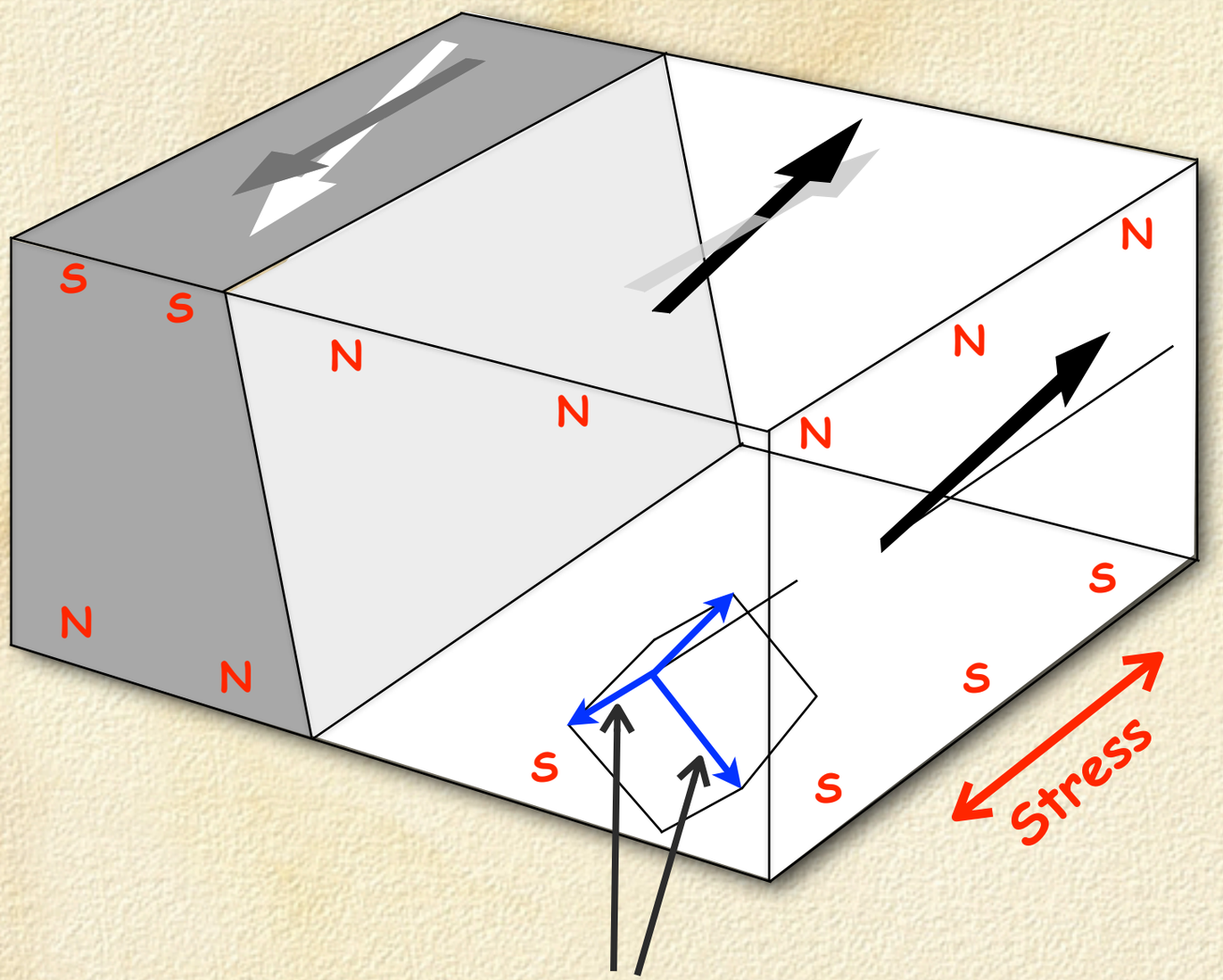

Grain-oriented FeSi transformer material

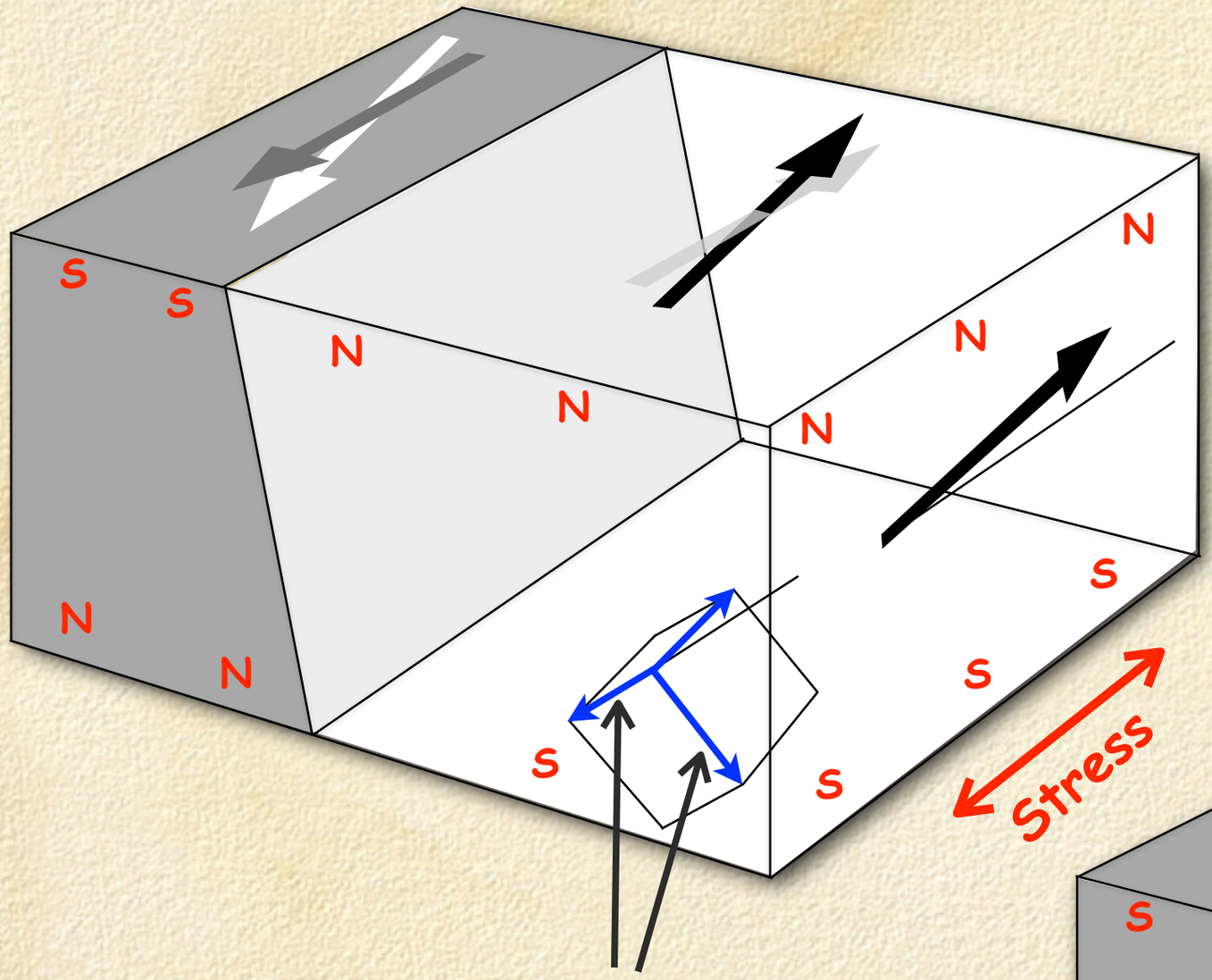

transverse easy axes
disfavored

Domain refinement

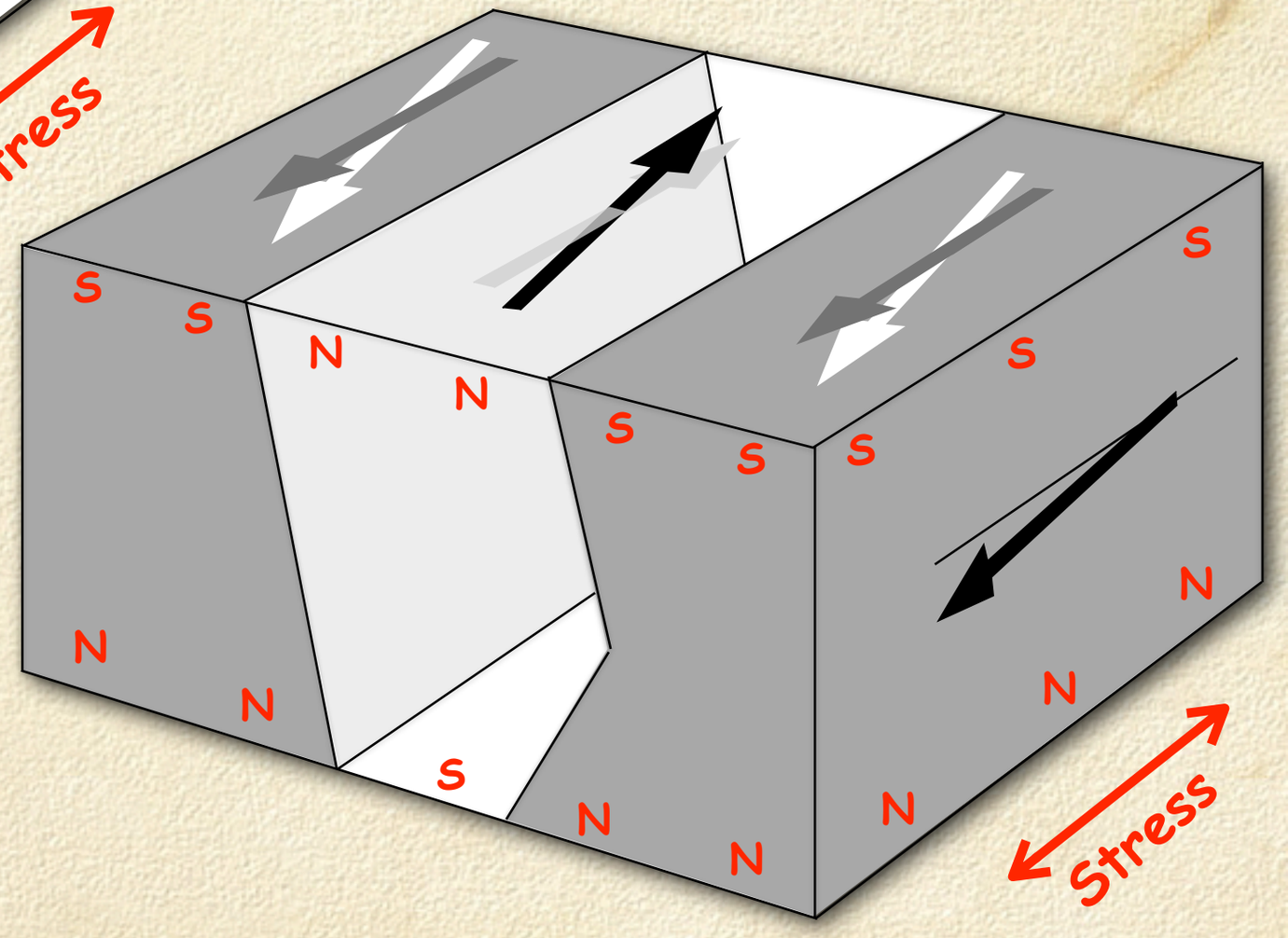

Grain-oriented FeSi transformer material

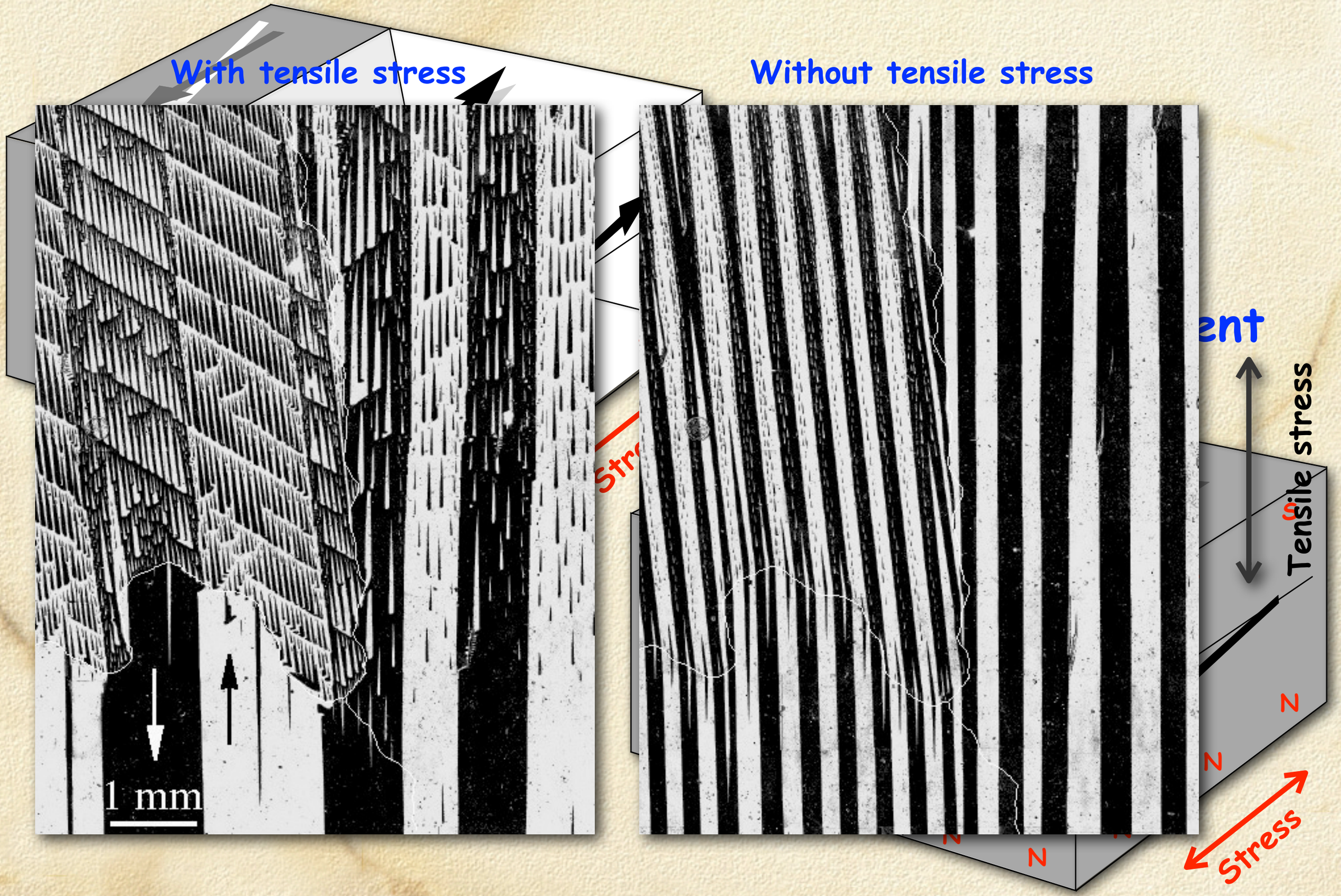

Excursus

Dynamic aspects of domains (eddy current dominated)

Domain multiplication in transformer steel

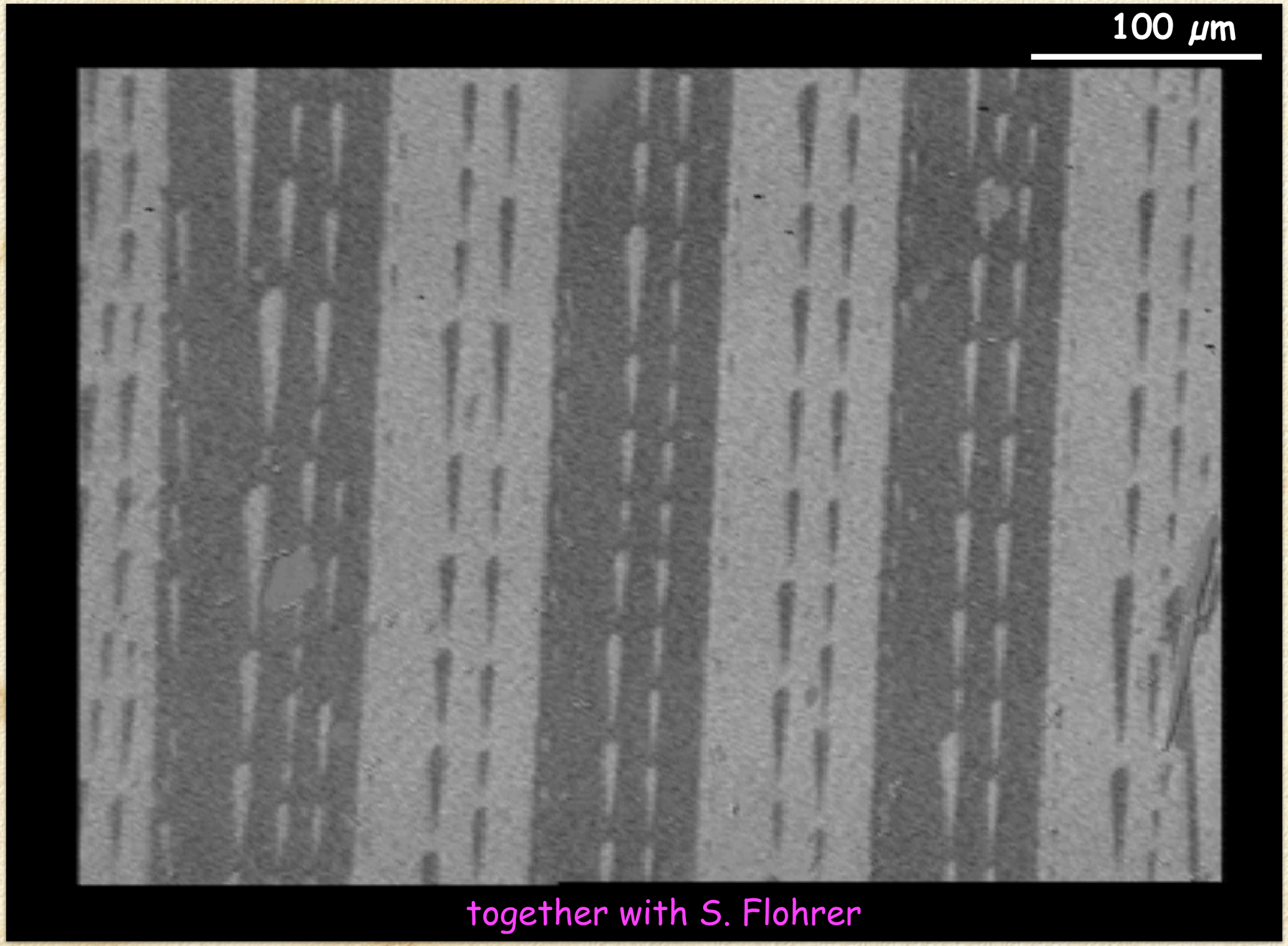

Domain multiplication in transformer steel

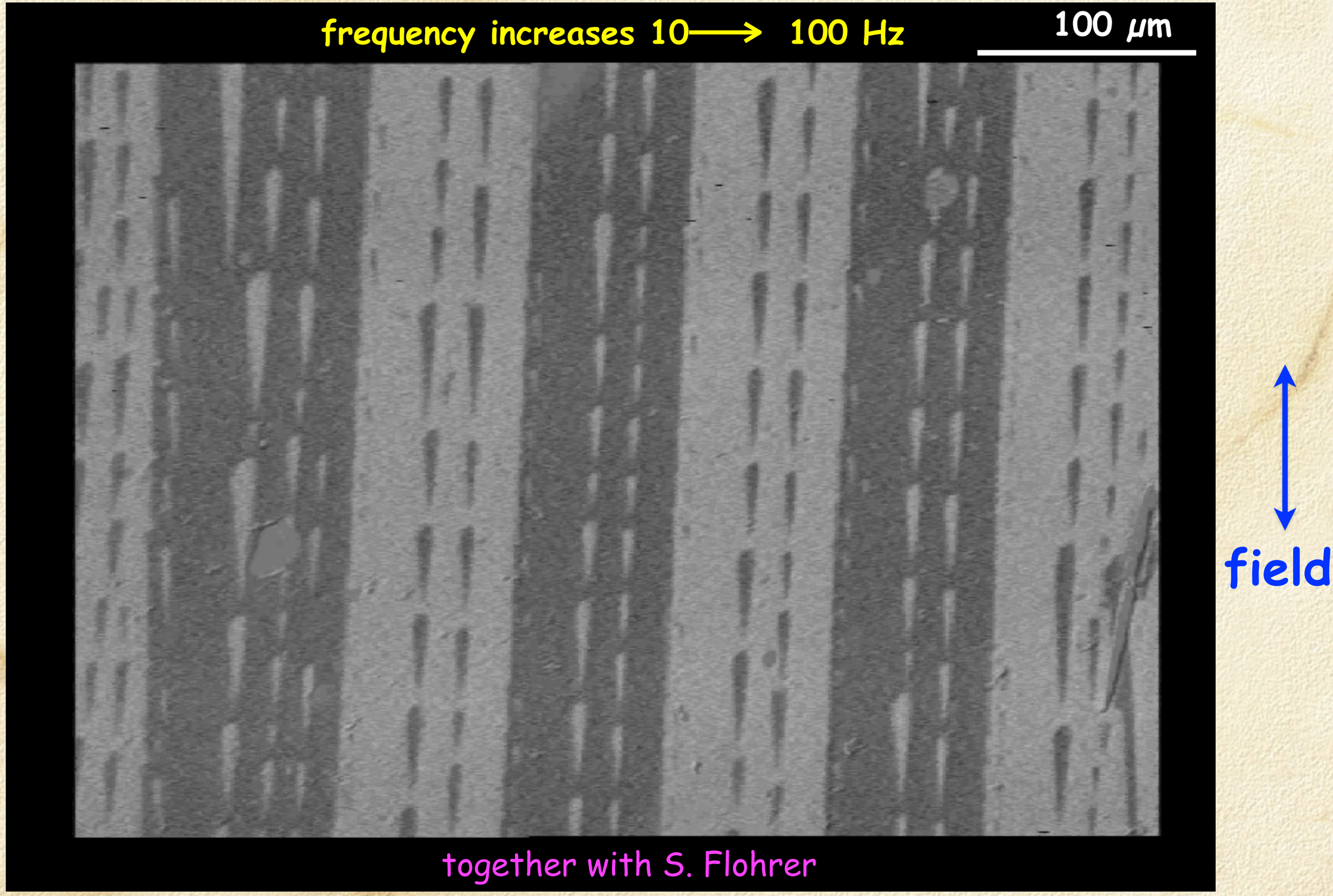

Dynamic magnetization loss

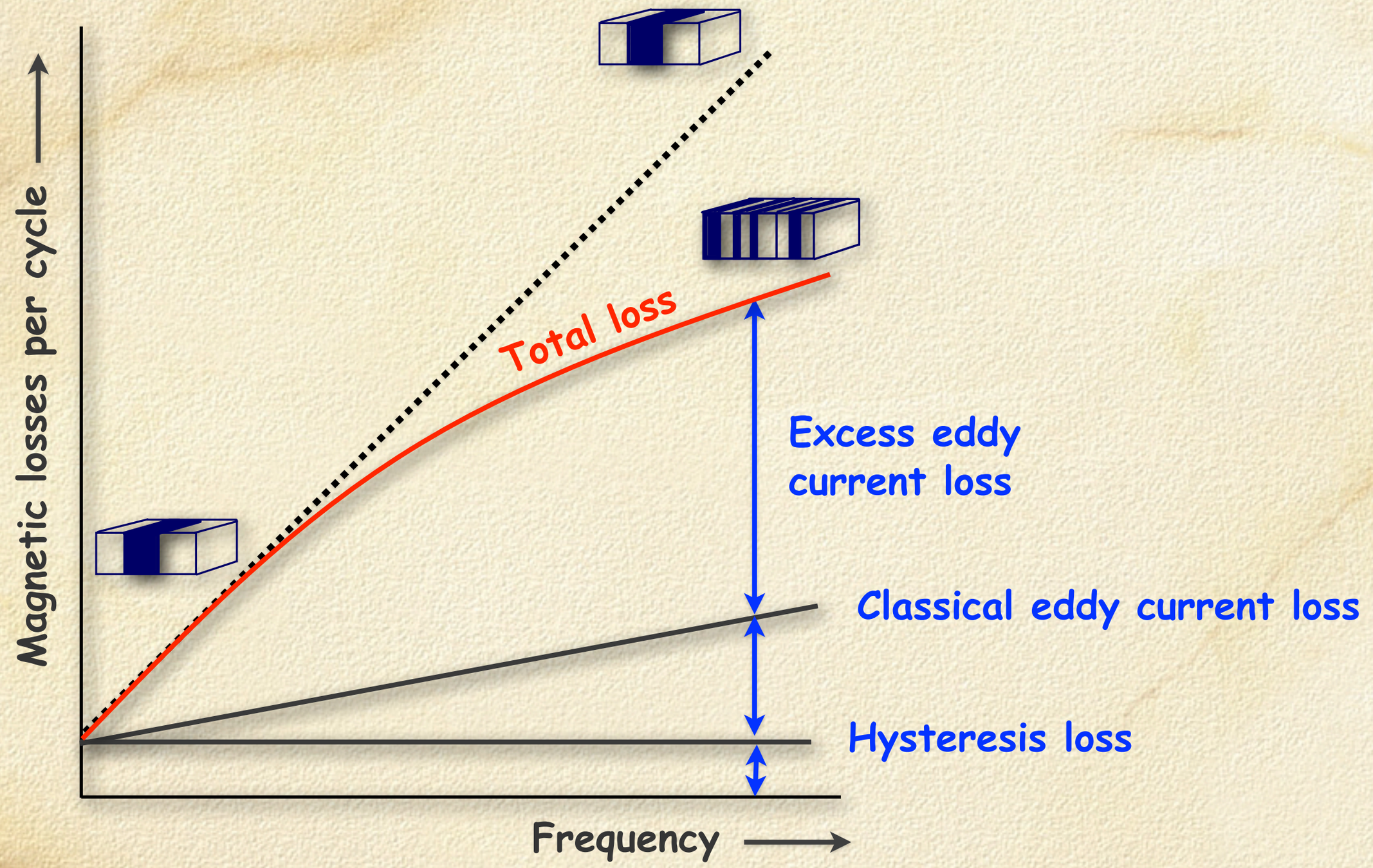

R.H. Pry , C.P. Bean, J. Appl. Phys. 29 (1958) 532
G.L. Houze, J. Appl. Phys. 38 (1967) 1089
G. Bertotti. Hysteresis in magnetism. Academic Press, Inc., San Diego, (2001)

Domain multiplication in transformer steel

after ac demagnetization with different frequency

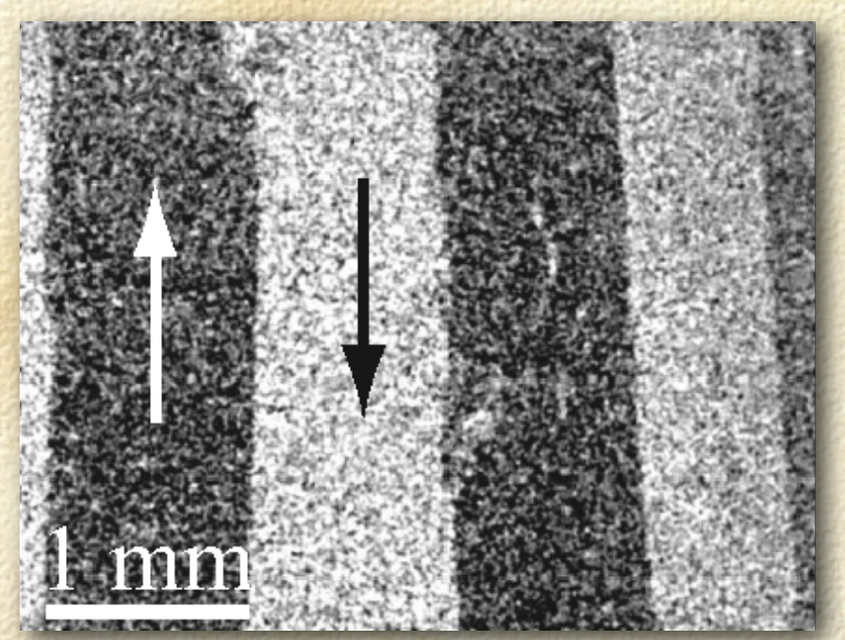

1 Hz

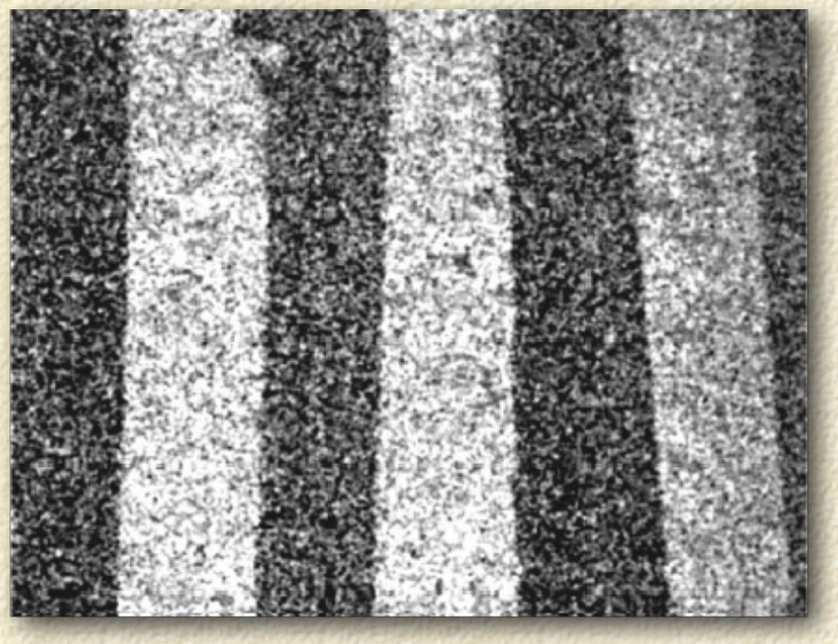

50 Hz

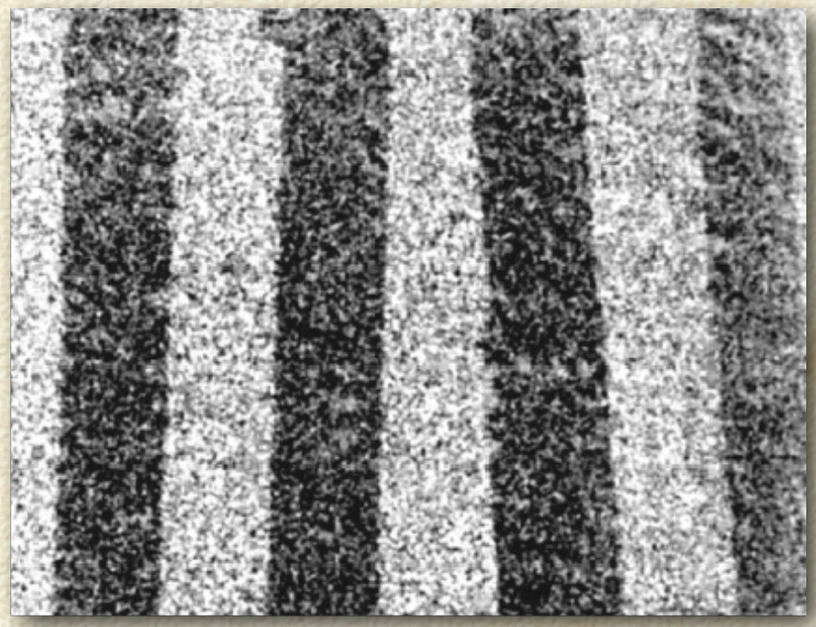

500 Hz

Domain wall damping by eddy currents

(nanocrystalline ribbon, 20 μm thick)

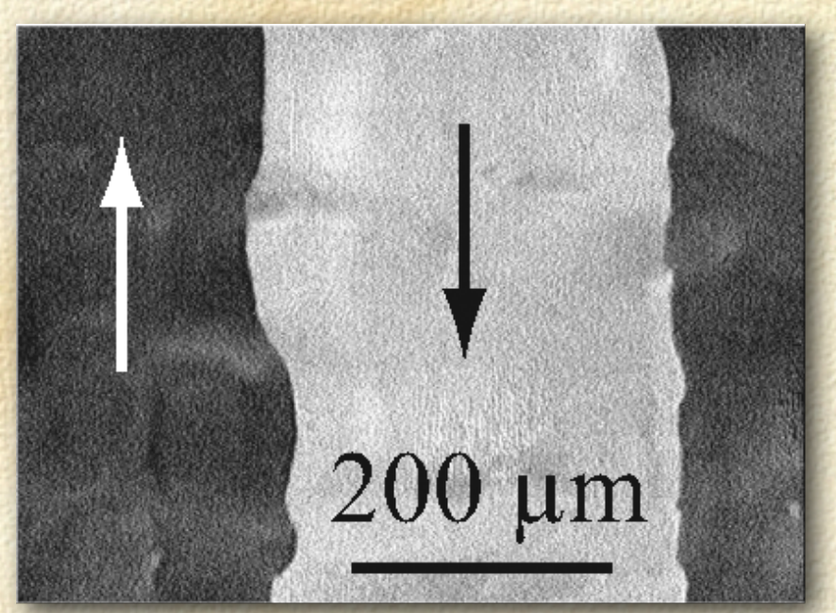

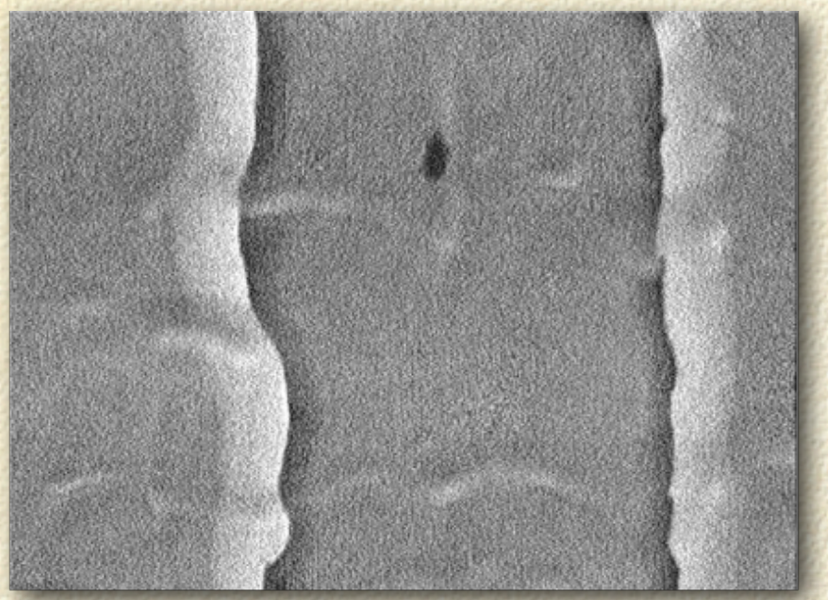

500 Hz

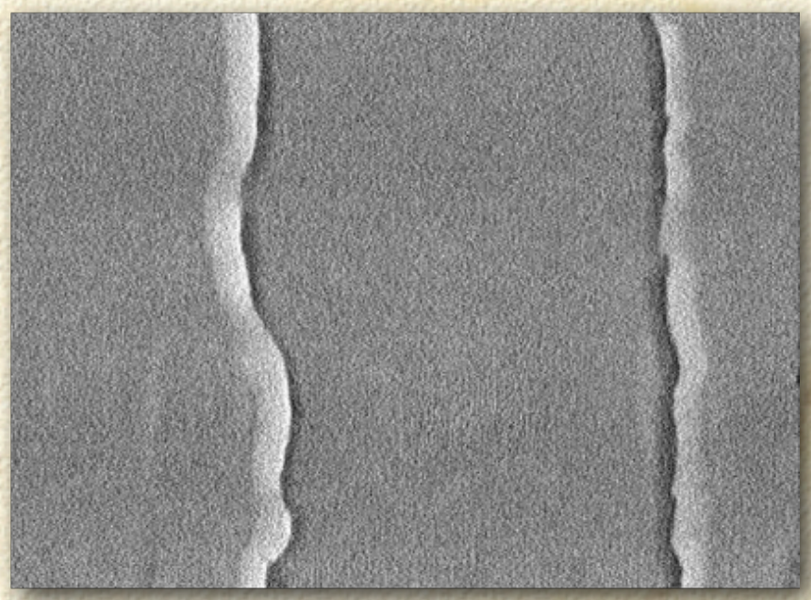

1000 Hz

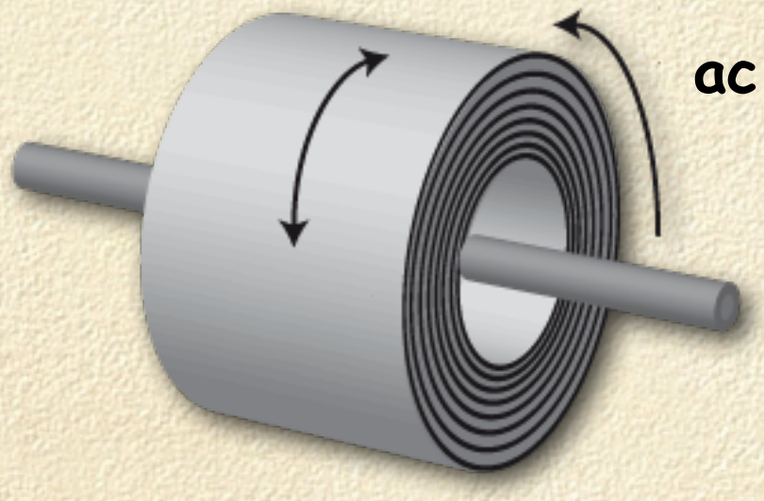

ac magnetic field

Domain wall damping by eddy currents

(nanocrystalline ribbon, 20 μm thick)

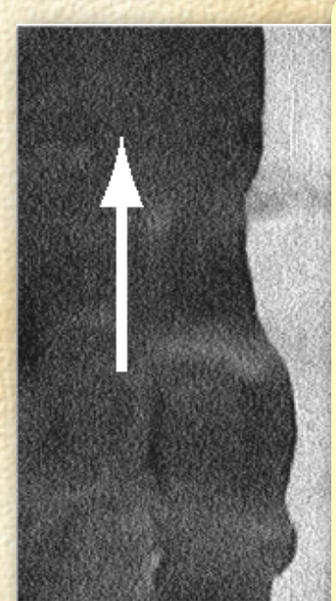

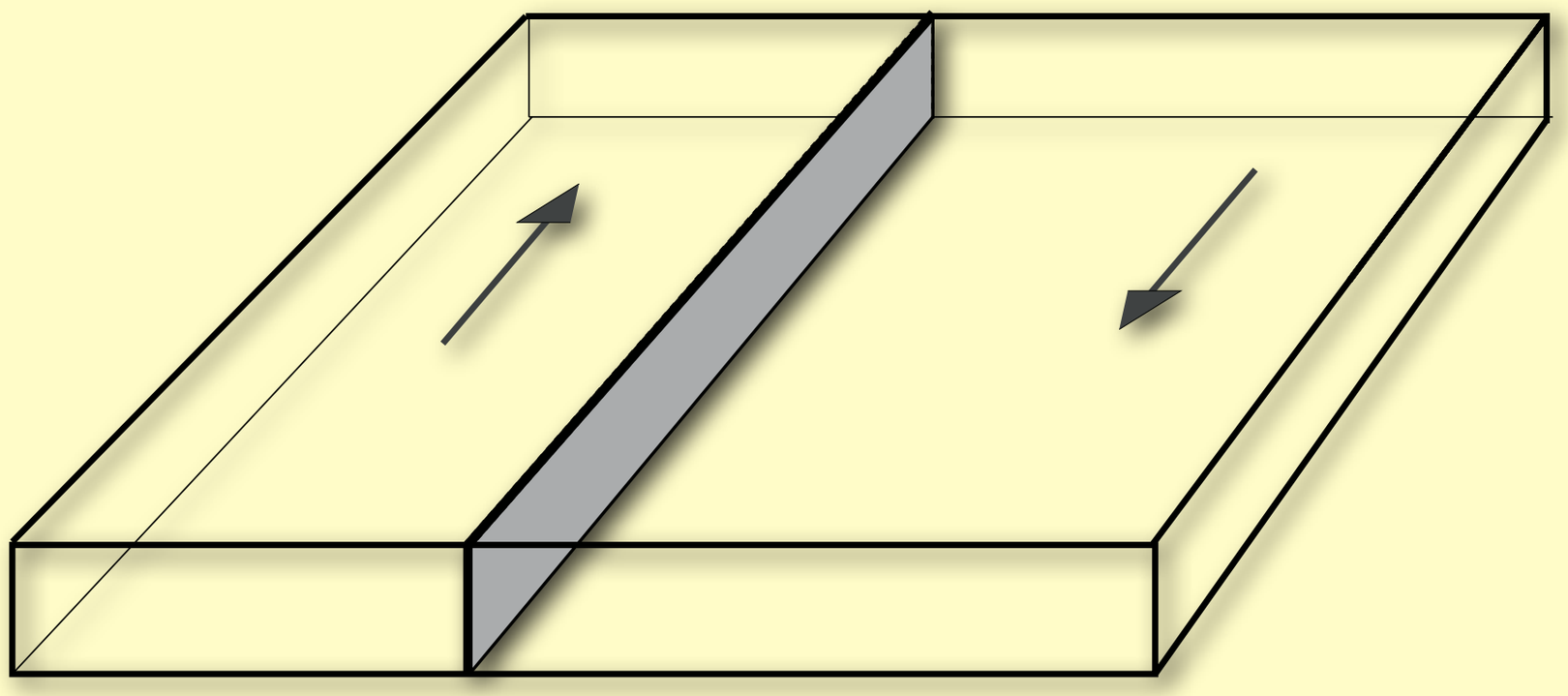

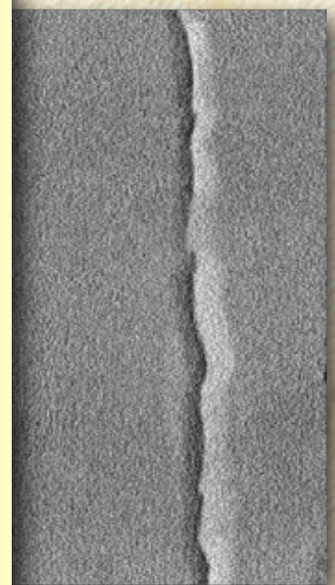

Hz

Domain wall damping by eddy currents

(nanocrystalline ribbon, 20 μm thick)

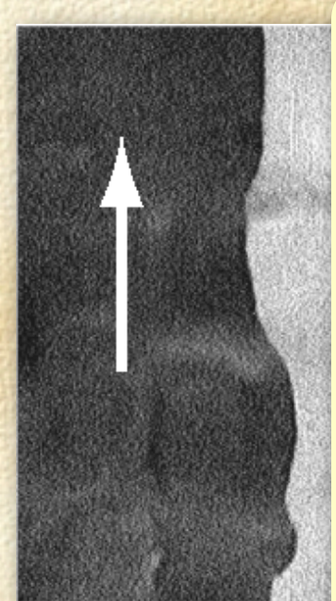

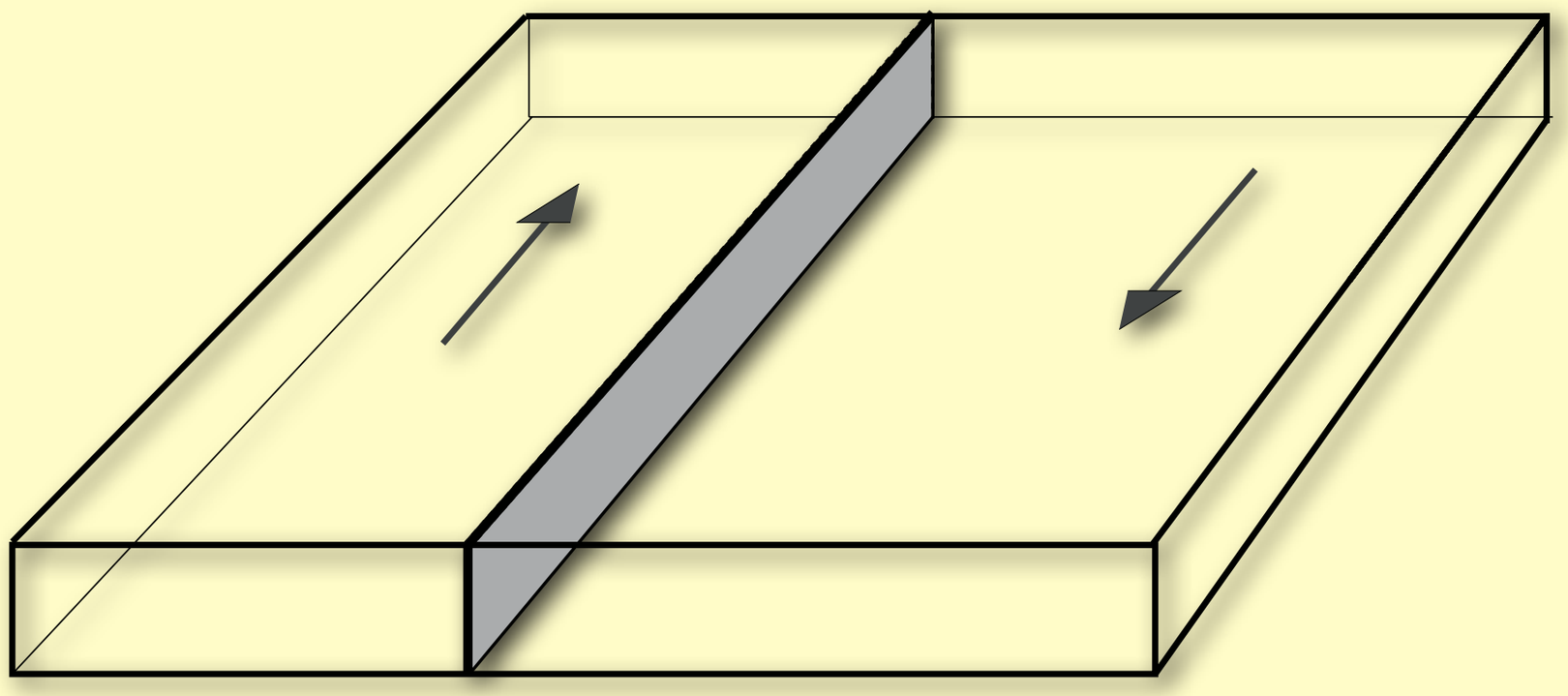

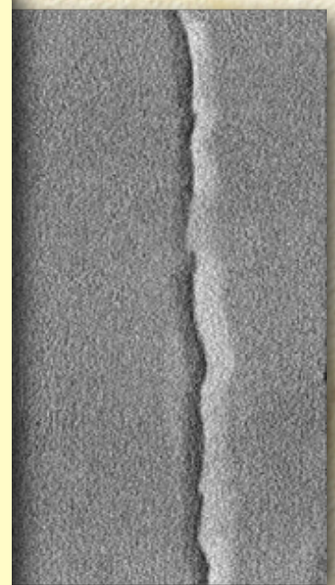

Hz

external magnetic field

Domain wall damping by eddy currents

(nanocrystalline ribbon, 20 μm thick)

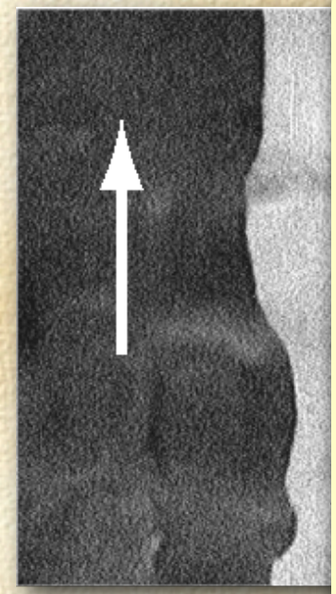

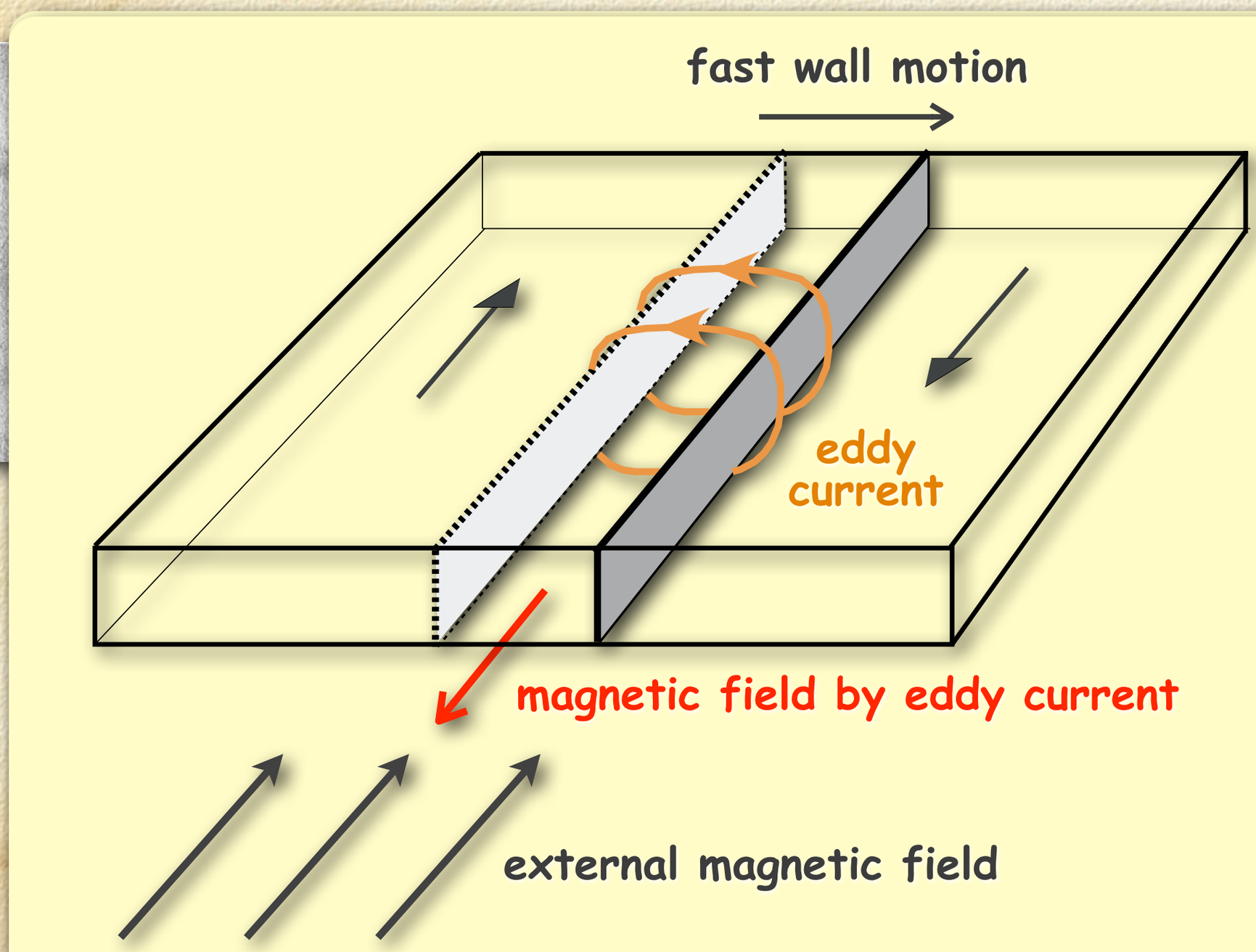

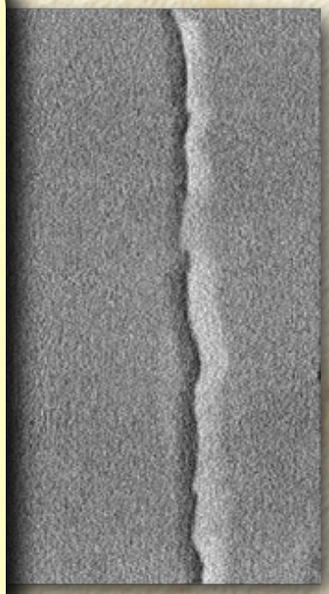

Hz

Domain wall deformation by eddy currents

(schematically)

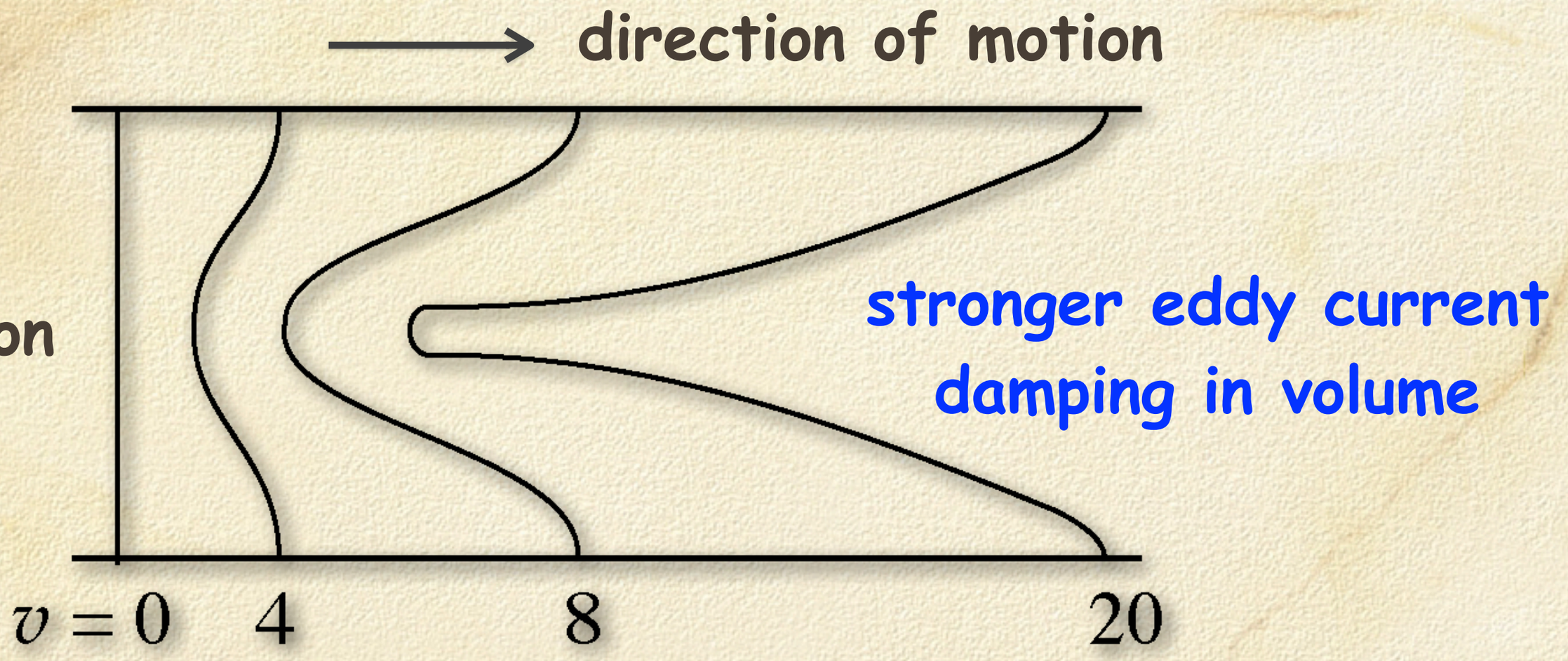

high velocity ⟶ walls run parallel to surface ⟶ skin effect

Magneto-acoustic Article Surveillance

semihard metall
(on-/off-switch)

amorphous ribon
(Sensor)

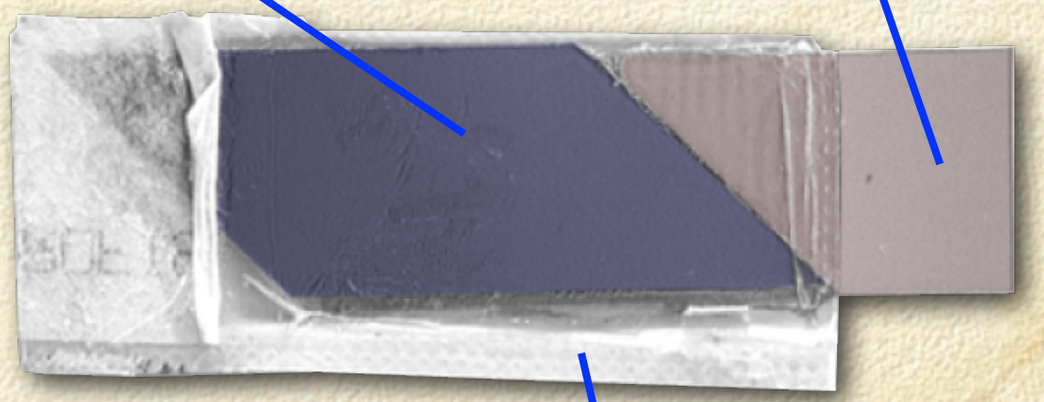

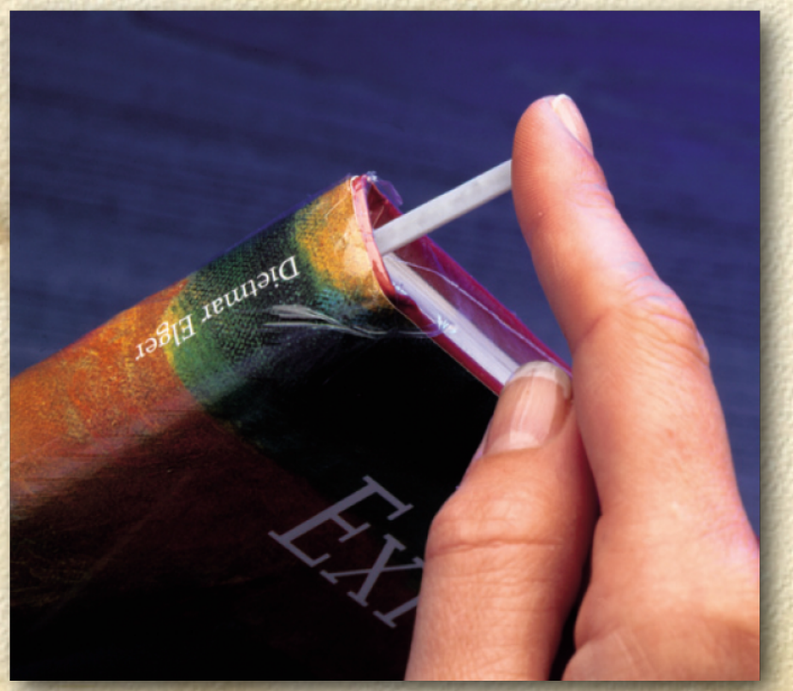

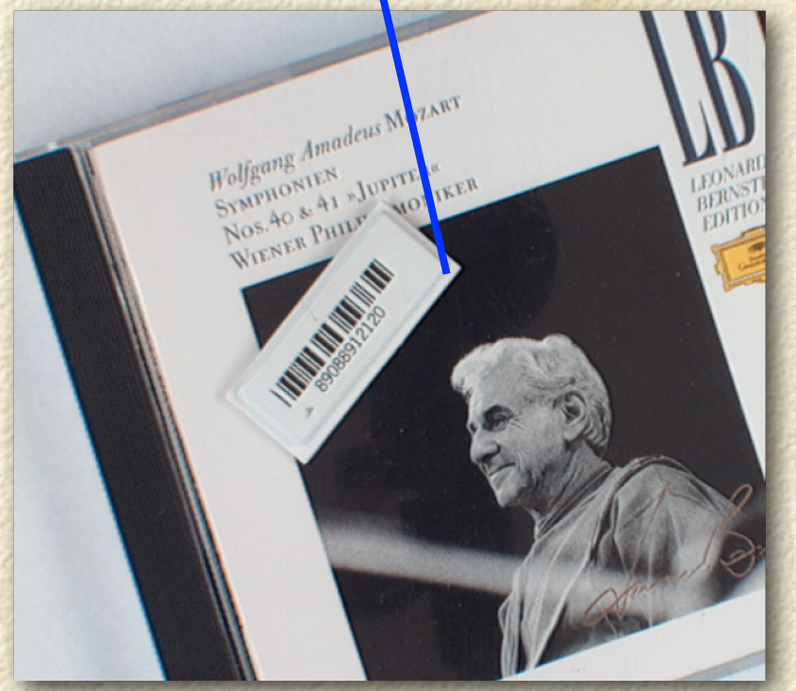

Magneto-acoustic Article Surveillance

deactivated

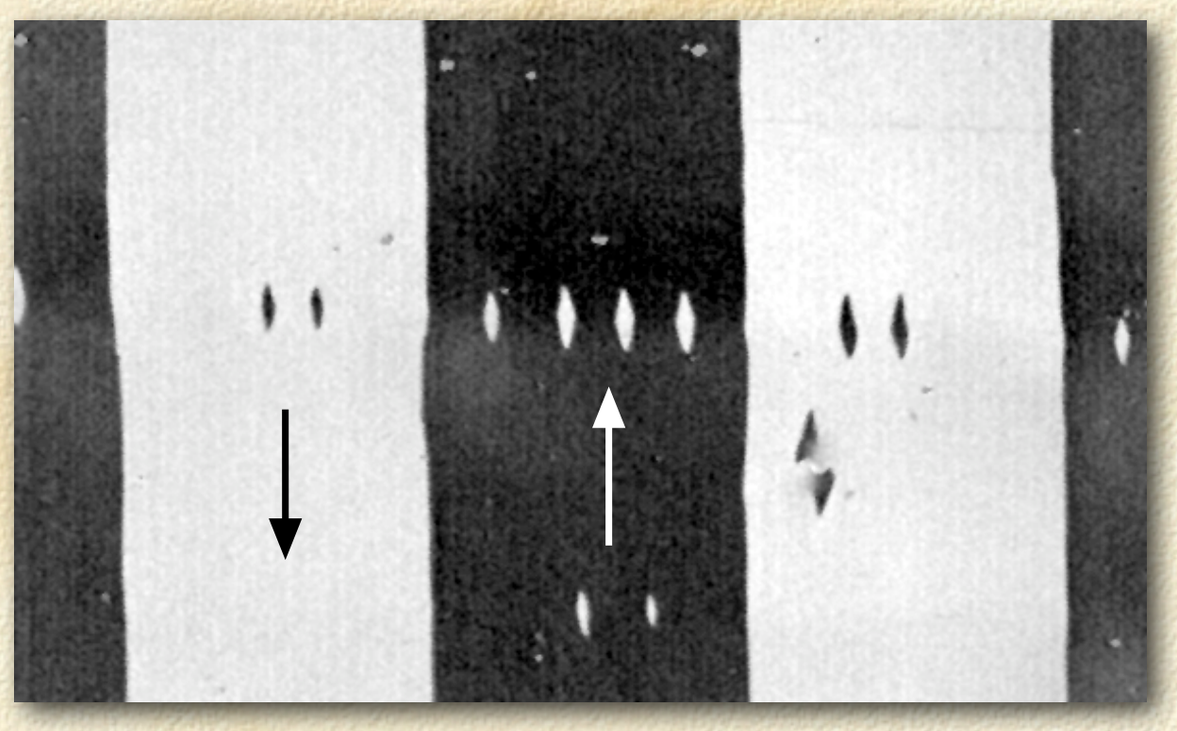

active

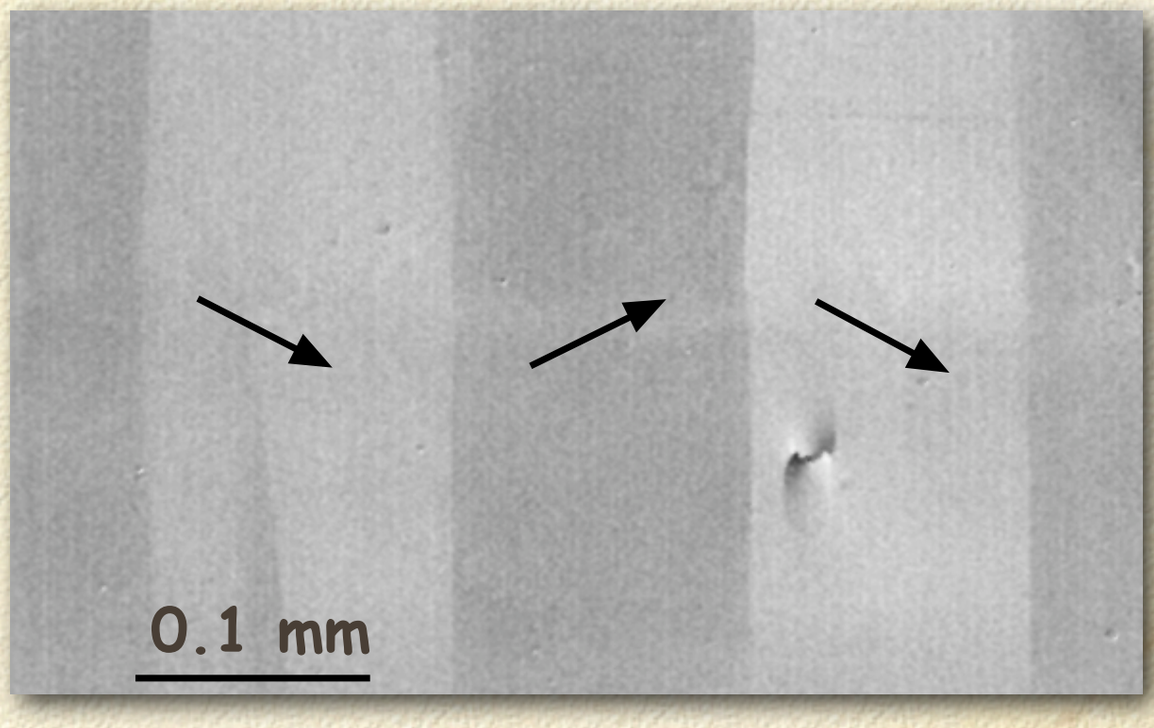

metallic glass without magnetic field

metallic glass in magnetic field

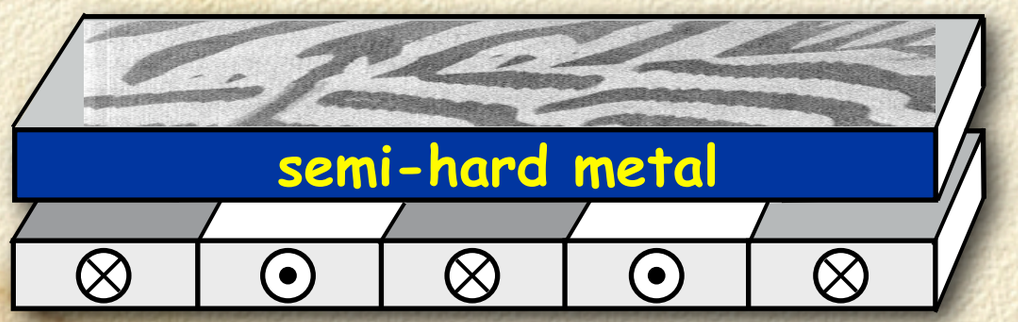

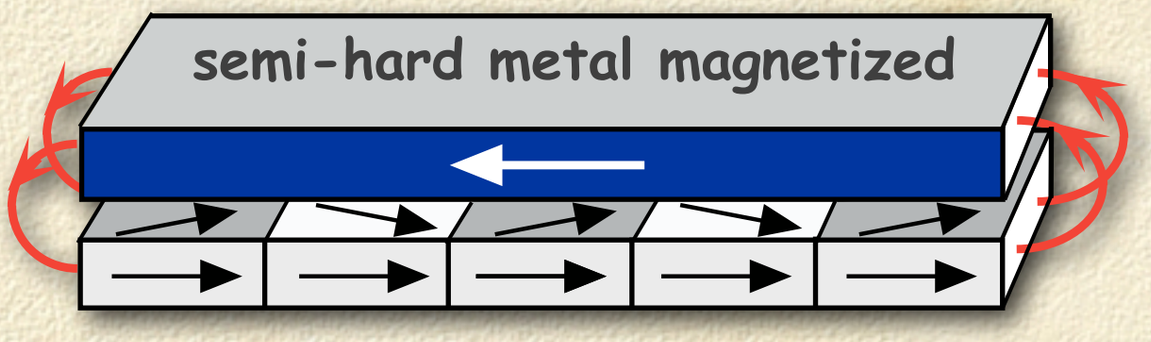

semi-hard metal
(on-/off-switch)

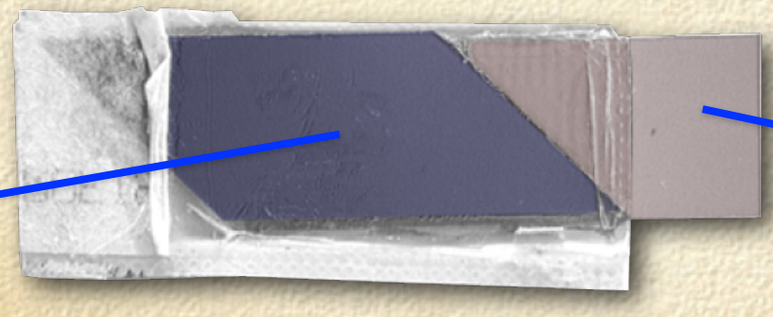

metallic glass
(sensor)

Magneto-acoustic Article Surveillance

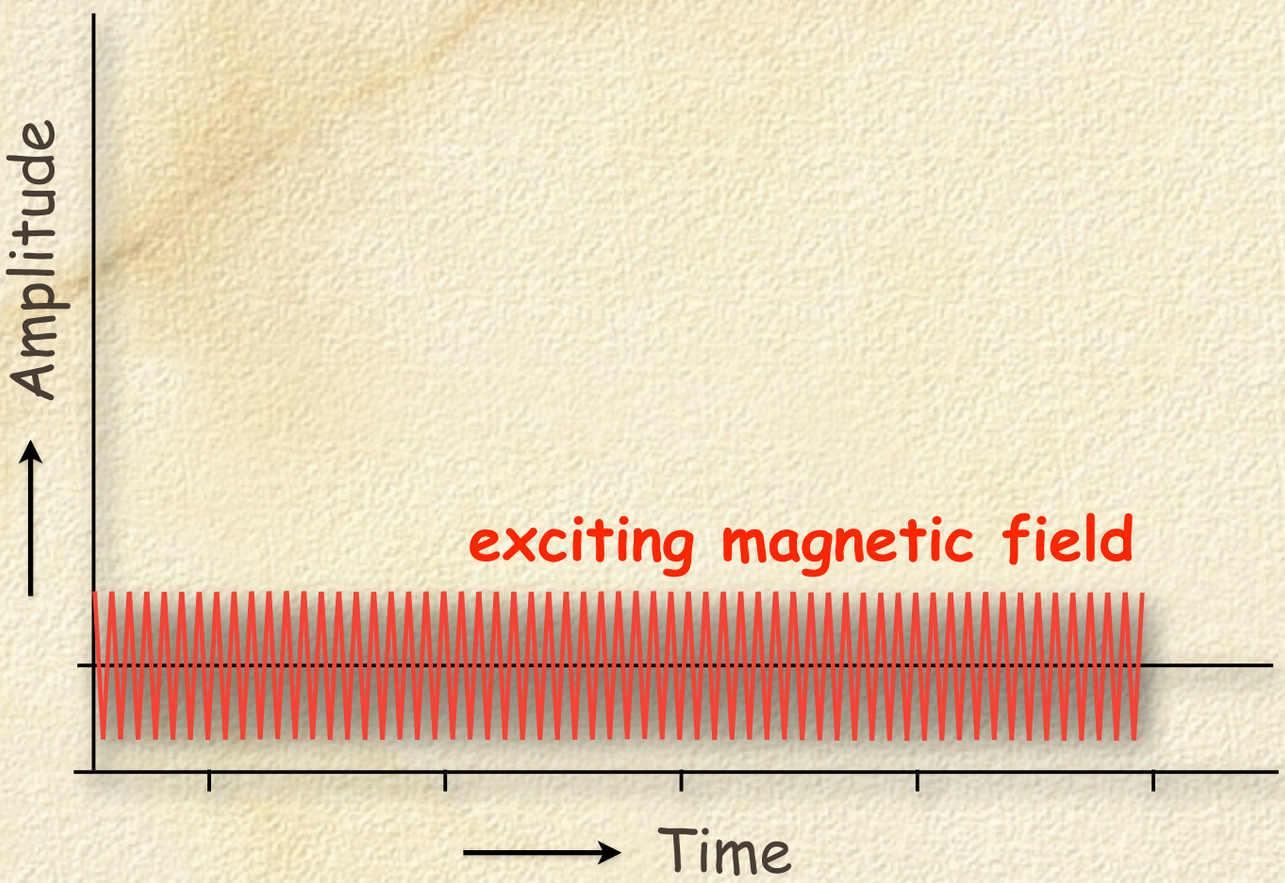

magnetic ac-field

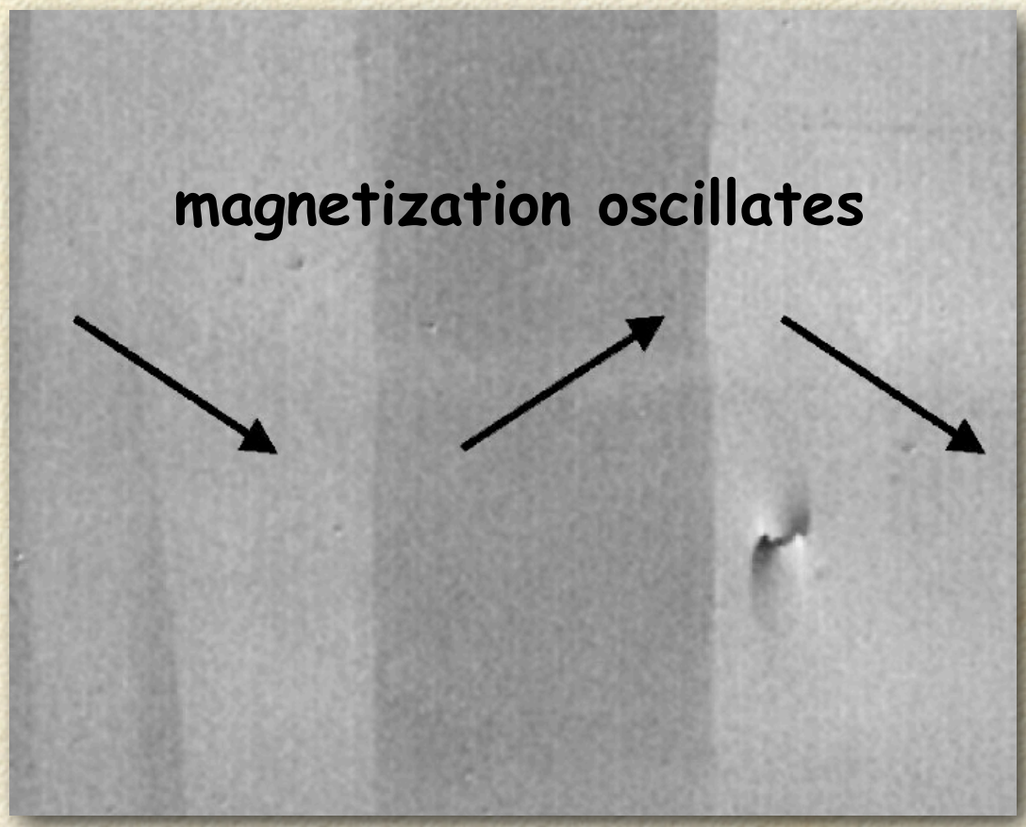

Magneto-acoustic Article Surveillance

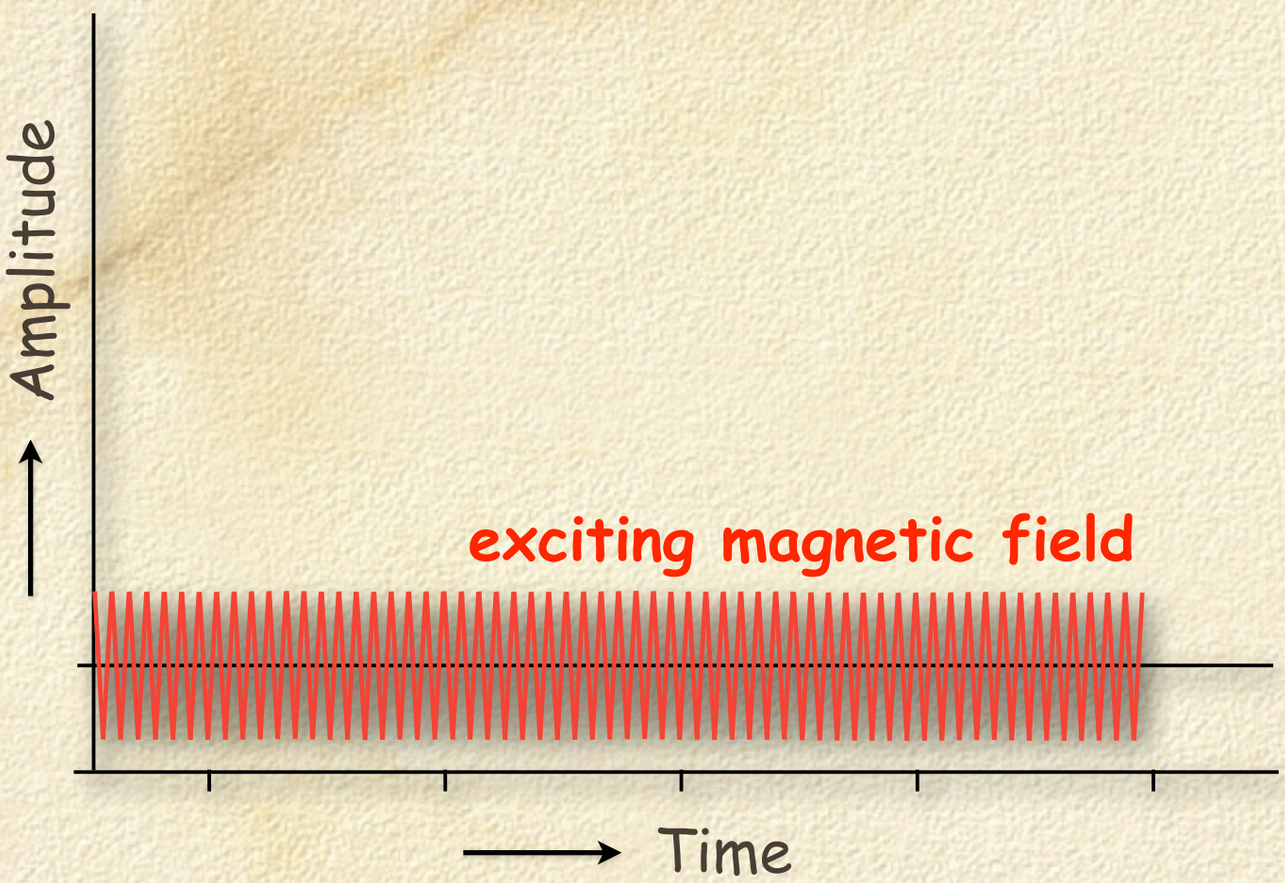

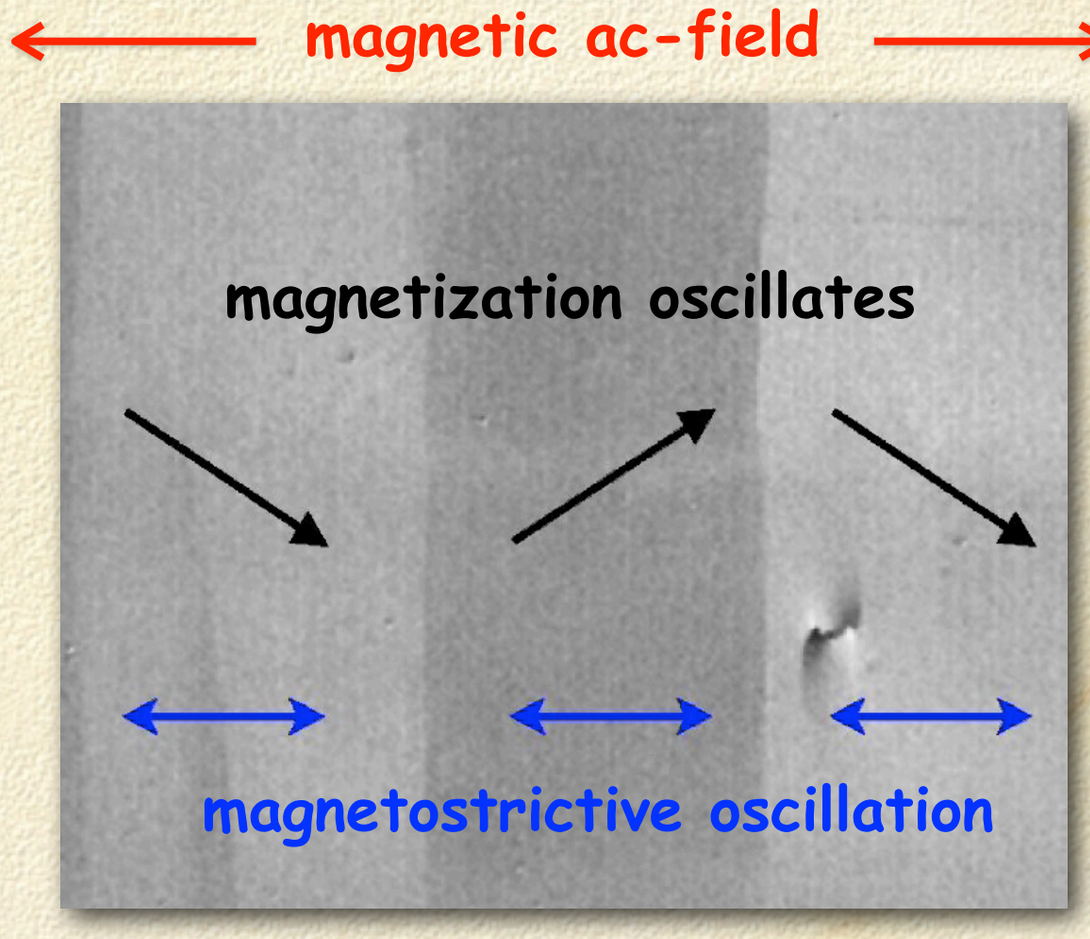

Magneto-acoustic Article Surveillance

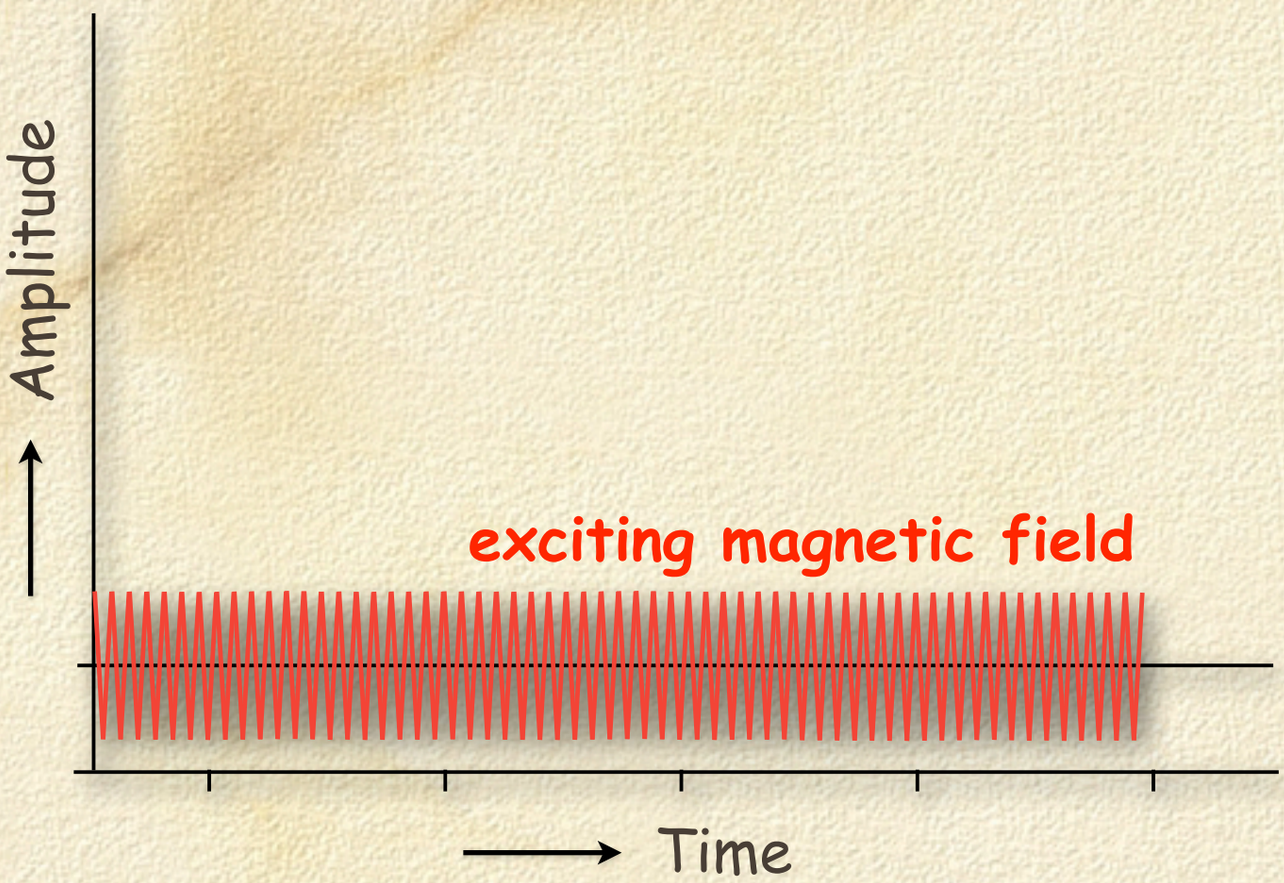

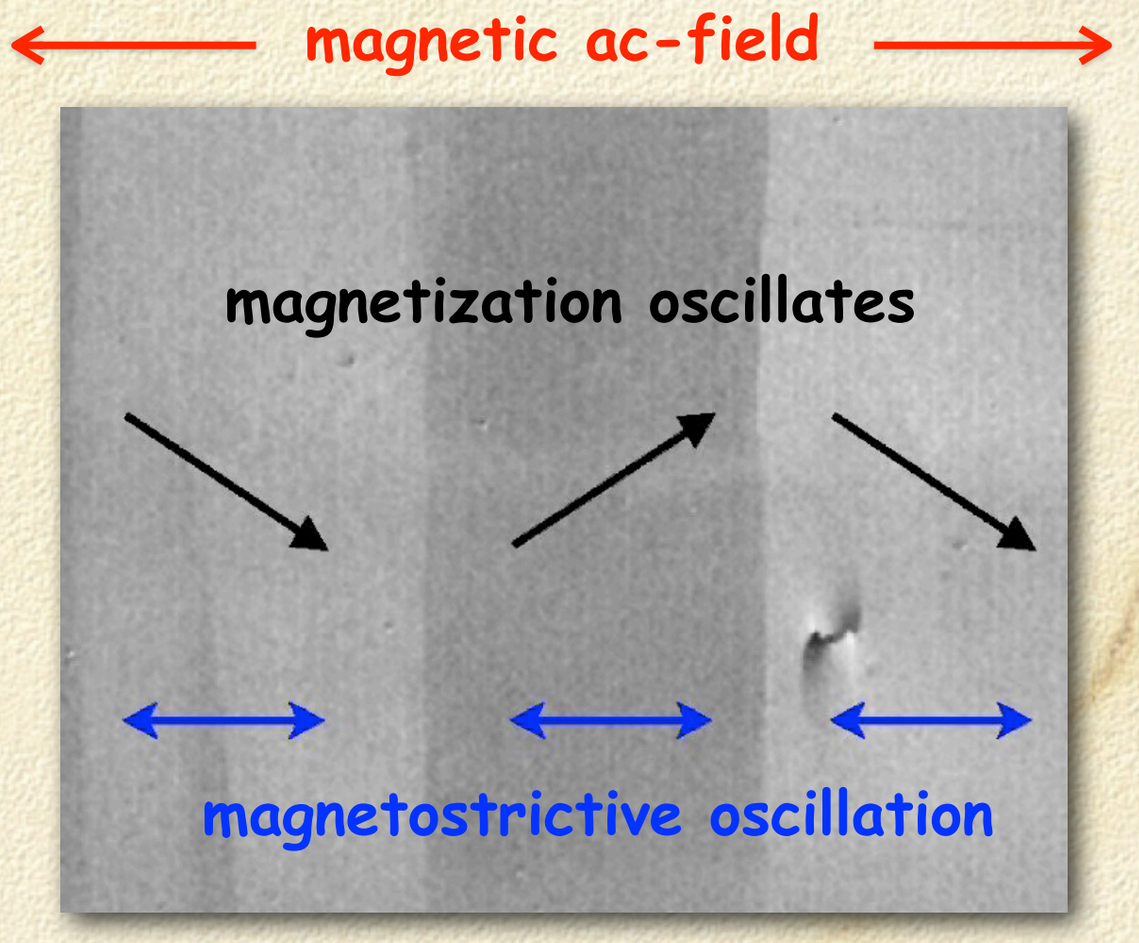

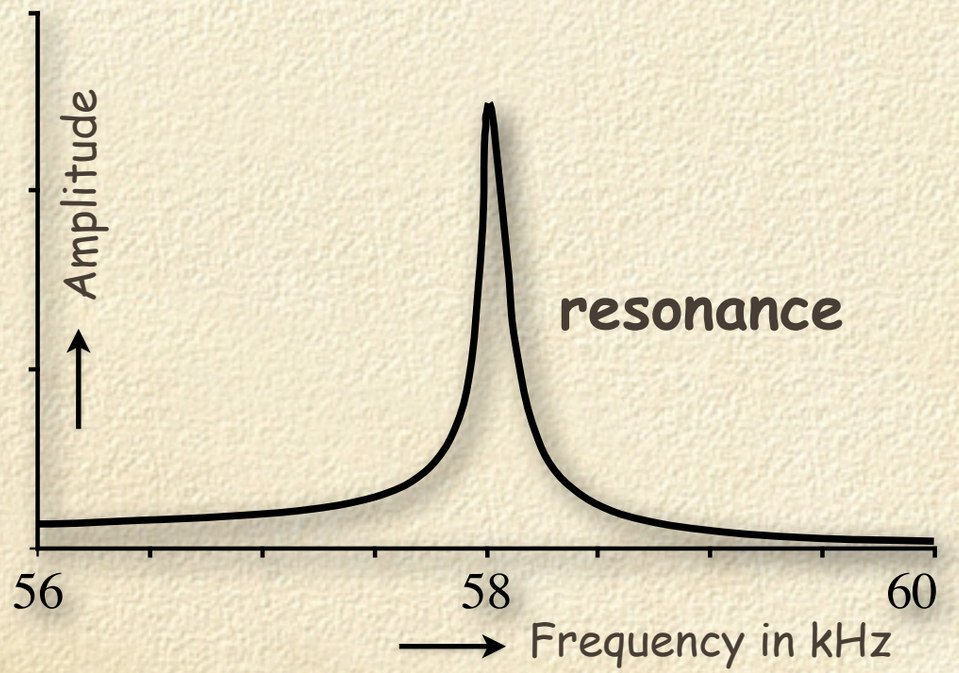

Magneto-acoustic Article Surveillance

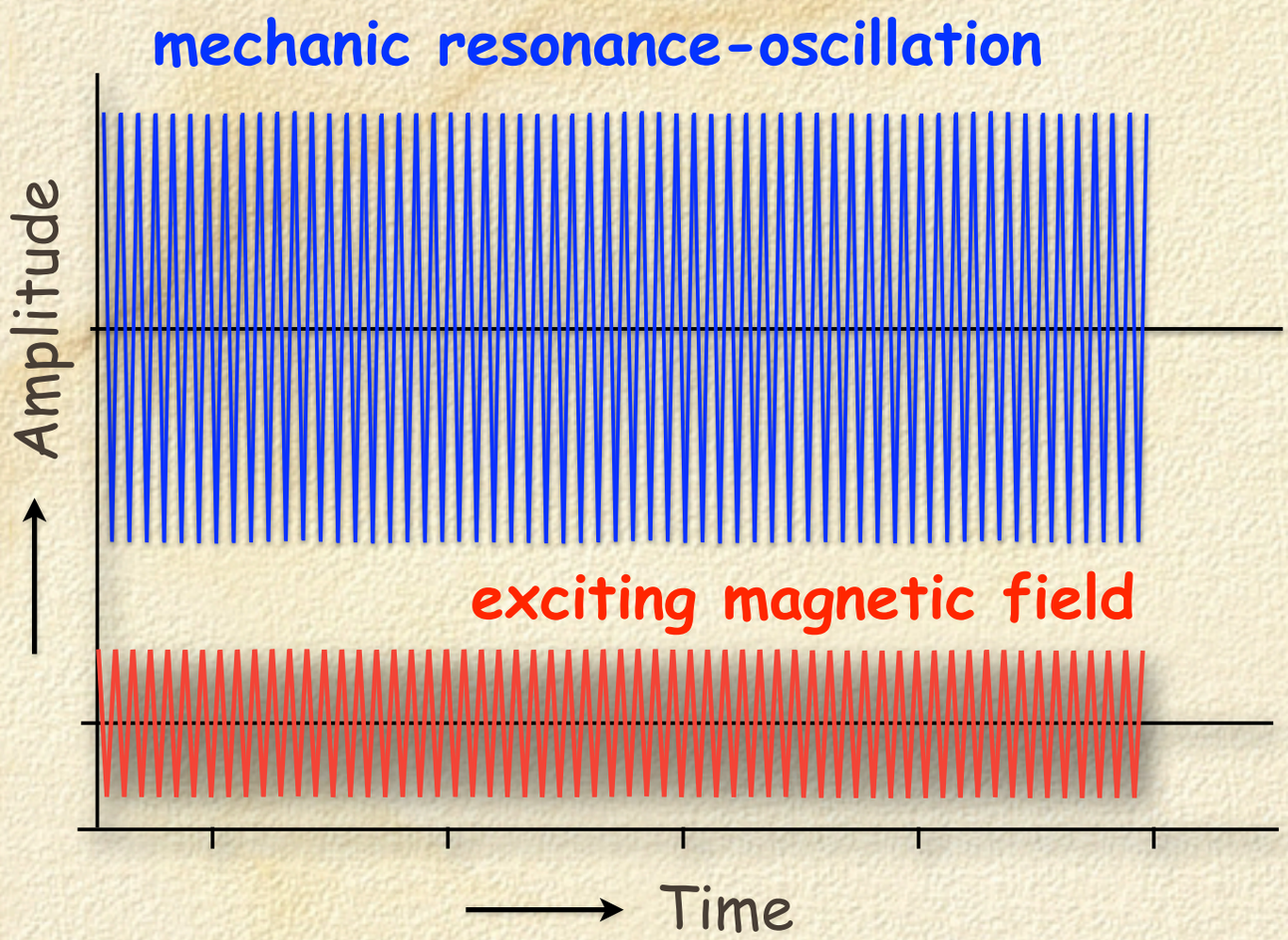

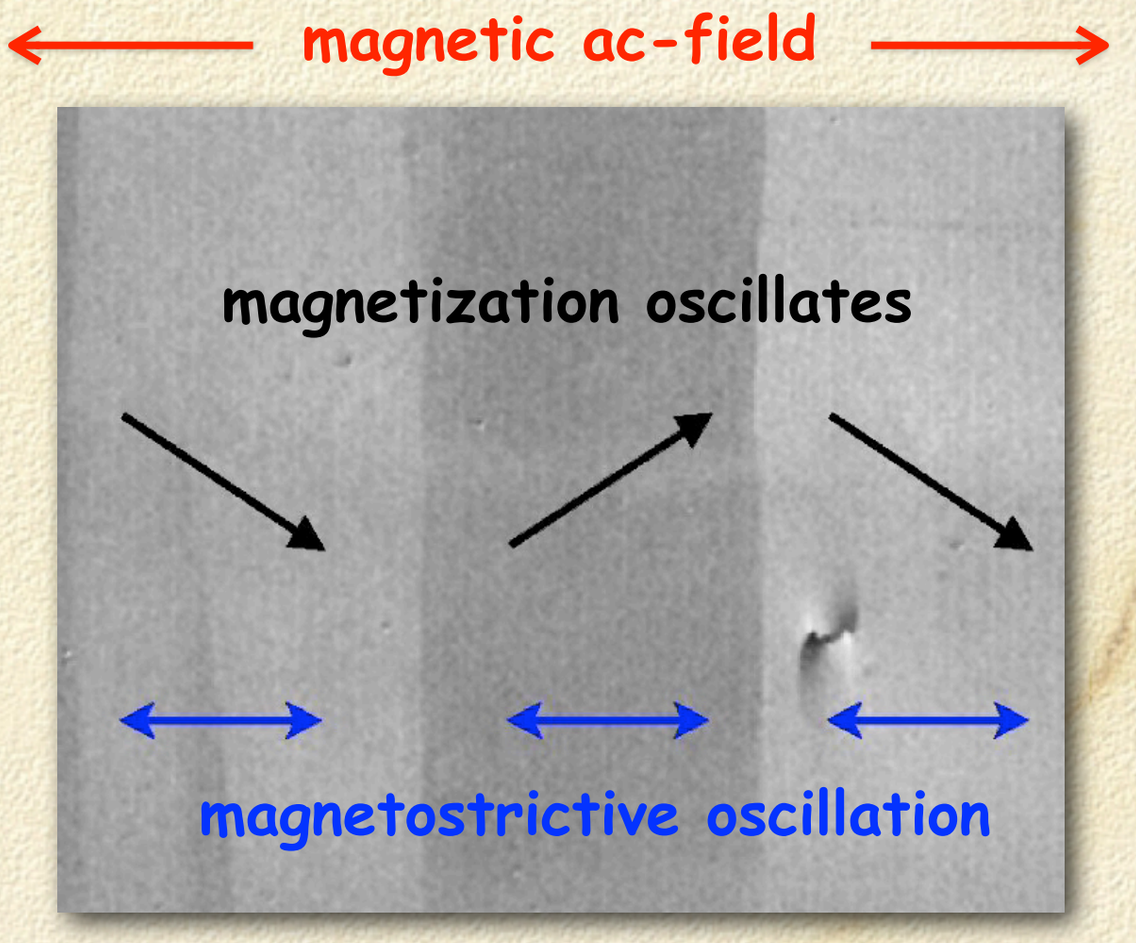

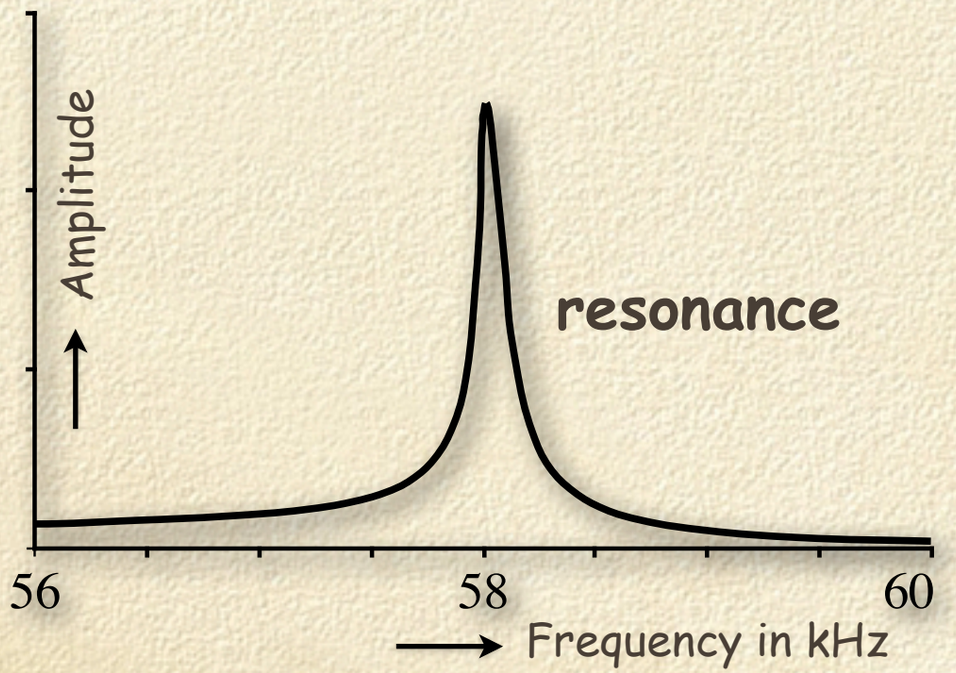

Magneto-acoustic Article Surveillance

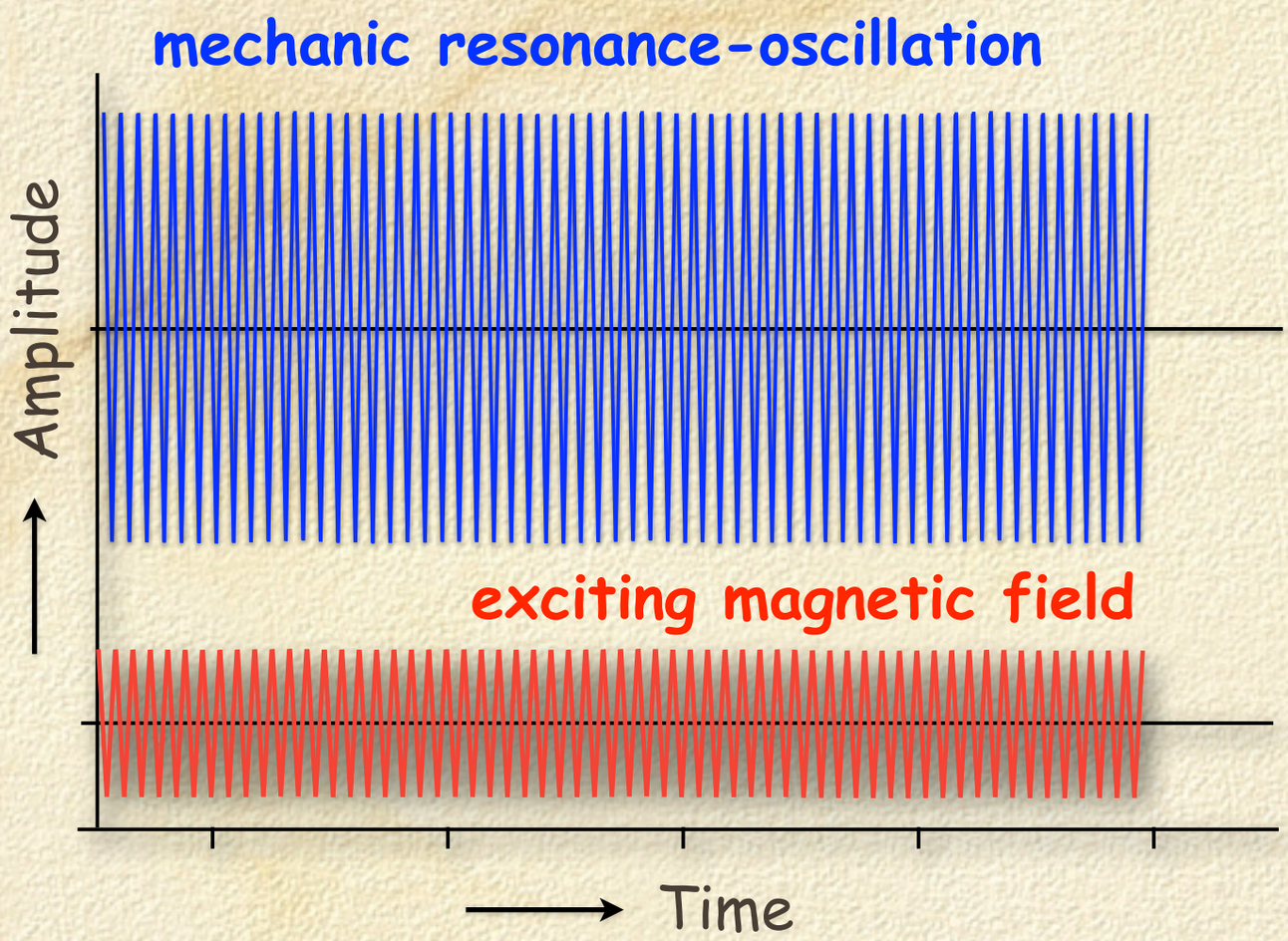

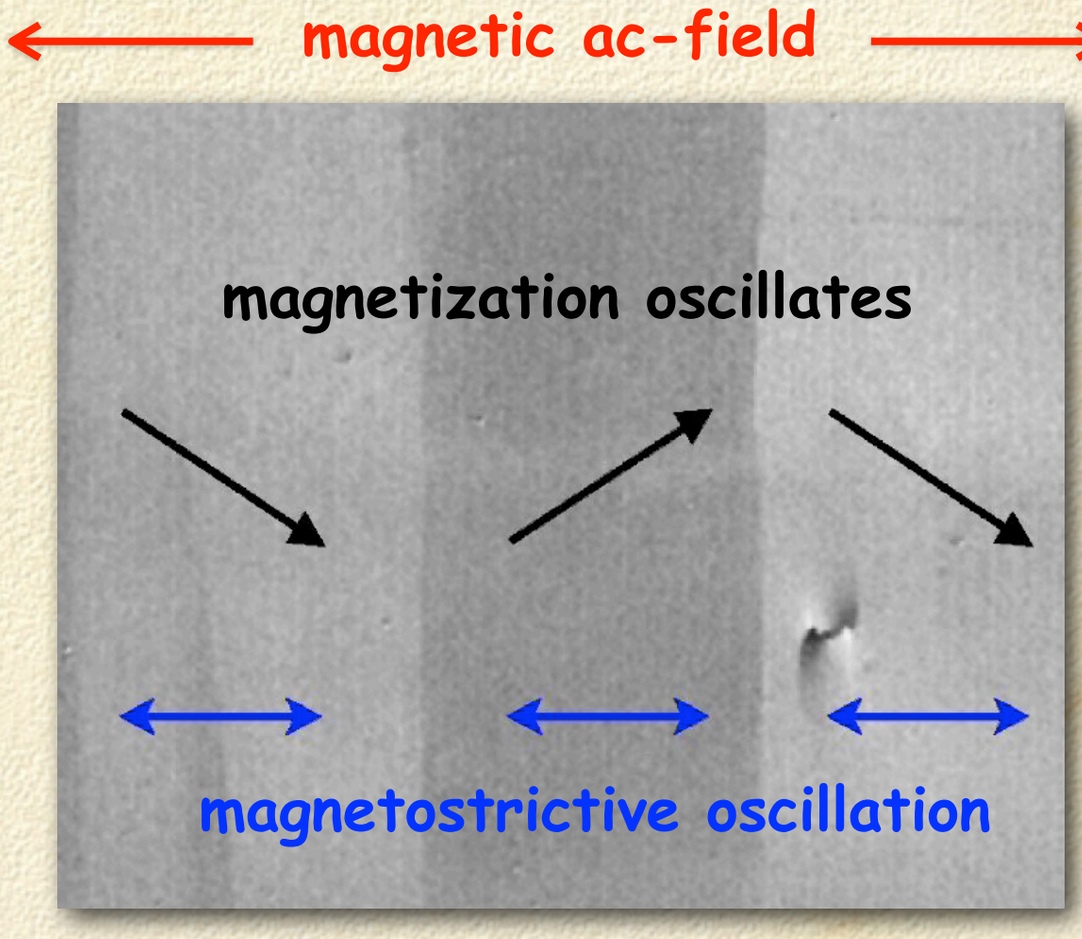

Magneto-acoustic Article Surveillance

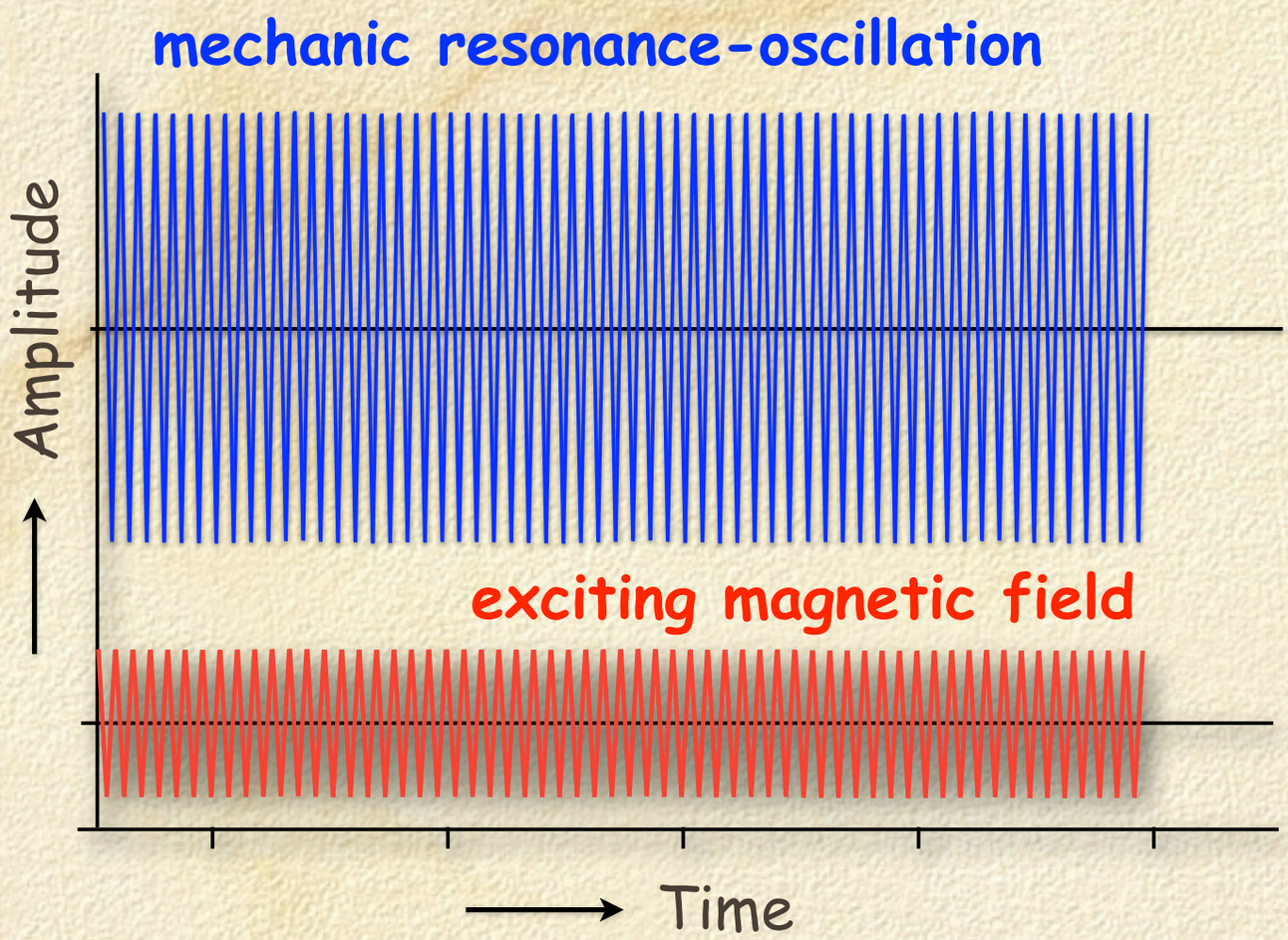

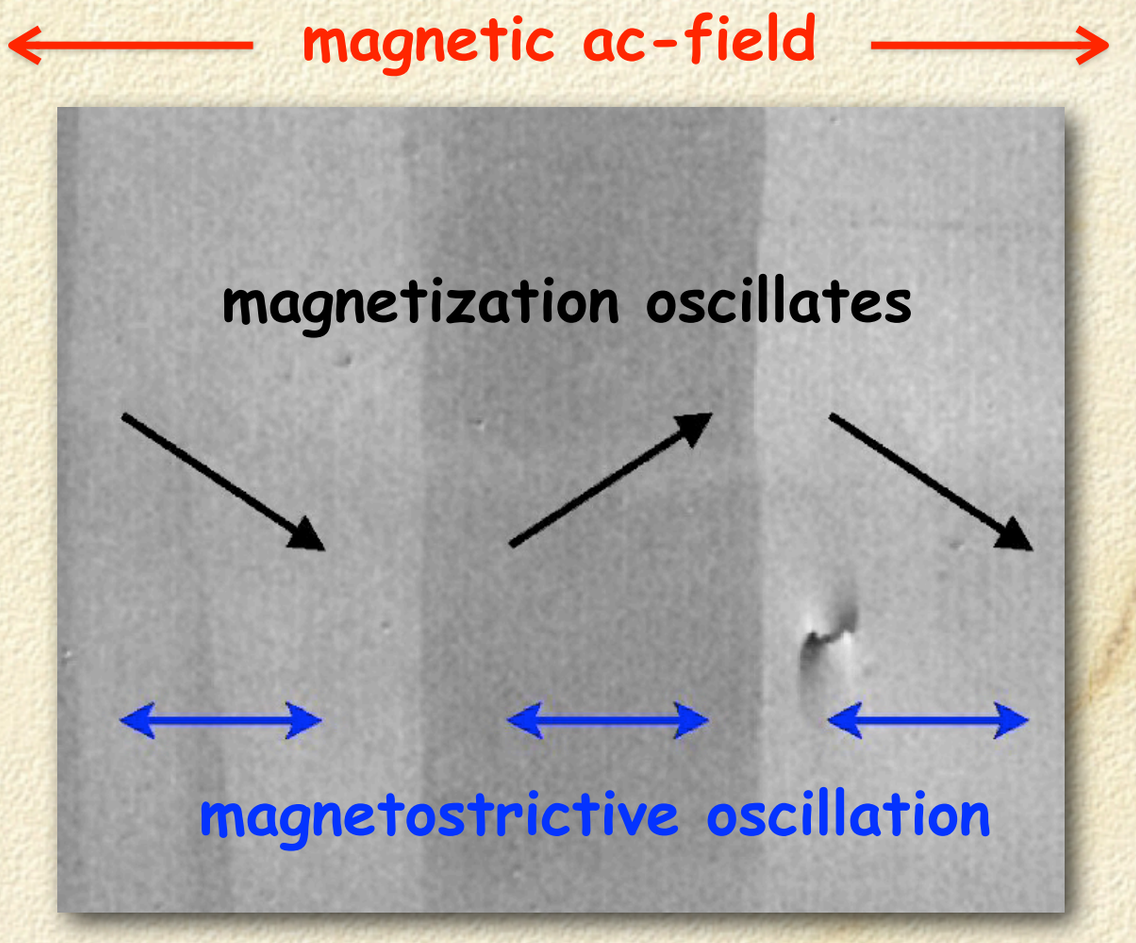

Magneto-acoustic Article Surveillance

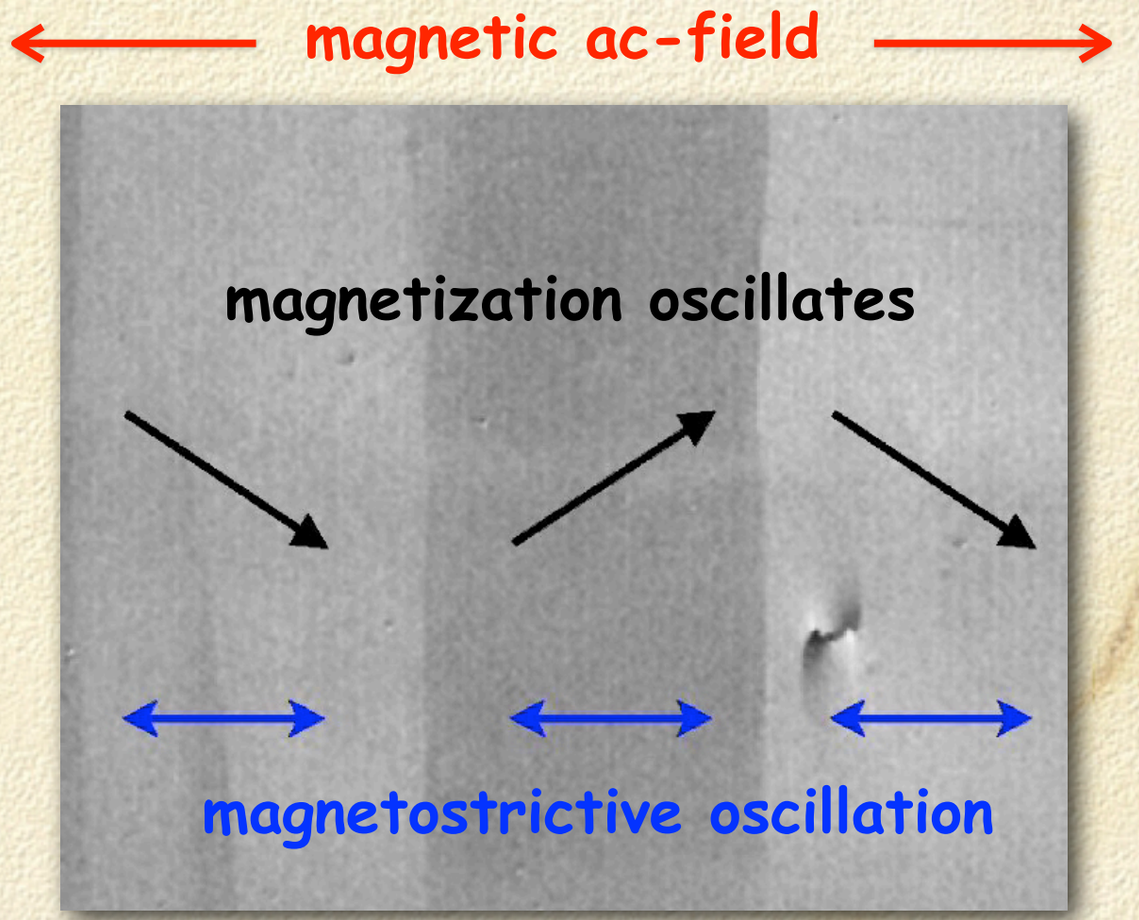

Magneto-acoustic Article Surveillance

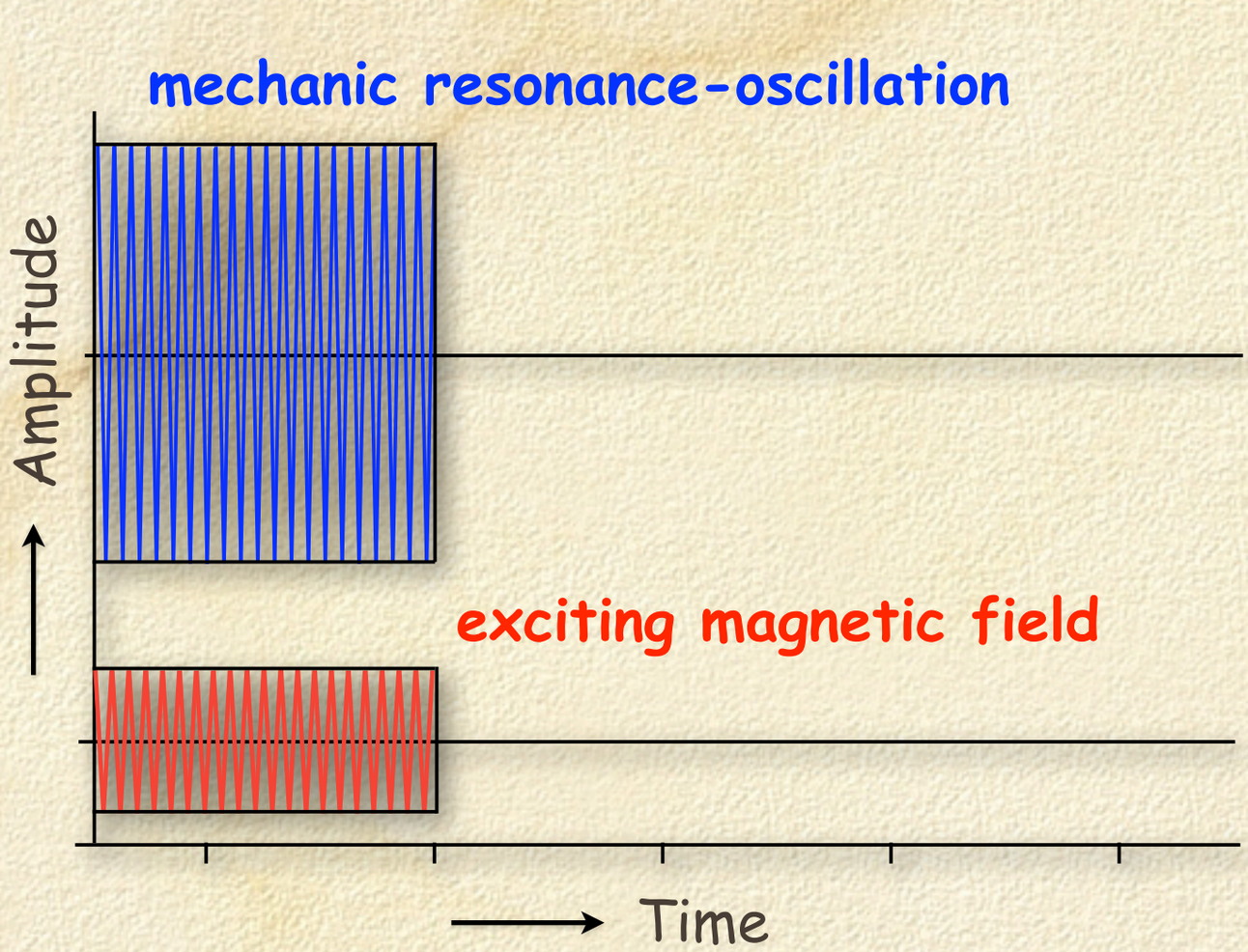

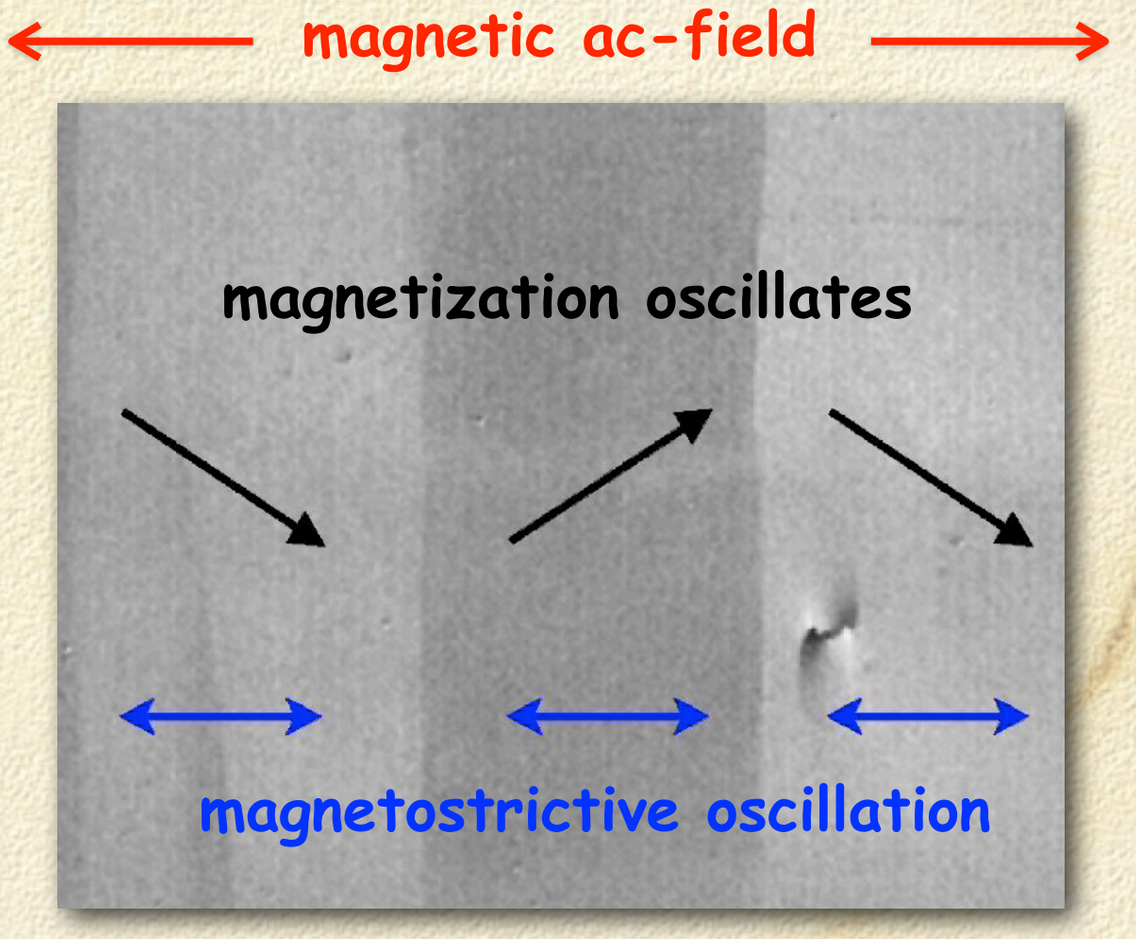

Magneto-acoustic Article Surveillance

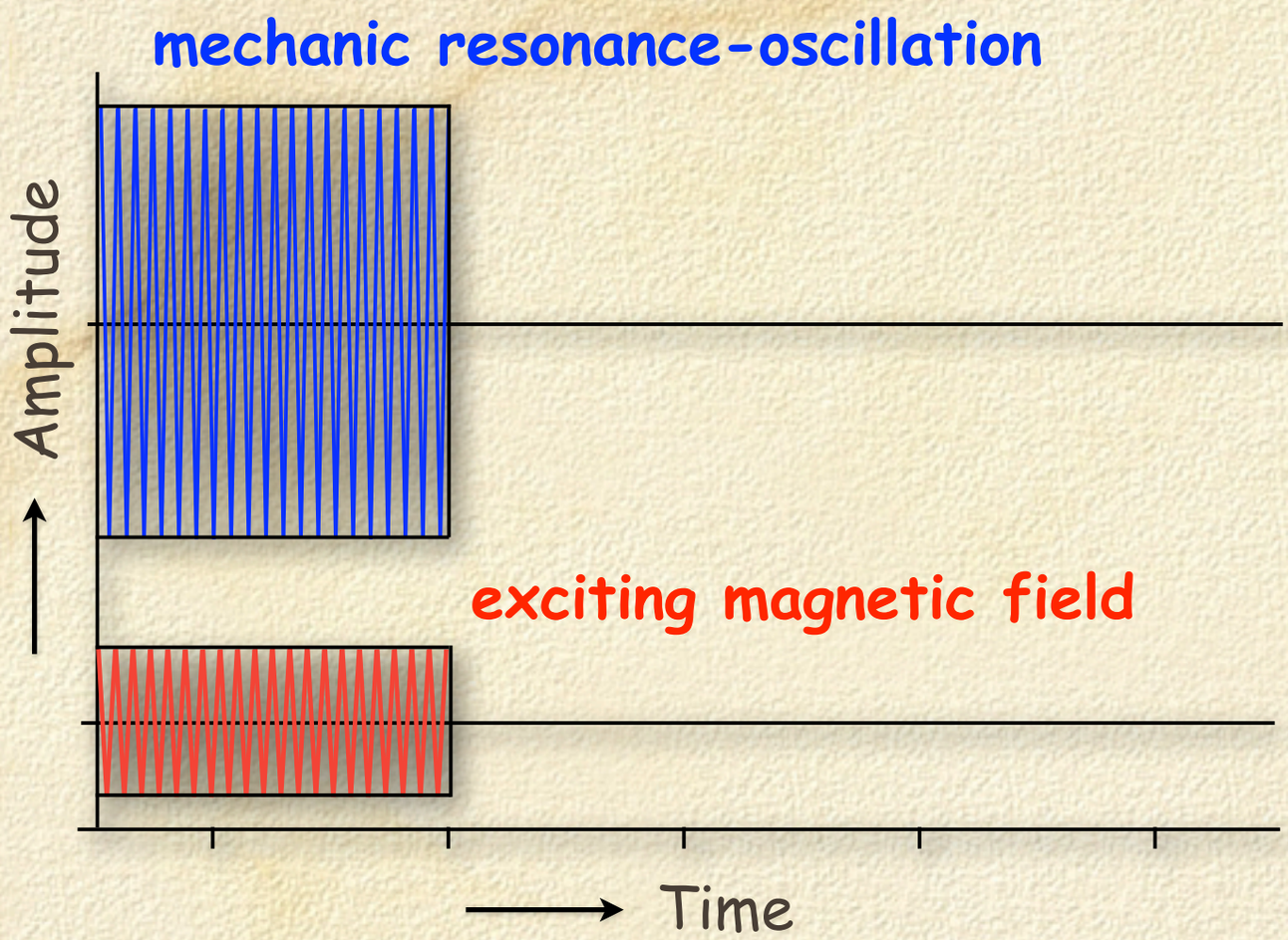

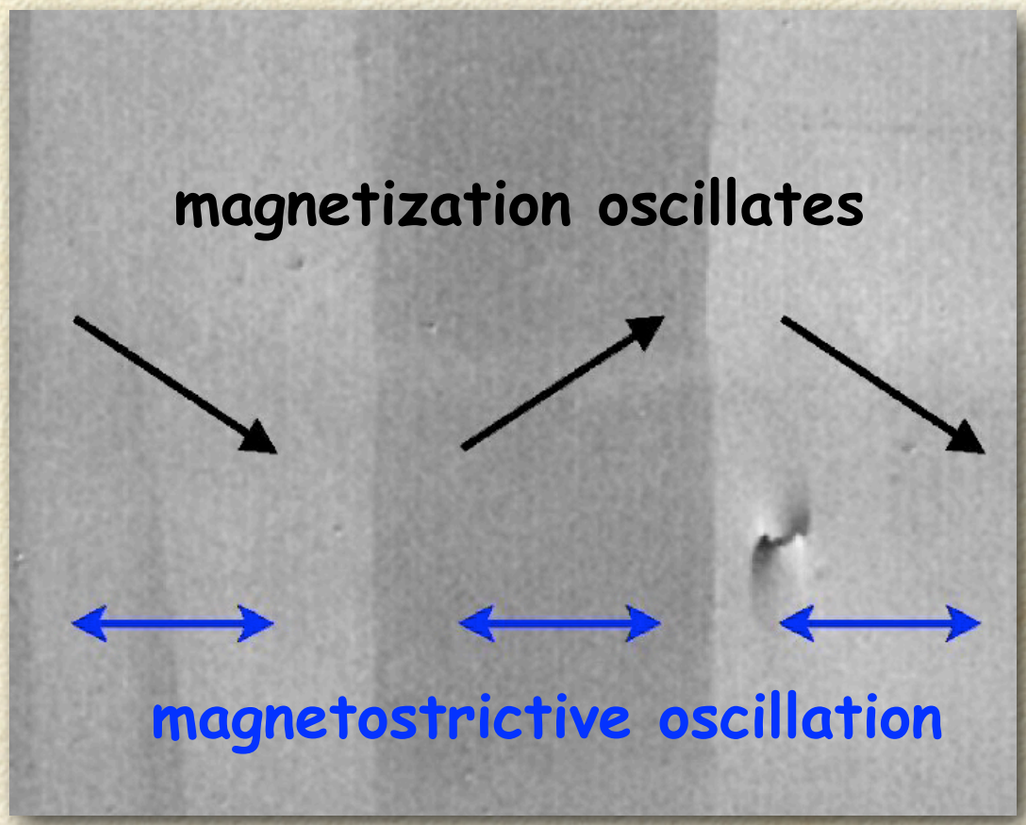

Magneto-acoustic Article Surveillance

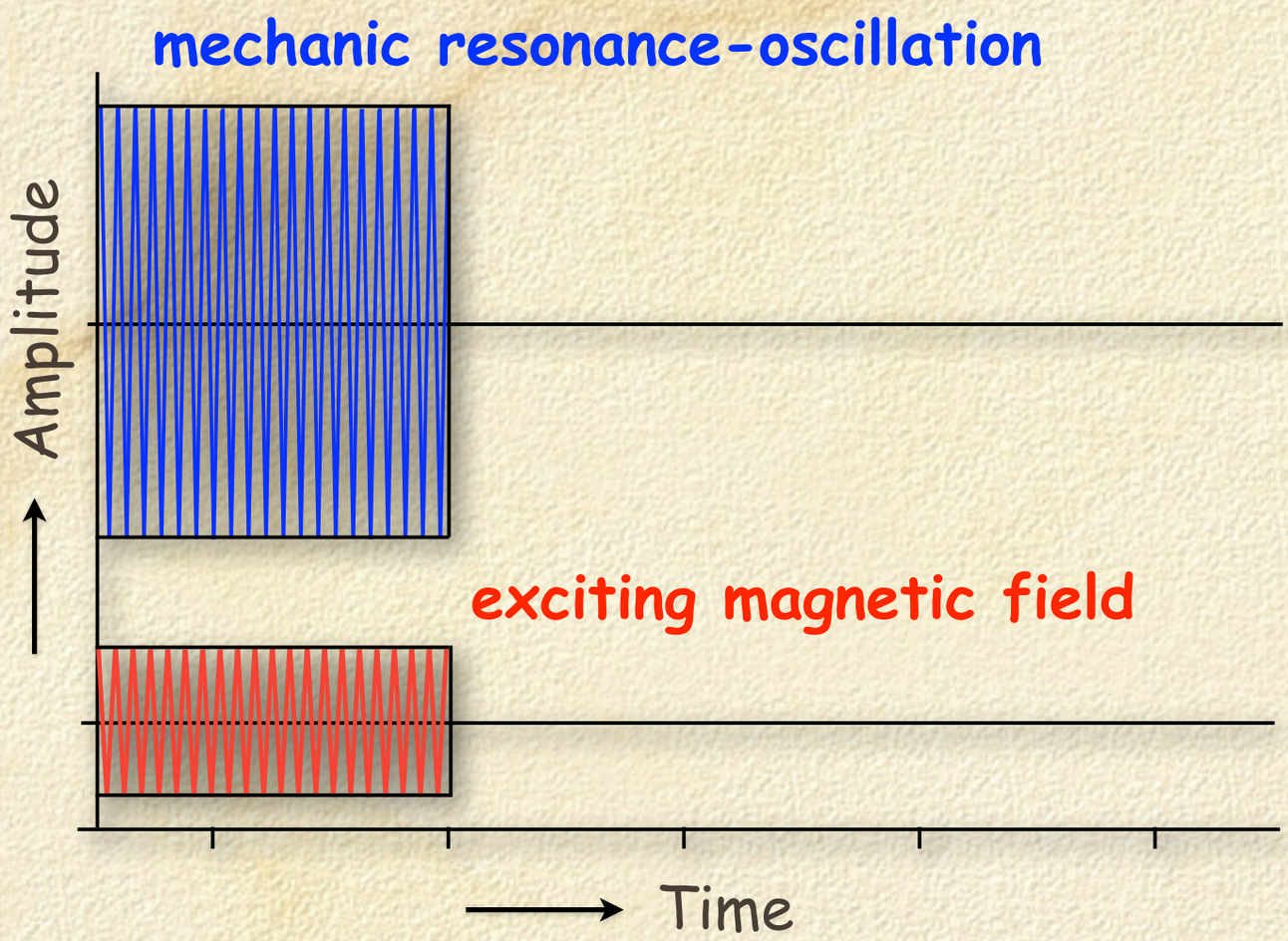

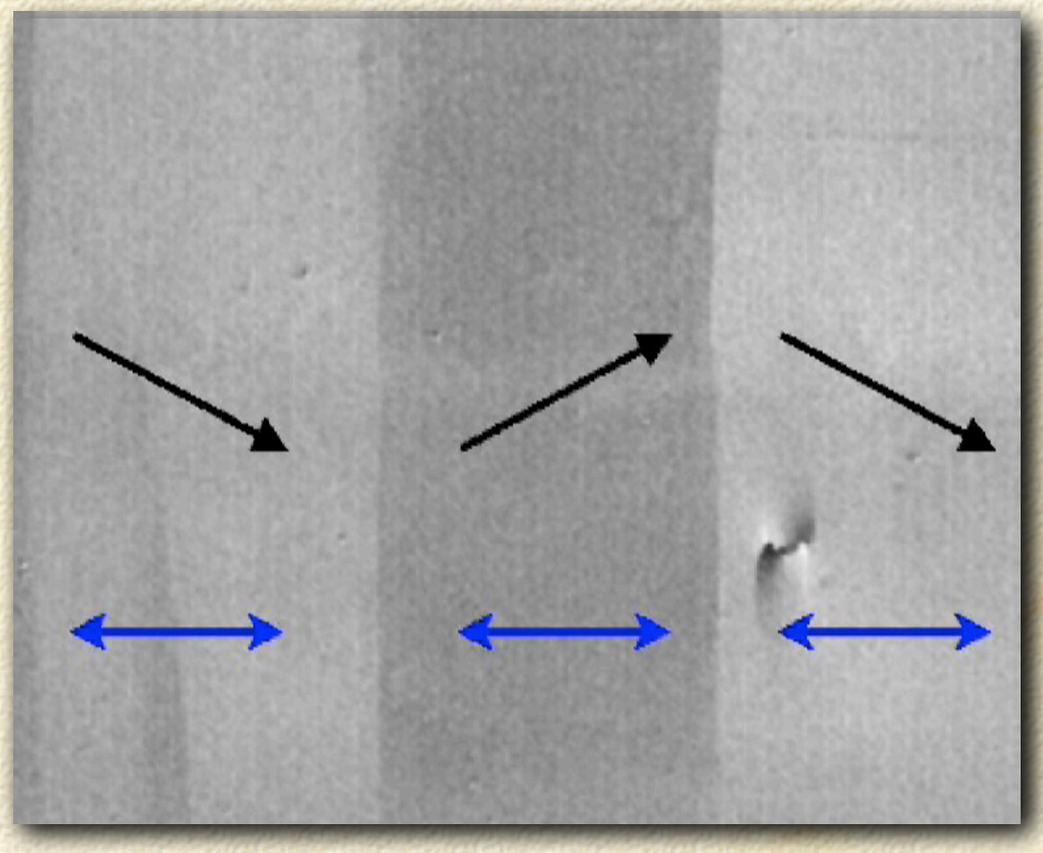

Magneto-acoustic Article Surveillance

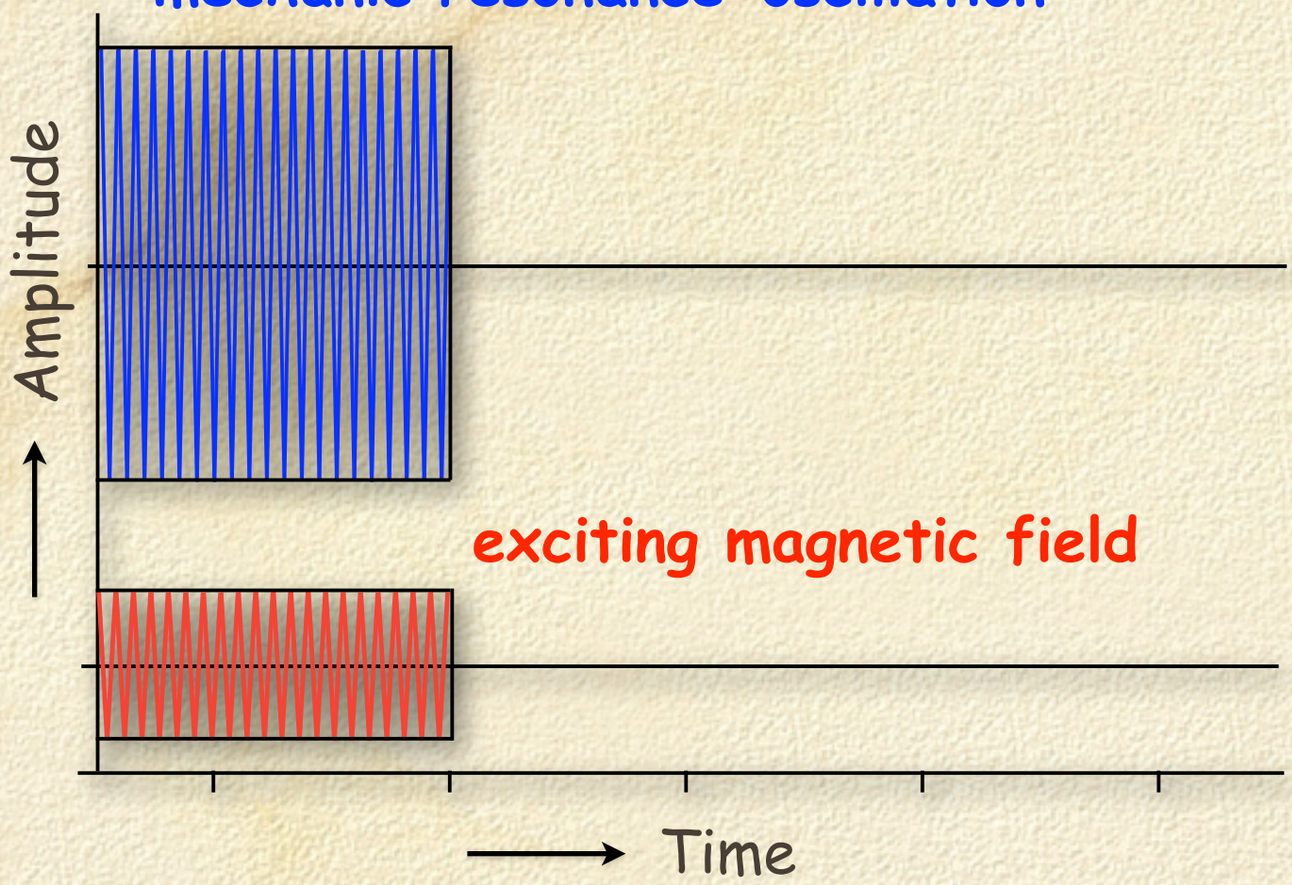

after switching-off pulse

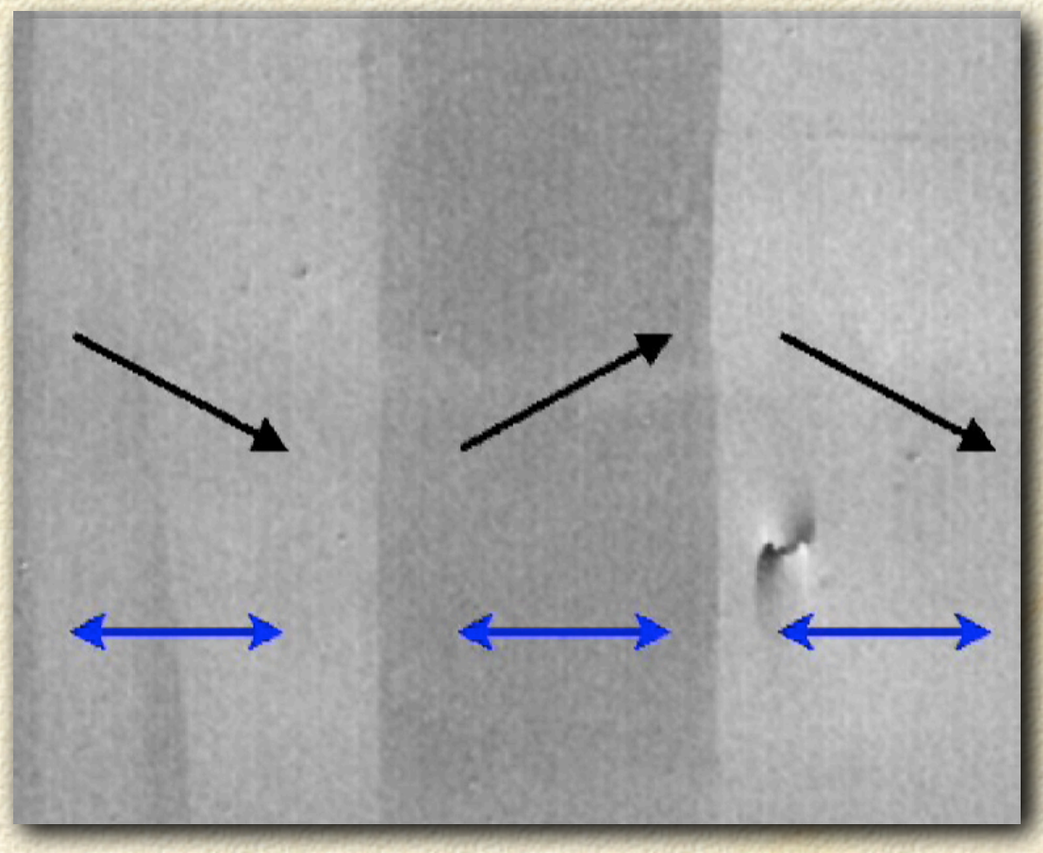

Magneto-acoustic Article Surveillance

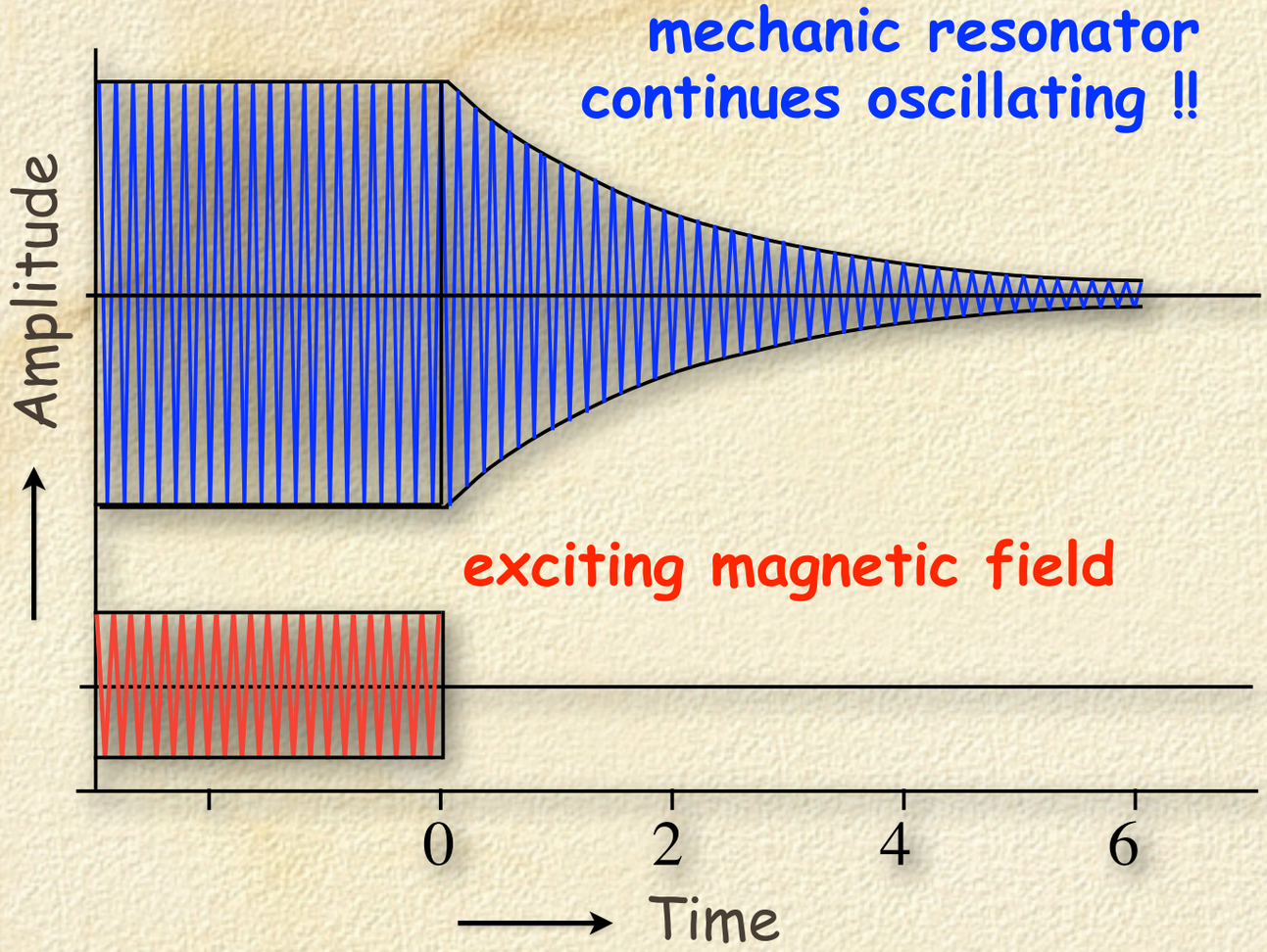

after switching-off pulse

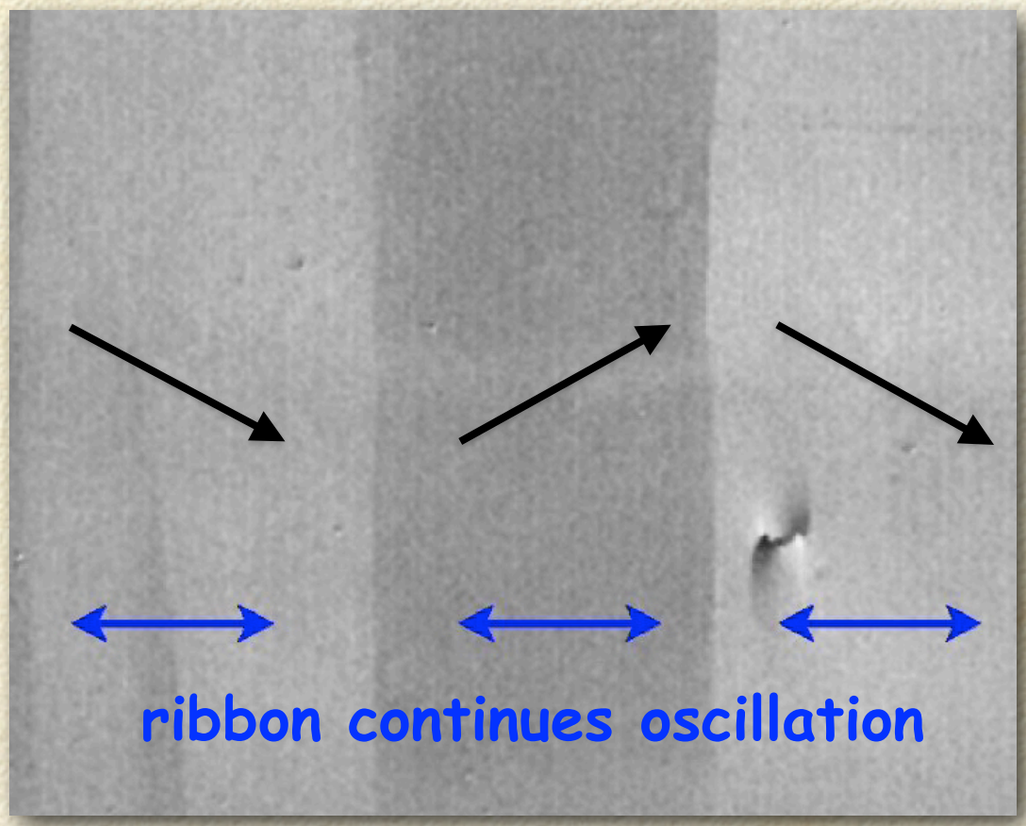

Magneto-acoustic Article Surveillance

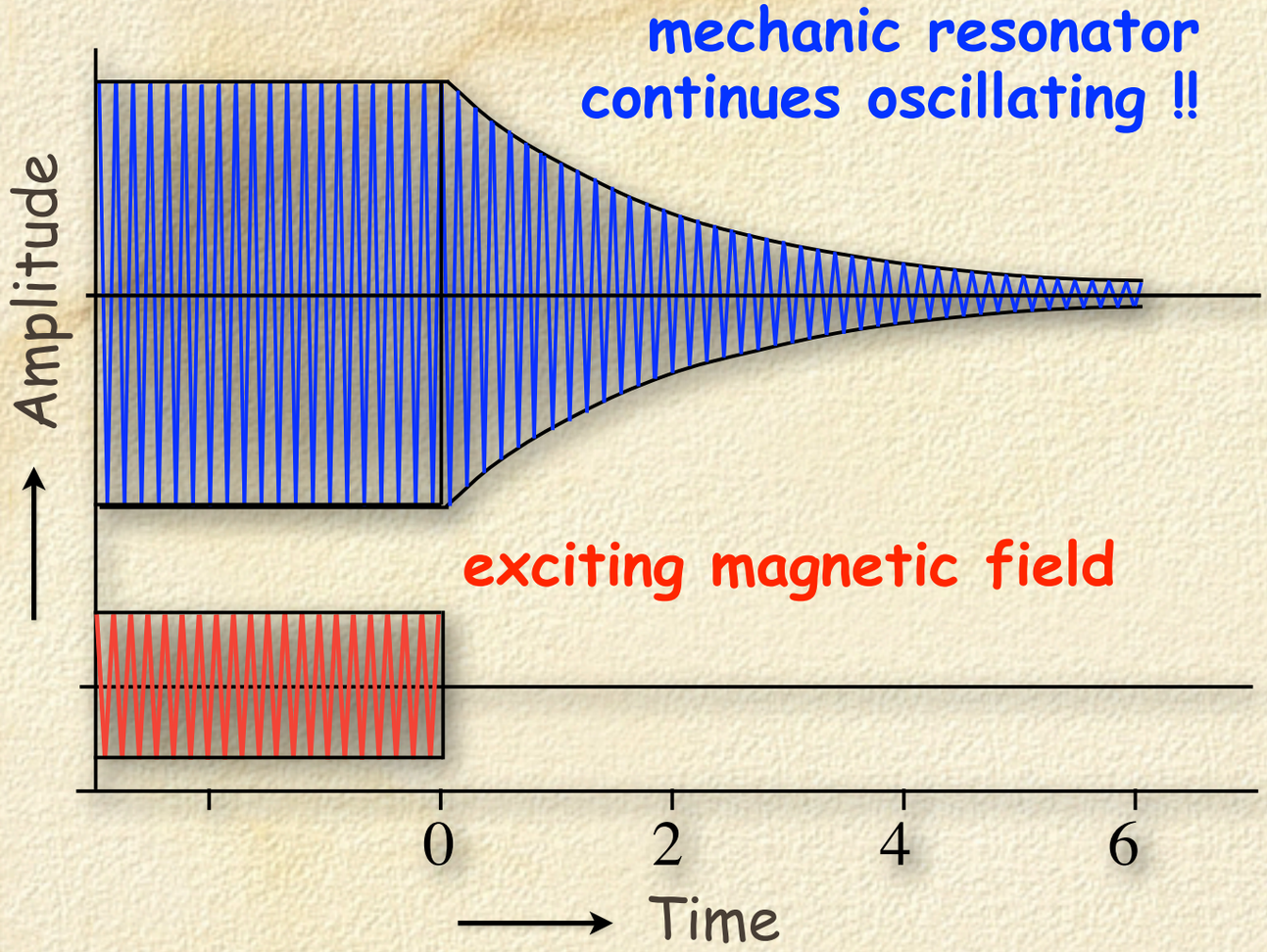

after switching-off pulse

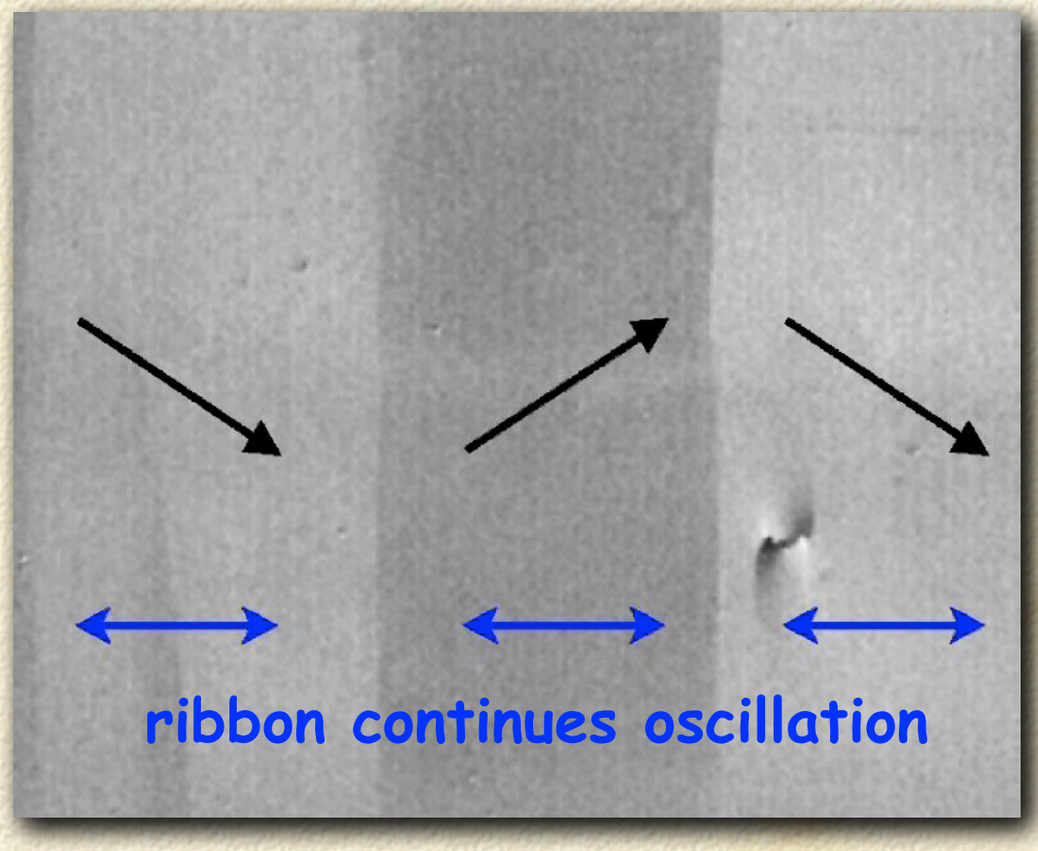

Magneto-acoustic Article Surveillance

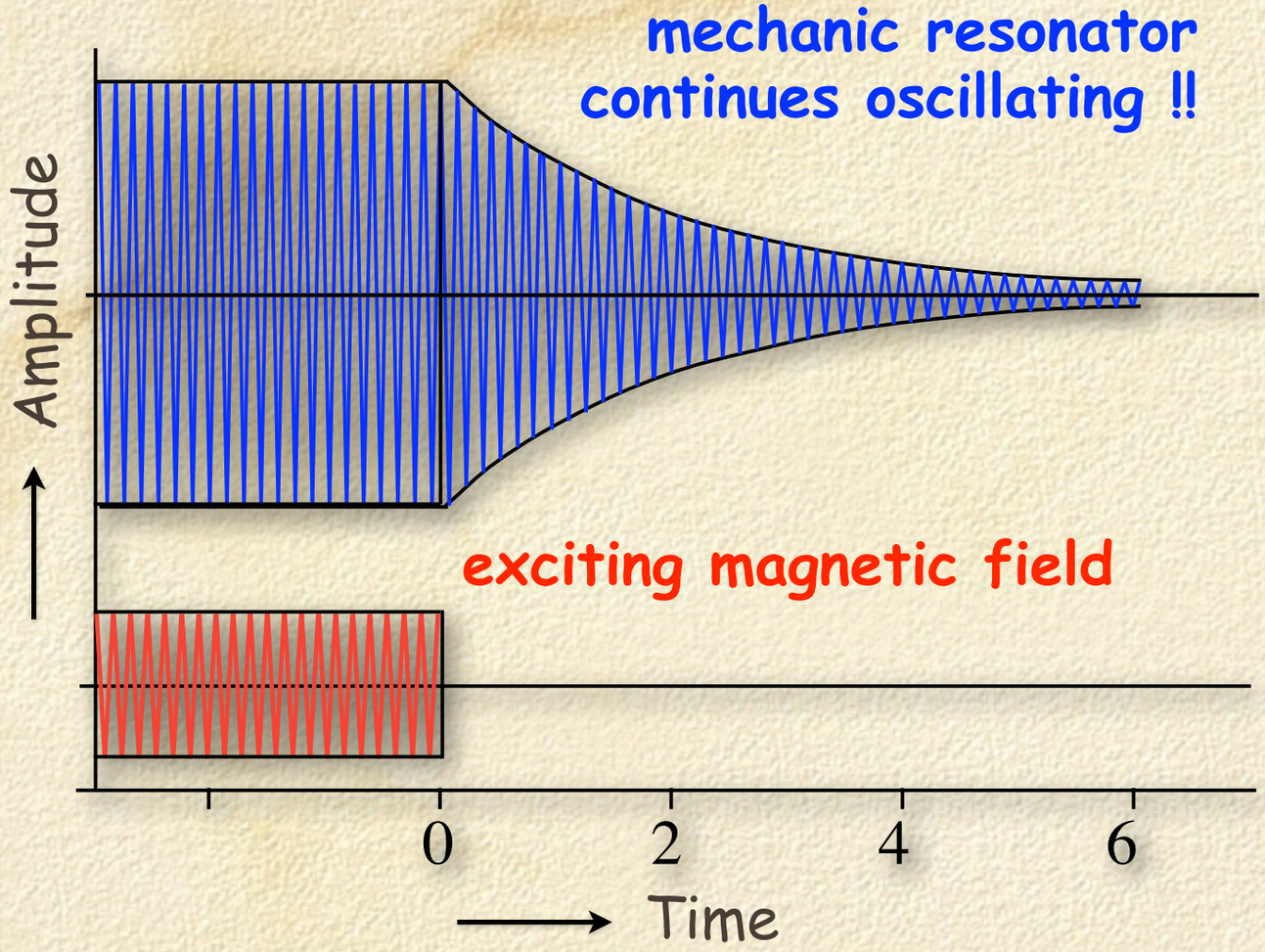

after switching-off pulse

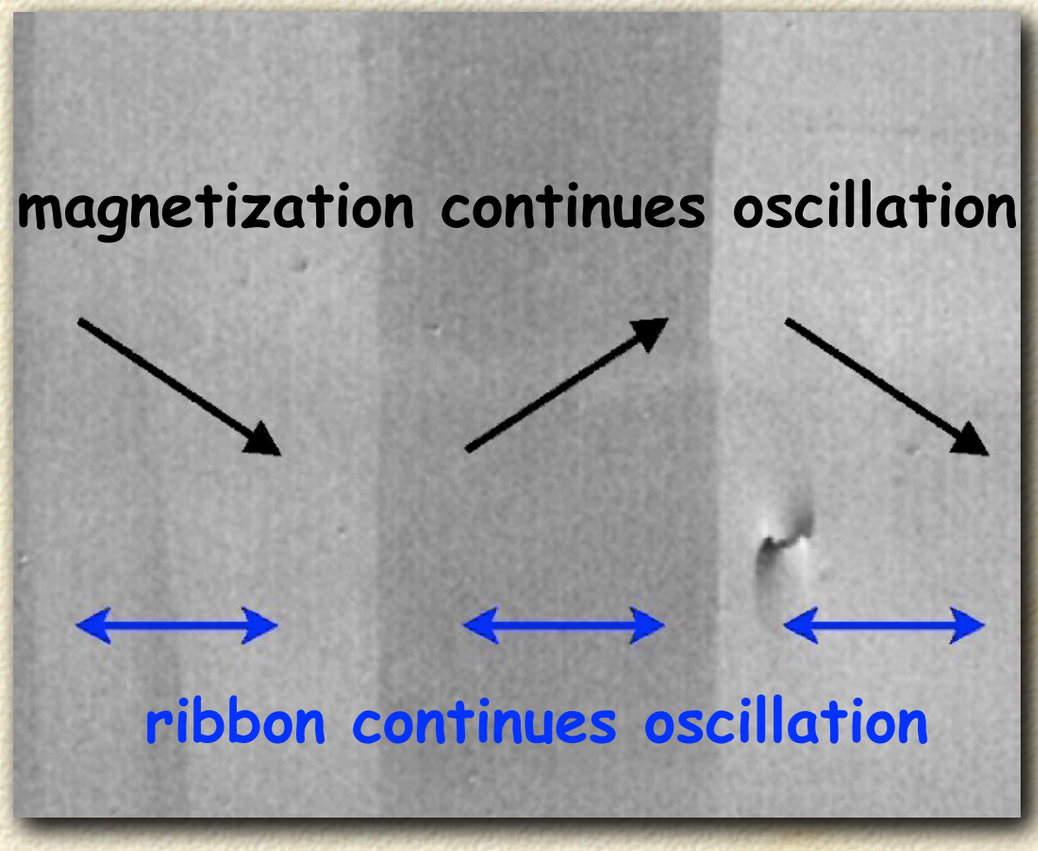

Induction-signal after
switching-off field pulse

Alarm

Magneto-acoustic Article Surveillance

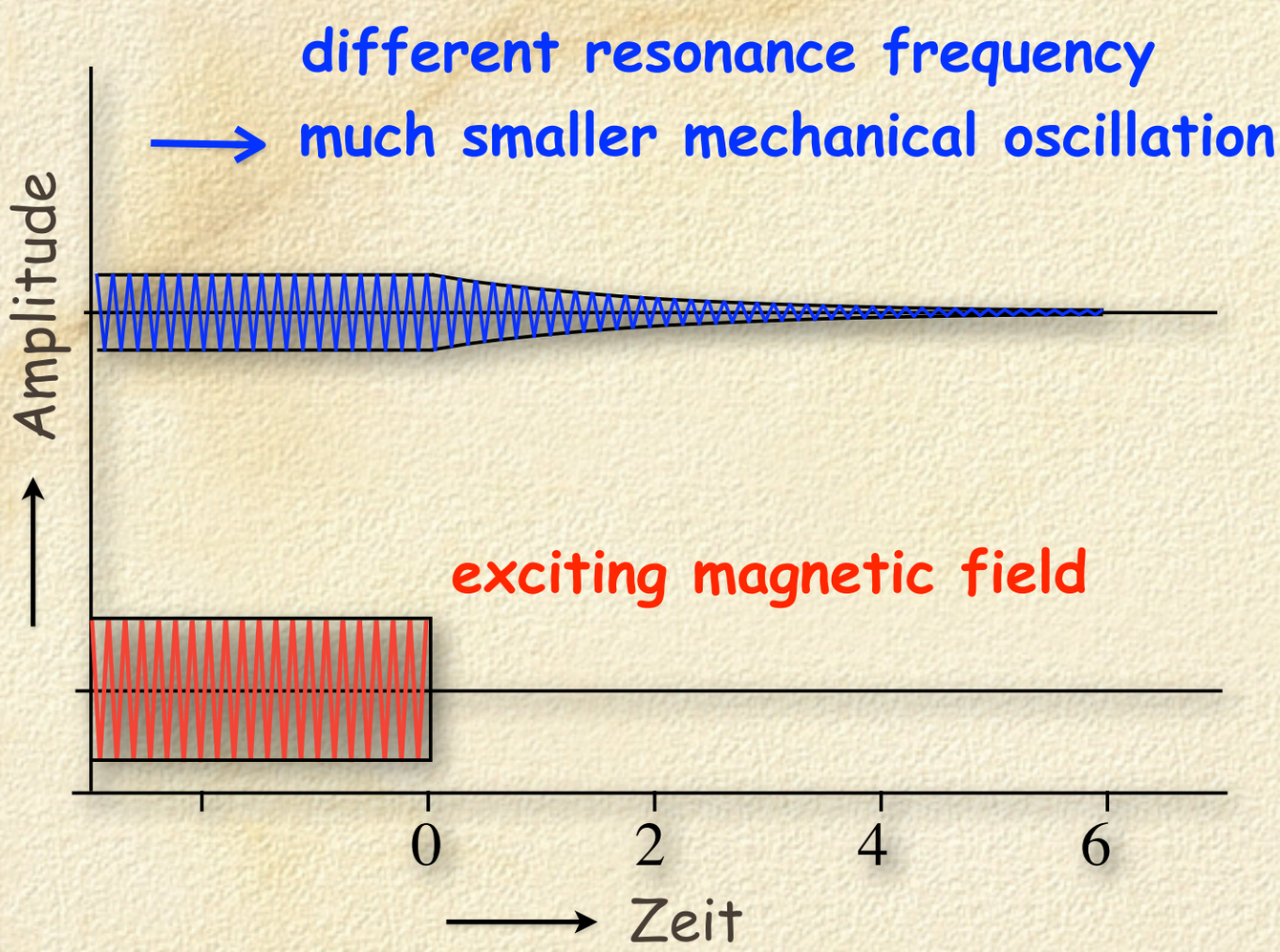

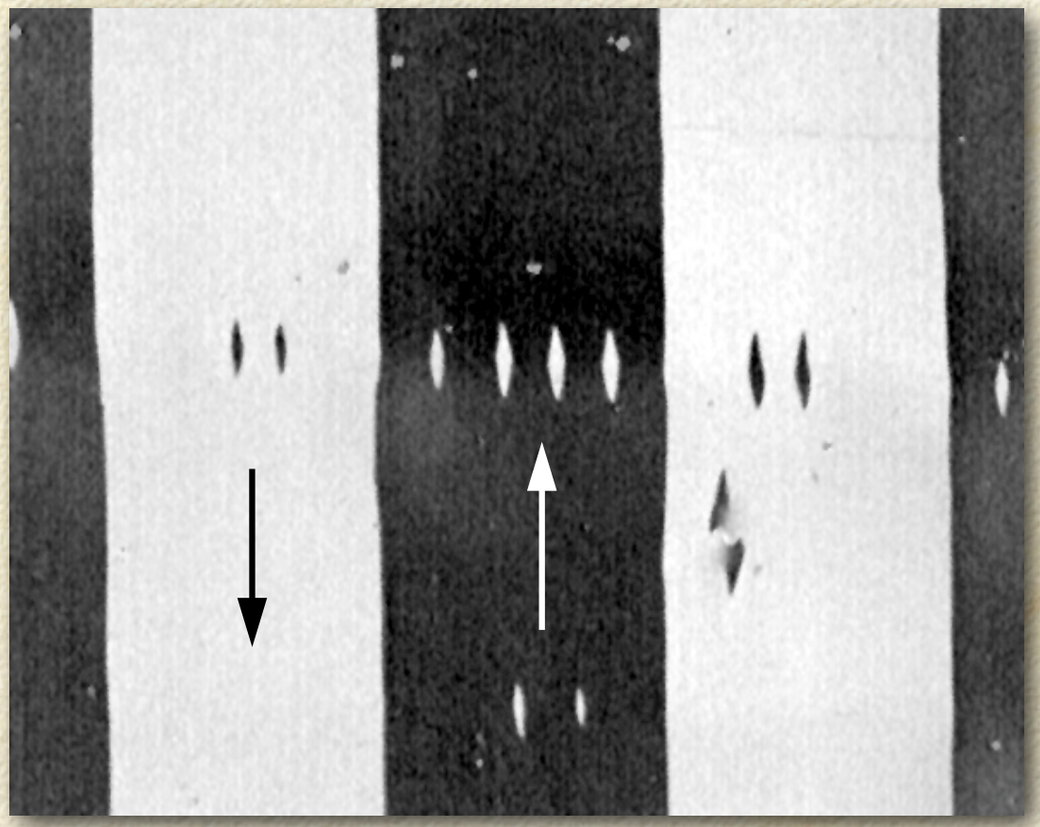

after deactivation

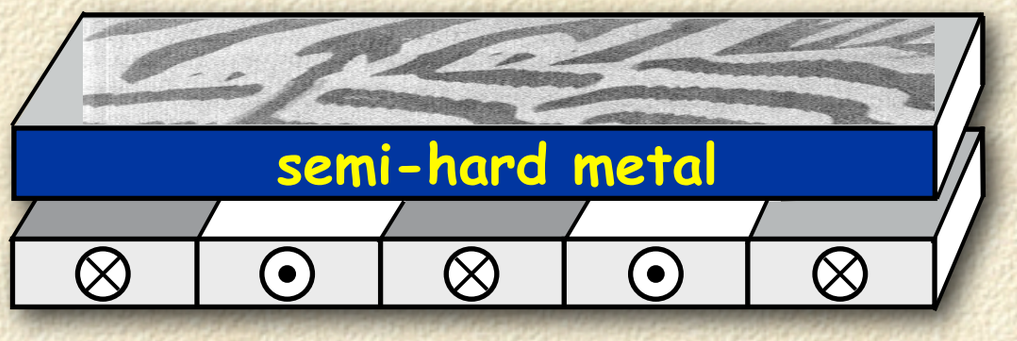

Magnetic Energies

Exchange energy

$e_A = 0$

$e_A > 0$

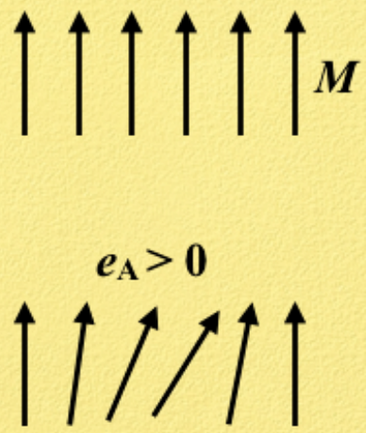

Stray field energy

$$\operatorname{div} \boldsymbol{H}_d = -\operatorname{div} \boldsymbol{M}$$

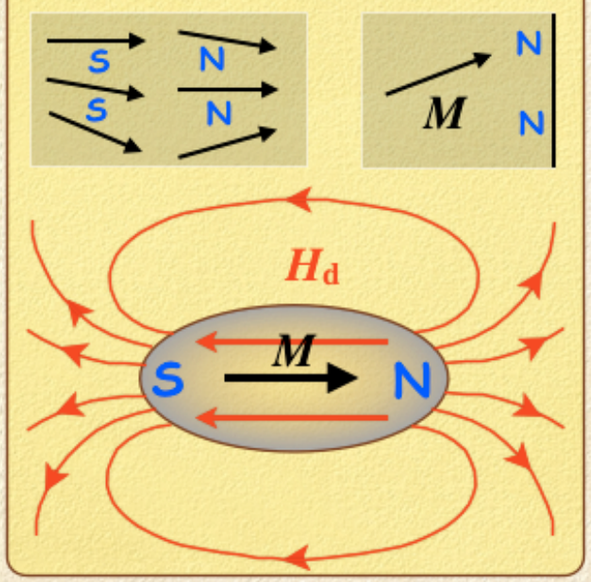

Magnetostrictive self energy

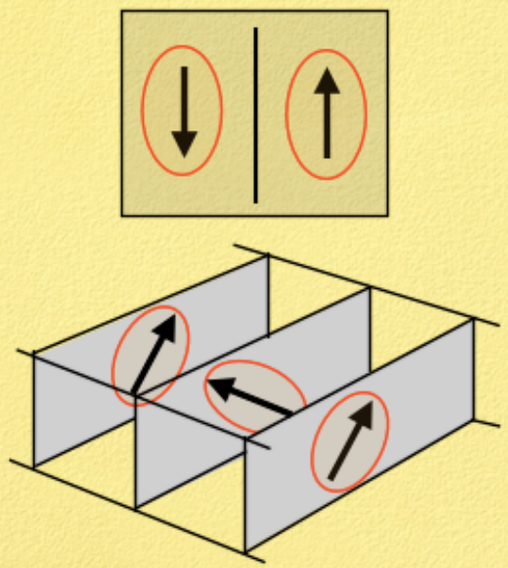

External stress energy

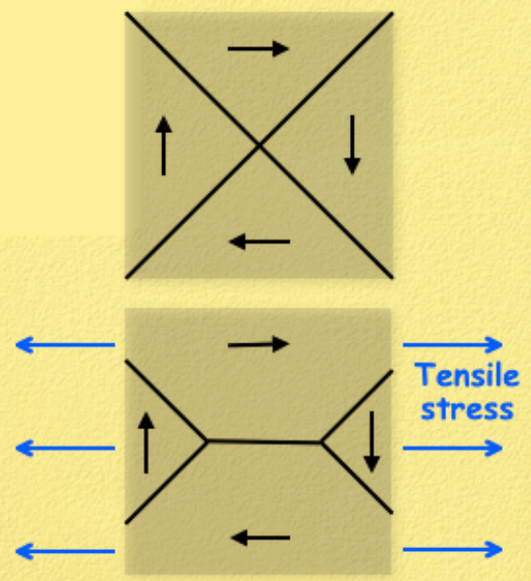

Anisotropy energy

Easy axis

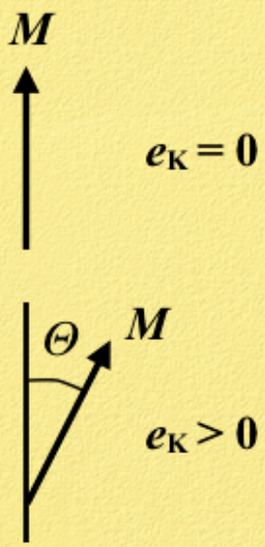

External field energy

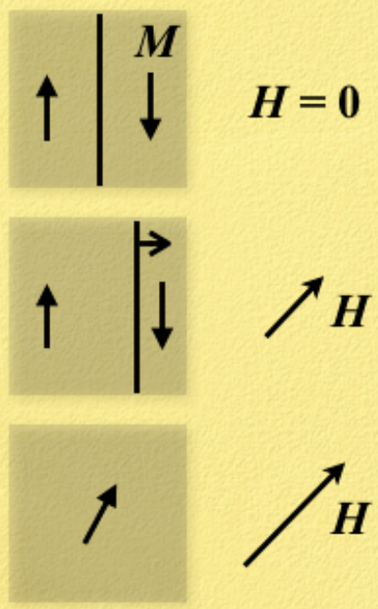

Magnetic Energies

Exchange energy

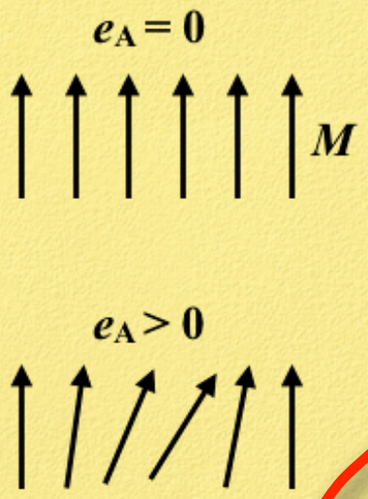

Stray field energy

$$\text{div}\, \boldsymbol{H}_d = -\,\text{div}\, \boldsymbol{M}$$

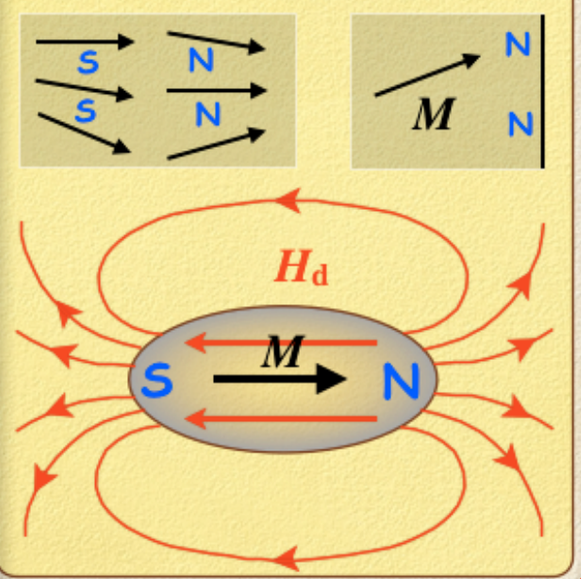

Magnetostrictive self energy

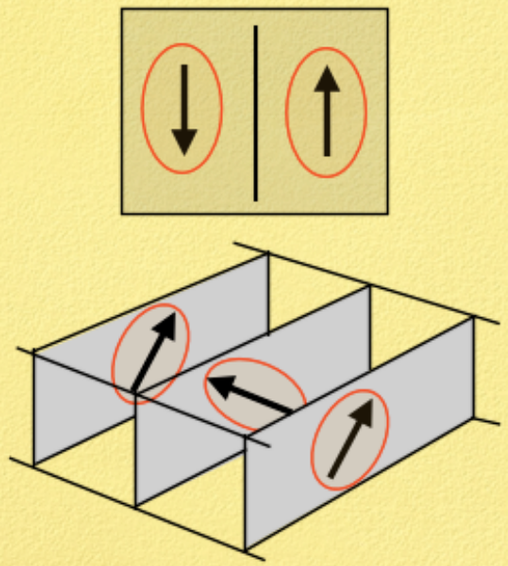

External stress energy

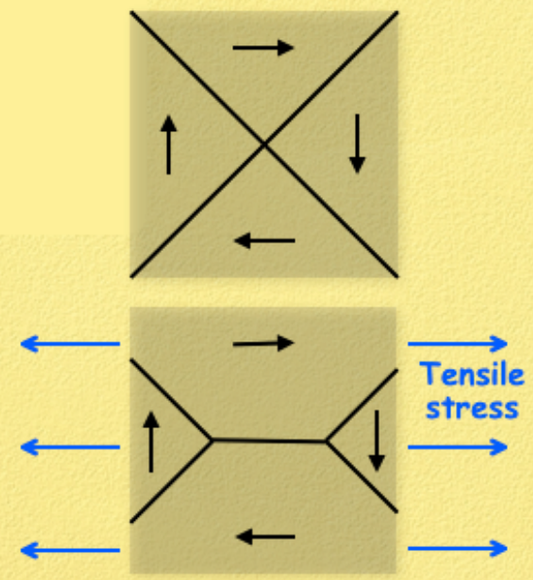

Anisotropy energy

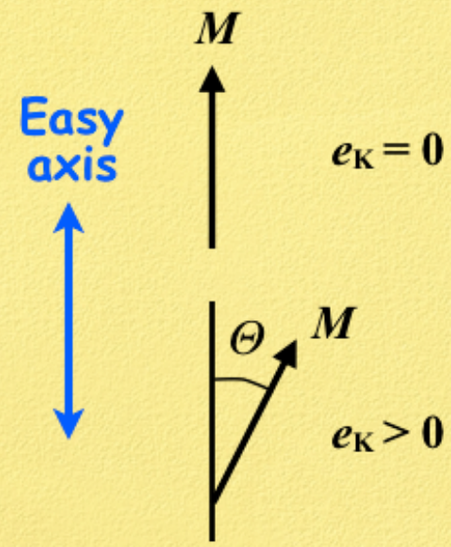

External field energy

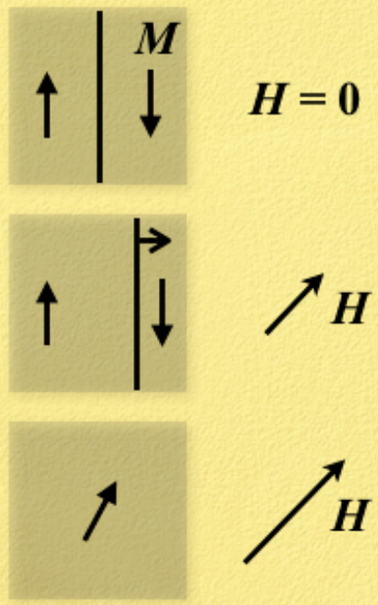

Magnetic Energies

Exchange energy

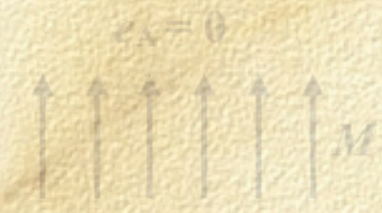

Stray field energy

$$\operatorname{div} H_0 = -\operatorname{div} M$$

Magnetostrictive self energy

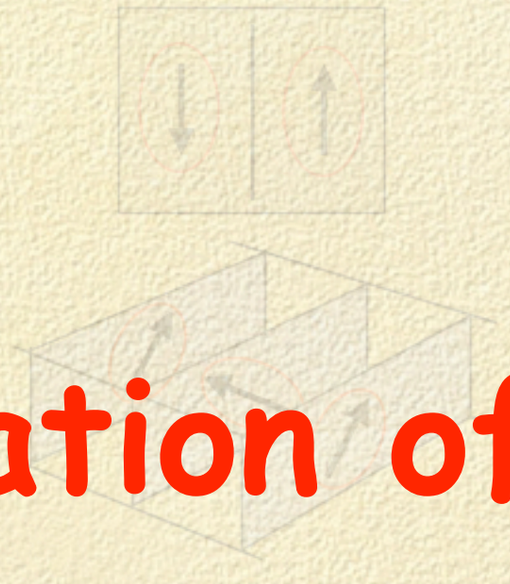

External stress energy

Anisotropy energy

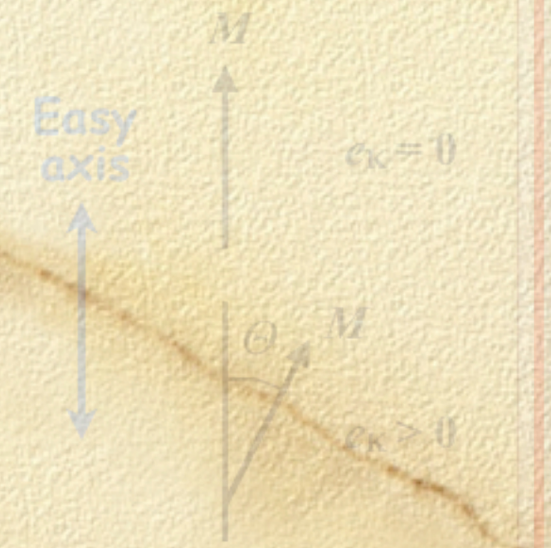

External field energy

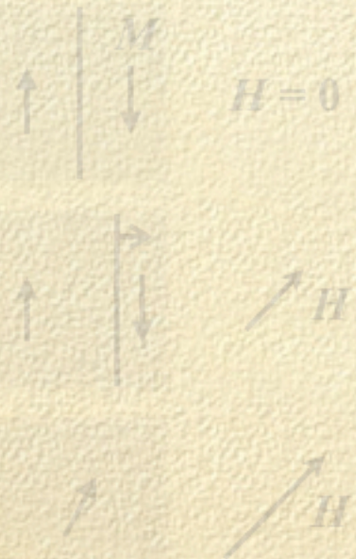

General Classification of Domains

General Classification of Domains

$$Q = \frac{\text{Anisotropy constant } K}{\text{Stray-field energy coefficient } (K_d = \mu_0 M_S^2/2)}$$

$Q >> 1$

Anisotropy energy dominates

↓

avoid anisotropy energy

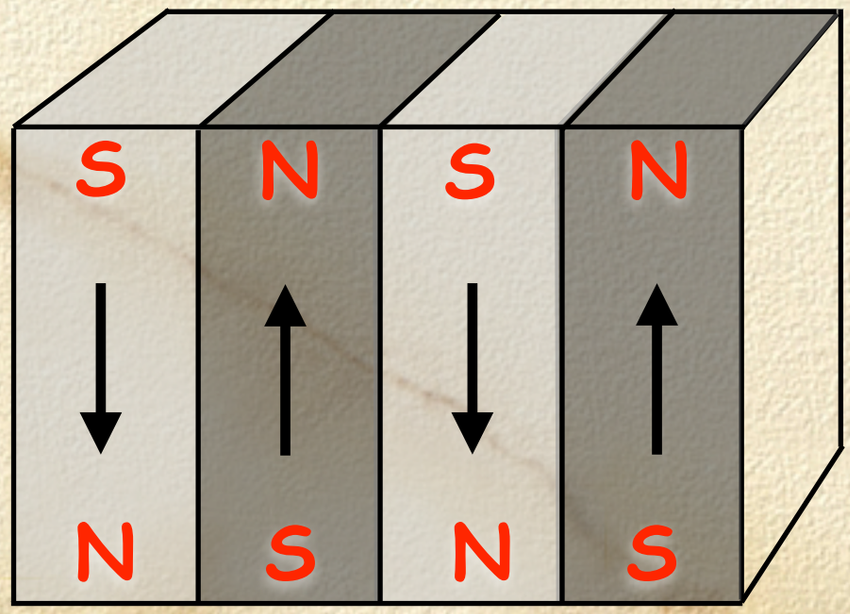

Anisotropy axis (uniaxial)

$Q << 1$

Stray-field energy dominates

↓

avoid stray-field energy

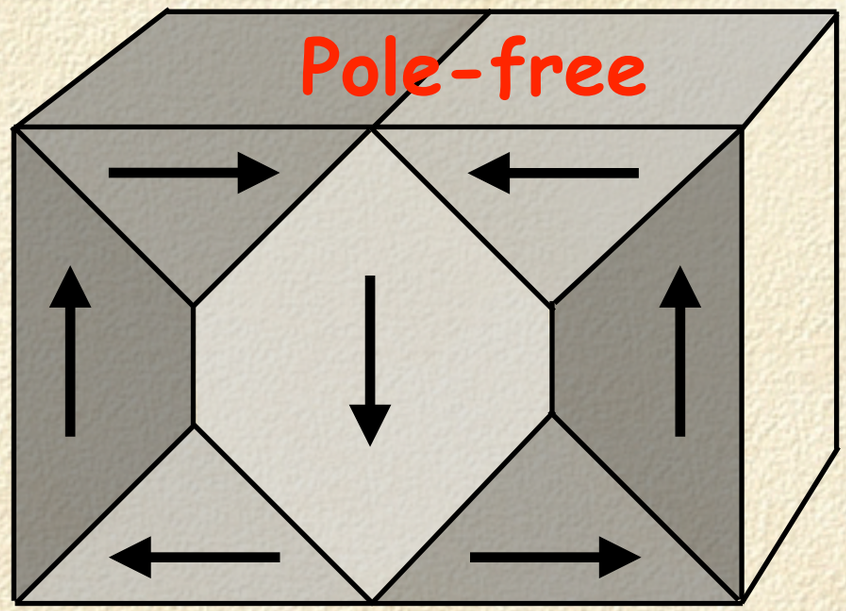

General Classification of Domains

$$Q = \frac{\text{Anisotropy constant } K}{\text{Stray-field energy coefficient } (K_d = \mu_0 M_S^2/2)}$$

Excursus

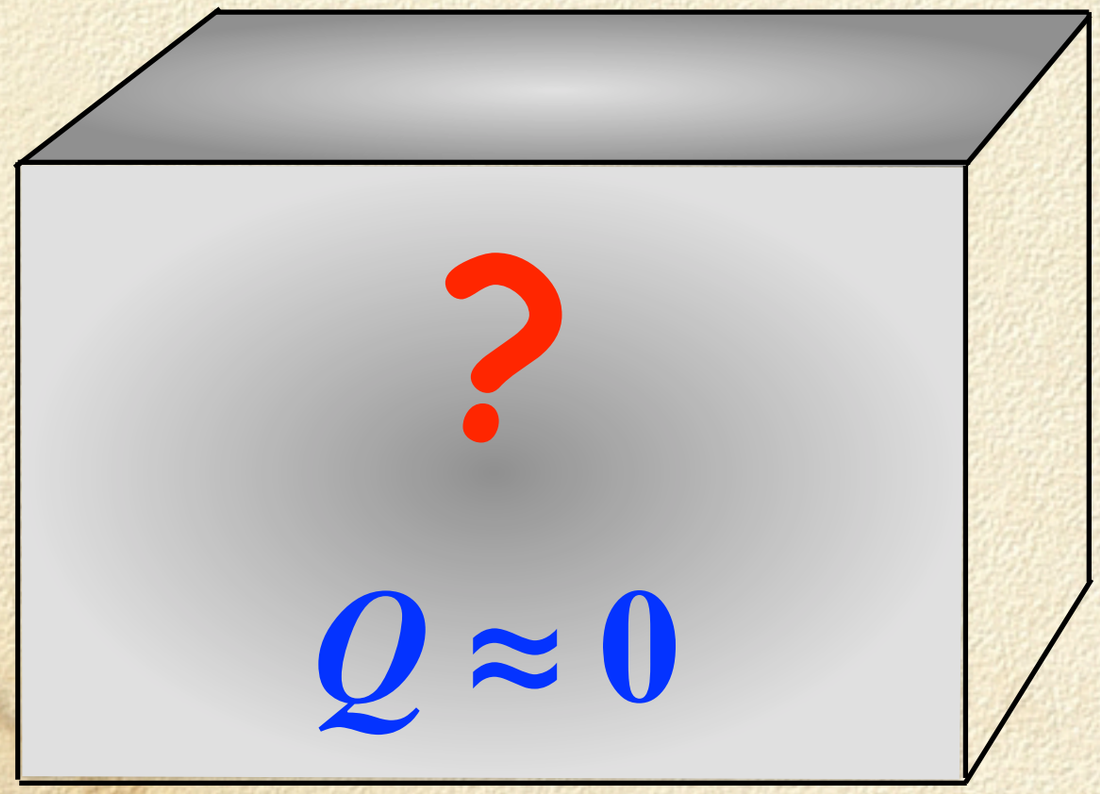

Excursus: Q = 0

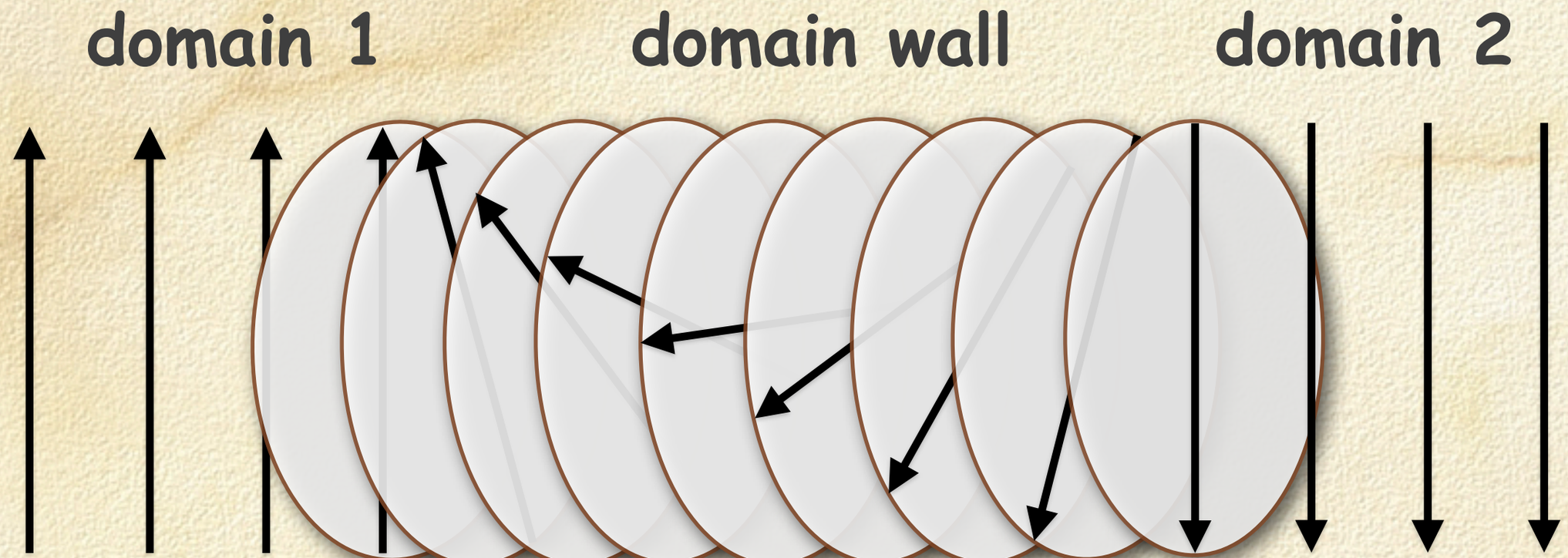

$$\pi \sqrt{A/K}$$

K: anisotropy constant
A: exchange constant

Excursus: Q = 0

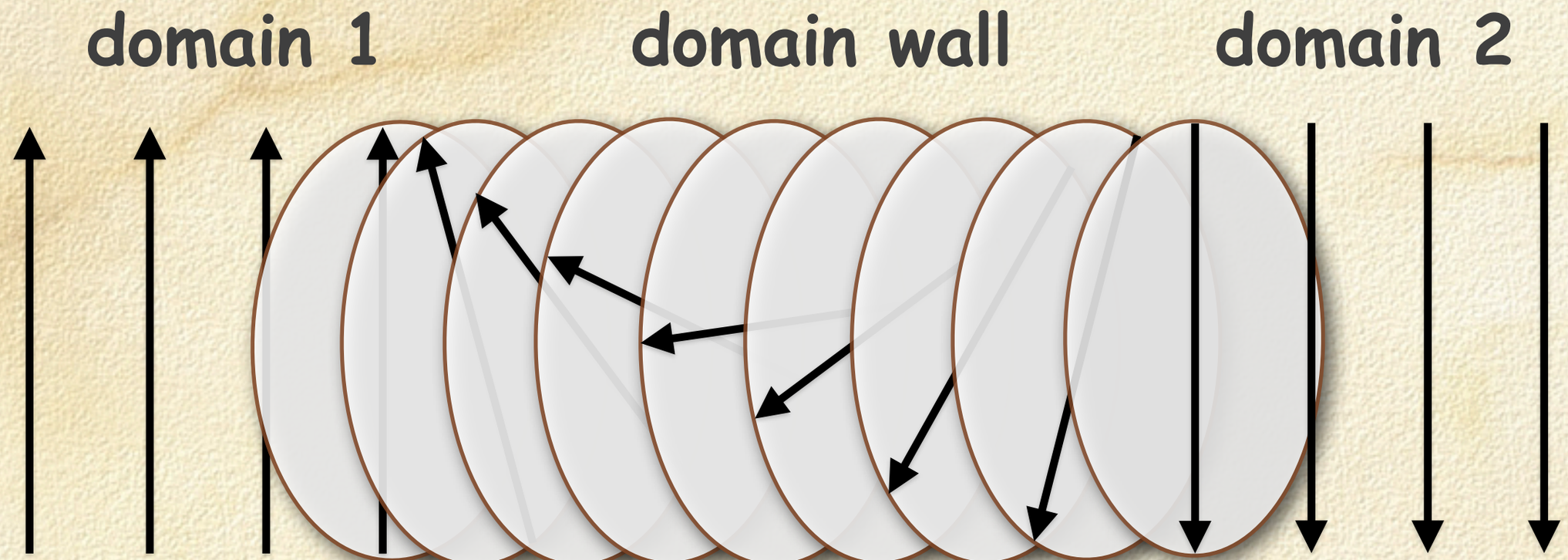

$$\pi \sqrt{A/K}$$

K: anisotropy constant
A: exchange constant

Q = 0: Domain walls not defined anymore

↓

We do <u>not</u> expect homogeneously magnetized domains with well defined walls, but continuous patterns

Excursus: Q = 0

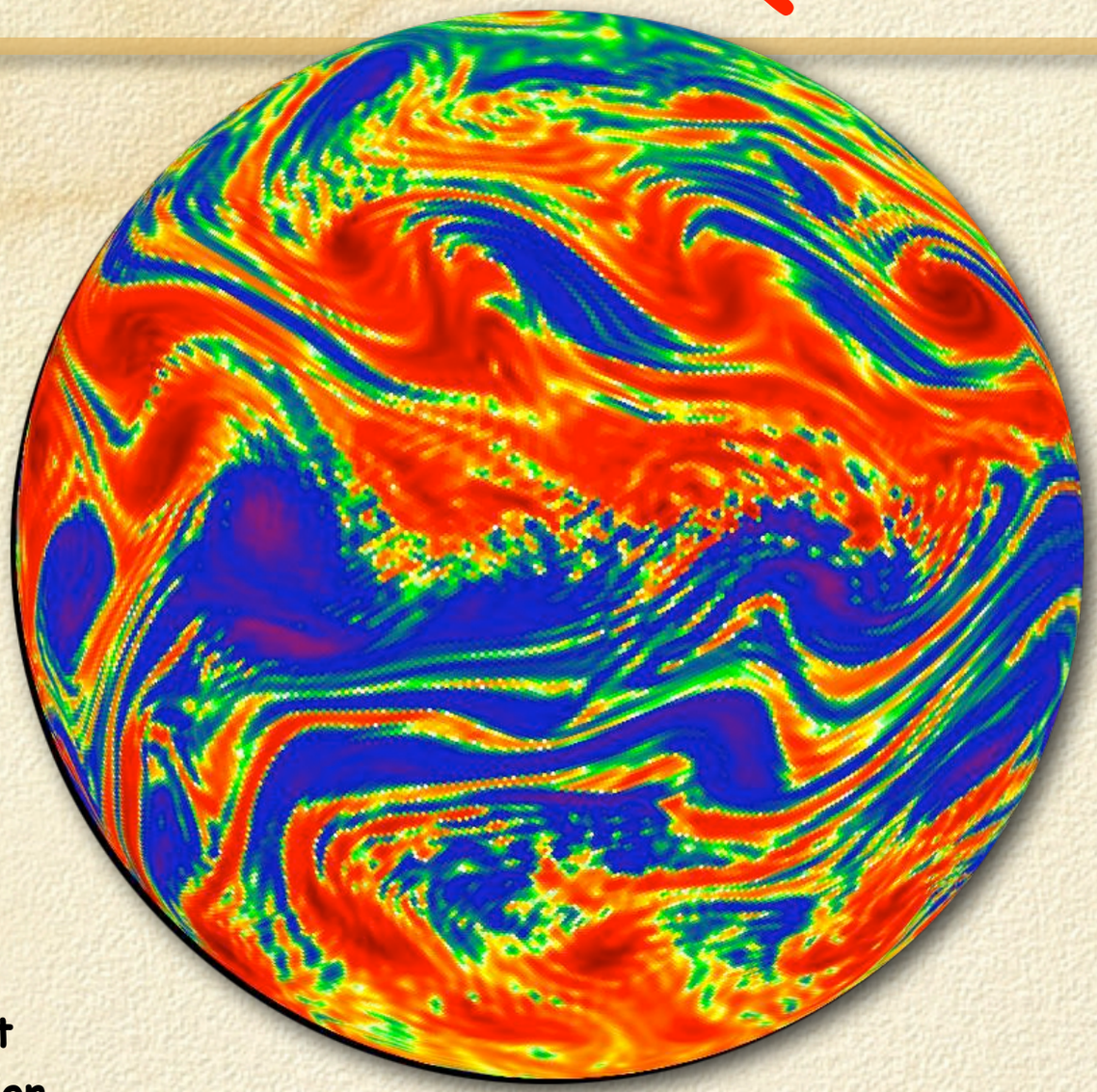

Astrophysical Fluid Dynamics via Direct Statistical Simulation.
S.M. Tobias et al. Astrophys.J. 727 (2011) 127

Q = 0: Domain walls not defined anymore

↓

We do <u>not</u> expect homogeneously magnetized domains with well defined walls, but continuous patterns

Excursus: Q = 0

Magnetostriction-free metallic glass after annealing in rotating field

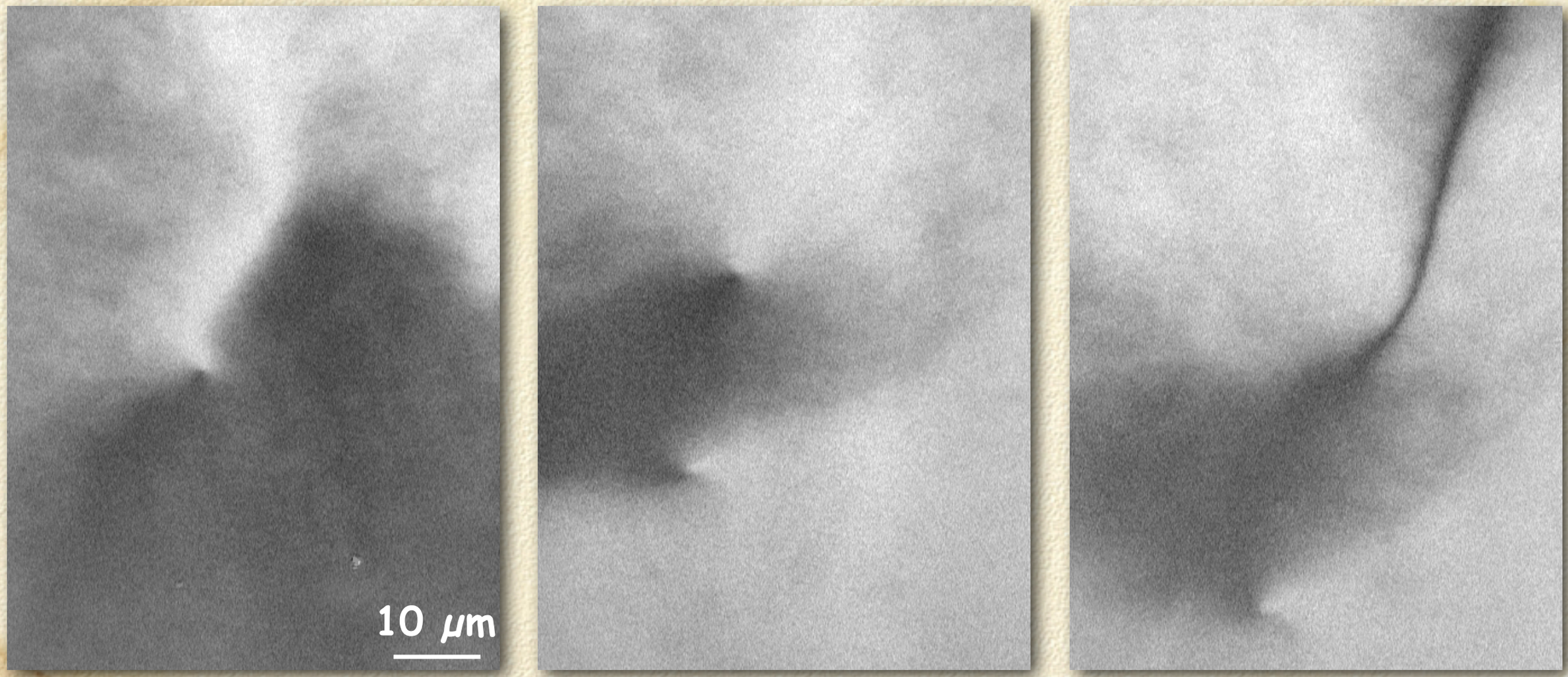

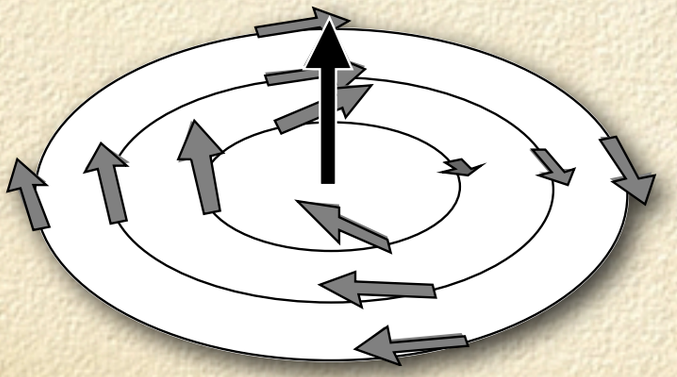

Swirl

Excursus: Q = 0

Permalloy sheet, 50 μm thick

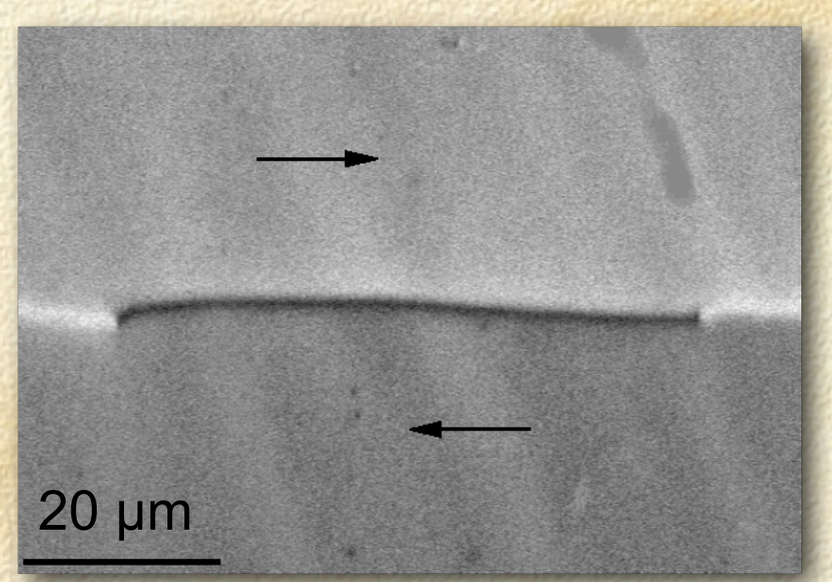

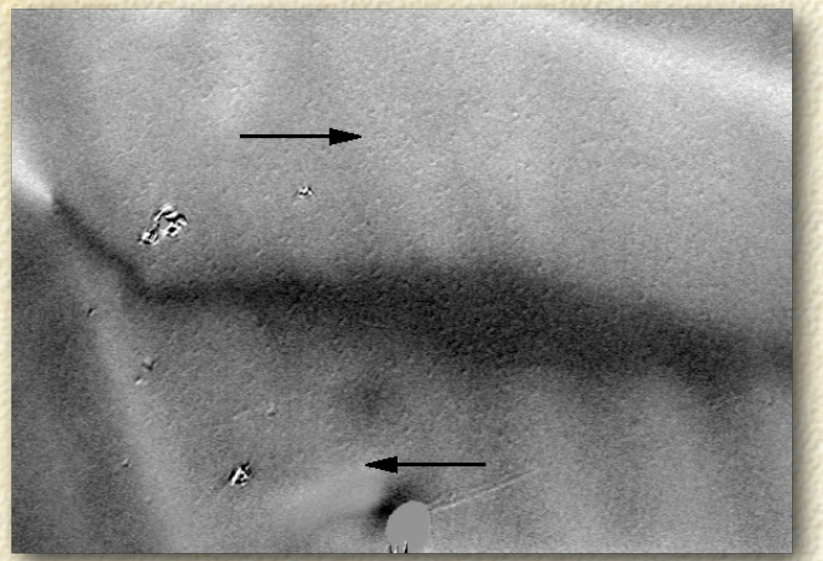
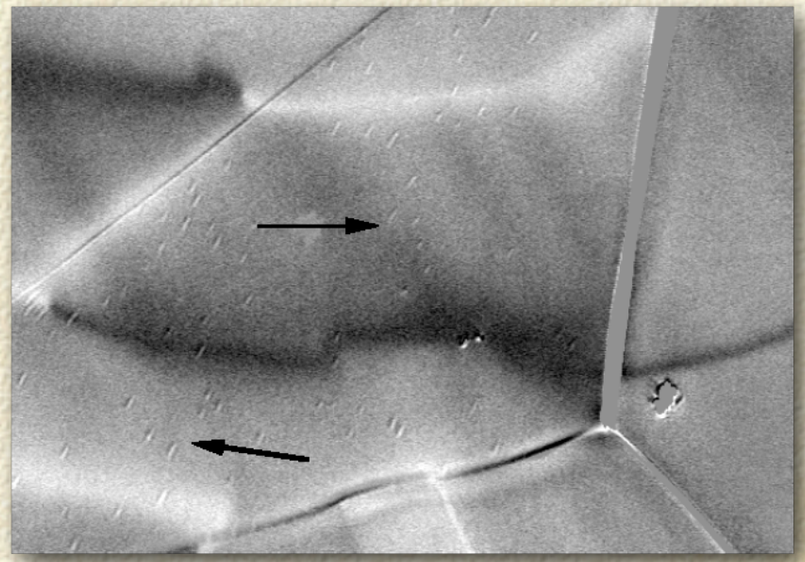
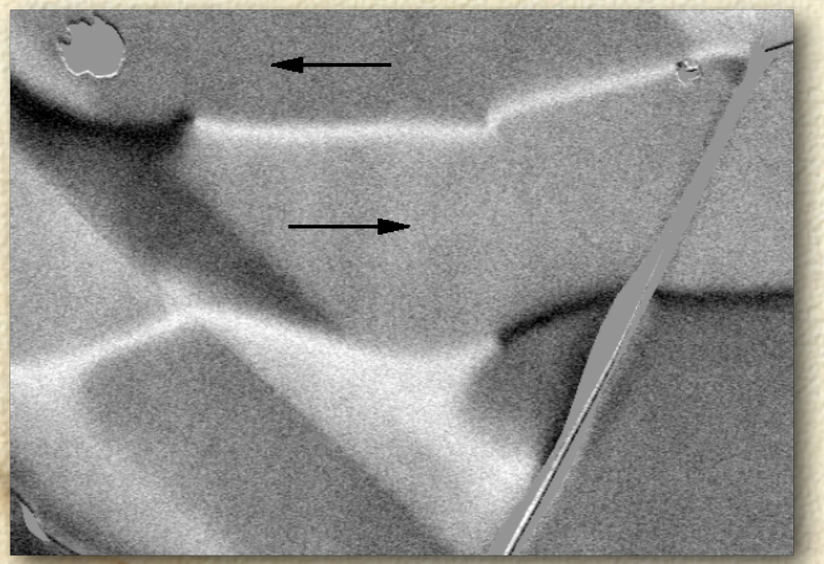
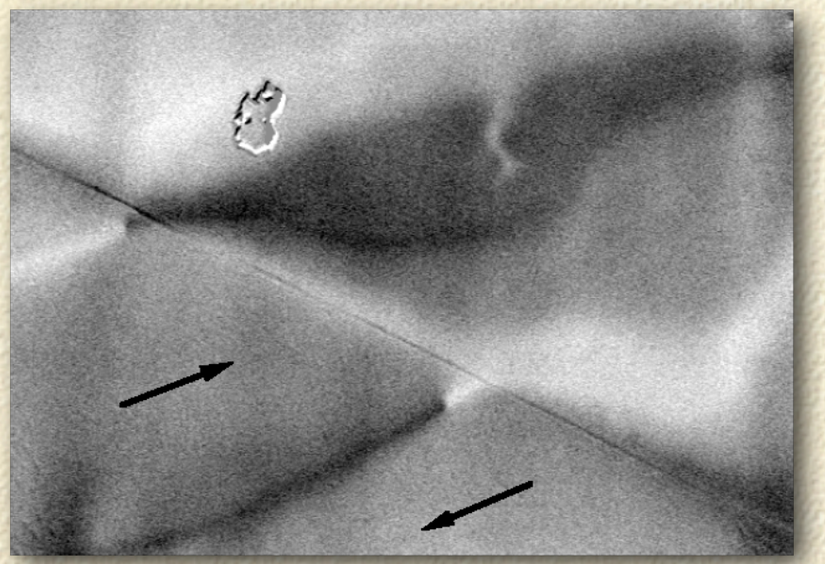
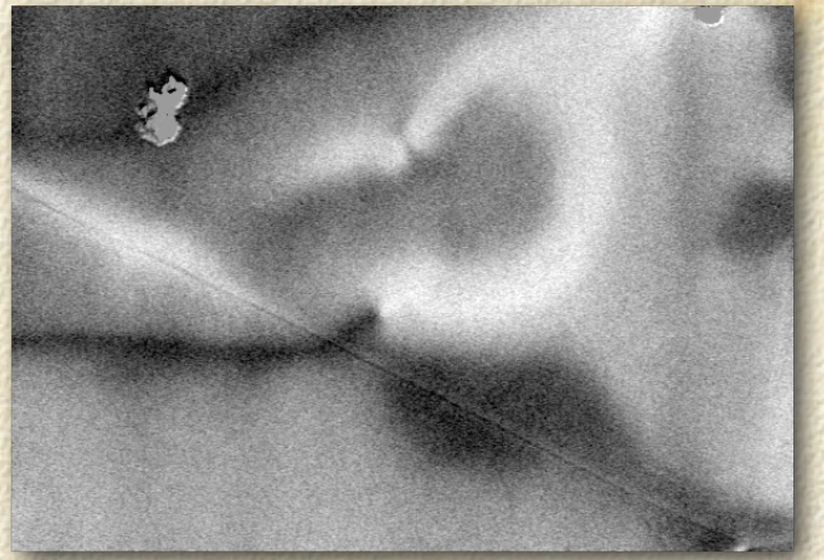

Fluctuations in local anisotropy

→ Domains walls and continuous patterns

General Classification of Domains

Dominating anisotropy energy (Q>>1)

Bubble garnet film (5 μm thick)

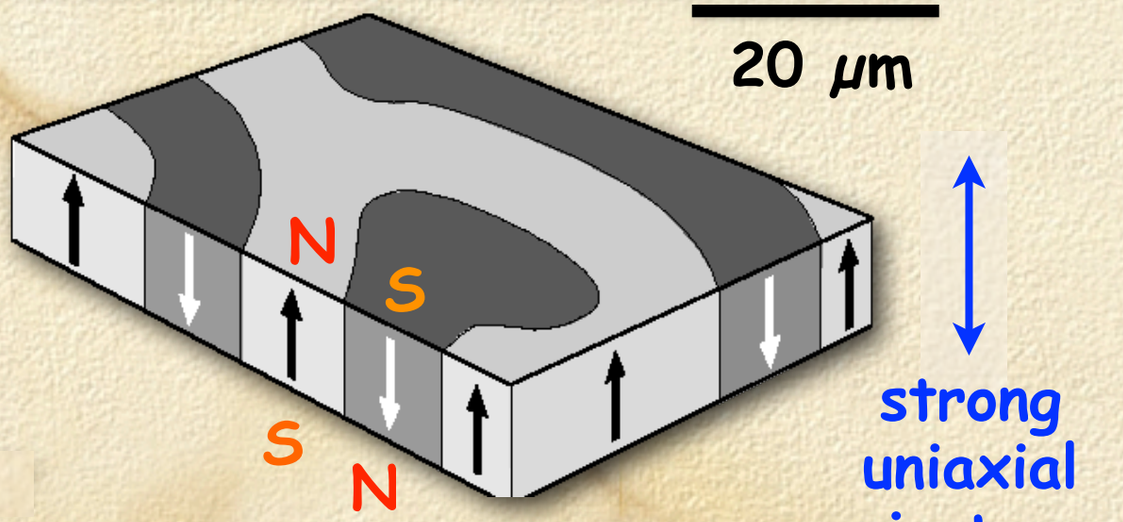

Dominating stray-field energy (Q<<1)

General Classification of Domains

Dominating anisotropy energy (Q>>1)

Bubble garnet film (5 μm thick)

20 μm

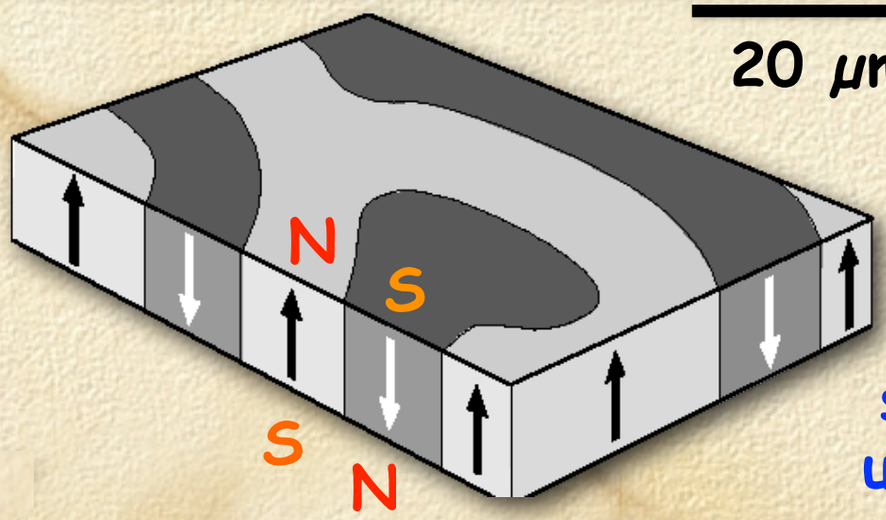

strong uniaxial anisotropy

Dominating stray-field energy (Q<<1)

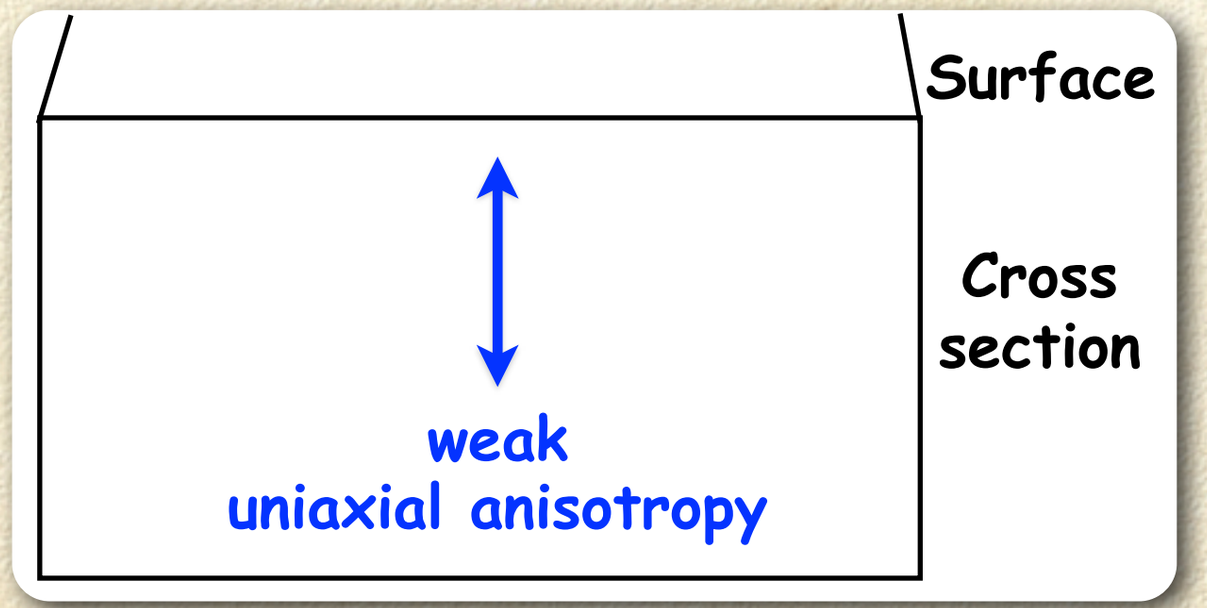

General Classification of Domains

Dominating anisotropy energy (Q>>1)

Bubble garnet film (5 μm thick)

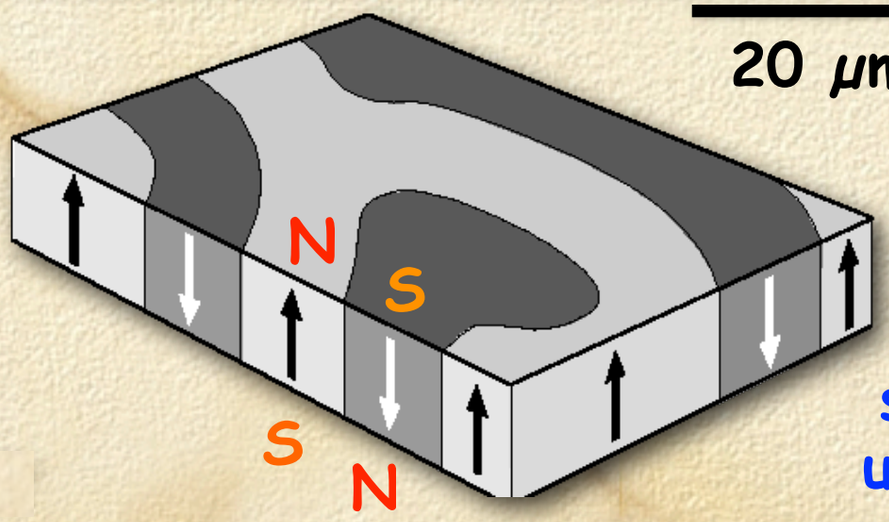

strong uniaxial anisotropy

Dominating stray-field energy (Q<<1)

Amorphous FeSiBCuNb film (2 μm thick)

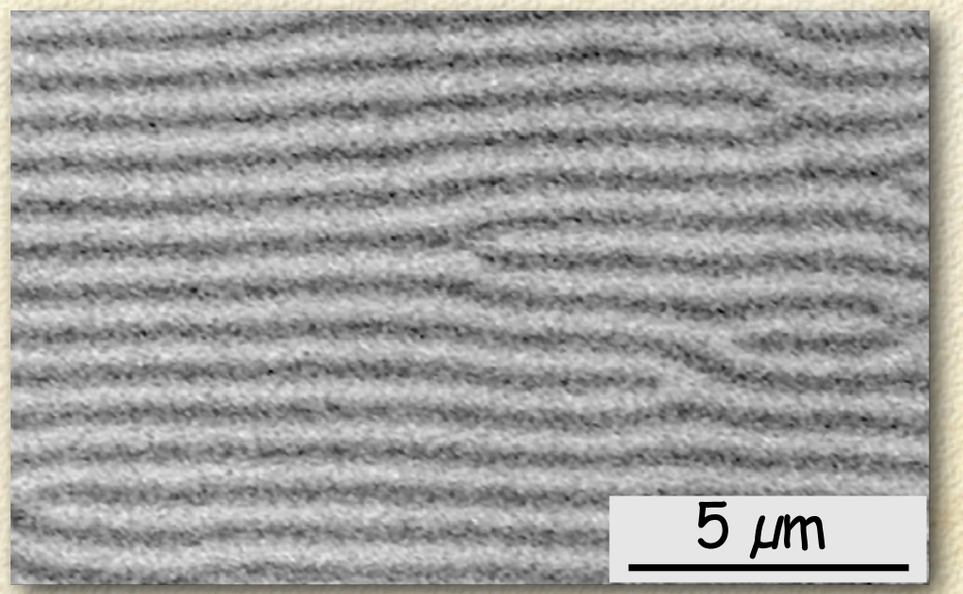

Stripe domains

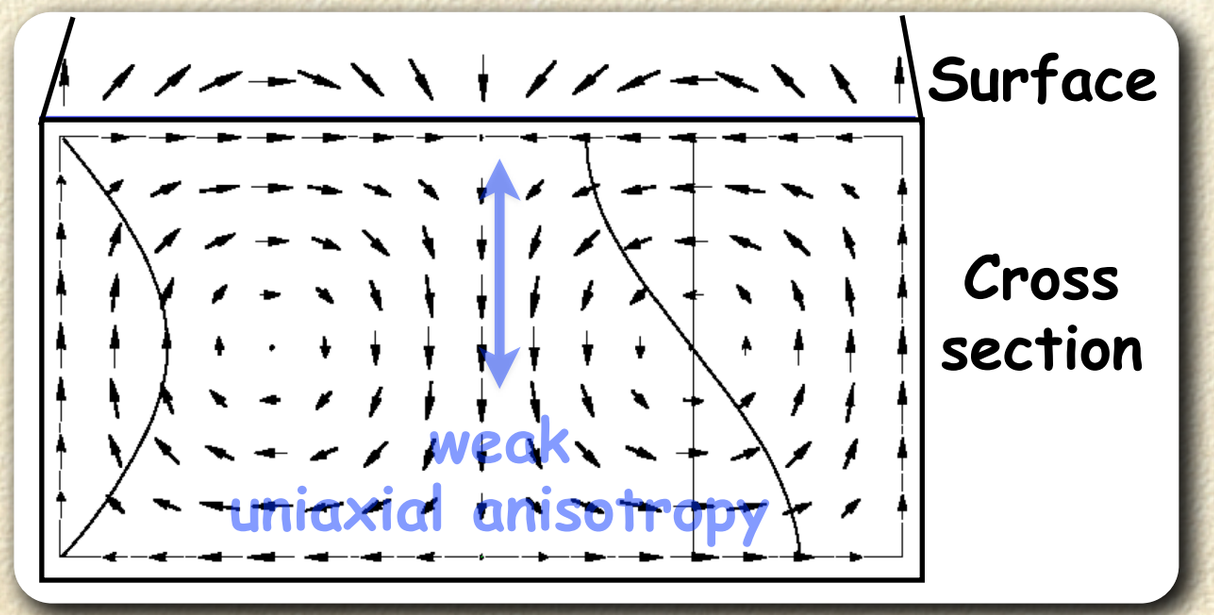

General Classification of Domains

Dominating anisotropy energy (Q>>1)

Bubble garnet film (5 μm thick)

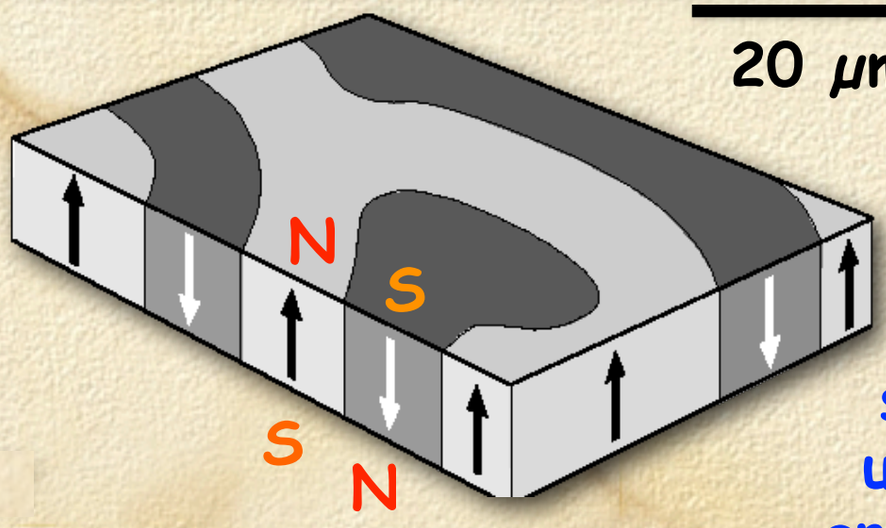

strong uniaxial anisotropy

Dominating stray-field energy (Q<<1)

Amorphous FeSiB ribbon (20 μm thick)

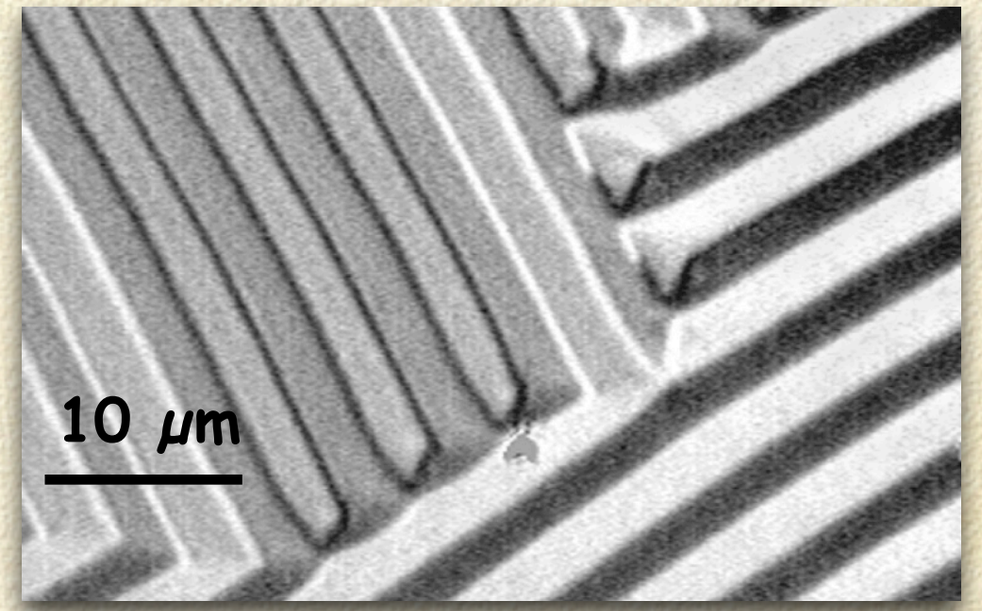

Landau domains

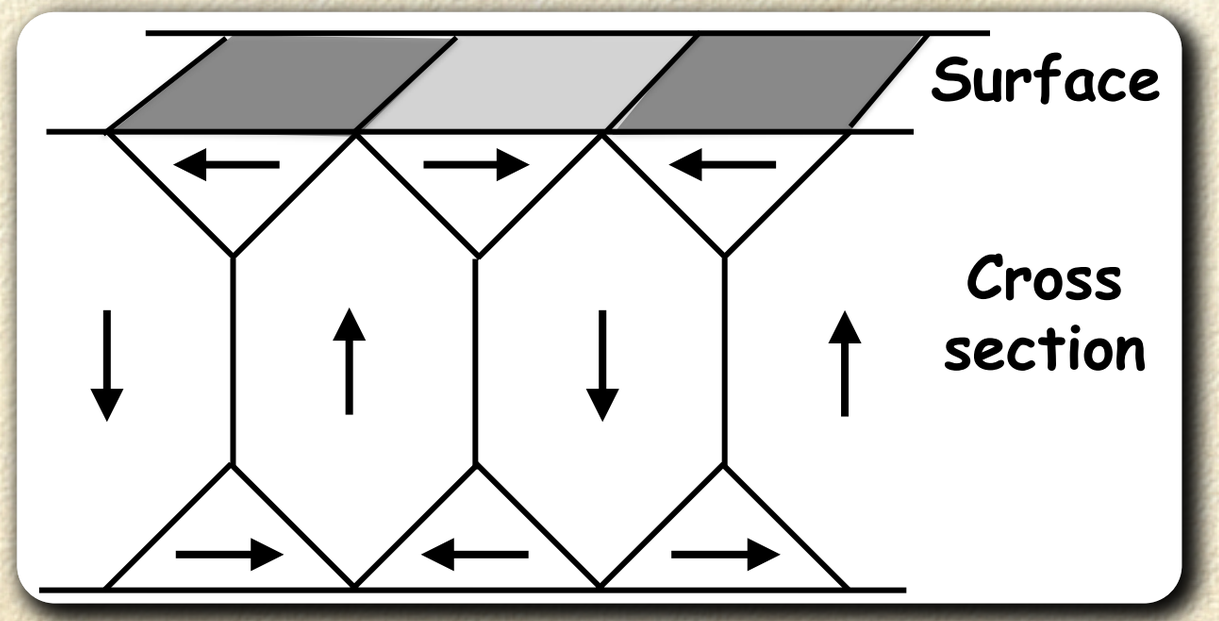

General Classification of Domains

Dominating anisotropy energy (Q>>1)

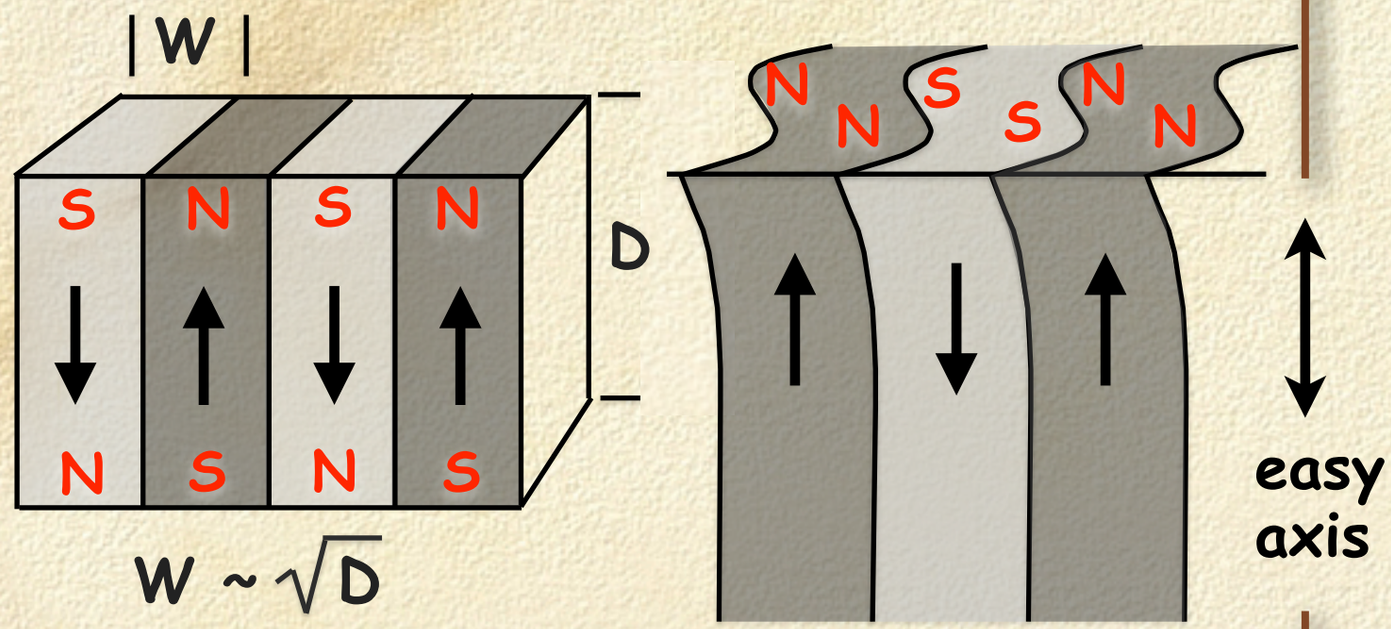

~1 μm NdFeB wedge 14 μm

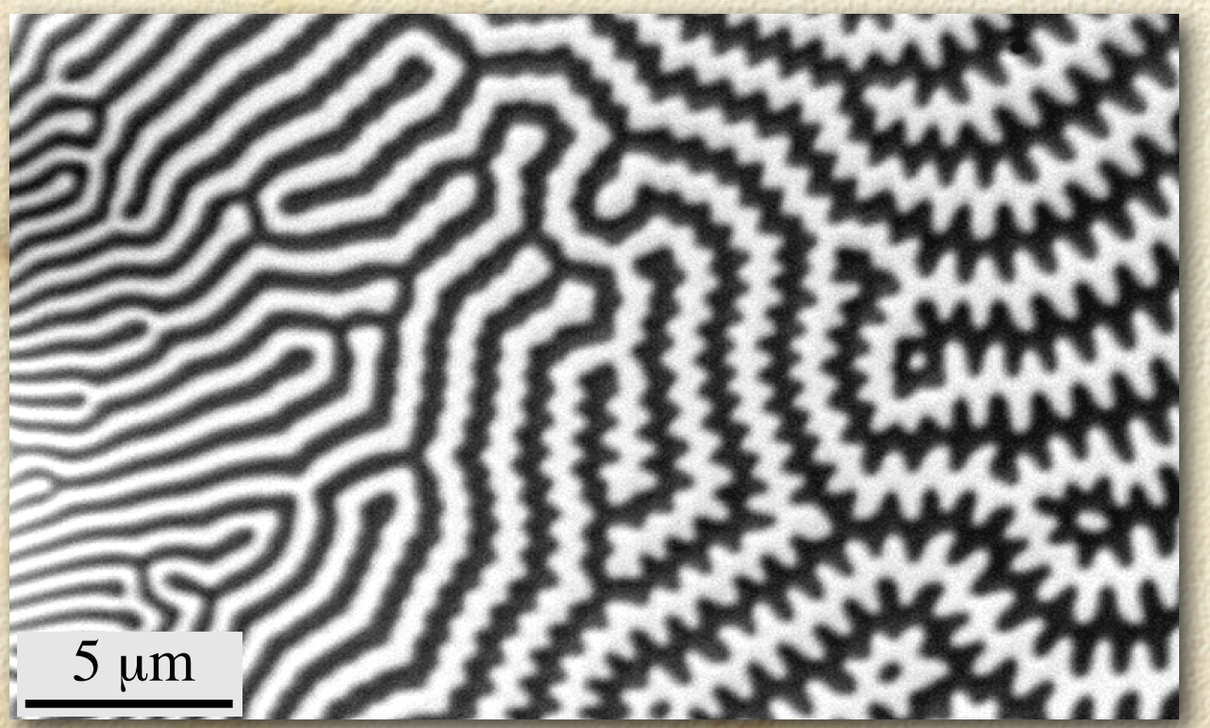

Dominating stray-field energy (Q<<1)

General Classification of Domains

Dominating anisotropy energy (Q>>1)

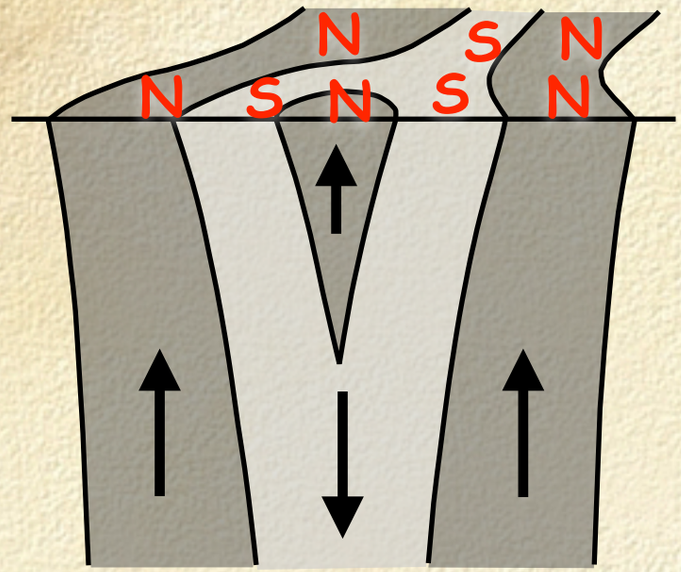

~ 40 μm

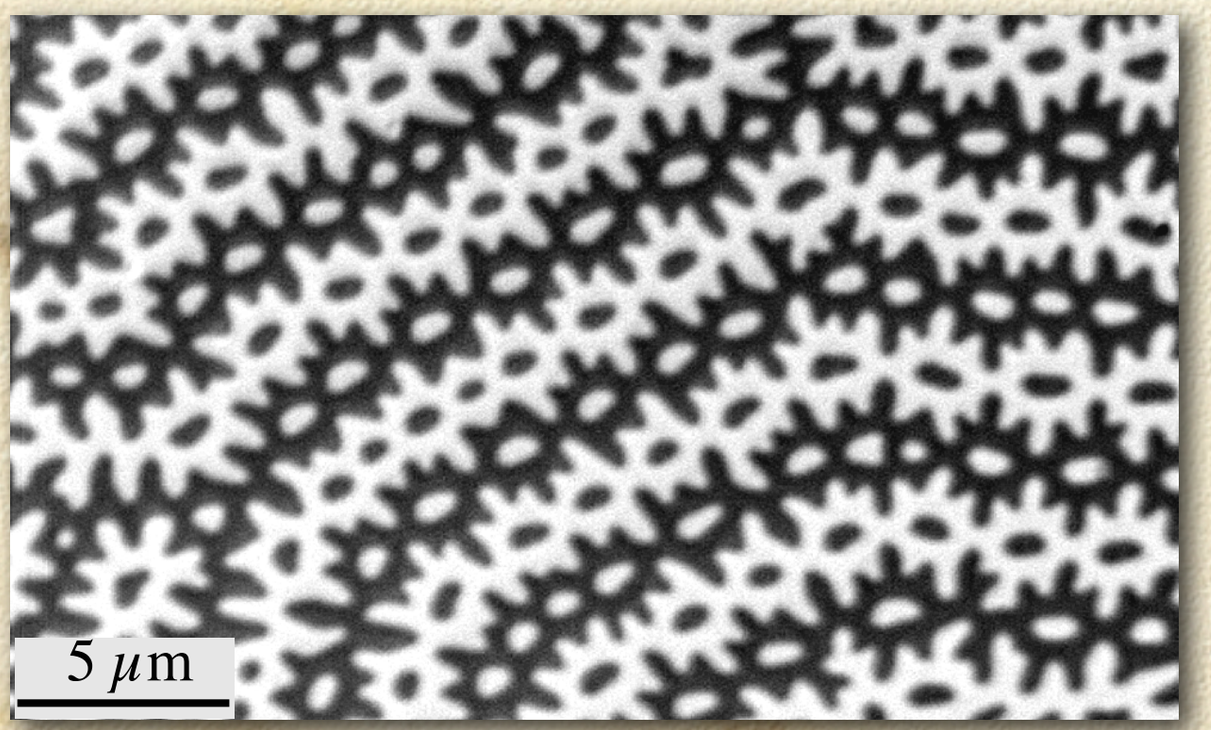

Dominating stray-field energy (Q<<1)

easy axis

General Classification of Domains

Dominating anisotropy energy (Q>>1)

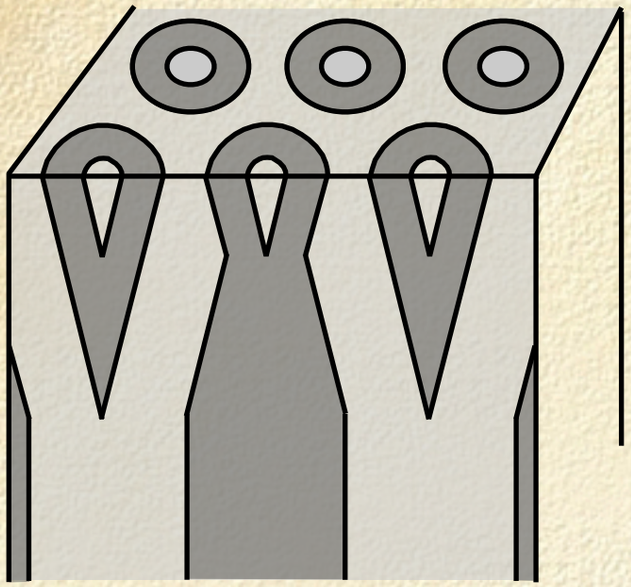

~ 120 μm

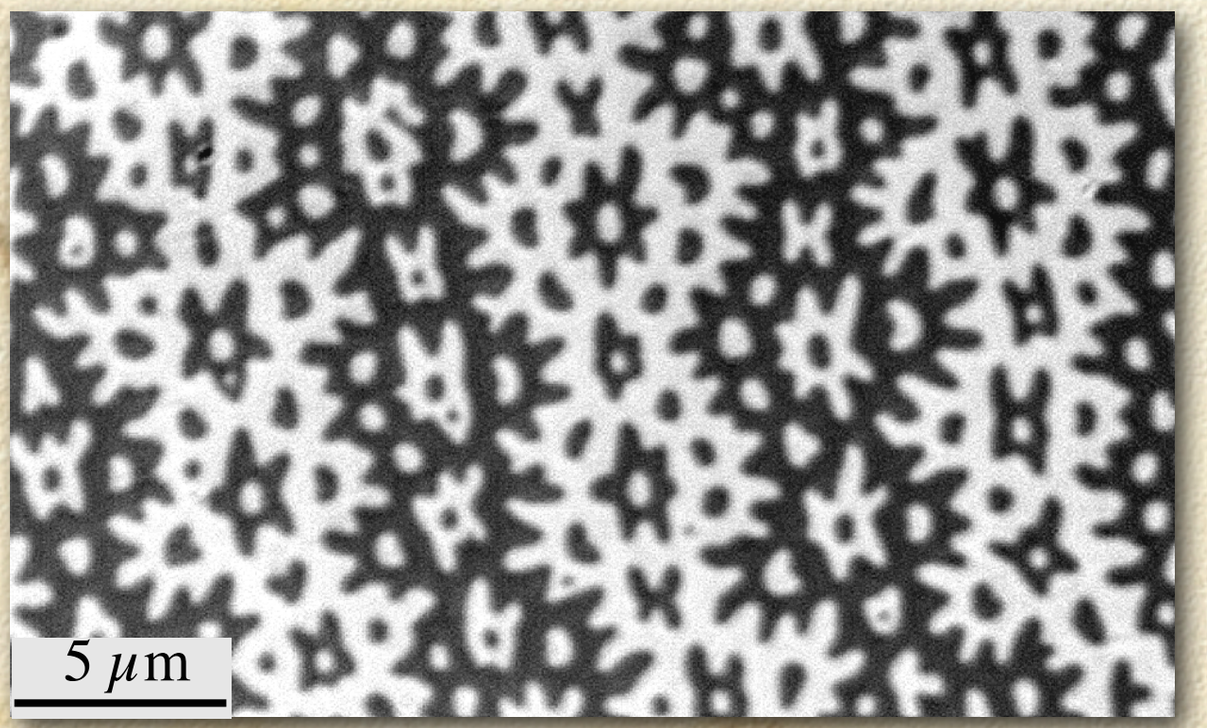

Dominating stray-field energy (Q<<1)

easy axis

General Classification of Domains

Dominating anisotropy energy (Q>>1)

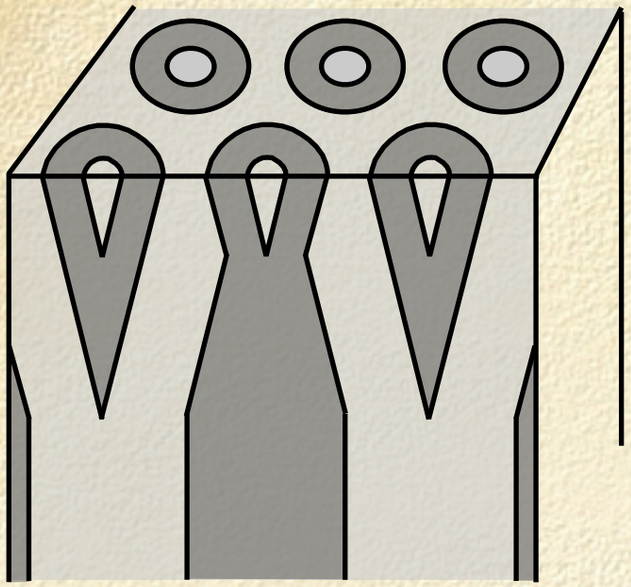

~ 600 μm

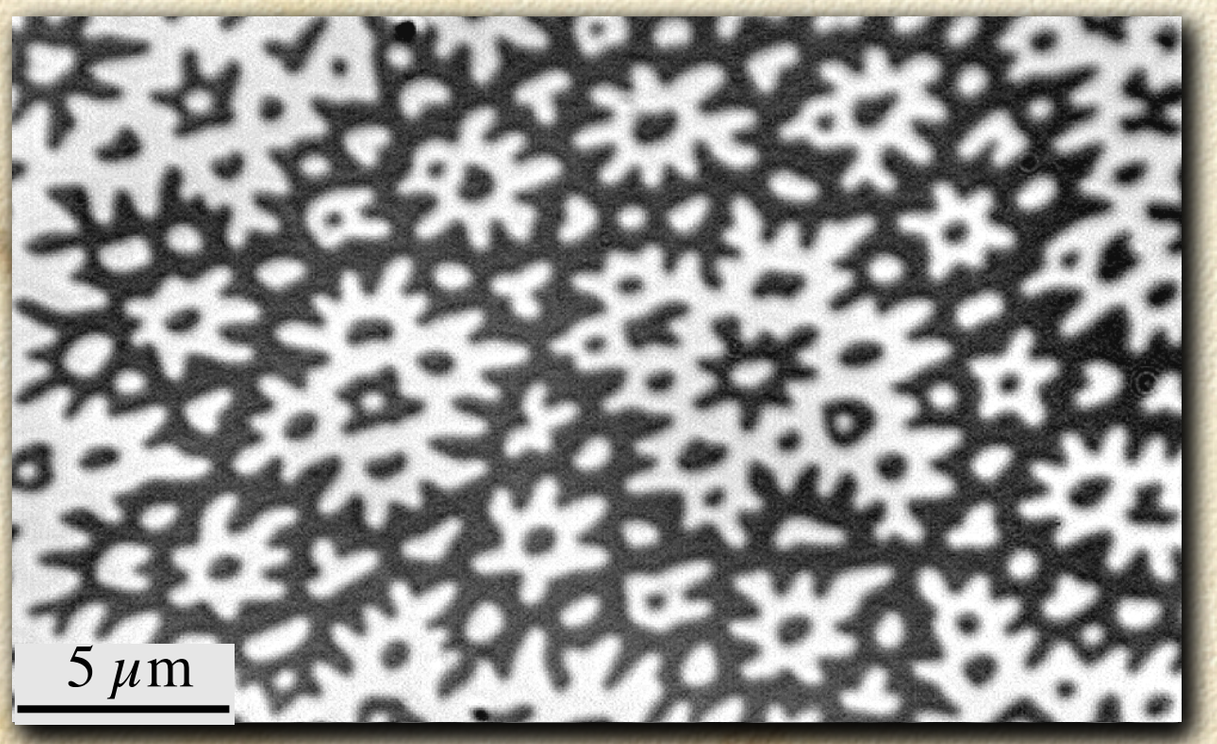

easy axis

Dominating stray-field energy (Q<<1)

General Classification of Domains

Dominating anisotropy energy (Q>>1)

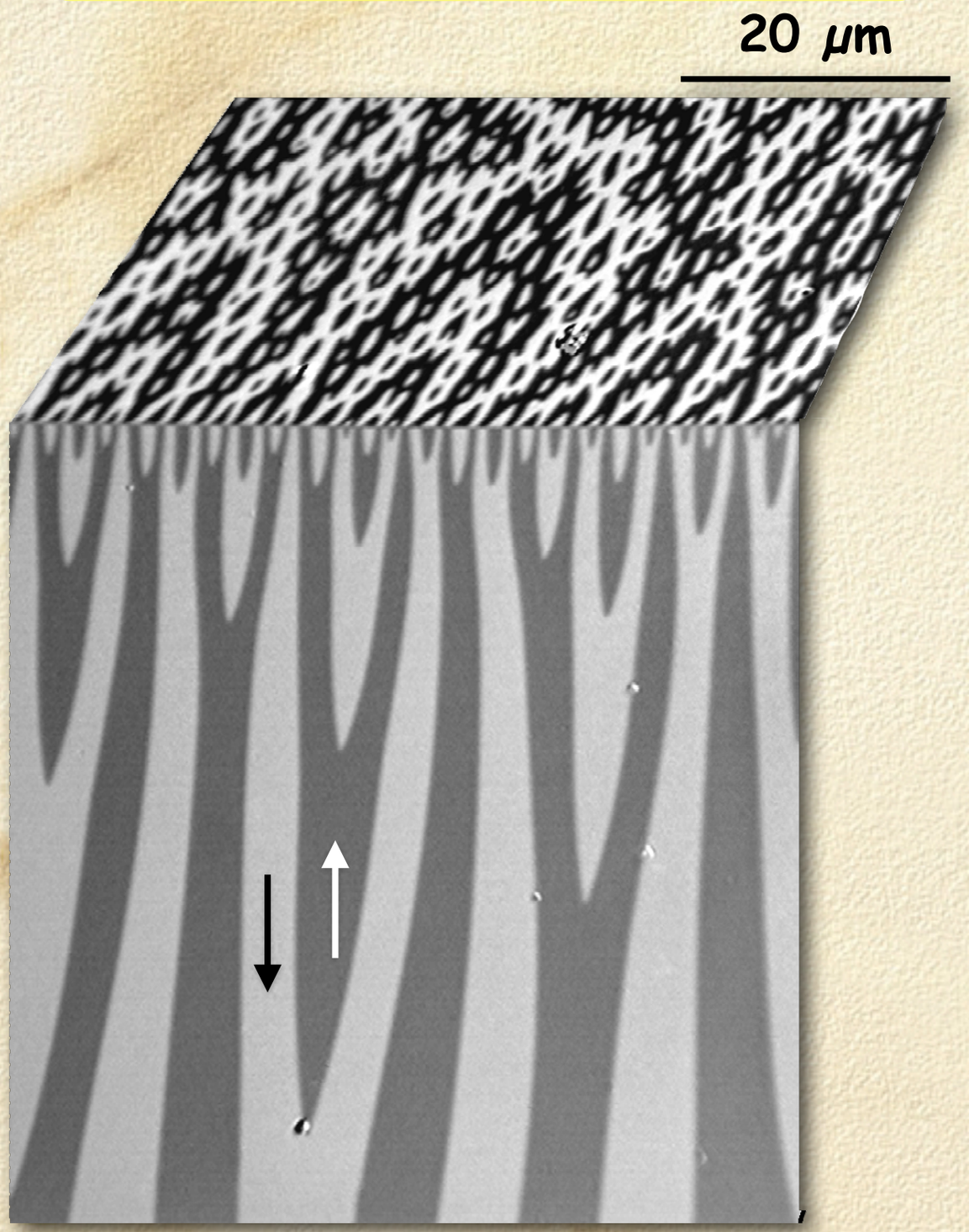

Dominating stray-field energy (Q<<1)

General Classification of Domains

Dominating anisotropy energy (Q>>1)

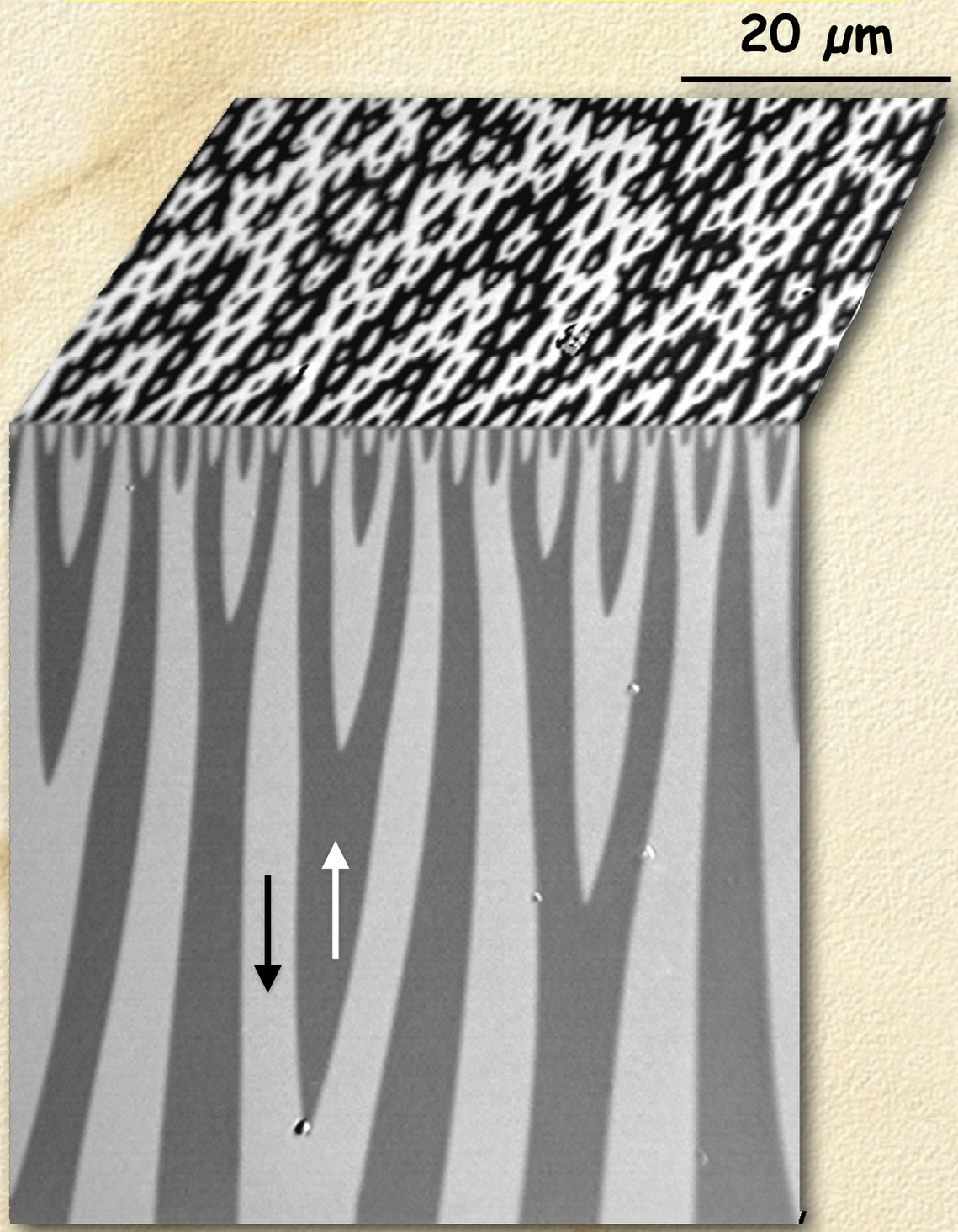

Dominating stray-field energy (Q<<1)

General Classification of Domains

Dominating anisotropy energy (Q>>1)

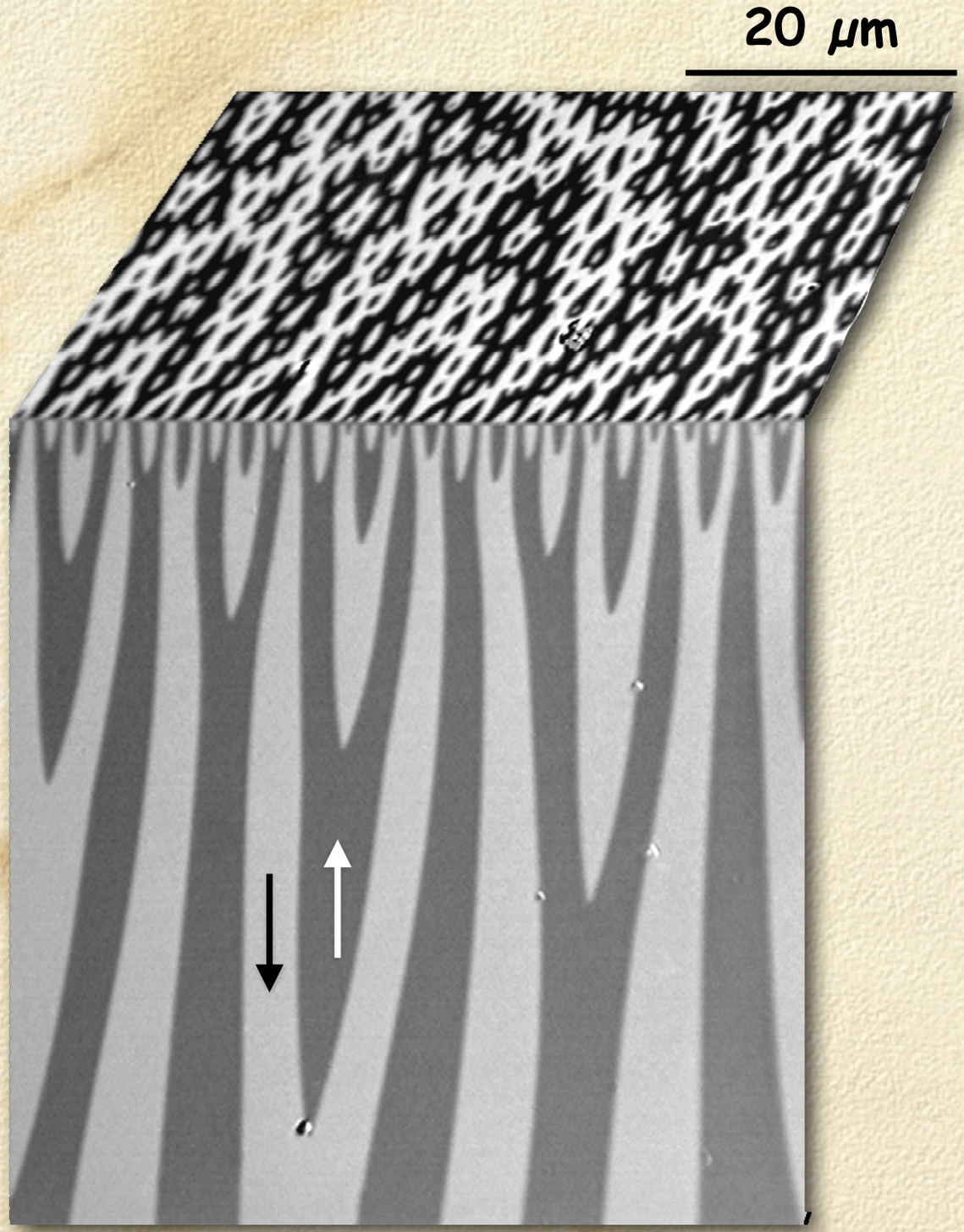

Dominating stray-field energy (Q<<1)

Amorphous FeSiB ribbon (20 μm thick)

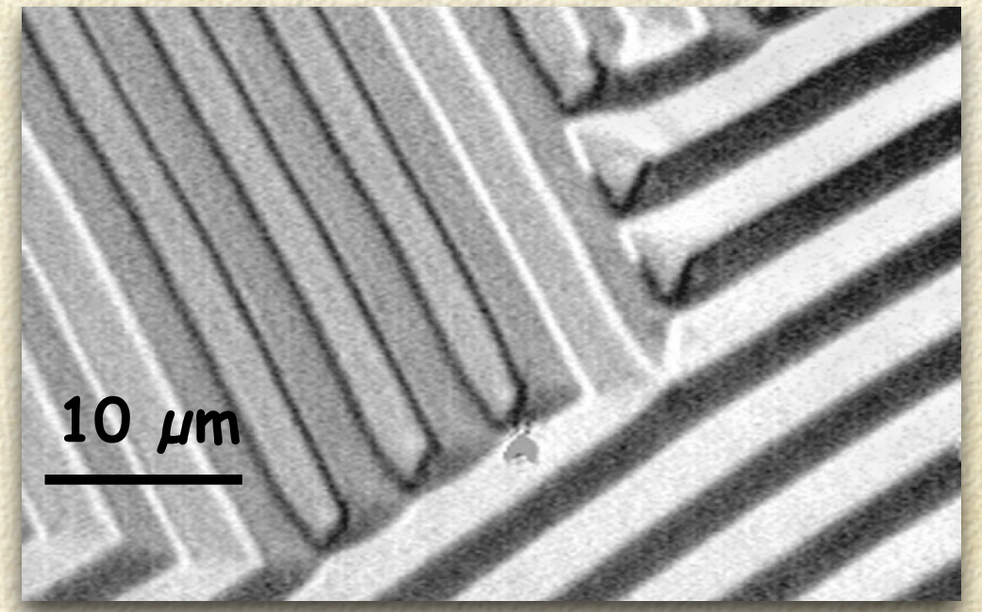

Landau domains

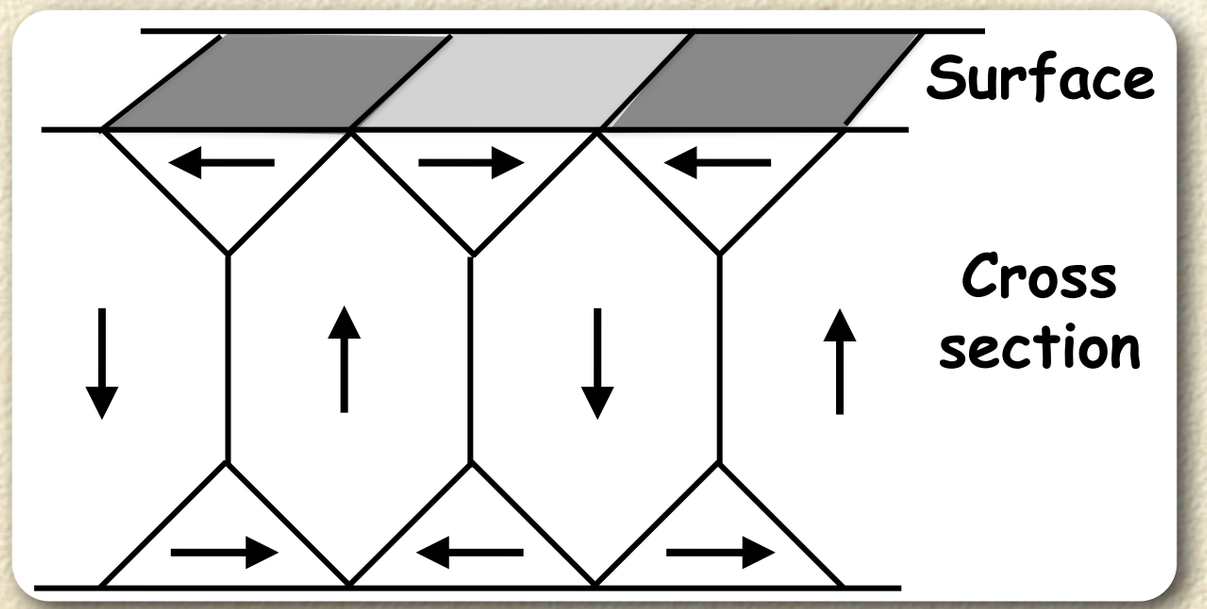

General Classification of Domains

$$Q << 1$$

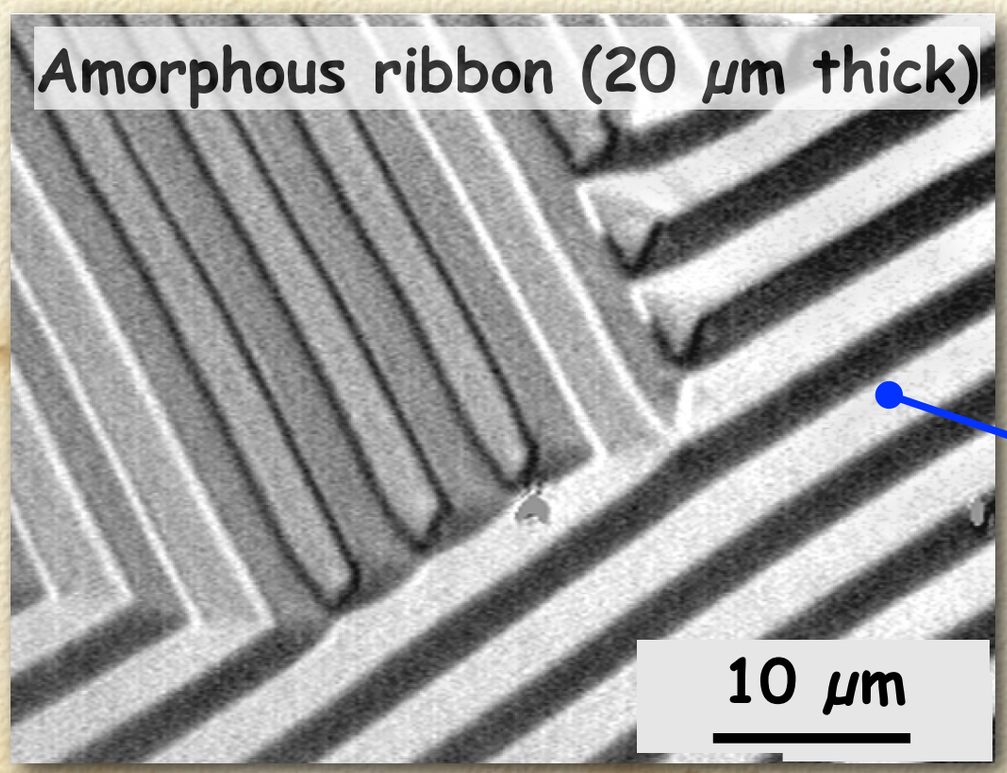

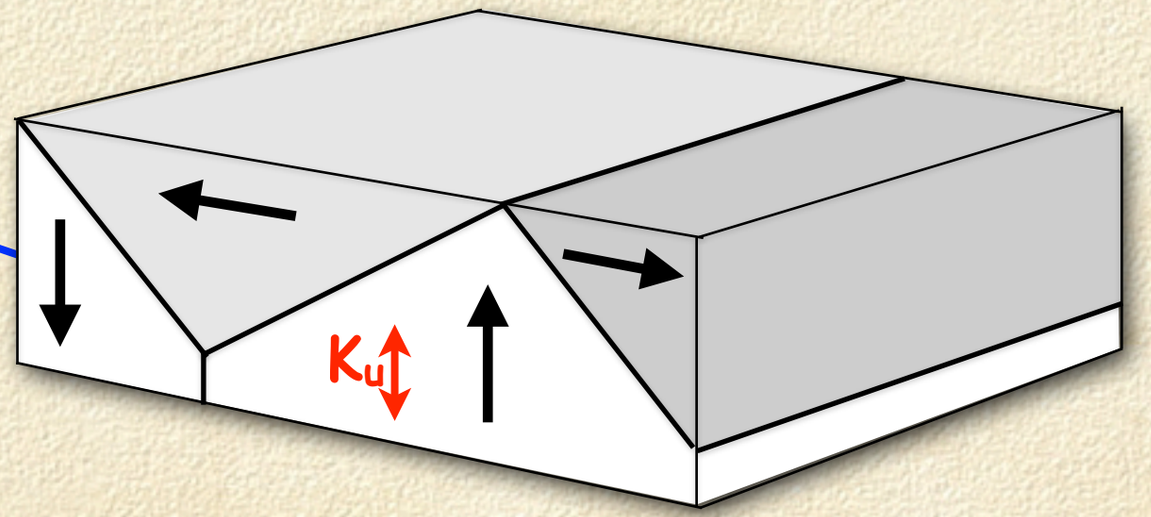

General Classification of Domains

$$Q << 1$$

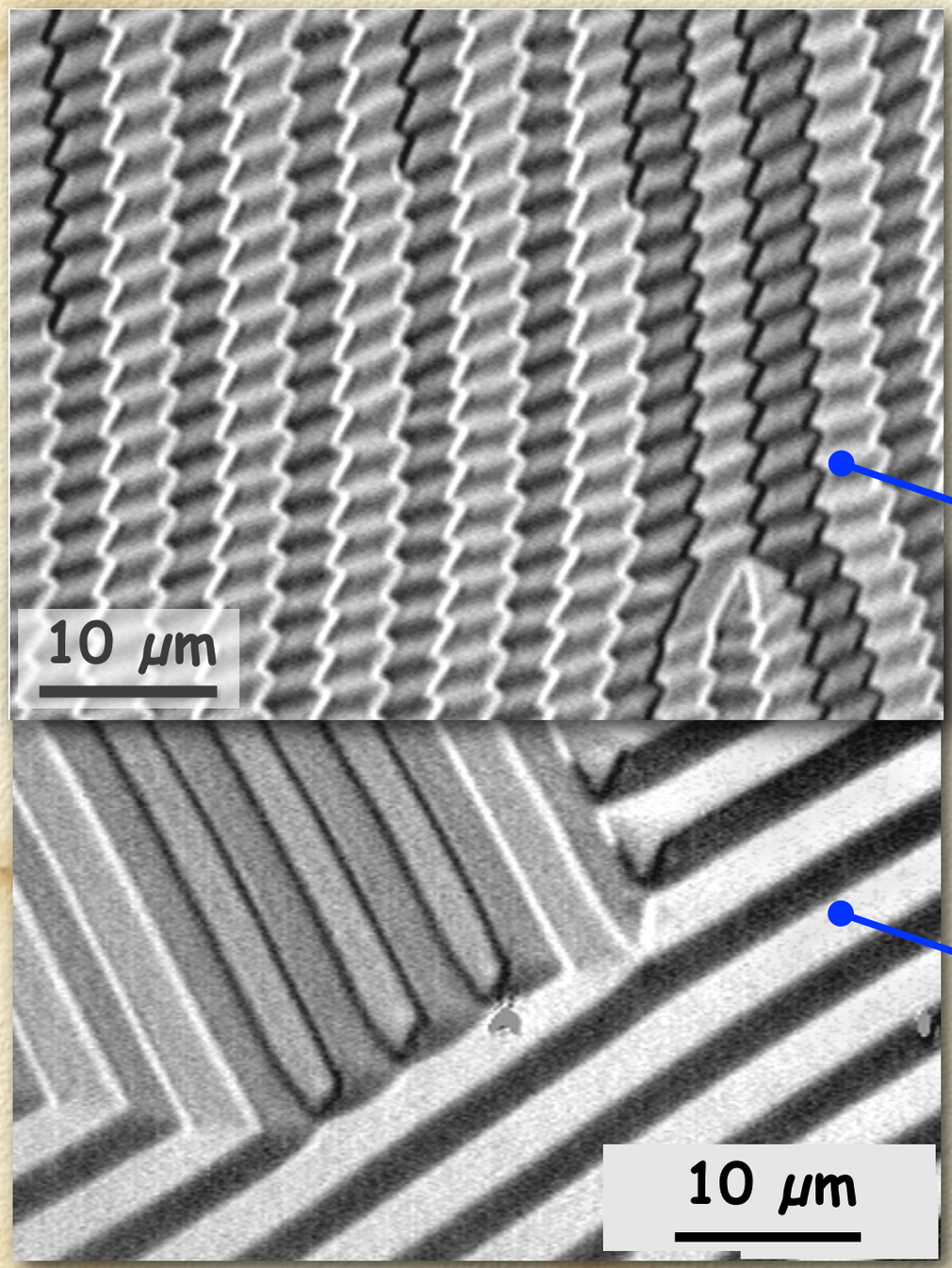

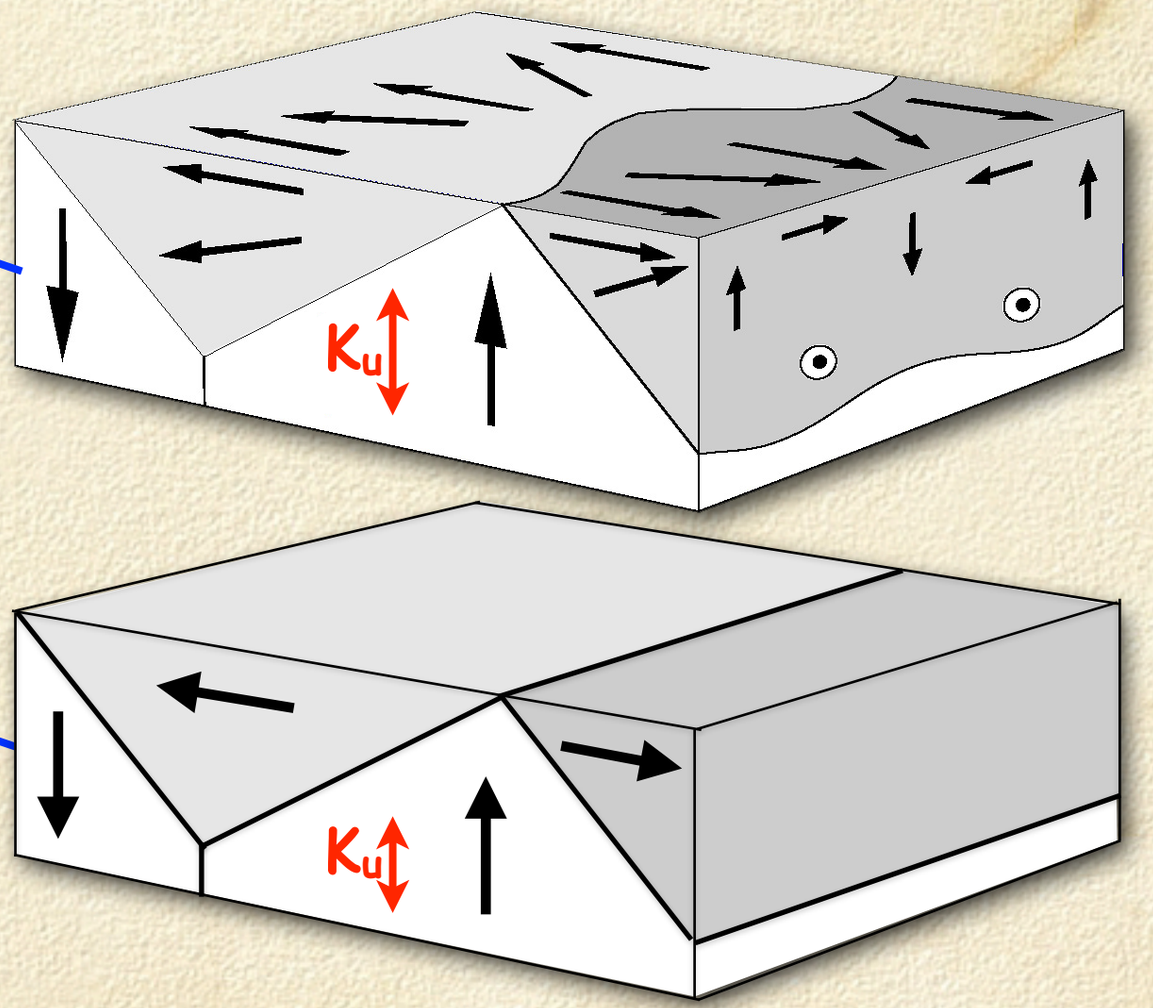

General Classification of Domains

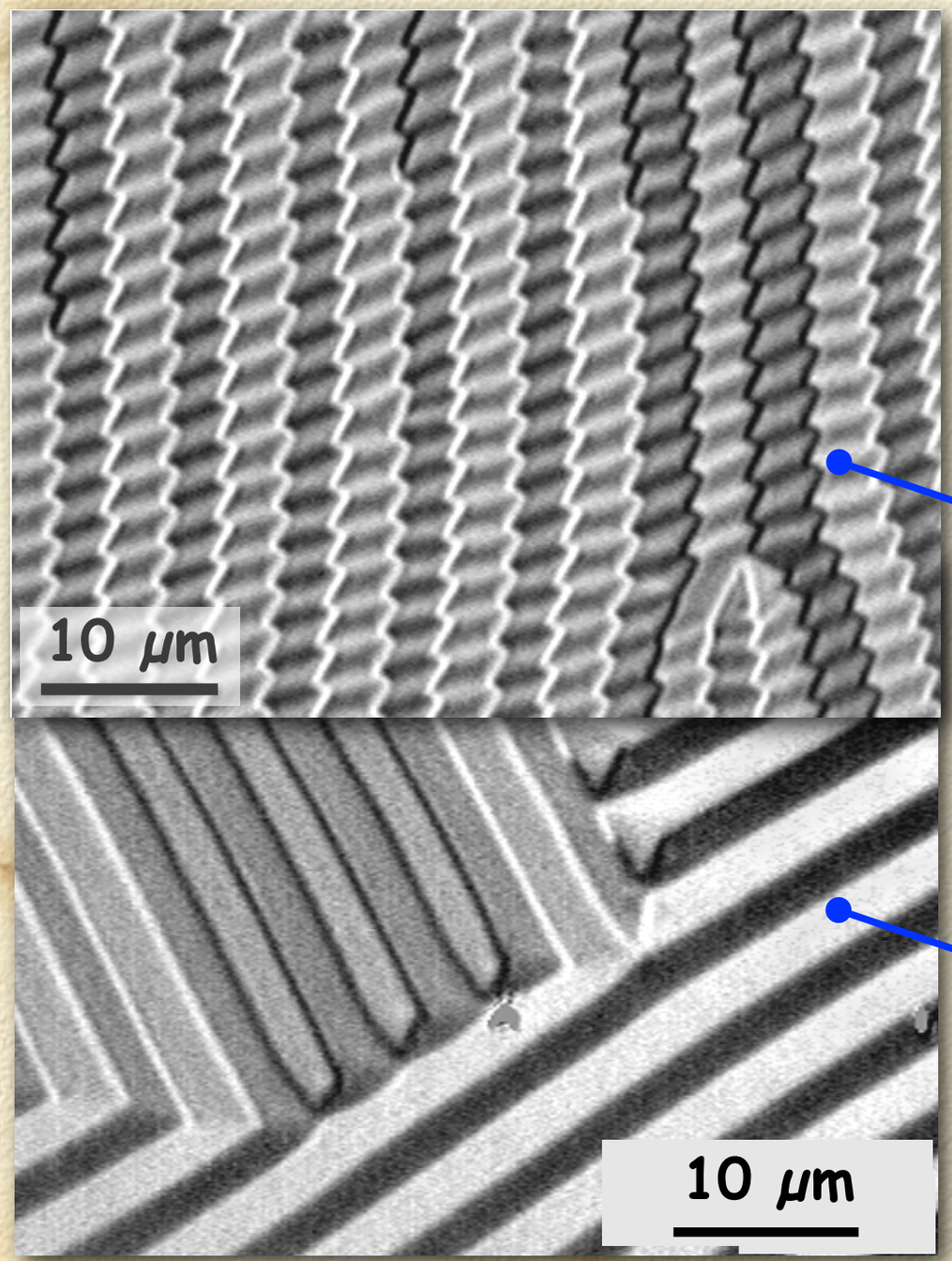

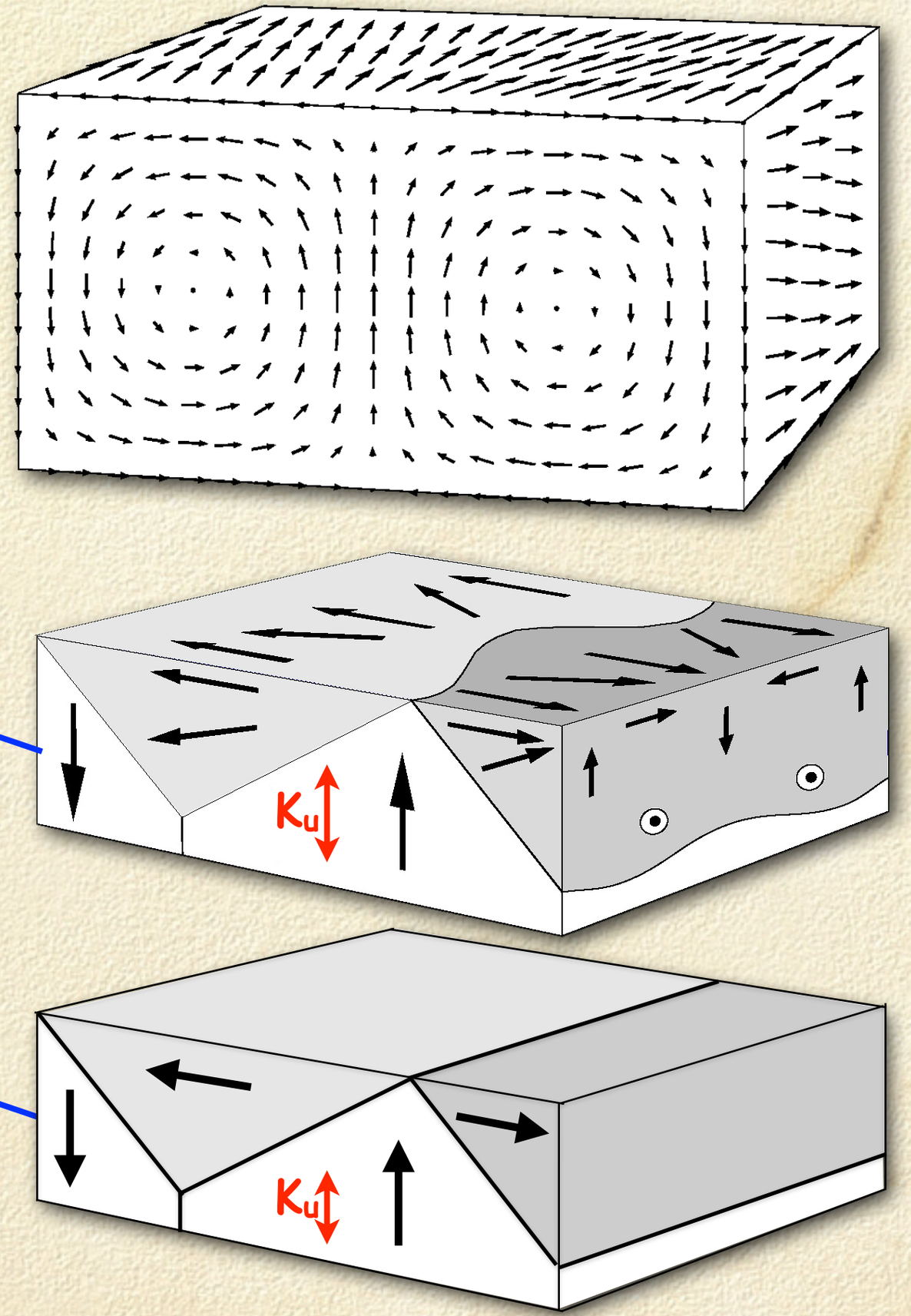

General Classification of Domains

$$Q << 1$$

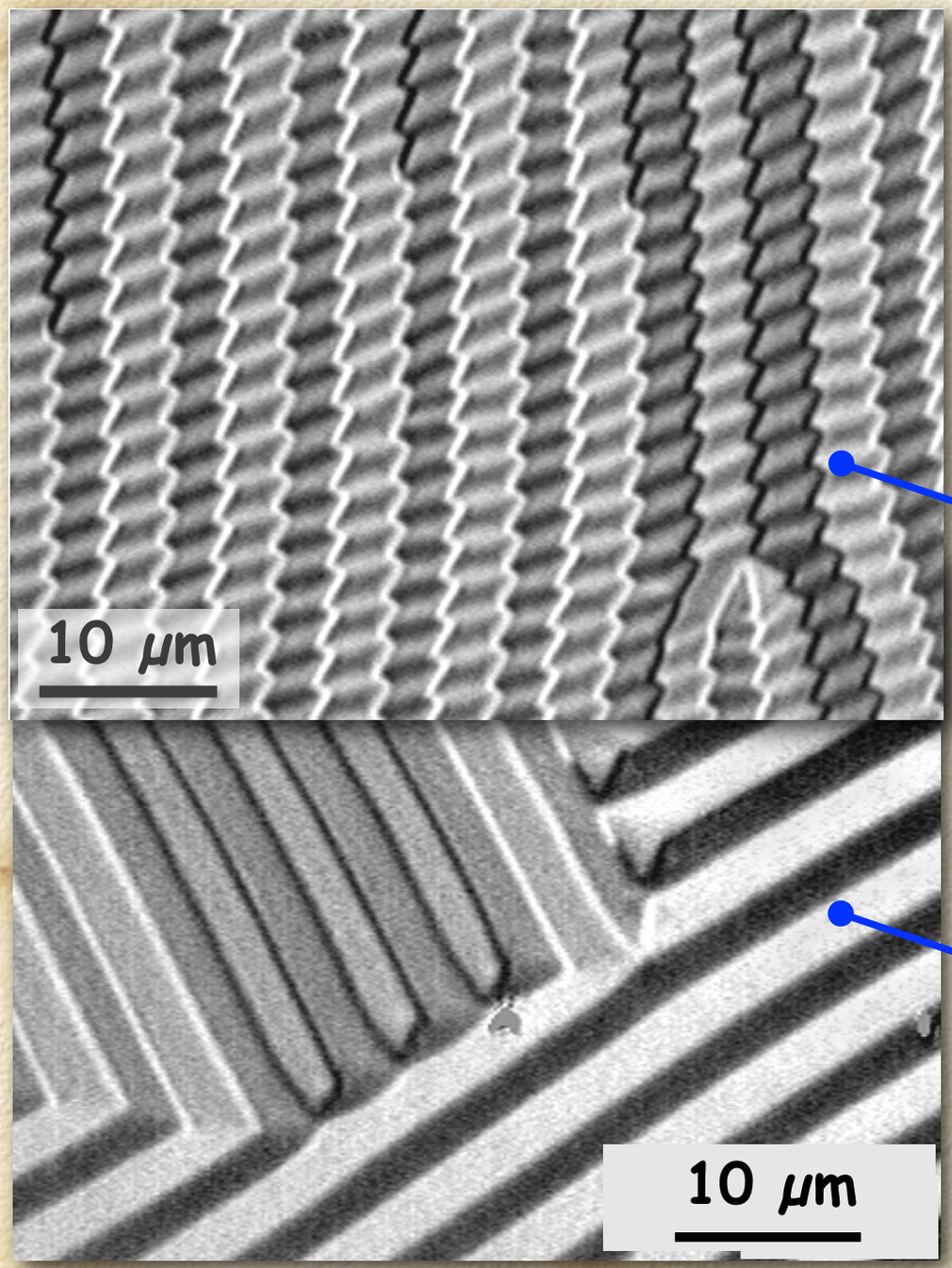

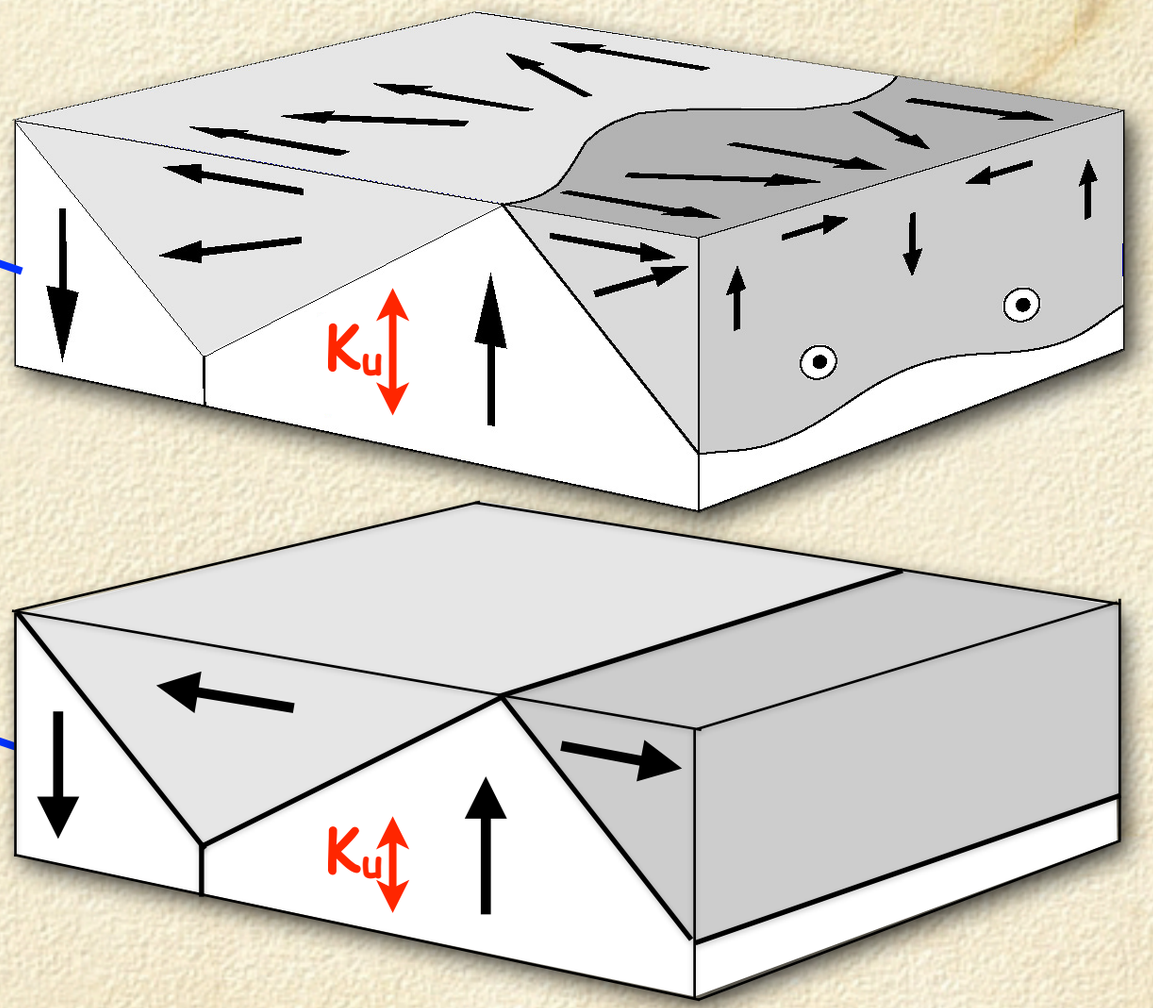

ification of Domains

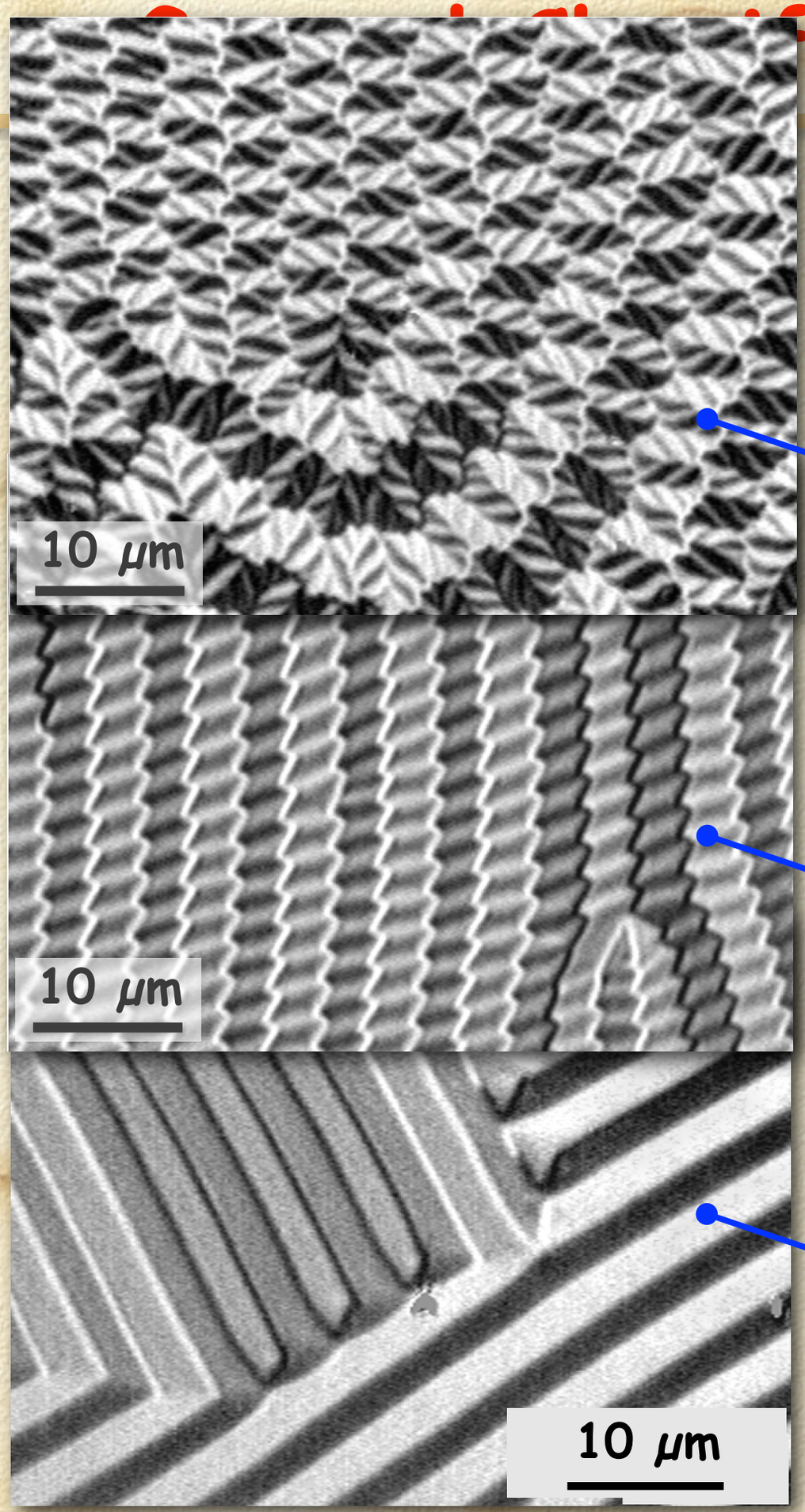

$Q \ll 1$

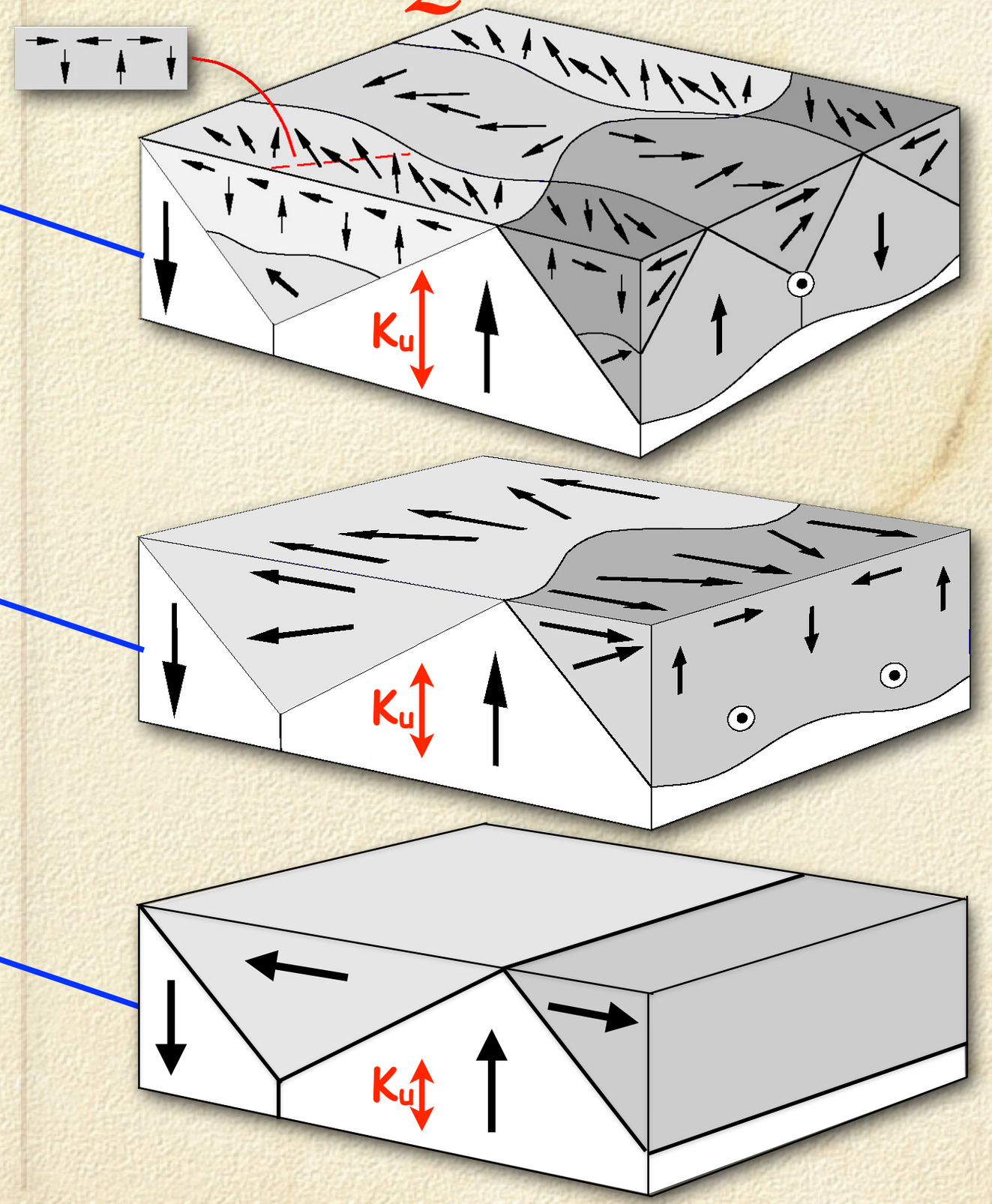

General Classification of Domains

$Q >> 1$

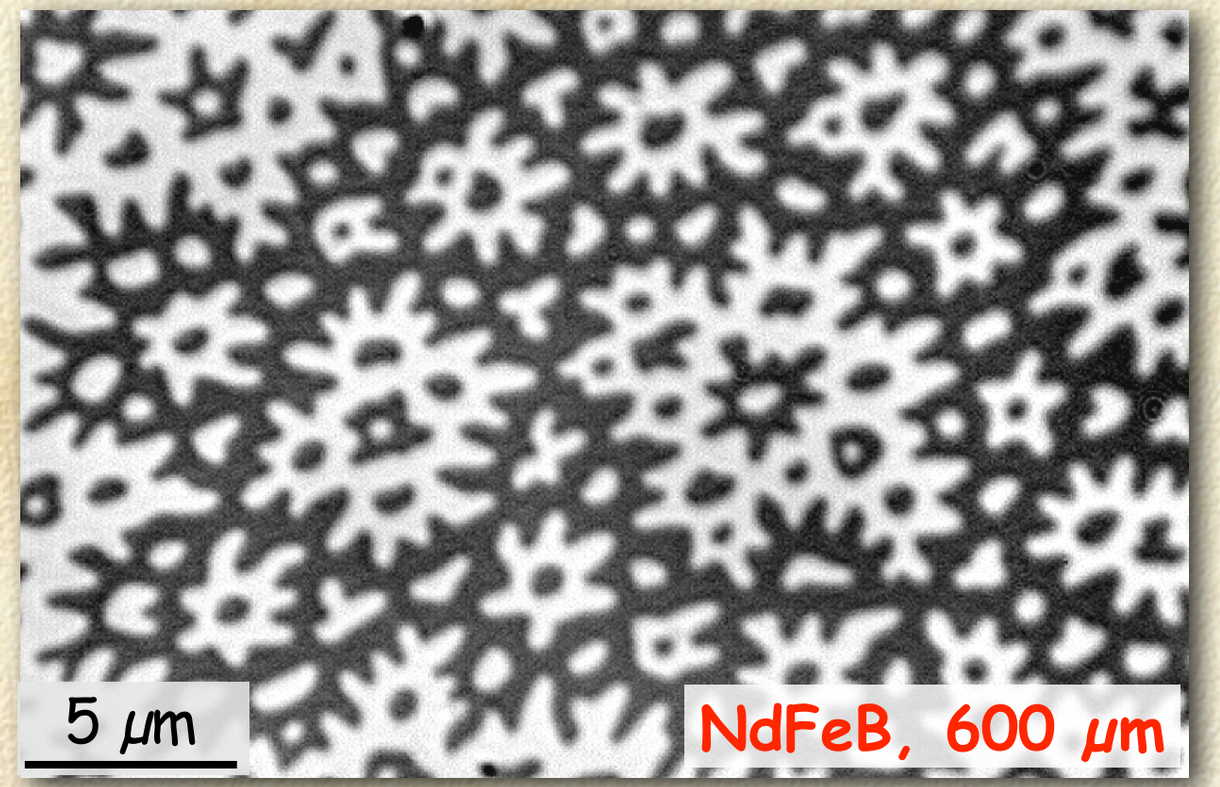

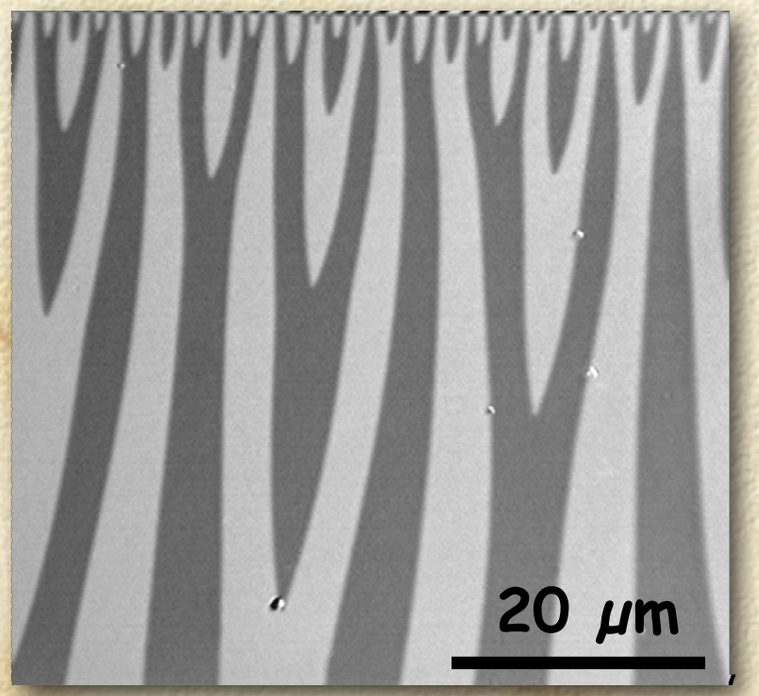

$Q << 1$

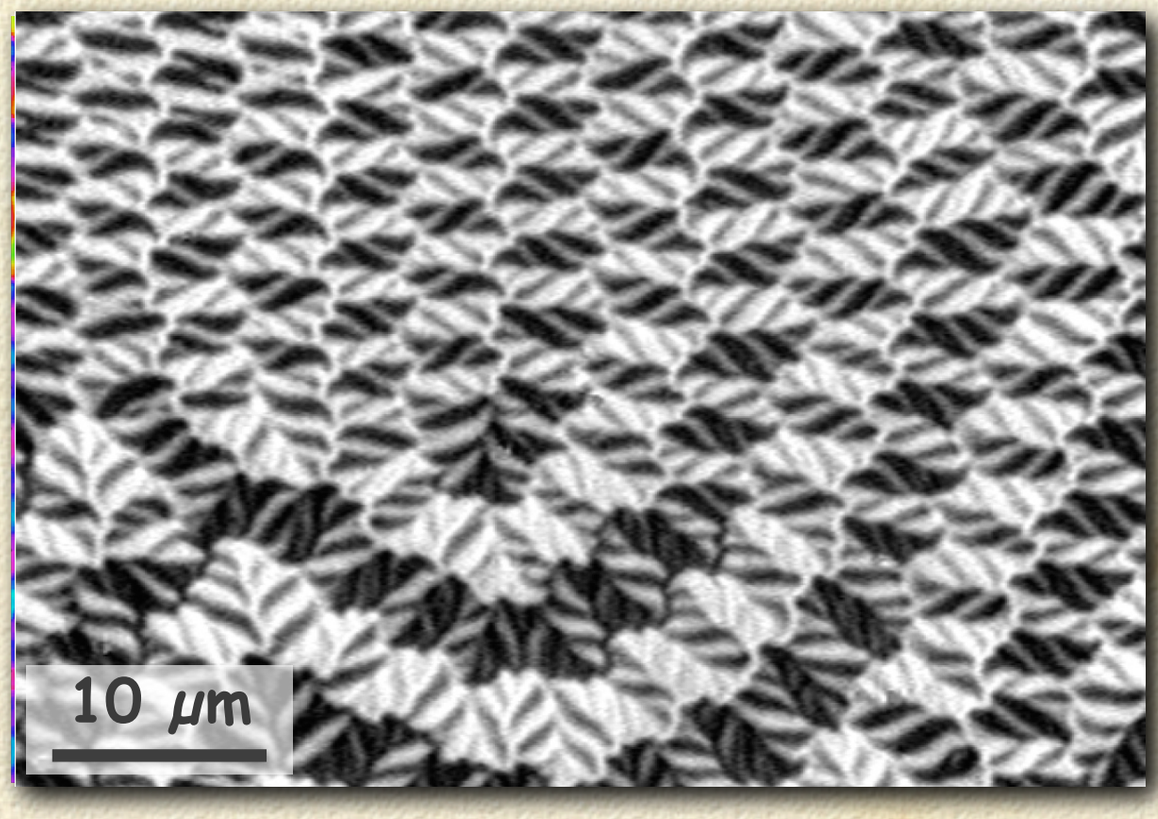

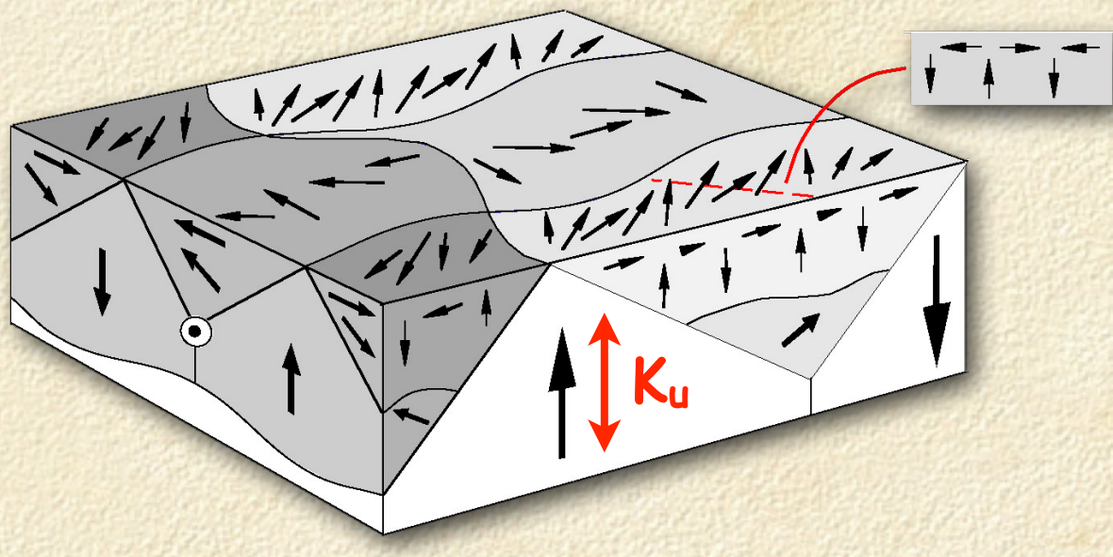

General Classification of Domains

$Q >> 1$

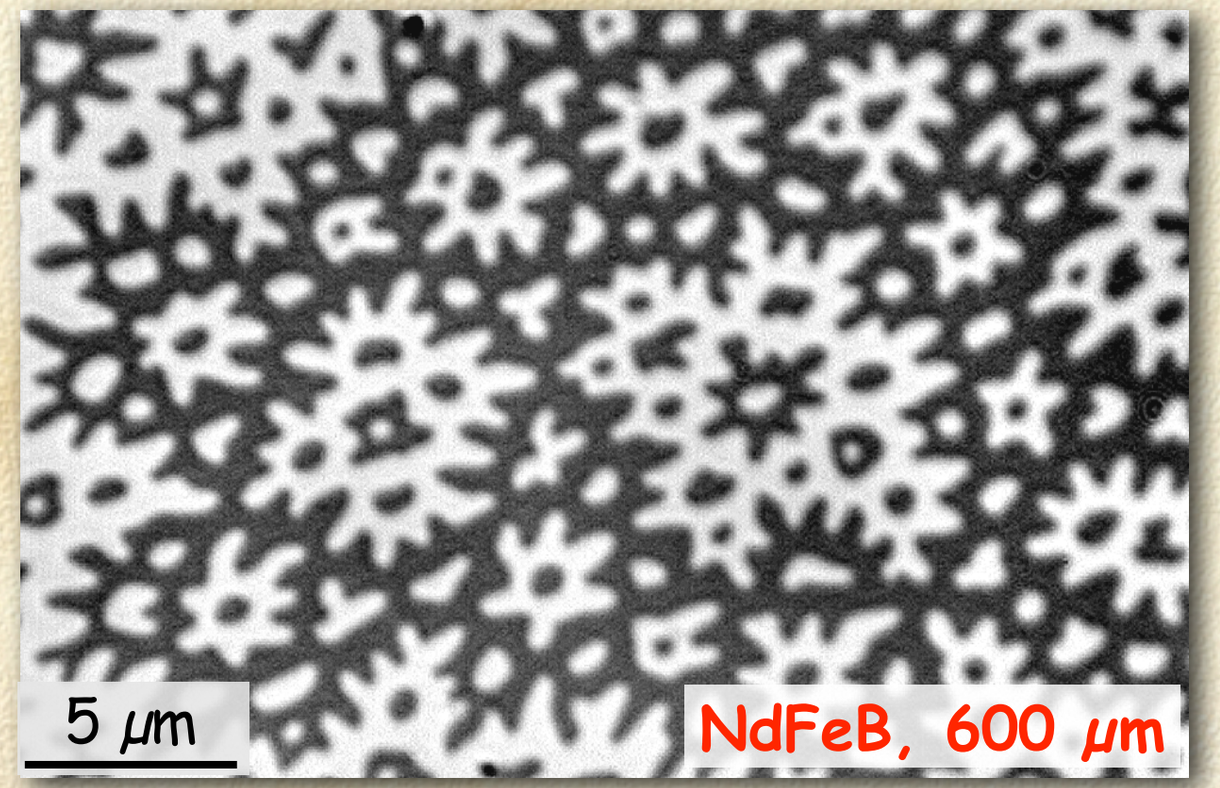

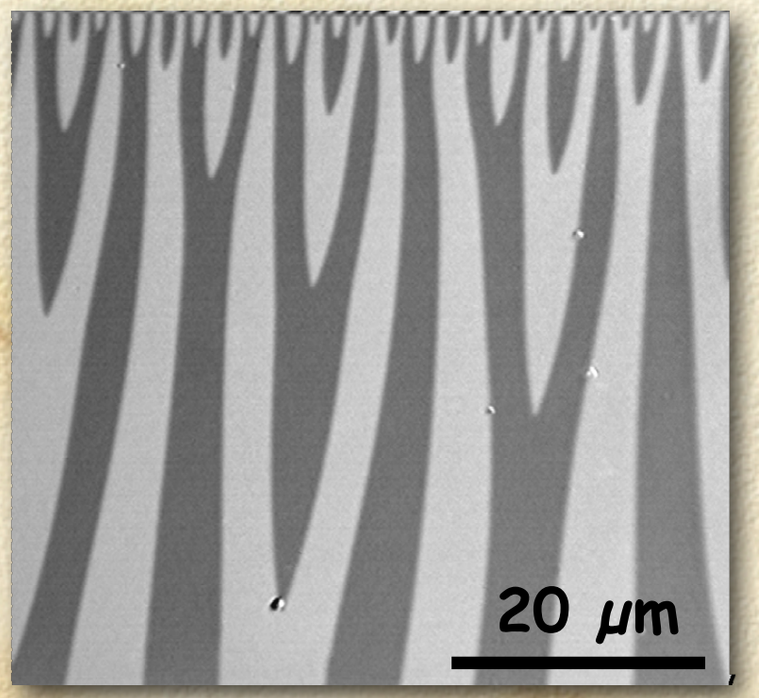

$Q << 1$

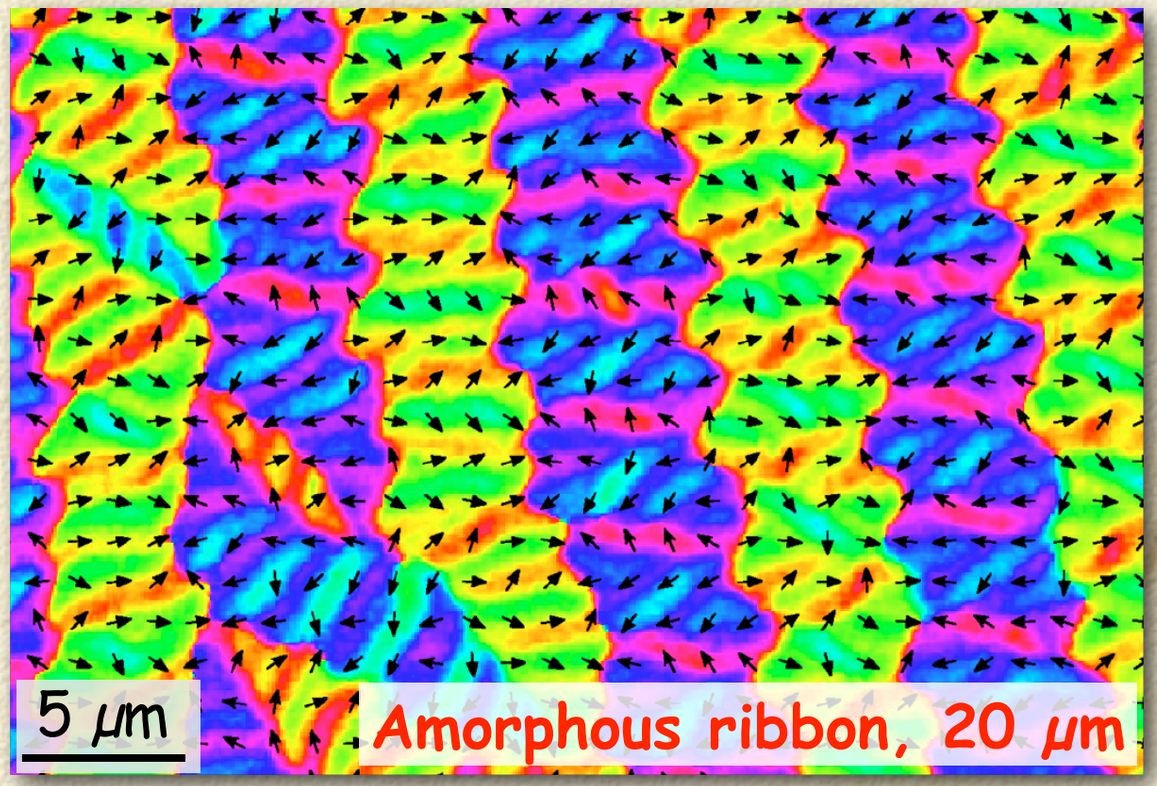

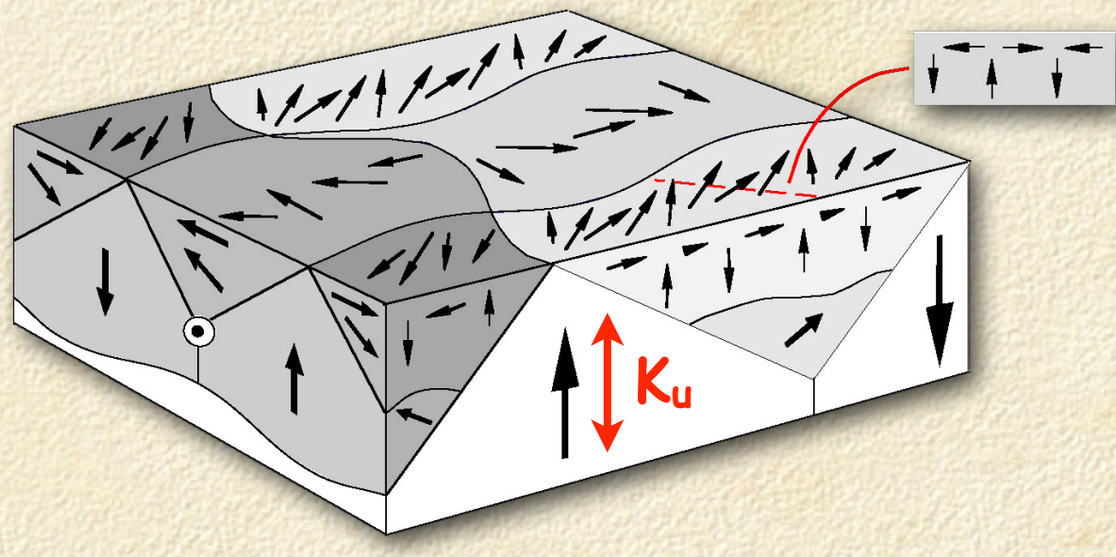

General Classification of Domains

$Q >> 1$

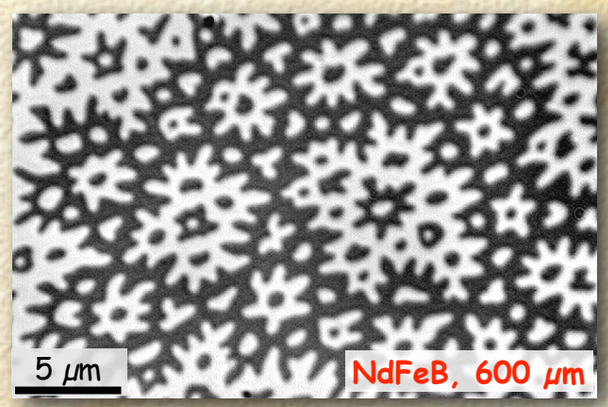

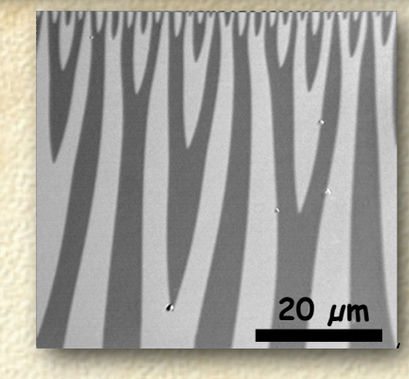

$Q << 1$

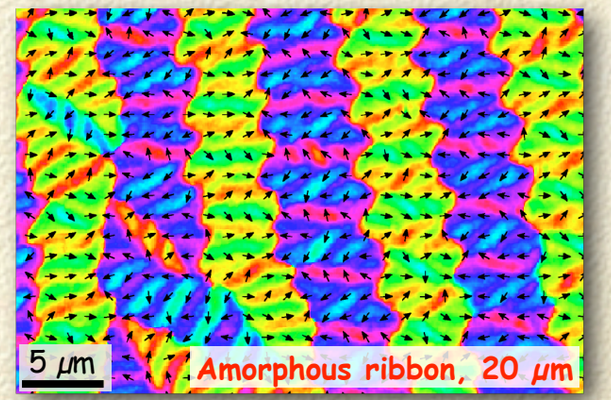

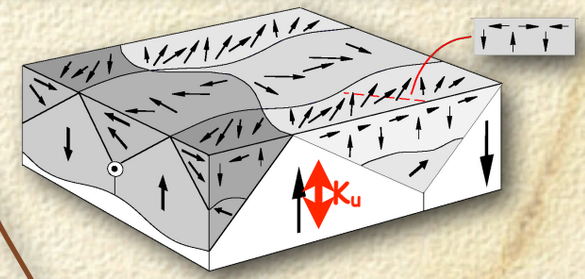

General Classification of Domains

$Q \gg 1$

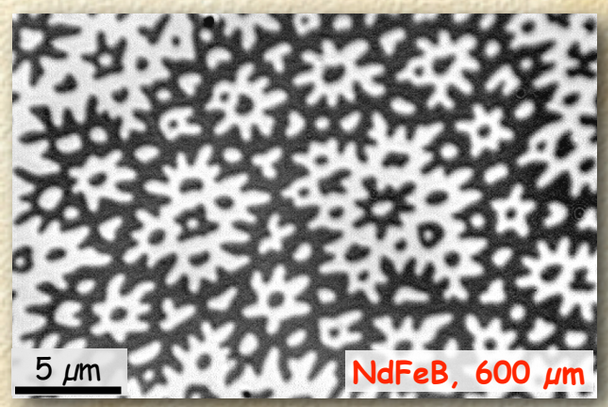

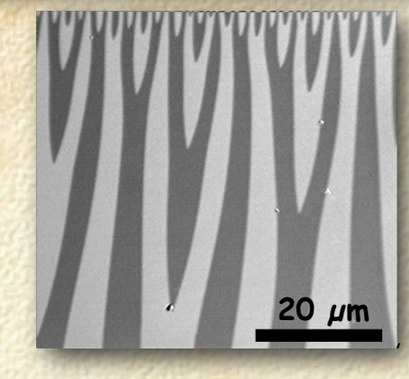

$Q \approx 1$

$Q \ll 1$

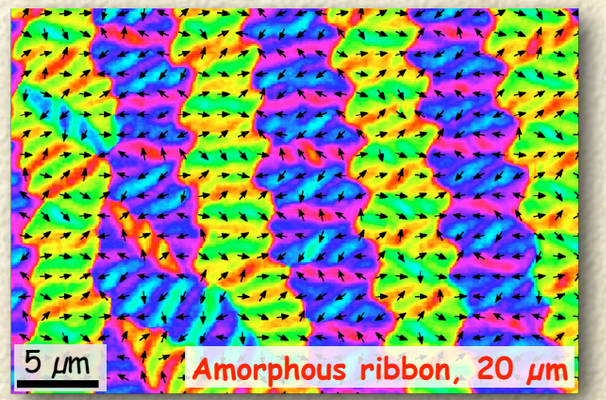

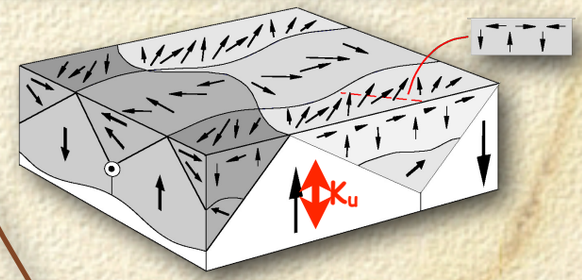

General Classification of Domains

$Q >> 1$

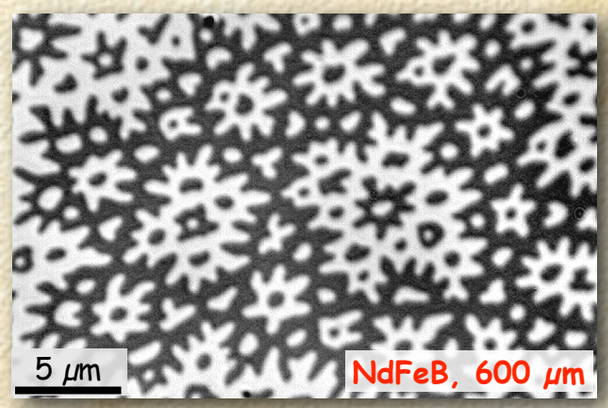

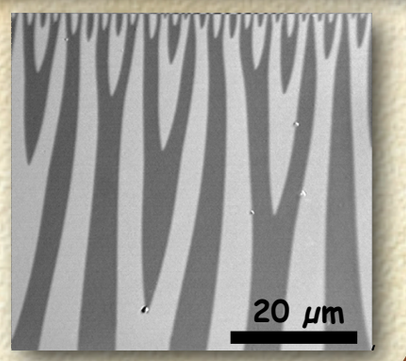

$Q \approx 1$

Cobalt: Q = 0.4

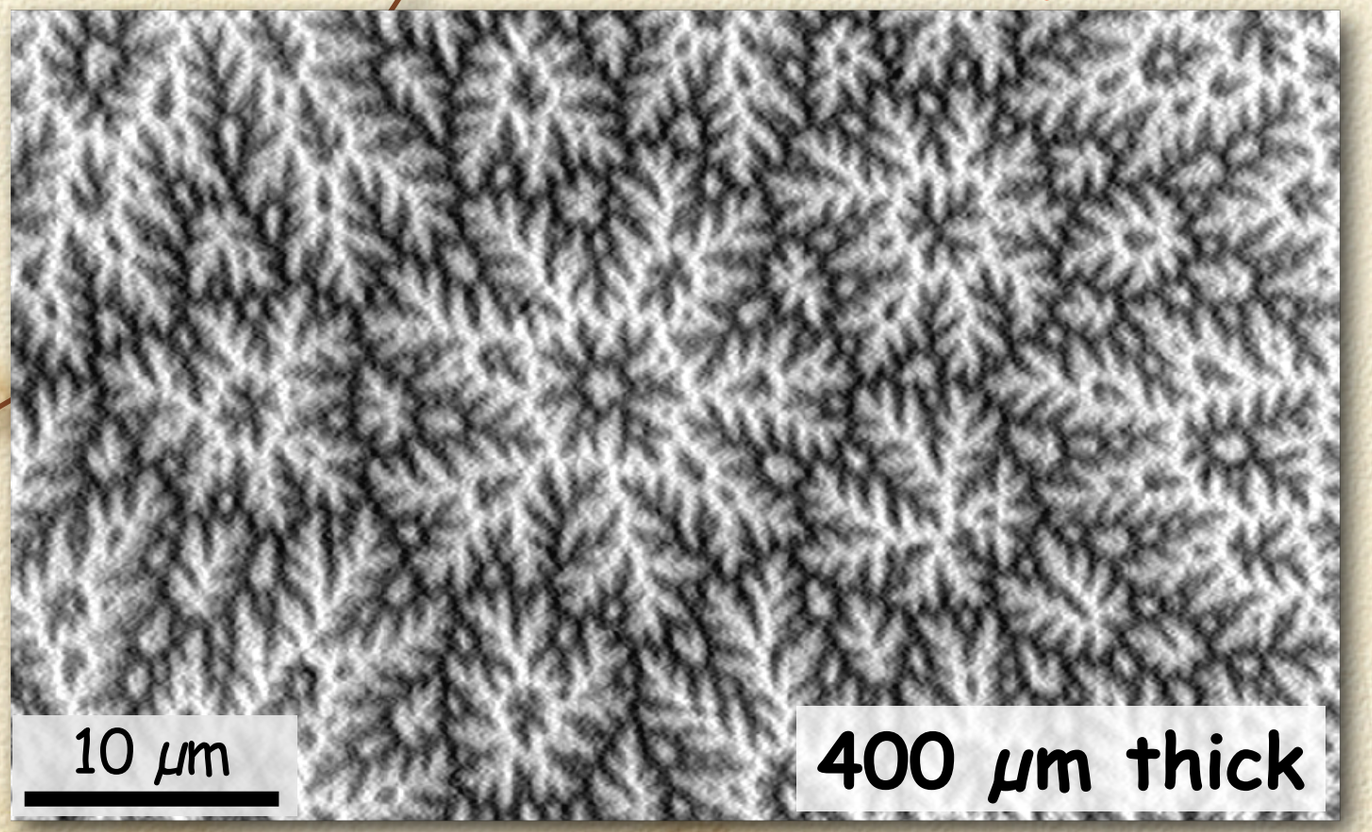

$Q << 1$

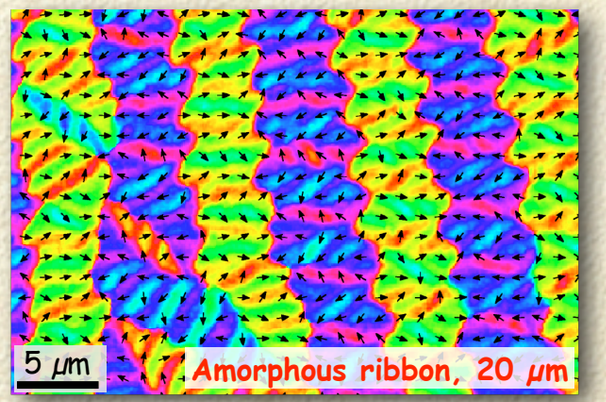

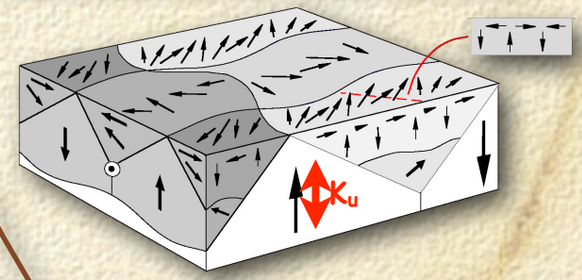

General Classification of Domains

$Q \gg 1$

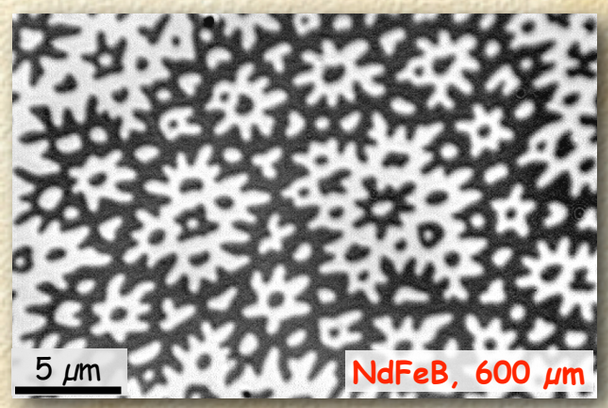

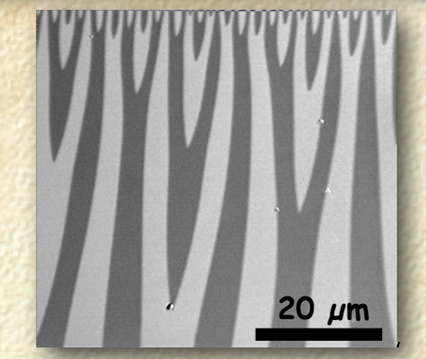

$Q \approx 1$

Cobalt: Q = 0.4

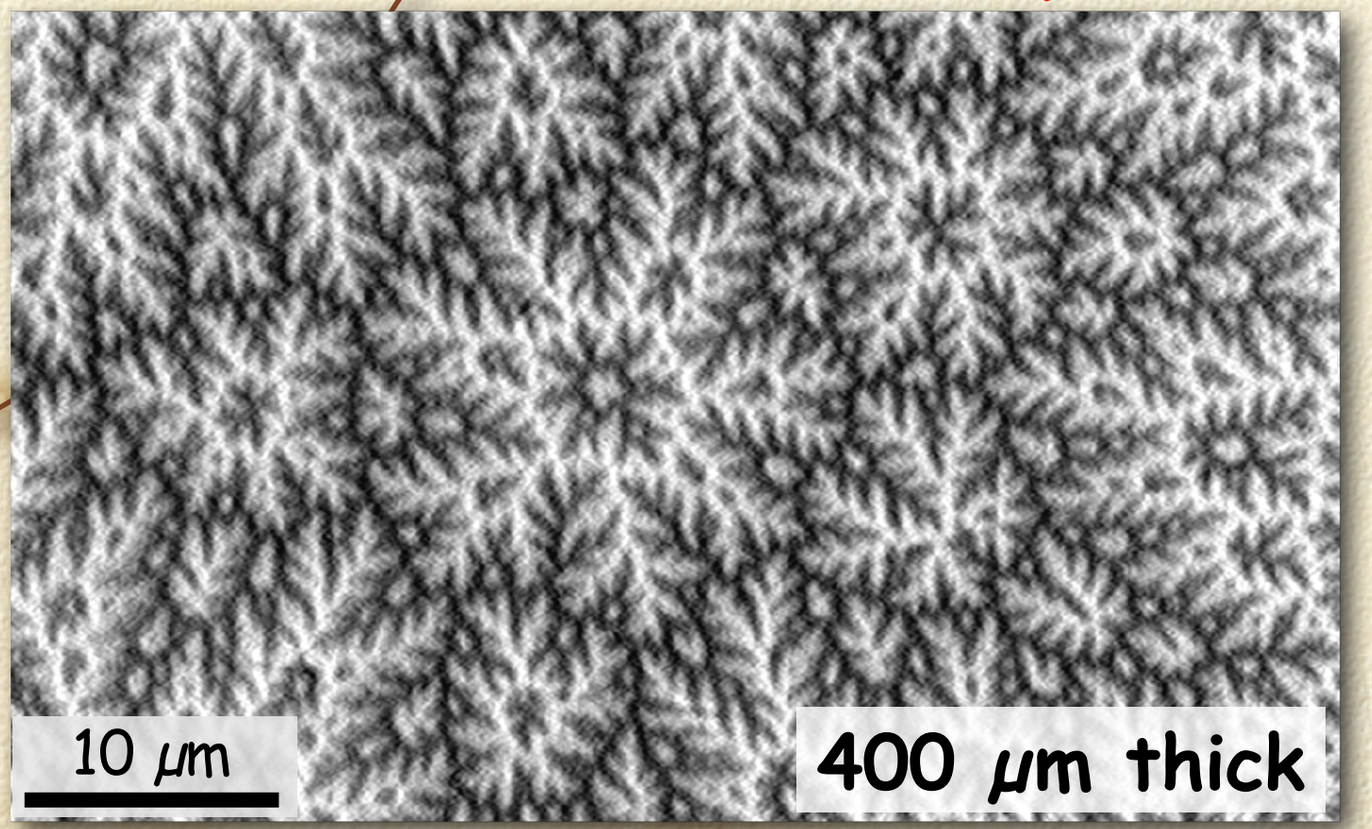

$Q \ll 1$

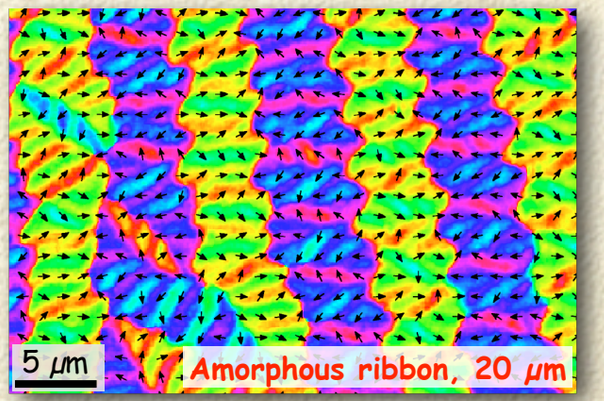

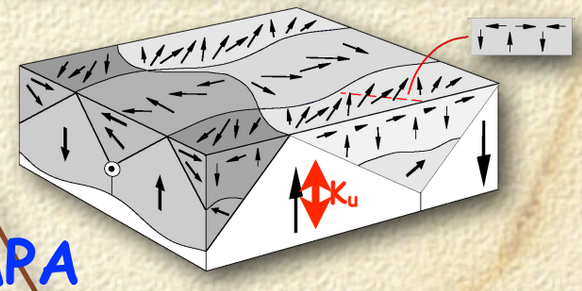

SEMPA
(courtesy John Unguris, NIST)

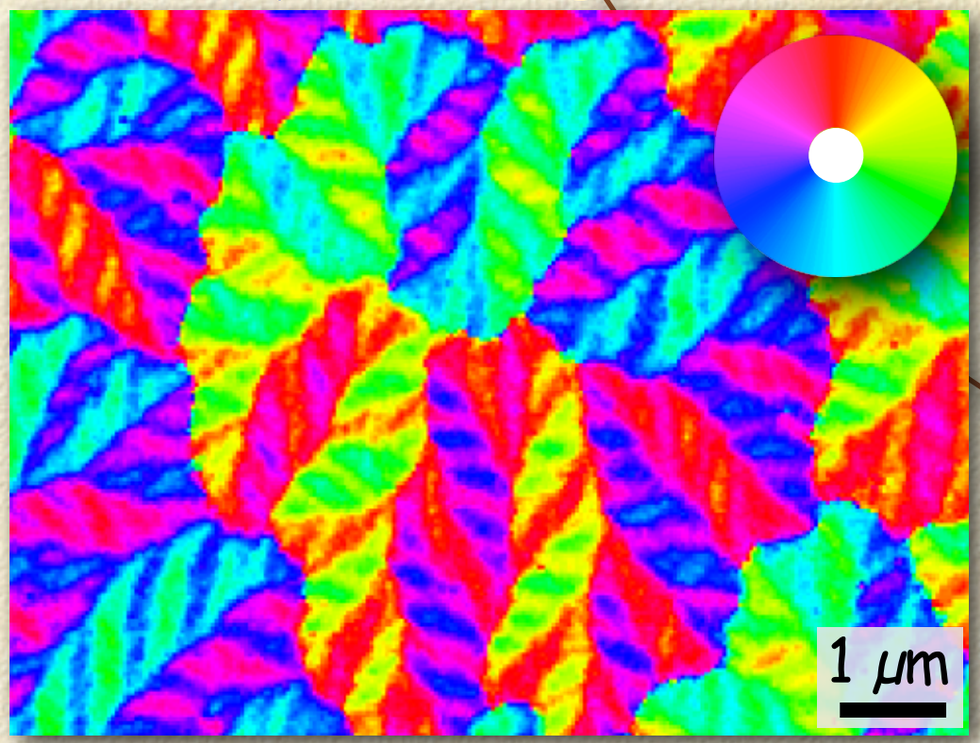

In-plane contrast at surface

General Classification of Domains

$Q >> 1$

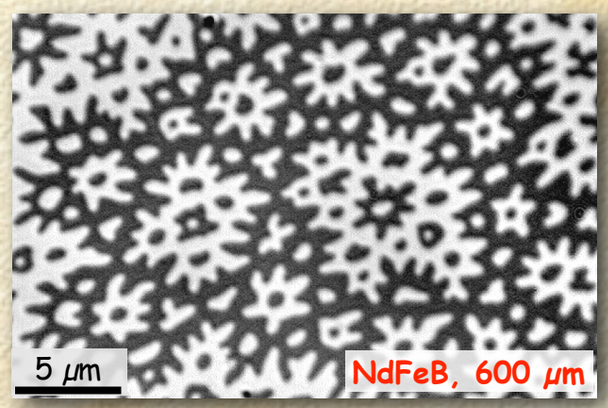

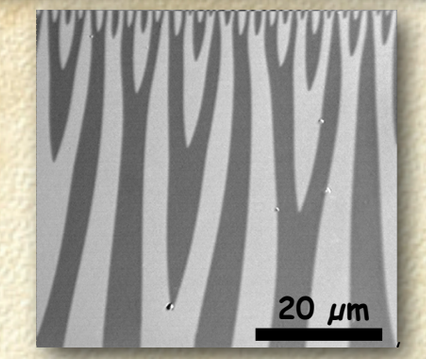

$Q \approx 1$

Partial closure

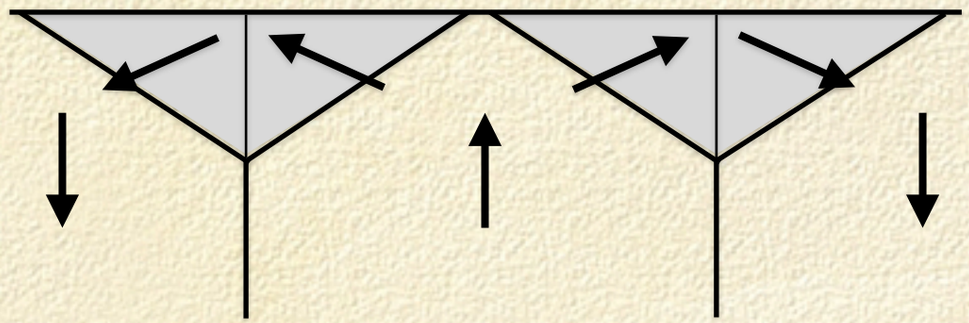

Cobalt: Q = 0.4

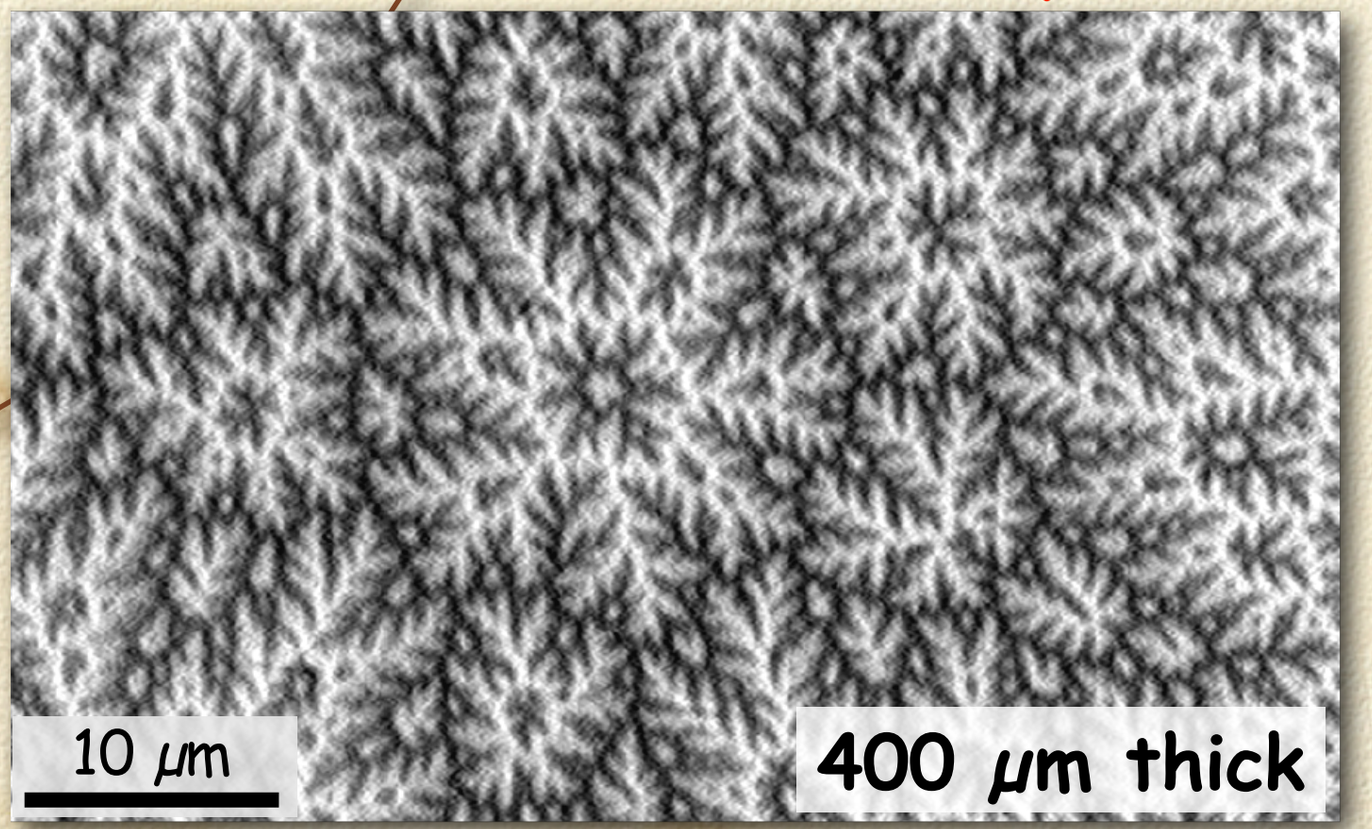

$Q << 1$

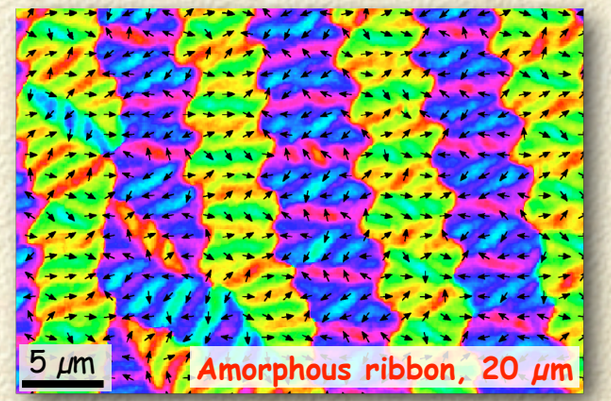

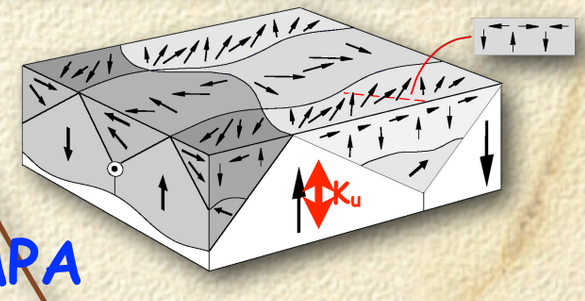

SEMPA
(courtesy John Unguris, NIST)

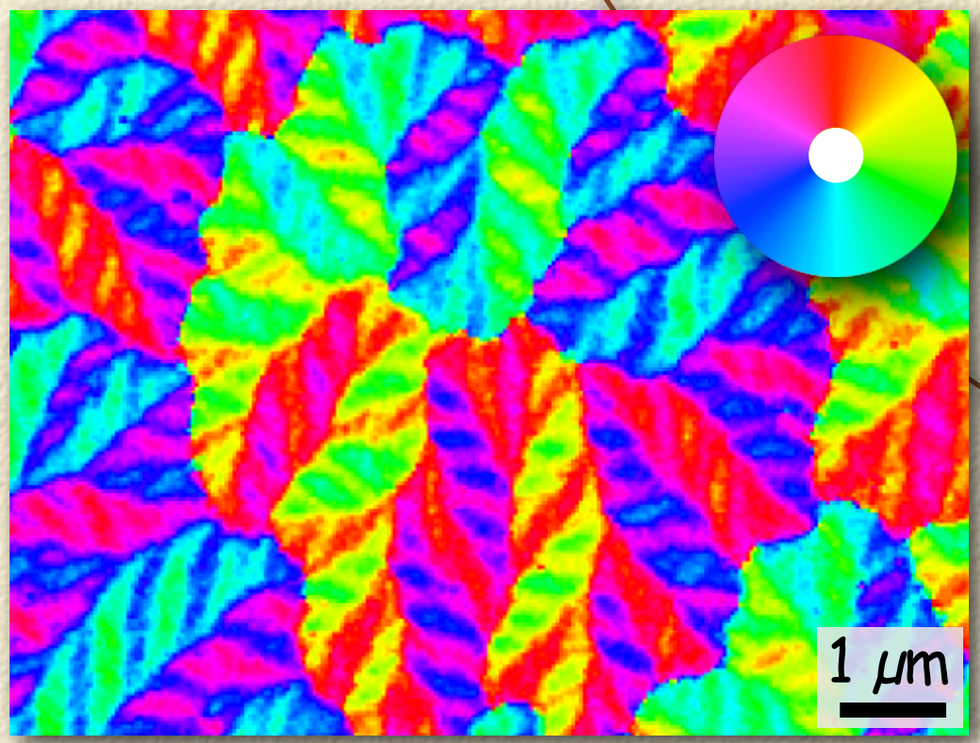

In-plane contrast at surface

General Classification of Domains

$Q >> 1$

N

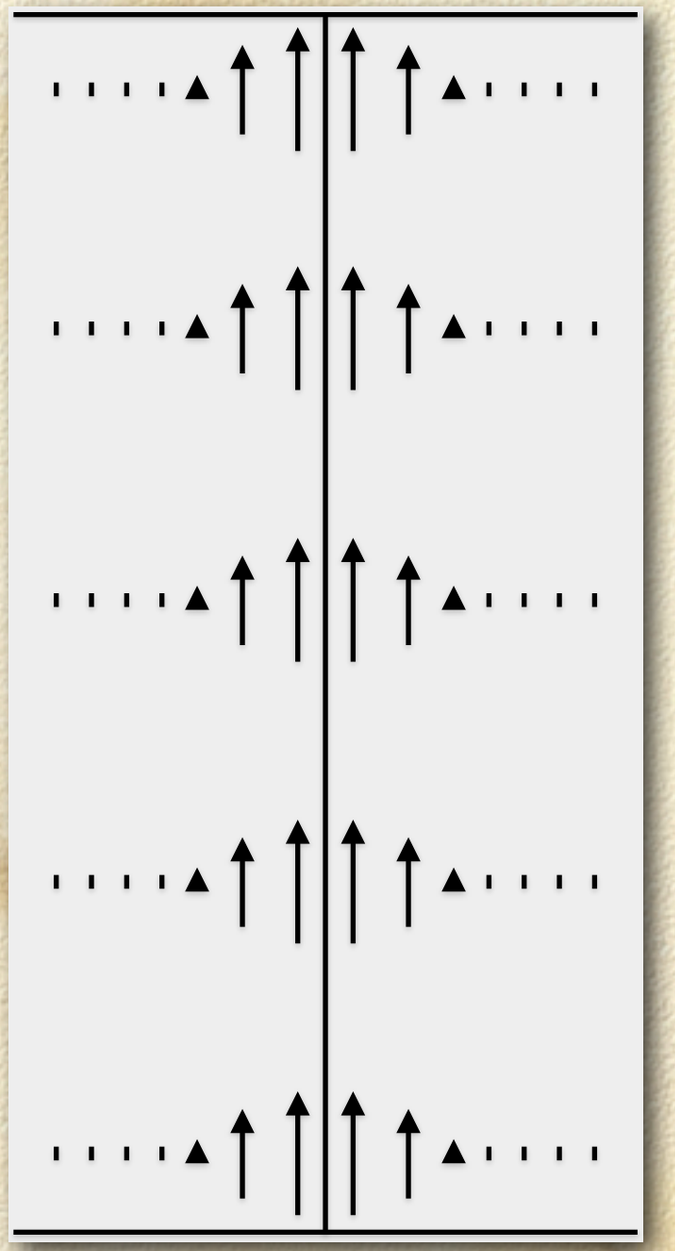

S

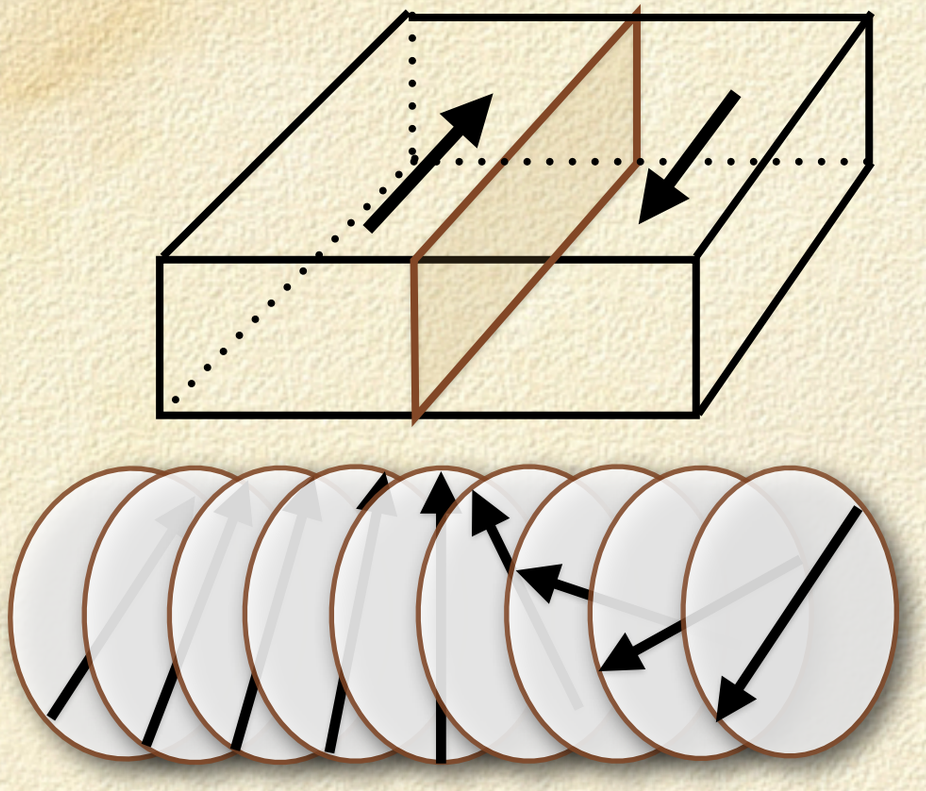

$Q << 1$

Pole-free

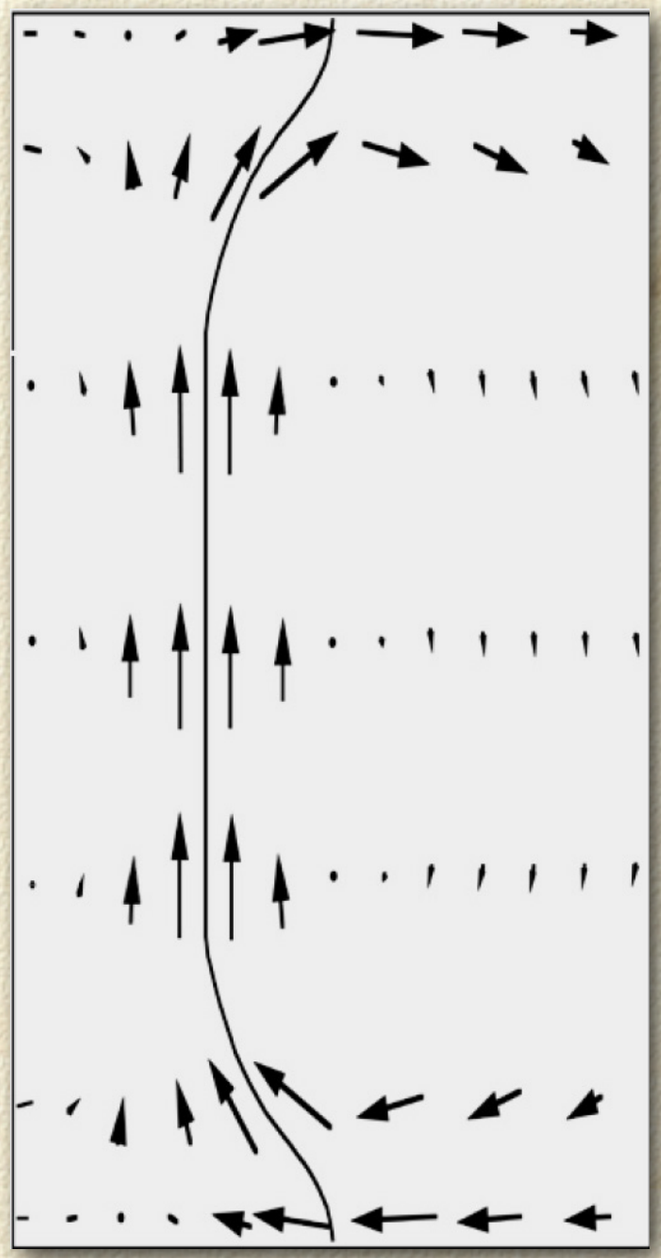

General Classification of Domains

Kerr observation on Fe whisker

$Q \ll 1$

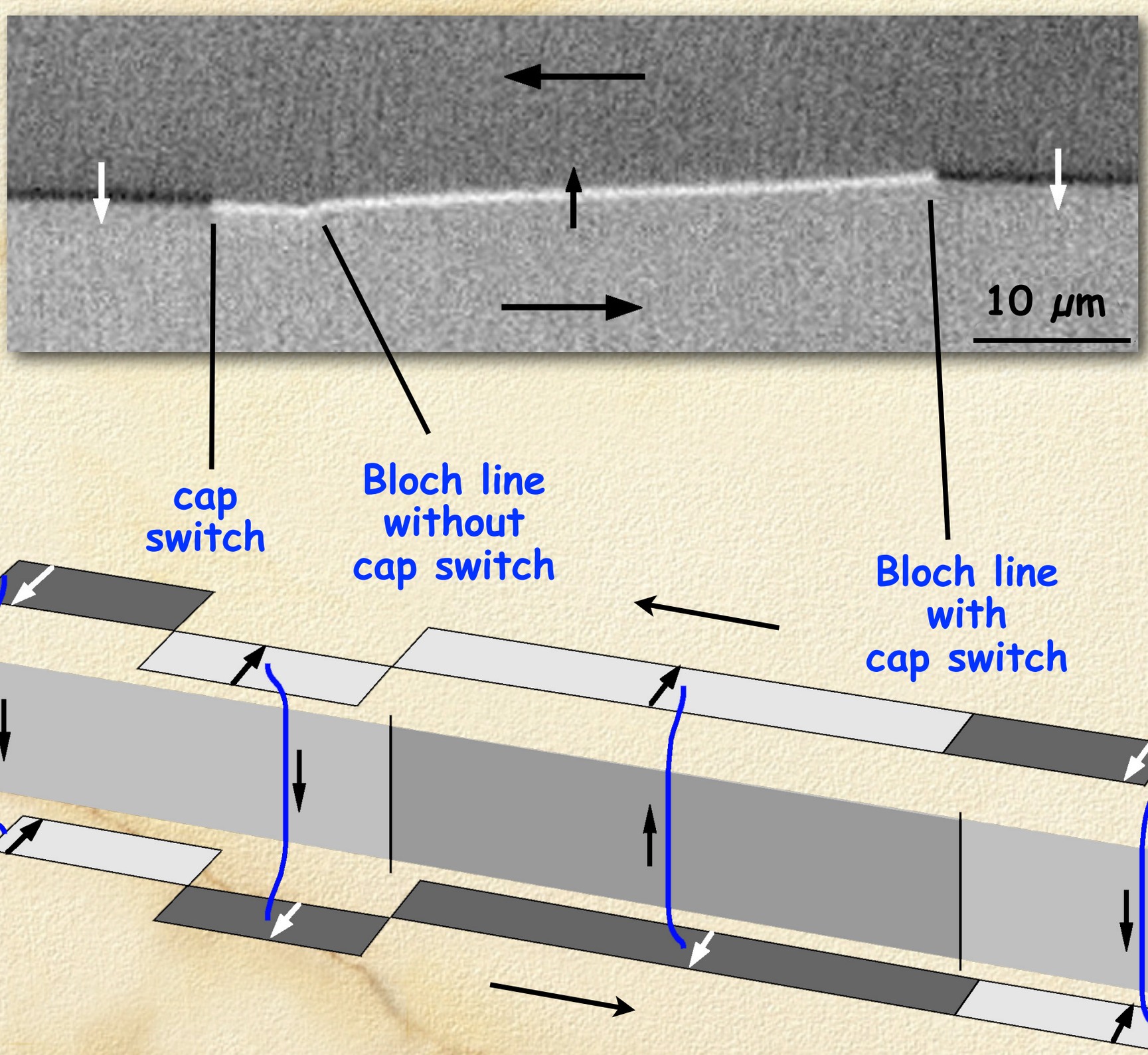

Pole-free

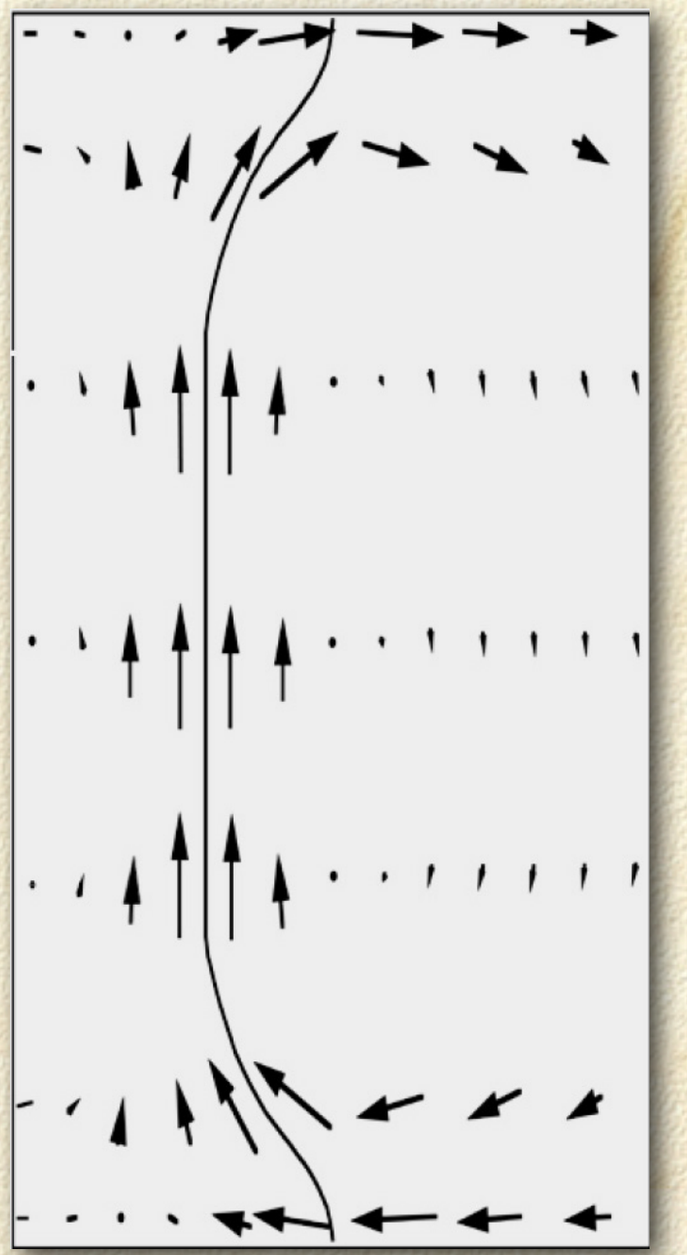

General Classification of Domains

$Q \ll 1$

servation on Fe whisker

Swirl

10 μm

cap switch

Bloch line without cap switch

Bloch line with cap switch

Pole-free

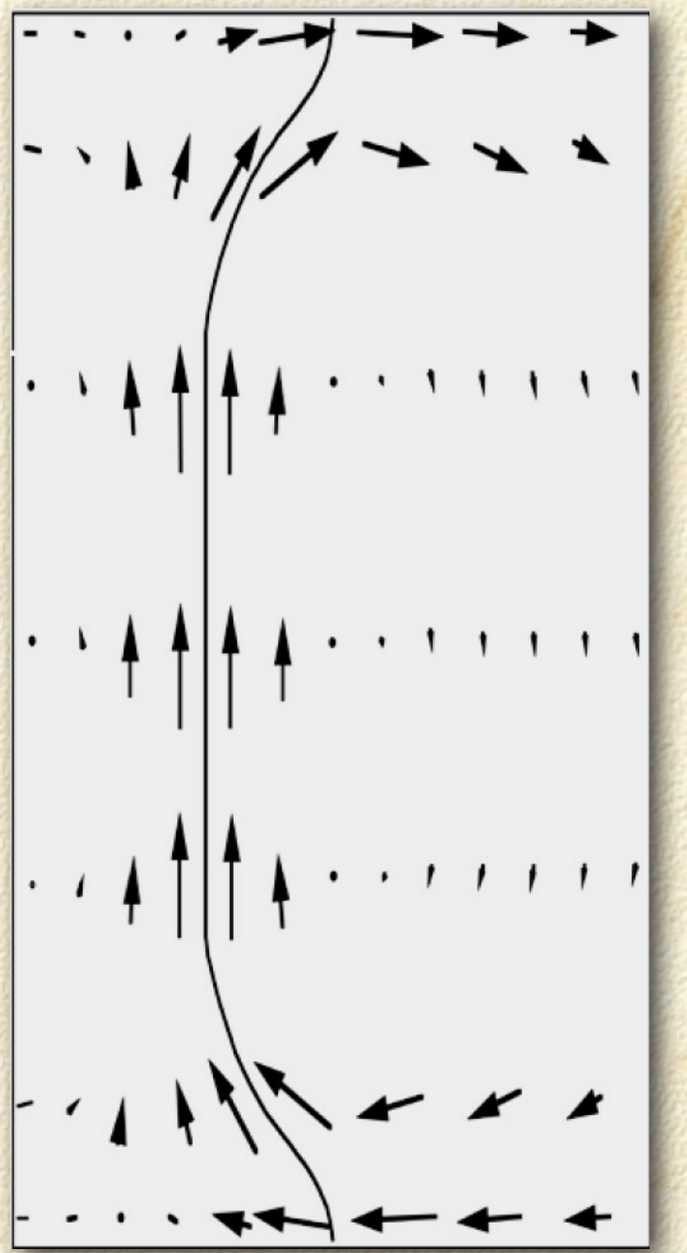

Analysis of Magnetic Domains

1) Experimental imaging

Amorphous ribbon (Co-rich, 45 μm thick)

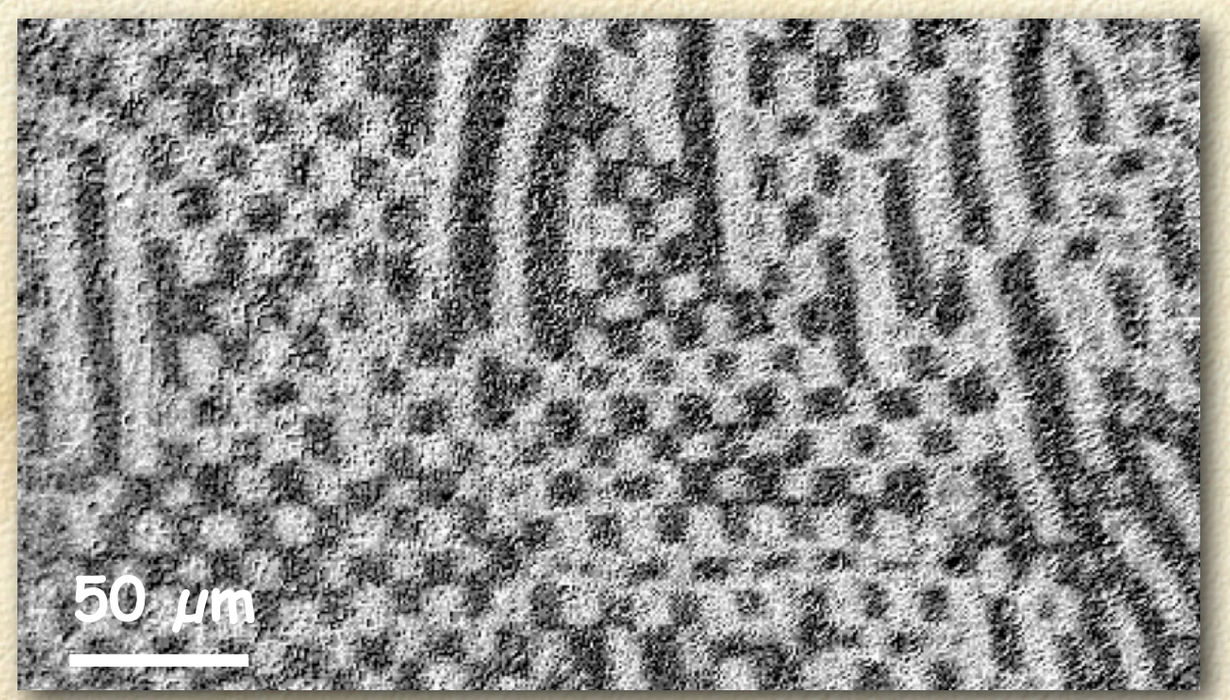

(image: courtesy G. Herzer, VAC)

Analysis of Magnetic Domains

1) Experimental imaging

Amorphous ribbon (Co-rich, 45 μm thick)

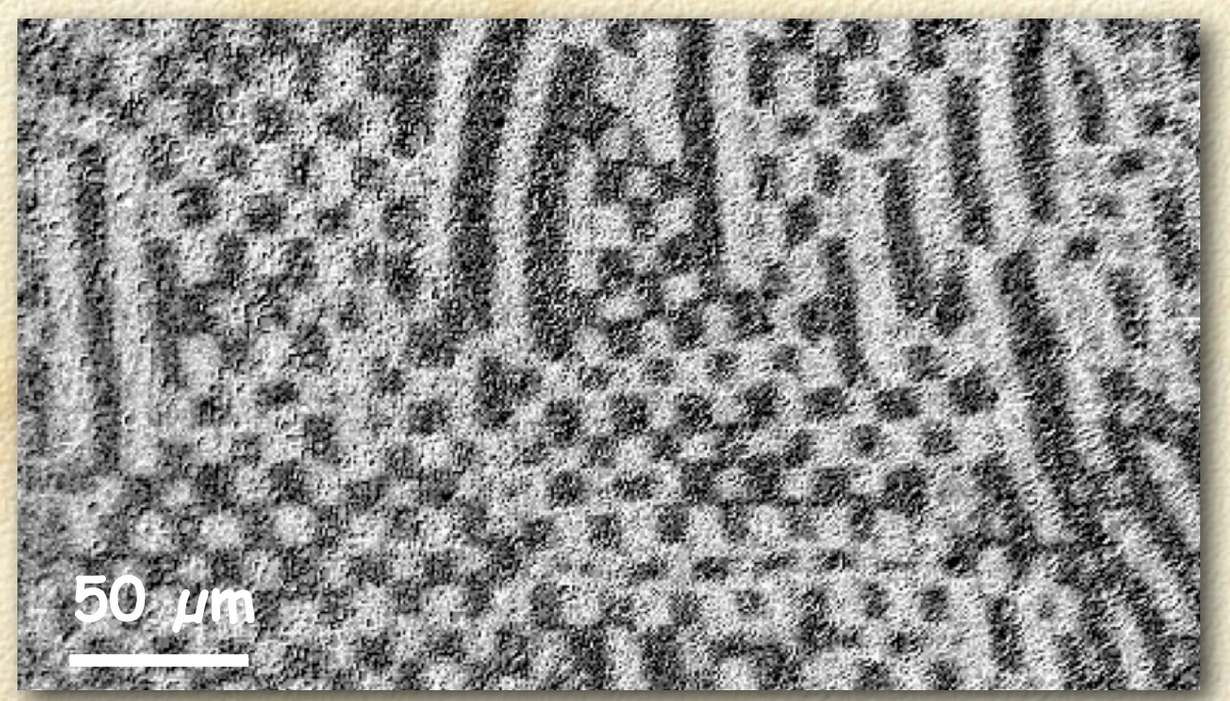

(image: courtesy G. Herzer, VAC)

2) Domain model

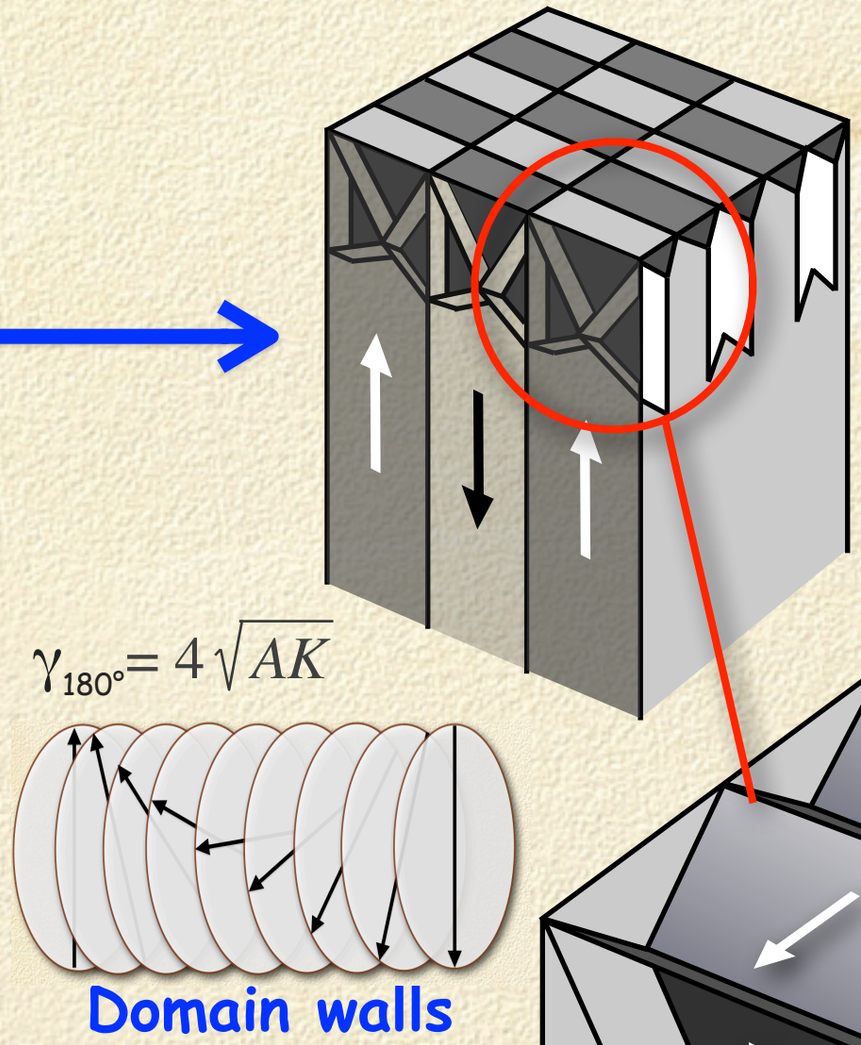

$Q \ll 1$

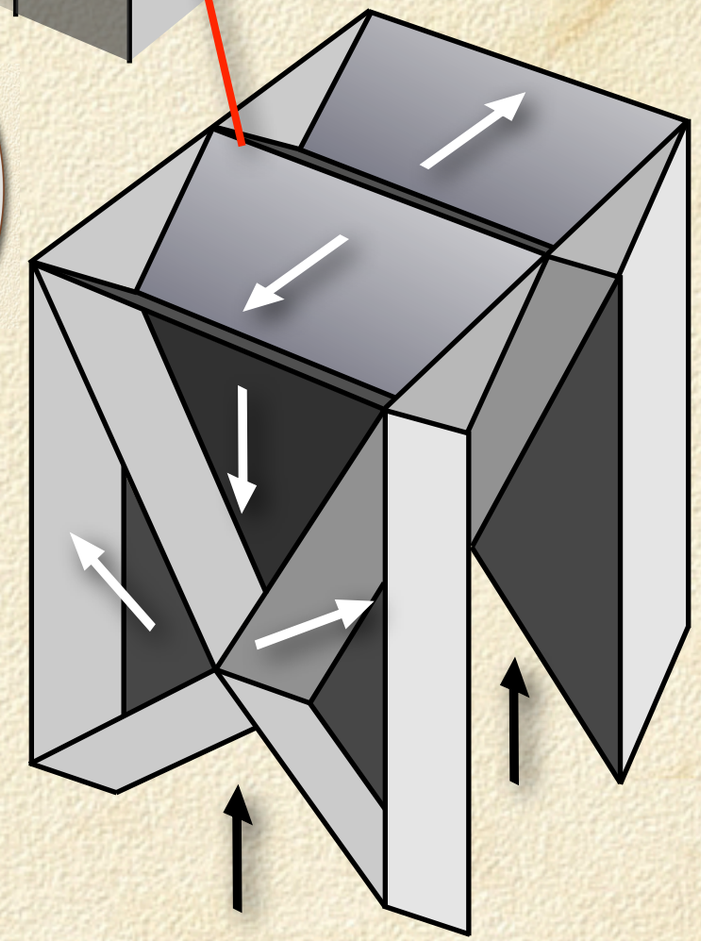

Analysis of Magnetic Domains

1) Experimental imaging

Amorphous ribbon (Co-rich, 45 μm thick)

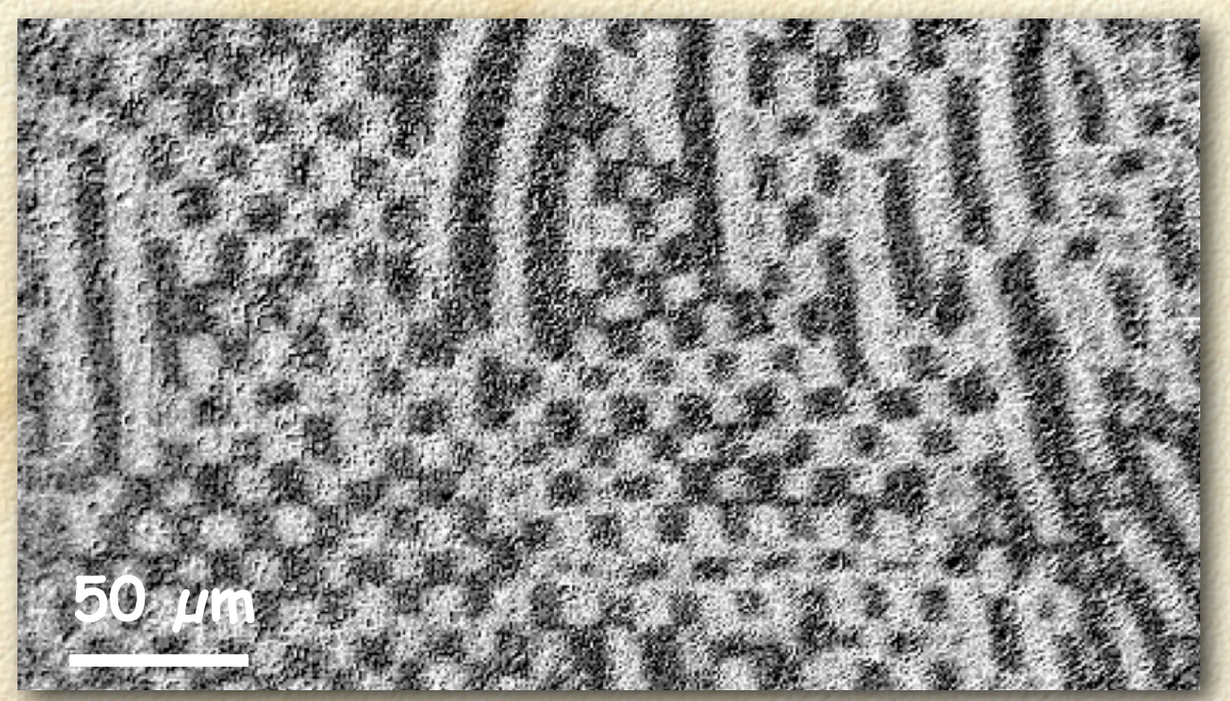

(image: courtesy G. Herzer, VAC)

2) Domain model

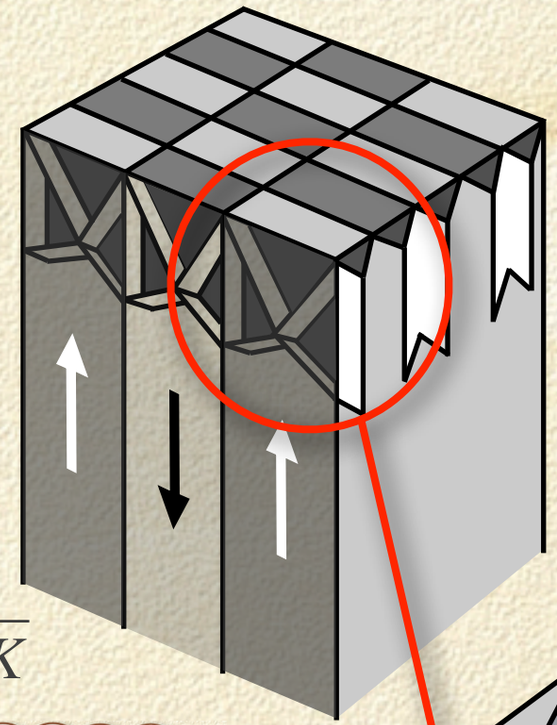

$Q \ll 1$

$\gamma_{180°} = 4\sqrt{AK}$

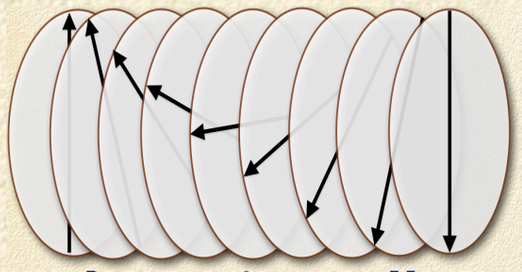

Domain walls

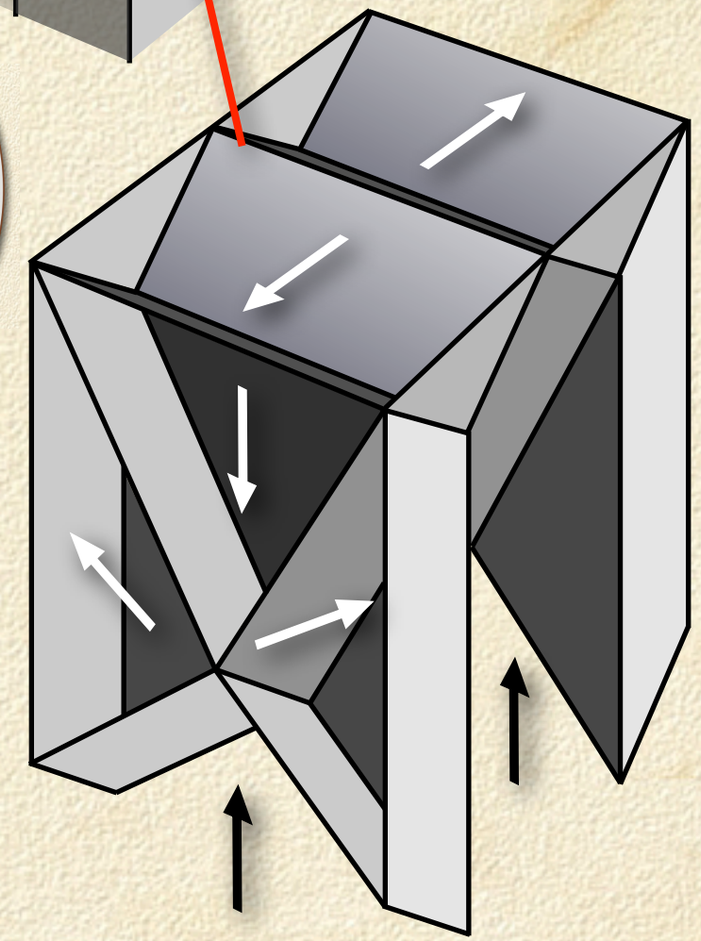

3) Optimization of model for minimum energy

Analysis of Magnetic Domains

1) Experimental imaging

Amorphous ribbon (Co-rich, 45 μm thick)

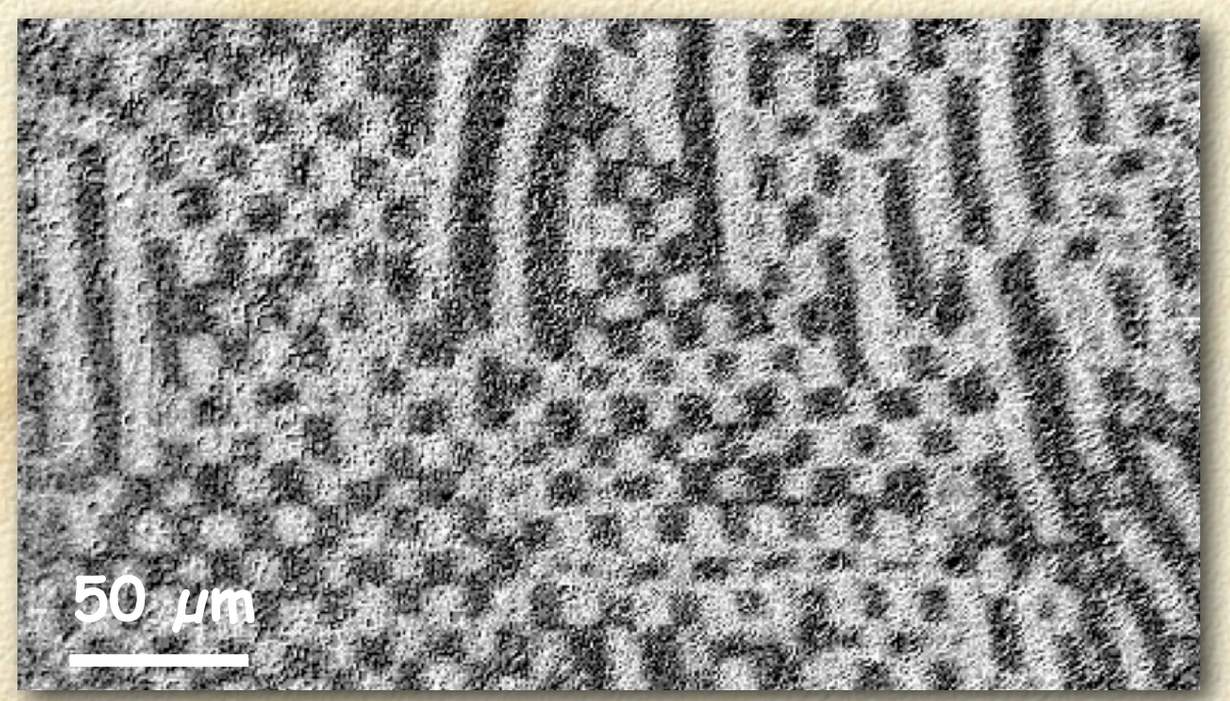

(image: courtesy G. Herzer, VAC)

2) Domain model

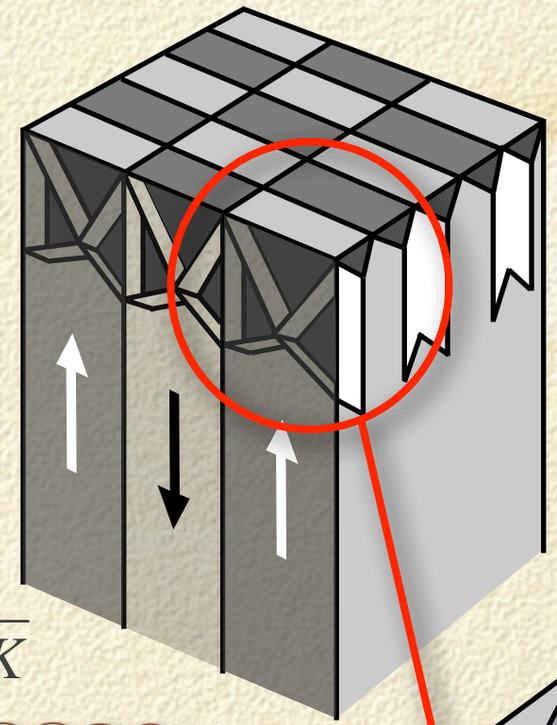

$Q \ll 1$

$\gamma_{180°} = 4\sqrt{AK}$

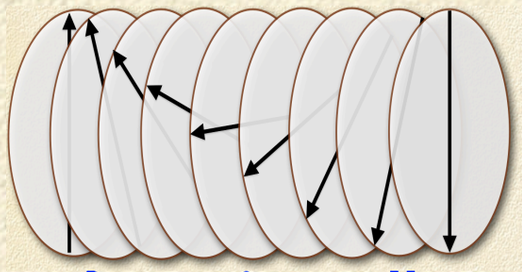

Domain walls

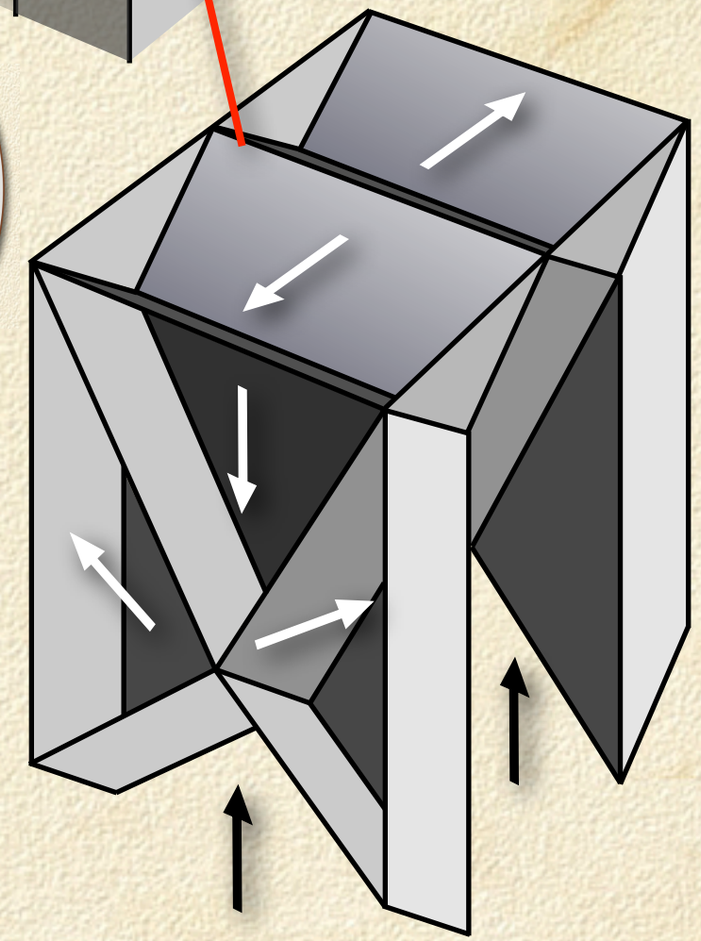

3) Optimization of model for minimum energy

4) Comparison with observation

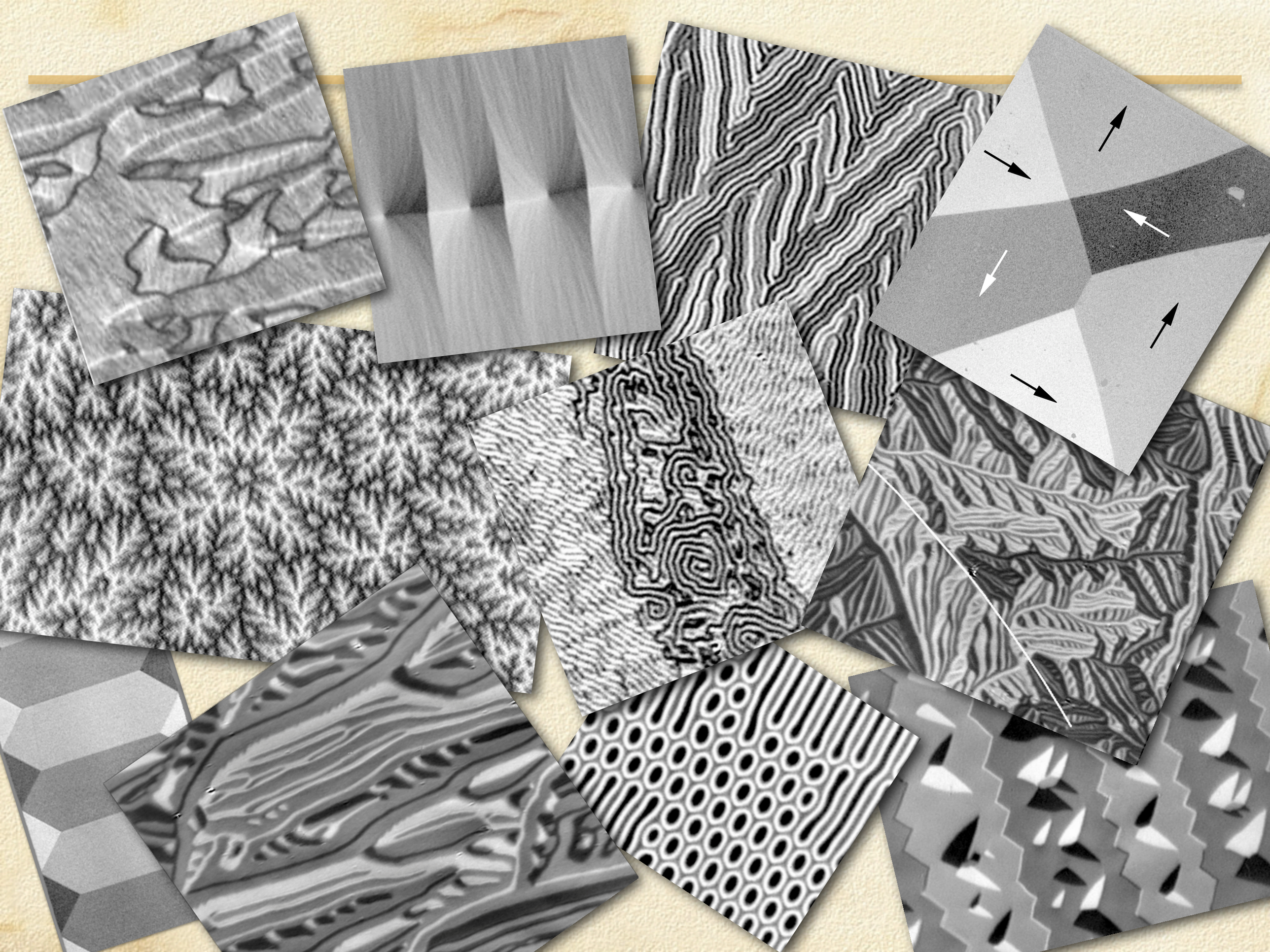

Domain analysis based on magneto-optical microscopy

Transparent films:
Domain analysis easily possible

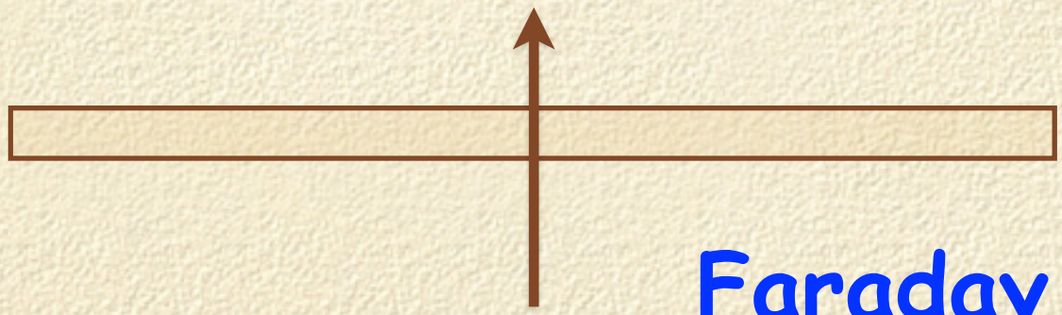

Faraday microscopy

Bubble garnet film

Band domains

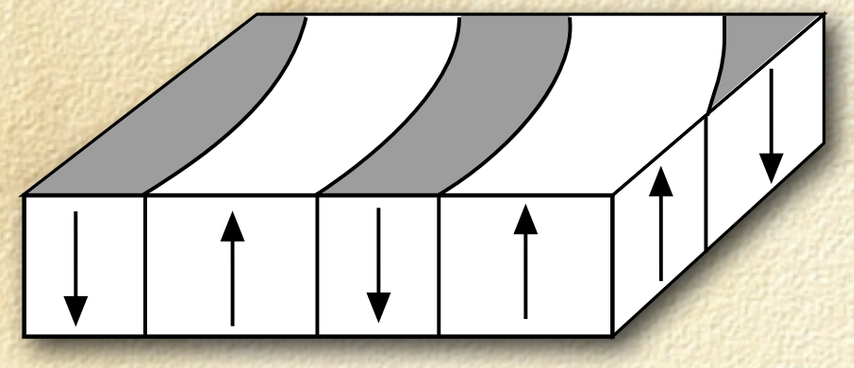

Bubble domains

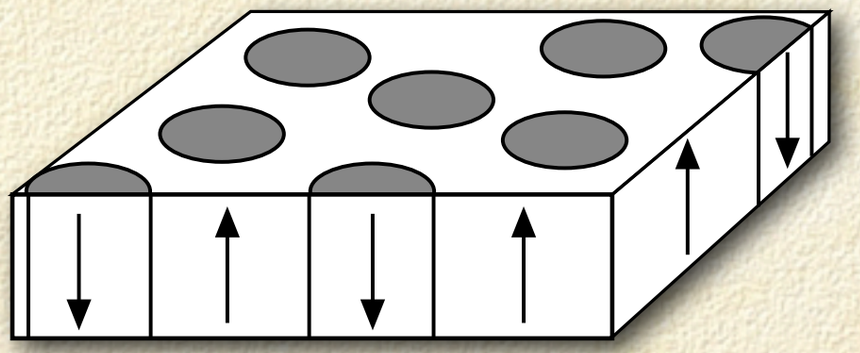

20 μm

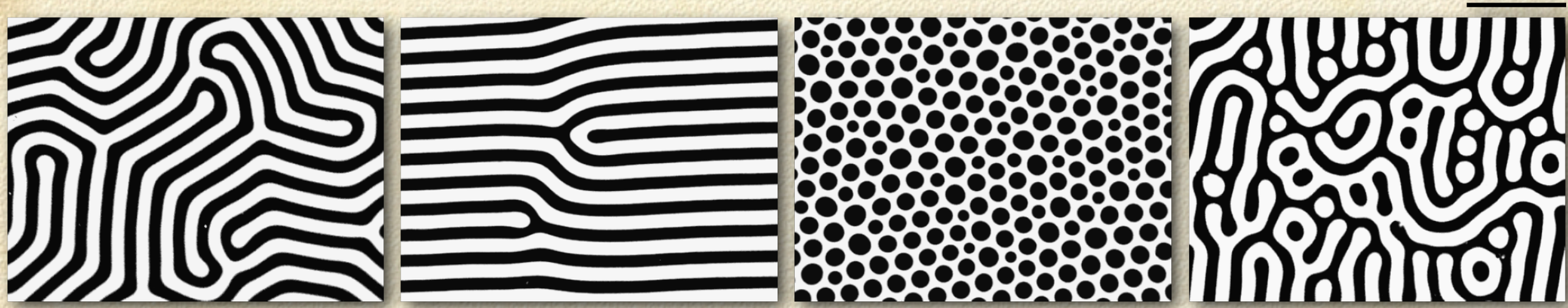

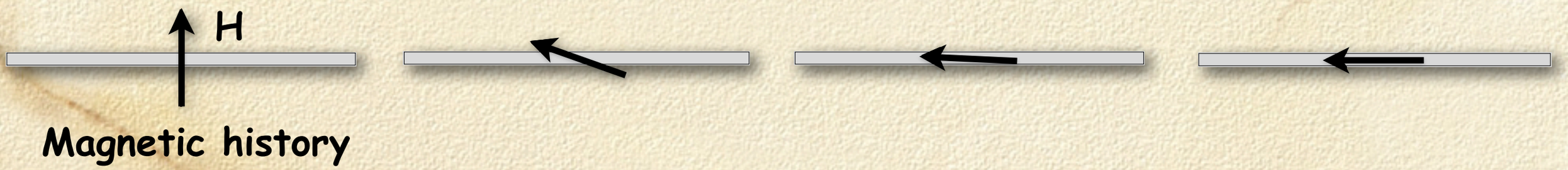

Magnetic history

Magnetic field history matters

Bubble garnet film

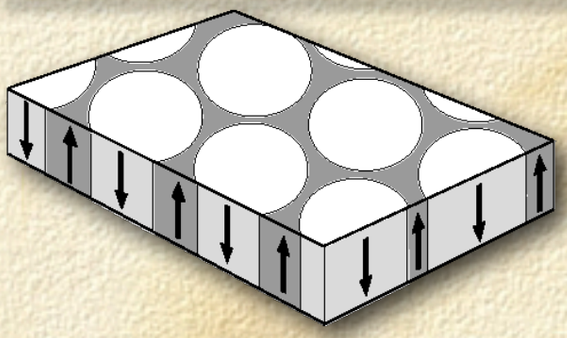

Configurational hysteresis

50 μm

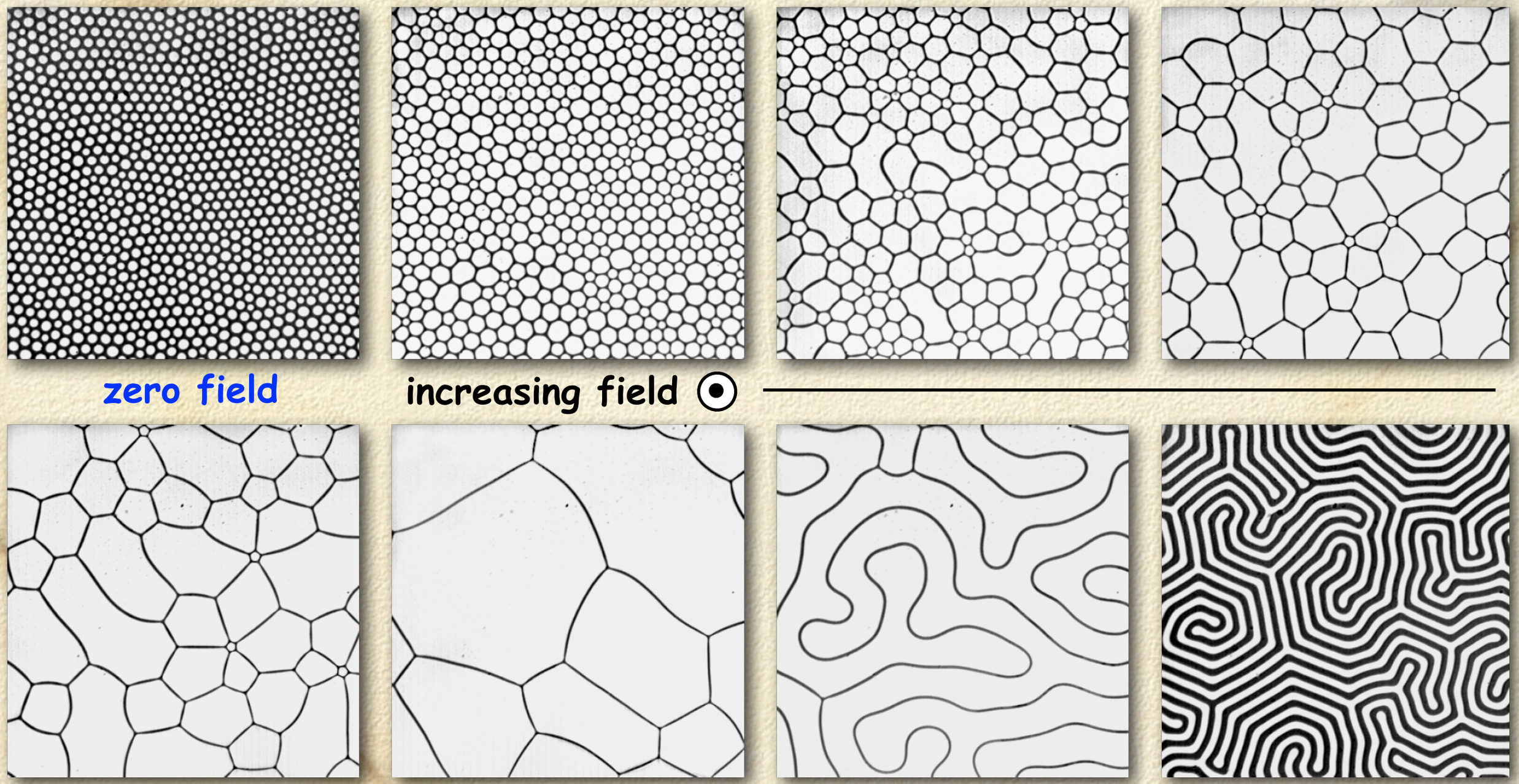

zero field

increasing field ⊙

decreasing field

zero field

Bubble garnet film

20 μm

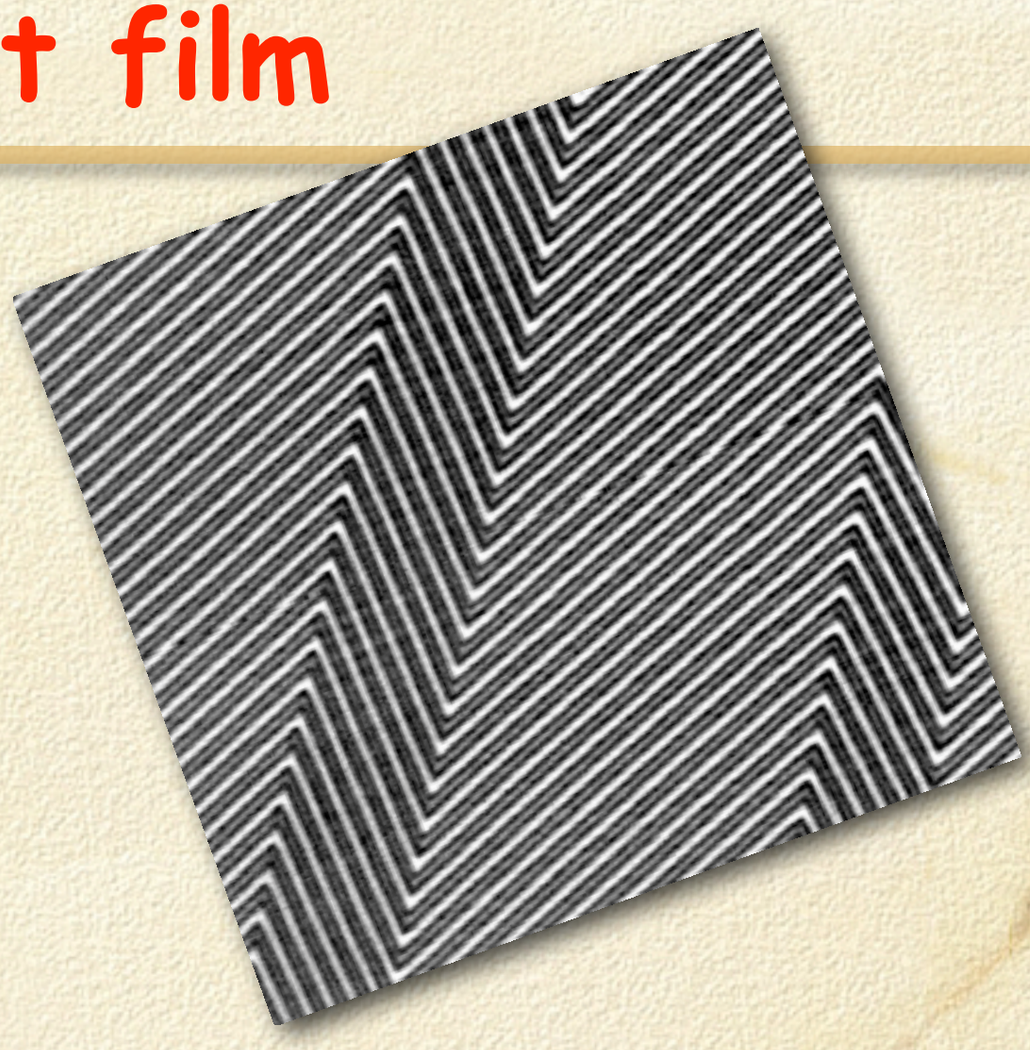

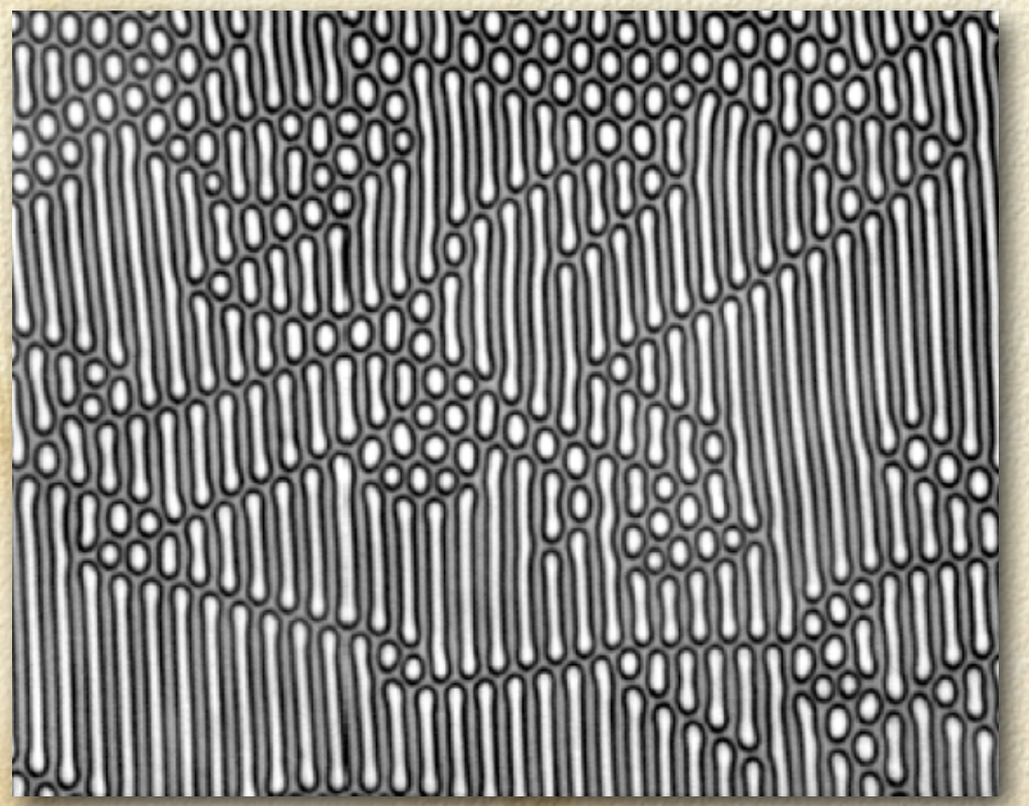

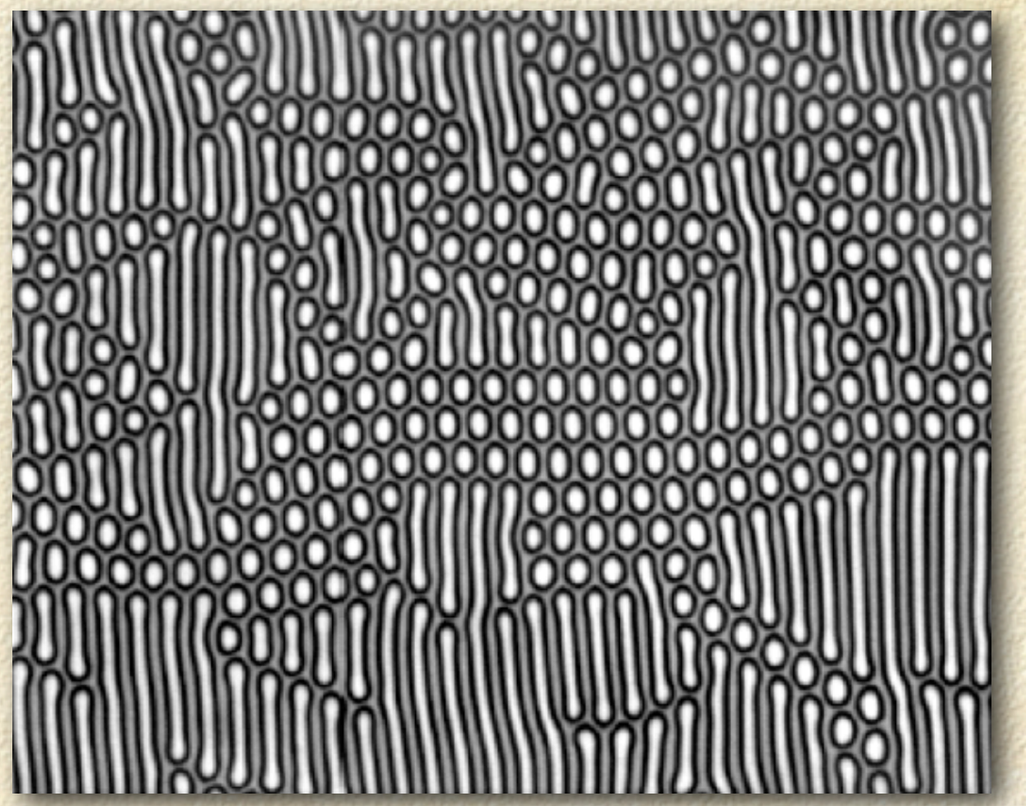

Bubble garnet film

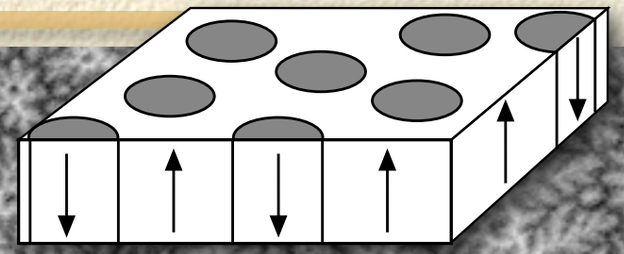

50 μm

GdYbBi garnet, 500 μm thick

Image: A. Stupaviewicz, M. Tekielak, A. Maziewski (Bialystok)

Sample: T. Satoh (Tokyo)

Metallic (single) films:

Domain analysis often easily possible …

Metallic (single) films:

Domain analysis often easily possible …

Permalloy film, 240 nm thick

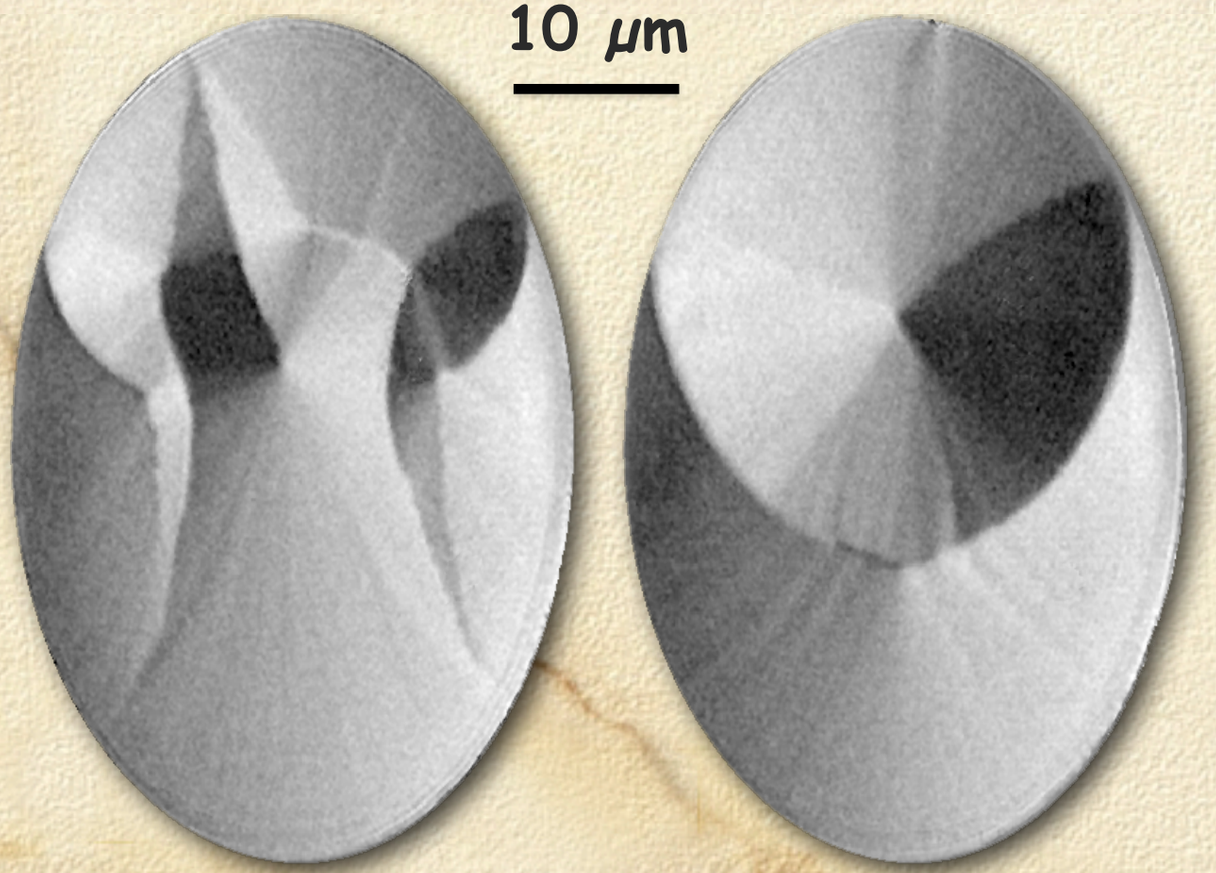

Epitaxial (100)-iron film, 40 nm thick

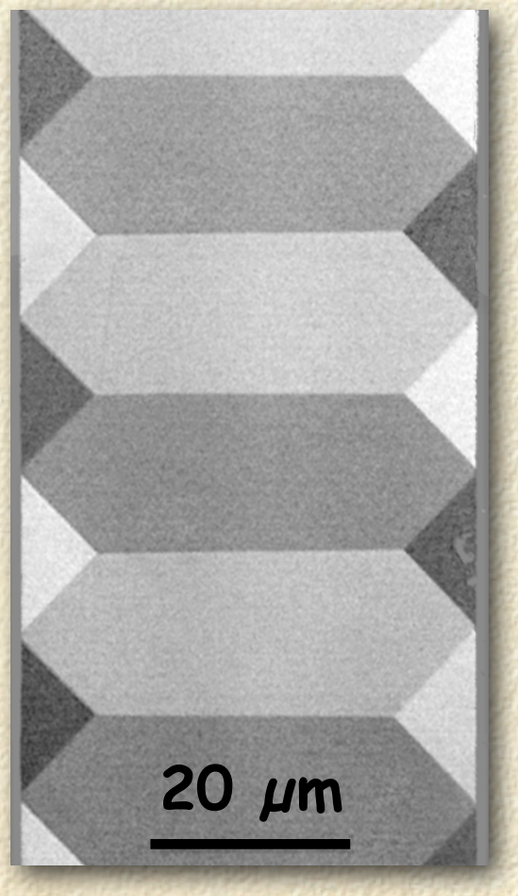

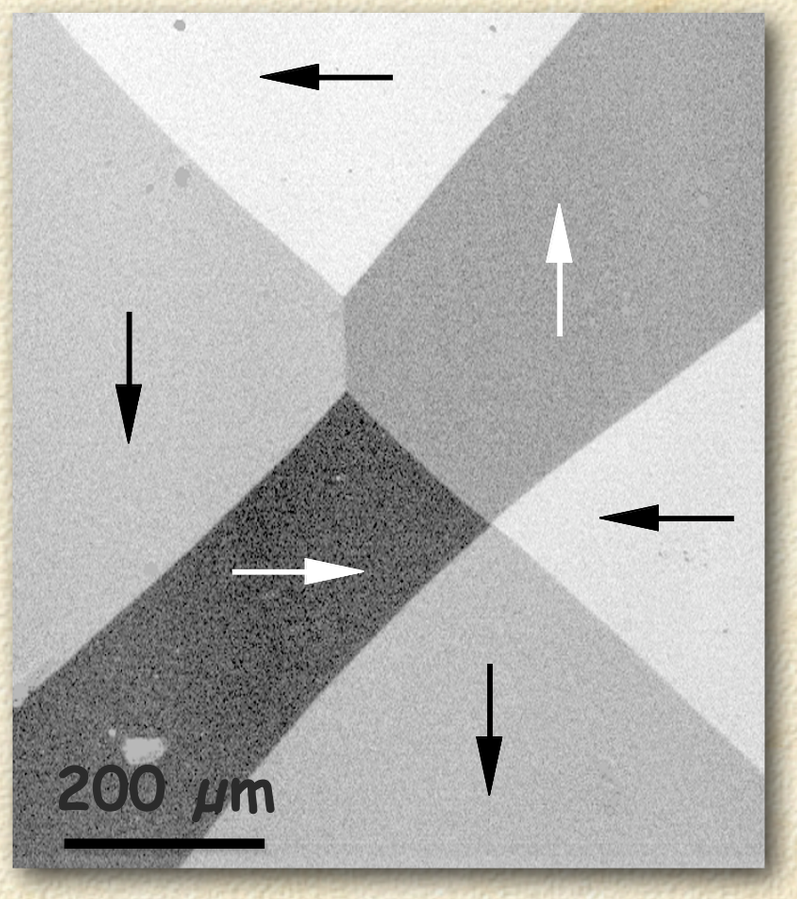

Metallic (single) films:

… sometimes combination with some micromagnetic theory may be required

Amorphous FeSiBCuNb film, 2 μm thick

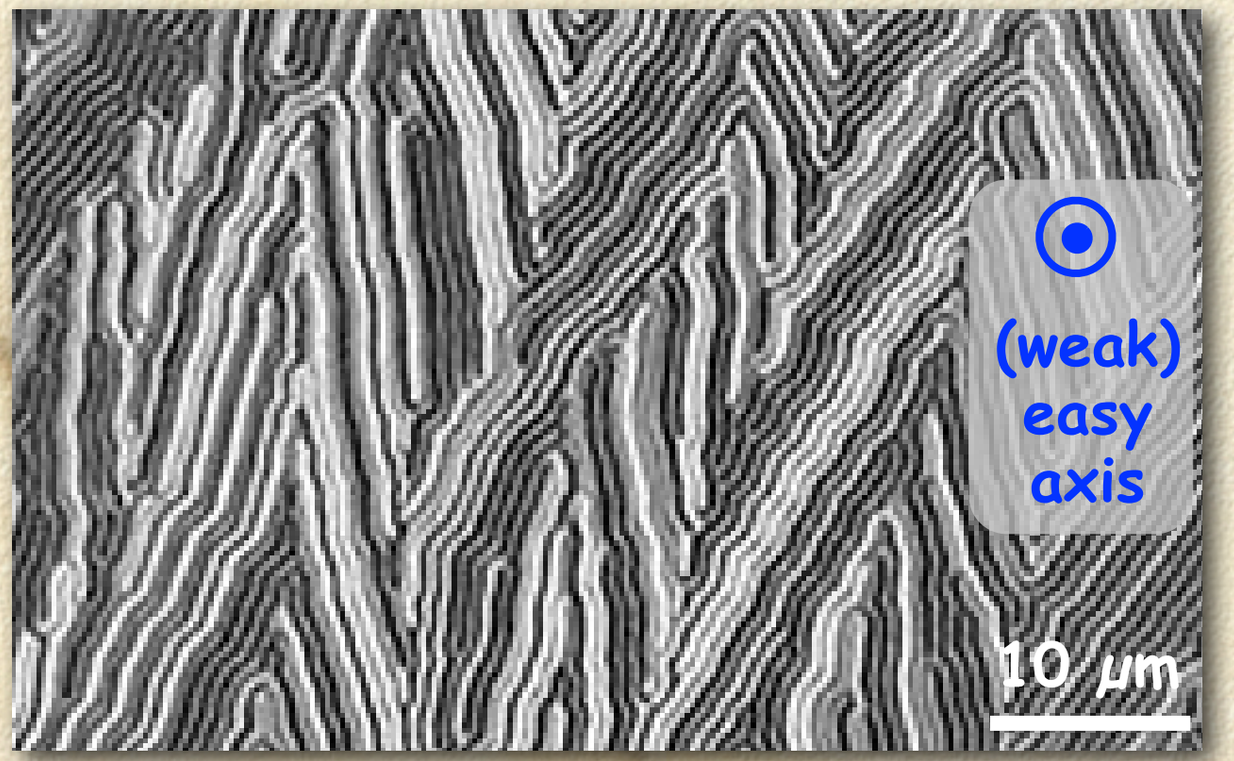

Stripe domains

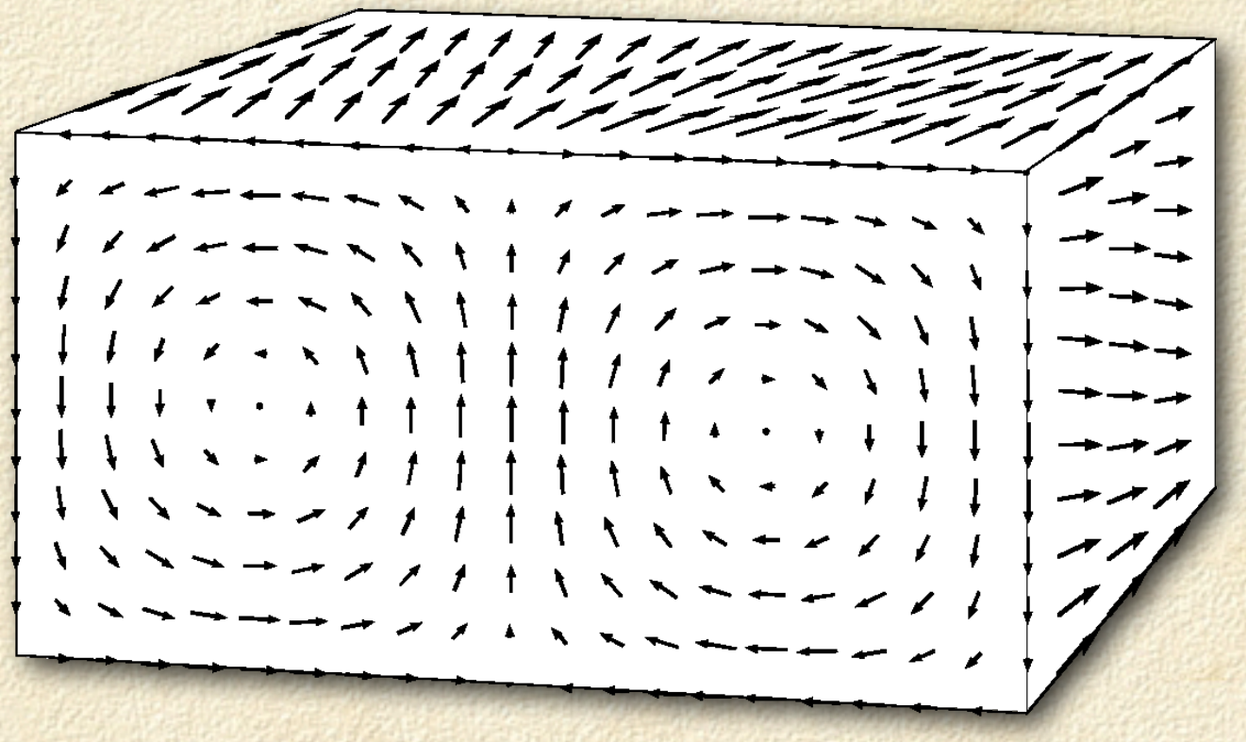

Metallic (single) films:

… sometimes combination with some micromagnetic theory may be required

Asymmetric Bloch wall

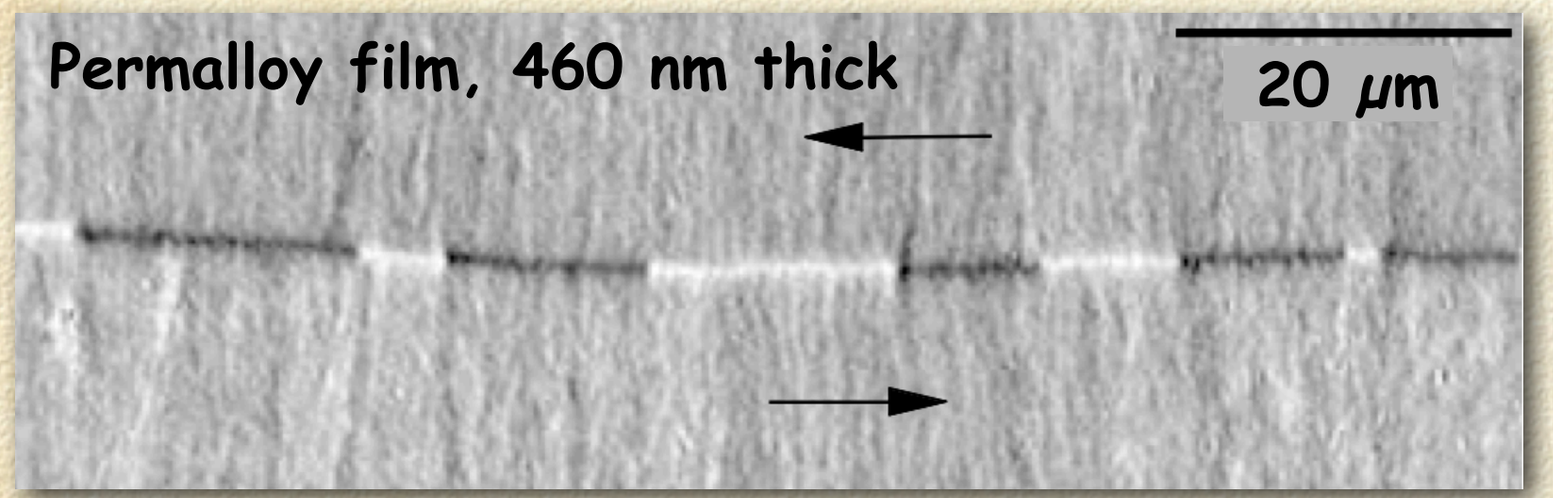

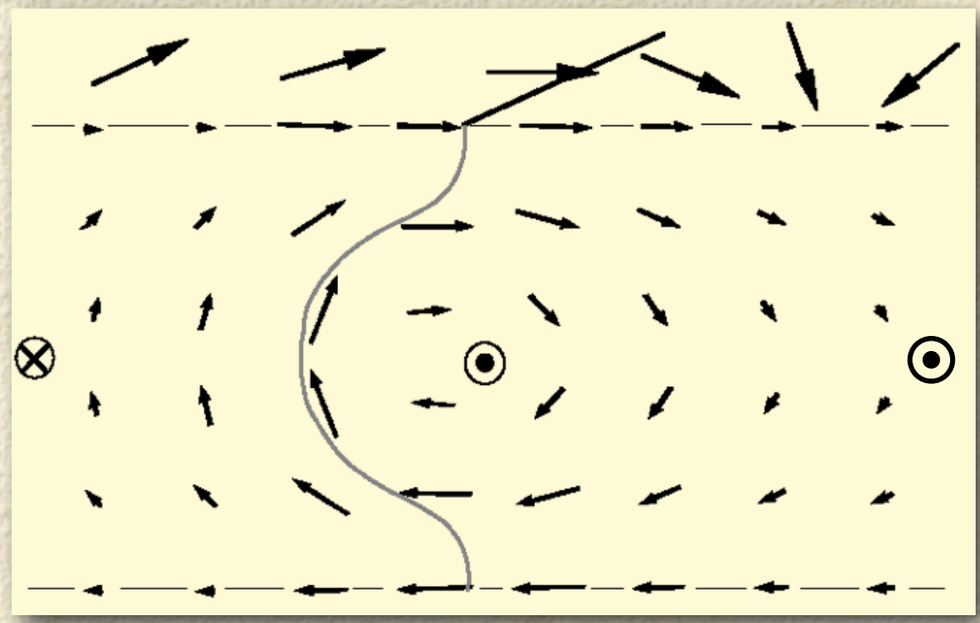

Asymmetric Néel wall

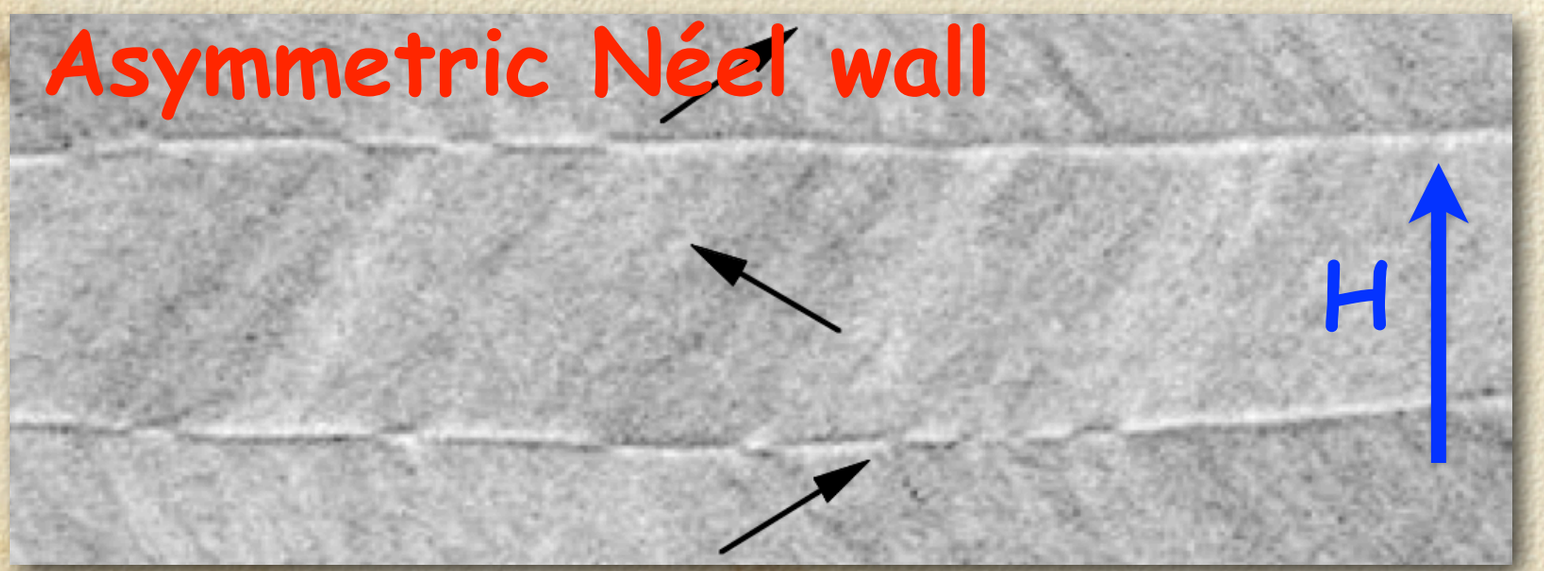

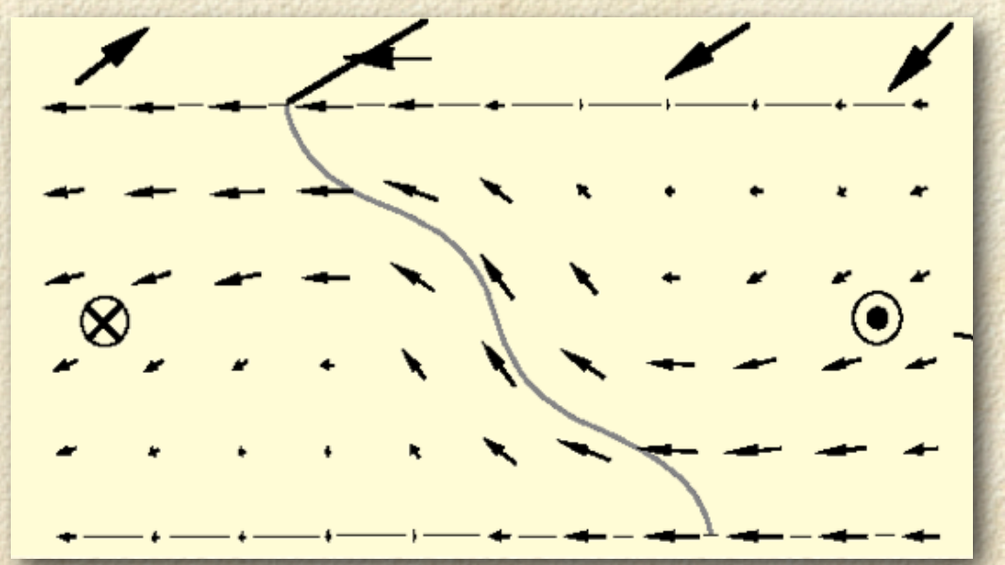

Multilayer films:

Domain analysis more challenging

Domain analysis in multilayers

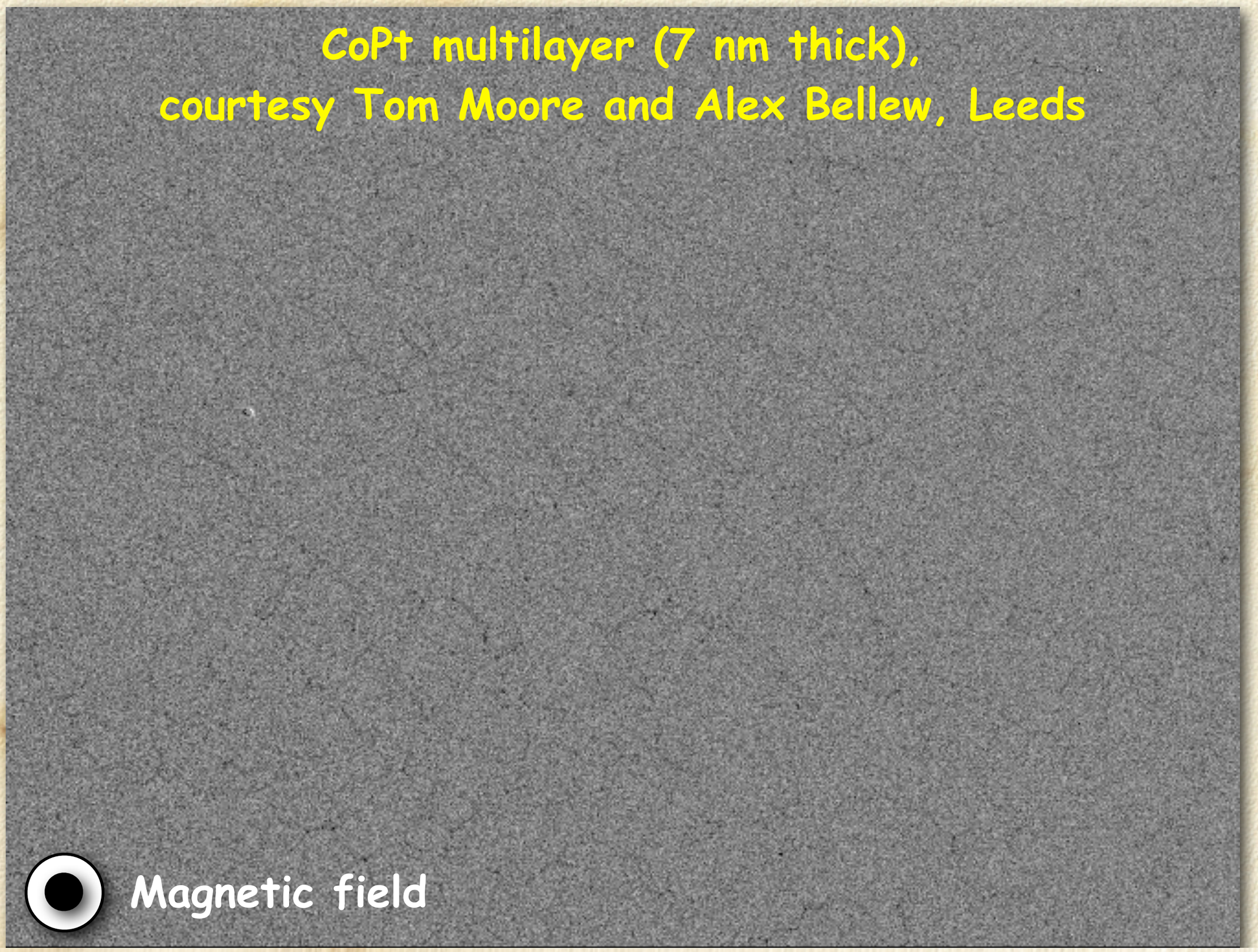

Domain analysis in multilayers

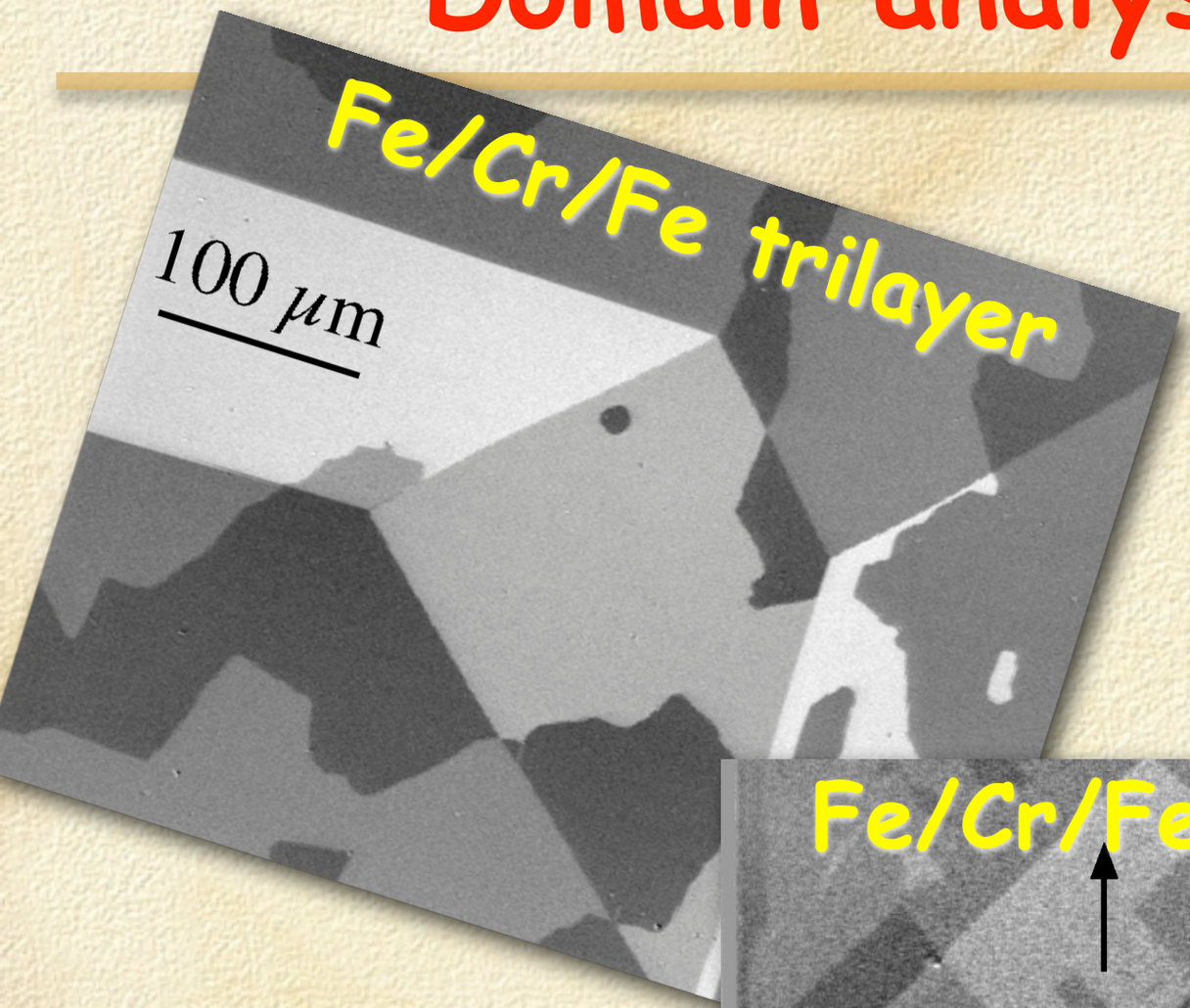

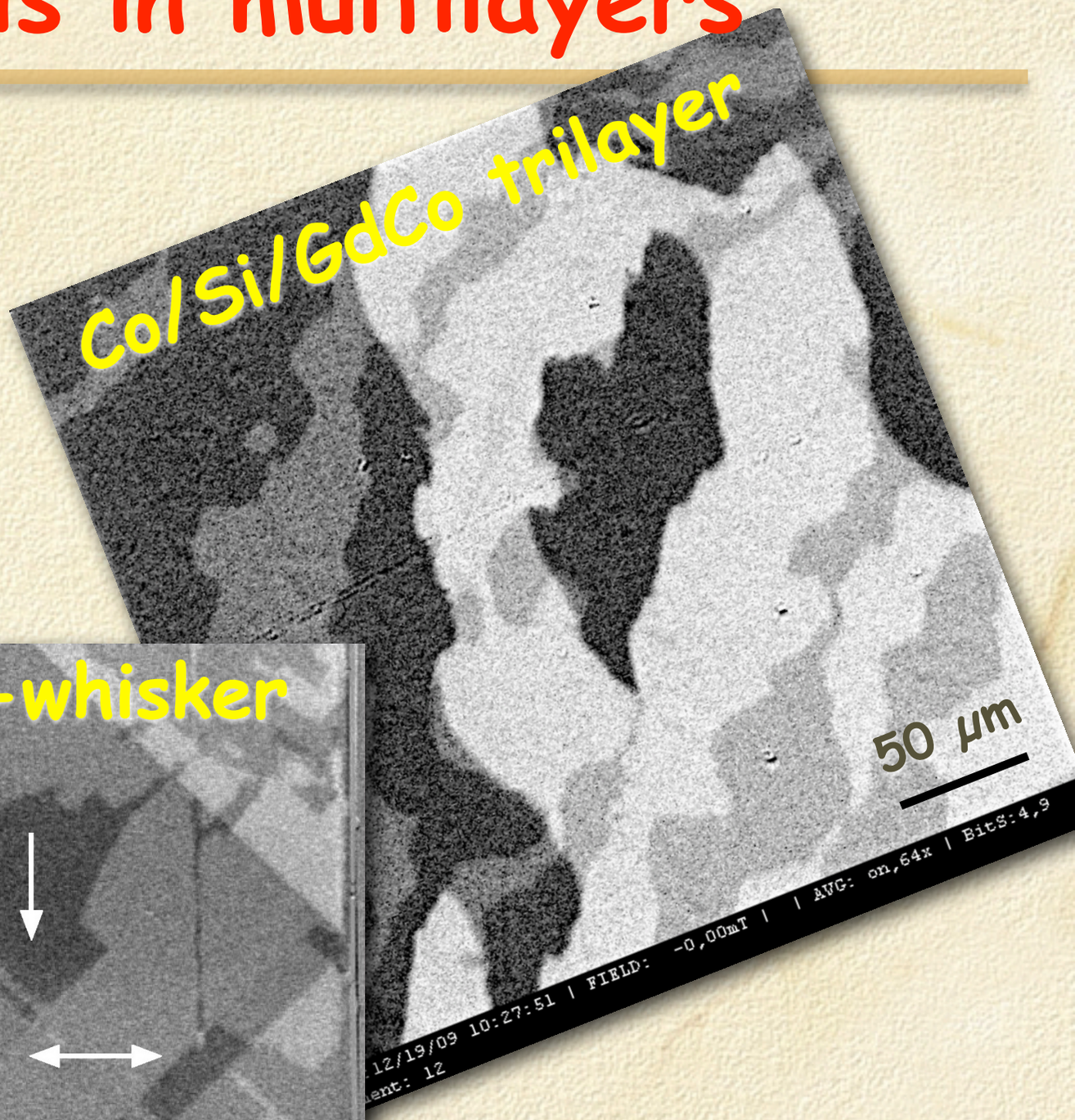

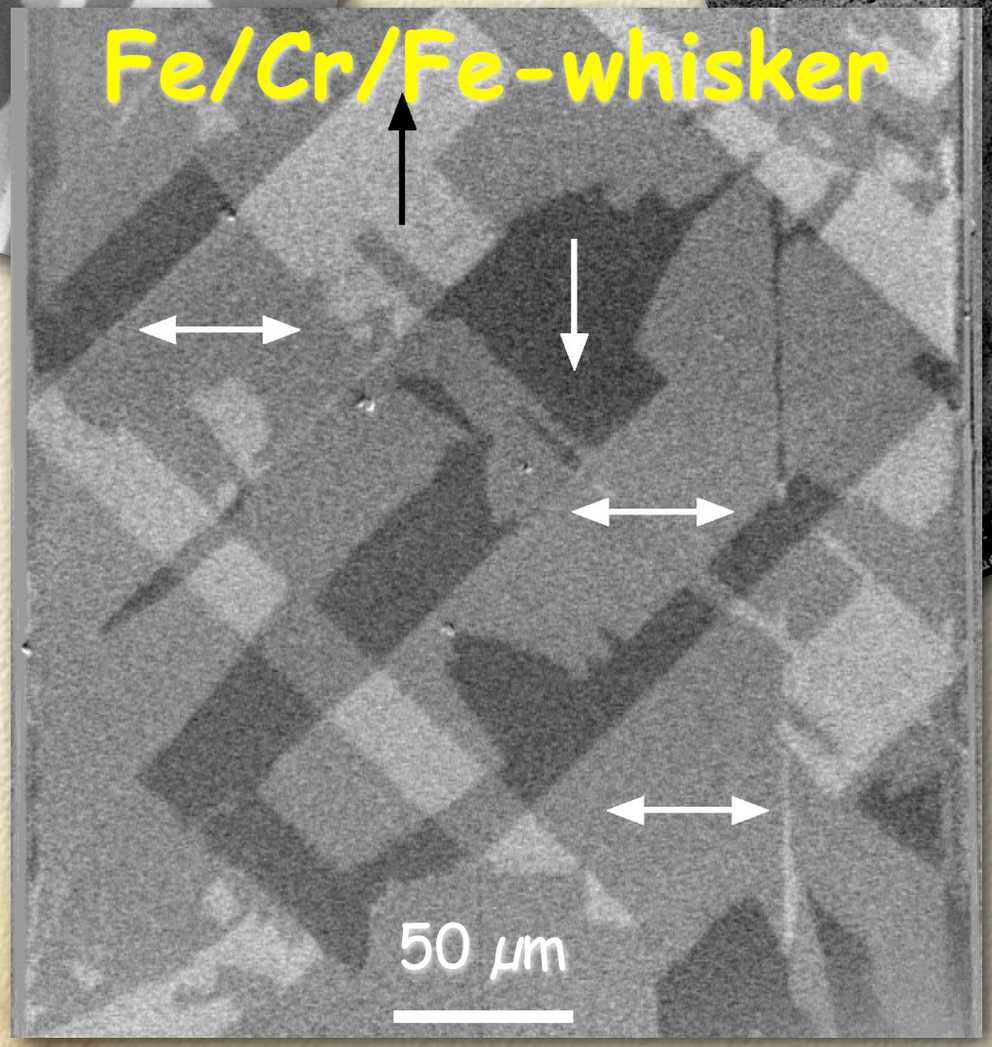

Domain analysis in multilayers

Co/Si/GdCo trilayer

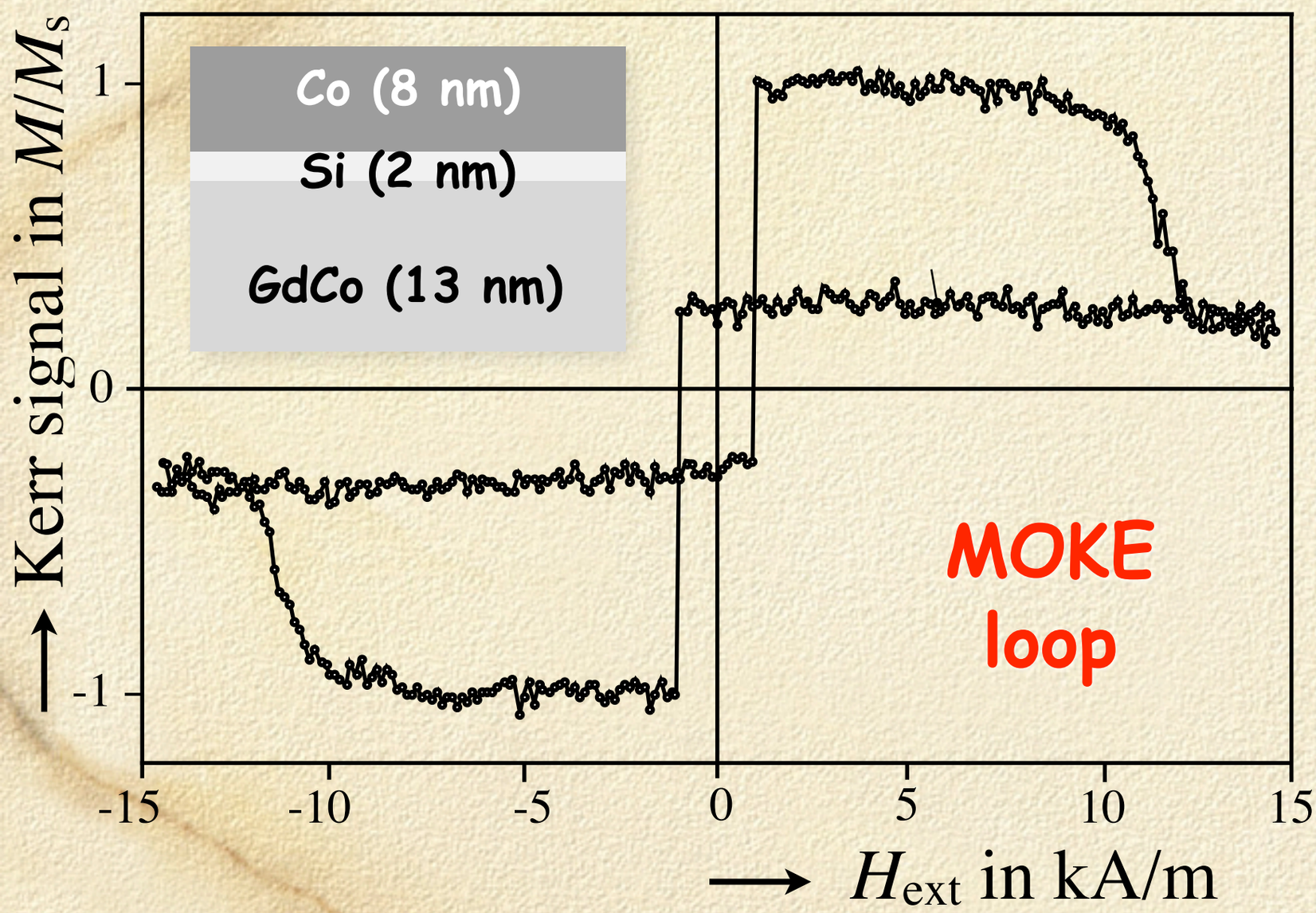

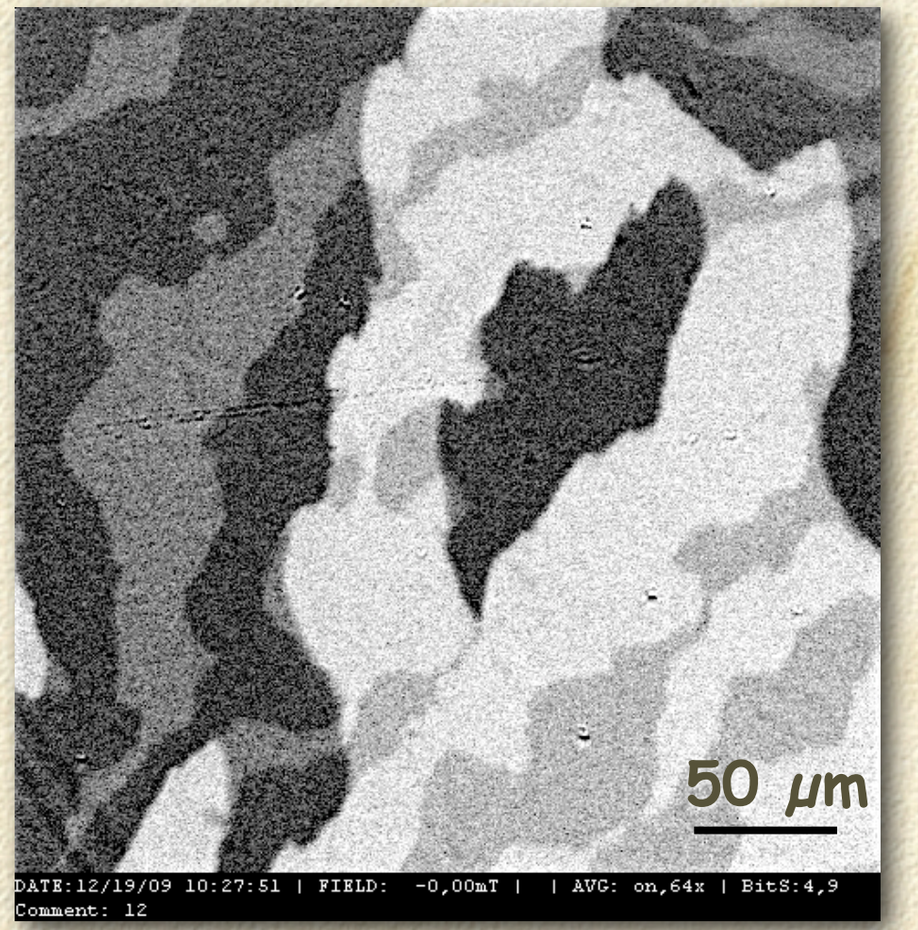

Sample: A. Svalov and G. Kurlyandskaya, Ekaterinburg

Imaging: together with L. Lokamani, Dresden (unpublished)

Depth selective Kerr microscopy

Compensator = „phase shifter“

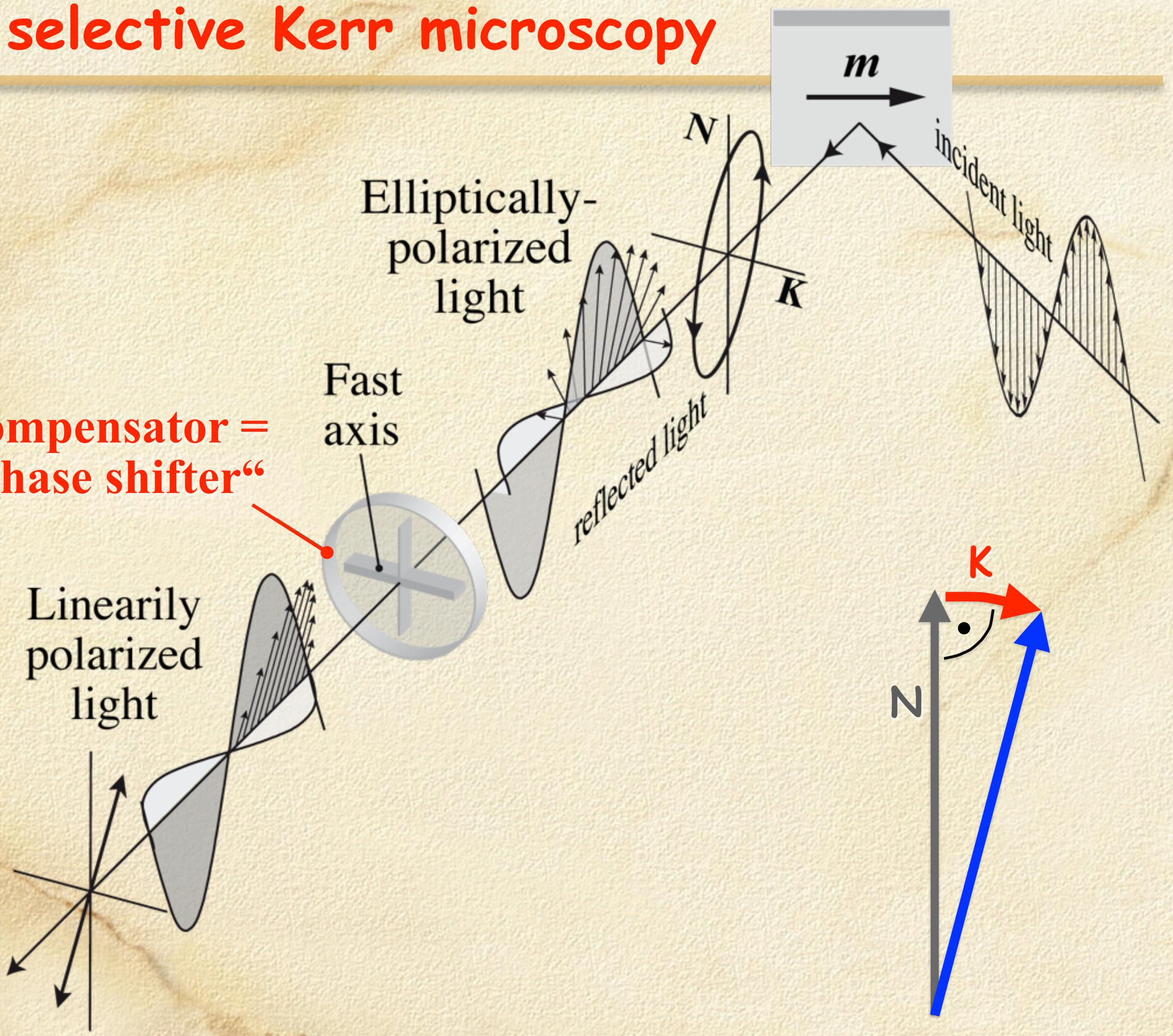

Depth selective Kerr microscopy

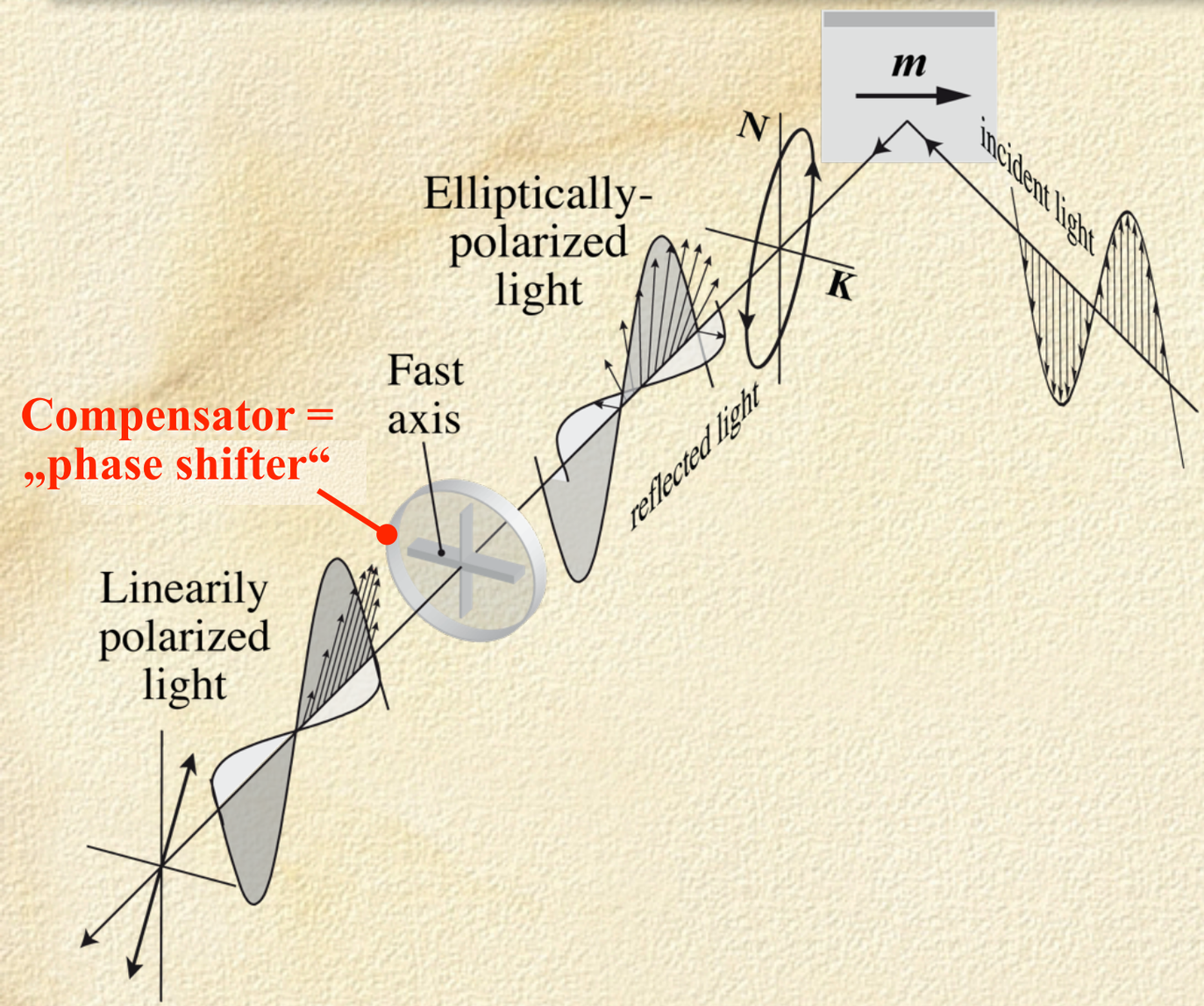

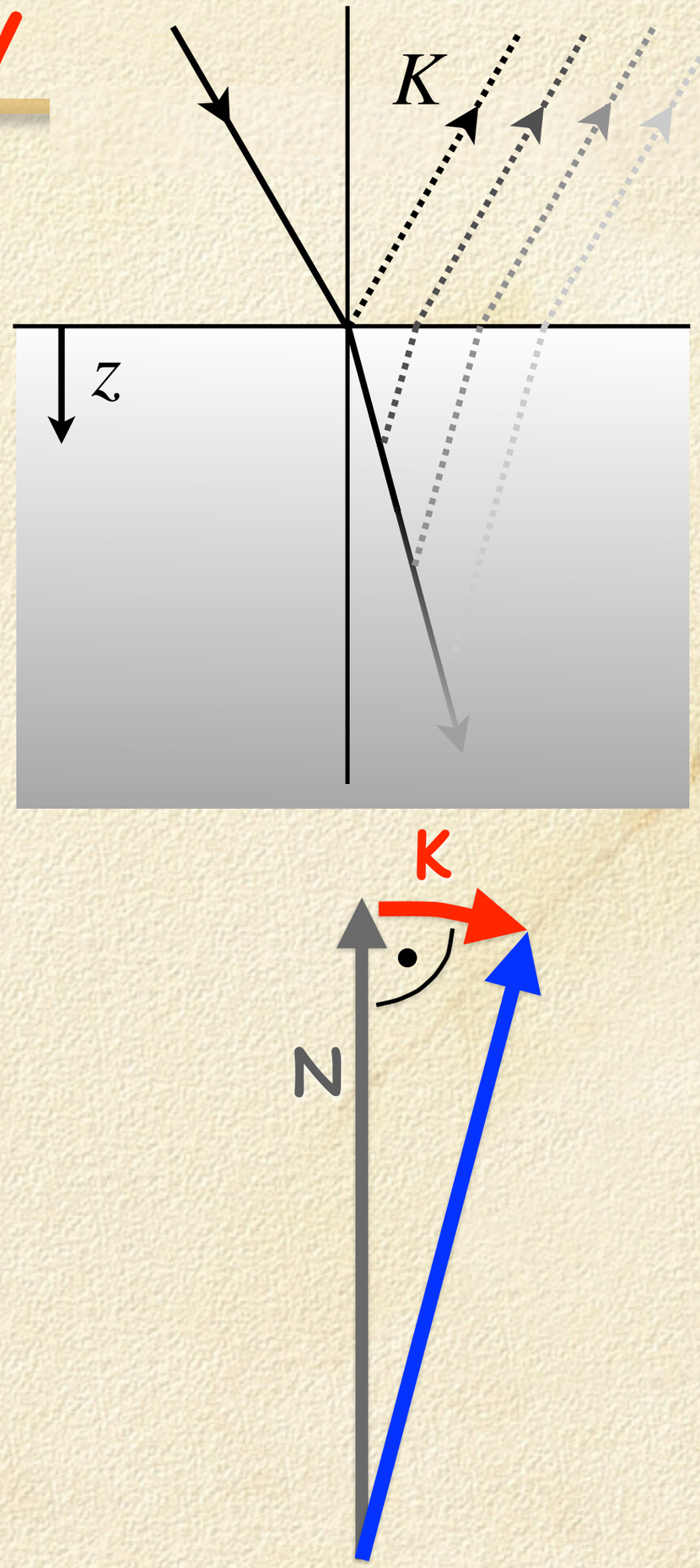

Depth selective Kerr microscopy

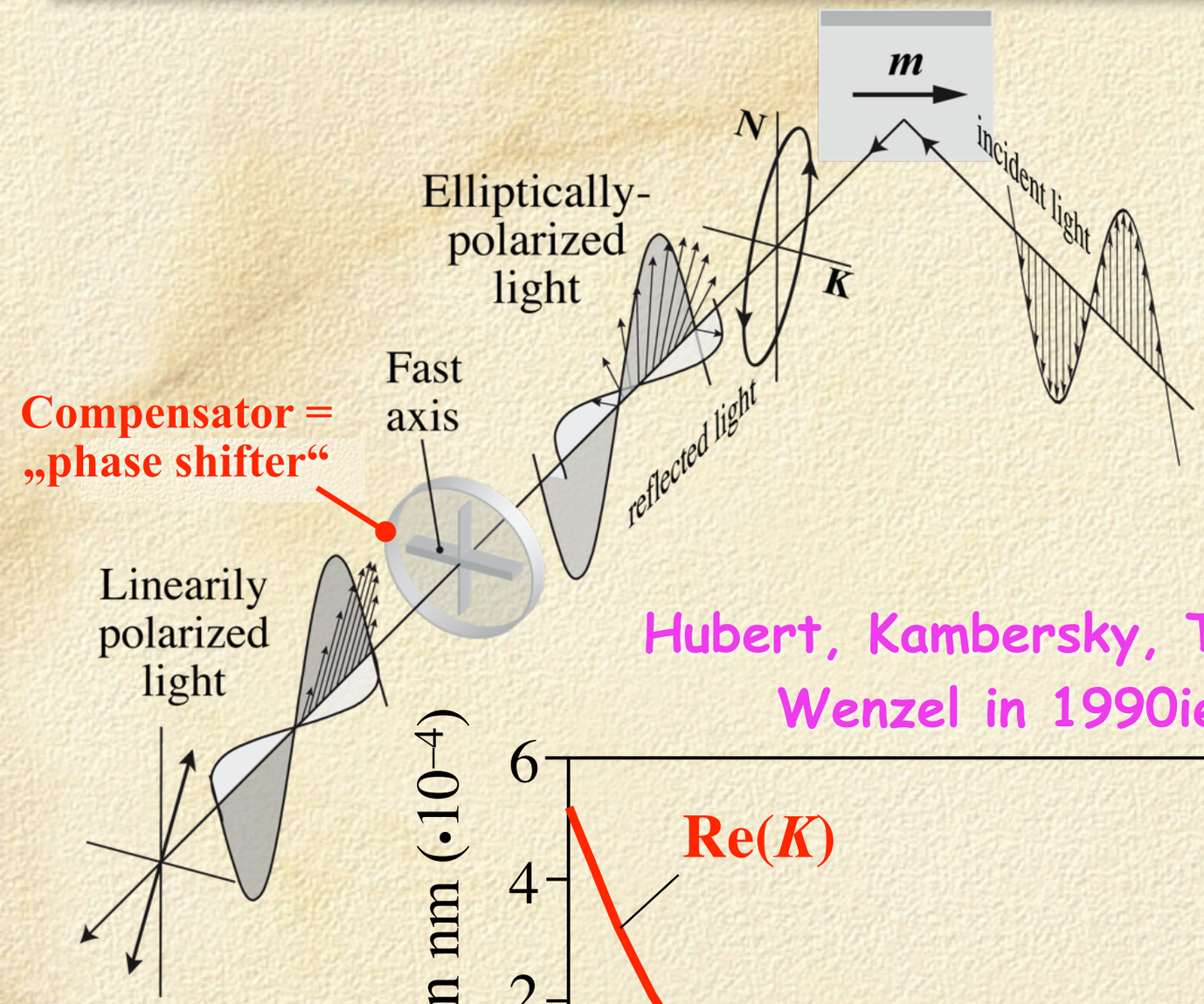

Hubert, Kambersky, Träger, Wenzel in 1990ies

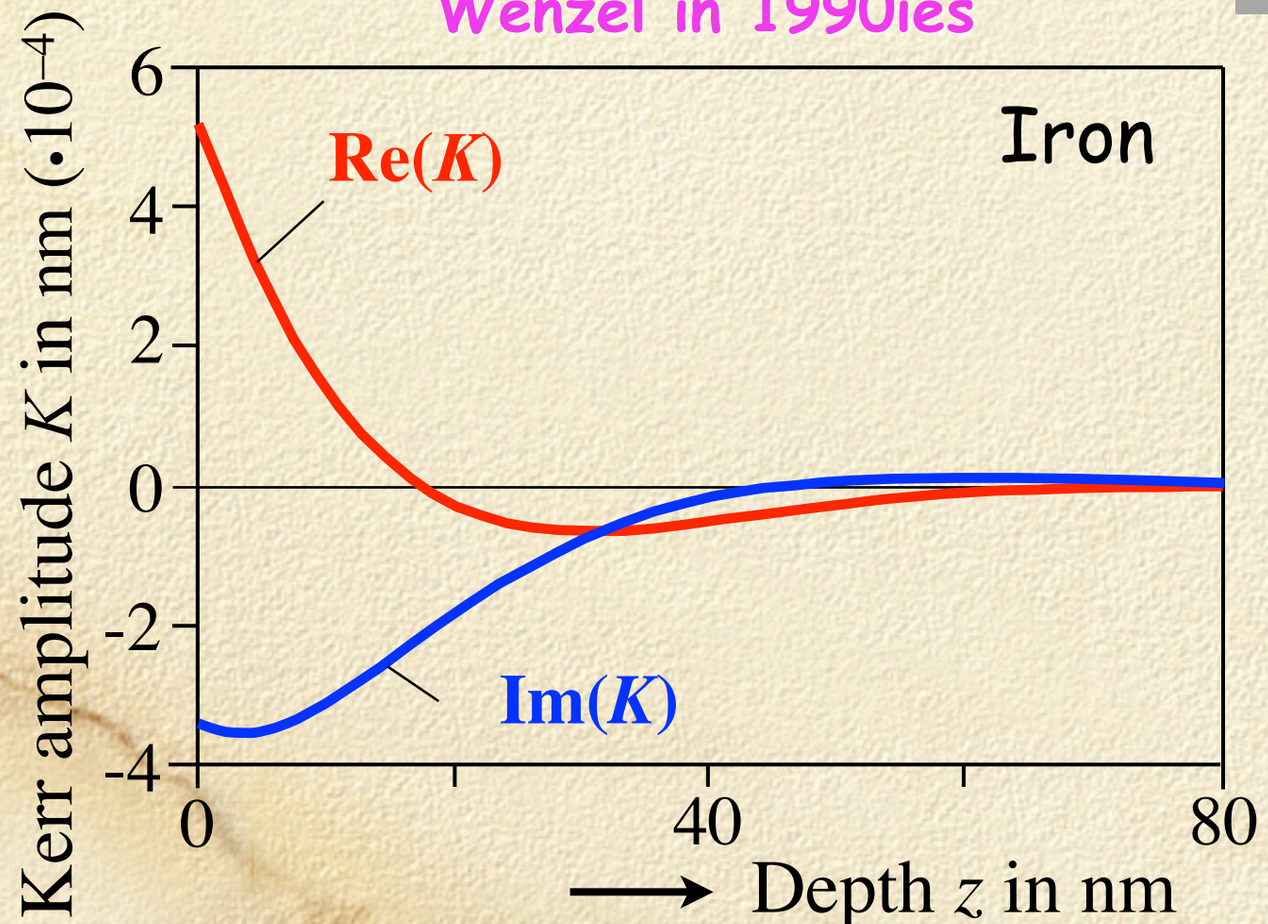

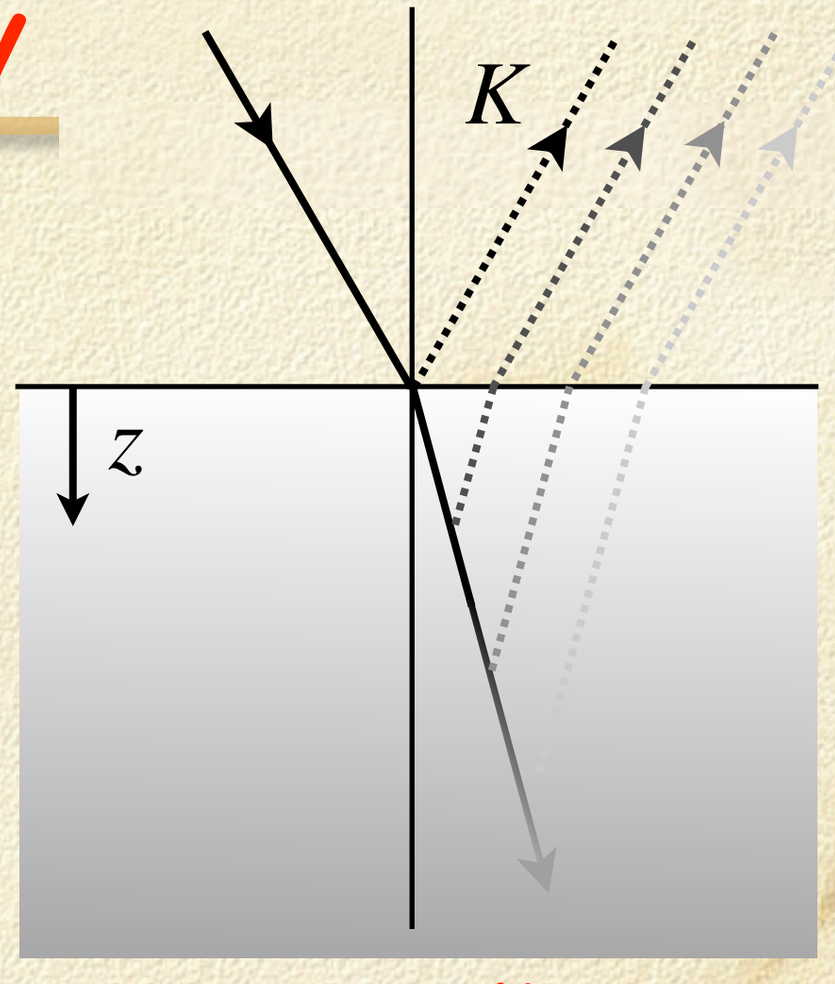

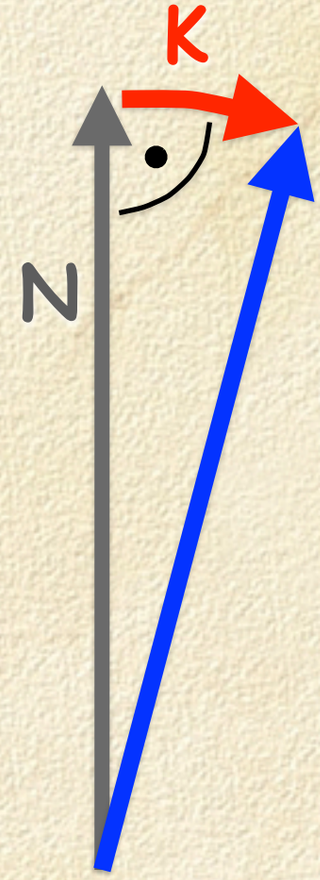

Depth selective Kerr microscopy

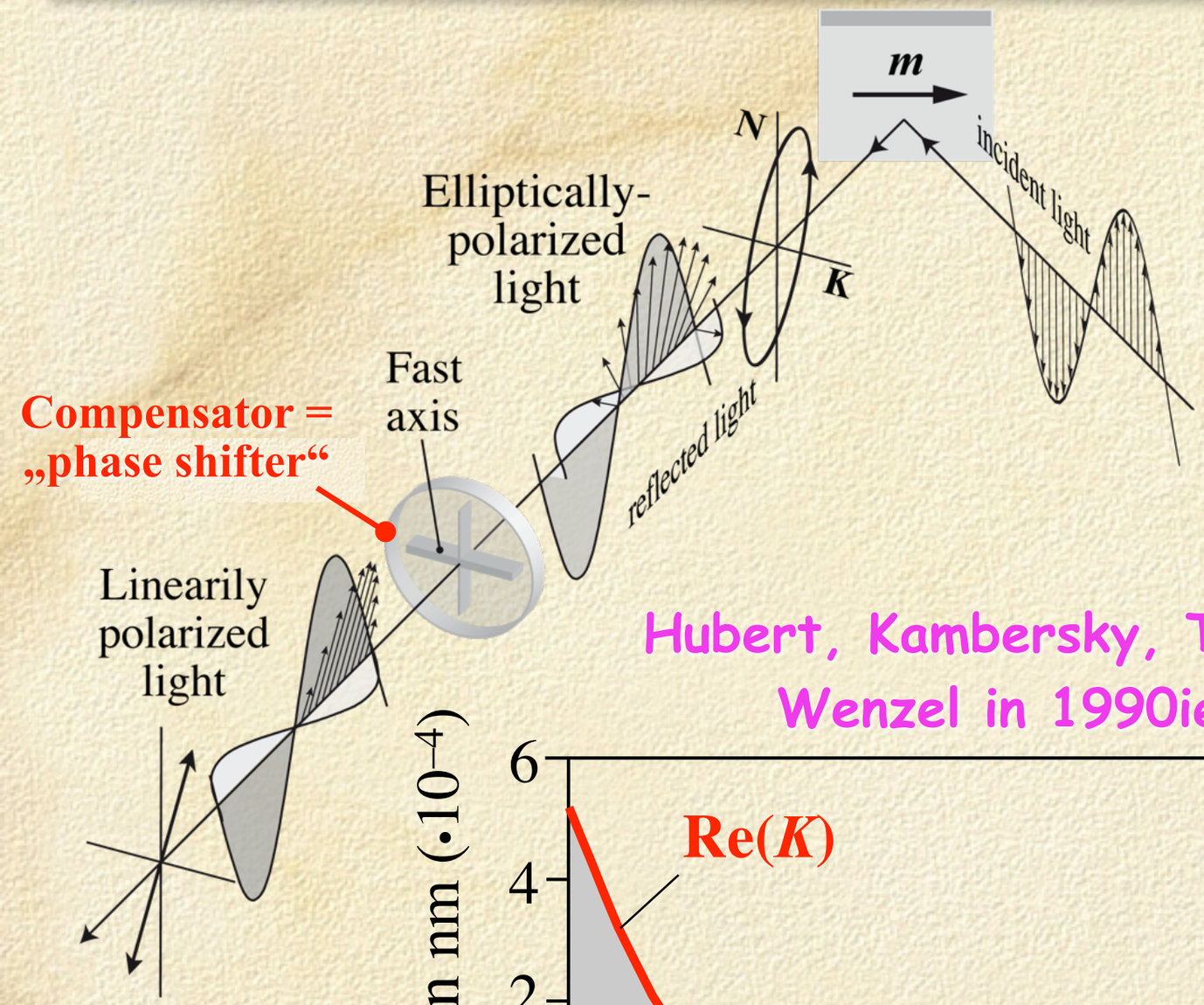

Hubert, Kambersky, Träger, Wenzel in 1990ies

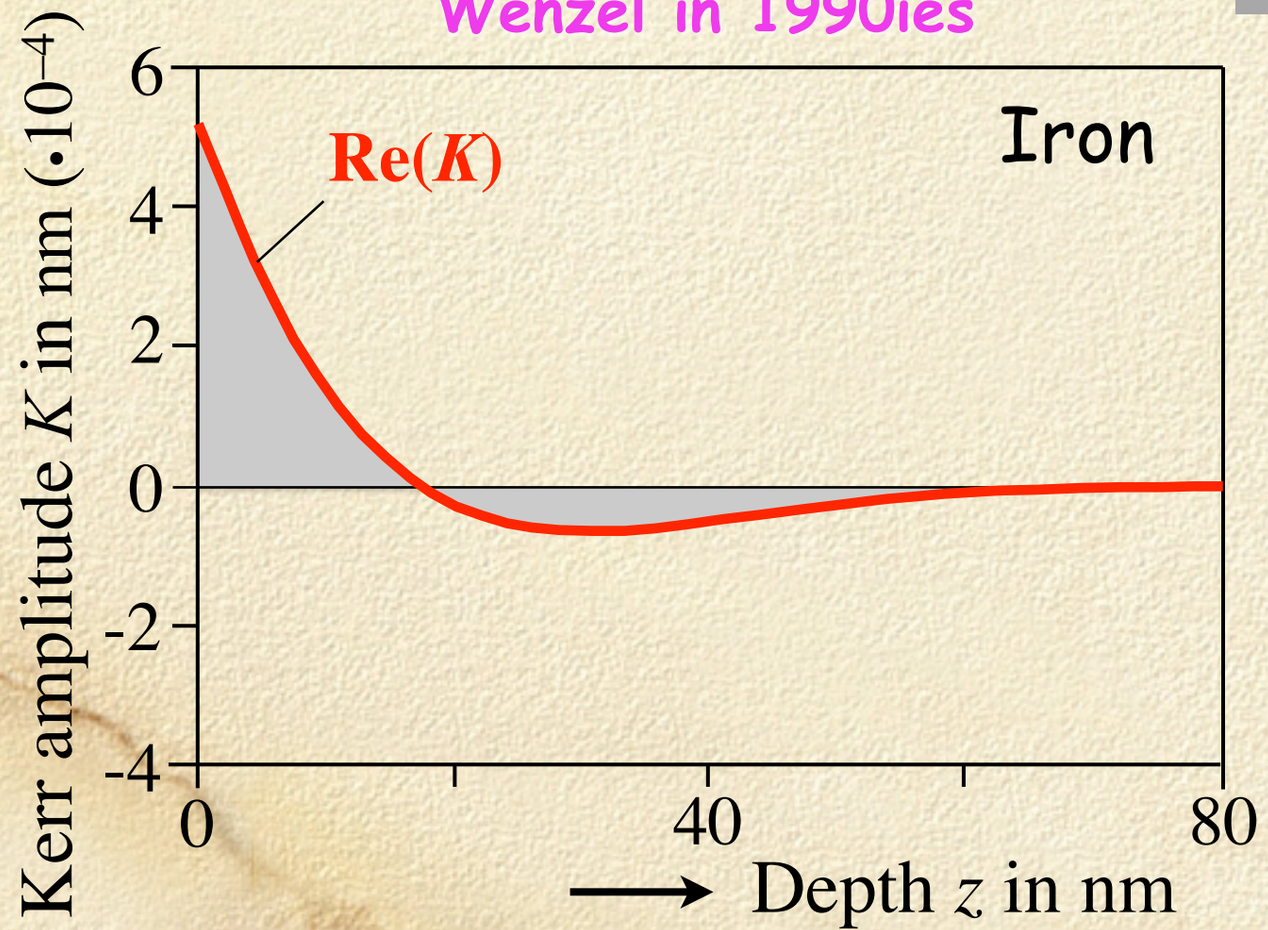

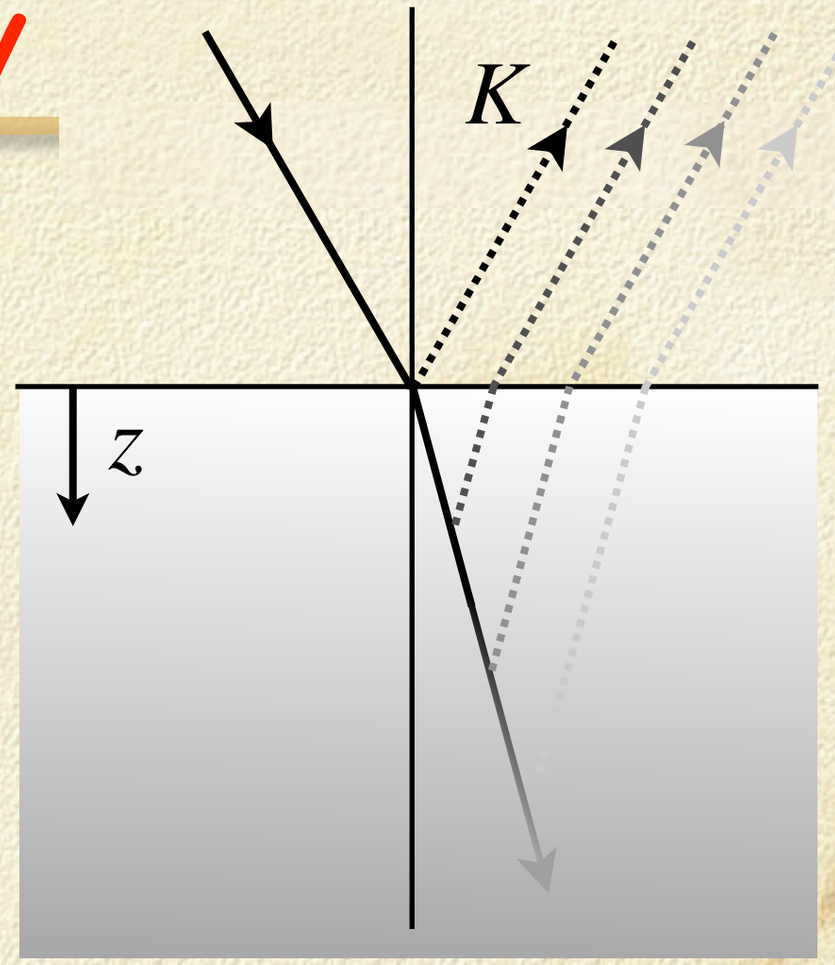

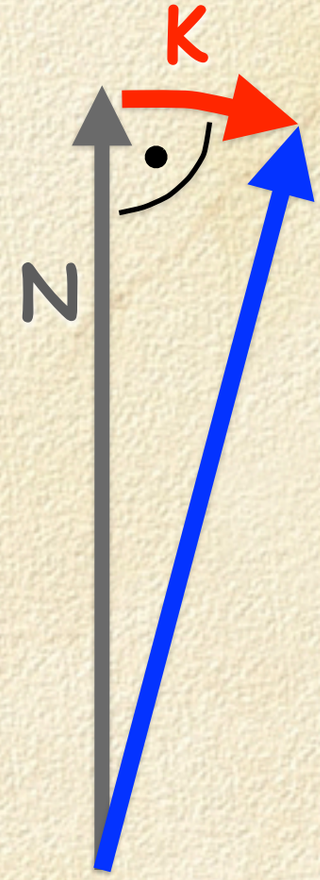

Depth selective Kerr microscopy

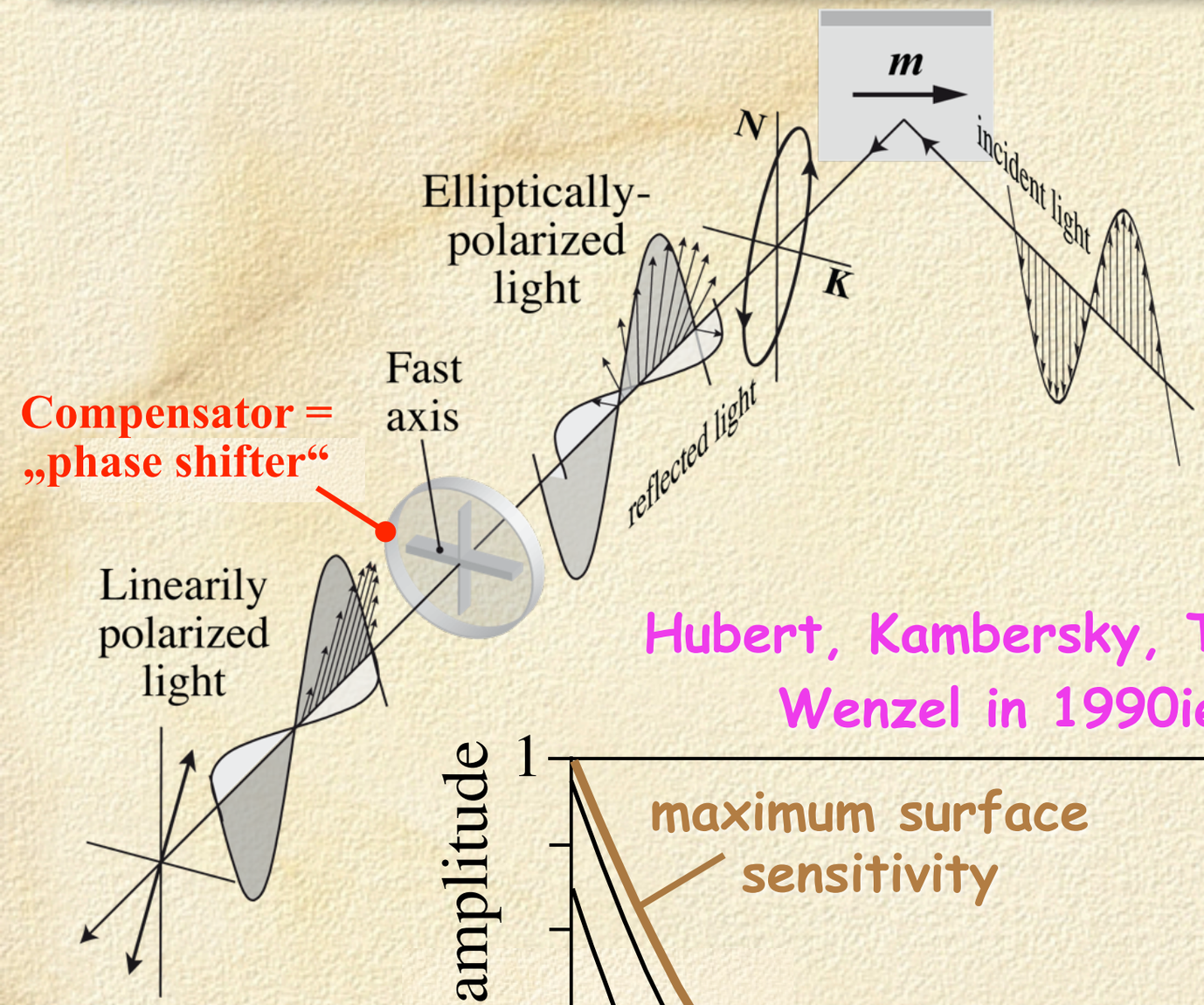

Hubert, Kambersky, Träger, Wenzel in 1990ies

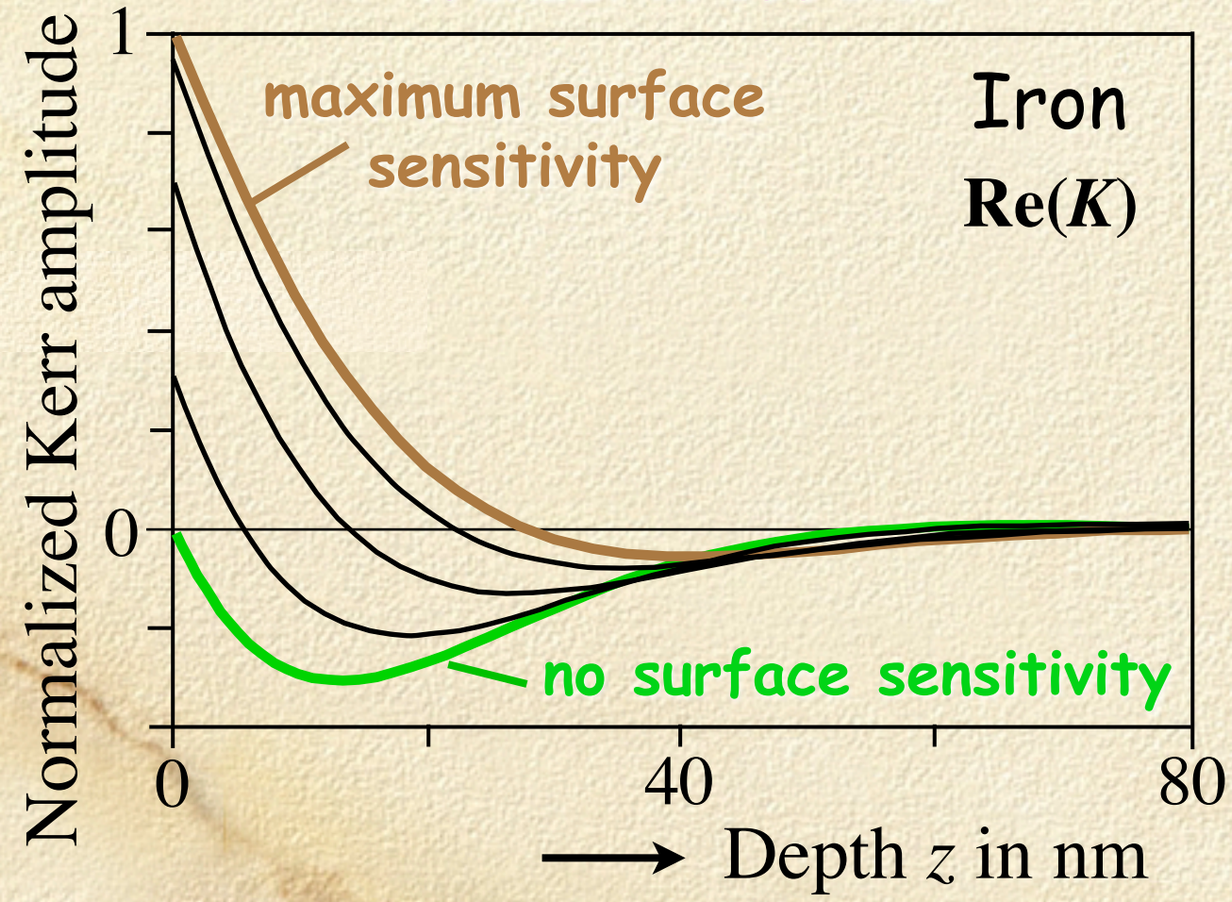

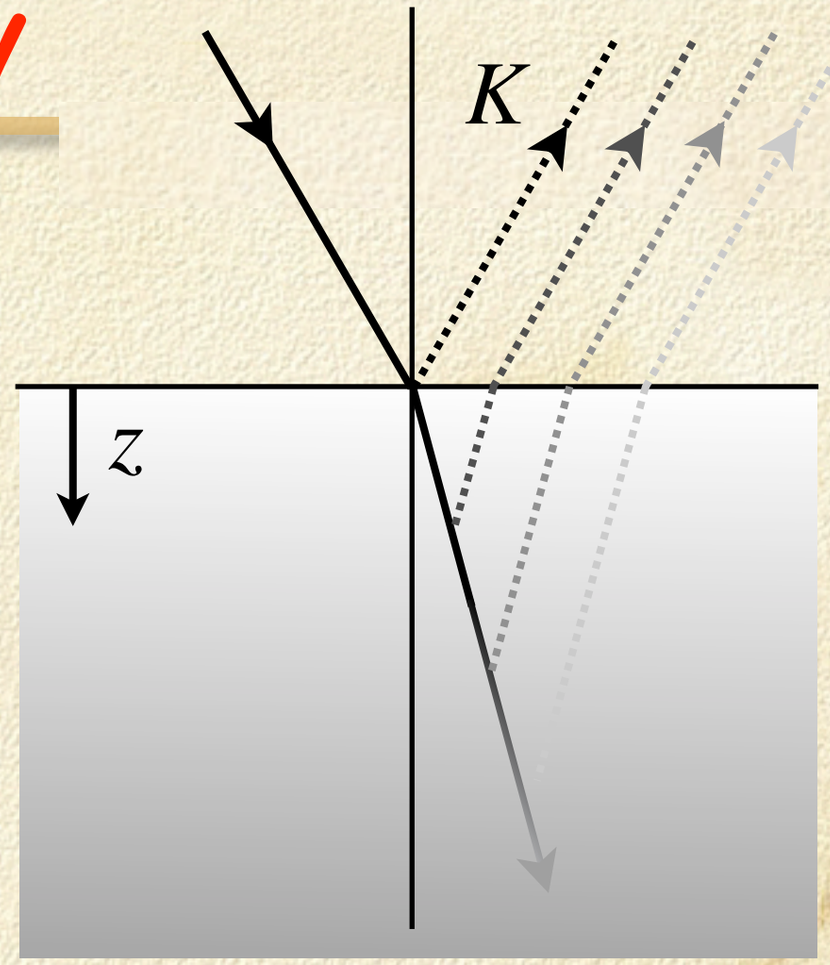

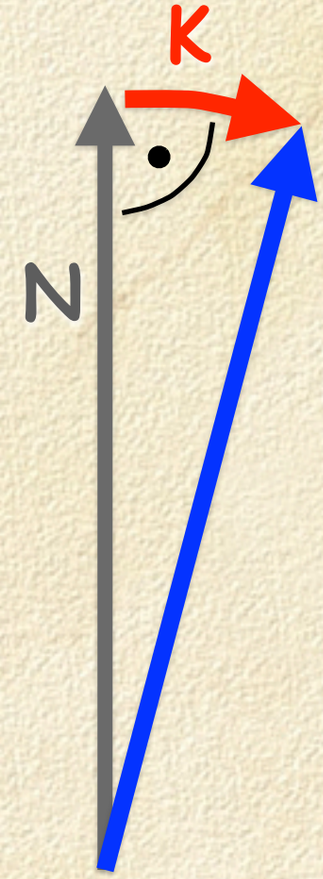

Layer-selective Kerr microscopy

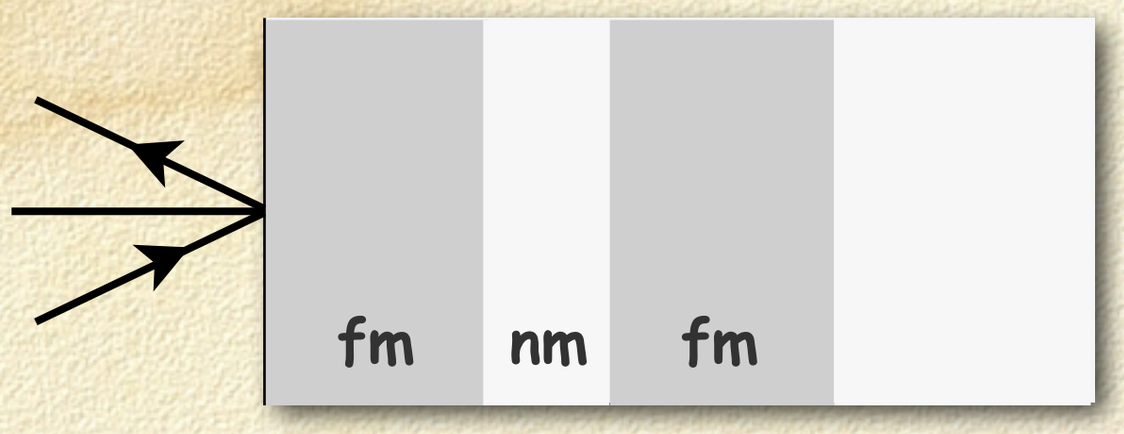

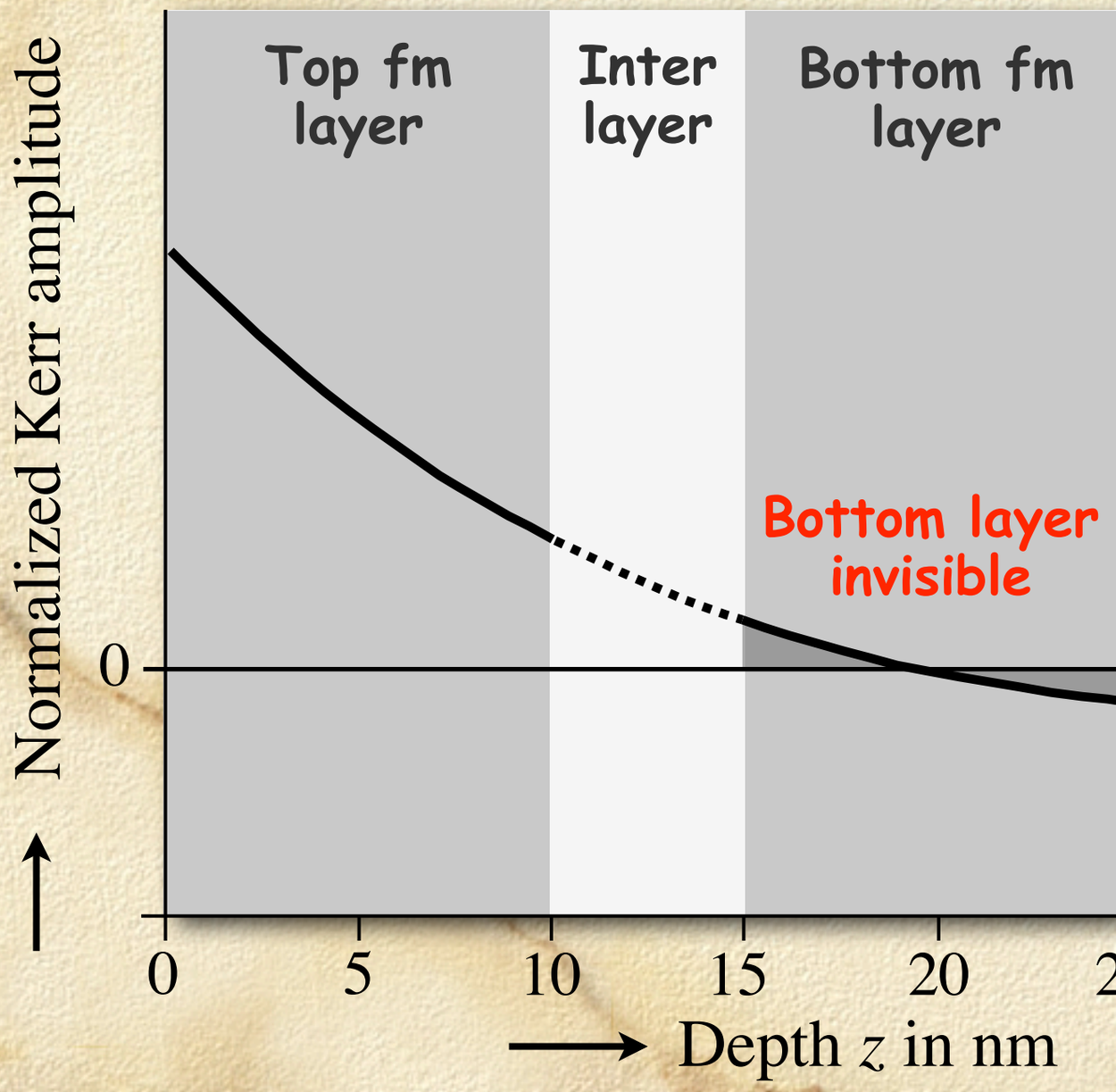

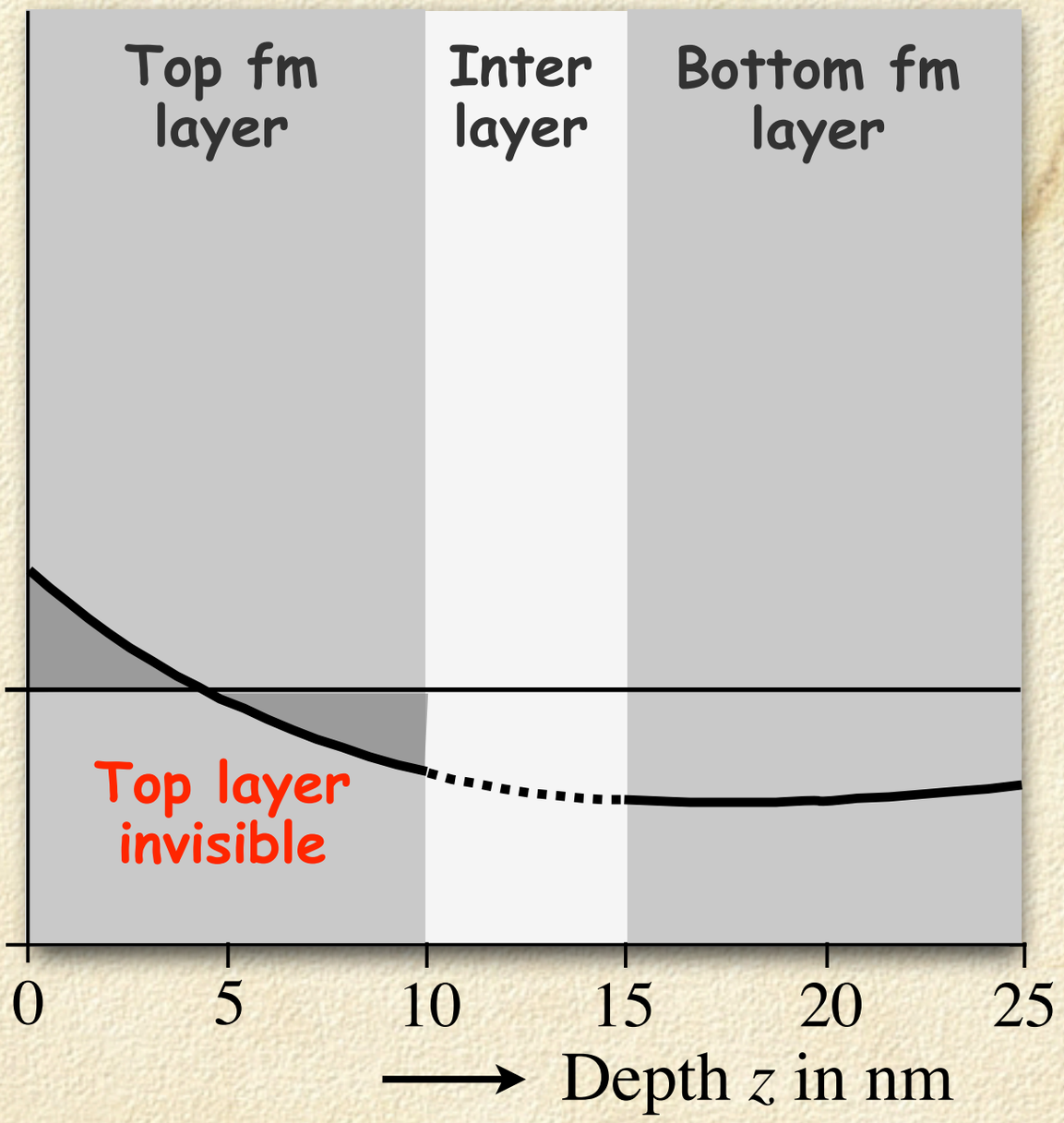

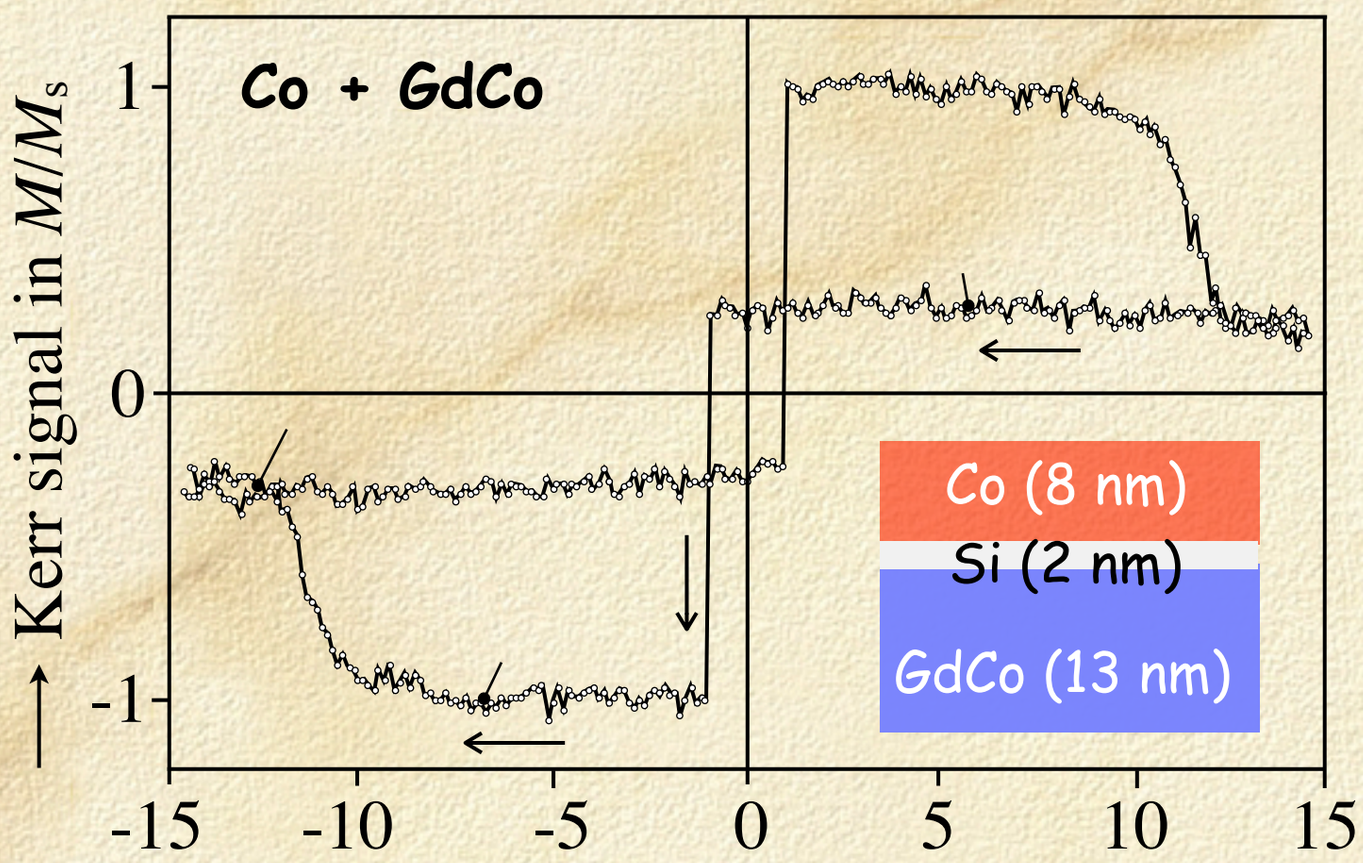

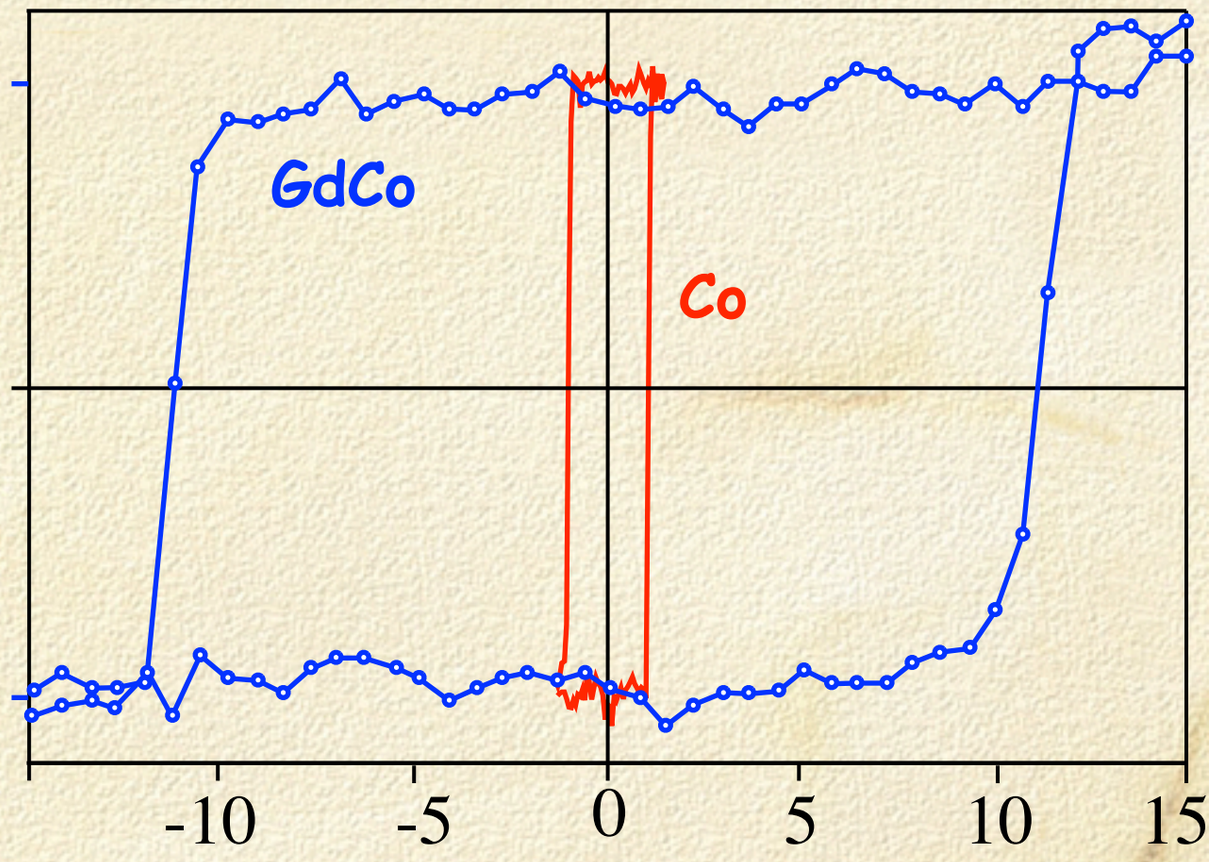

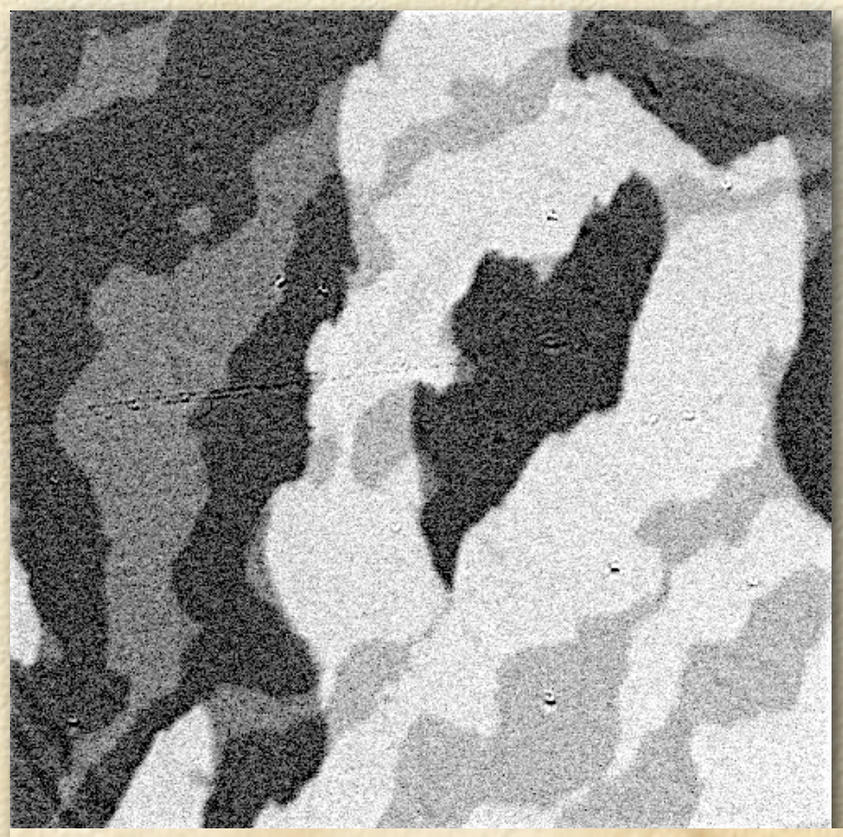

Mixed Kerr signal

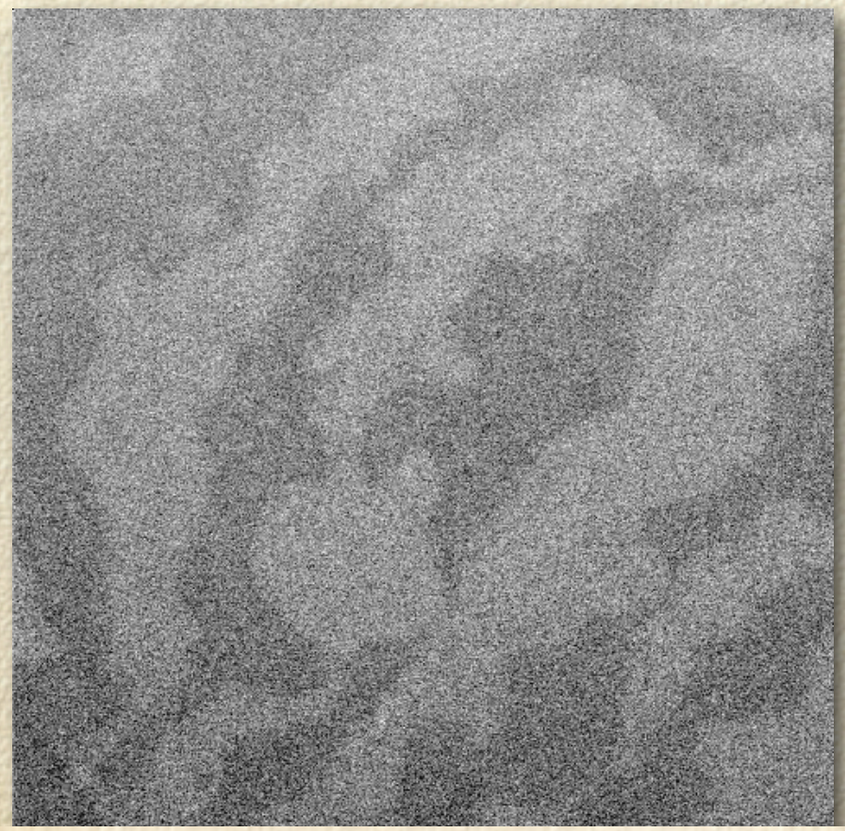

GdCo layer

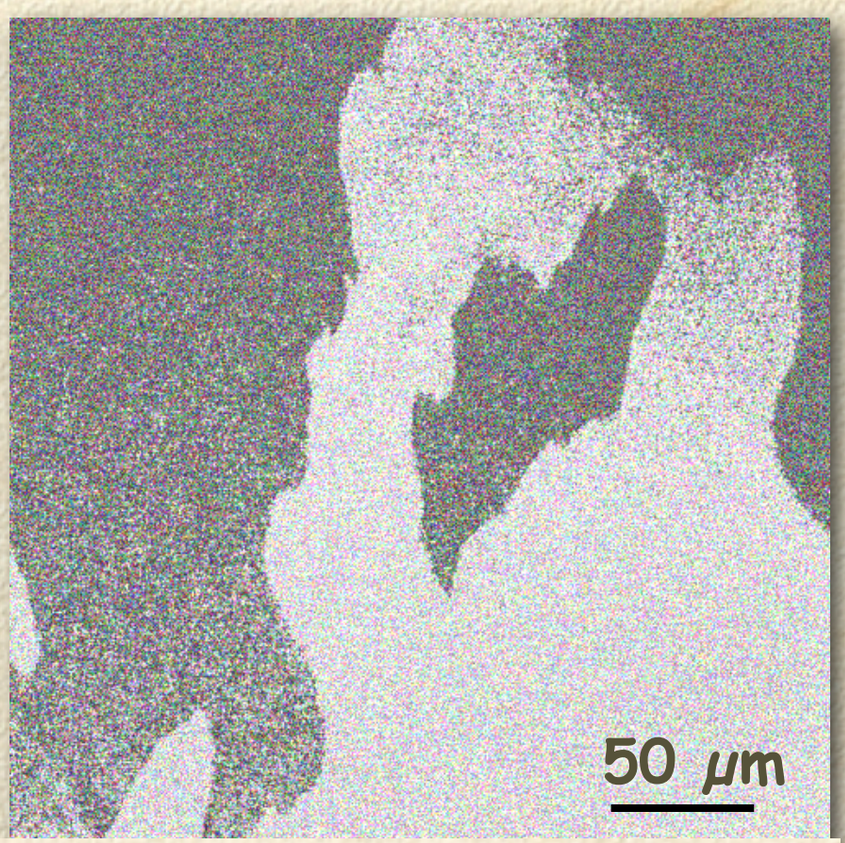

Co layer

Co + GdCo

Co
Gd Co

Co
Co Gd

Co
Gd Co

Co (8 nm)

Si (2 nm)

GdCo (13 nm)

→ Kerr signal in M/M_s

→ H_{ext} in kA/m

GdCo

Co

→ H_{ext} in kA/m

Mixed Kerr signal

GdCo layer

Co layer

50 µm

Layer-selective Kerr microscopy

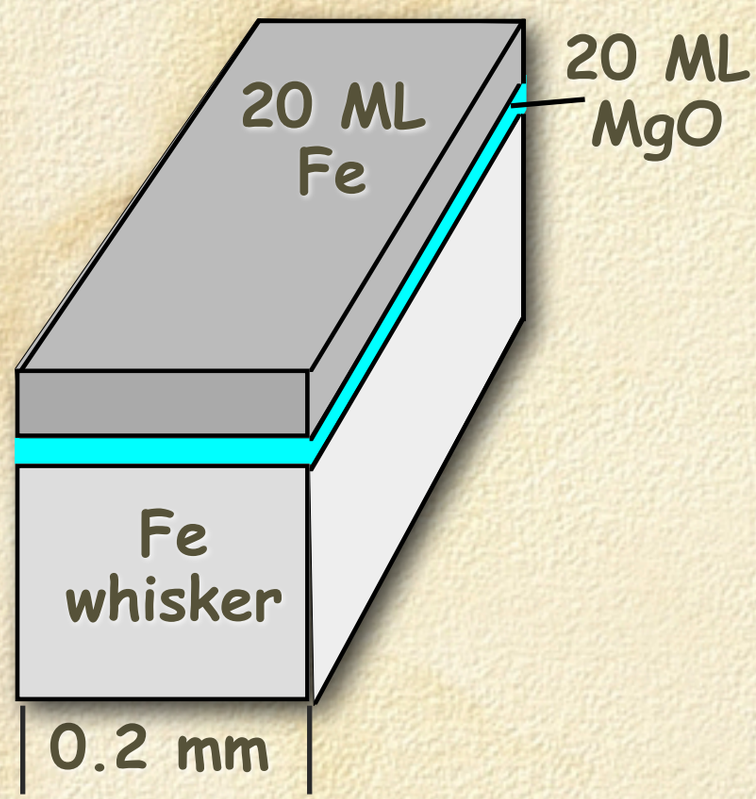

Domains in Fe-film

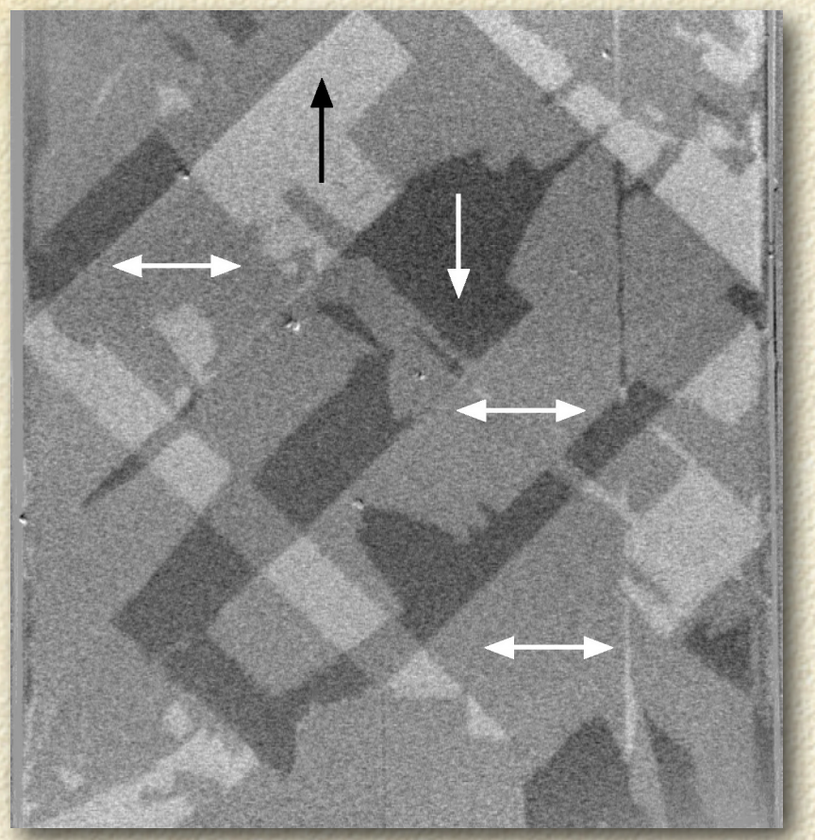

Whisker domains

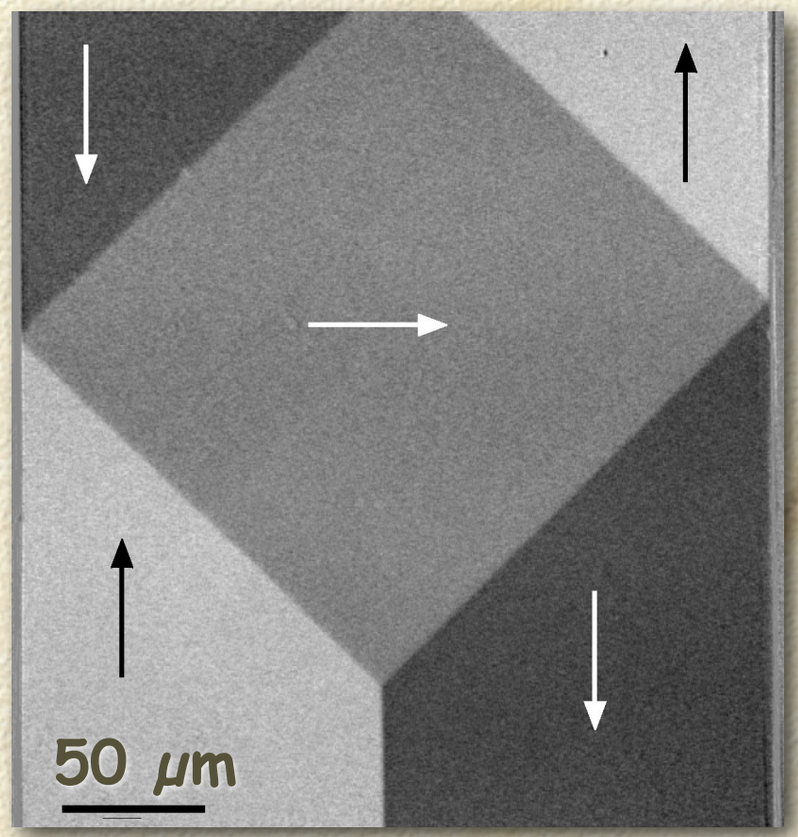

R. S., R. Urban, D. Ullmann, H. L. Meyerheim, B. Heinrich, L. Schultz, J. Kirschner, PRB 65, 144405 (2003)

Bulk materials:

Domain analysis can be more or less difficult

... less difficult

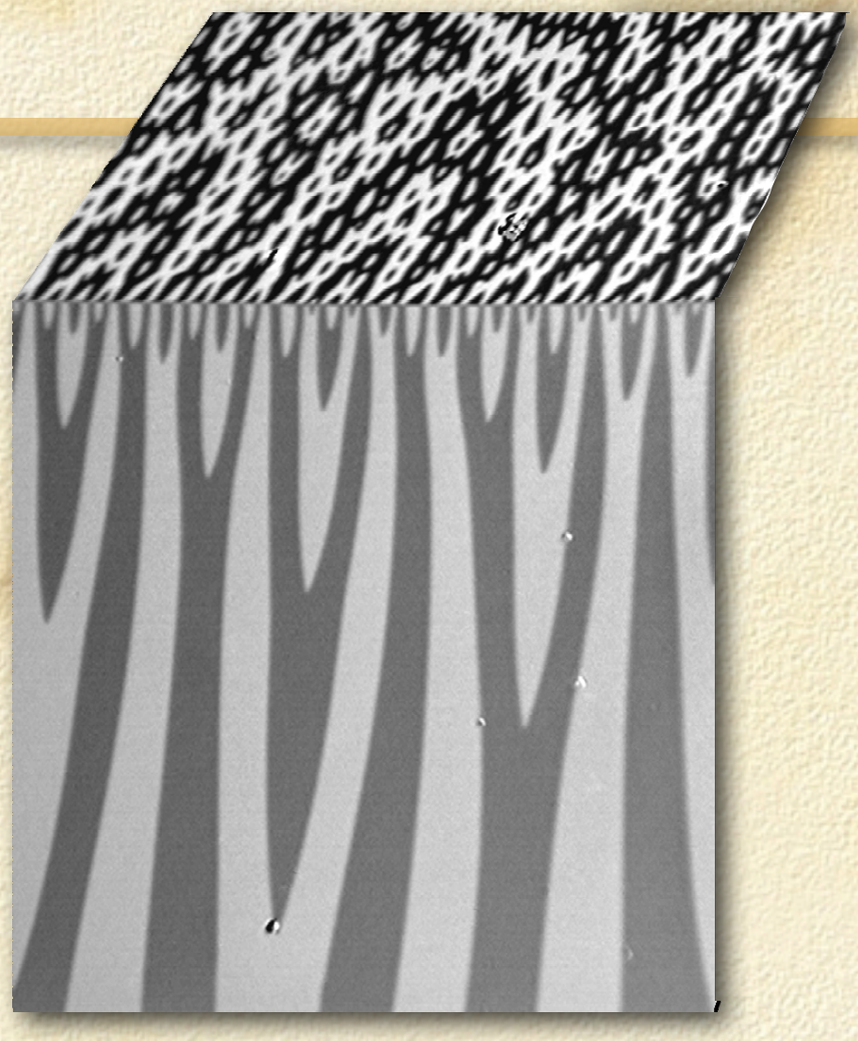

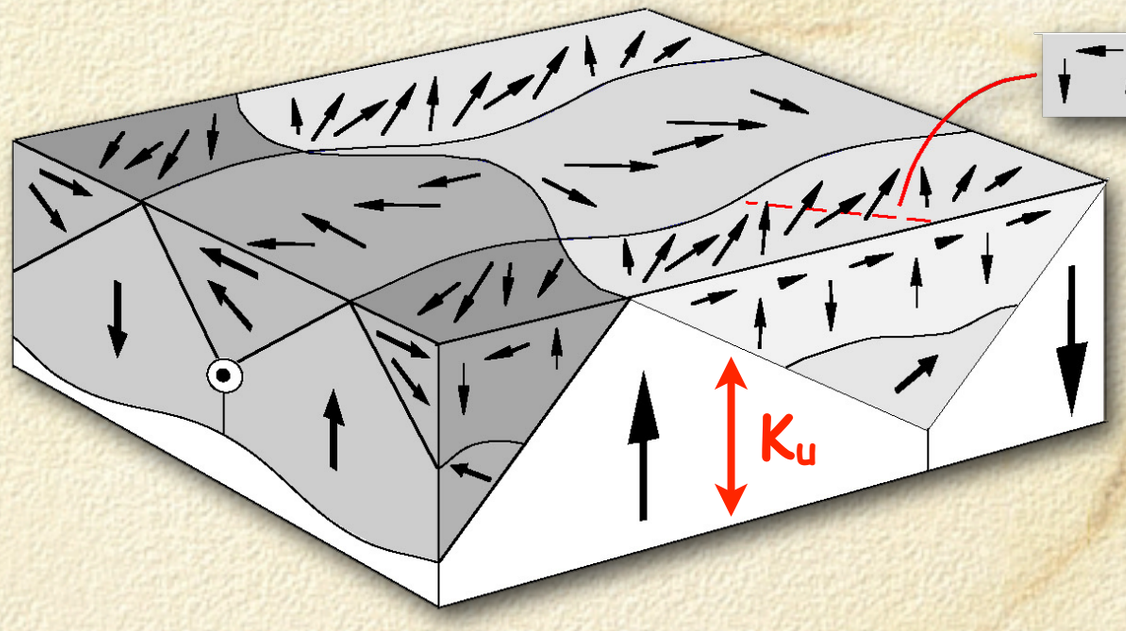

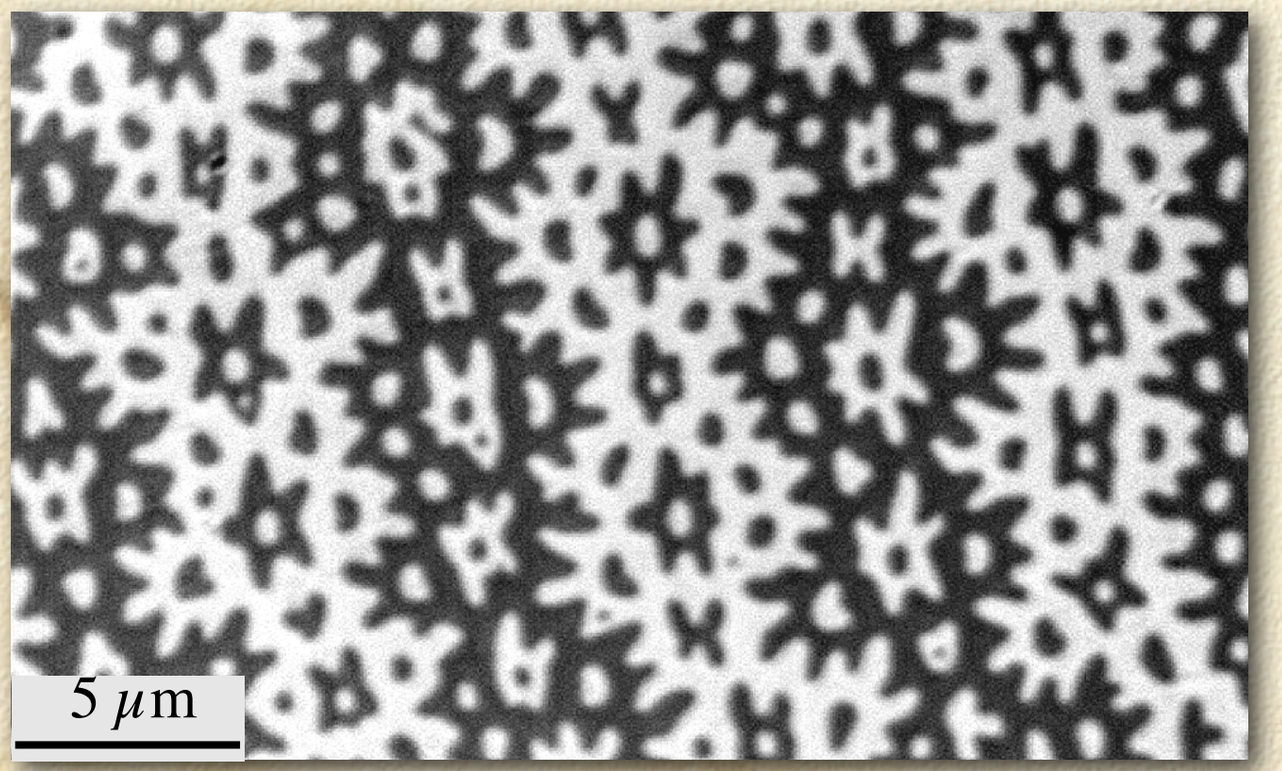

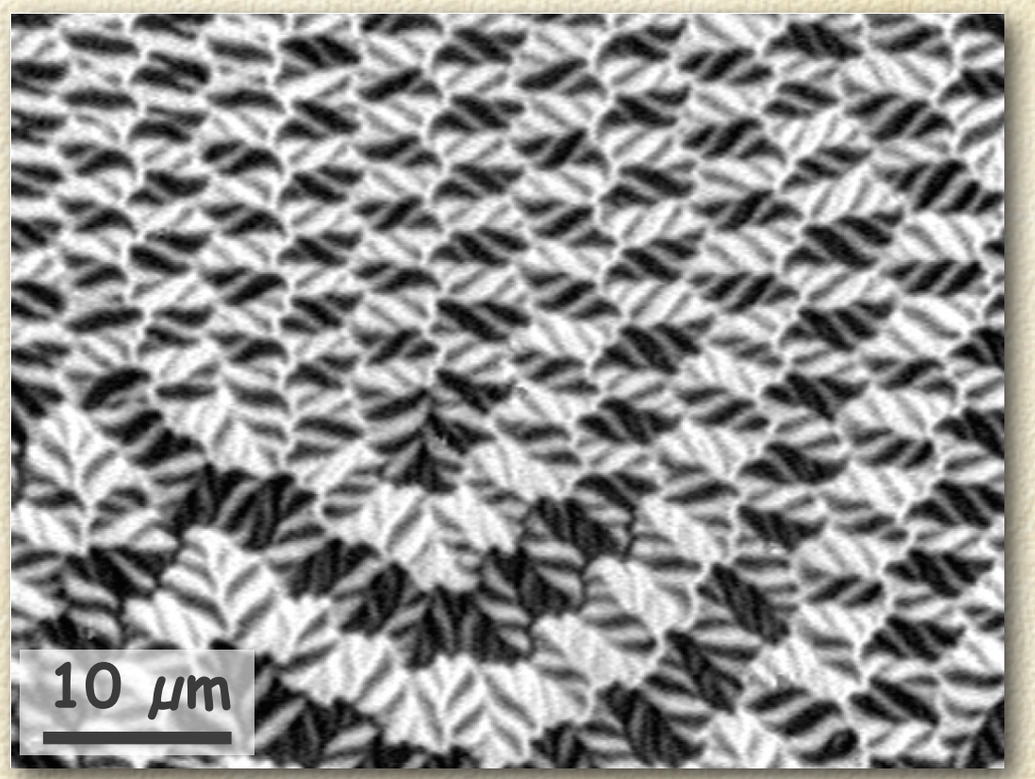

... less difficult

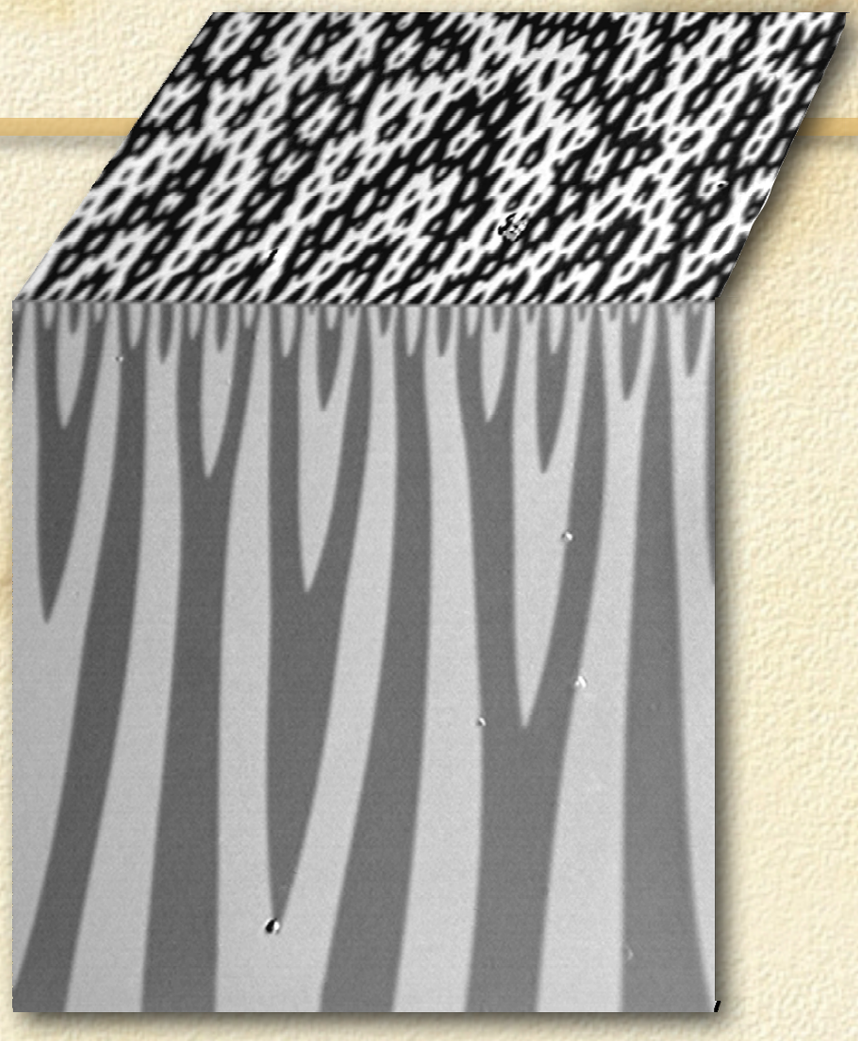

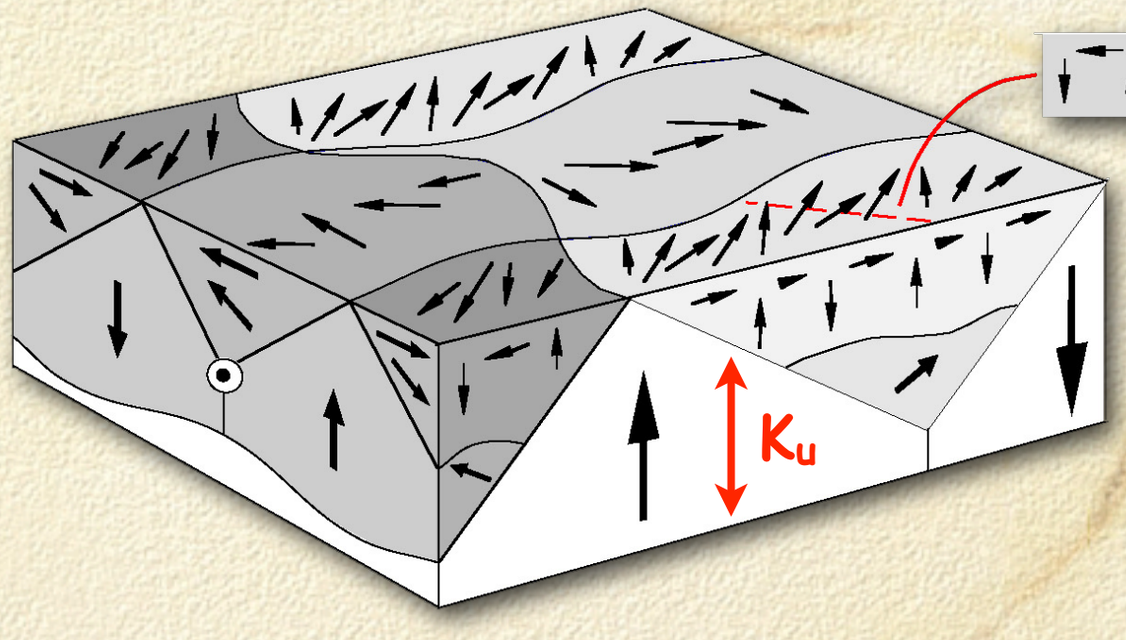

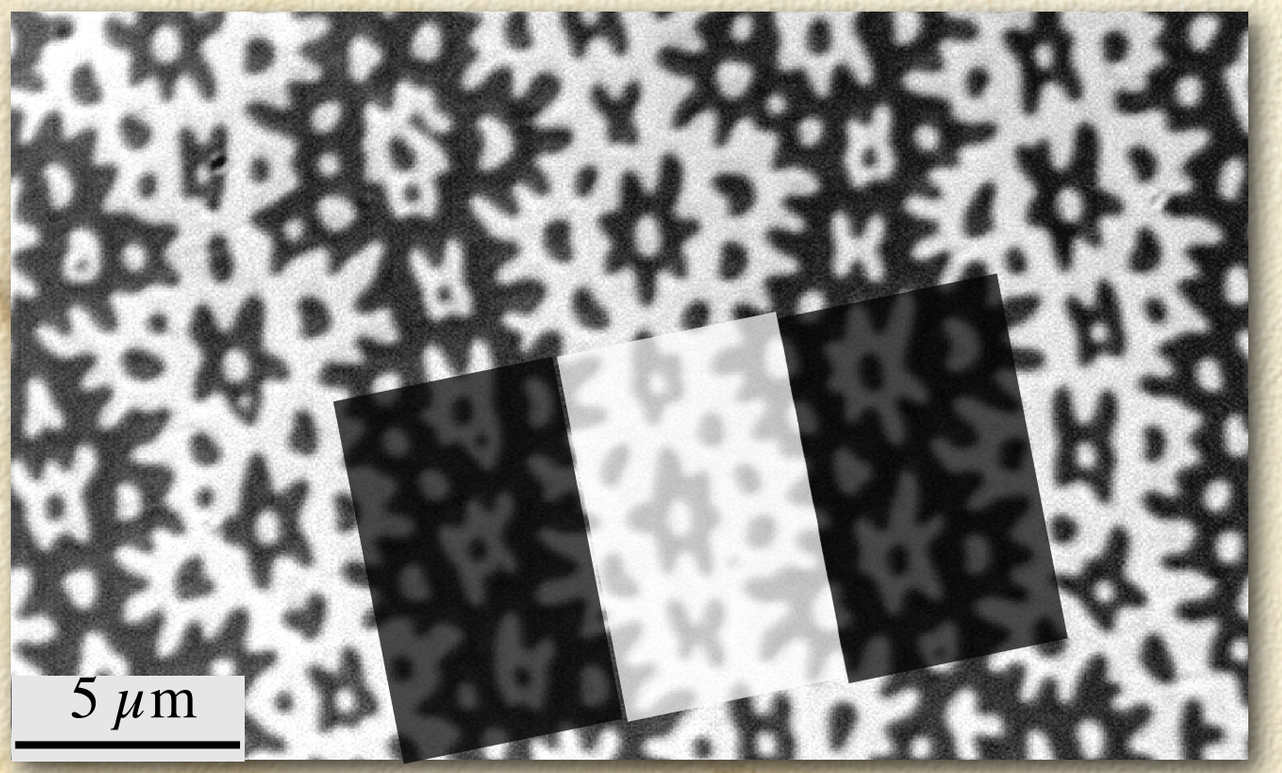

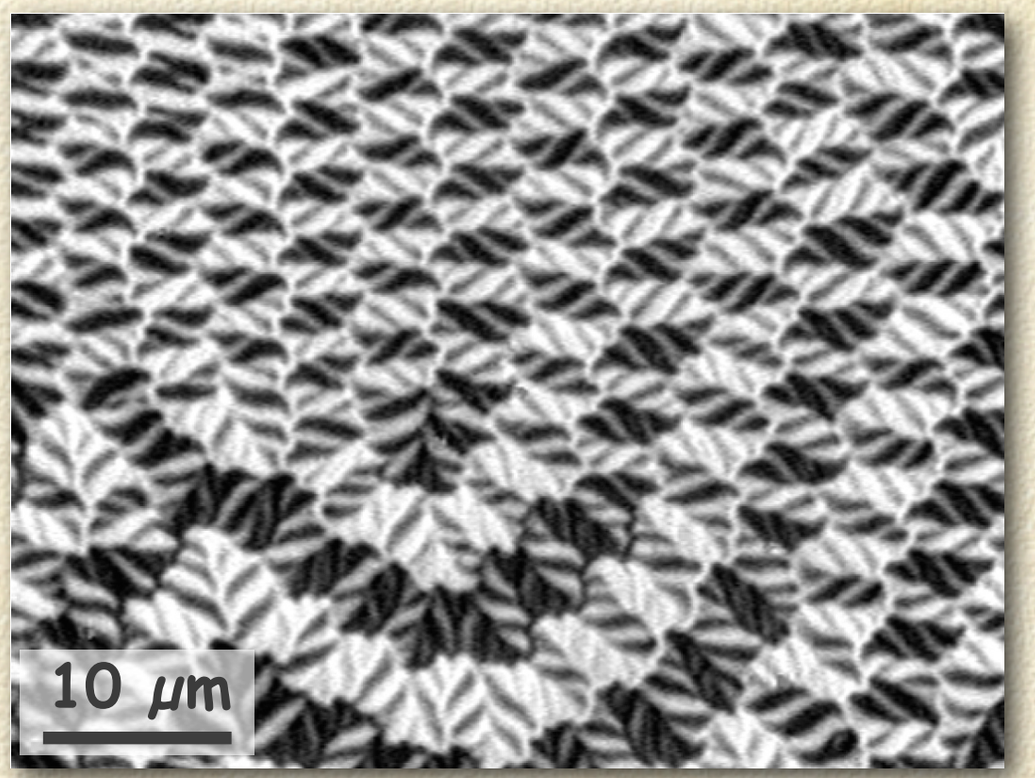

... however

Amorphous ribbons: Layered domain patterns

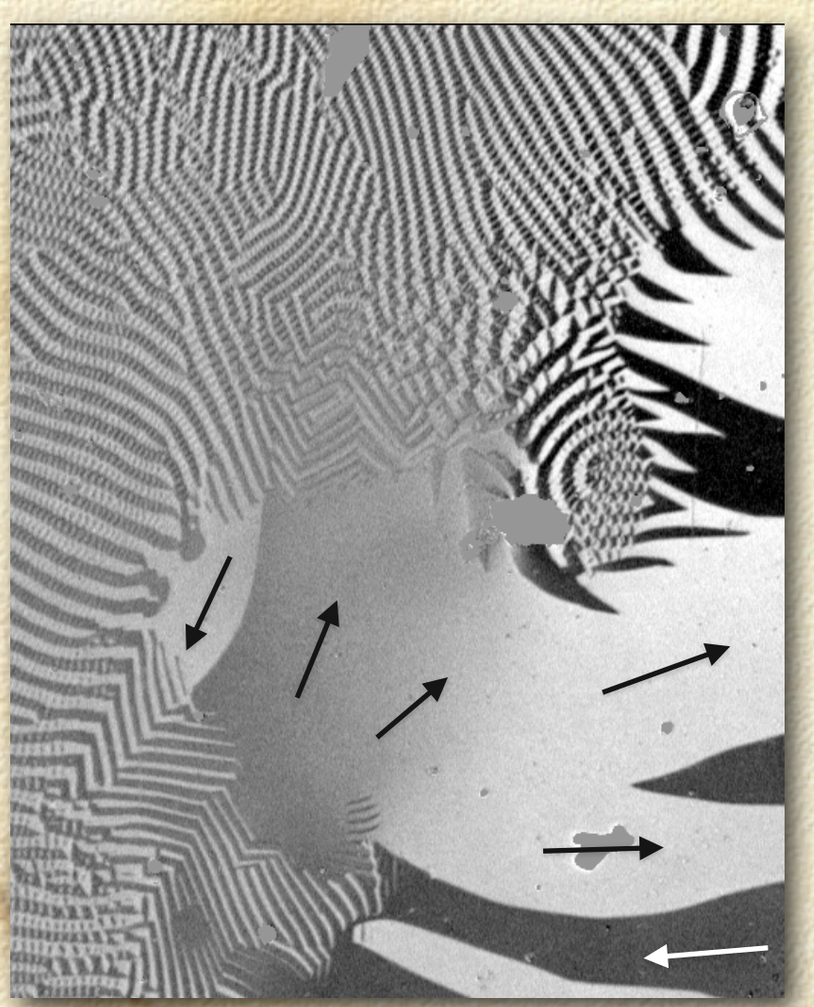

initial state
(reference image)

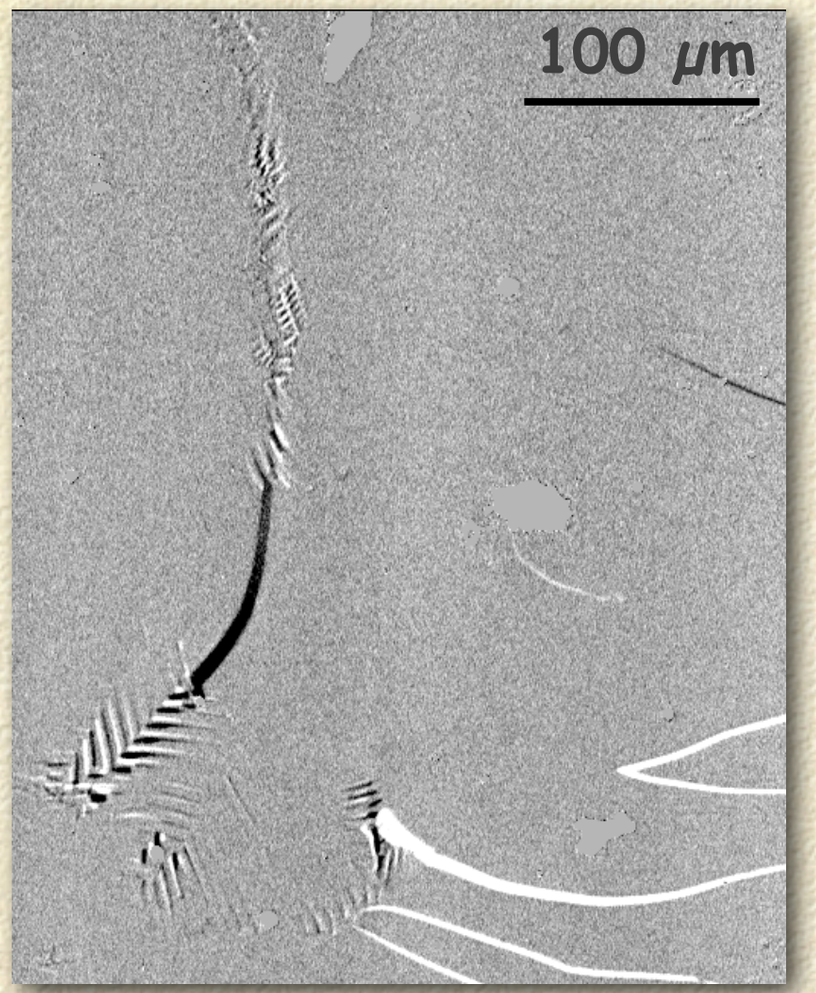

difference image
after application
of small field

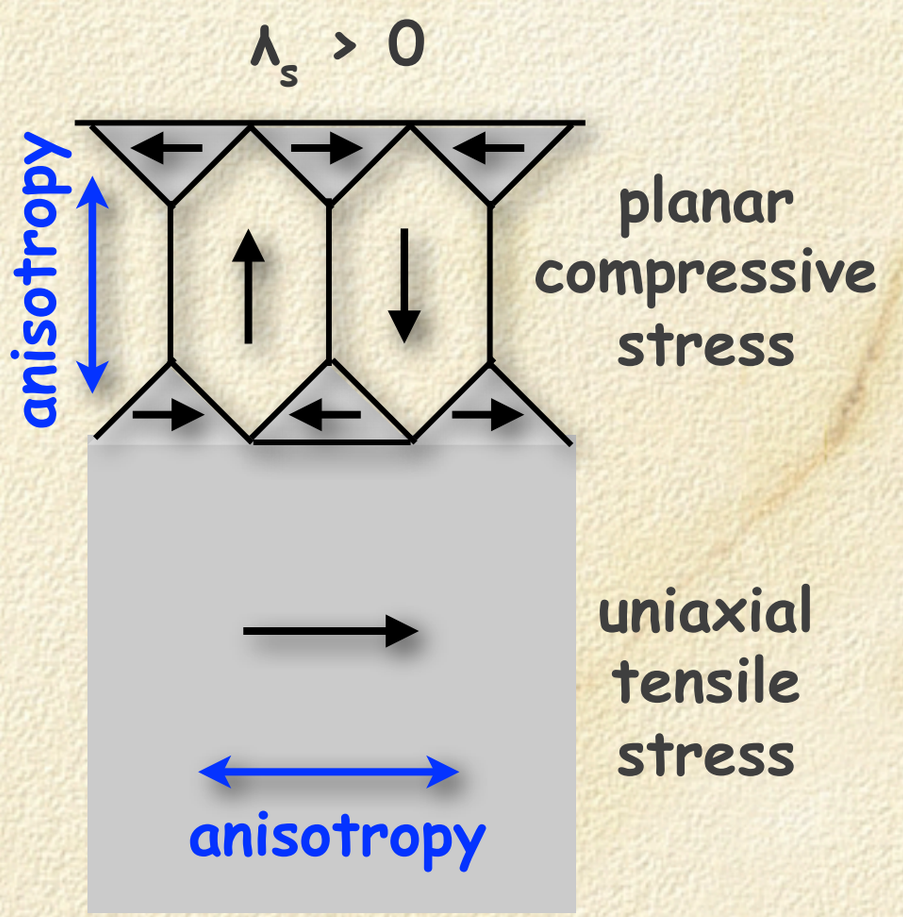

Most complicated:

Bulk multiaxial material

Non-oriented FeSi sheet

0.5 mm

(Fe-3%Si,
non-oriented electrical steel
0.5 mm thick)

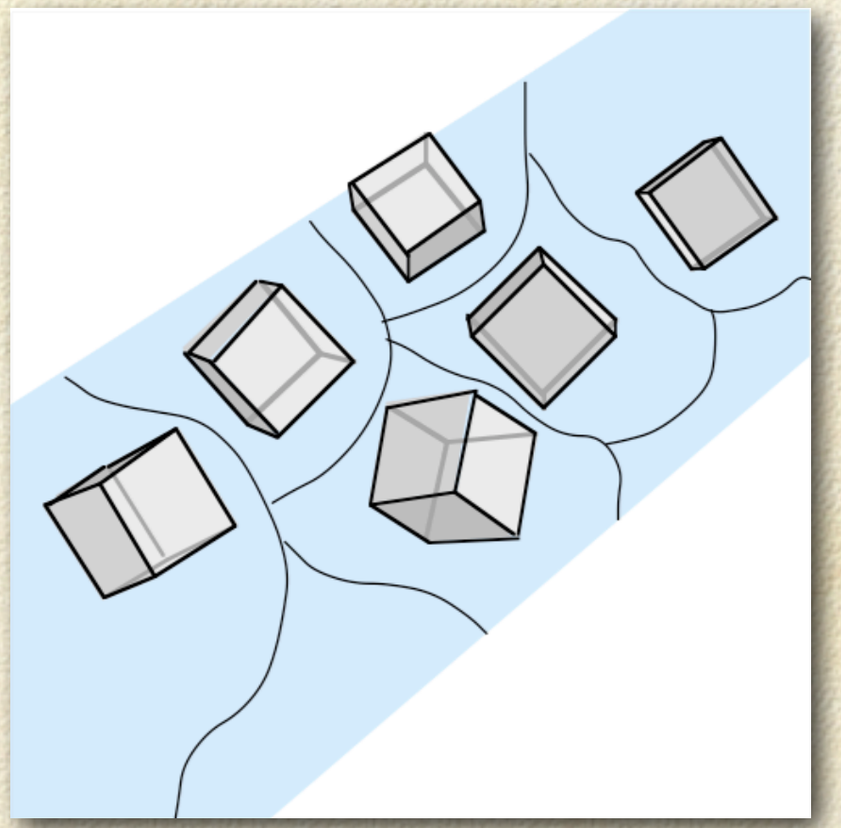

Surface orientation determines domain character

Non-oriented FeSi sheet

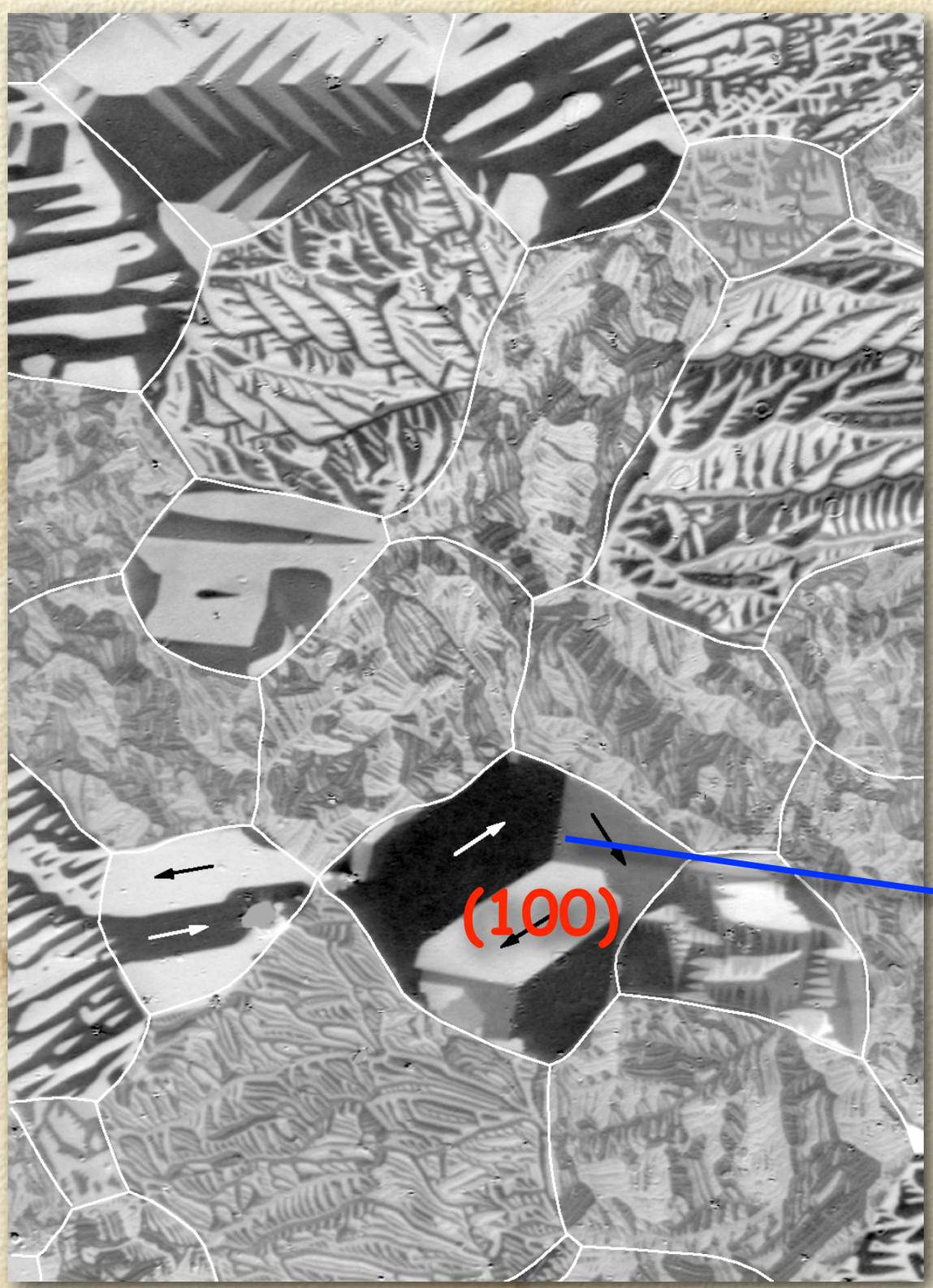

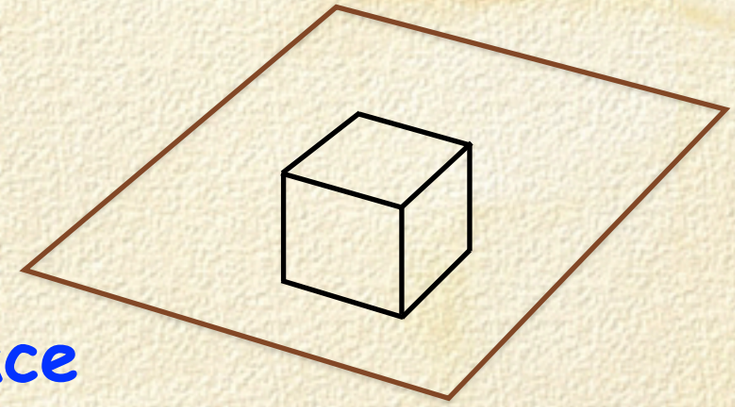

(100)-surface

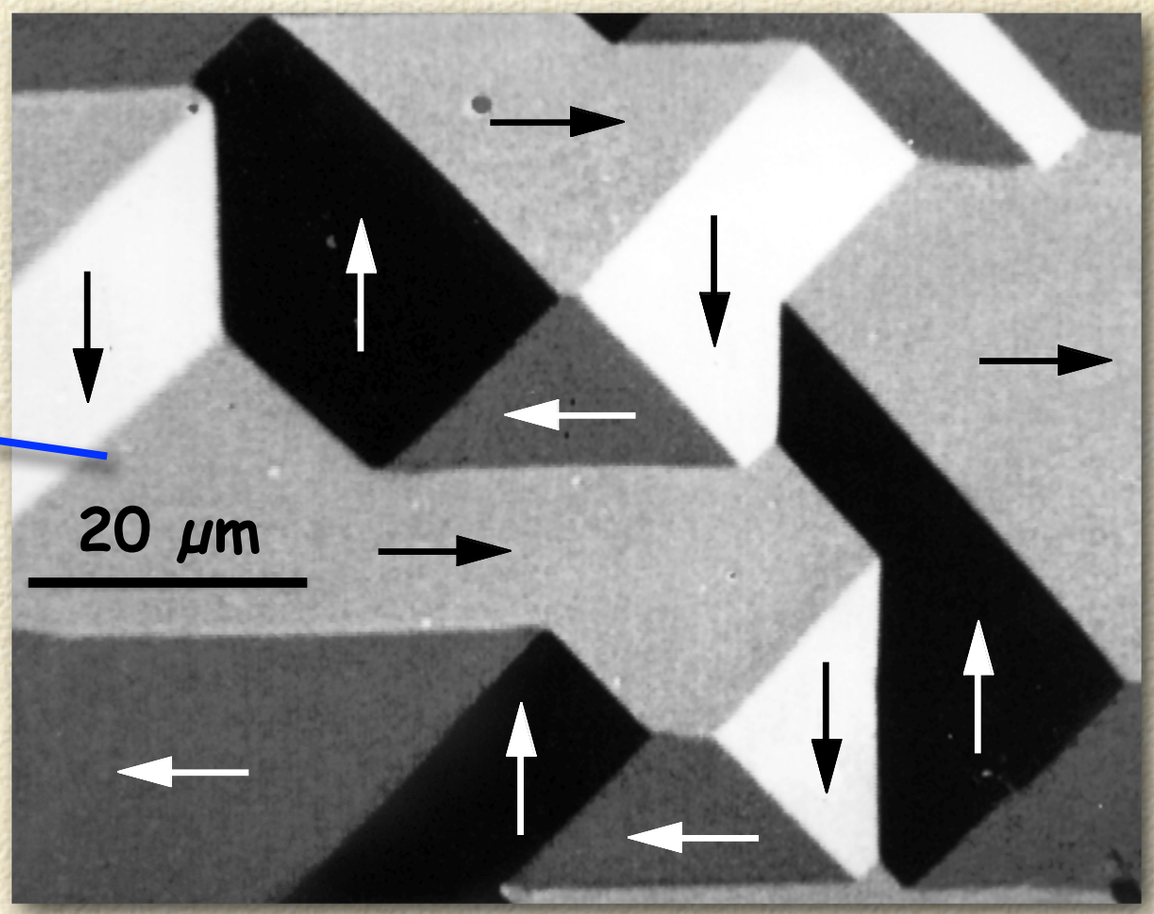

Non-oriented FeSi sheet

0.5 mm

Non-oriented FeSi sheet

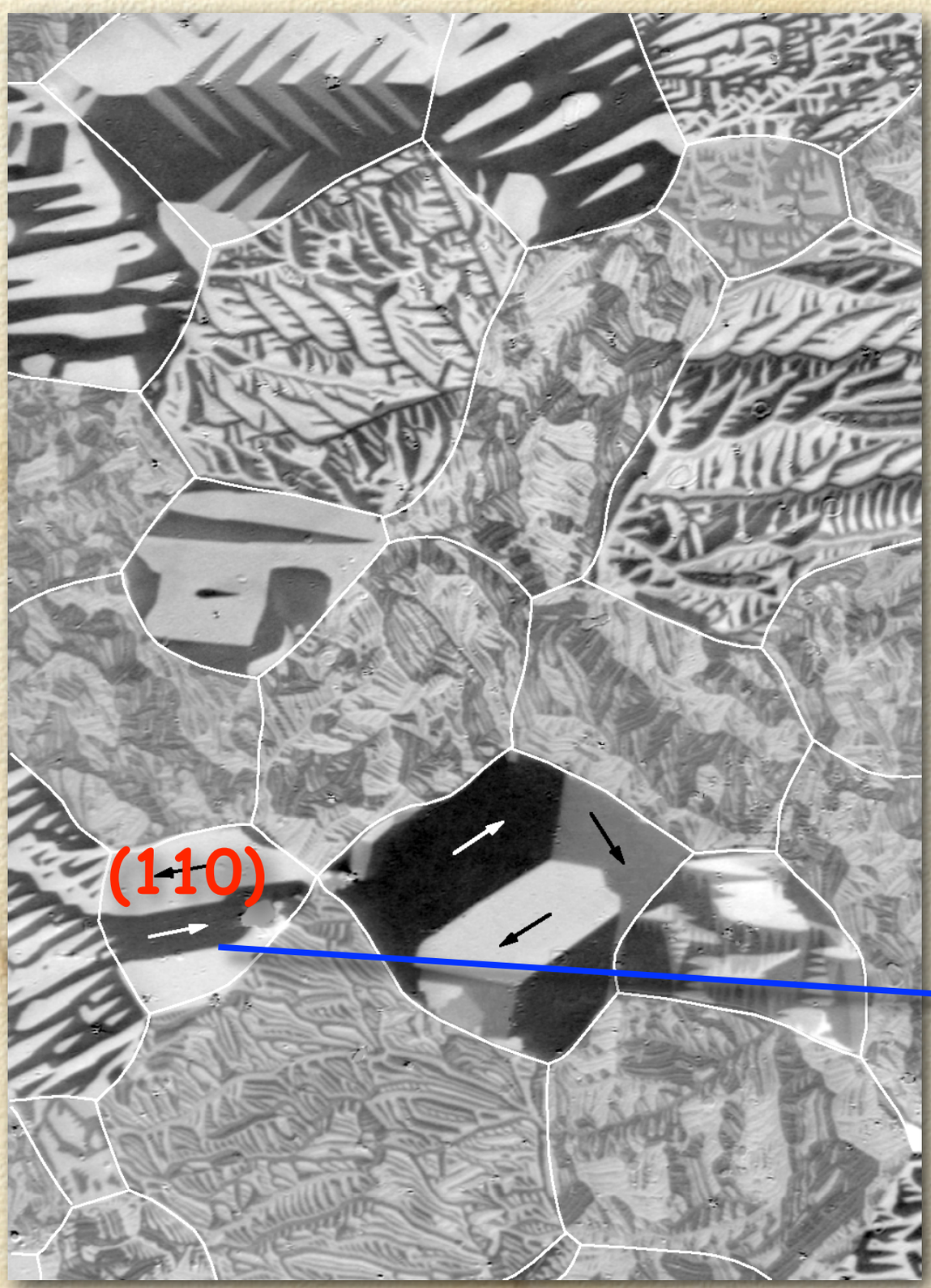

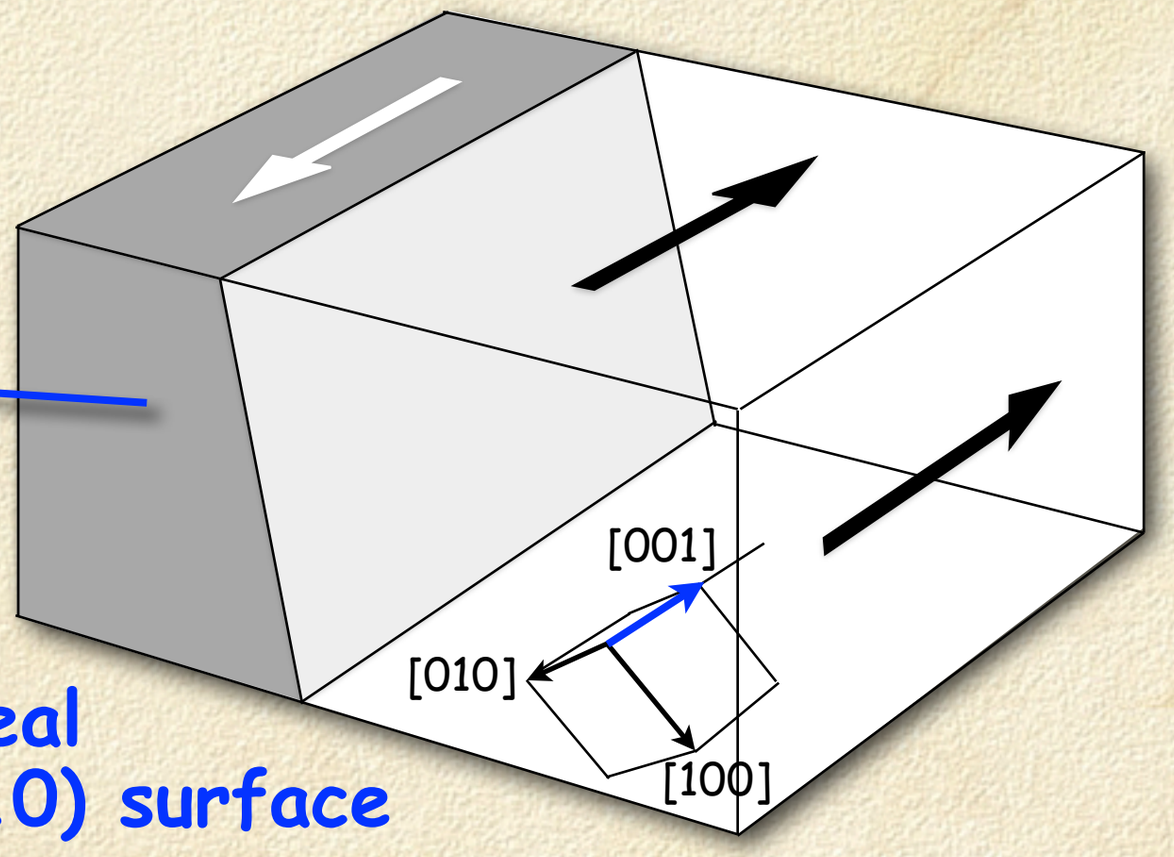

Ideal
(110) surface

Non-oriented FeSi sheet

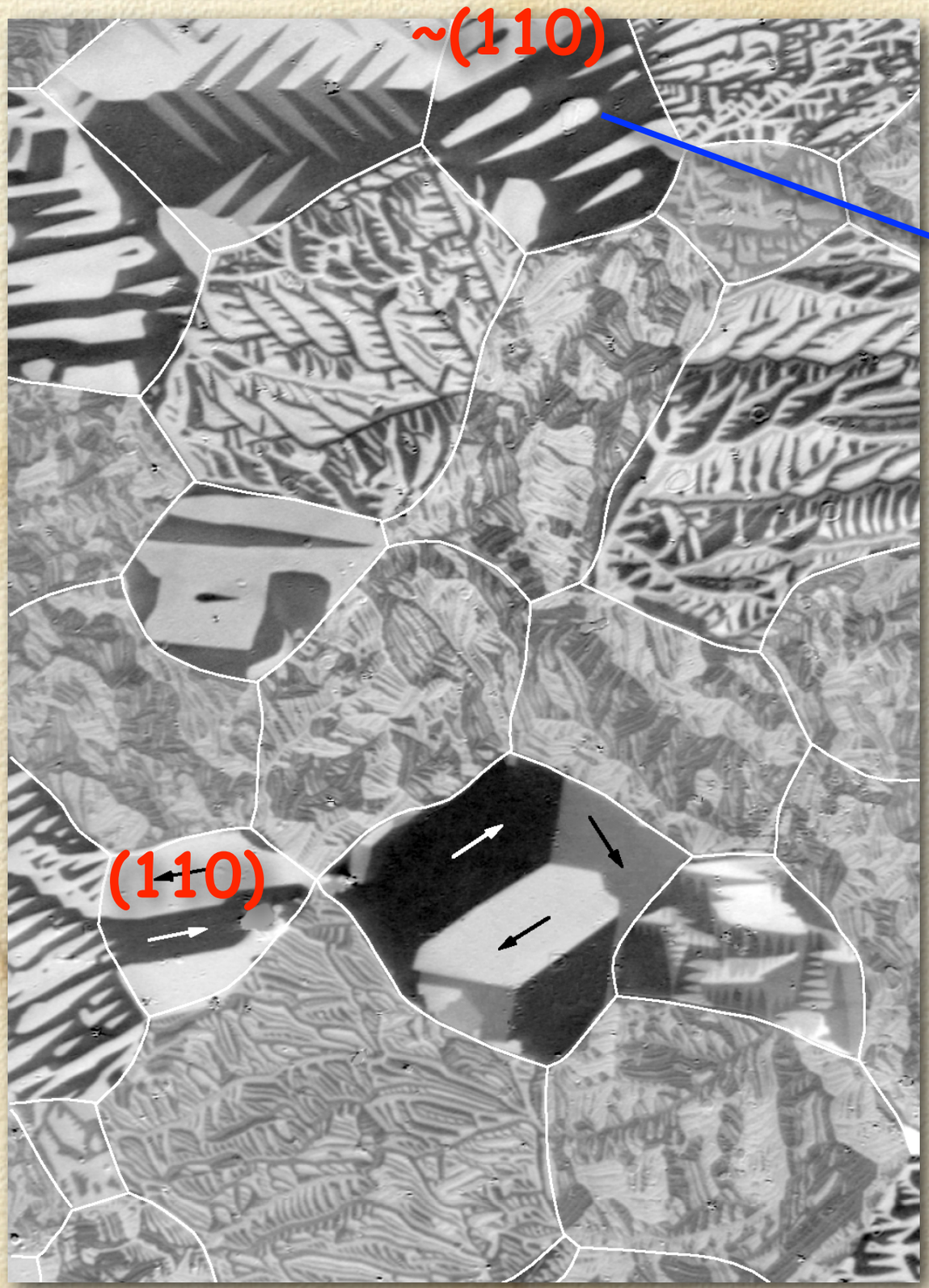

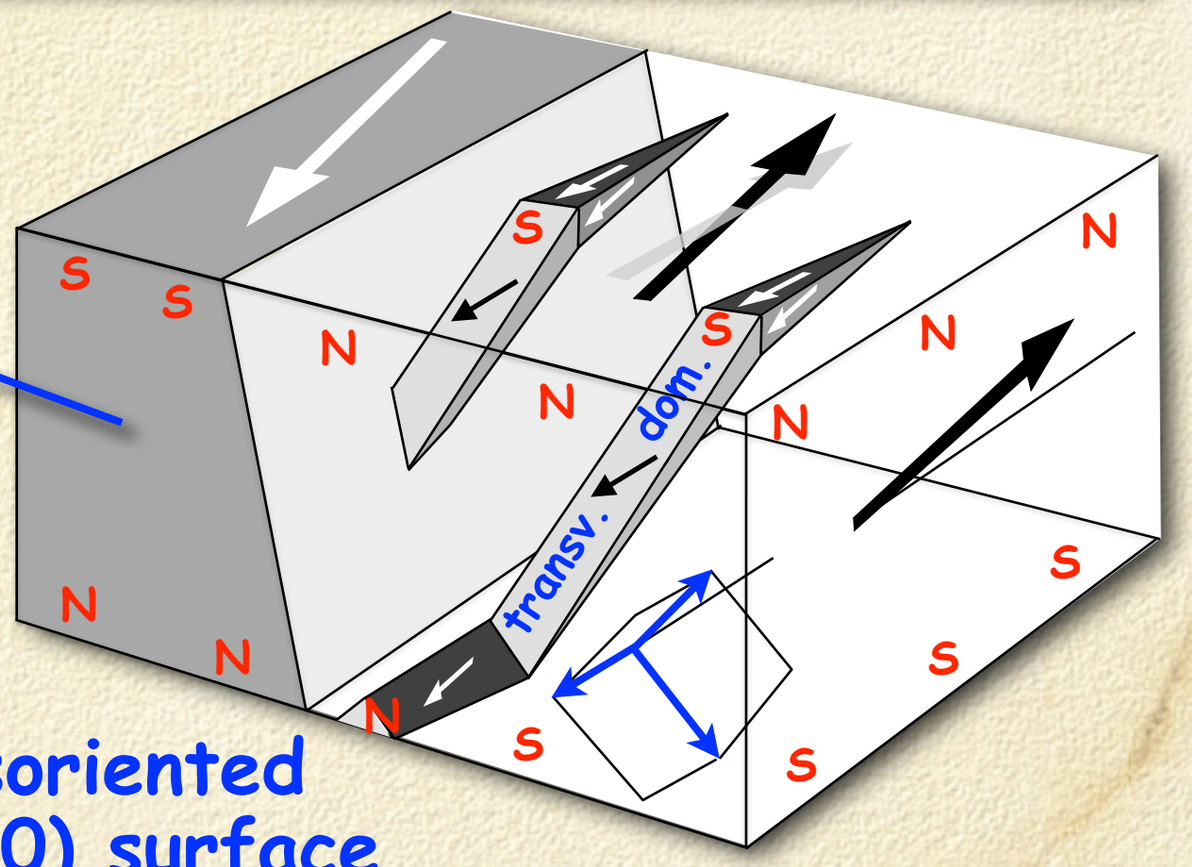

Misoriented
(110) surface

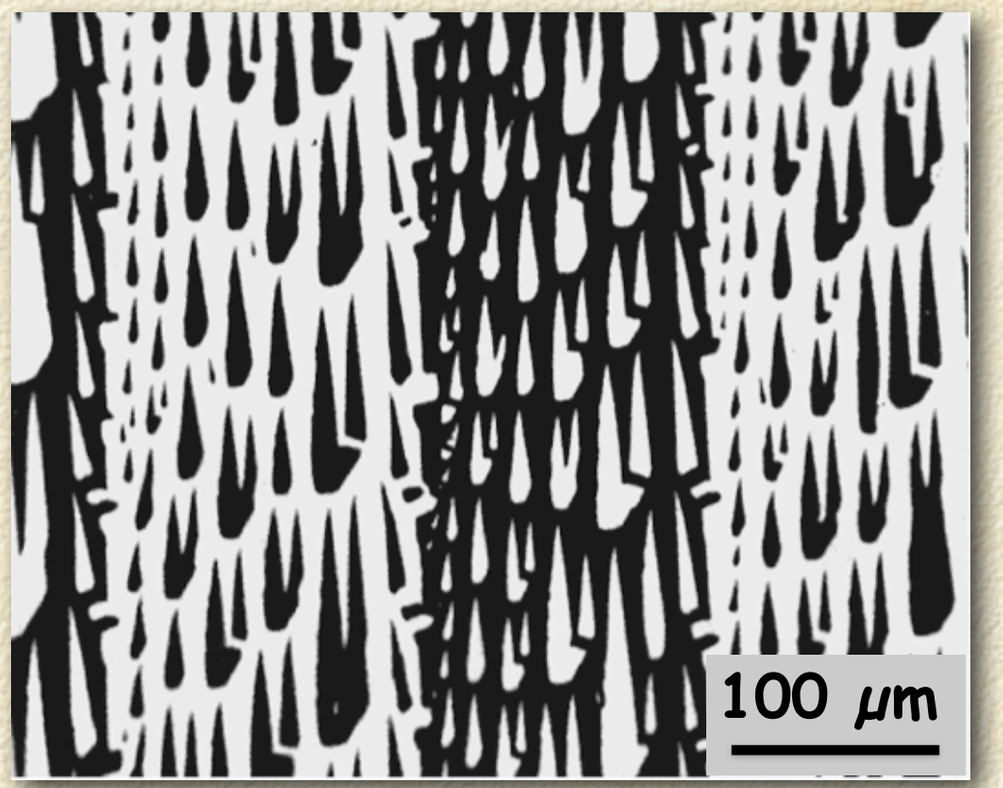

Non-oriented FeSi sheet

0.5 mm

Non-oriented FeSi sheet

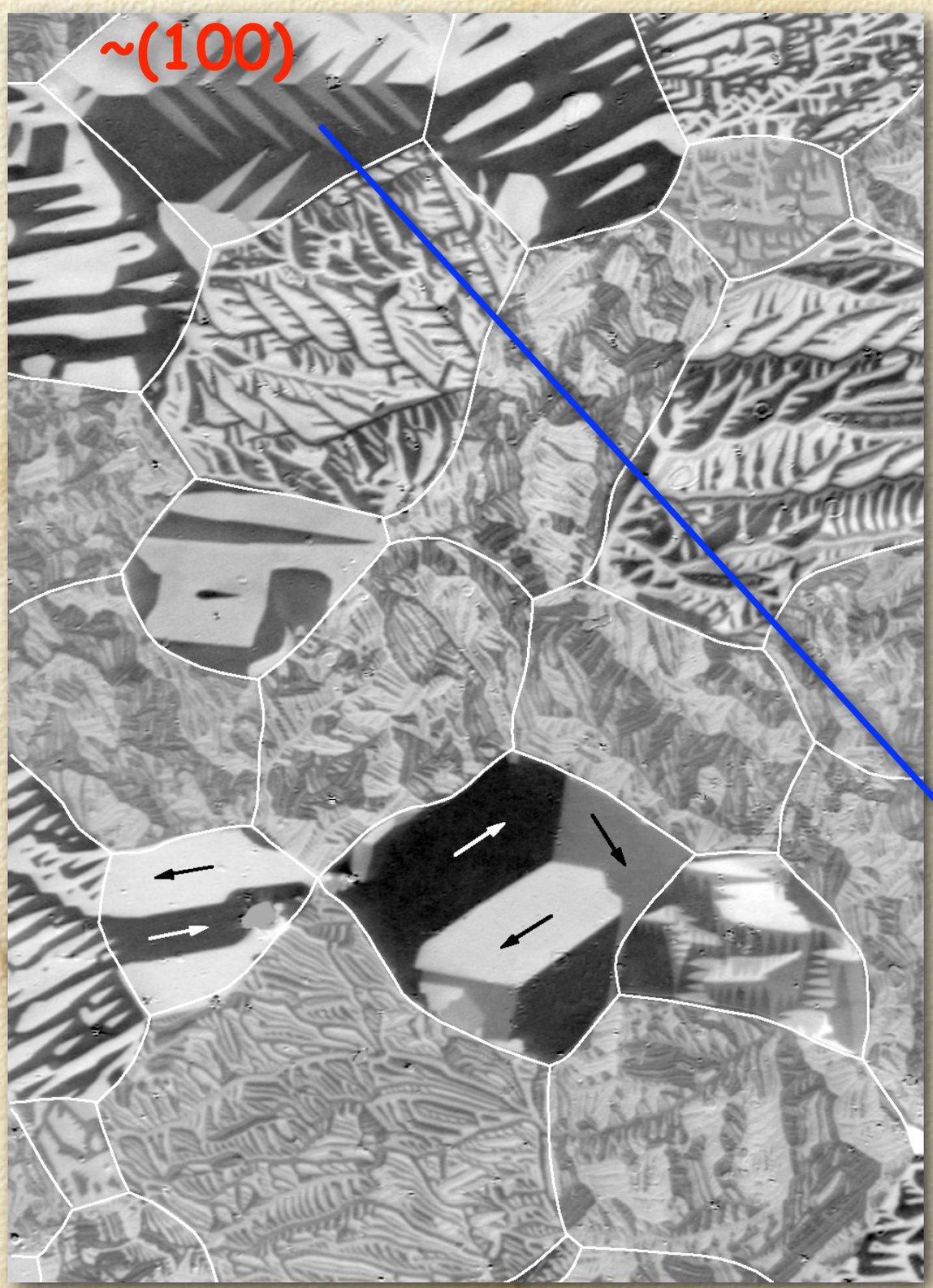

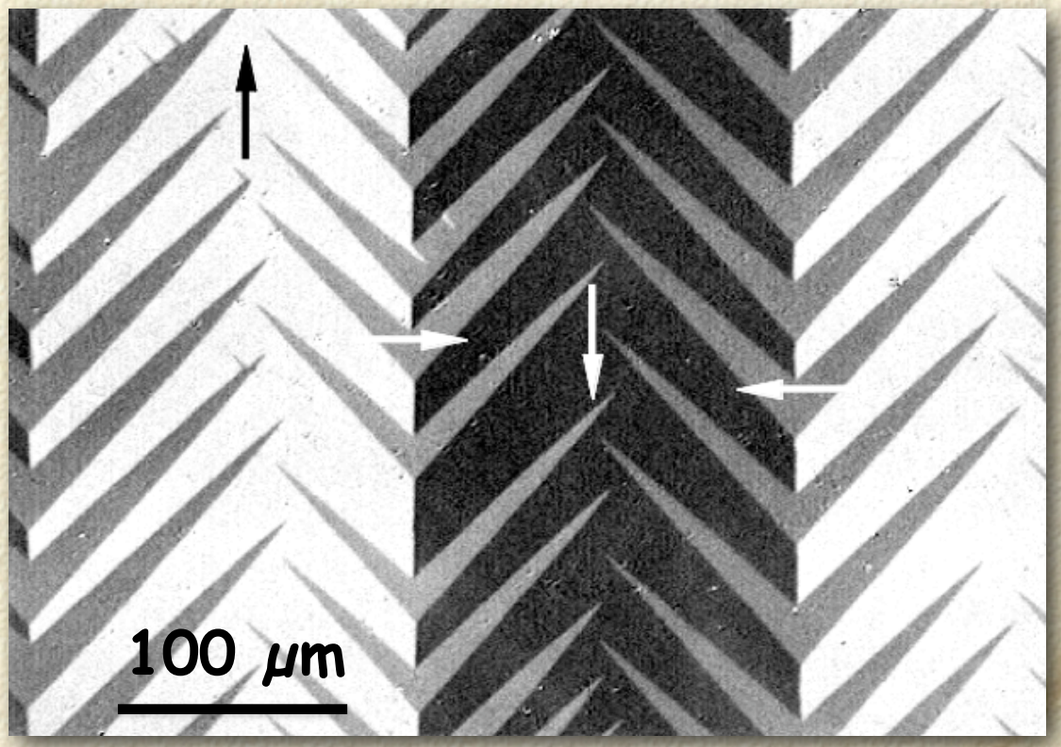

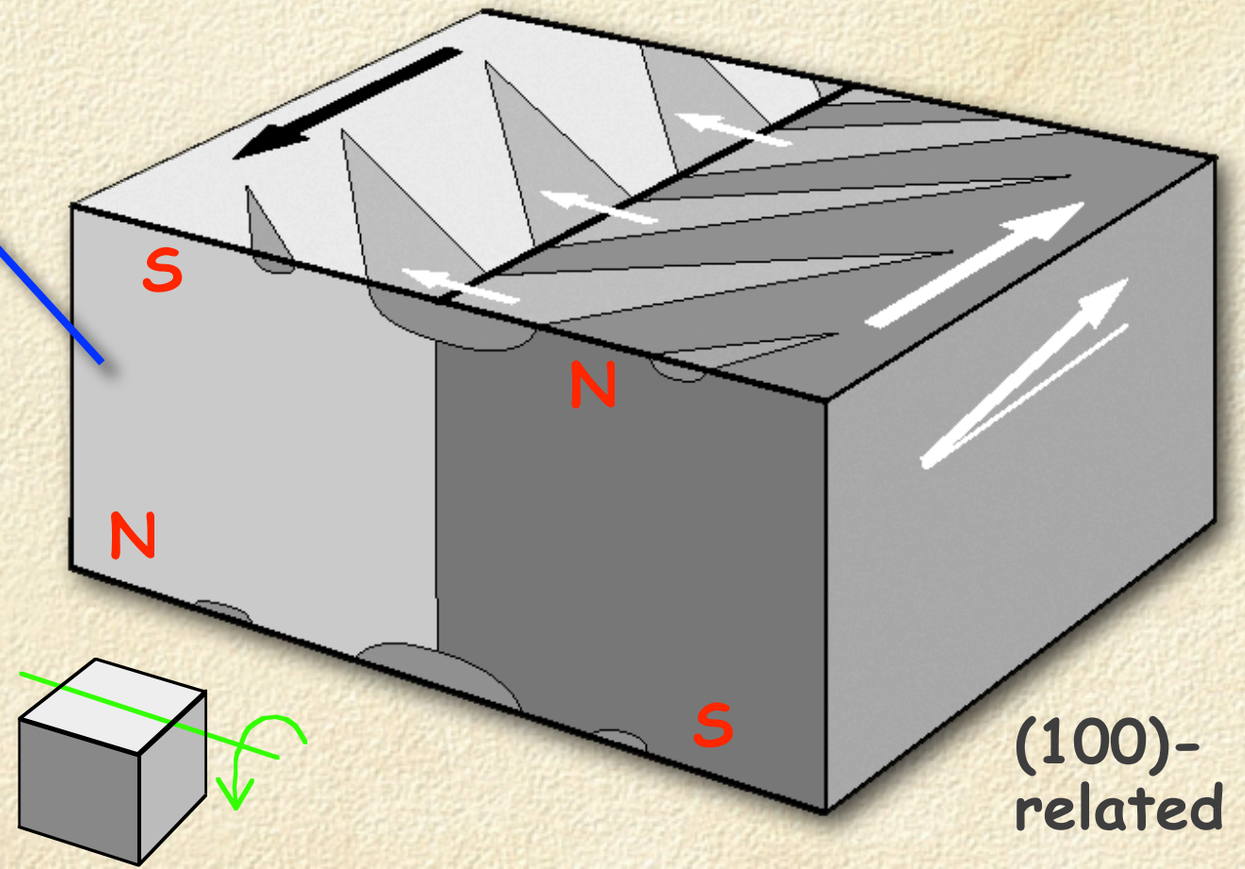

(100)-related

Weak misorientation: Supplementary Domains

Weak misorientation: Supplementary Domains

Iron, (100)- and (110)-related surfaces

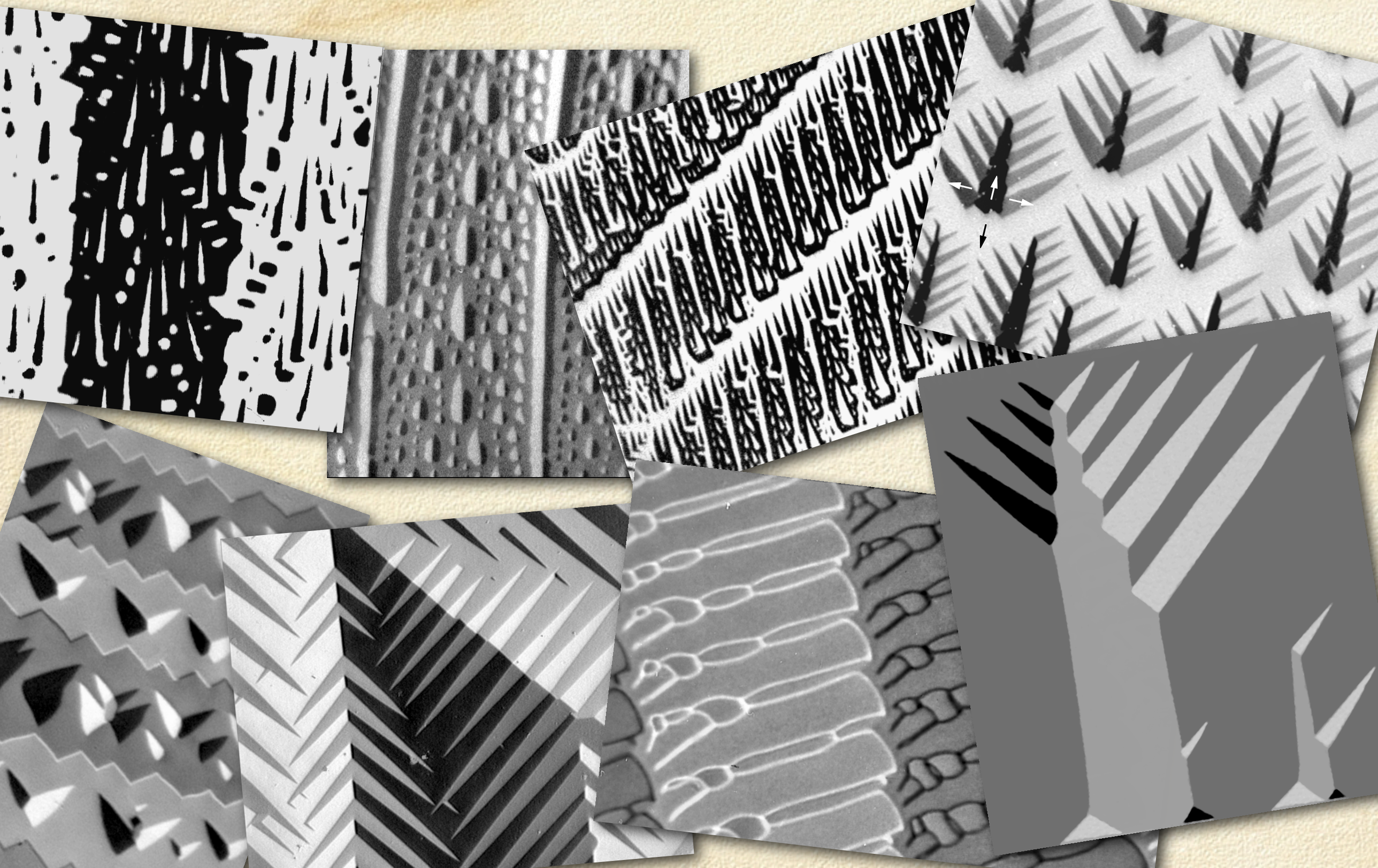

Non-oriented FeSi sheet

For well-oriented and slightly misoriented grains domains can be interpreted:

basic domains and supplementary pattern

Non-oriented FeSi sheet

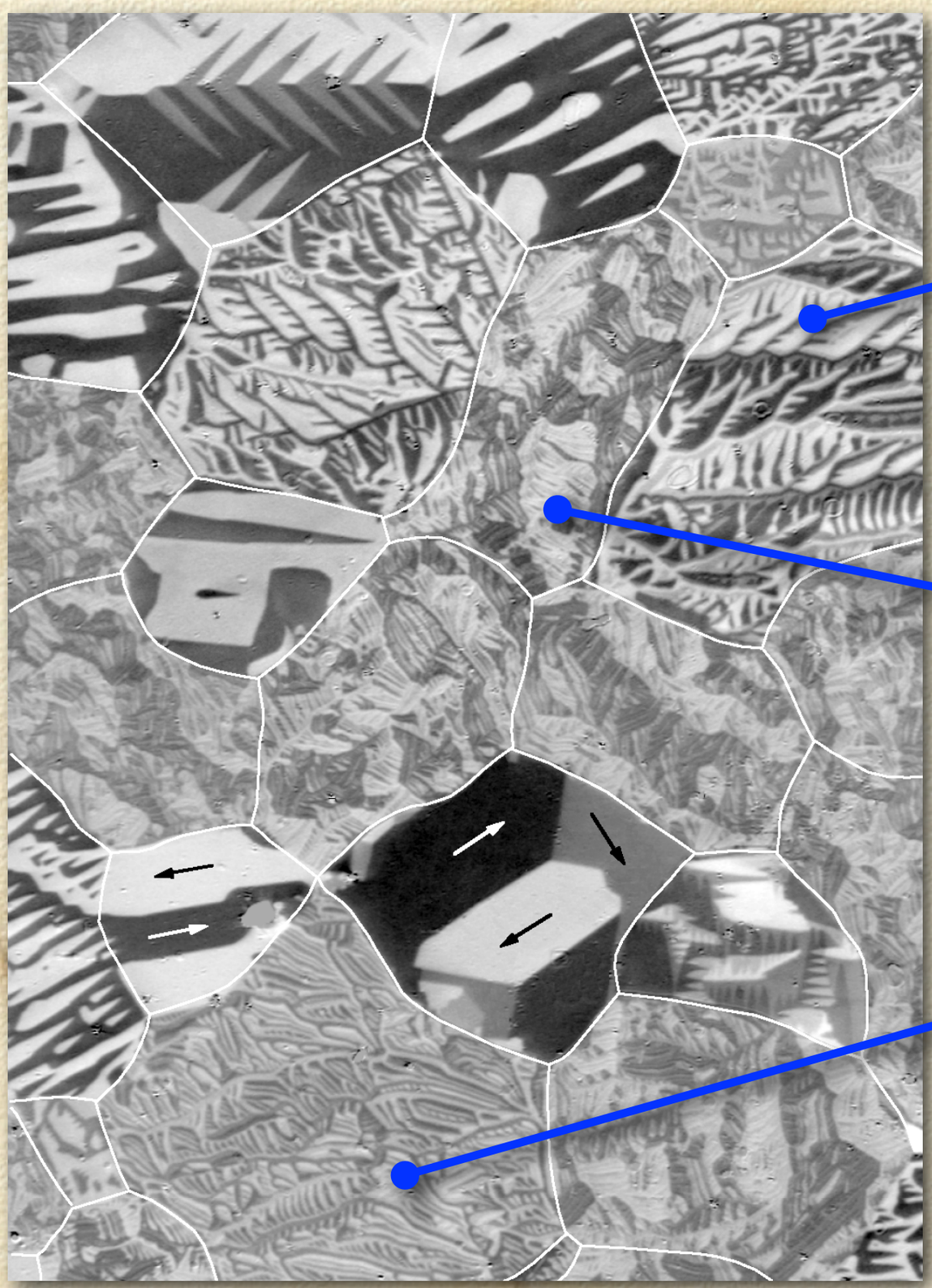

0.5 mm

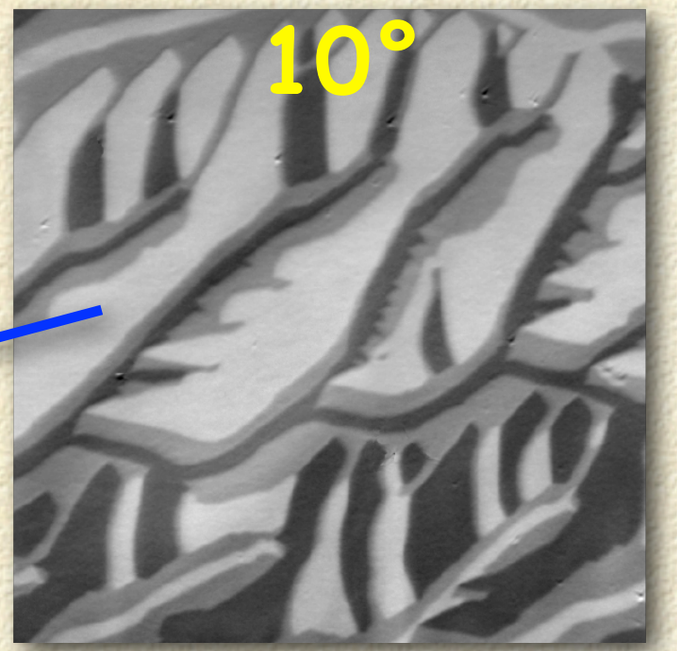

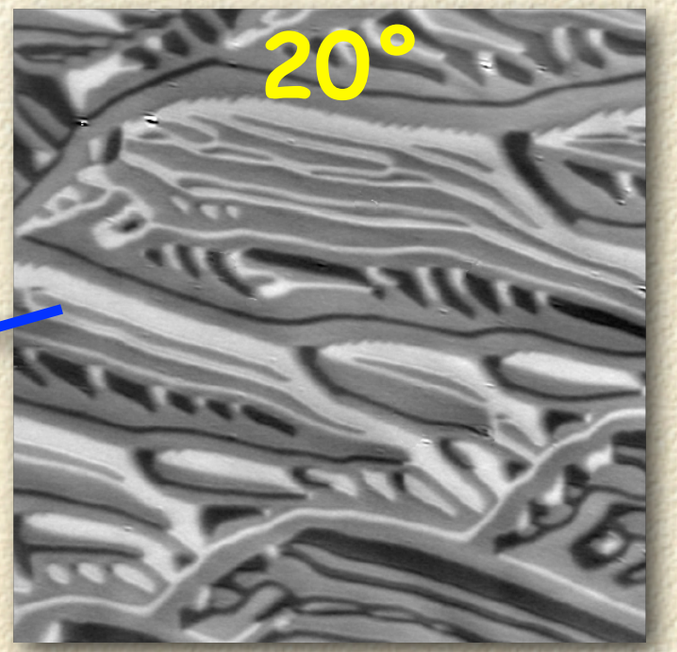

10 μm

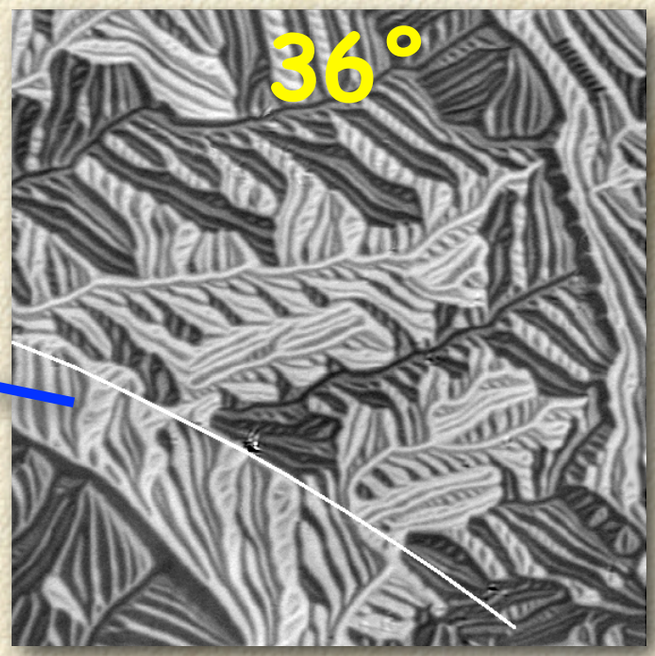

(111)-surface

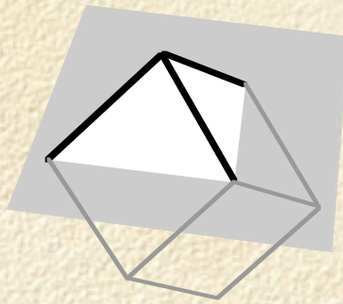

Extreme misorientation: Domain branching

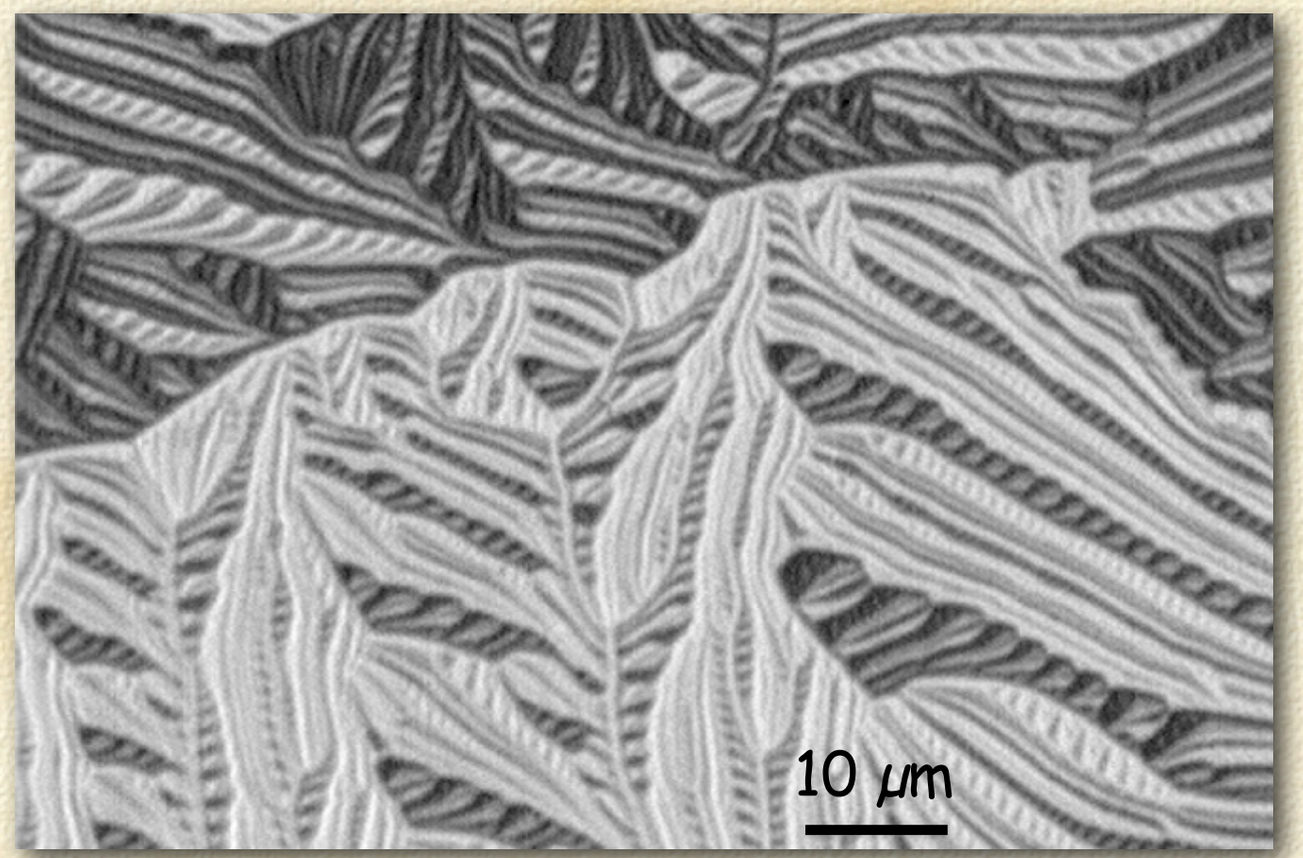

Iron: $Q = 0.02$

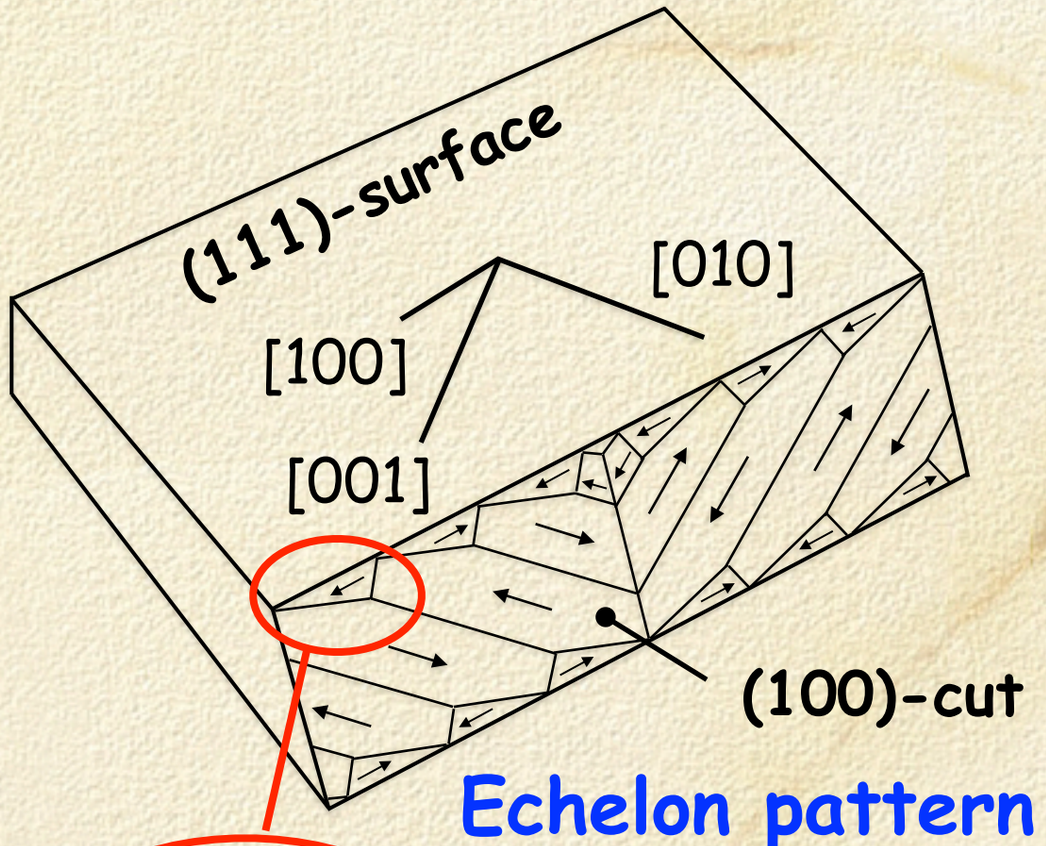

Echelon pattern

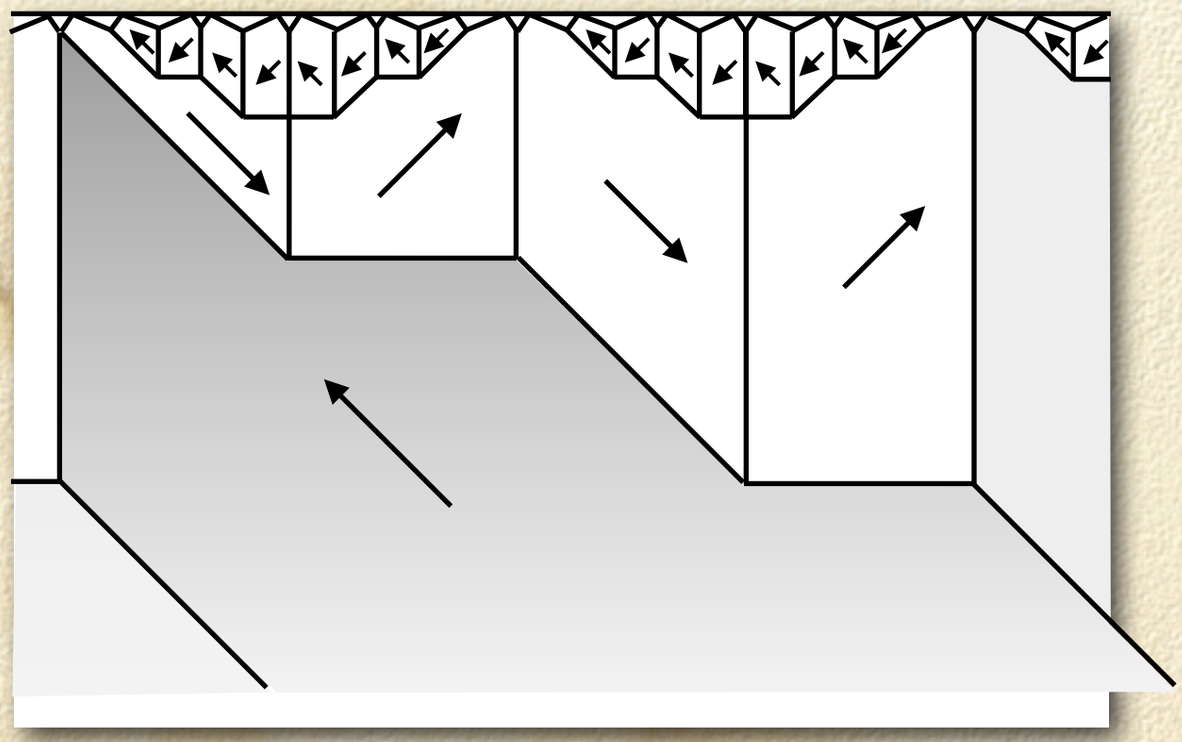

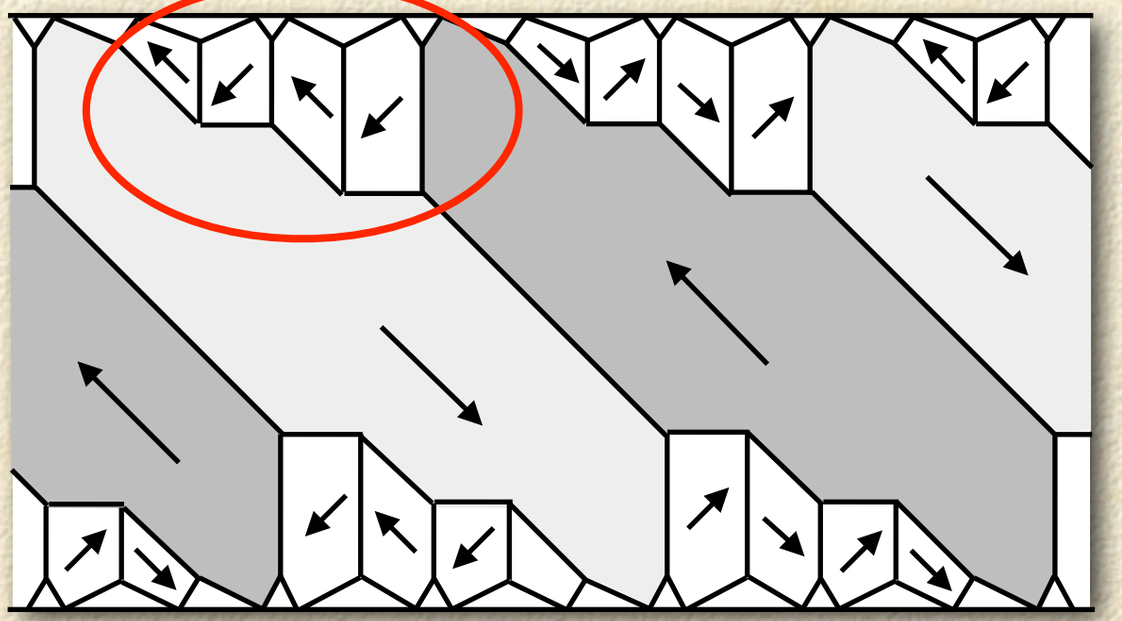

Problem: only surface domains can be seen

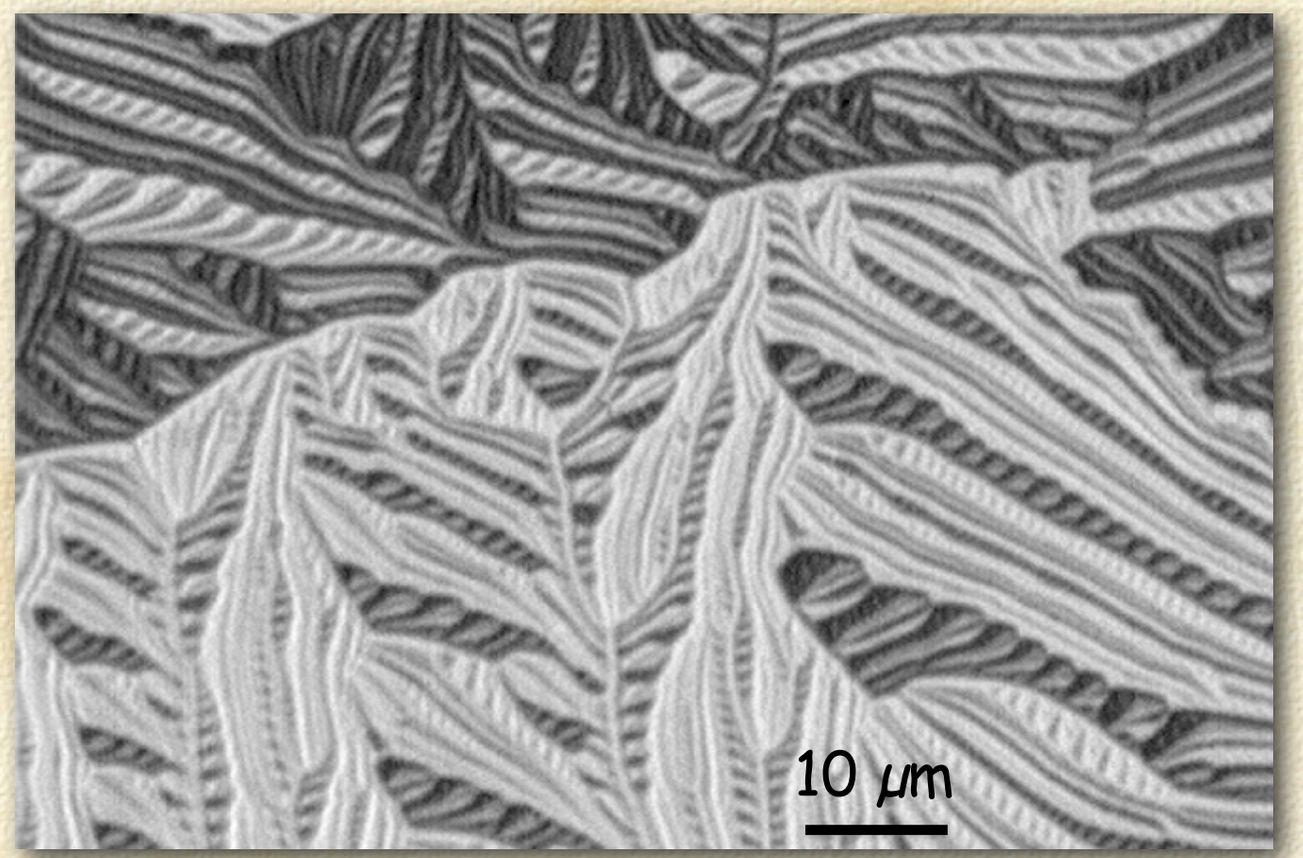

Iron: $Q = 0.02$

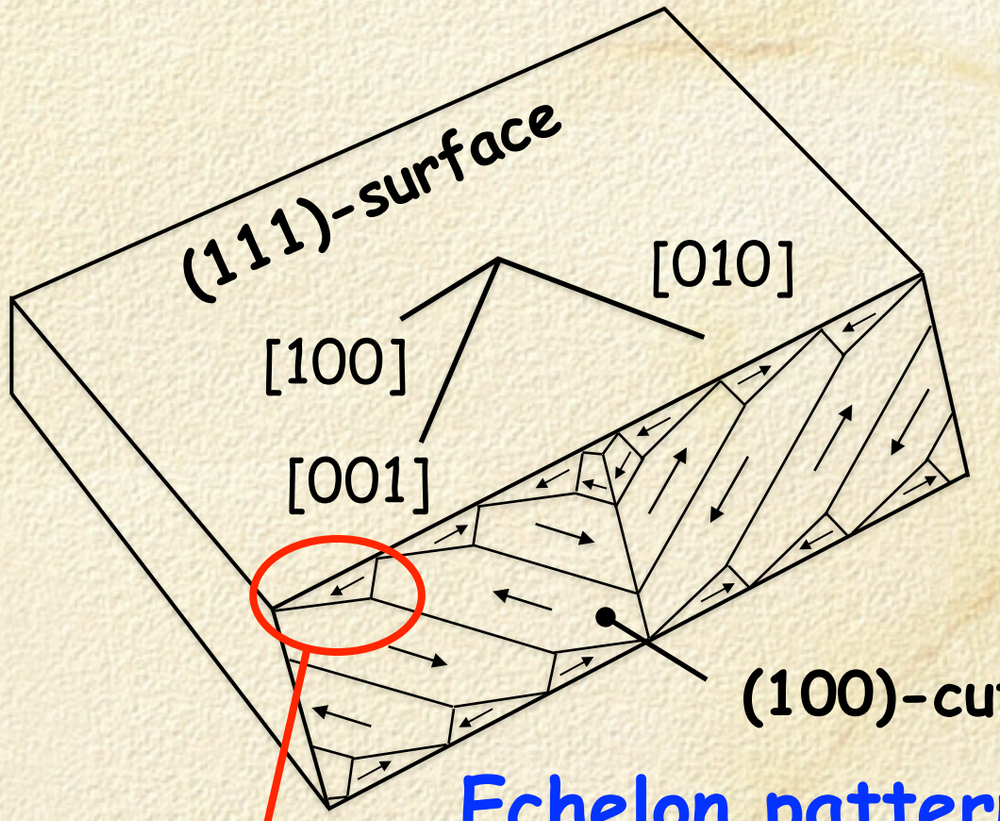

Echelon pattern

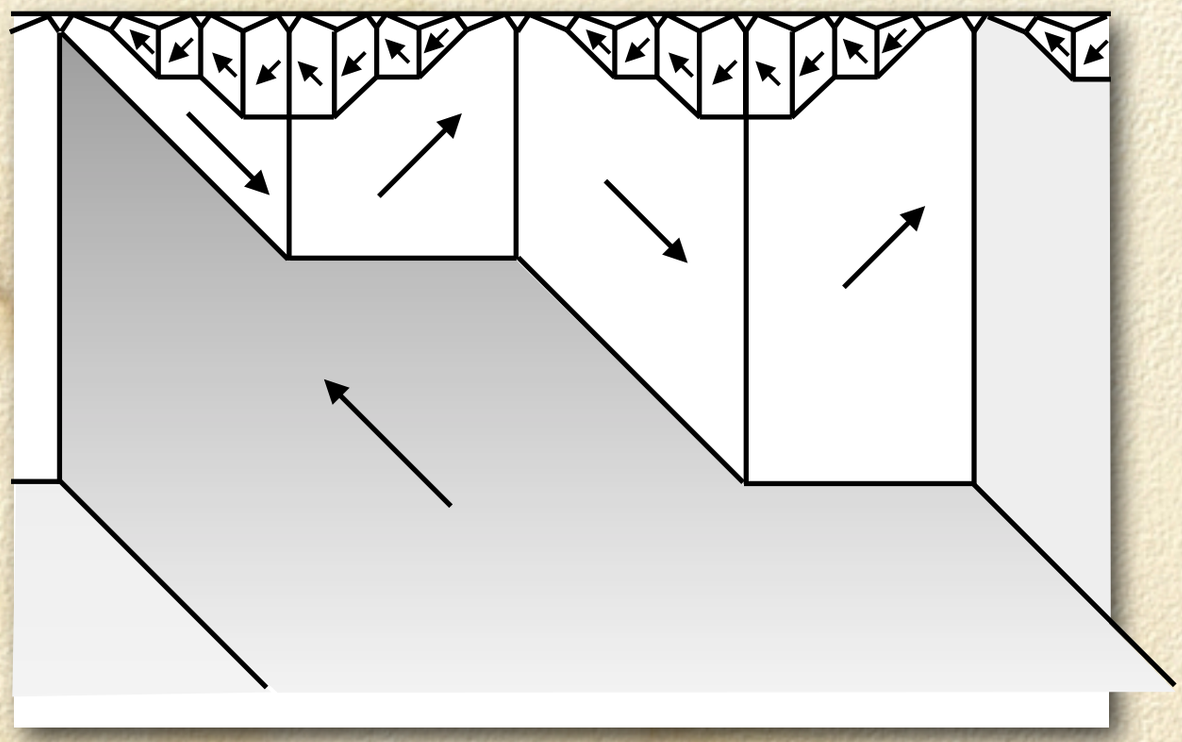

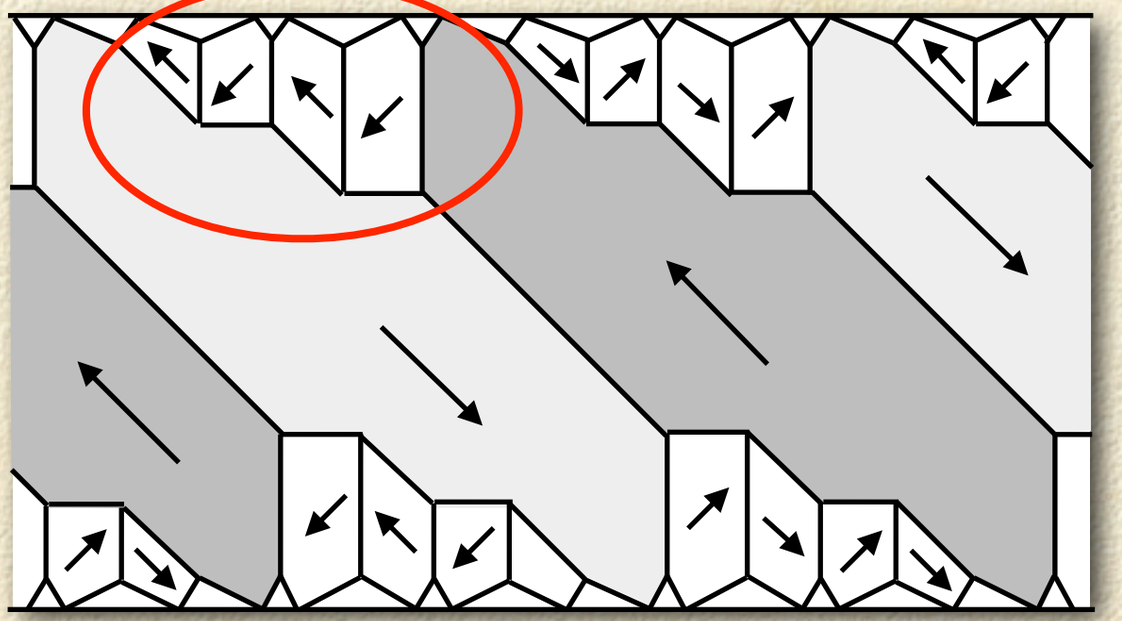

Problem: only surface domains can be seen

Iron: $Q = 0.02$

Bulk Domain Analysis

Echelon pattern

Direct imaging of volume domains by neutron dark-field microscopy

together with

C. Grünzweig and coworkers,
Paul Scherrer Institut, Villigen, Switzerland

I. Manke, N. Kardjilov, A. Hilger,
Helmholtz Centre Berlin for Materials and Energy

C. Grünzweig, et al.: Neutron decoherence imaging for visualizing bulk magnetic domain structure. Phys. Rev. Lett. 101, 025504 (2008)

I. Manke, et al.: Three-dimensional imaging of magnetic domains. Nature Communications, 1:125 doi: 10.1038/ncomms1125 (2010)

Neutron dark-field microscopy

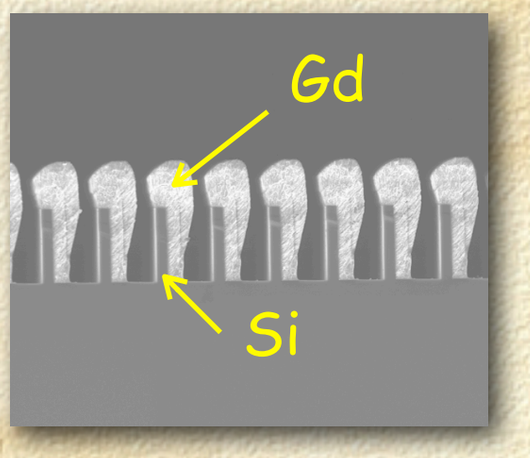

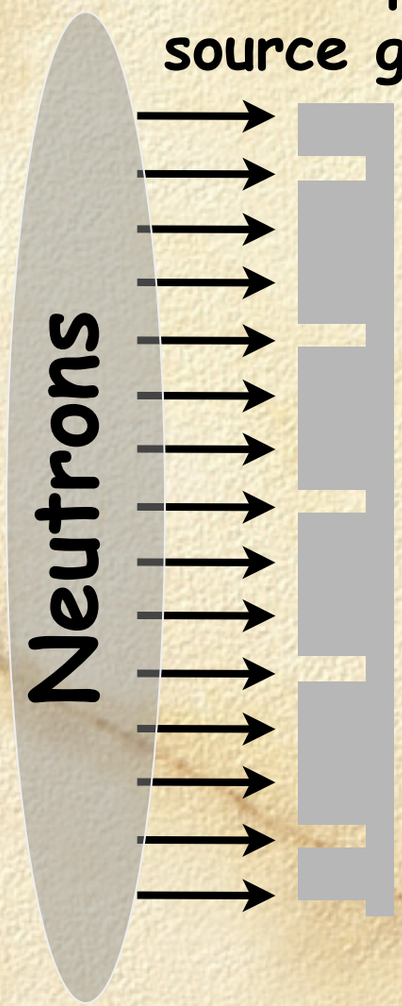

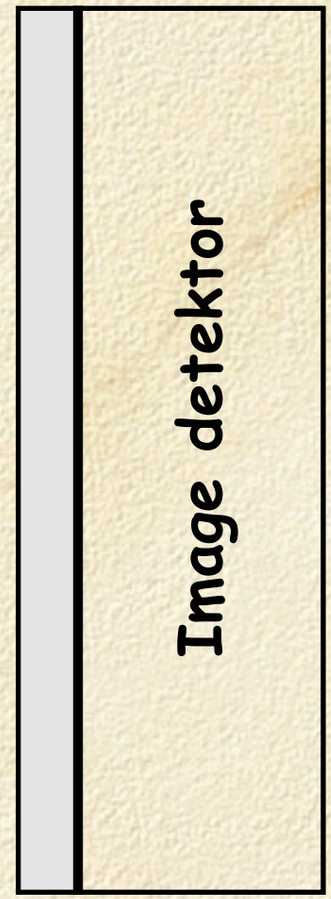

Neutron dark-field microscopy

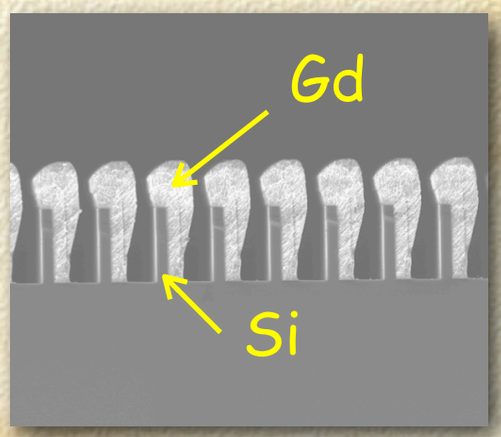

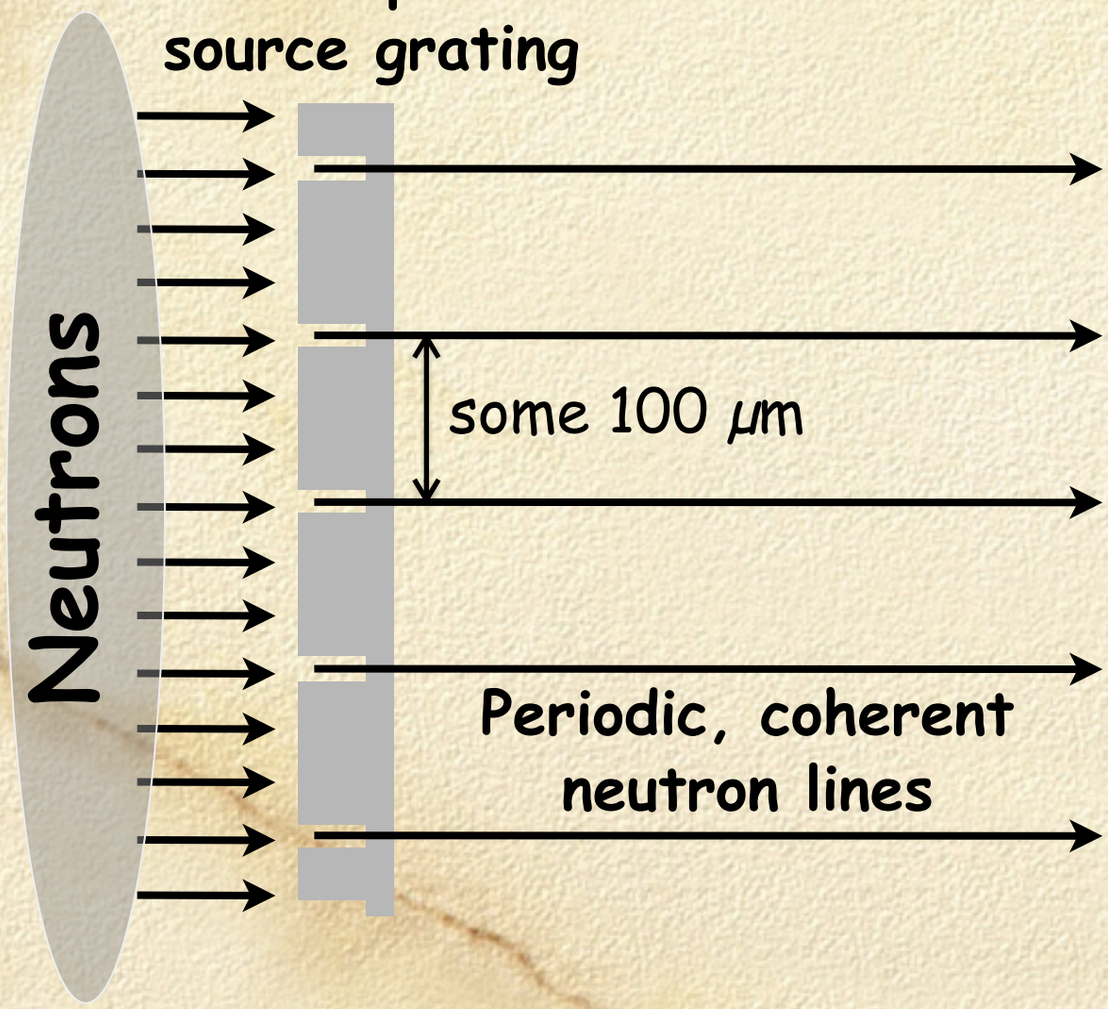

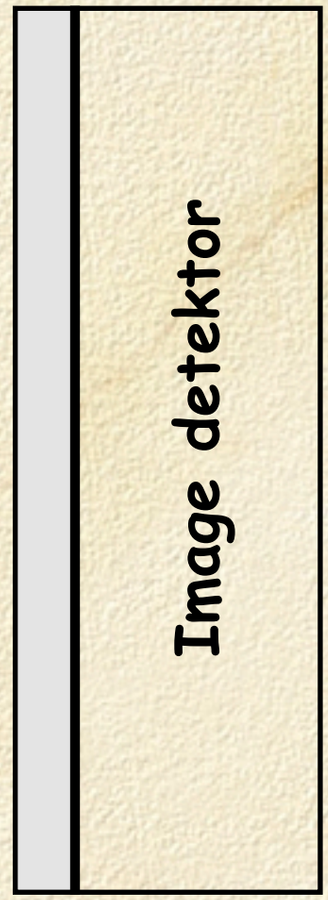

Neutron dark-field microscopy

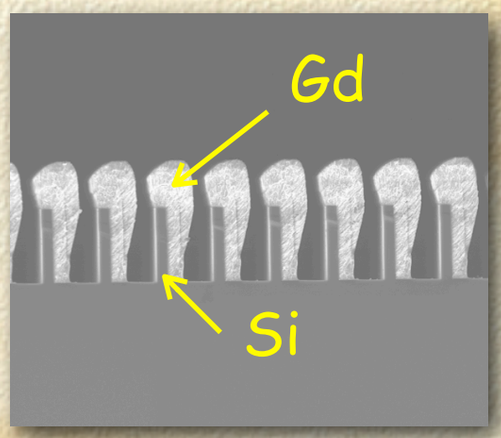

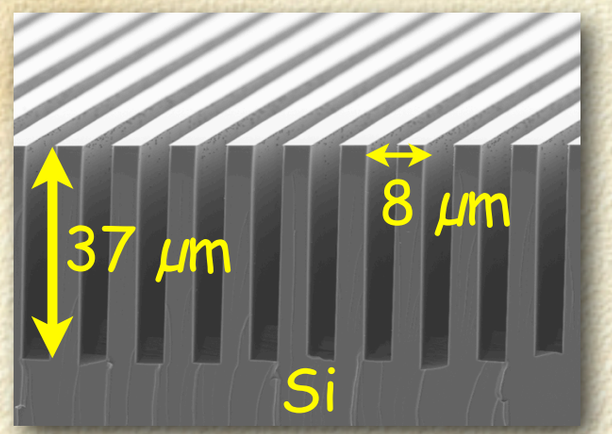

Absorption source grating

Phase grating

Neutrons

some 100 µm

Periodic, coherent neutron lines

Image detektor

Phase shift
→ periodic phase modulation
→ Talbot effect

Neutron dark-field microscopy

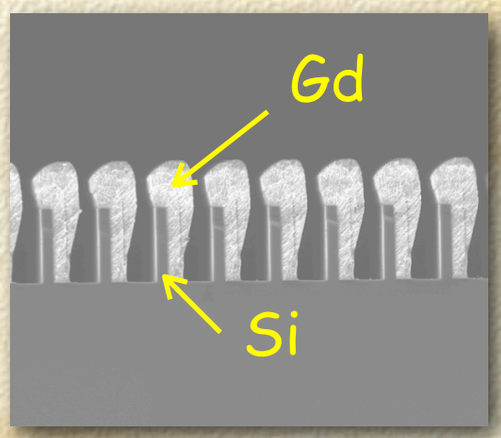

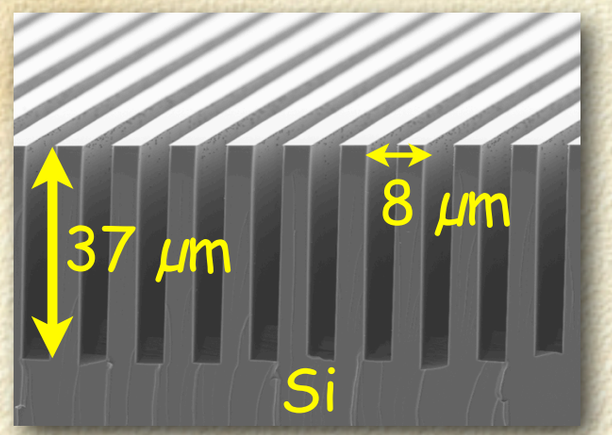

Absorption source grating

Phase grating

Neutrons

some 100 µm

Periodic, coherent neutron lines

Image detektor

Phase shift
→ periodic phase modulation
→ Talbot effect

Interference pattern (period 4 µm)

Neutron dark-field microscopy

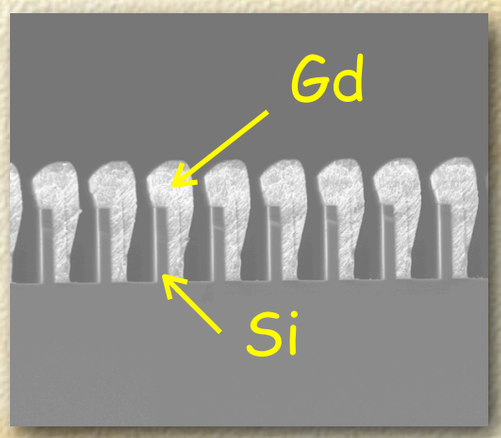

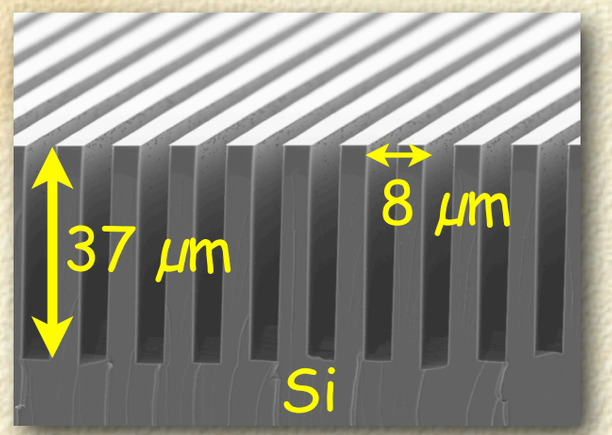

Absorption source grating

Phase grating

Absorption analyser grating

Neutrons

some 100 µm

Periodic, coherent neutron lines

Image detektor

Phase shift
→ periodic phase modulation
→ Talbot effect

Interference pattern (period 4 µm)

Neutron dark-field microscopy

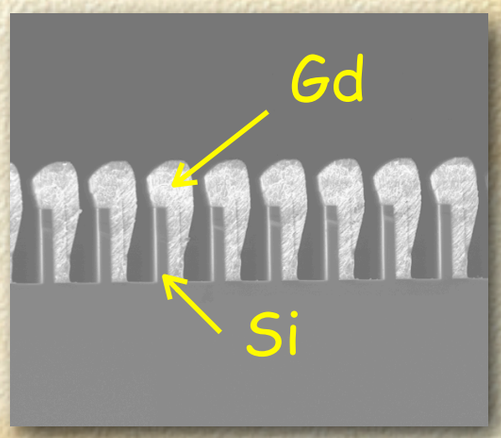

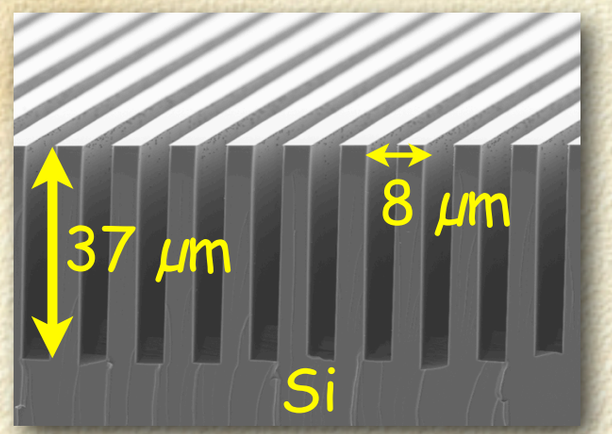

Absorption source grating

Phase grating

Absorption analyser grating

Neutrons

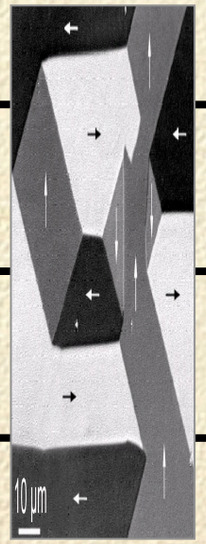

Image detektor

Phase shift
→ periodic phase modulation
→ Talbot effect

Interference pattern
(period 4 µm)

Neutron dark-field microscopy

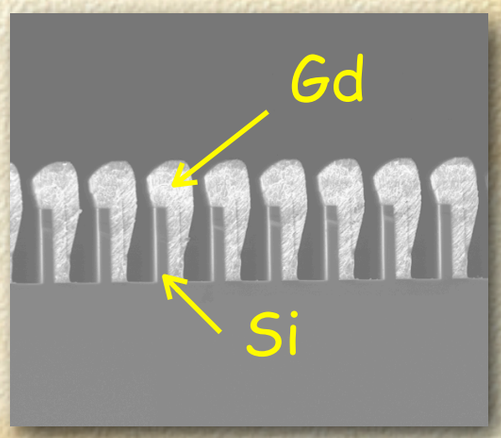

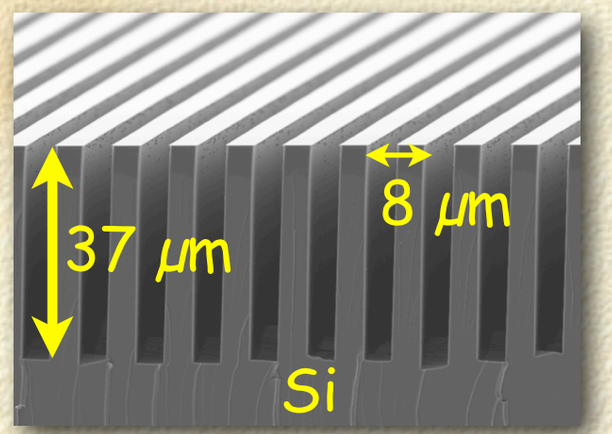

Absorption source grating

Phase grating

Absorption analyser grating

Neutrons

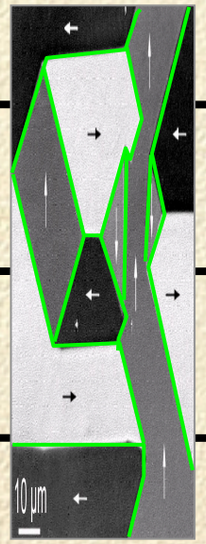

Image detektor

Phase shift
→ periodic phase modulation
→ Talbot effect

Interference pattern
(period 4 µm)

Neutron dark-field microscopy

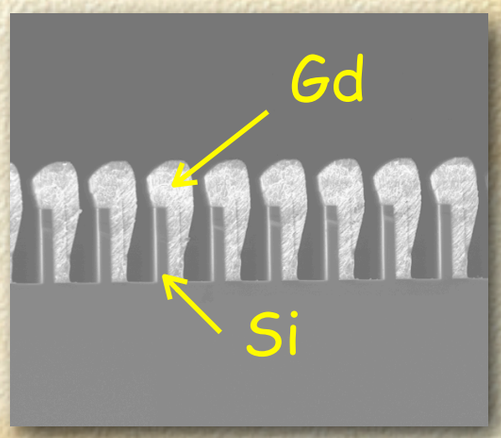

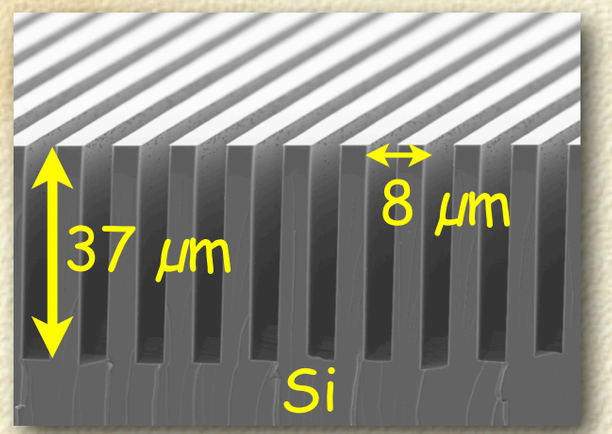

Absorption source grating

Phase grating

Absorption analyser grating

Neutrons

Image detektor

Phase shift
→ periodic phase modulation
→ Talbot effect

Interference pattern
(period 4 µm)

Neutron dark-field microscopy

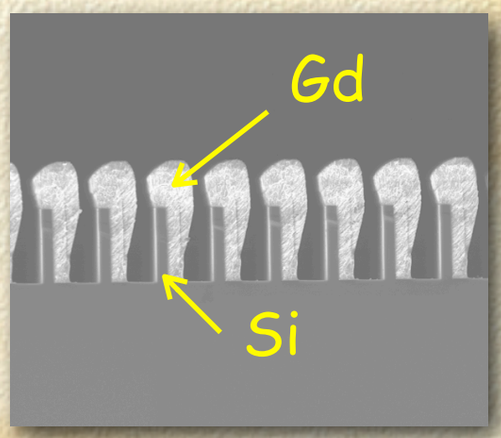

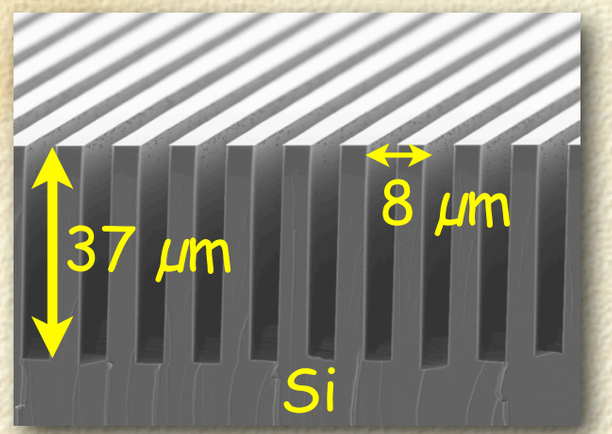

Absorption source grating

Phase grating

Absorption analyser grating

Neutrons

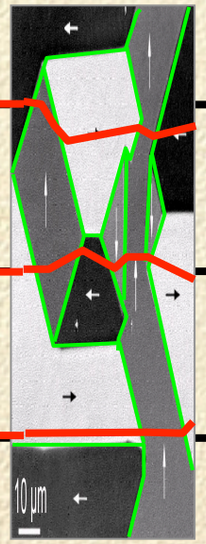

Image detektor

Phase shift
→ periodic phase modulation
→ Talbot effect

Interference pattern
(period 4 µm)

Neutron dark-field microscopy

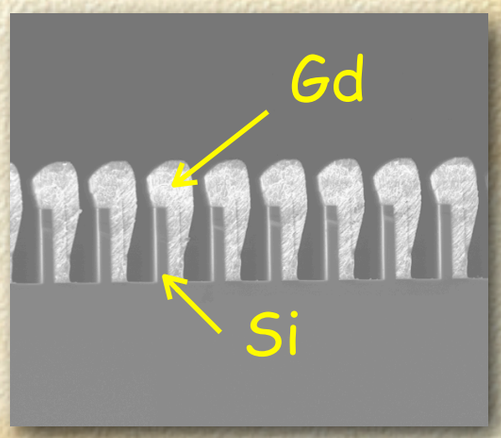

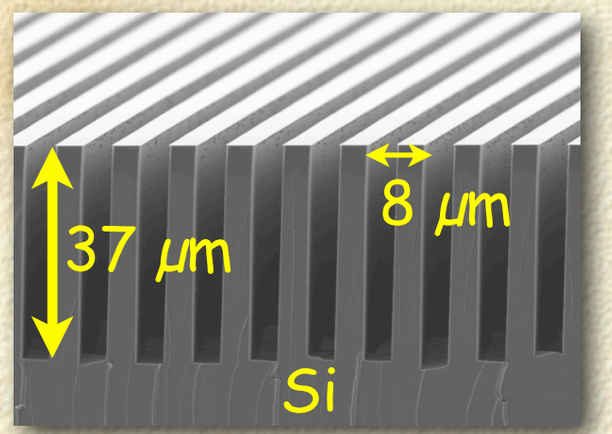

Absorption source grating

Phase grating

Absorption analyser grating

Neutrons

Image detektor

Phase shift
→ periodic phase modulation
→ Talbot effect

Interference pattern
(period 4 µm)

Neutron dark-field microscopy

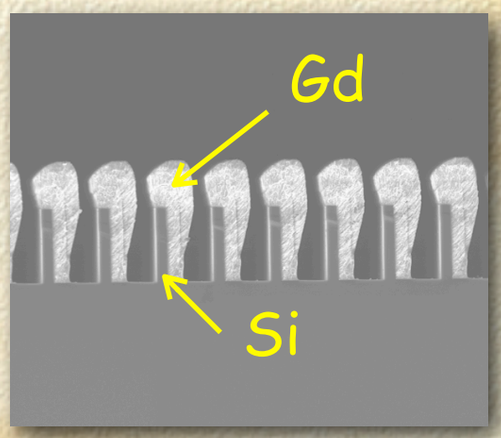

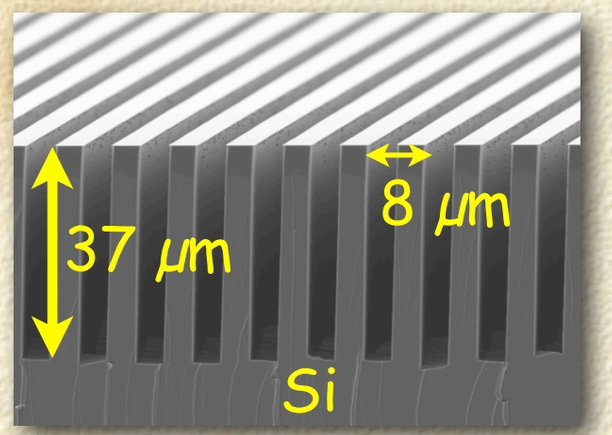

Absorption source grating

Phase grating

Absorption analyser grating

Neutrons

Image detektor

Phase shift
→ periodic phase modulation
→ Talbot effect

Neutron dark-field microscopy

Principle:

Unpolarized neutrons, refracted at domain walls, locally destroy the interference pattern

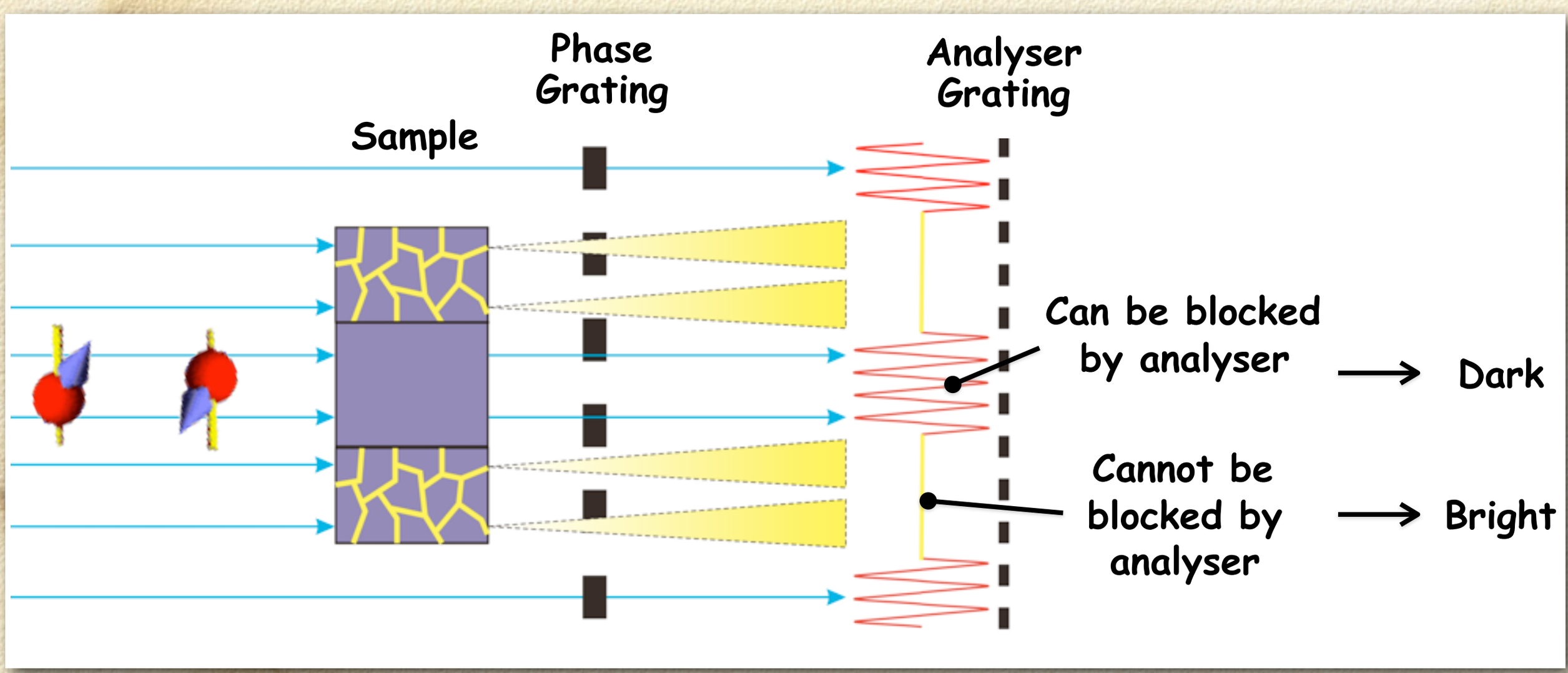

→ Bright contrast is caused by refraction

→ Dark field imaging

Neutron dark-field microscopy

Resolution:

Determined by pixel size of detector and scattering angle

↓

~100 μm

Unpolari… …in walls,
loc… …ern

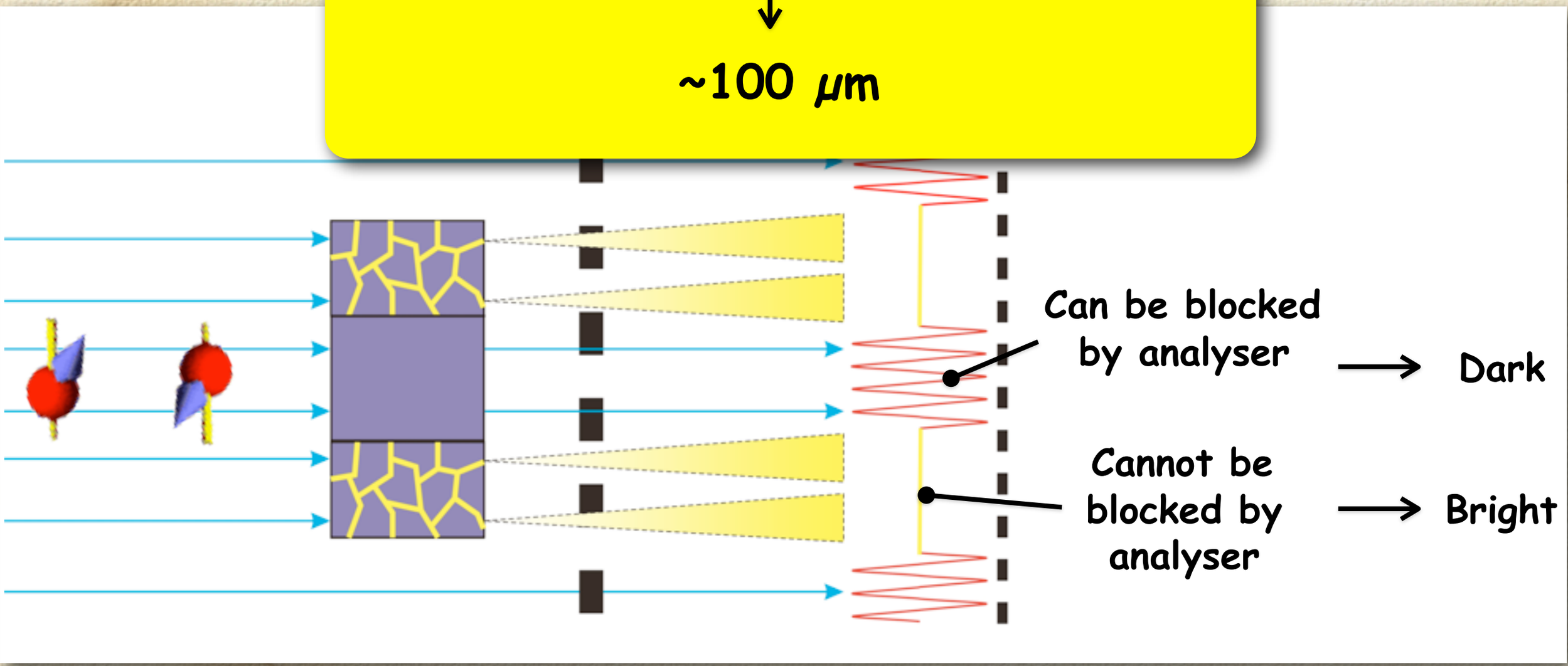

→ Bright contrast is caused by refraction

→ Dark field imaging

Neutron dark-field microscopy

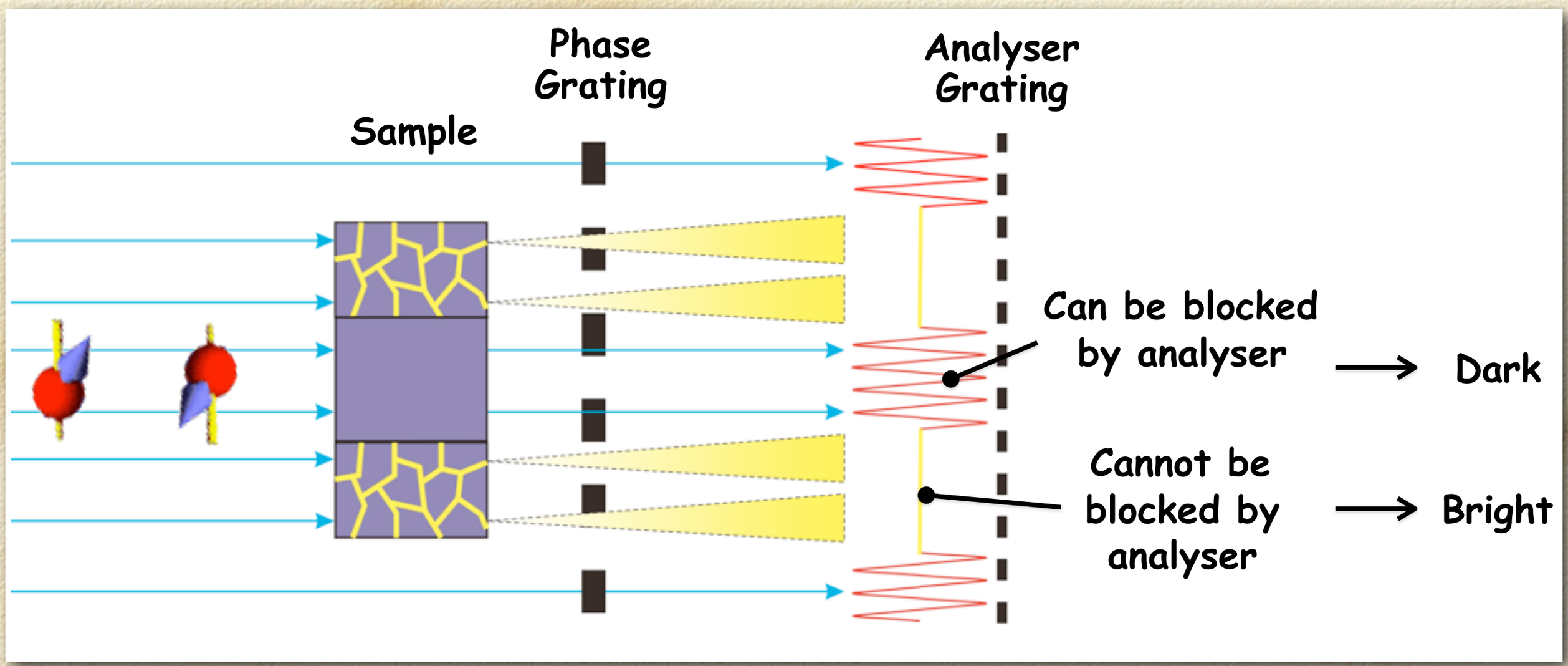

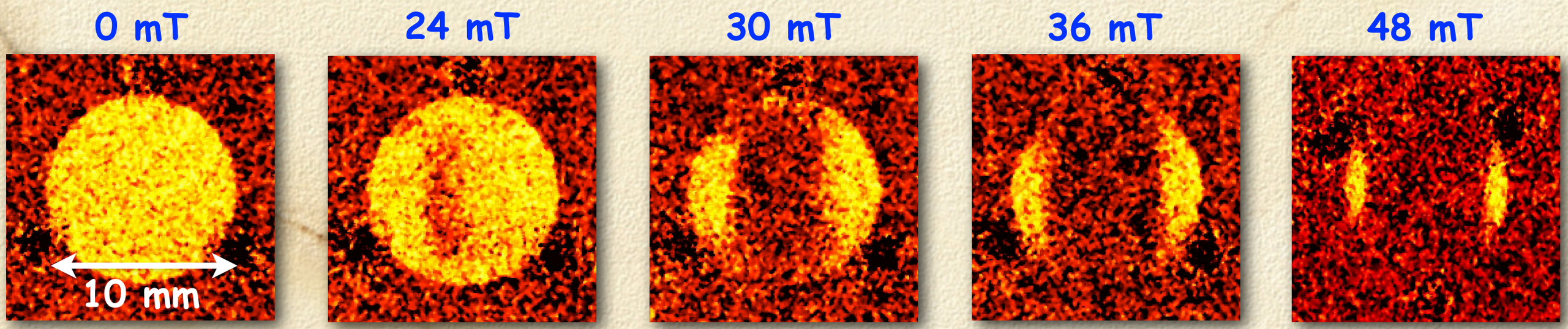

Phase Theory and M(H) curve

Infinite or closed sample

$N = 0 \rightarrow H_{in} = H_{ext}$

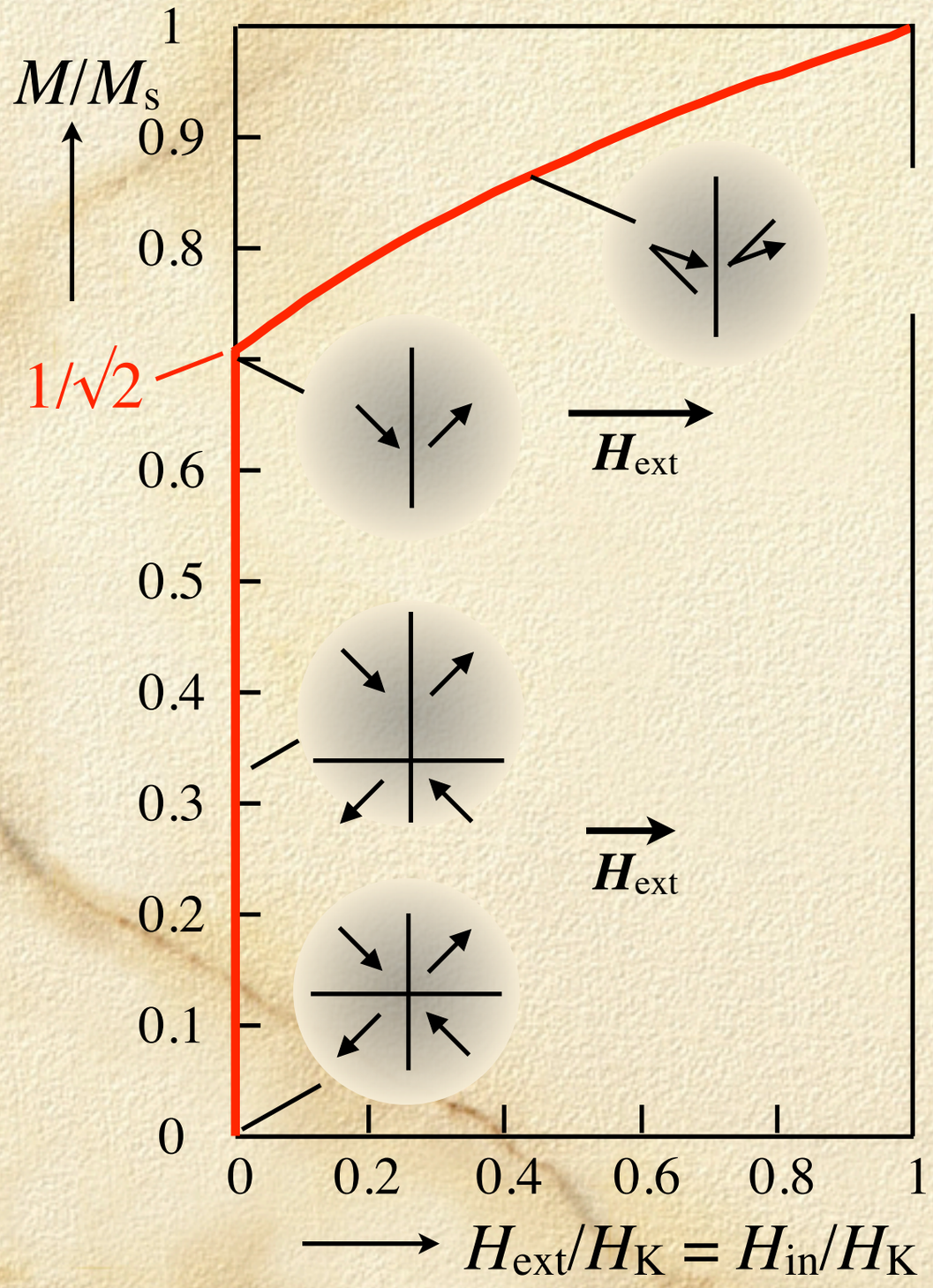

Finite sample

$N \neq 0 \rightarrow H_{ext} = H_{in} + N \cdot \overline{M} \rightarrow$ shearing

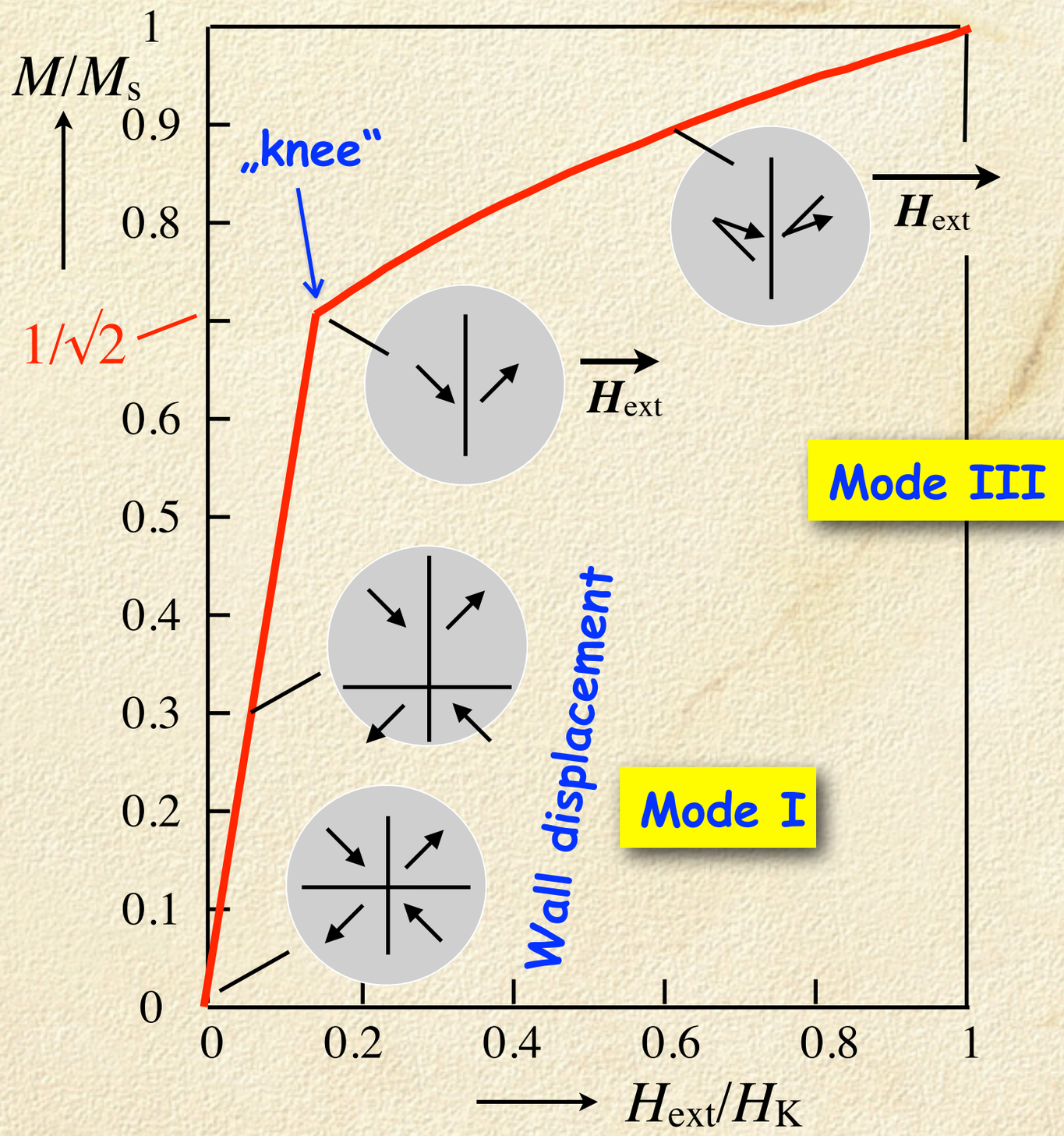

Phase Theory and M(H) curve

Infinite or closed sample

$N = 0 \rightarrow H_{in} = H_{ext}$

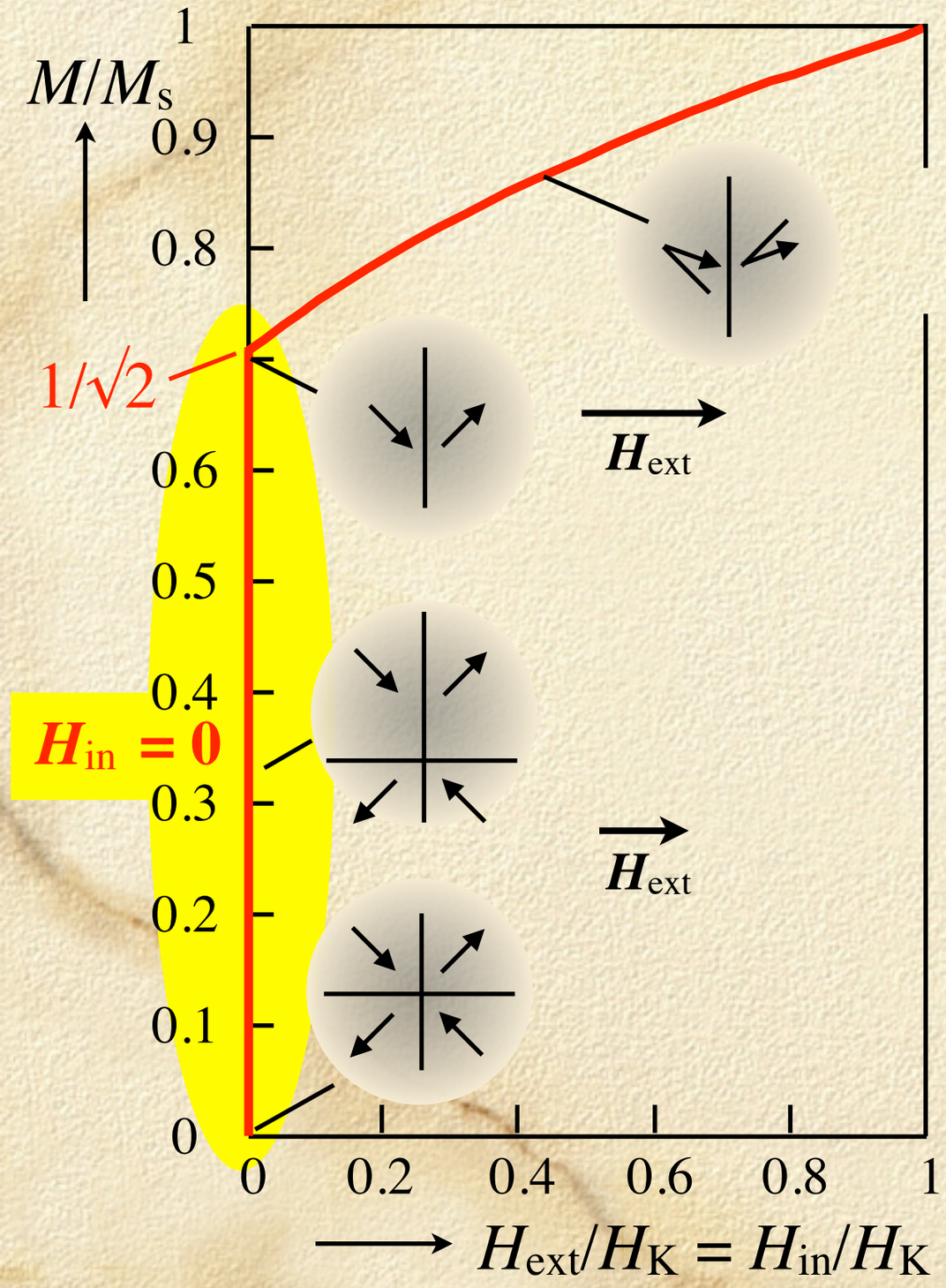

Finite sample

$N \neq 0 \rightarrow H_{ext} = H_{in} + N \cdot \overline{M} \rightarrow$ shearing

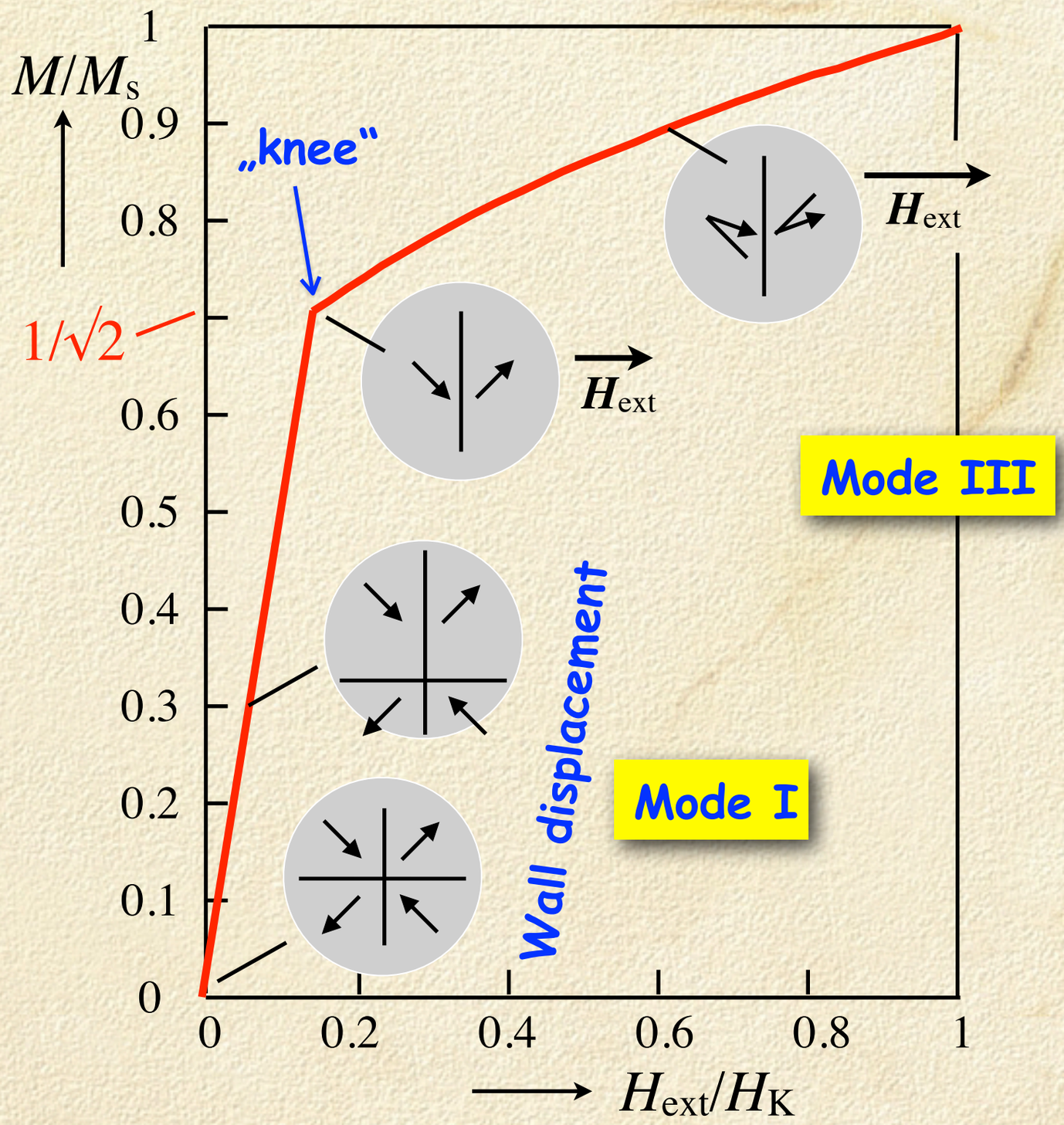

Phase Theory and M(H) curve

Infinite or closed sample

$N = 0 \rightarrow H_{in} = H_{ext}$

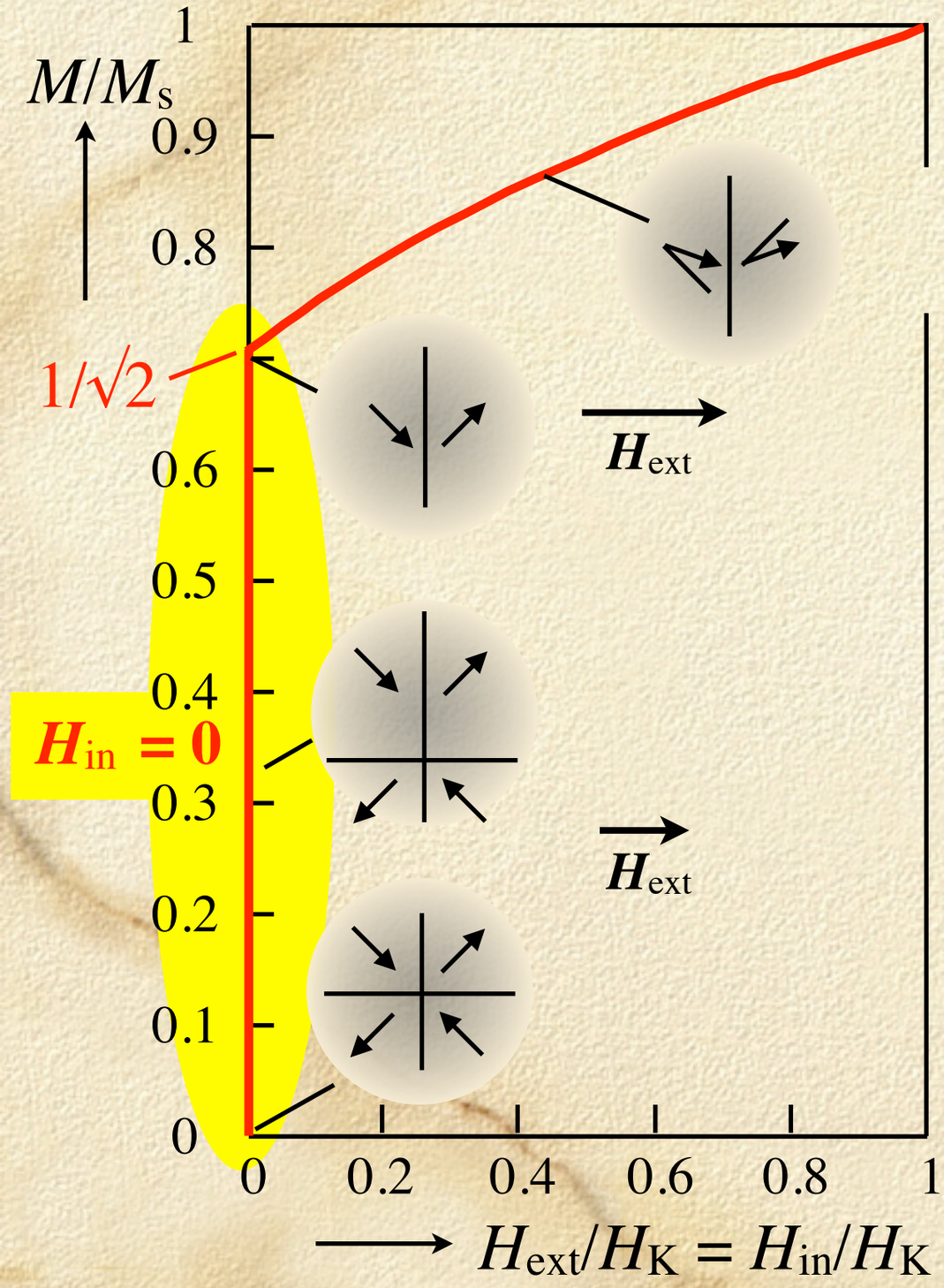

Finite sample

$N \neq 0 \rightarrow H_{ext} = H_{in} + N \cdot \overline{M} \rightarrow$ shearing

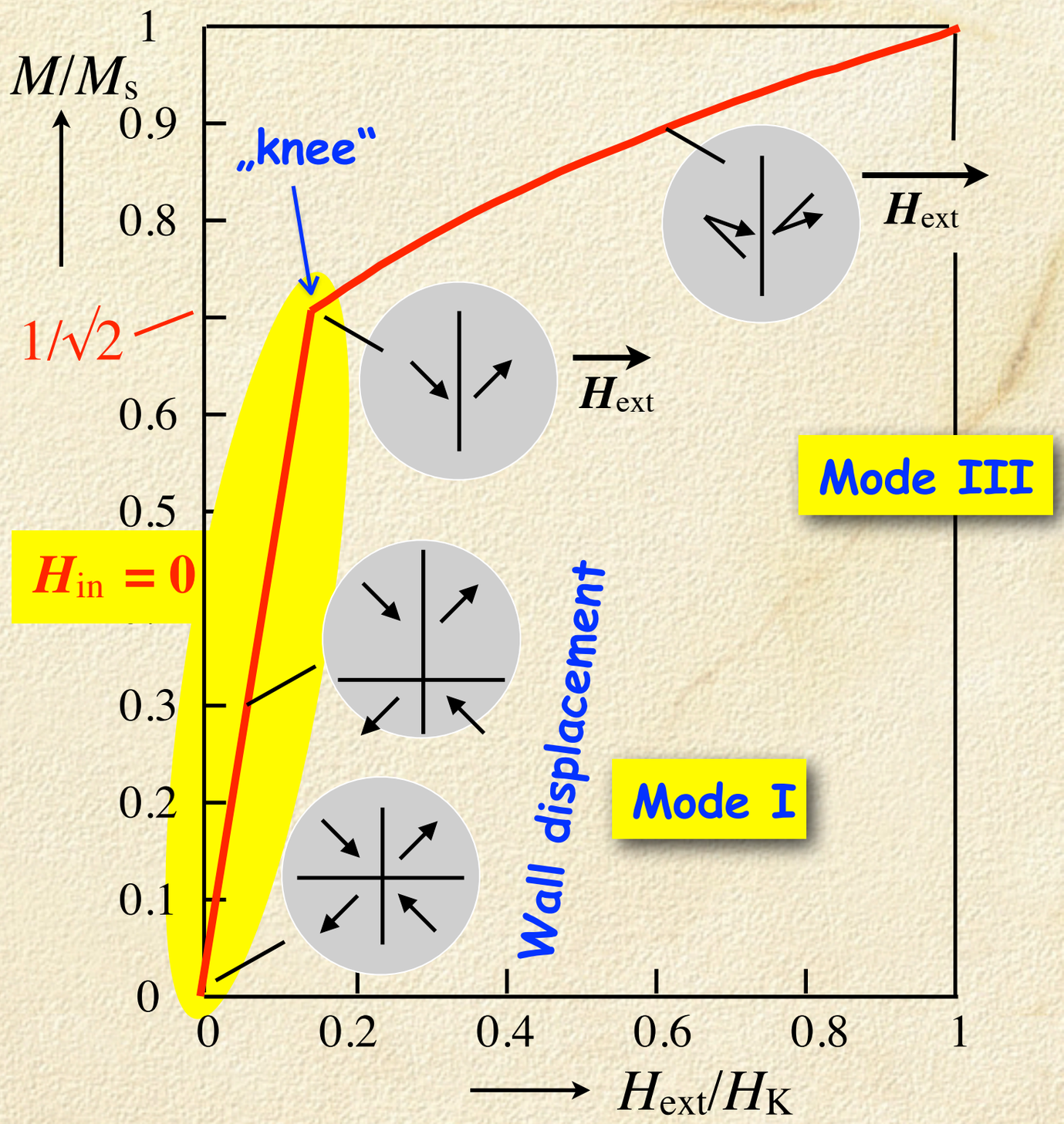

Neutron dark-field microscopy

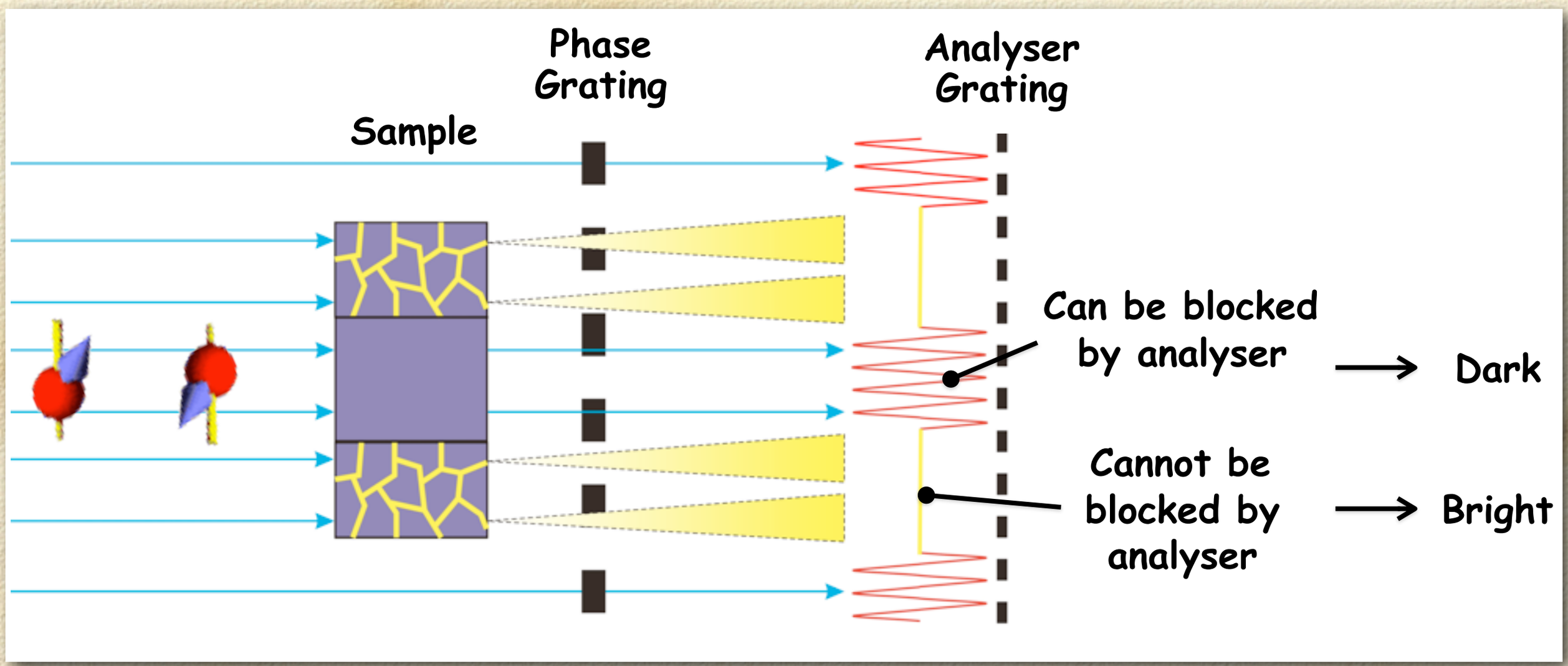

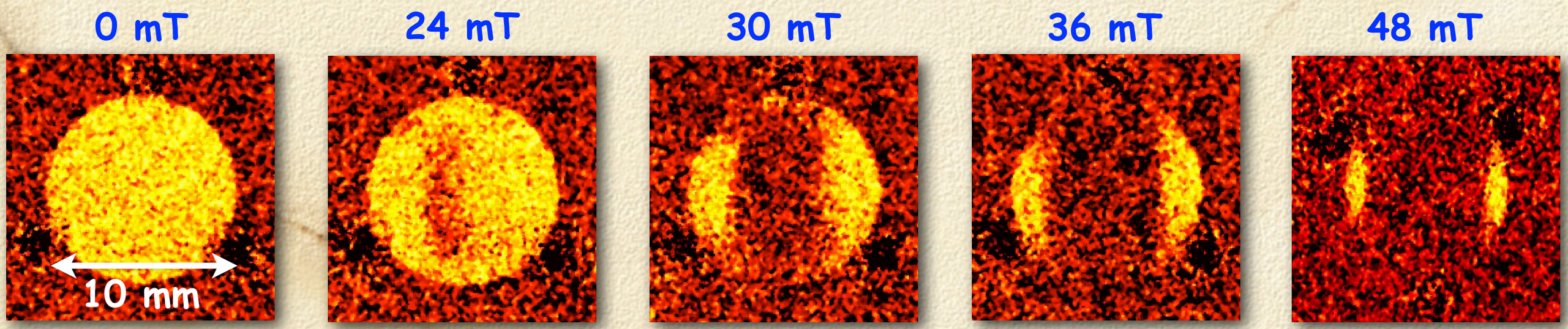

Neutron dark-field microscopy

Courtesy C. Grünzweig, PSI

Kerr image

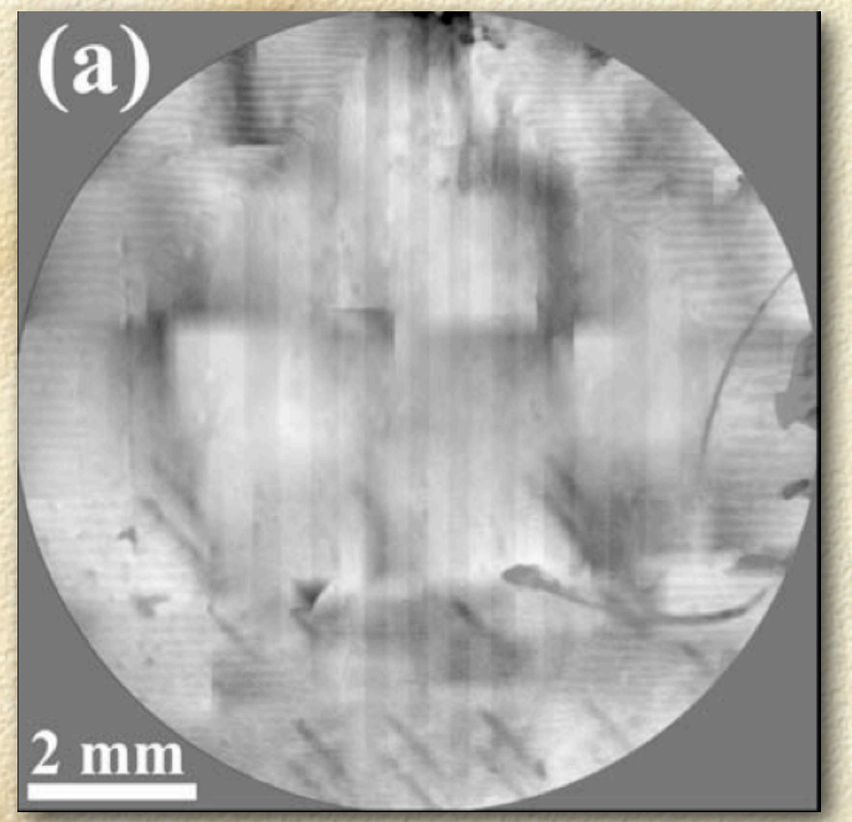

FeSi disk with (110) surface

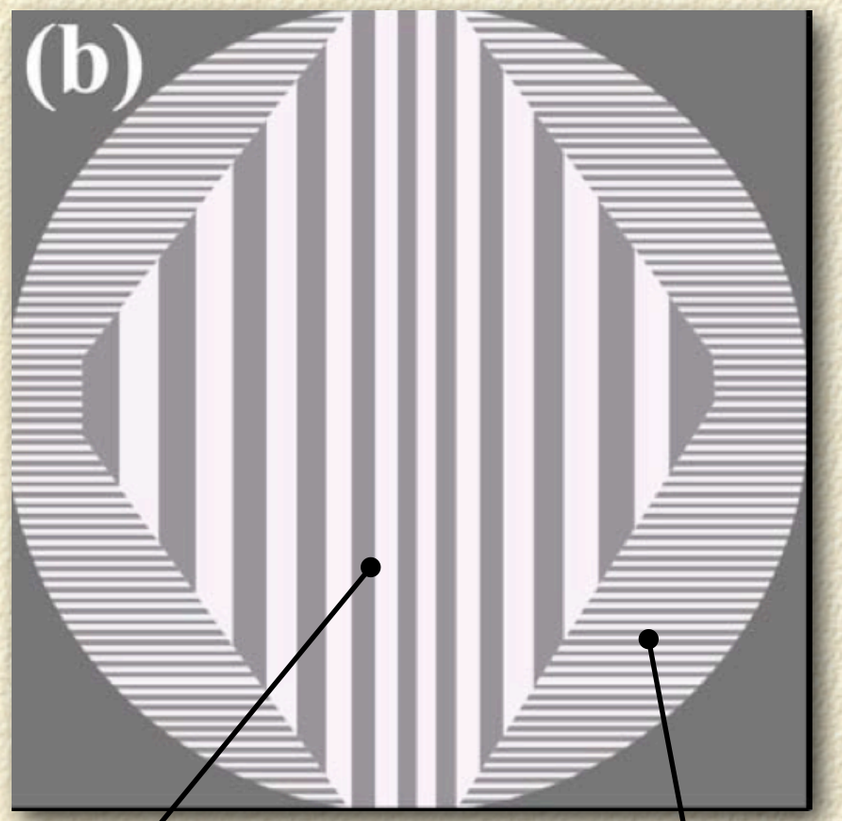

Neutron image

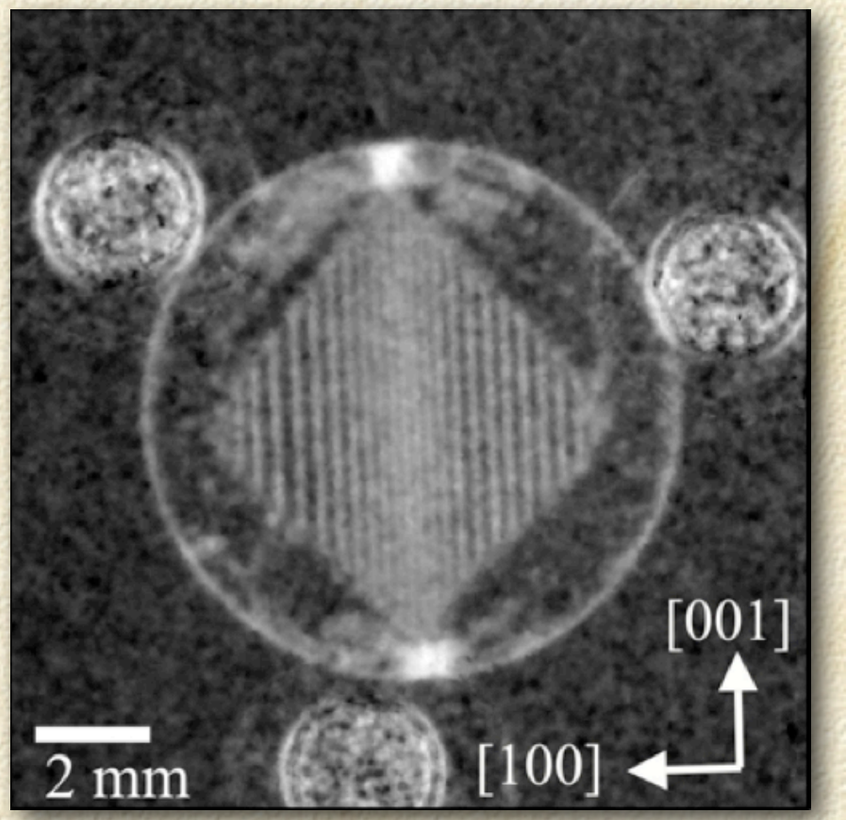

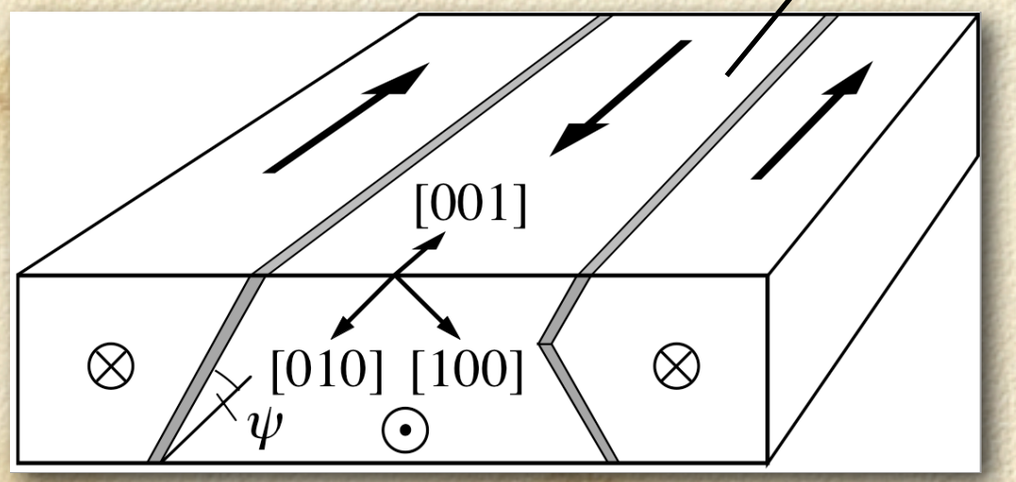

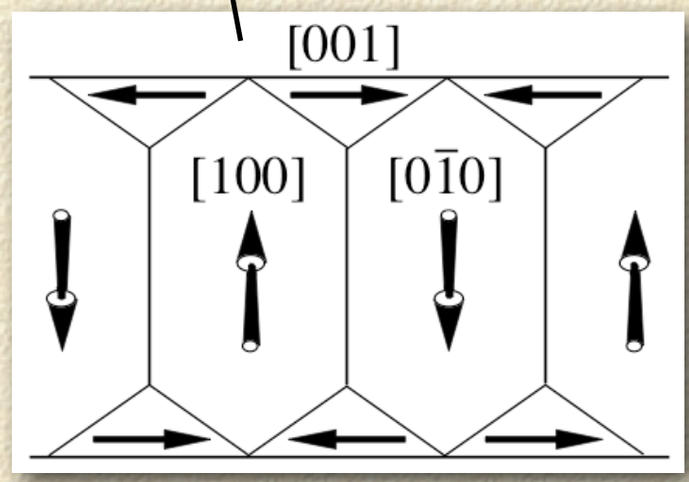

Neutron dark-field microscopy

Courtesy C. Grünzweig, PSI

Kerr image

Goss sheet, laser-scribed

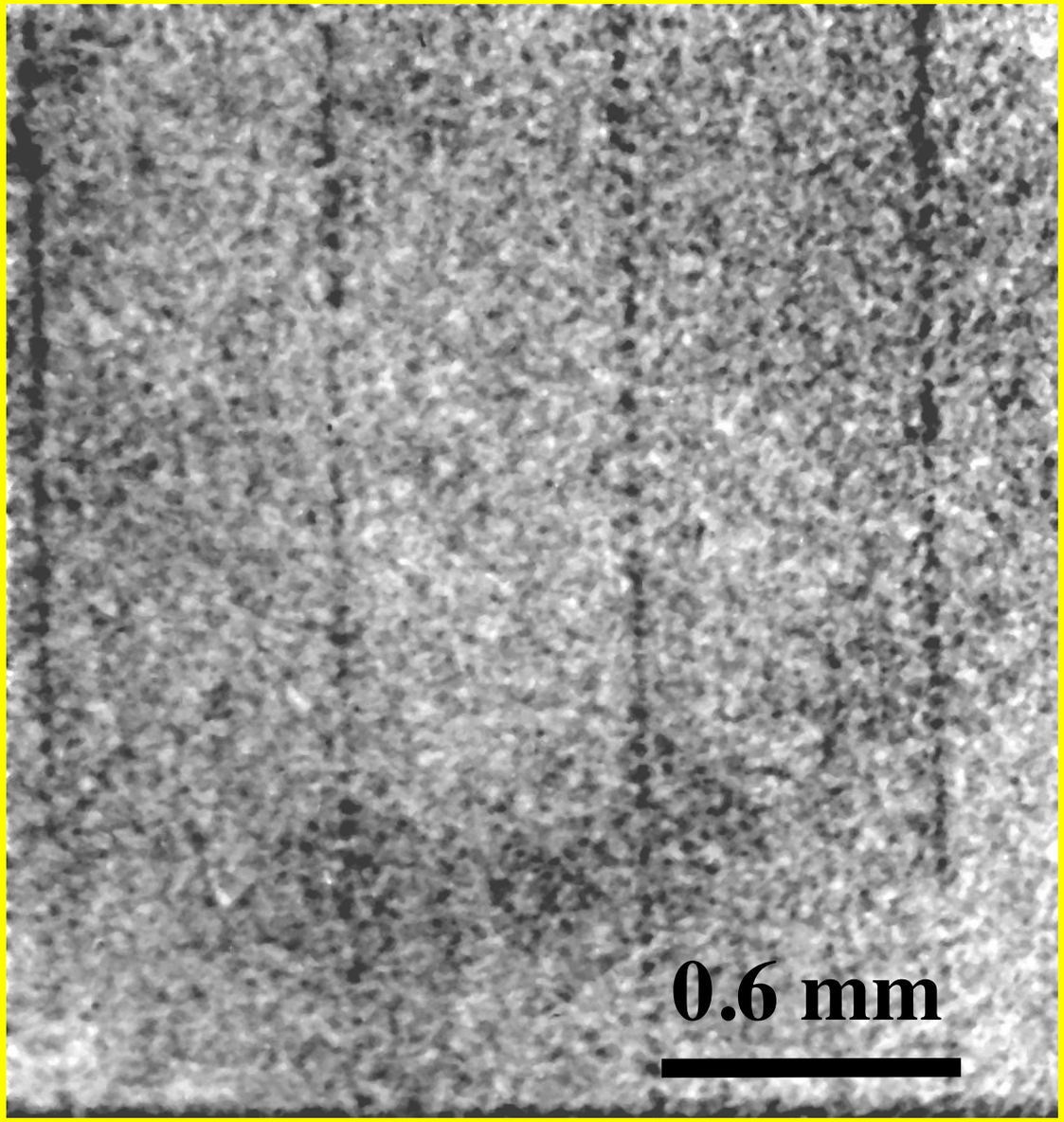

eutron image

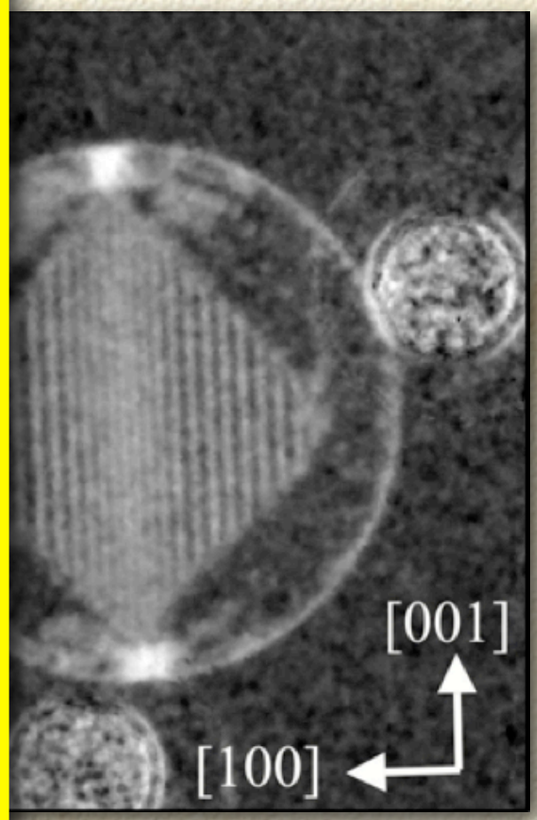

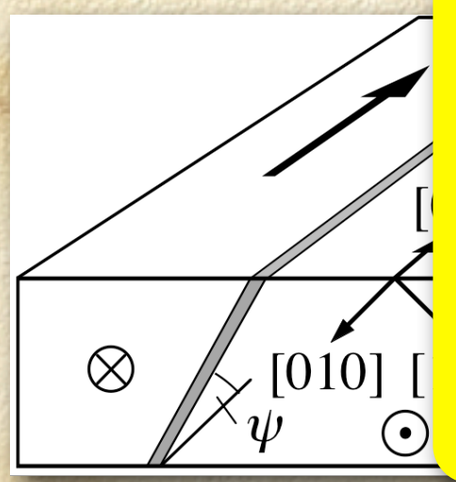

Neutron dark-field tomography

I. Manke et al.

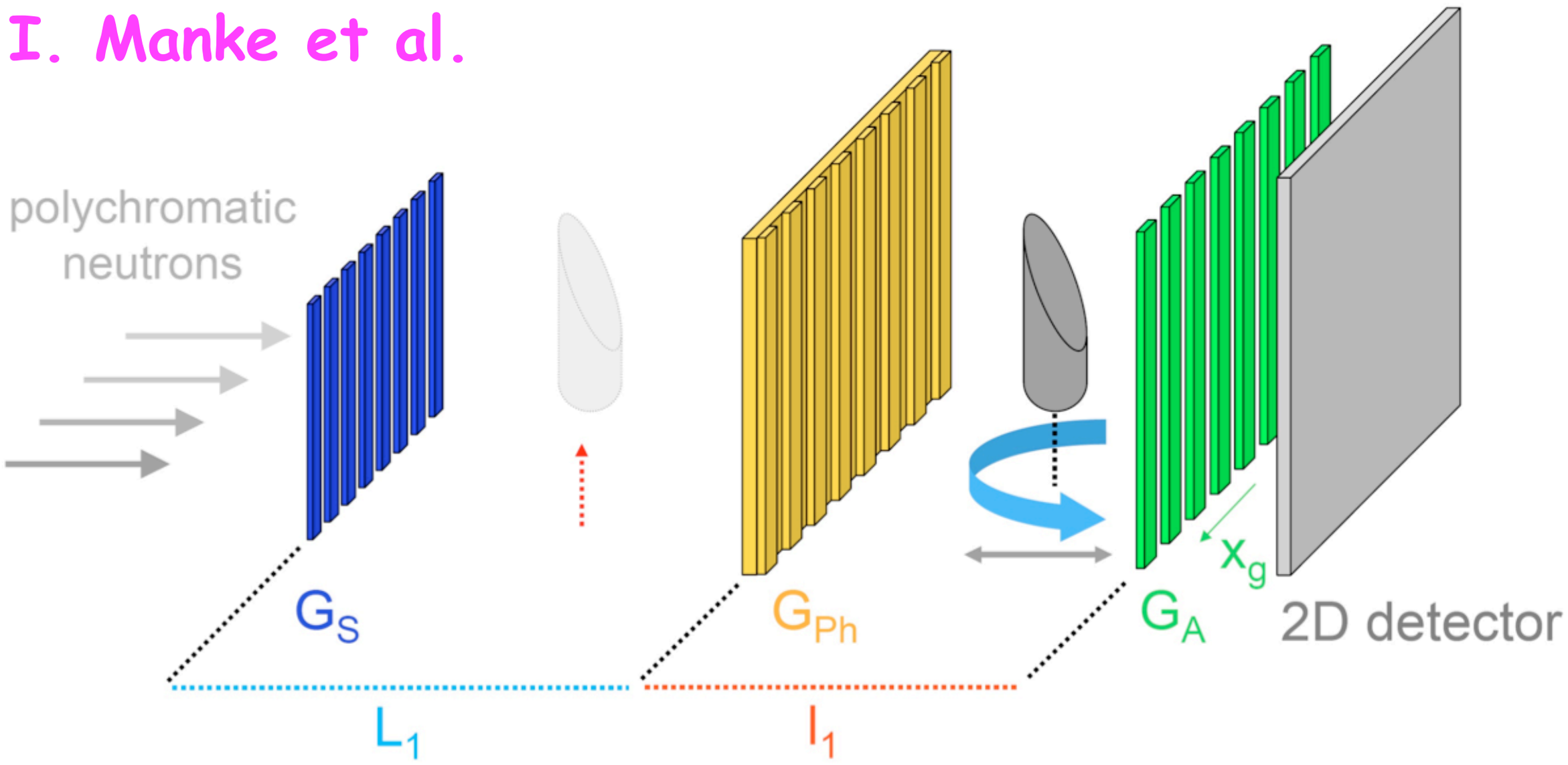

Sample closer to detector: effective opening angle of diffracted beam is smaller at the detector ⟶ higher resolution (<35 nm)

Sample rotated stepwise by 360°,
recording of projection images at each angle ⟶ tomographic image

Neutron dark-field tomography

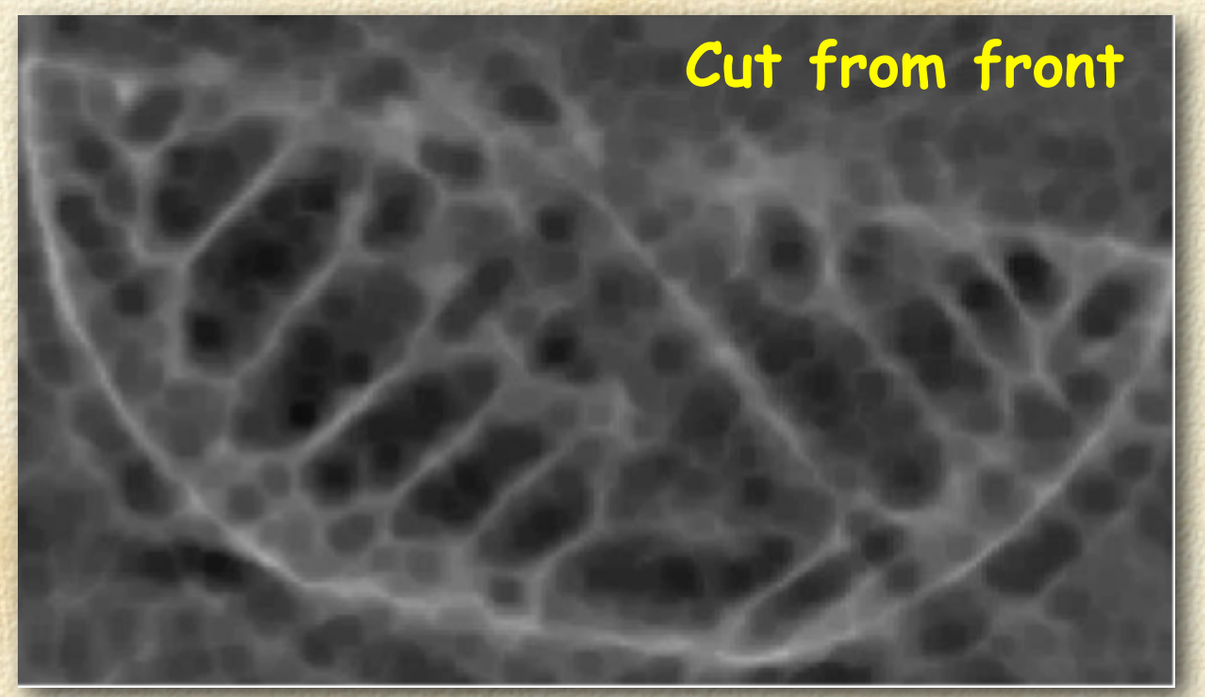

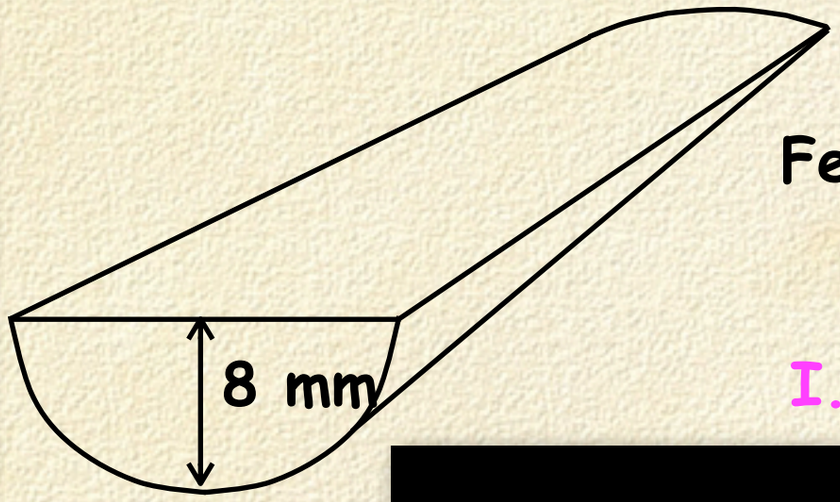

FeSi crystal

I. Manke, HMI

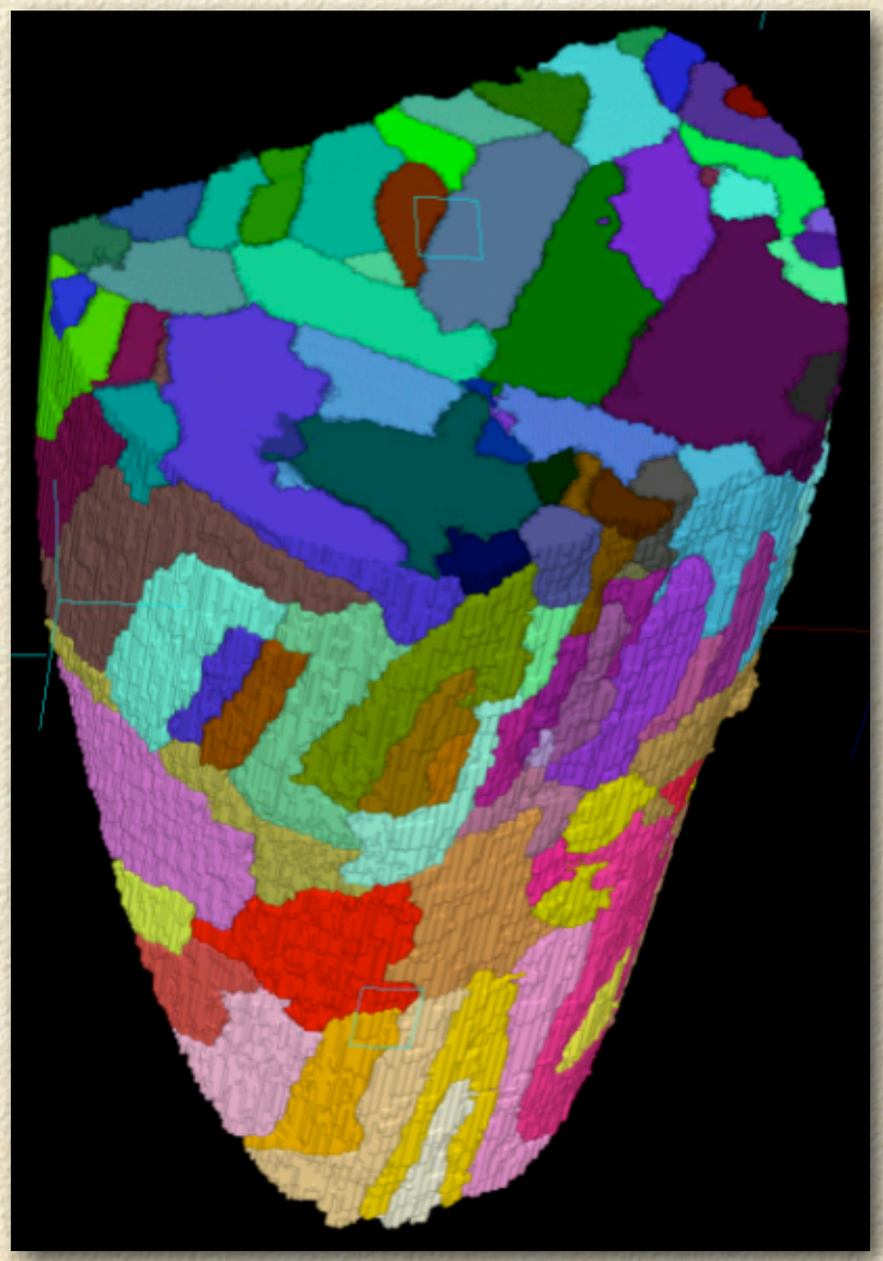

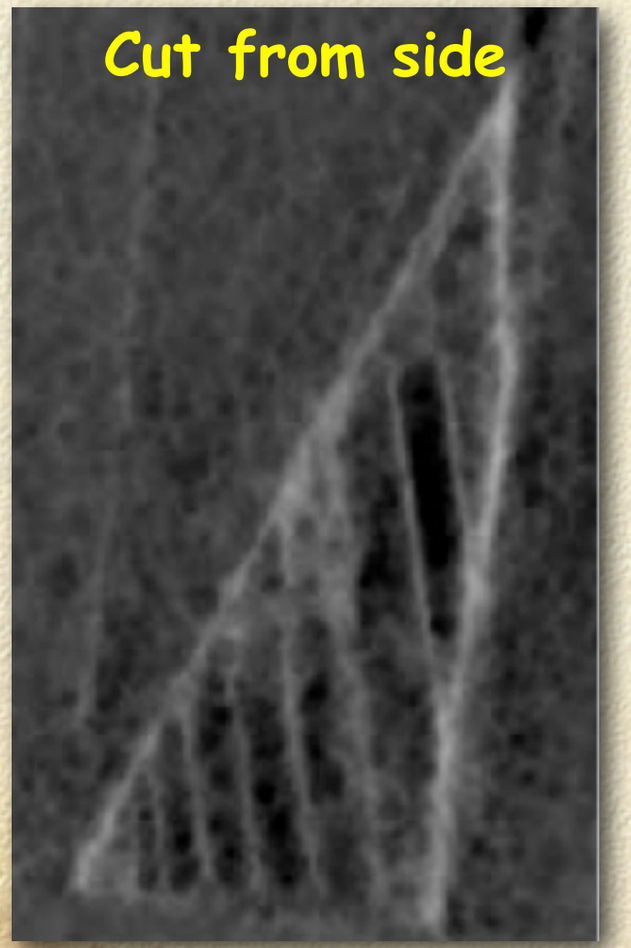

Volume domain observation in FeSi (111) sheet

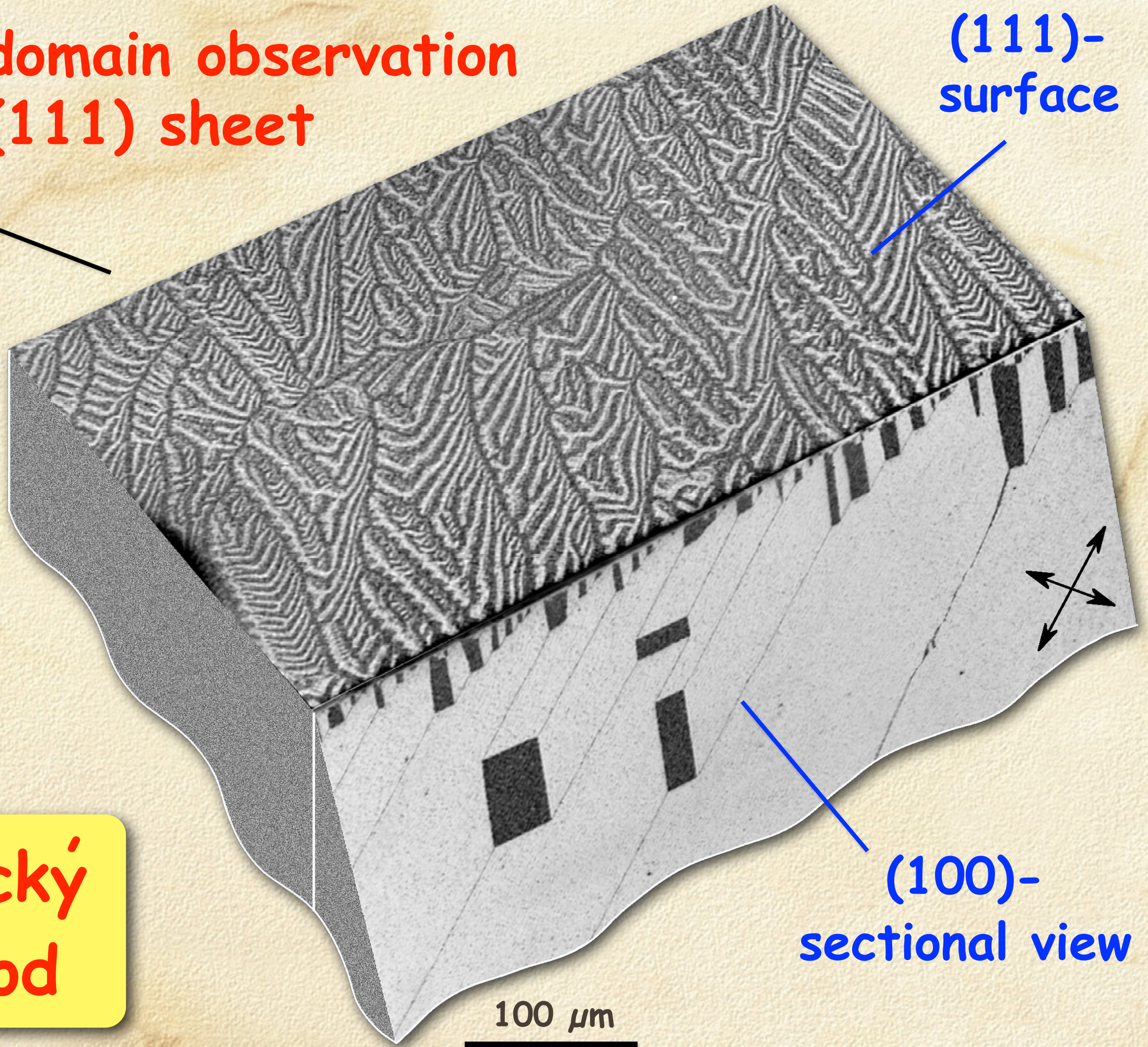

Libovický method

Bulk domain observation by Libovický-method

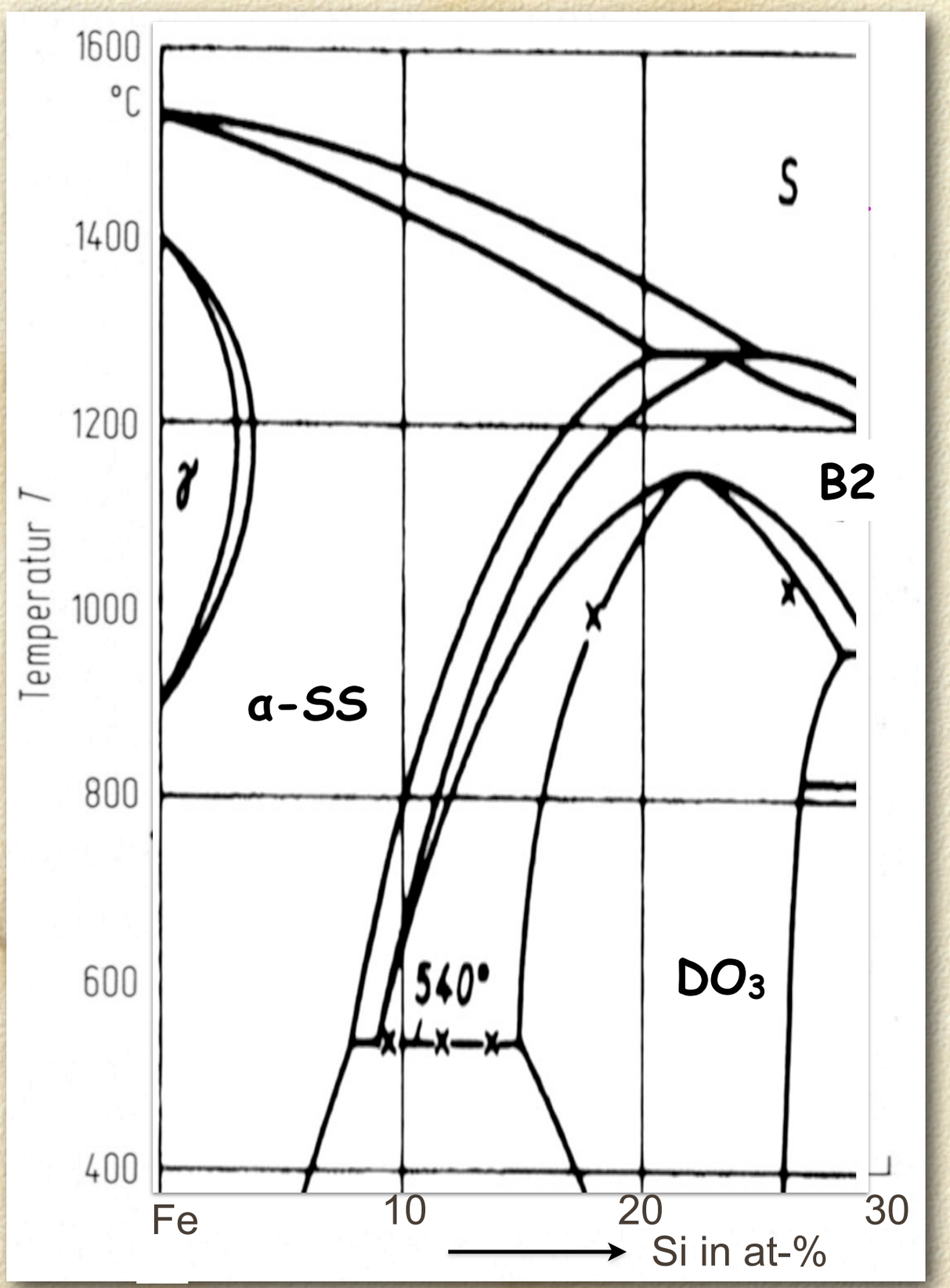

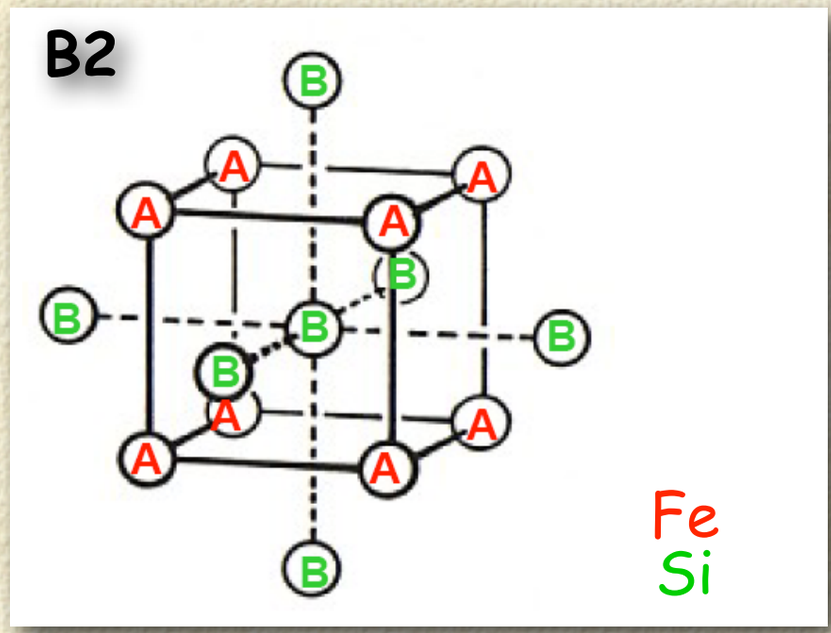

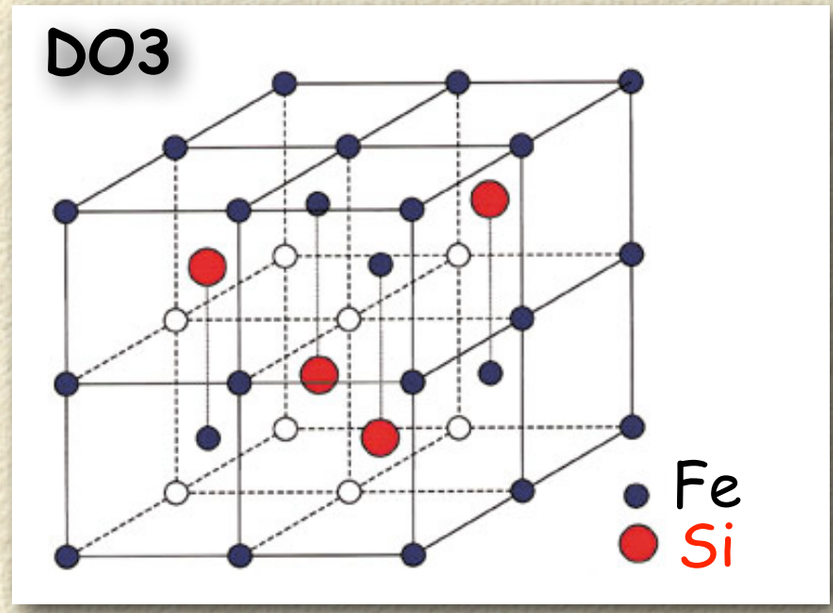

H. Warlimont:
Elektronenmikroskopische Untersuchung der α-Fe-Si-Phasen.
Z. Metallkunde 59, 598 (1968)

Bulk domain observation by Libovický-method

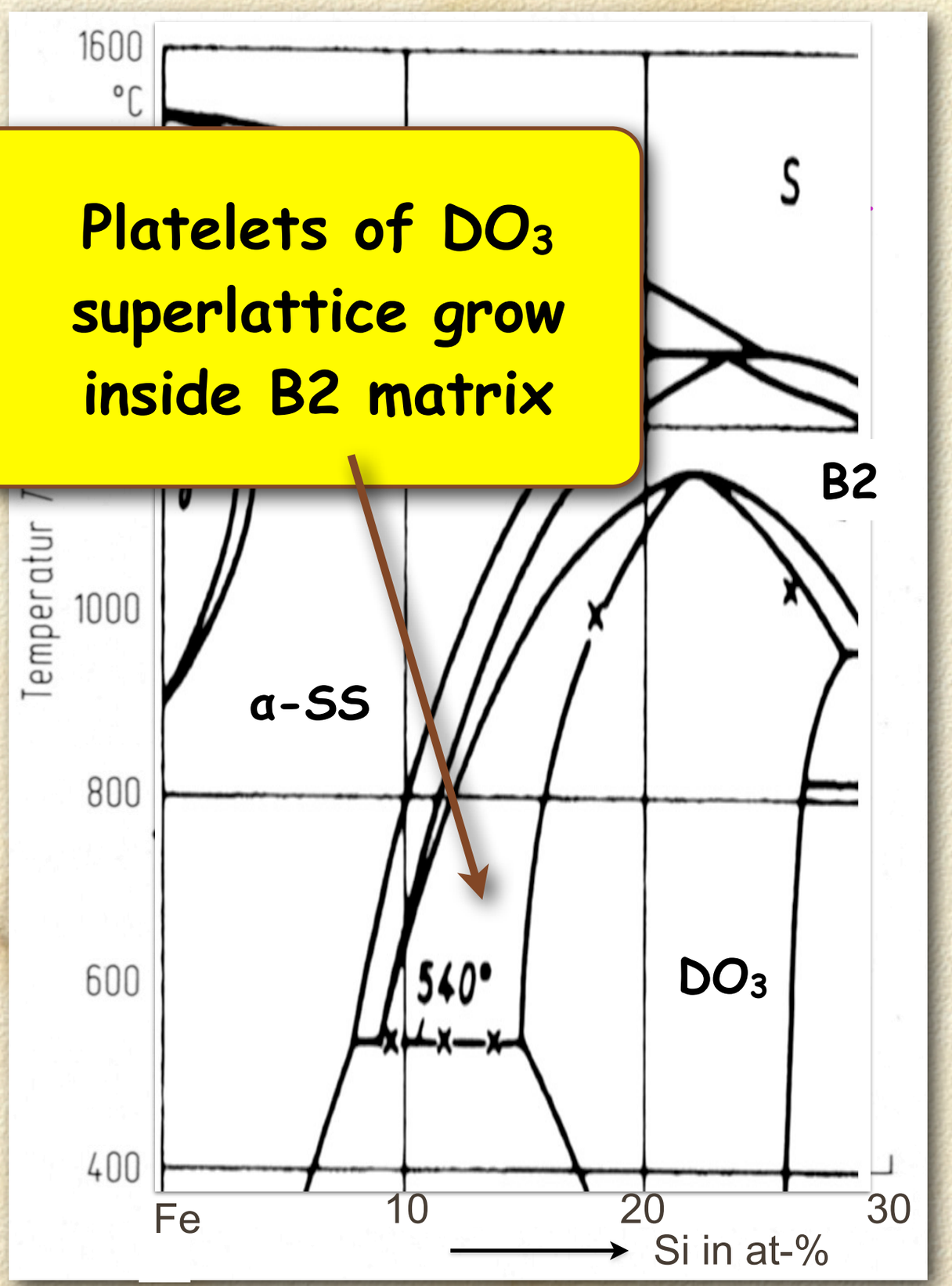

Platelets of DO_3 superlattice grow inside B2 matrix

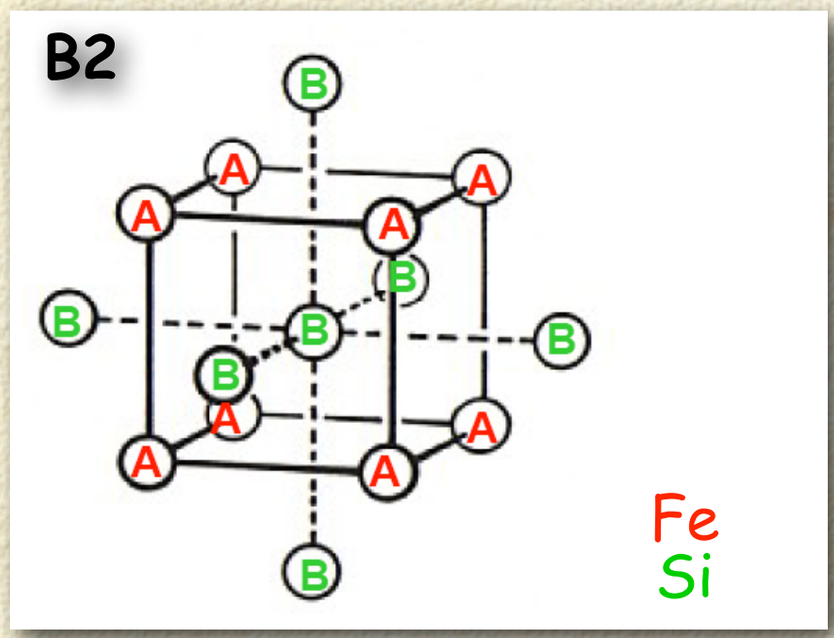

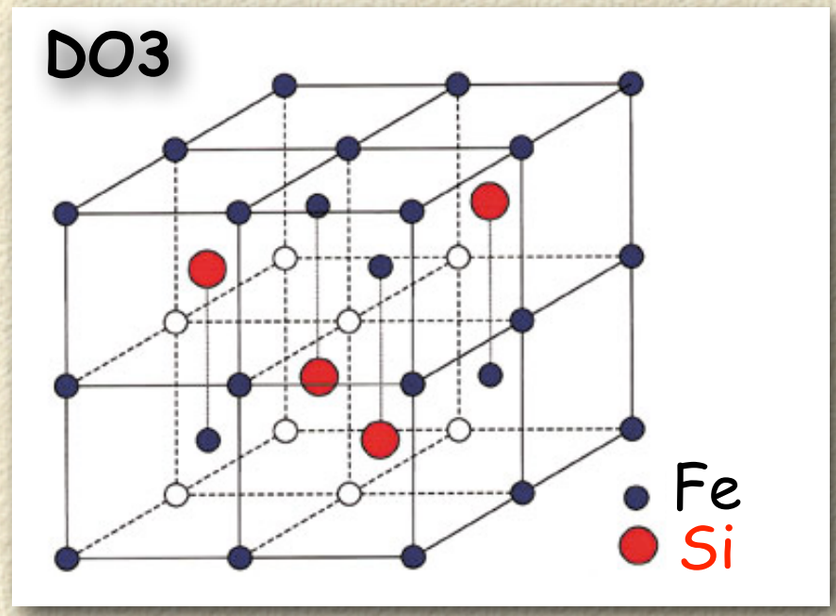

H. Warlimont:
Elektronenmikroskopische Untersuchung der a-Fe-Si-Phasen.
Z. Metallkunde 59, 598 (1968)

Bulk domain observation by Libovický-method

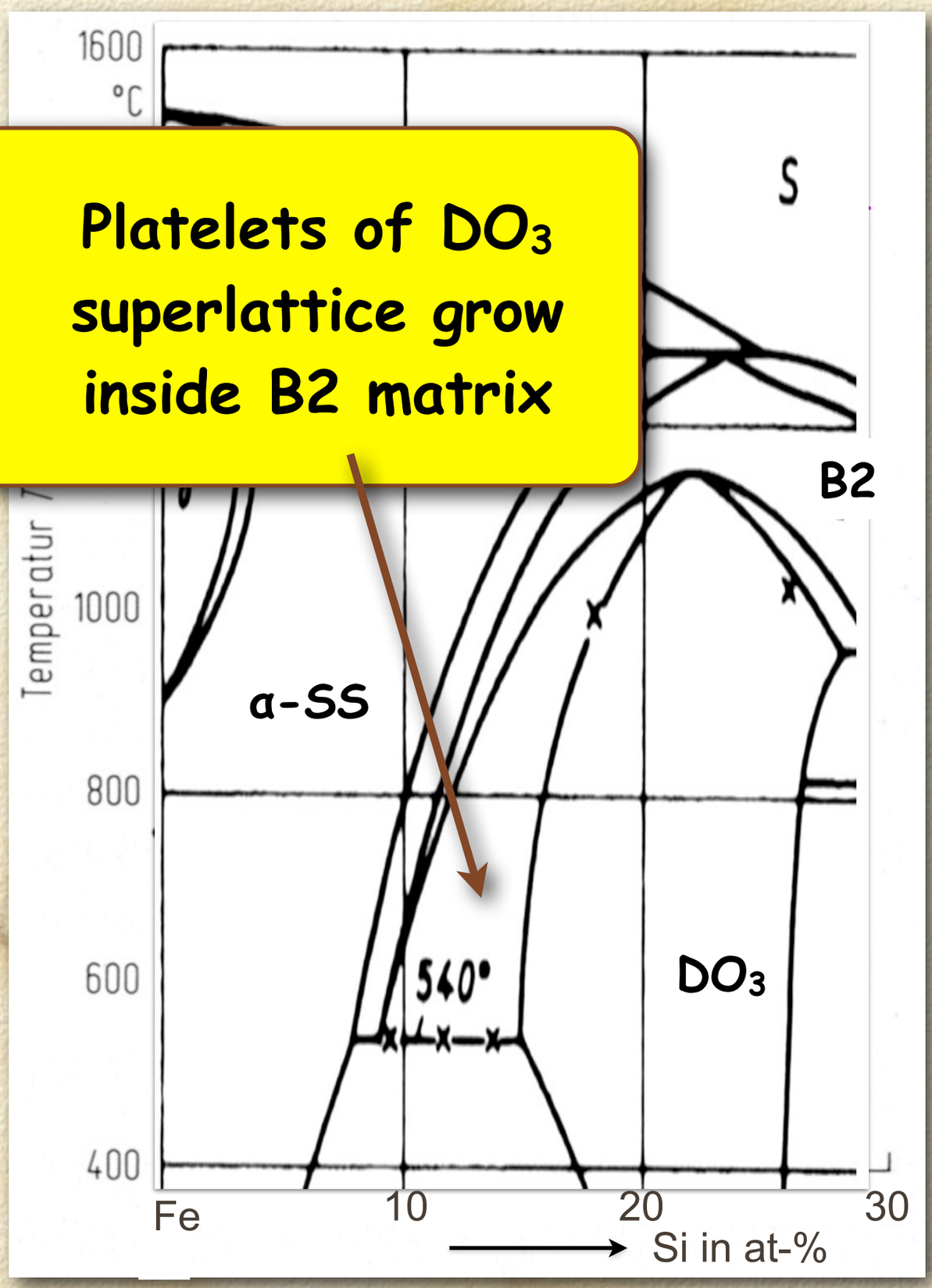

Platelets of DO_3 superlattice grow inside B2 matrix

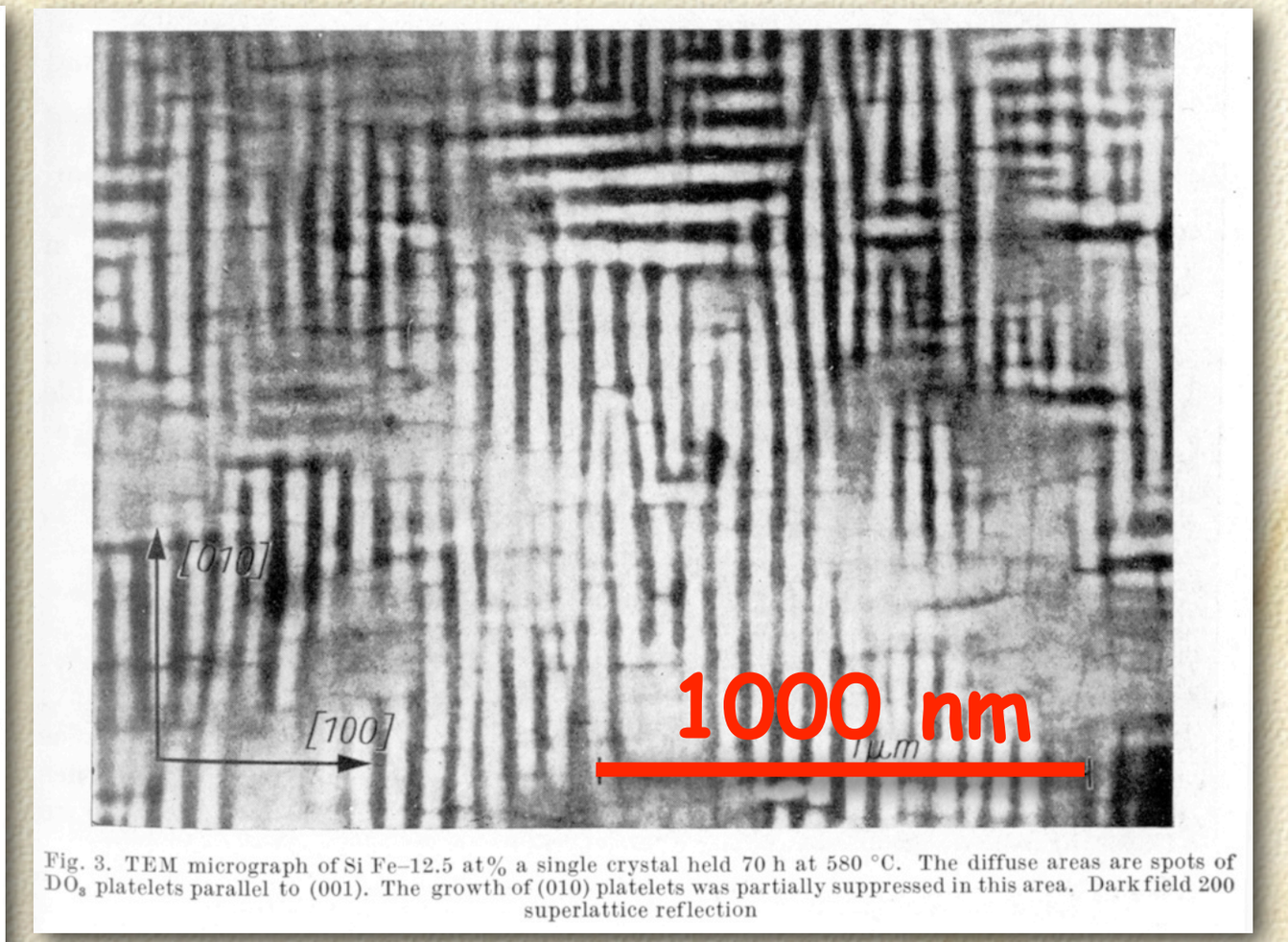

Fig. 3. TEM micrograph of Si Fe–12.5 at% a single crystal held 70 h at 580 °C. The diffuse areas are spots of DO_3 platelets parallel to (001). The growth of (010) platelets was partially suppressed in this area. Dark field 200 superlattice reflection

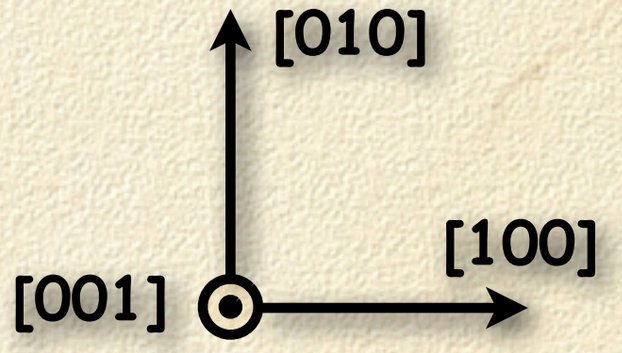

from: S. Libovicky: Spatial replica of ferromagnetic domains in iron-silicon alloys. Phys. Status Solidi A 12 (1972) 539

Bulk domain observation by Libovický-method

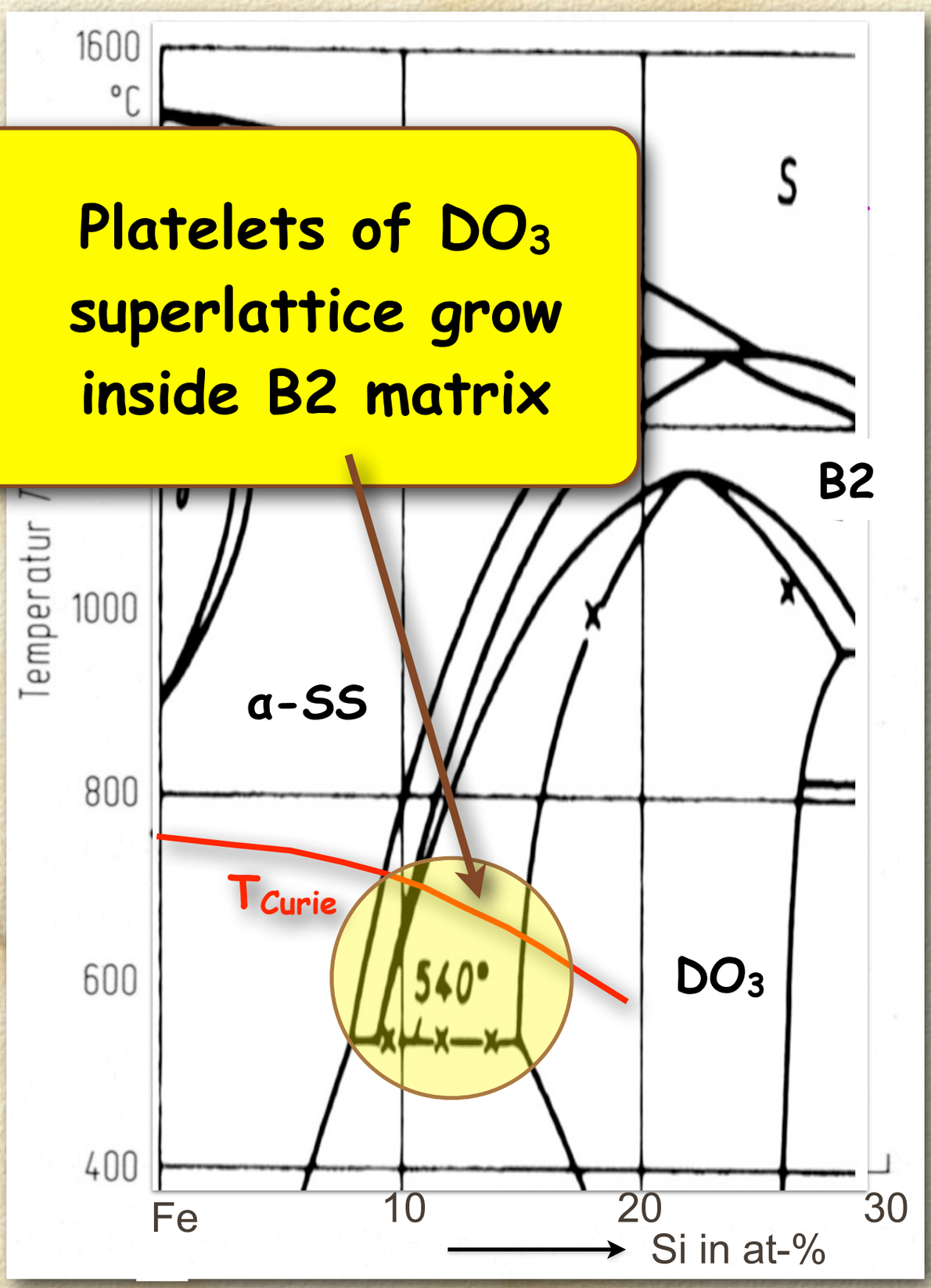

Platelets of DO_3 superlattice grow inside B2 matrix

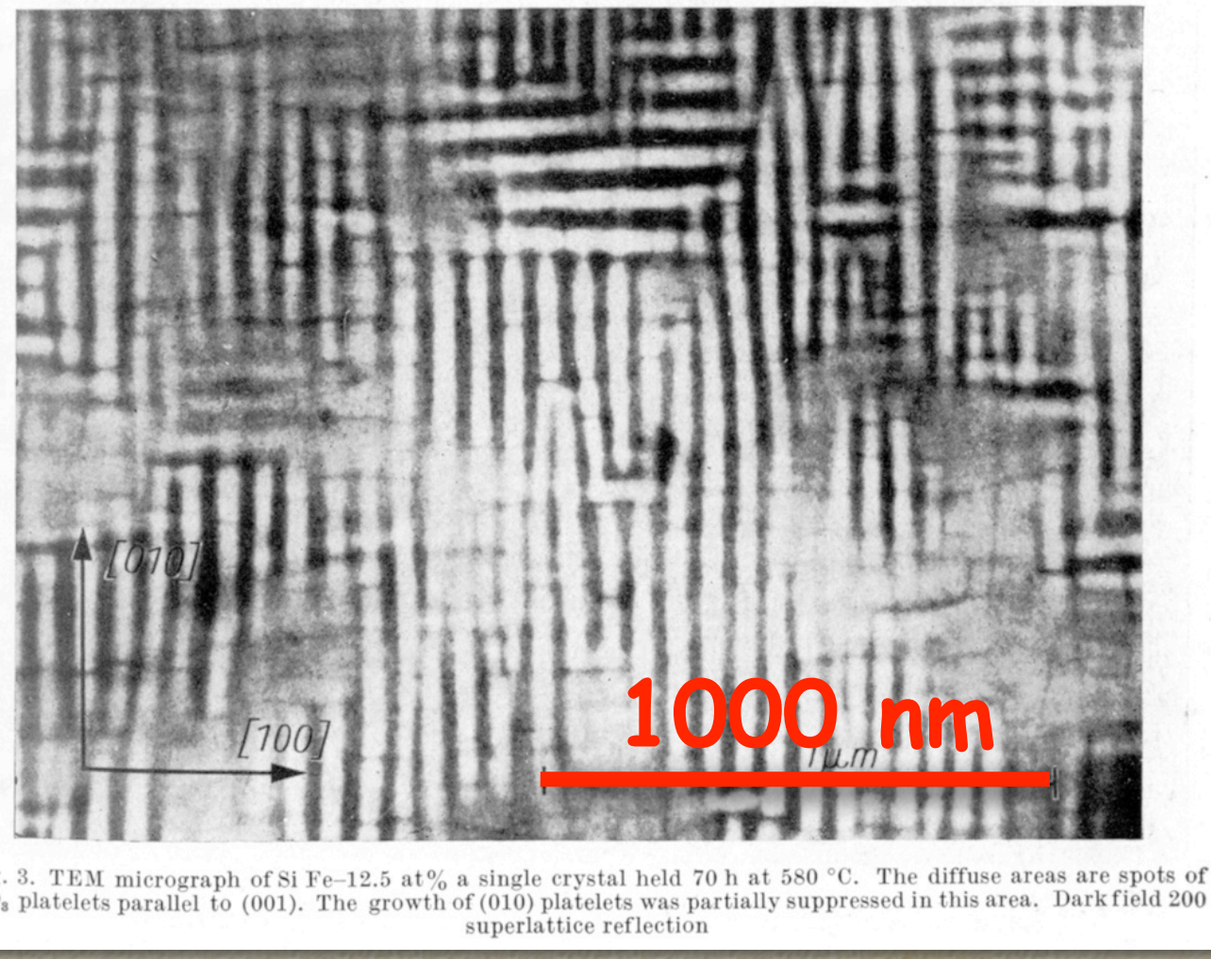

Fig. 3. TEM micrograph of Si Fe–12.5 at% a single crystal held 70 h at 580 °C. The diffuse areas are spots of DO_3 platelets parallel to (001). The growth of (010) platelets was partially suppressed in this area. Dark field 200 superlattice reflection

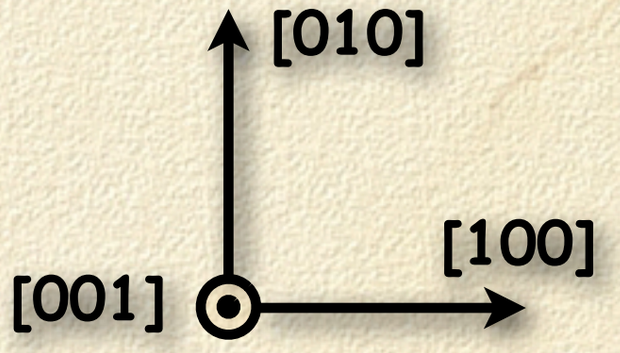

from: S. Libovicky: Spatial replica of ferromagnetic domains in iron-silicon alloys. Phys. Status Solidi A 12 (1972) 539

Bulk domain observation by Libovický-method

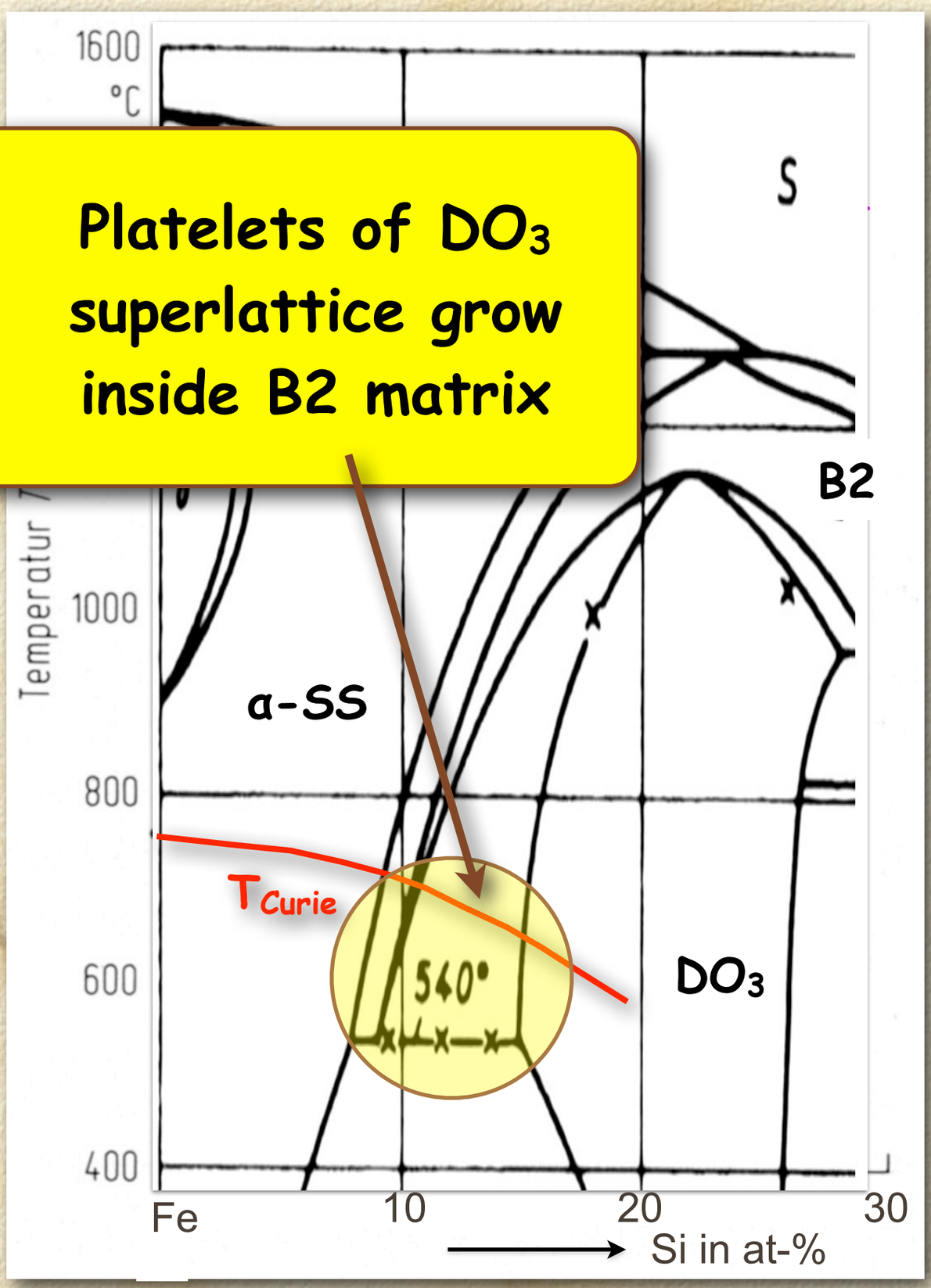

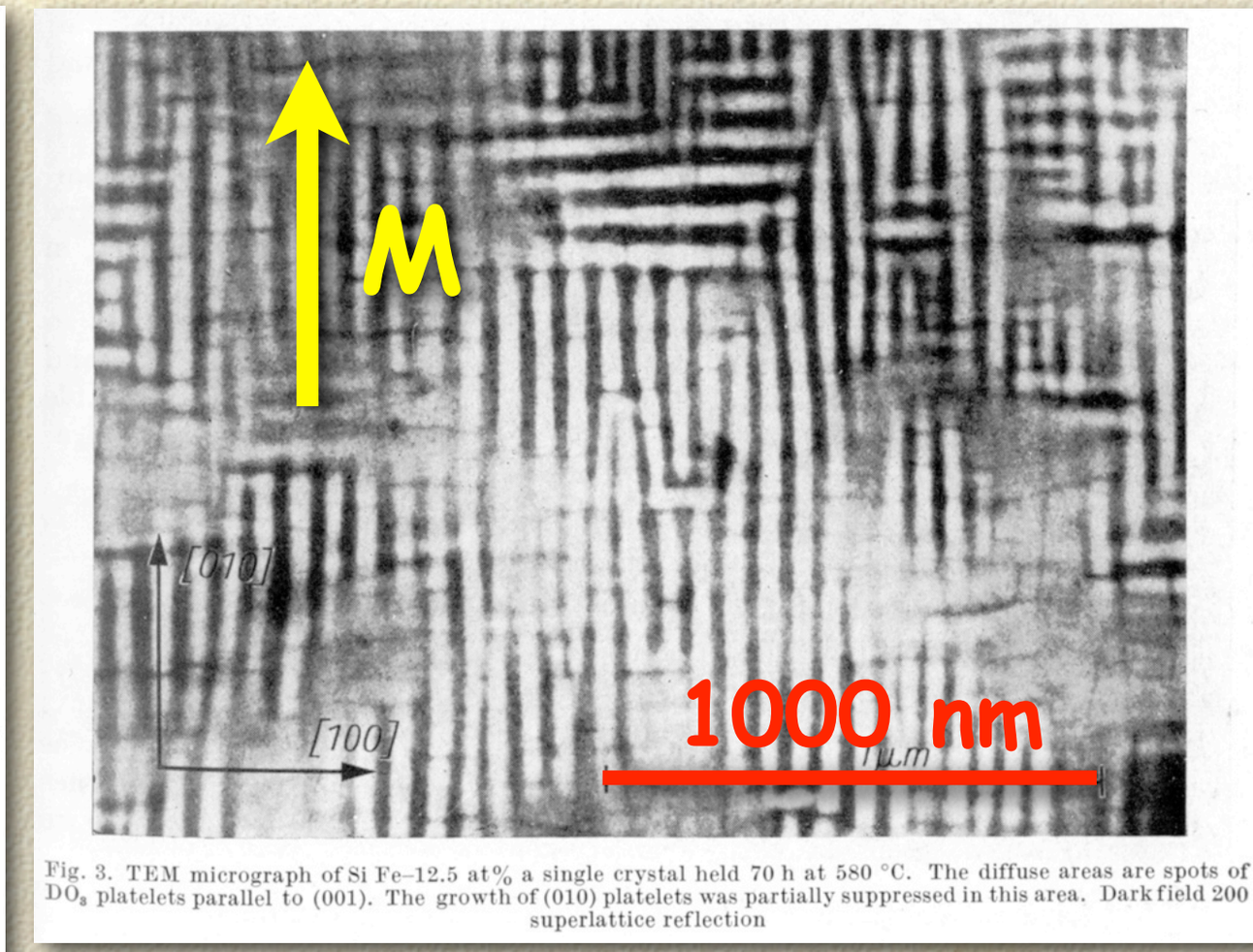

Fig. 3. TEM micrograph of Si Fe–12.5 at% a single crystal held 70 h at 580 °C. The diffuse areas are spots of DO_3 platelets parallel to (001). The growth of (010) platelets was partially suppressed in this area. Dark field 200 superlattice reflection

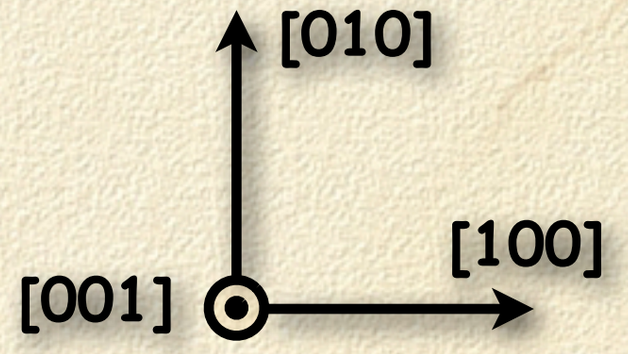

from: S. Libovicky: Spatial replica of ferromagnetic domains in iron-silicon alloys. Phys. Status Solidi A 12 (1972) 539

Bulk domain observation by Libovický-method

Orientation of magnetization vector (at annealing temperature) generates anisotropic distribution of DO_3 platelets

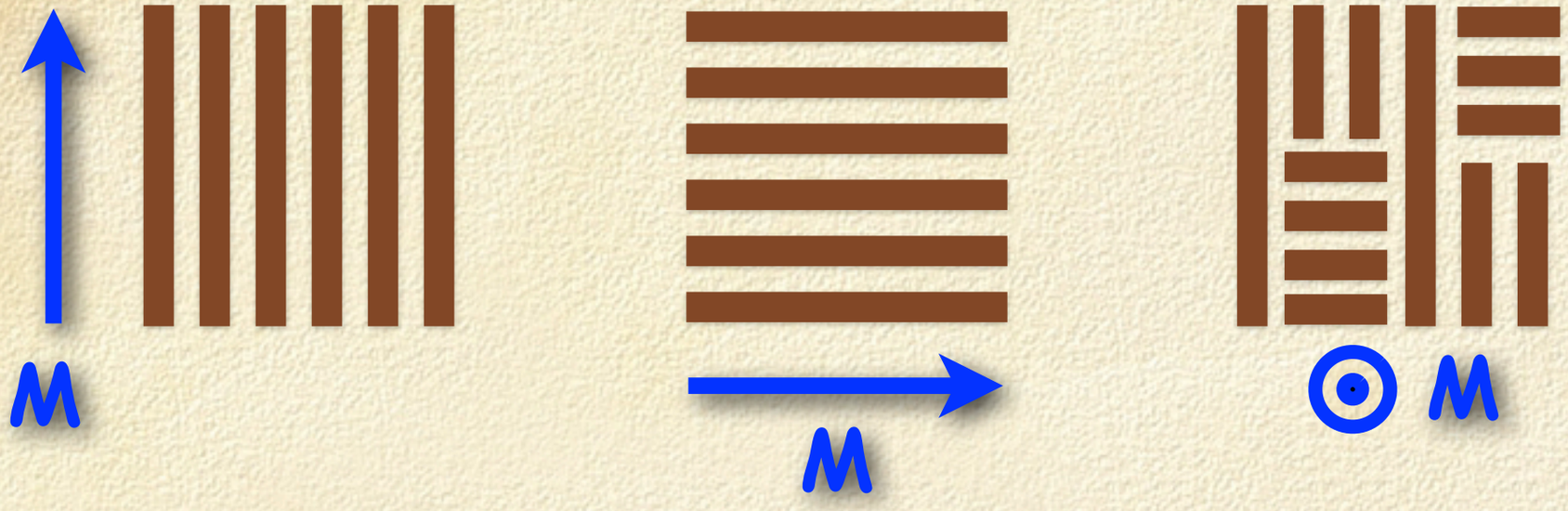

→ Creation of precipitation pattern by annealing >540°C (<T_c)

→ Cooling to room temperature

→ Domain pattern is „frozen" as submicroscopic precipitation pattern

→ Domain imaging in polarization microscope after etching due to optical birefringence effect (at room temperature)

"Metallographic" domain analysis

Bulk domain observation by Libovický-method

Branched domains on Fe12.8%Si (111) surface

(thickness 0.5 mm)

Bulk domain observation by Libovický-method

Branched domains on Fe12.8%Si (111) surface

(thickness 0.5 mm)

Bulk domain observation by Libovický-method

Branched domains on Fe12.8%Si (111) surface

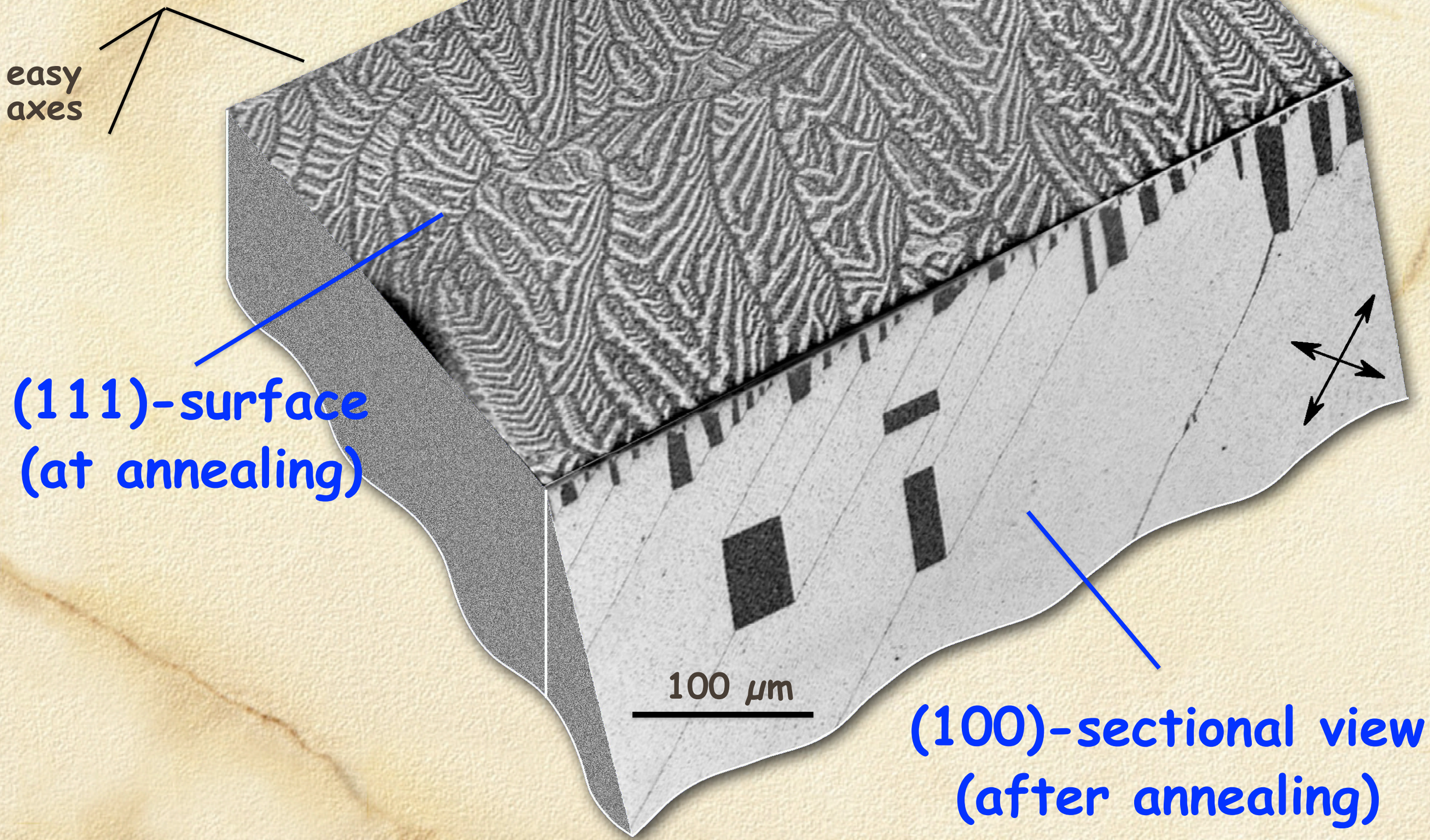

Butterfly domains on (100)-related surface

Kerr observations

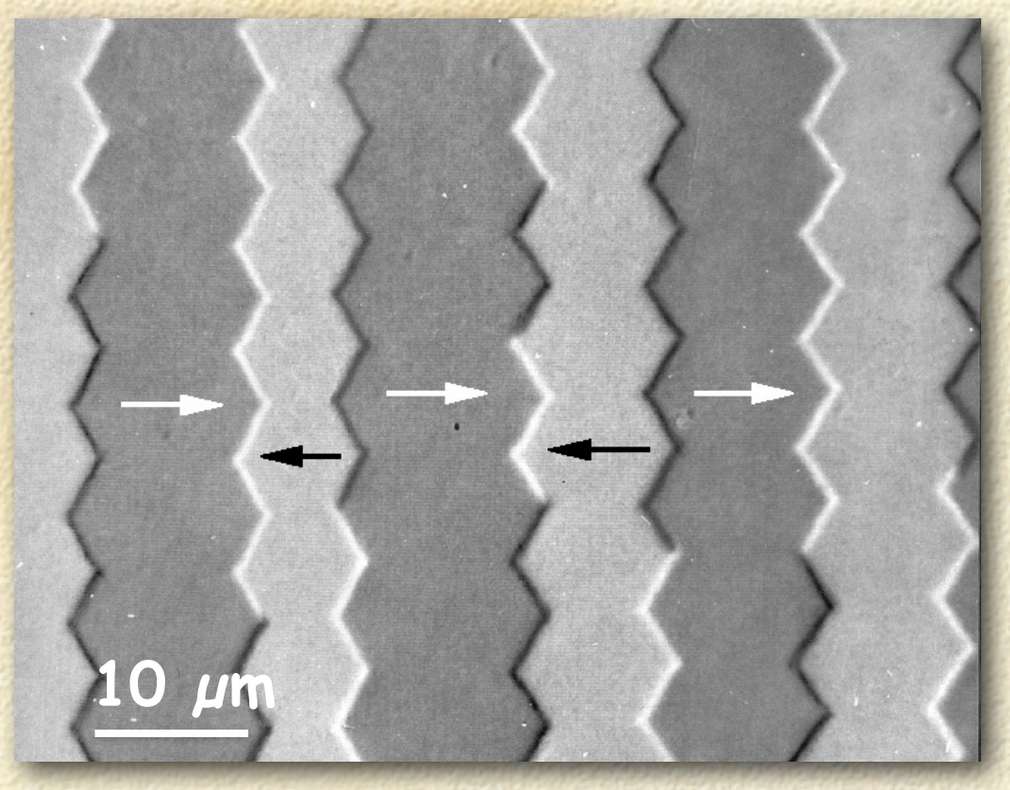

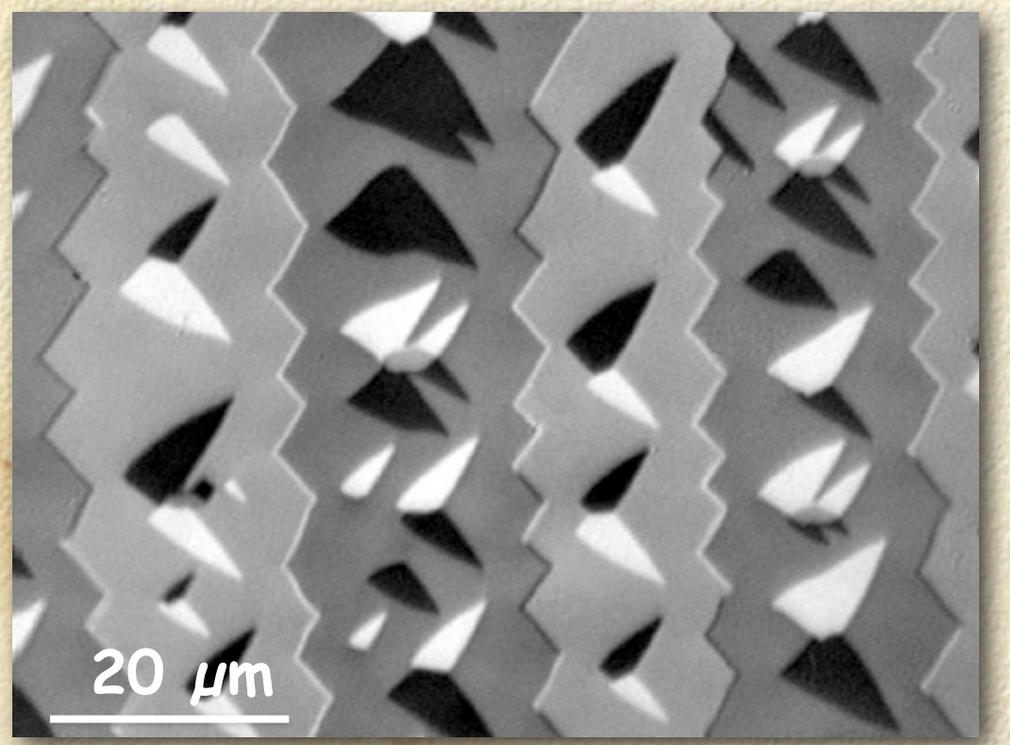

Fe (100)-surface, ideally oriented

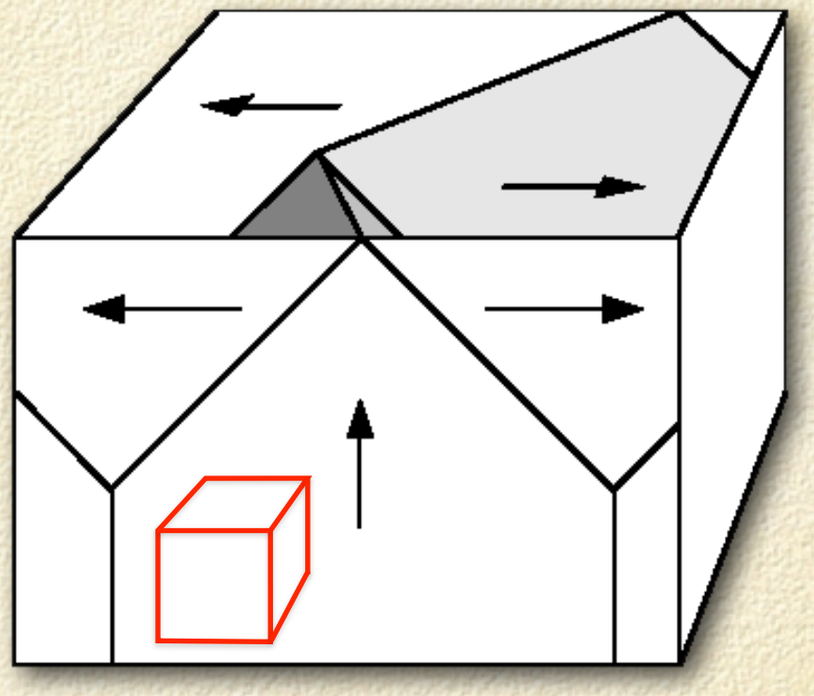

sligthly misoriented

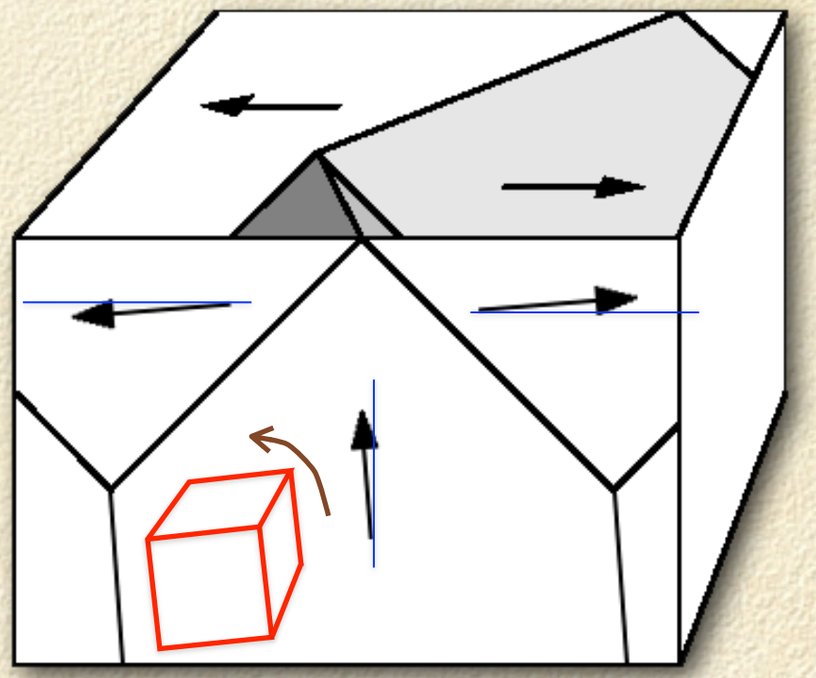

Butterfly domains on (100)-related surface

Kerr observations

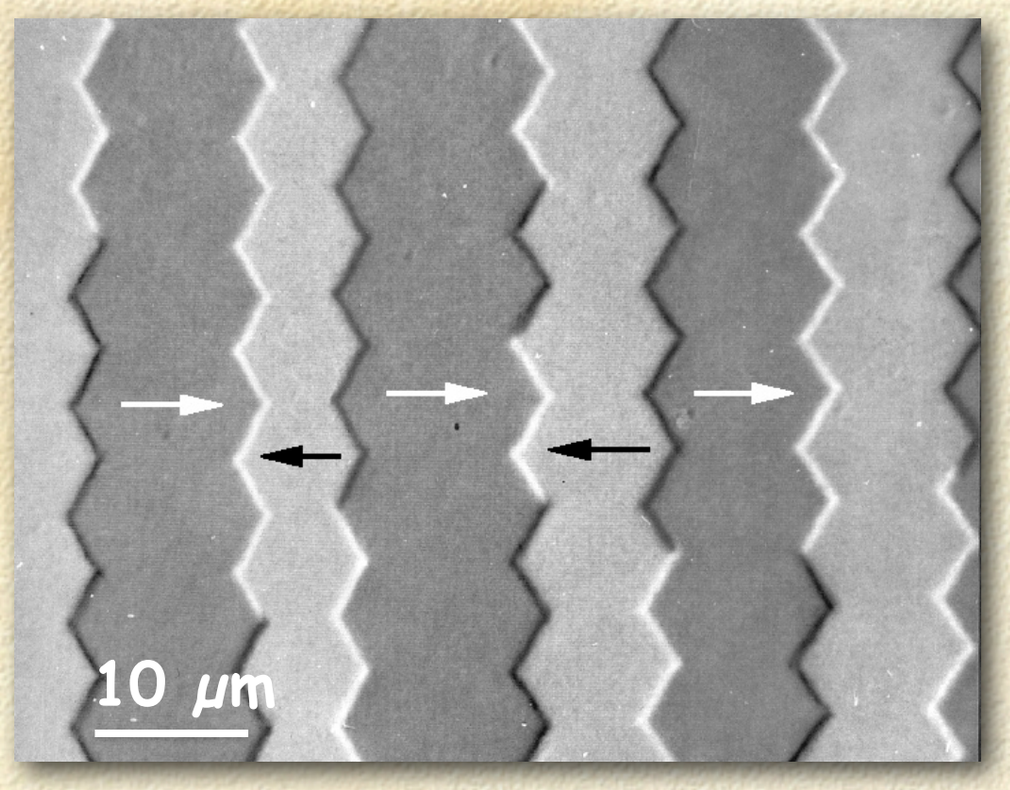

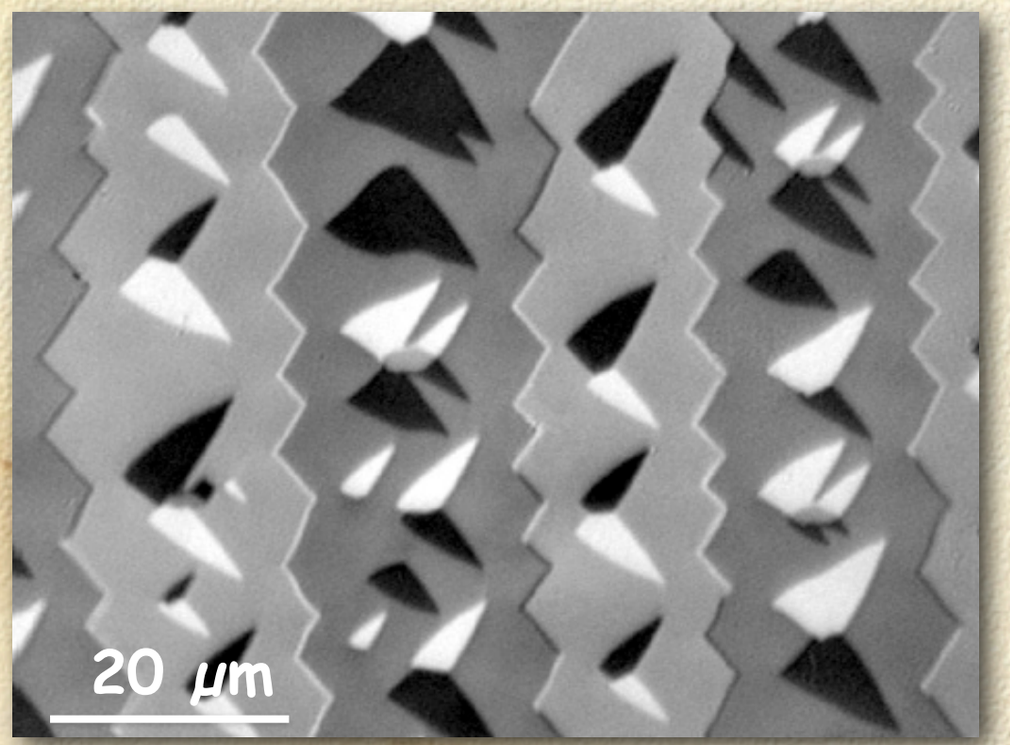

Fe (100)-surface, ideally oriented

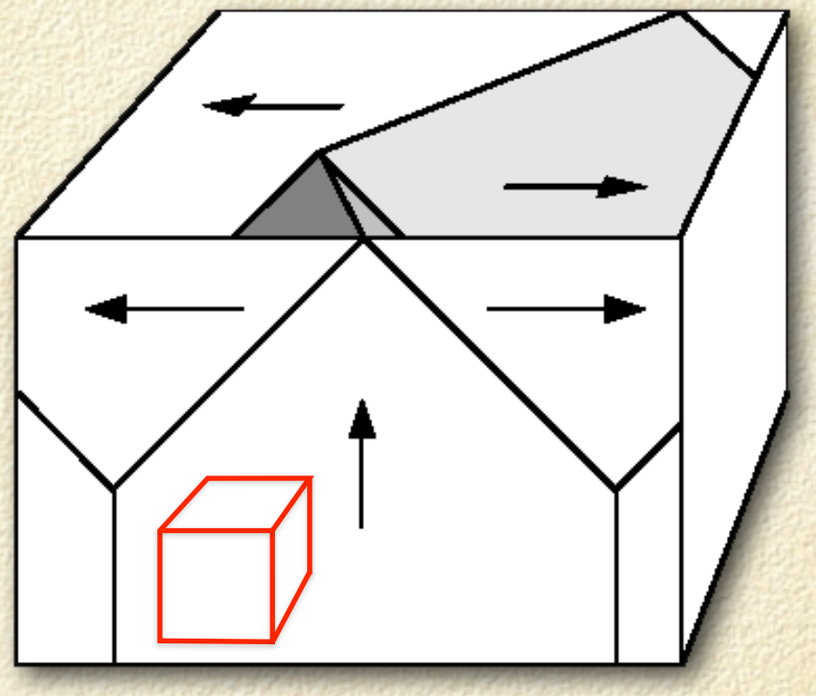

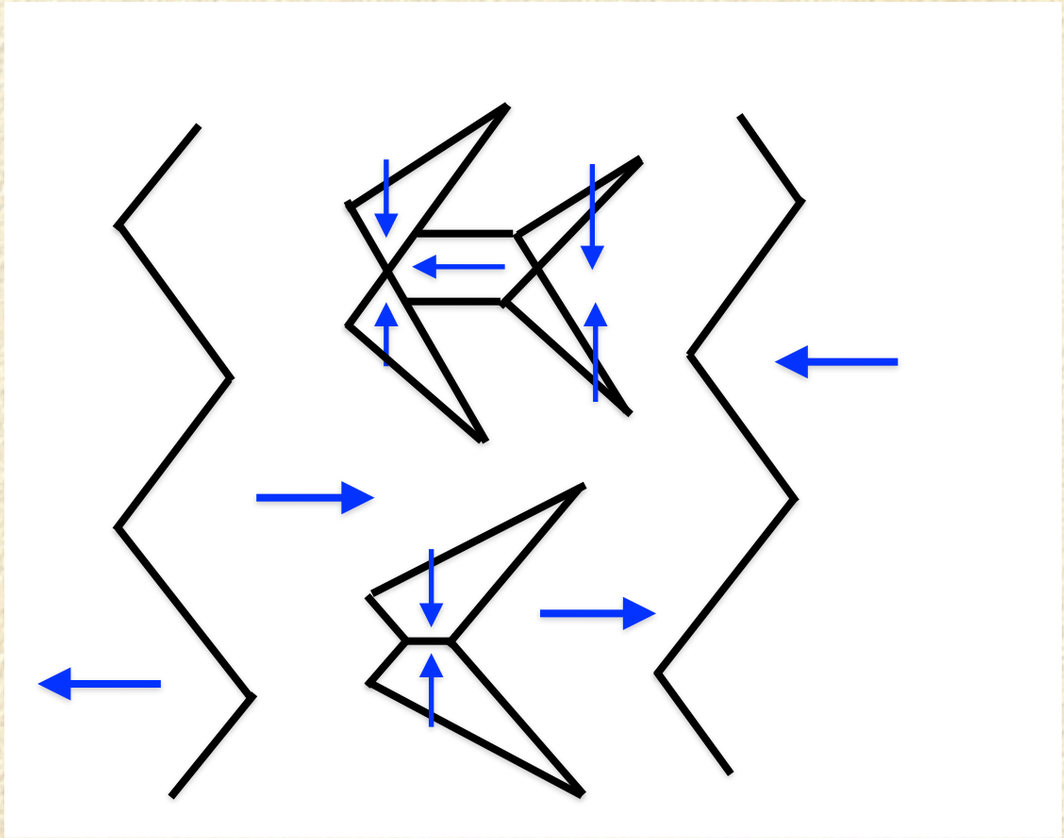

Butterfly domains on Fe12.8%Si crystal

frozen-in domains

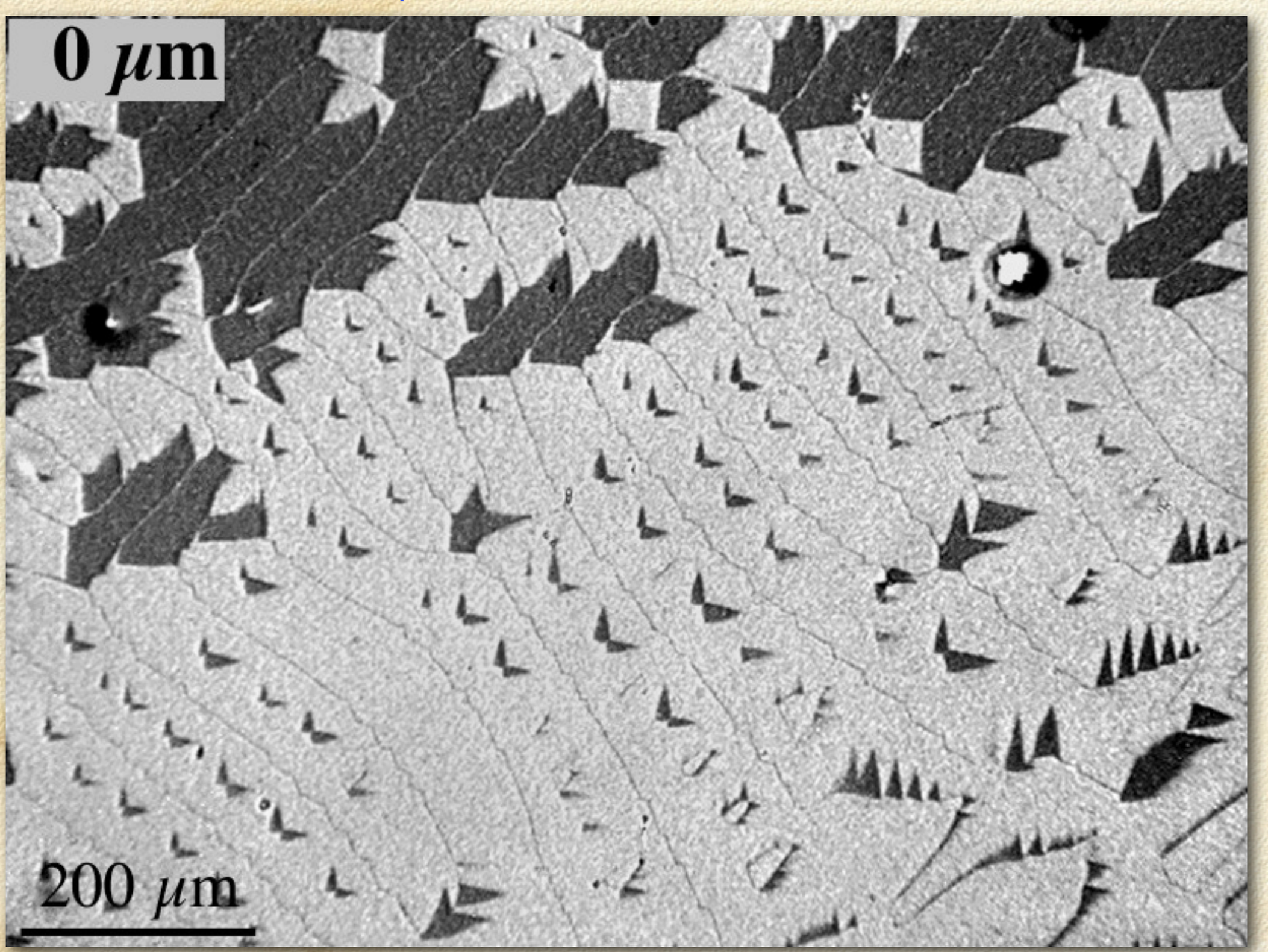

Butterfly domains on Fe12.8%Si crystal

frozen-in domains

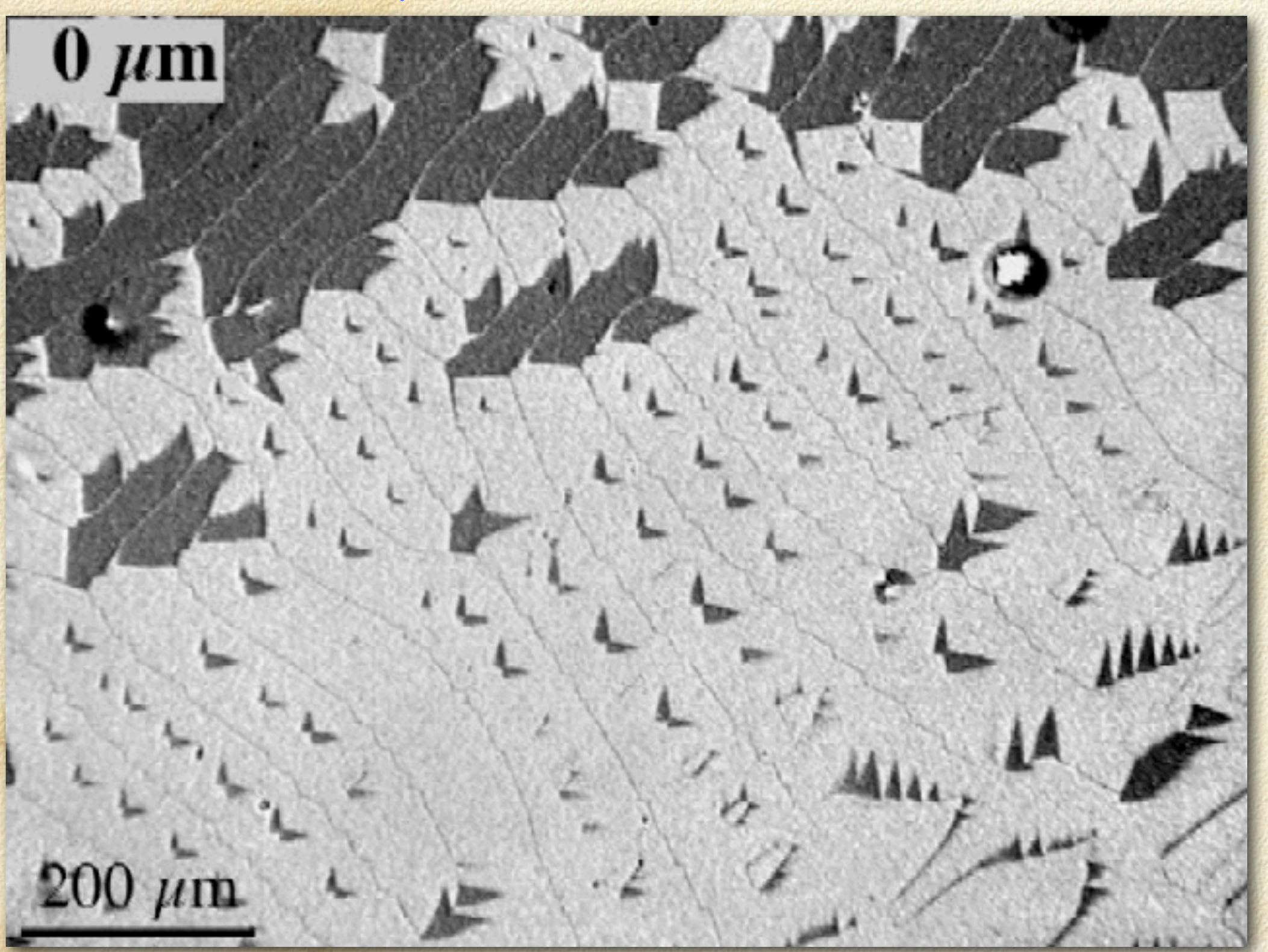

Butterfly domains on Fe12.8%Si crystal

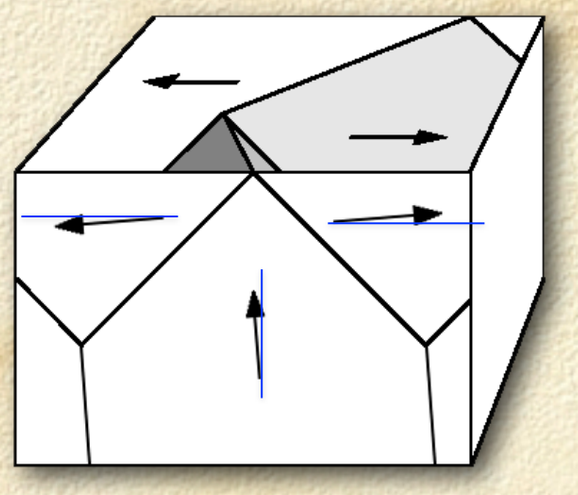

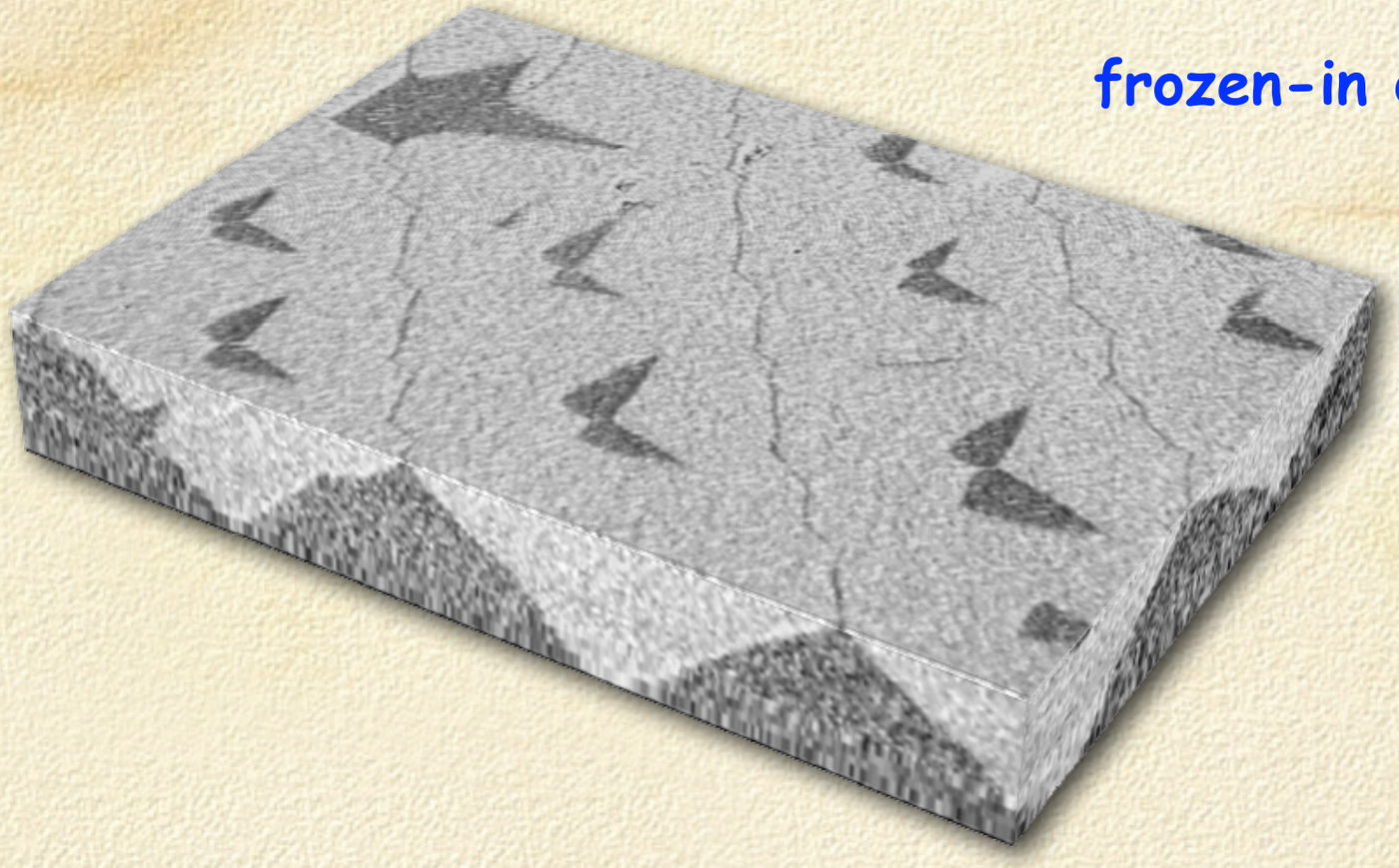

frozen-in domains

50 μm

Butterfly domains on Fe12.8%Si crystal

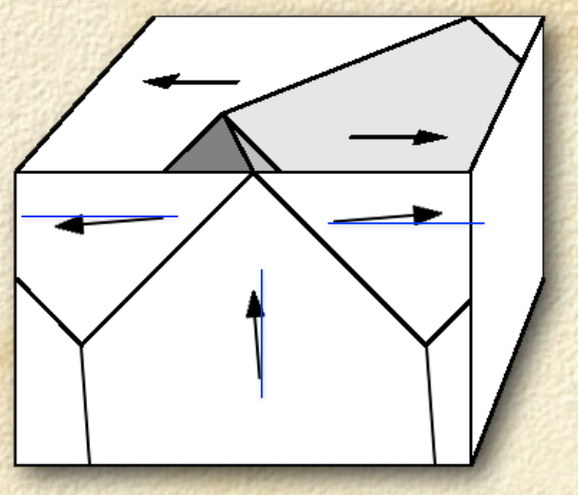

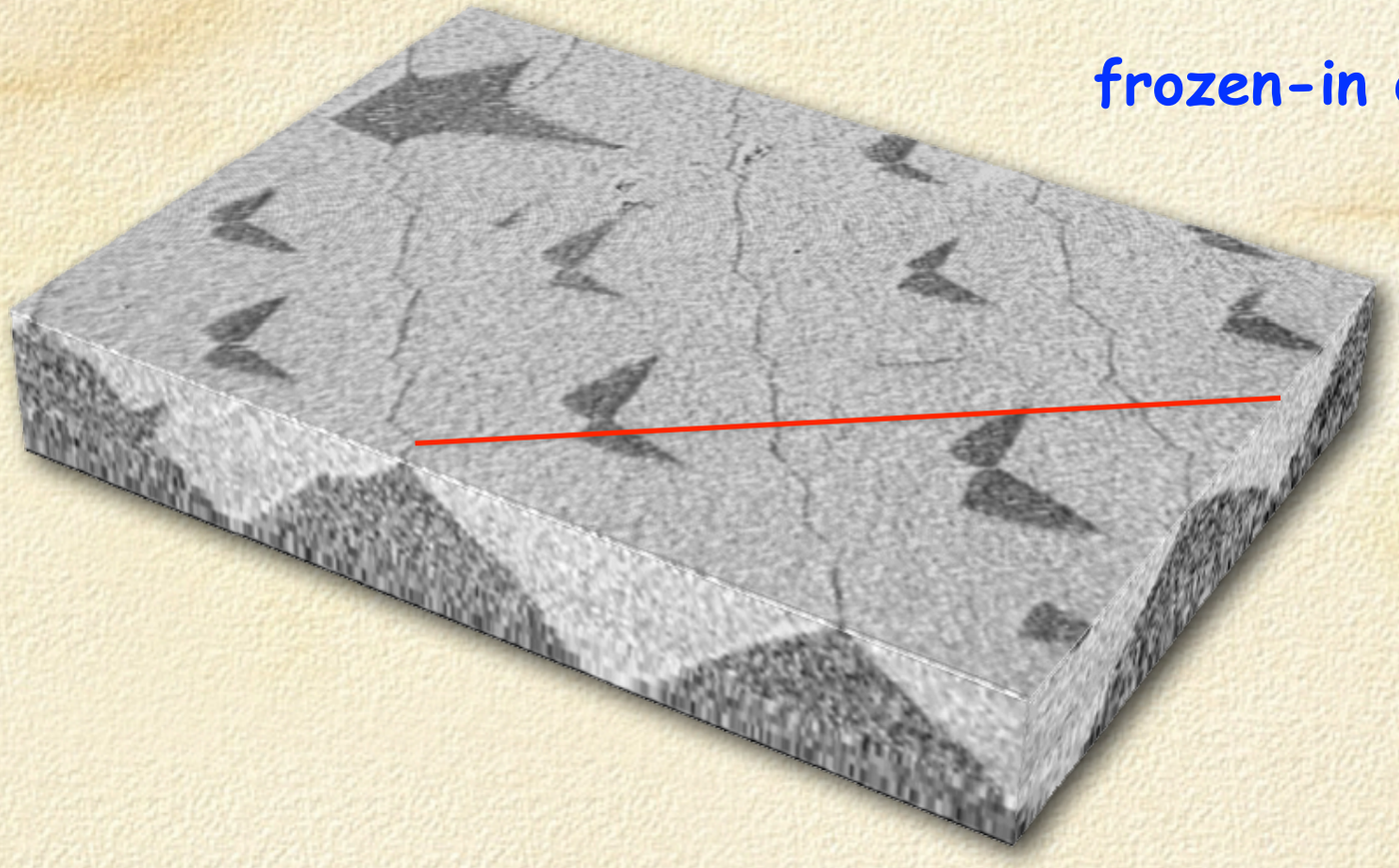

frozen-in domains

50 μm

Butterfly domains on Fe12.8%Si crystal

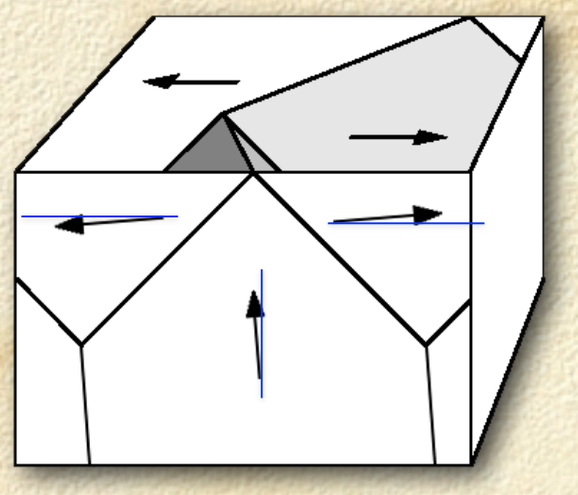

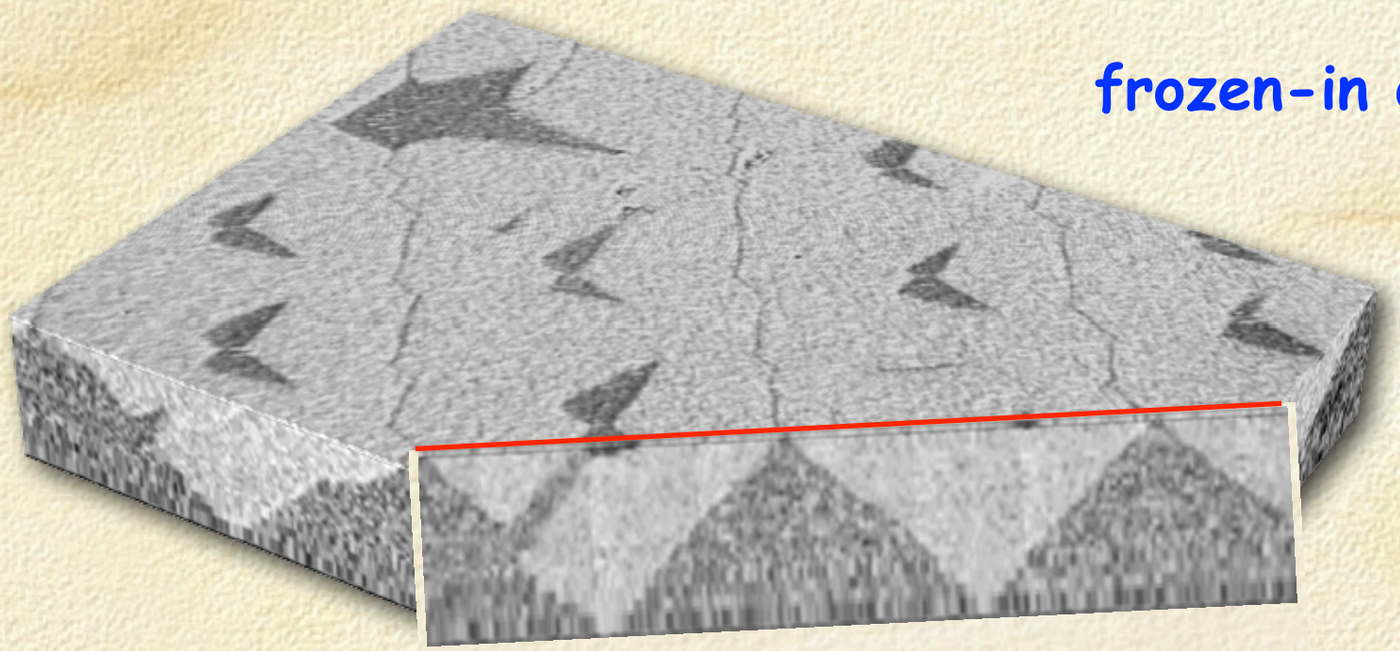

Butterfly domains on Fe12.8%Si crystal

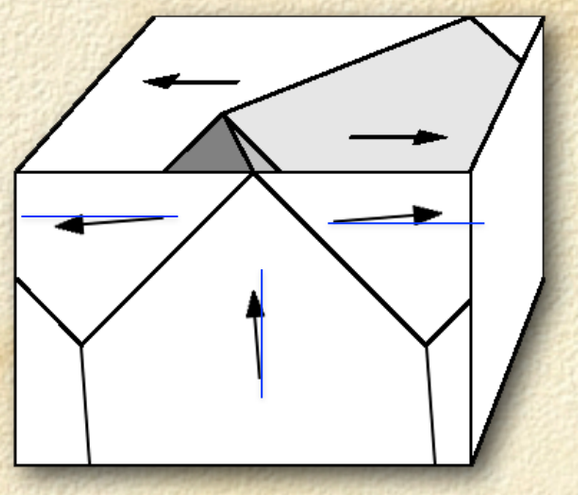

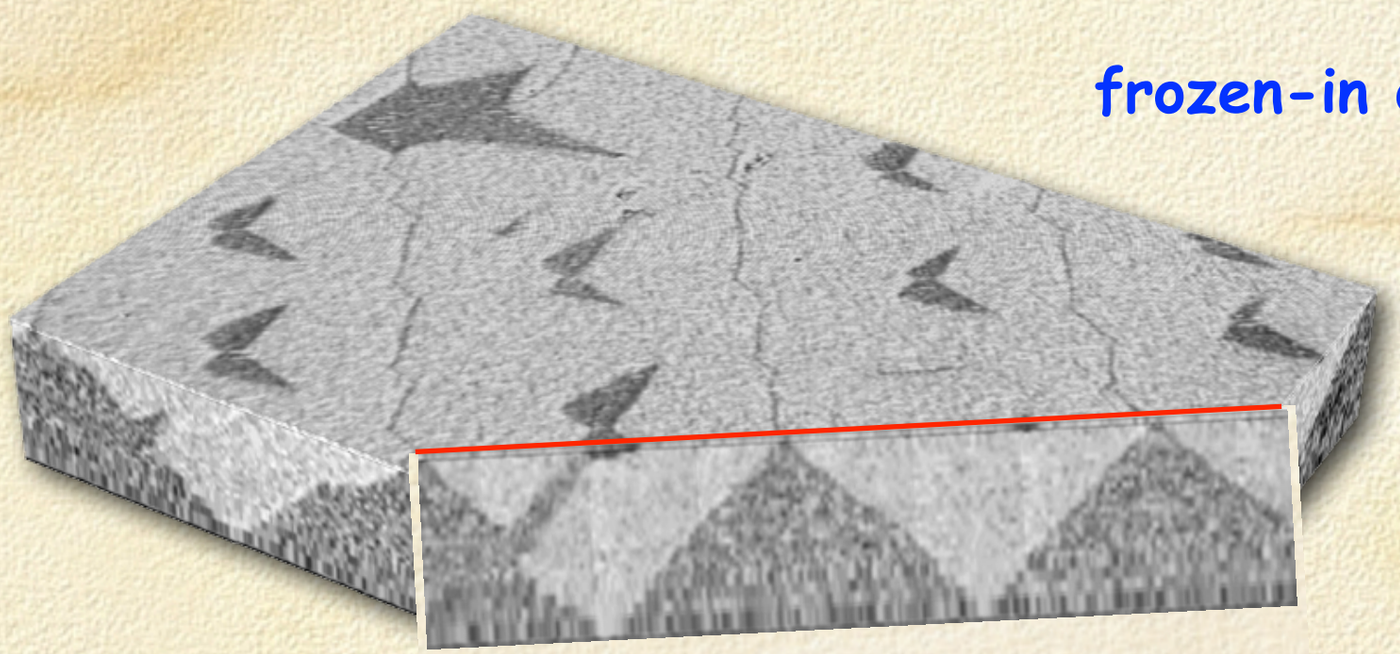

top view

surface

side view

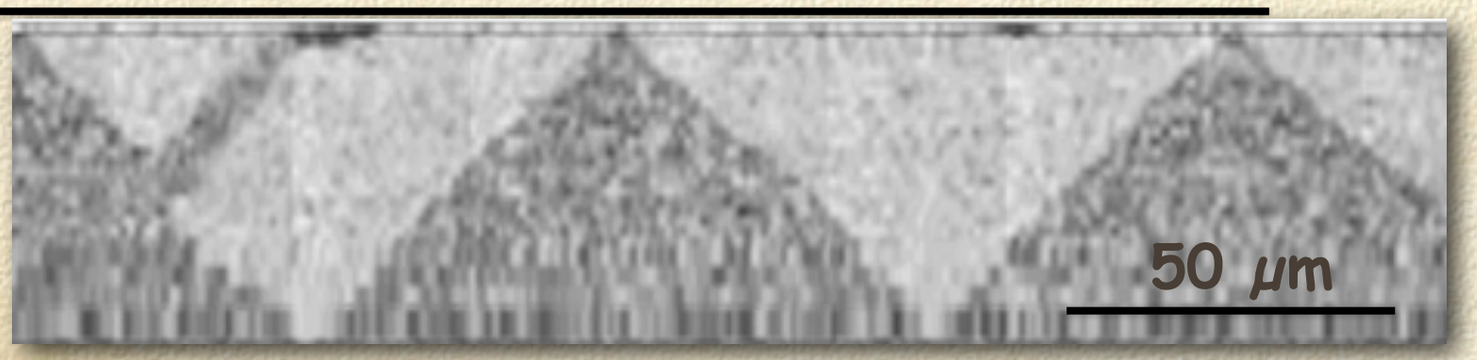

Butterfly domains on Fe12.8%Si crystal

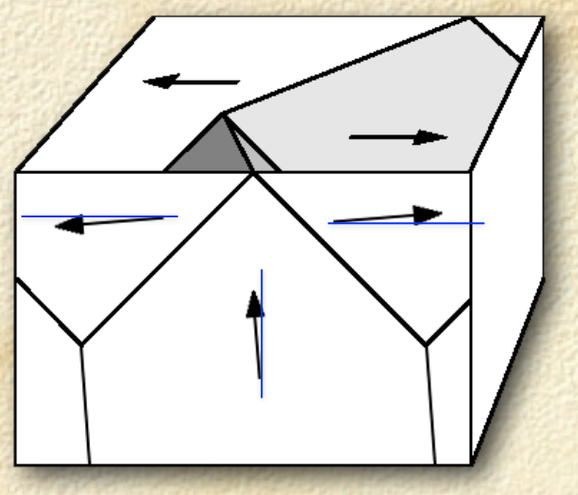

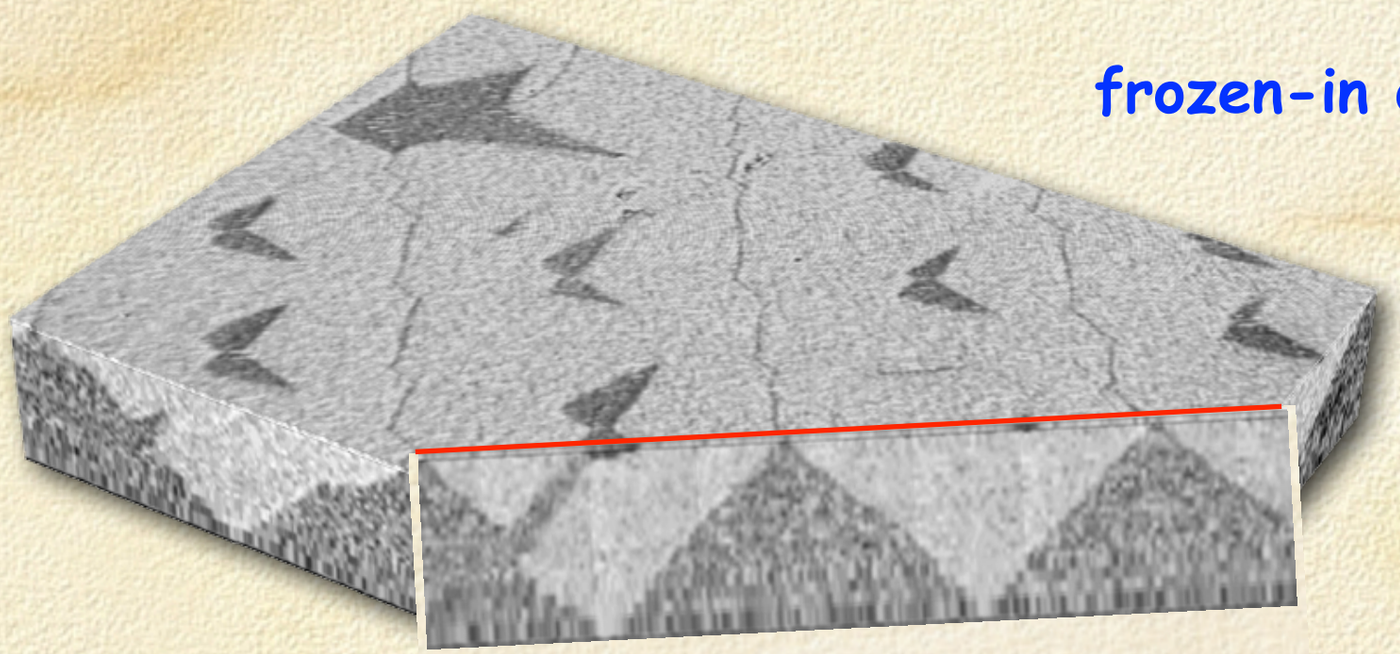

frozen-in domains

50 μm

cut

top view

surface

side view

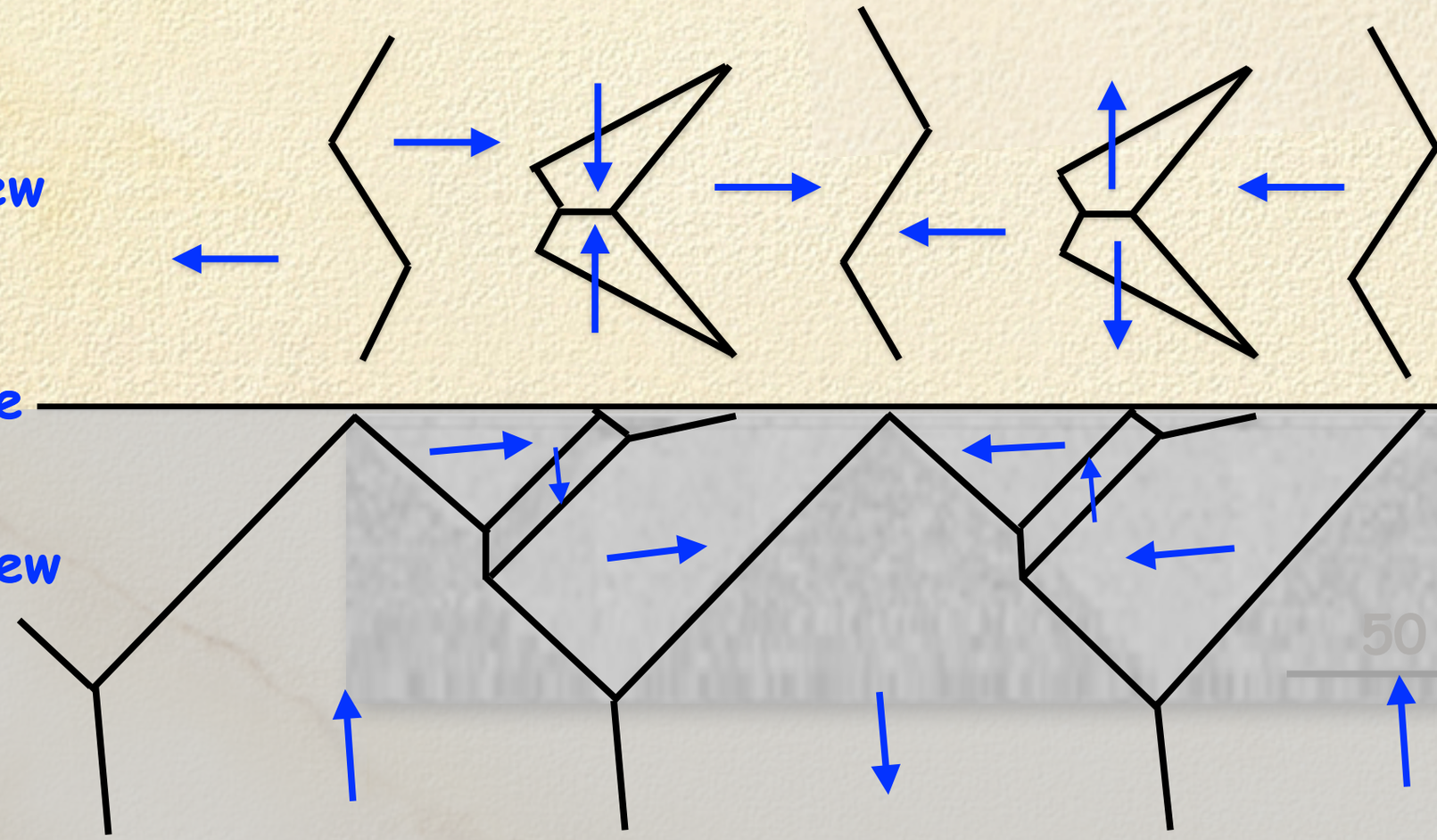

misorientation

easy axes

Néel Spikes on surface of FeSi sheet

Fe (100) sheet with cube texture, imaged by Bitter technique

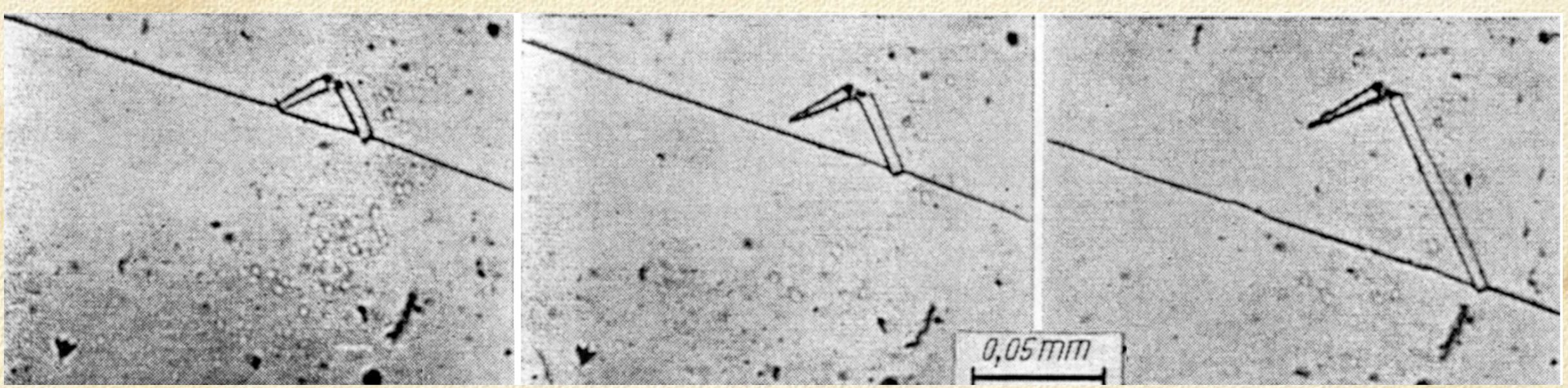

from: D. Ganz, Arch. Eisenhütten 35, 371 (1964)

L. Néel, Cah. de Phys. 25, 21(1944)	prediction
H. J. Williams, W. Shockley, Phys. Rev. 75, 178 (1949)	first observation
L. F. Bates, D. H. Martin, Proc. Phys. Soc. B69, 145 (1956)	calculation
L. F. Bates, R. Carey, Proc. Phys. Soc. 75, 880 (1956)	
etc.	

Néel Spikes in volume of Fe12.8%Si crystal with (100) surface

frozen-in domains

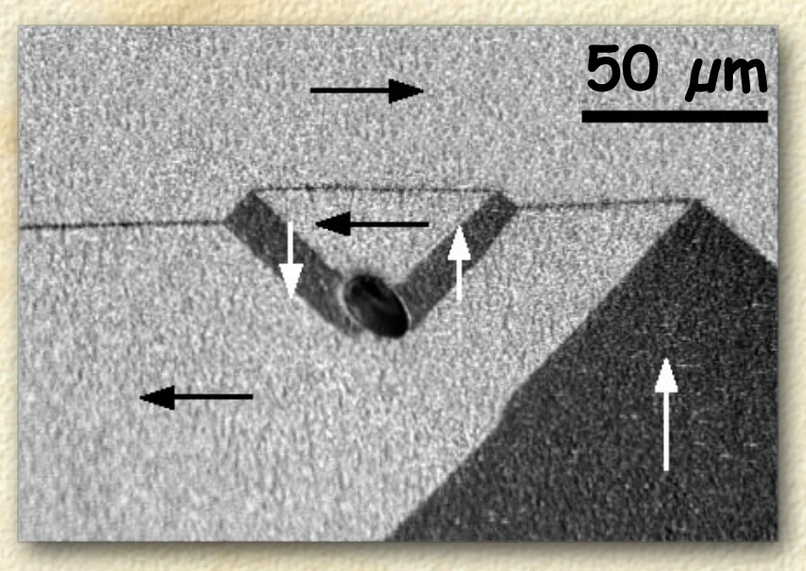

depth = 50 μm

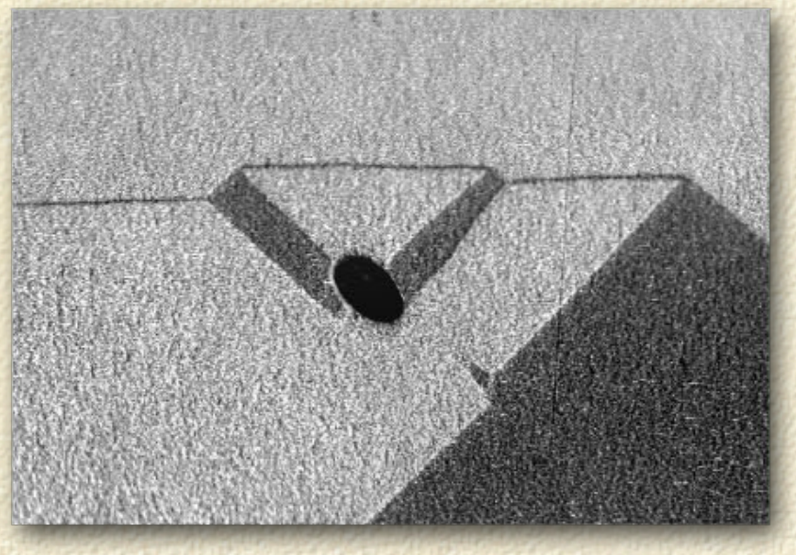

51 μm

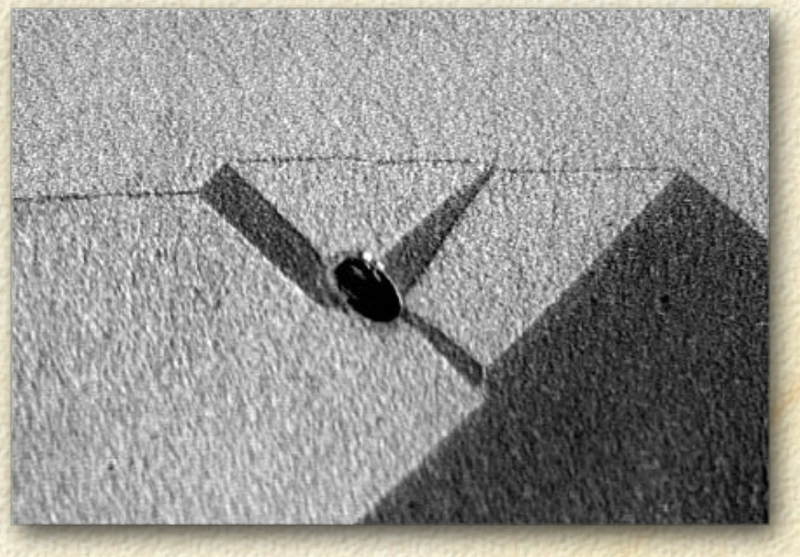

52 μm

53 μm

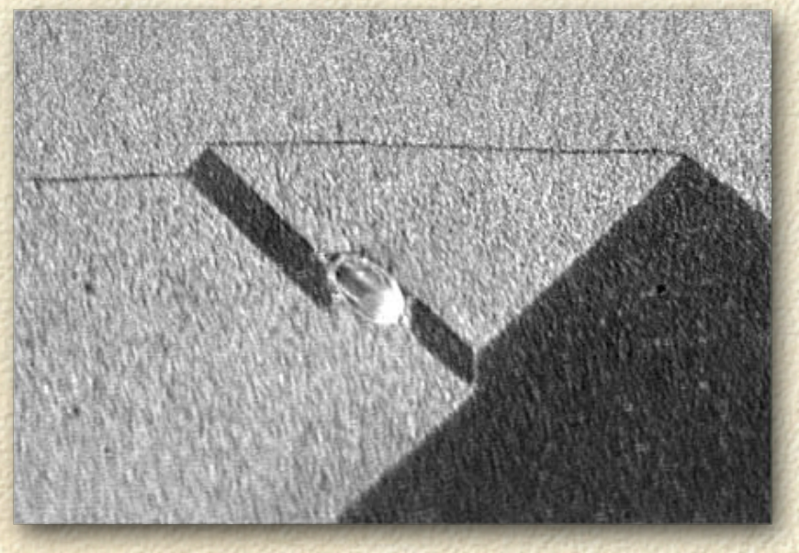

55 μm

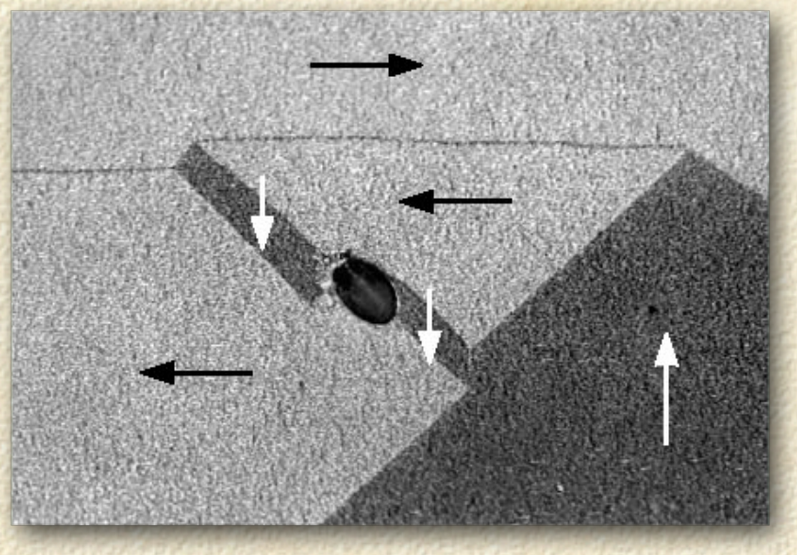

57 μm

Non-oriented FeSi sheet

0.5 mm

Non-oriented FeSi sheet

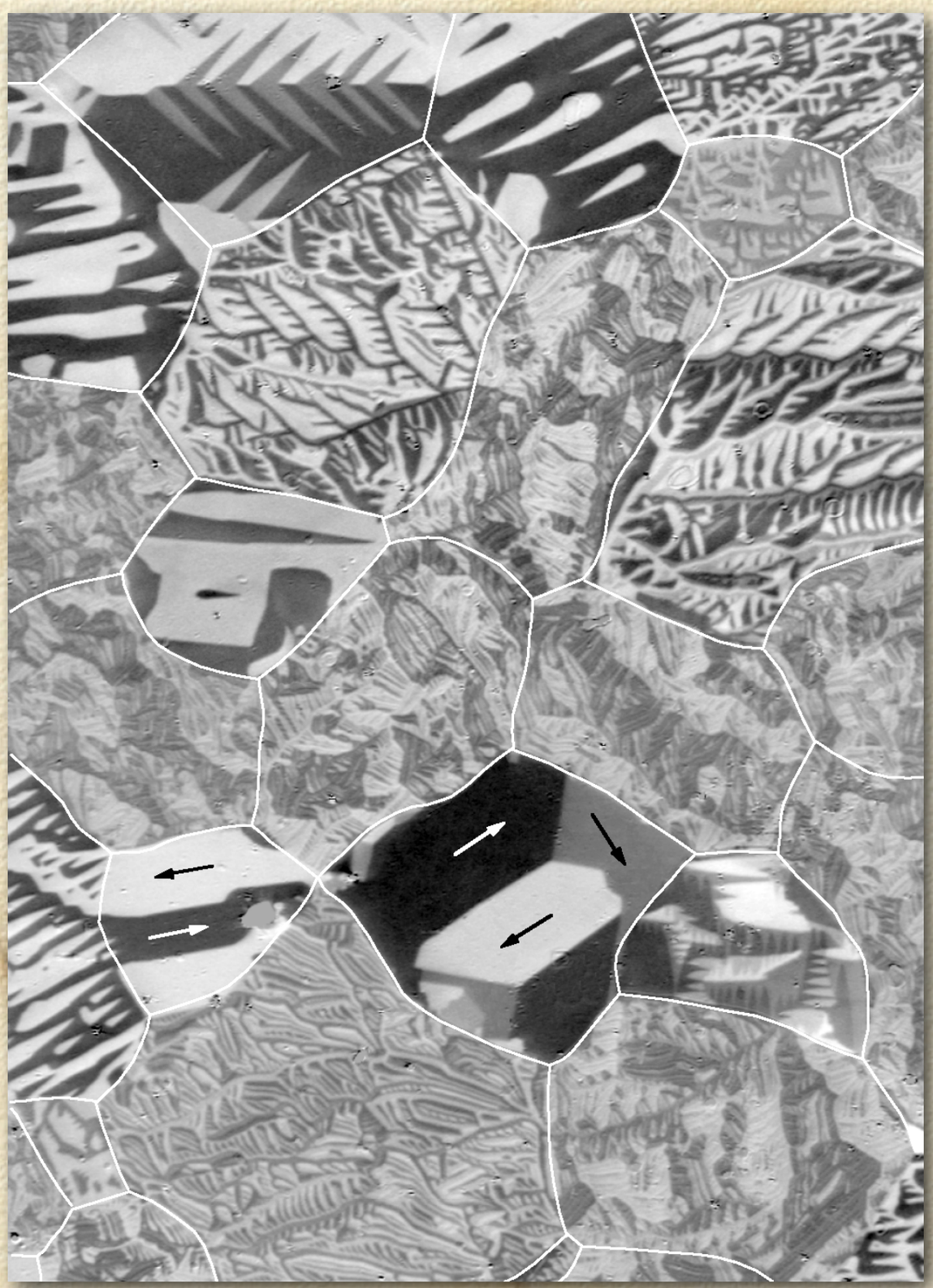

0.5 mm

Conclusion:

Strong misorientation:
Complex domains restricted to surface zone, in volume wide basic domains can be expected

Weak misorientation: wide basic domains with superimposed supplementary domains

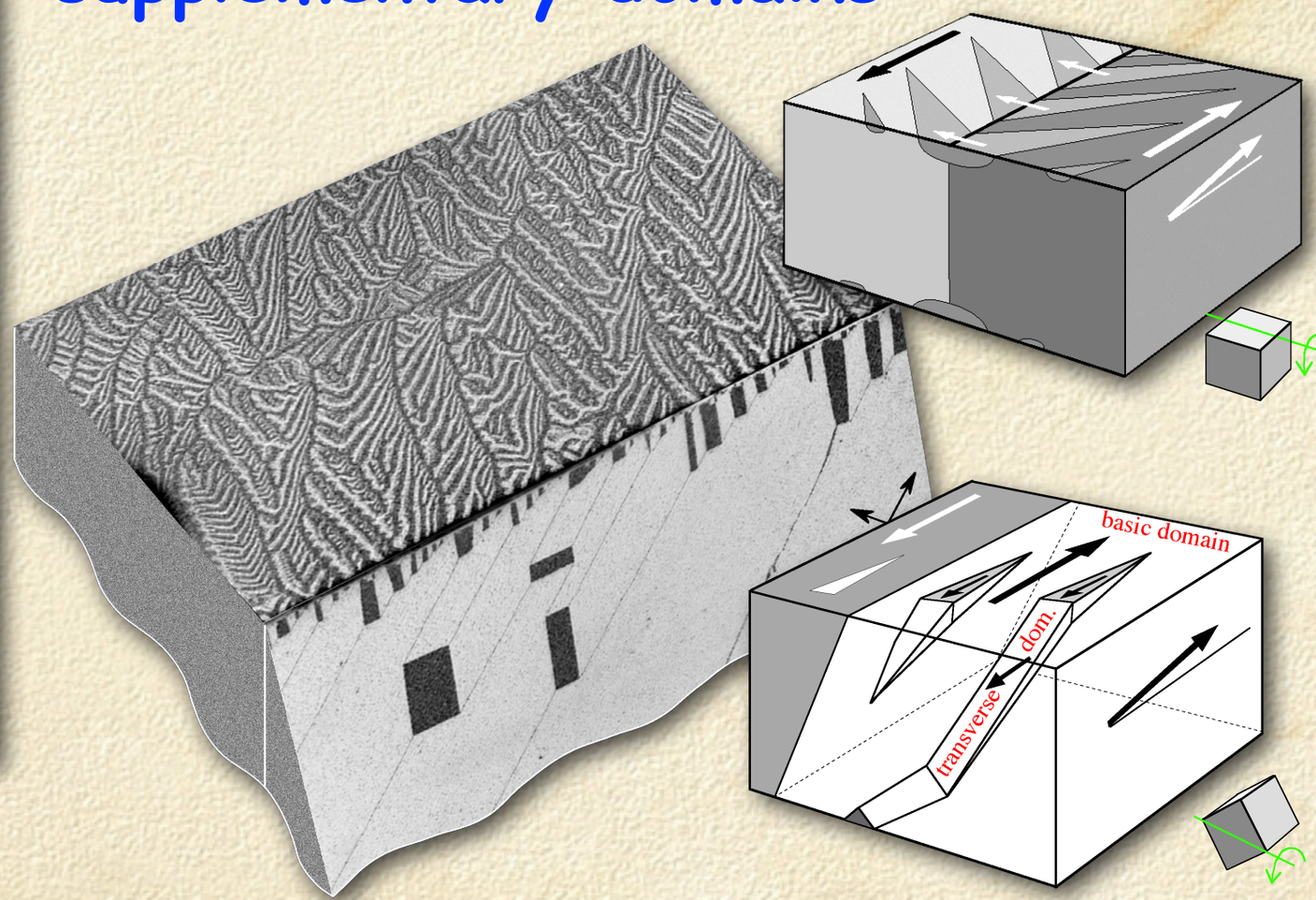

Non-oriented FeSi sheet

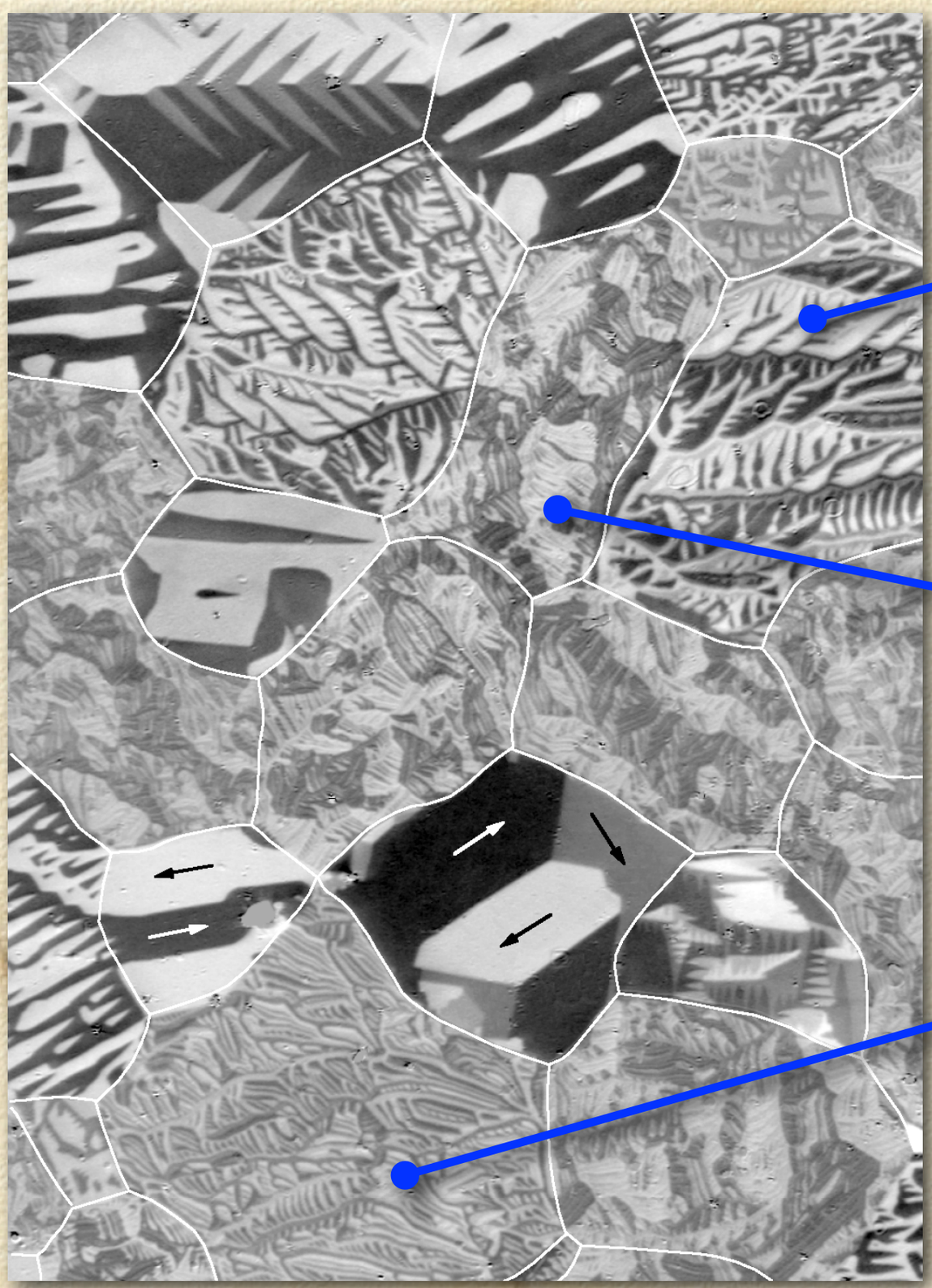

0.5 mm

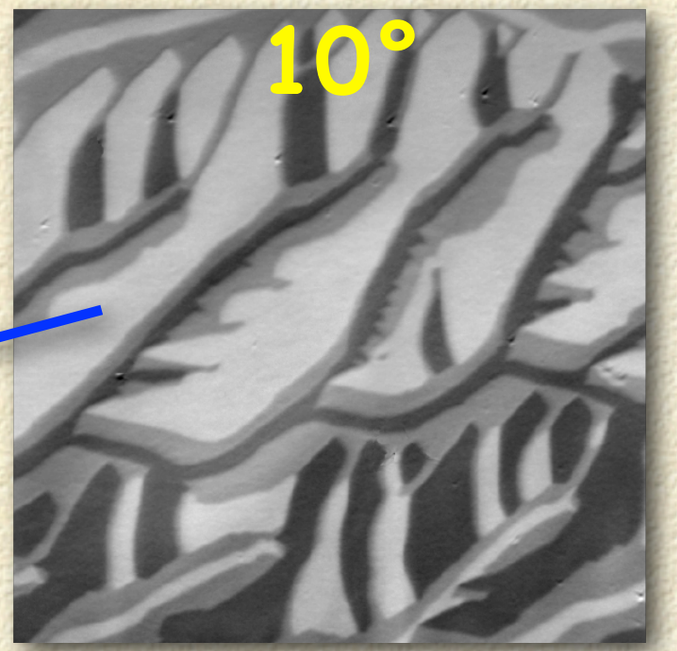

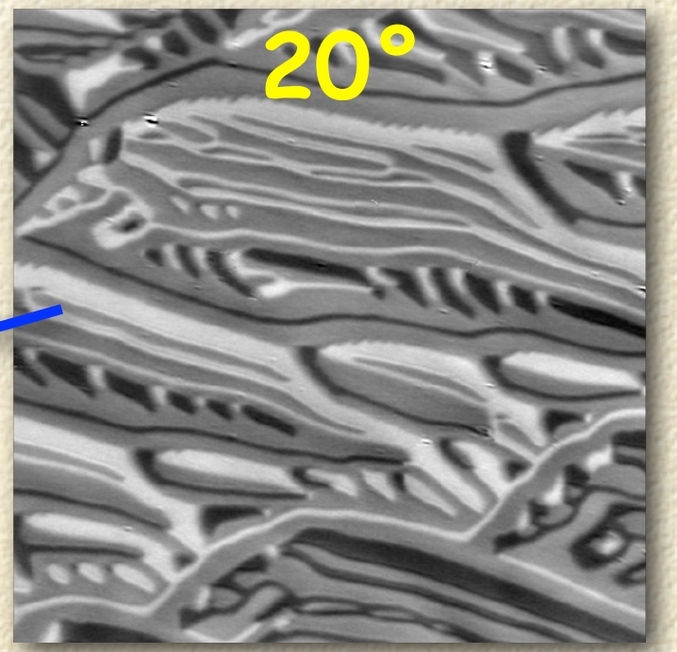

10 μm

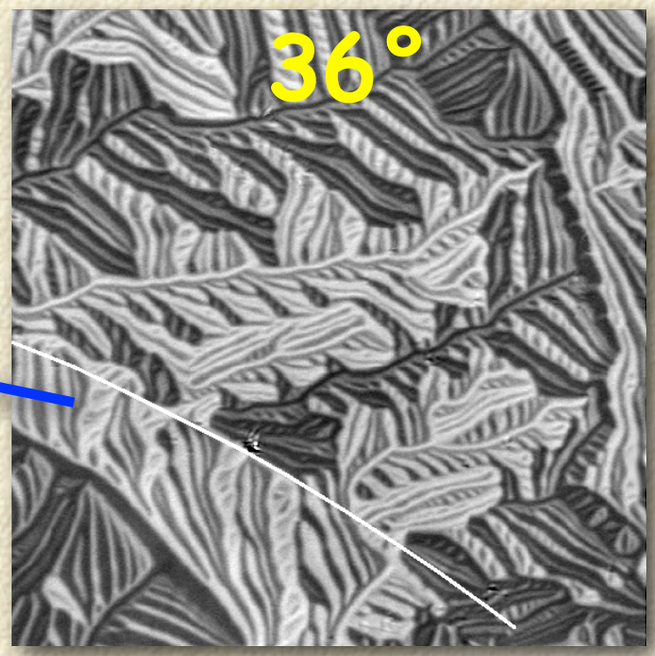

(111)-surface

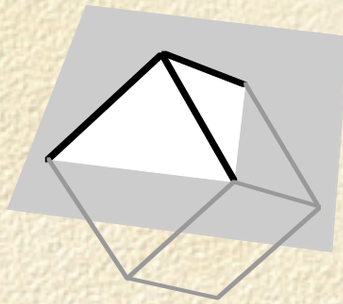

Non-oriented FeSi sheet

10 μm

(111)-surface

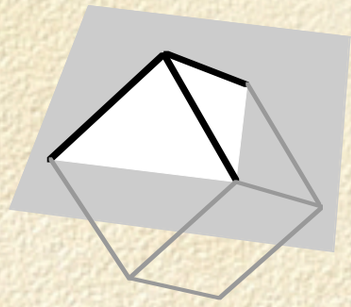

We expect wide volume domains in any case

0.5 mm

Non-oriented FeSi sheet

0.5 mm

Indication of wide volume domains by surface observation

Non-oriented FeSi sheet

0.5 mm

Indication of wide volume domains by surface observation

Non-oriented FeSi sheet

0.5 mm

Indication of wide volume domains by surface observation

Non-oriented FeSi sheet

0.5 mm

Indication of wide volume domains by surface observation

A. Hubert:
Quasi-domain model for domains and flux transport in interior

Quasi-Domains

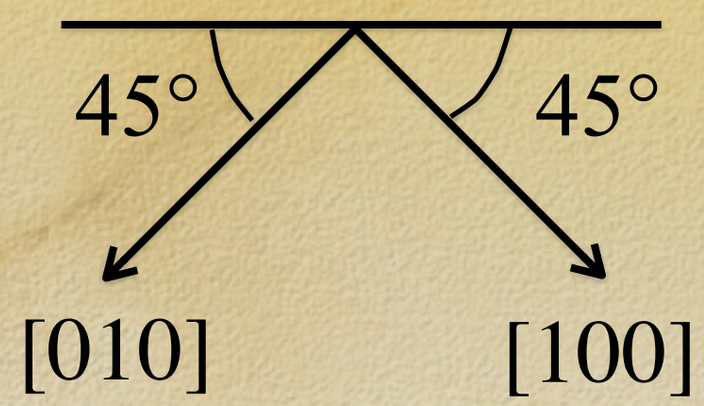

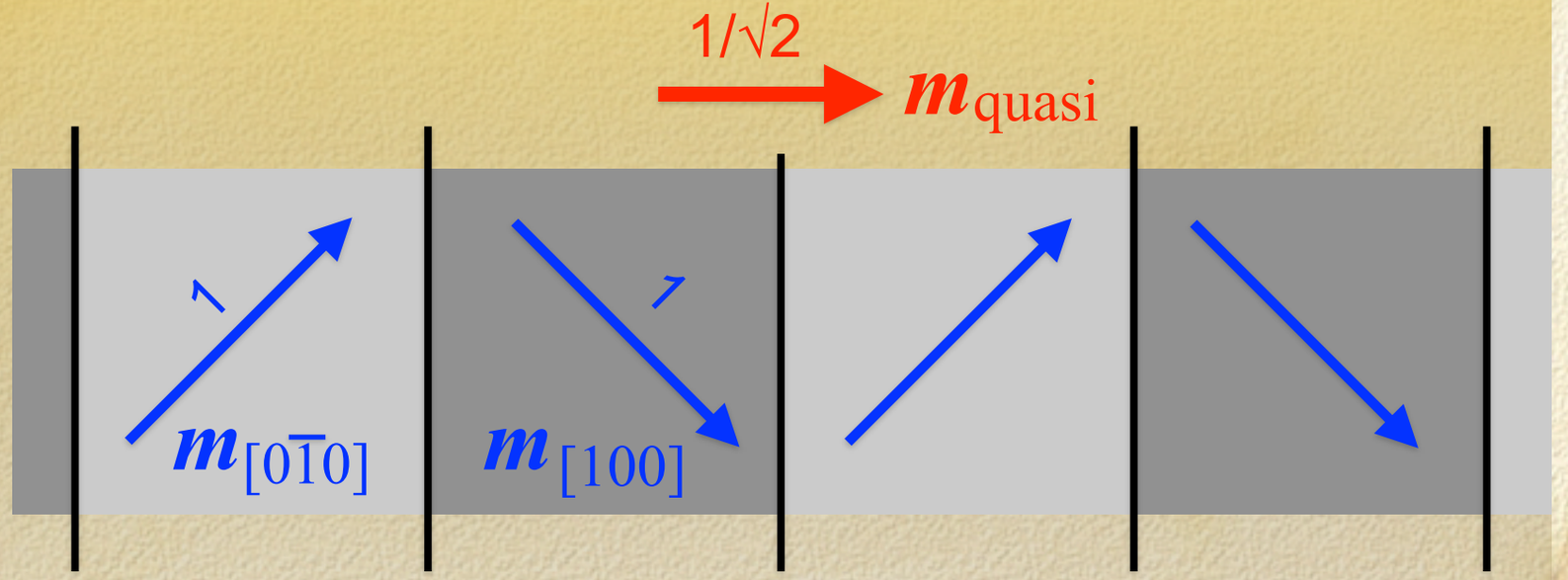

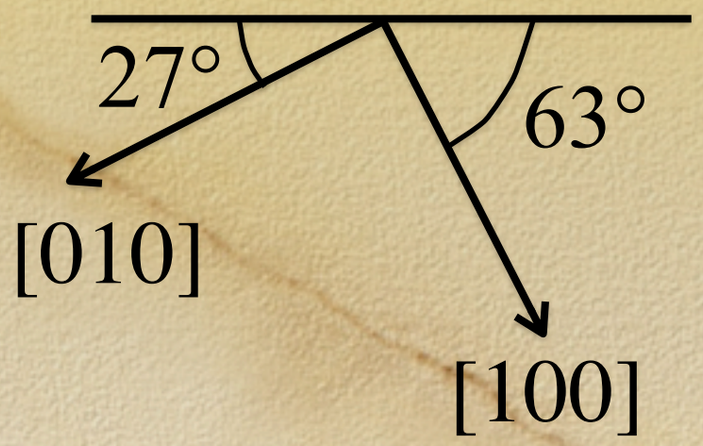

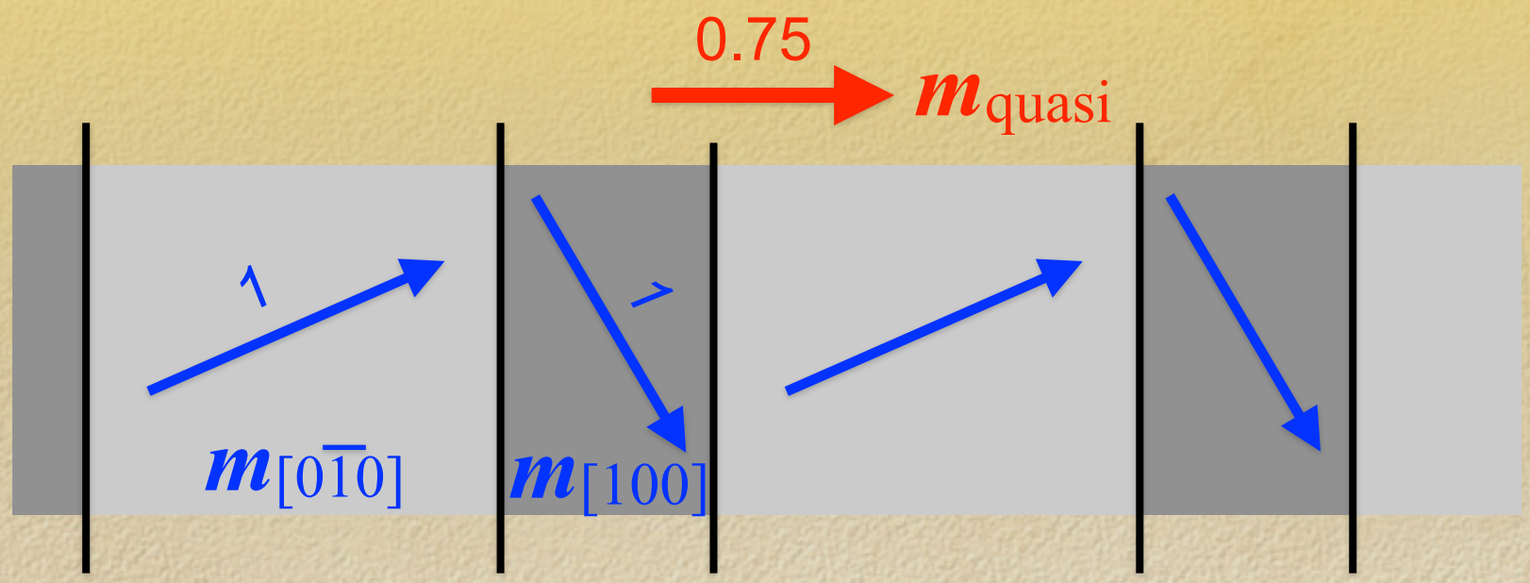

Quasi-Domains

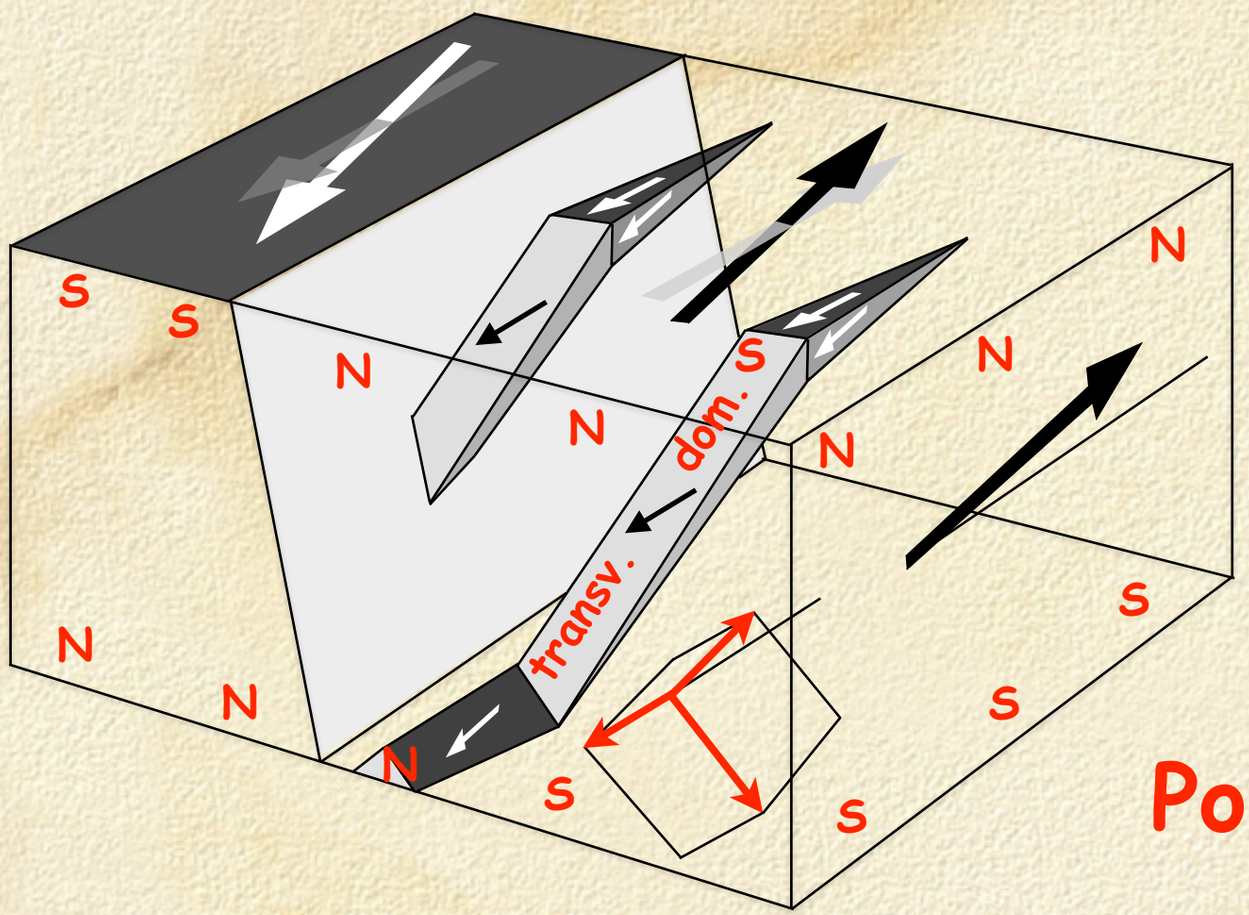

Lancet pattern on slightly misoriented (110) surface

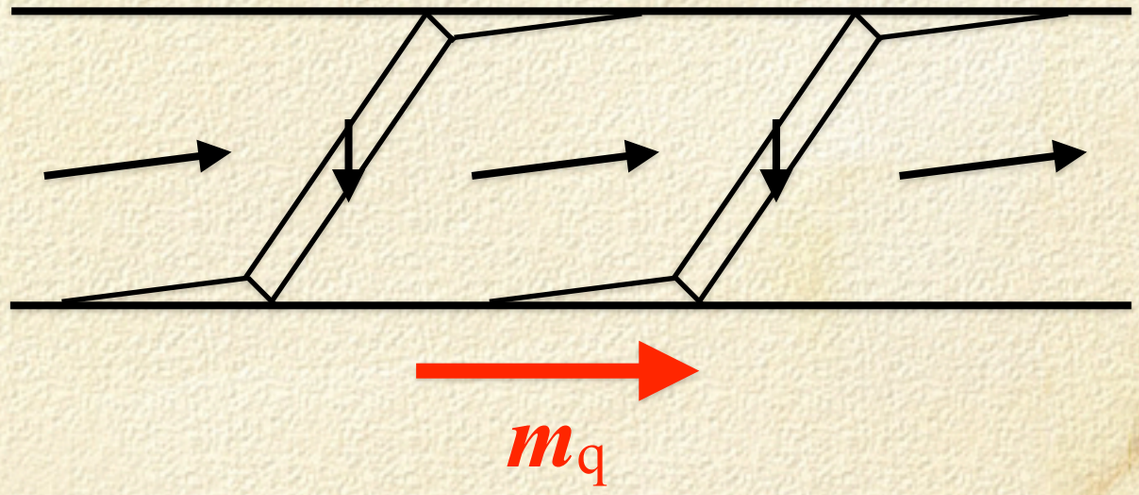

Pole-free on macroscopic scale

Misorientation: **2°** **4°** **8°**

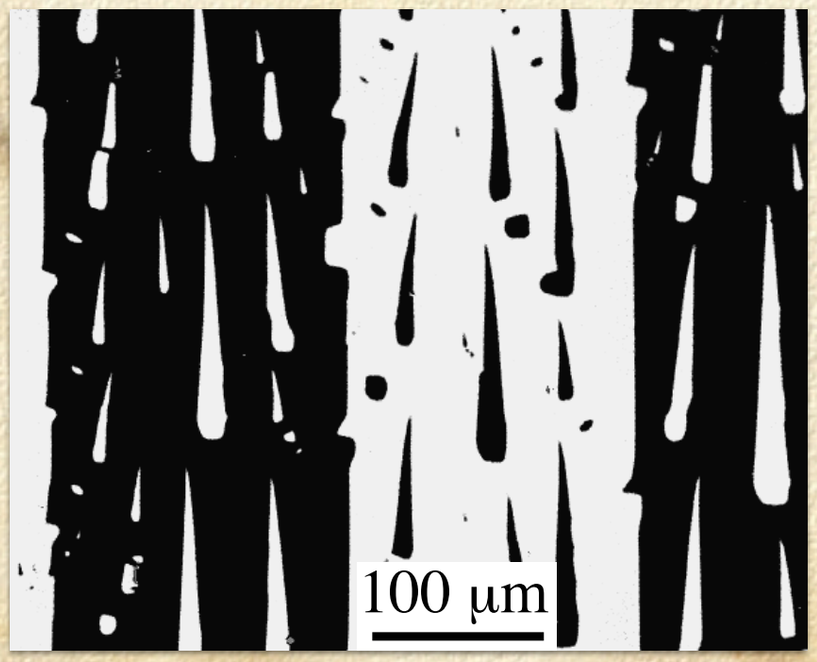

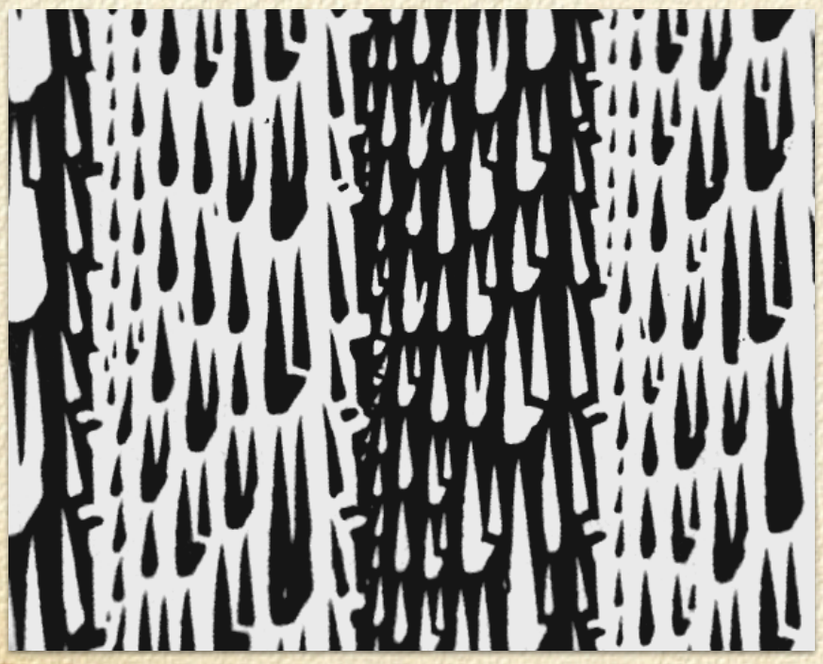

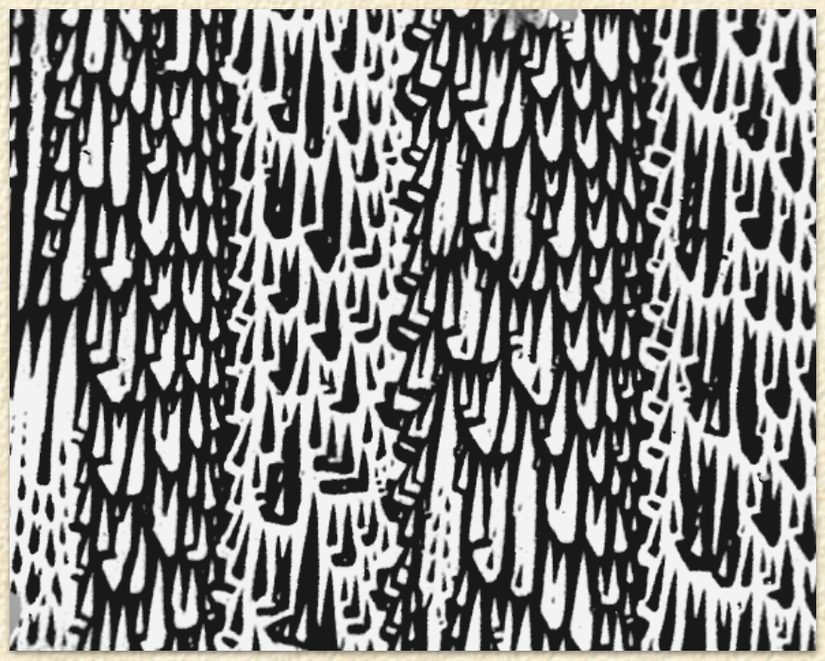

Non-oriented FeSi sheet

Folded bands and Quasi-domains [A. Hubert]

In bulk of non-oriented material:

Folded bands of "quasi-domains" that are able to carry the flux along the working direction

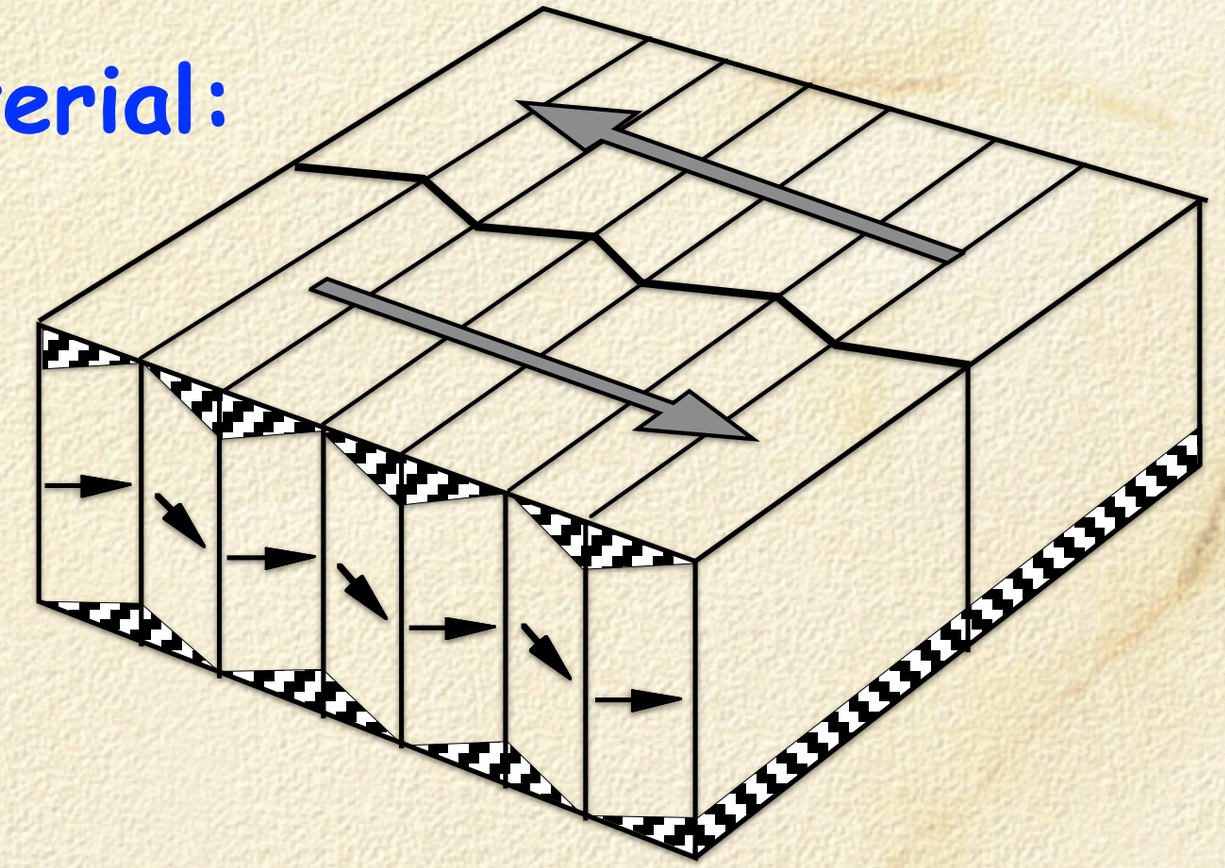

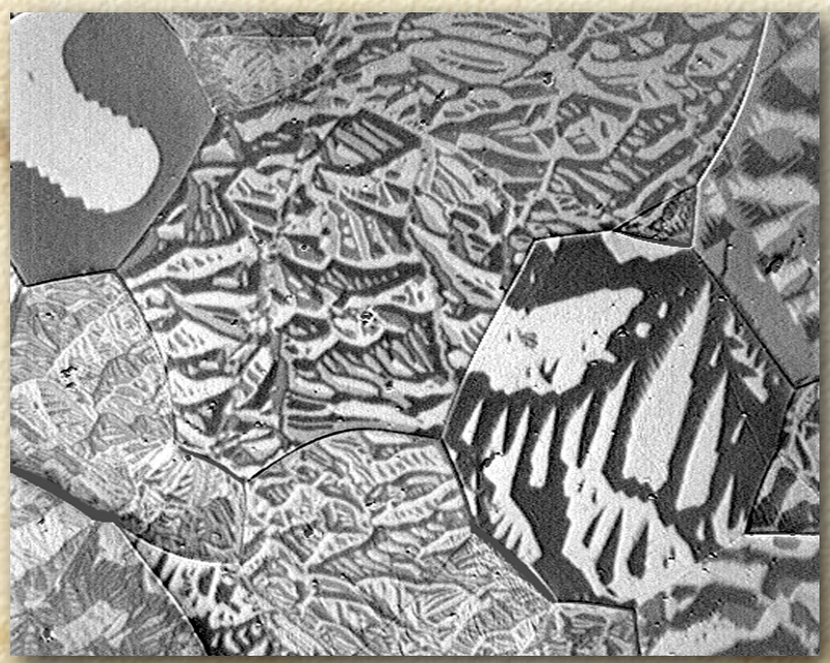

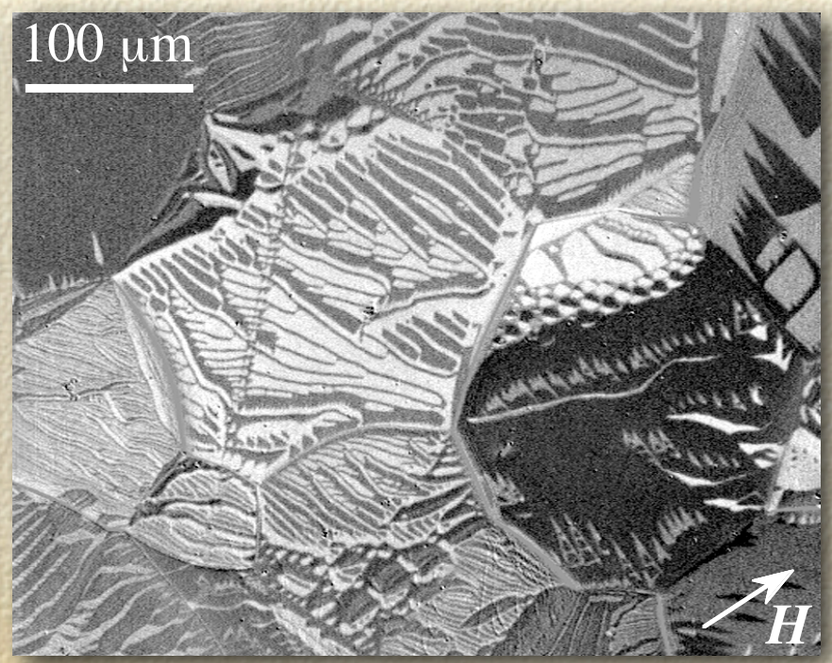

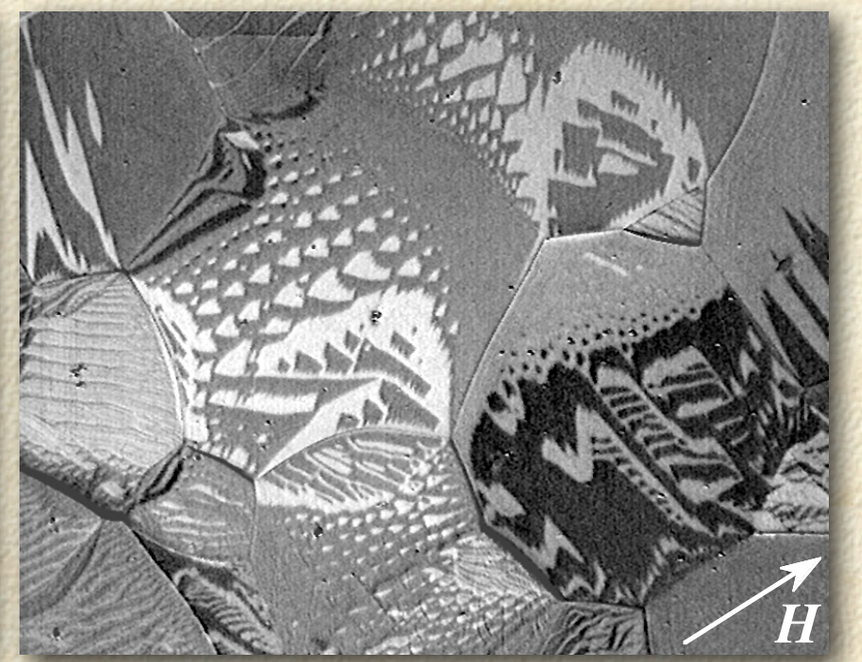

Non-oriented FeSi sheet

Folded bands and Quasi-domains [A. Hubert]

In bulk of non-oriented material:

Folded bands of "quasi-domains" that are able to carry the flux along the working direction

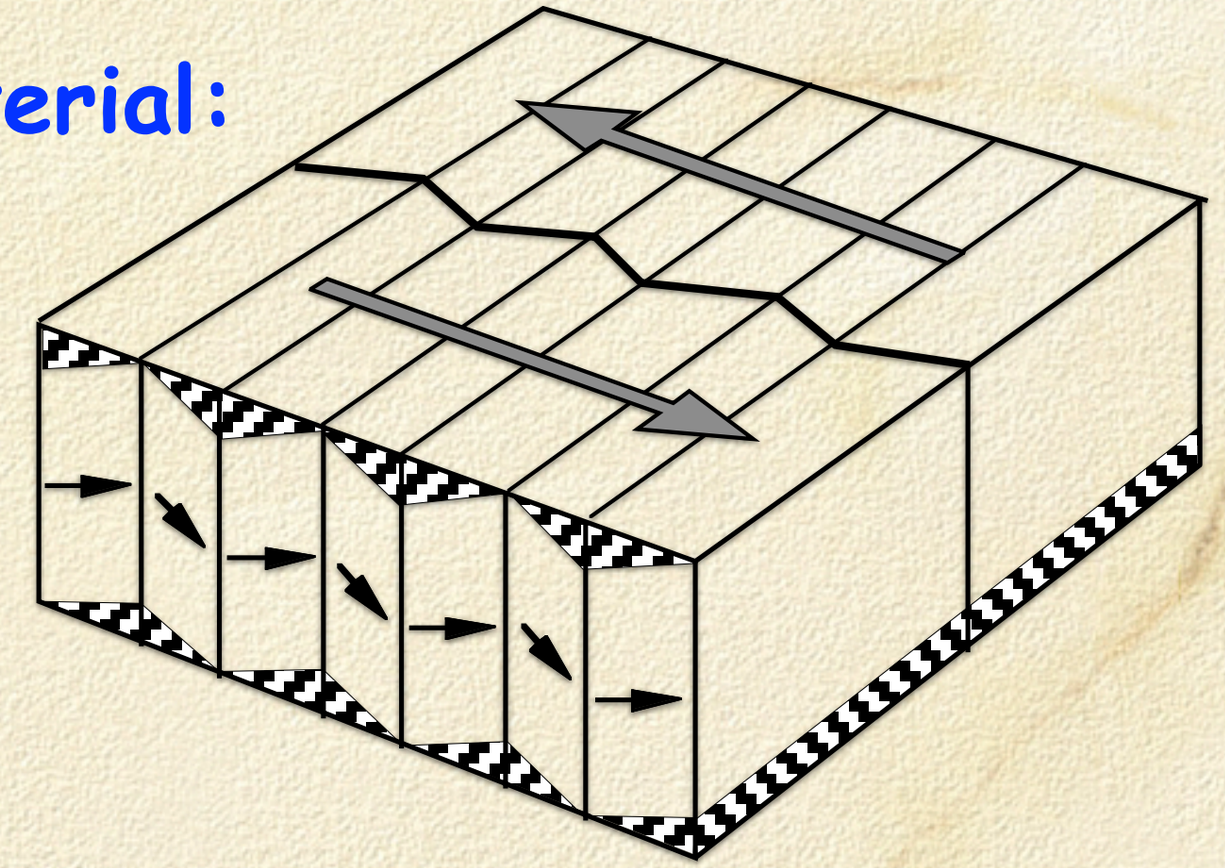

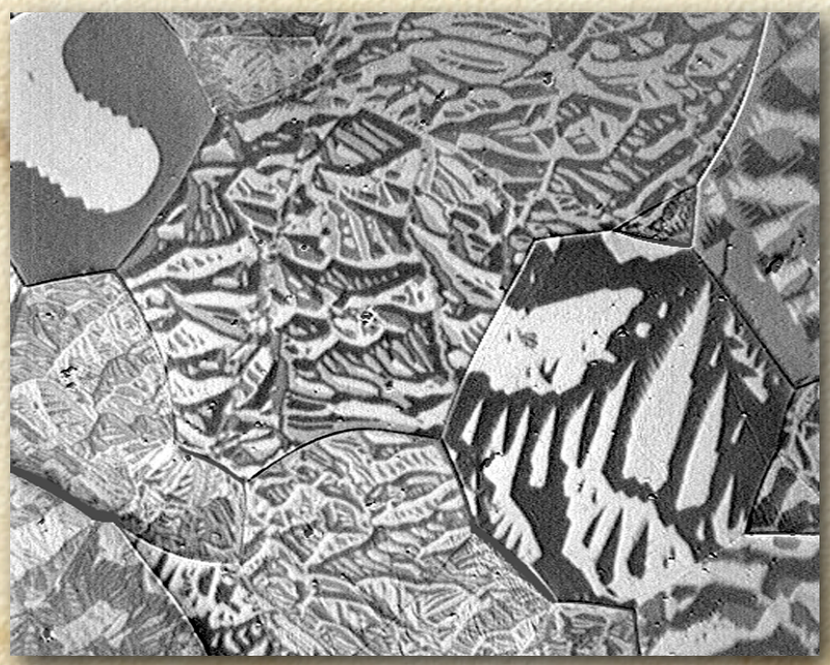

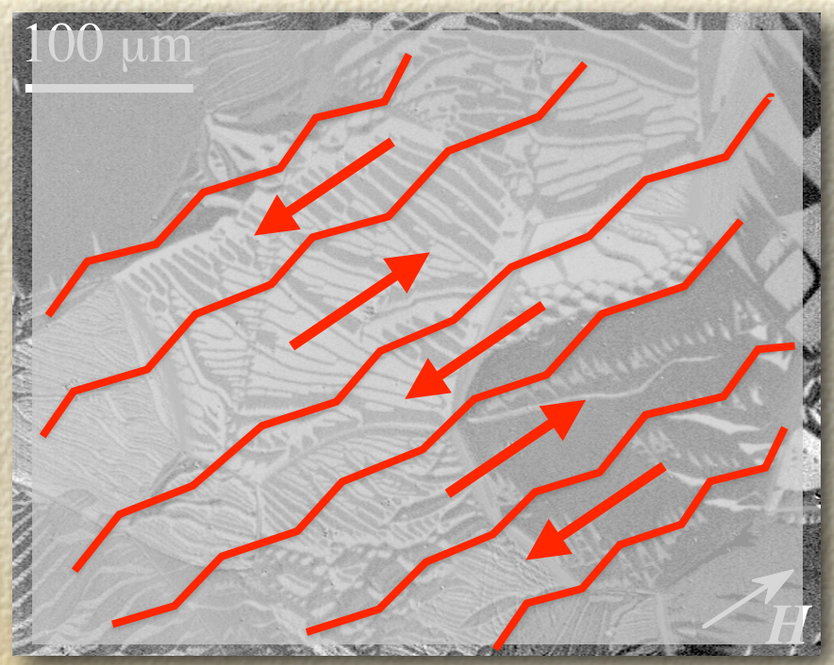

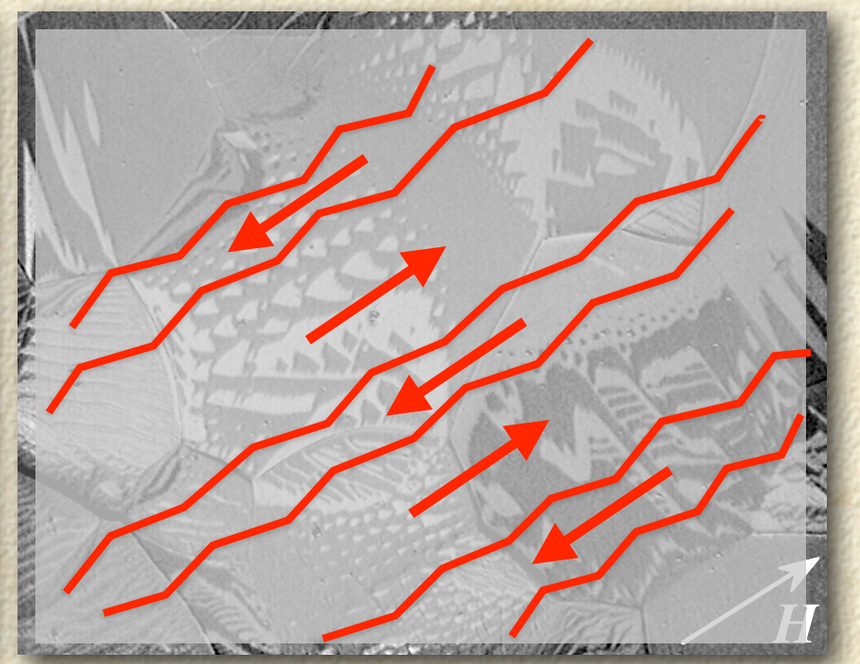

Non-oriented FeSi sheet

Indication of folded bands by surface observation

Non-oriented electrical steel (0.5 mm thick)

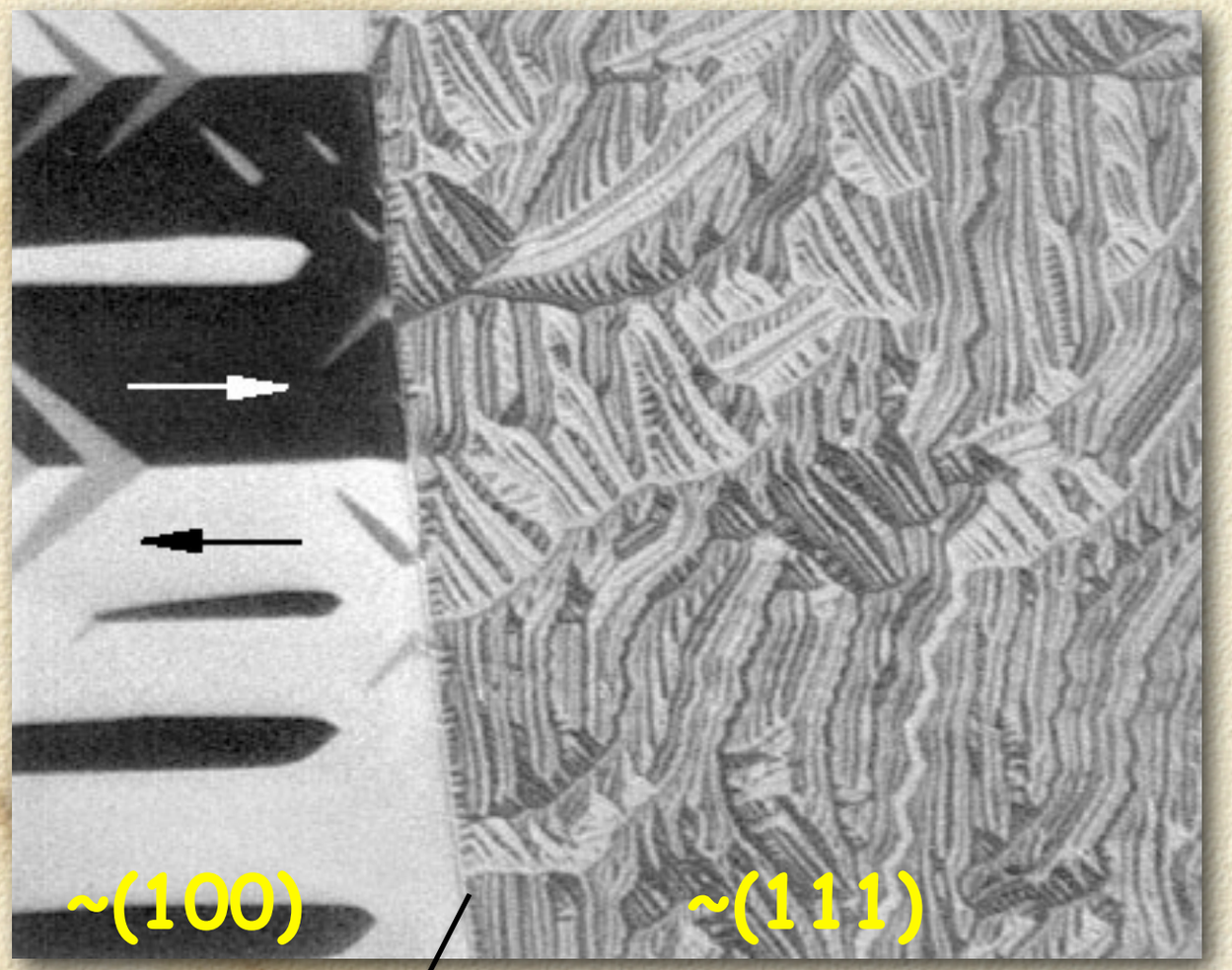

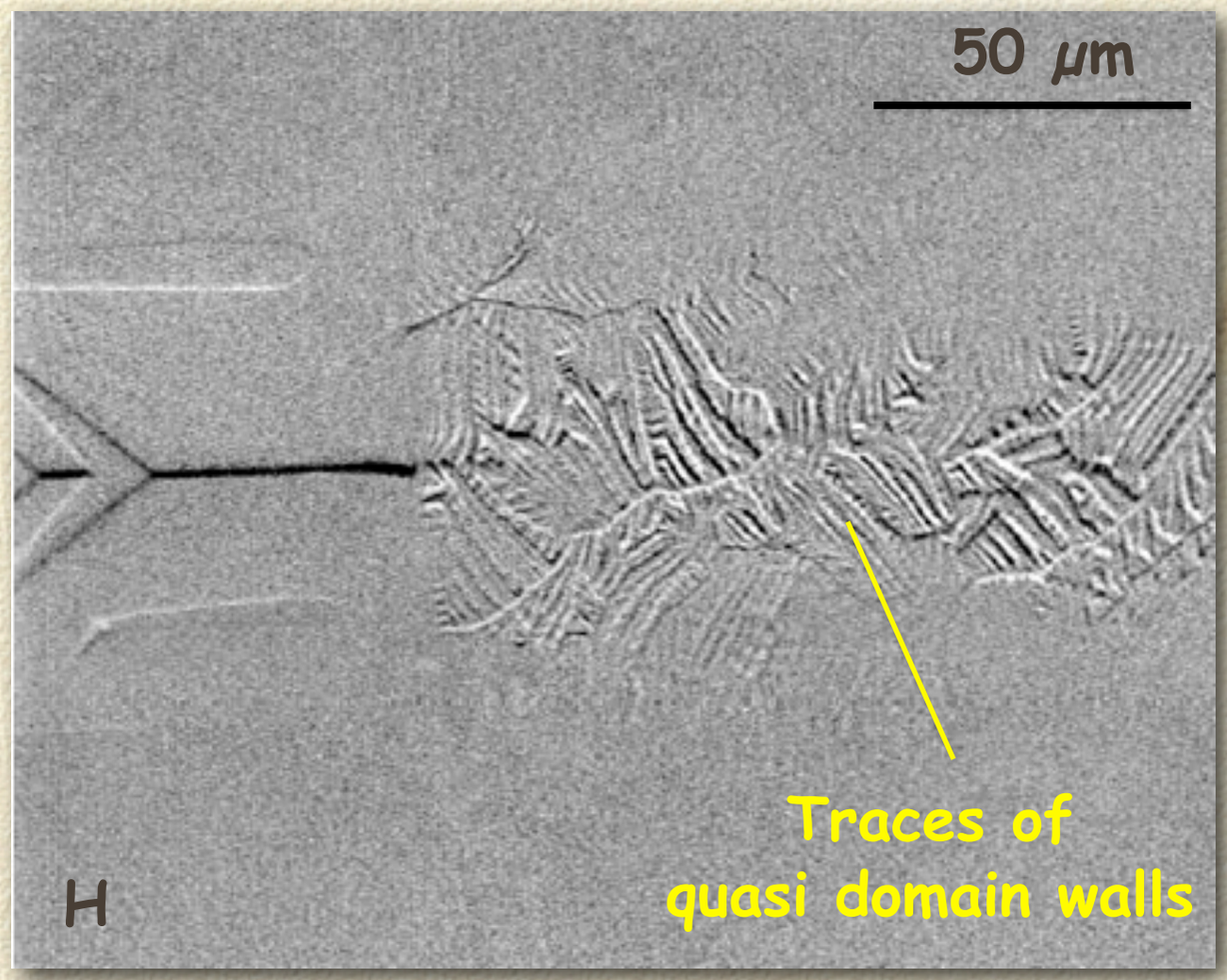

Difference between left image and image with field applied

Motor sheet

magnetic field

Motor sheet

magnetic ac field

Microstructure and Domains

What happens to domains, when grain size gets smaller ?

What happens to domains, when grain size gets smaller ?

Grain size: 100 μm range

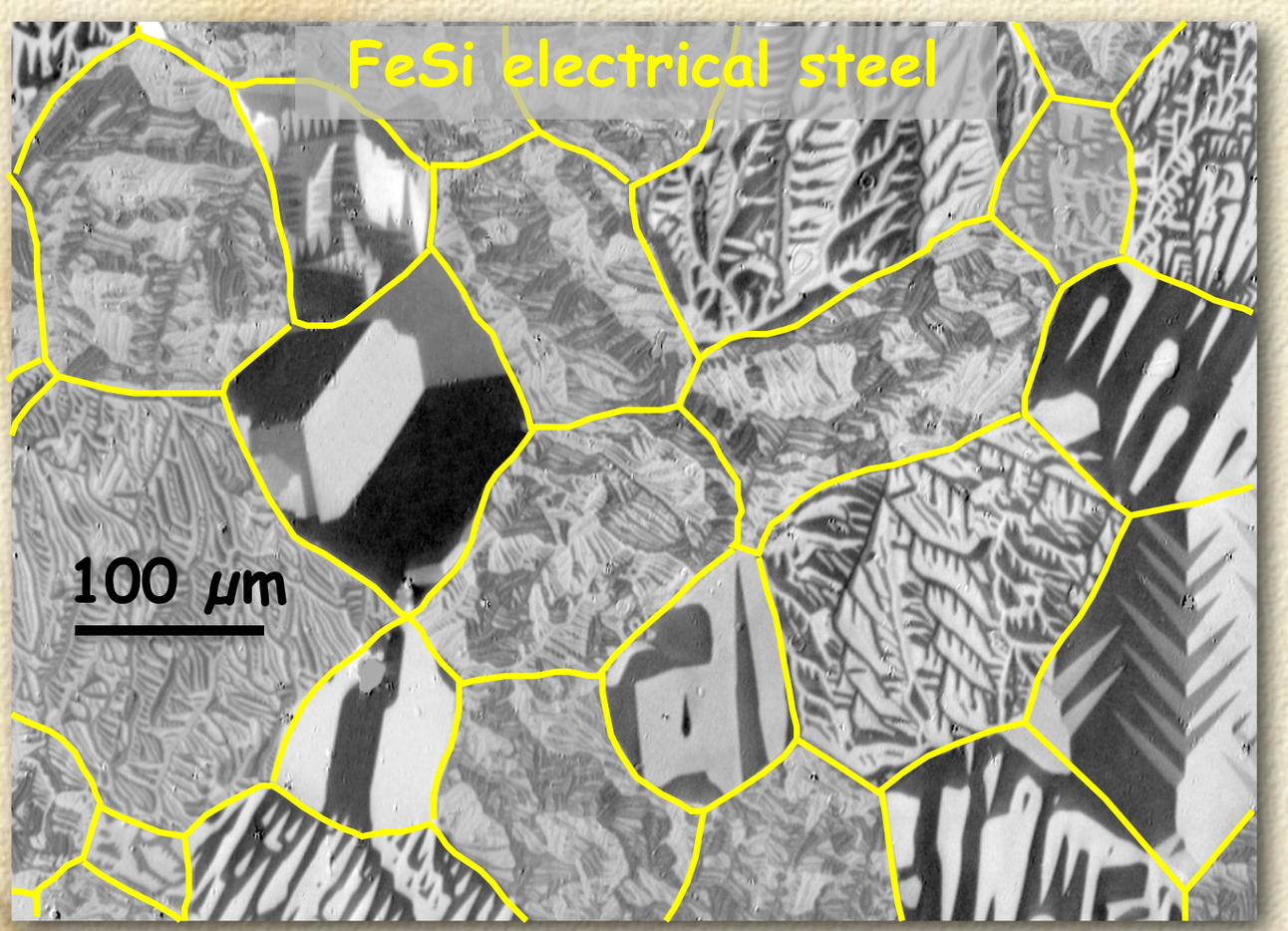

What happens to domains, when grain size gets smaller ?

Grain size:
100 μm range

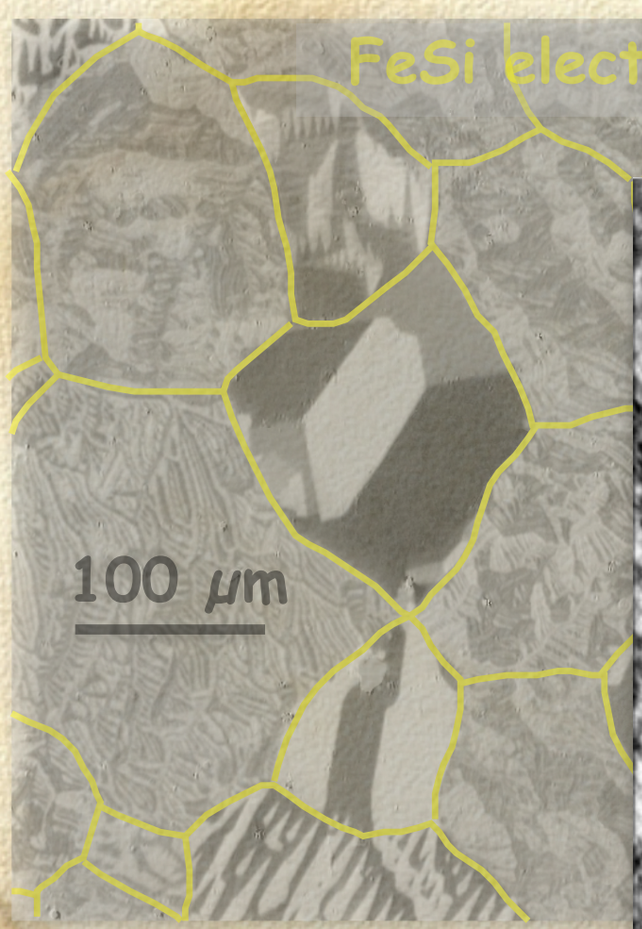

Grain size:
100 nm range

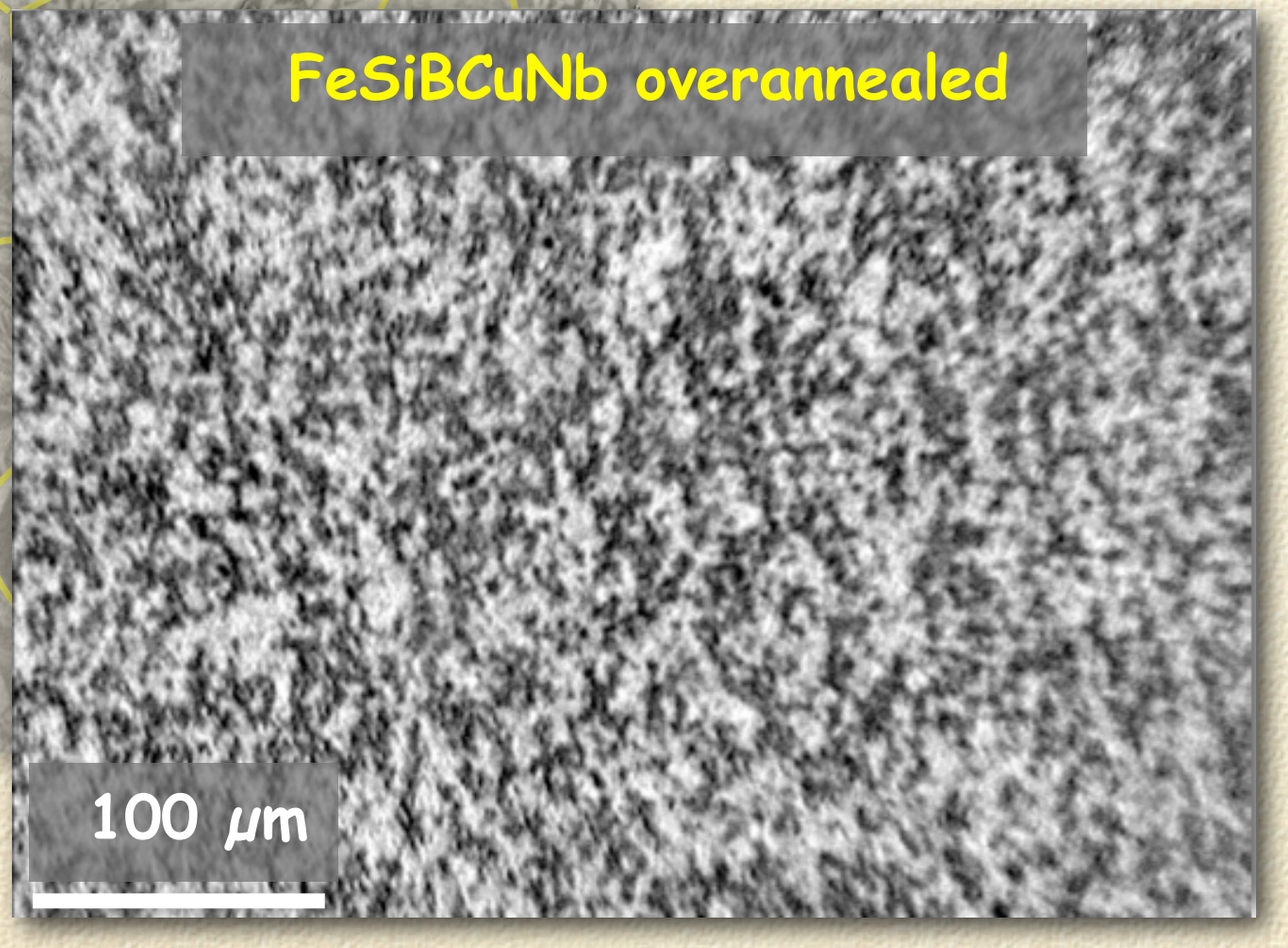

What happens to domains, when grain size gets smaller ?

Grain size:
100 μm range

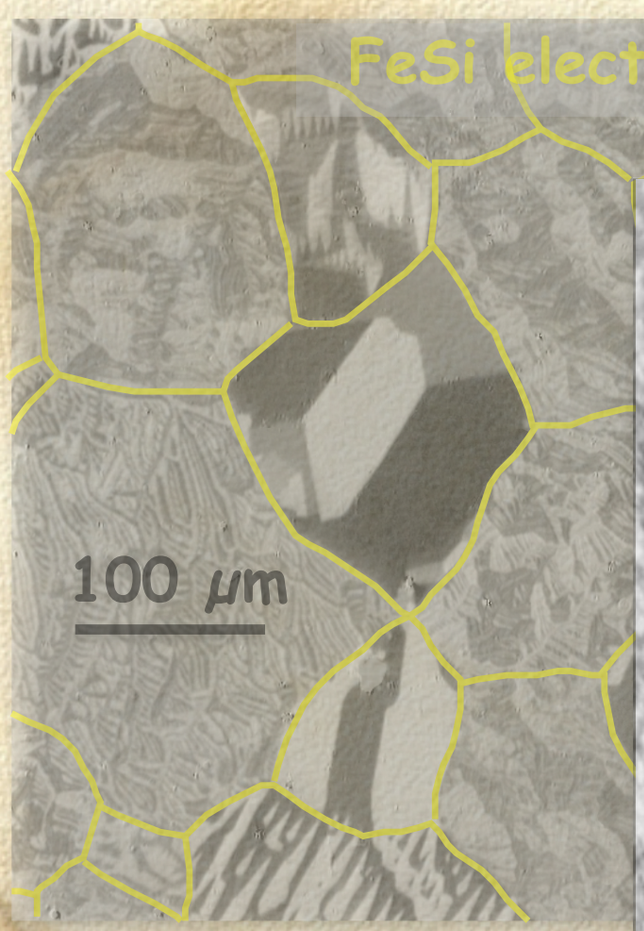

Grain size:
100 nm range

Grain size:
10 nm range

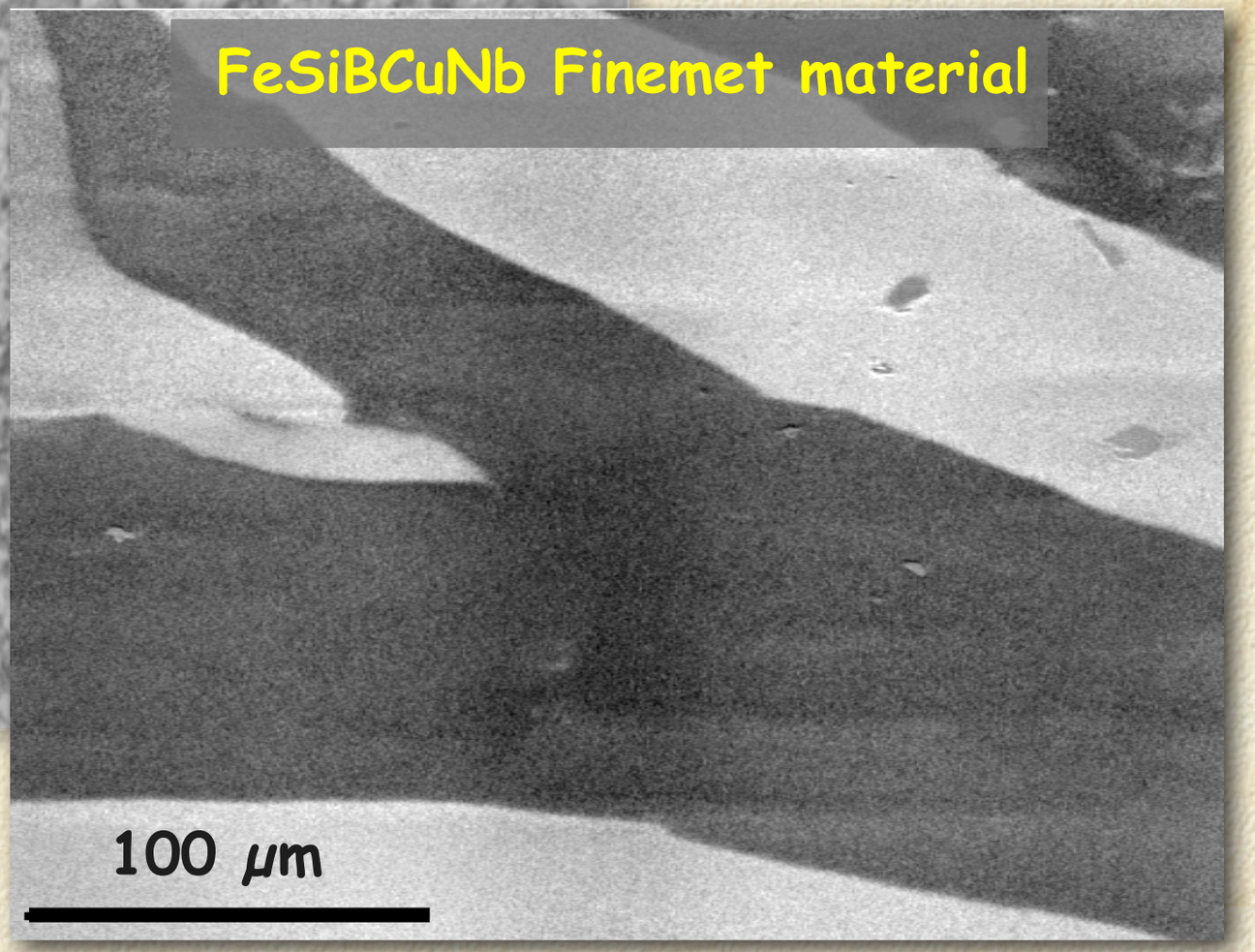

What happens to domains, when grain size gets smaller ?

Grain size:
100 μm range

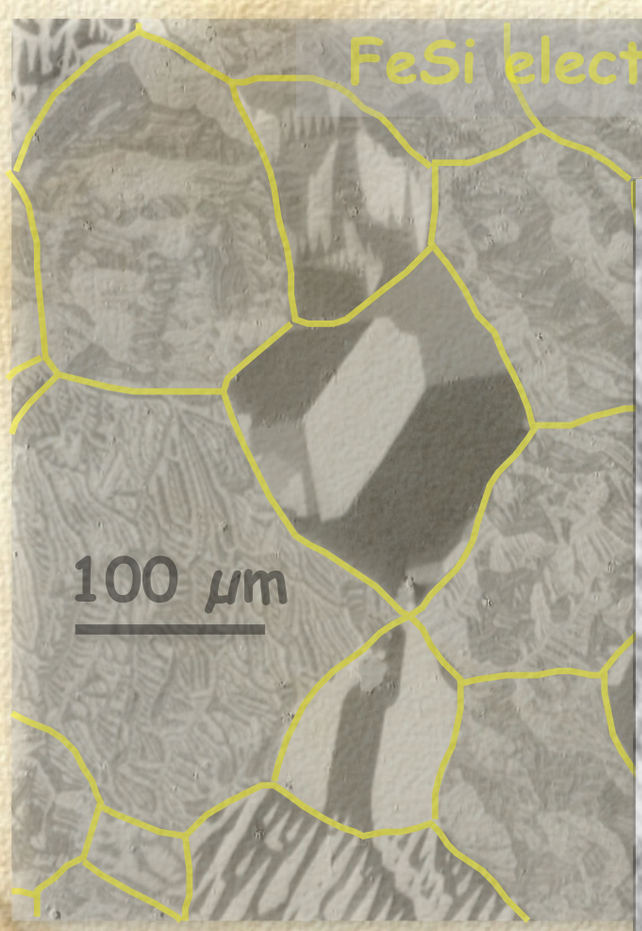

Grain size:
100 nm range

Grain size:
10 nm range

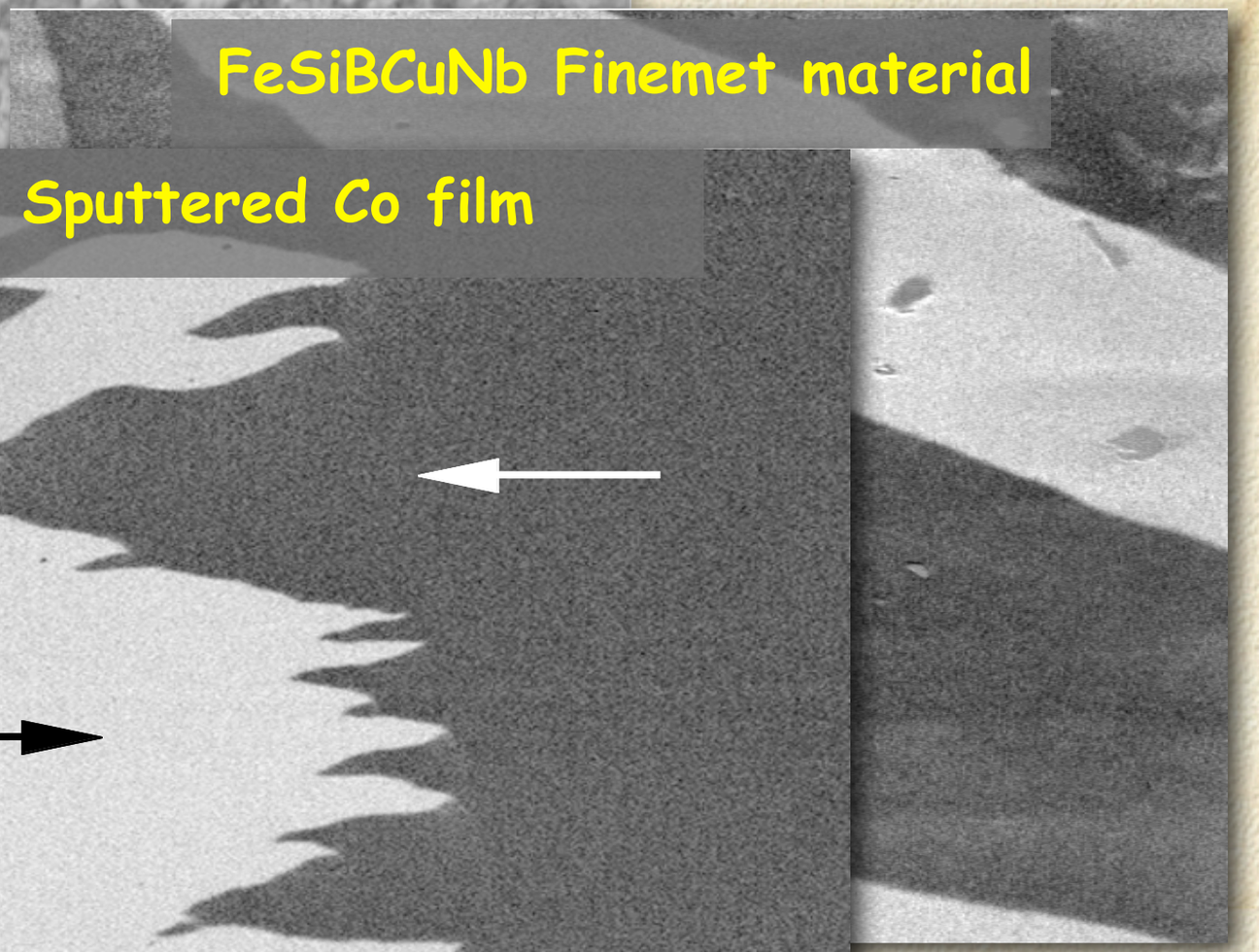

Nanocrystalline (Q<<1) materials

Low resolution

Nanocrystalline FeSiBCuNb ribbon (20 μm thick)

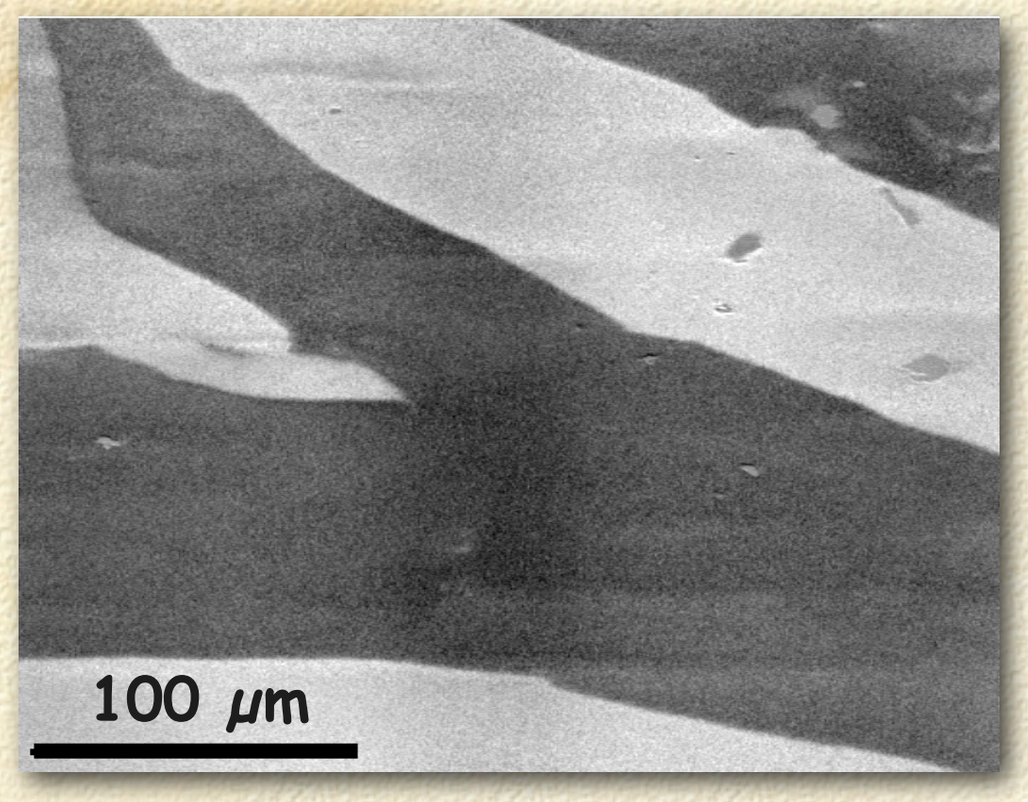

Sputtered Co film (60 nm thick)

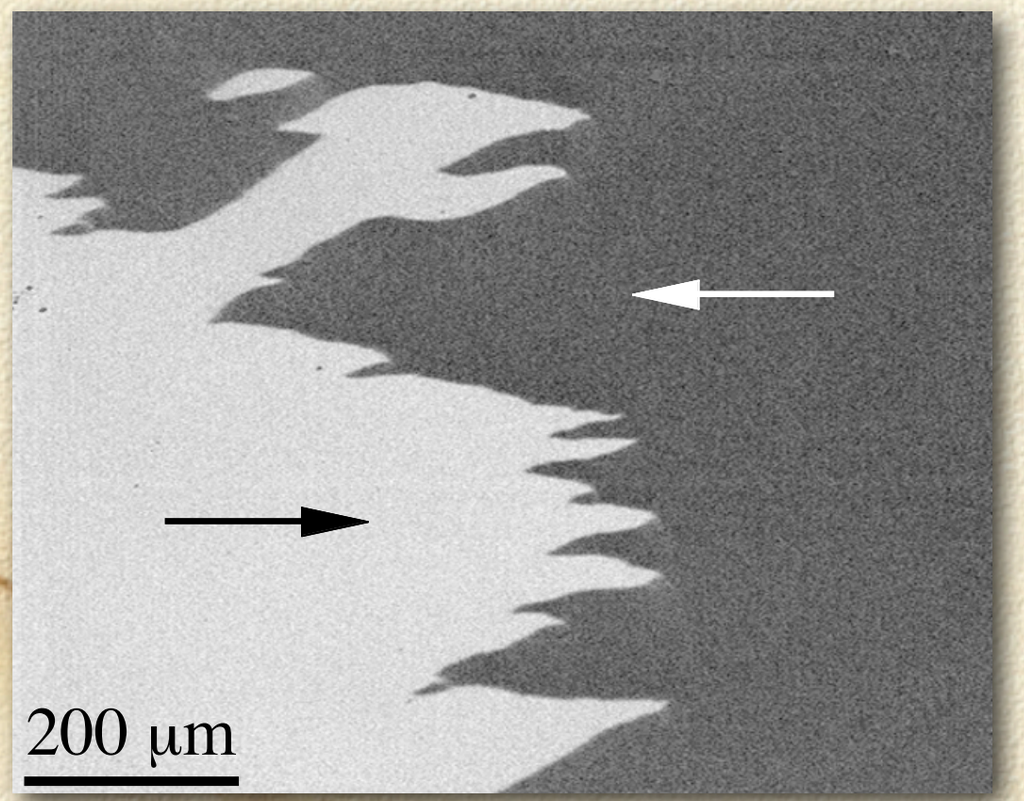

Nanocrystalline (Q<<1) materials

Low resolution

High resolution

Nanocrystalline FeSiBCuNb ribbon (20 μm thick)

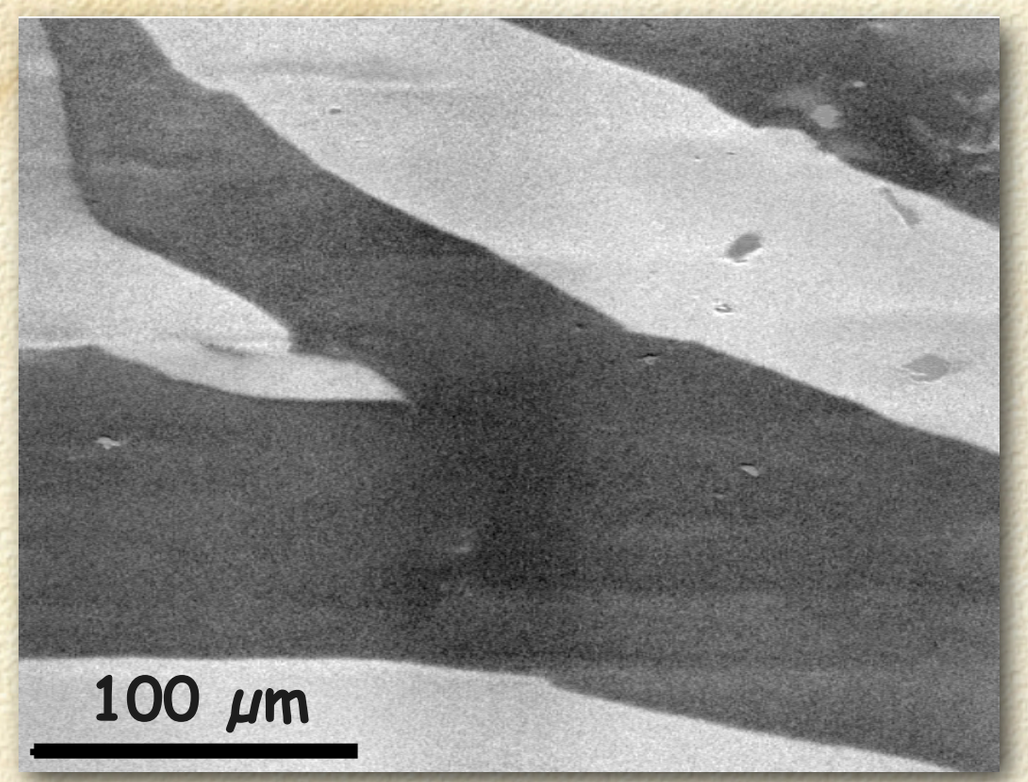

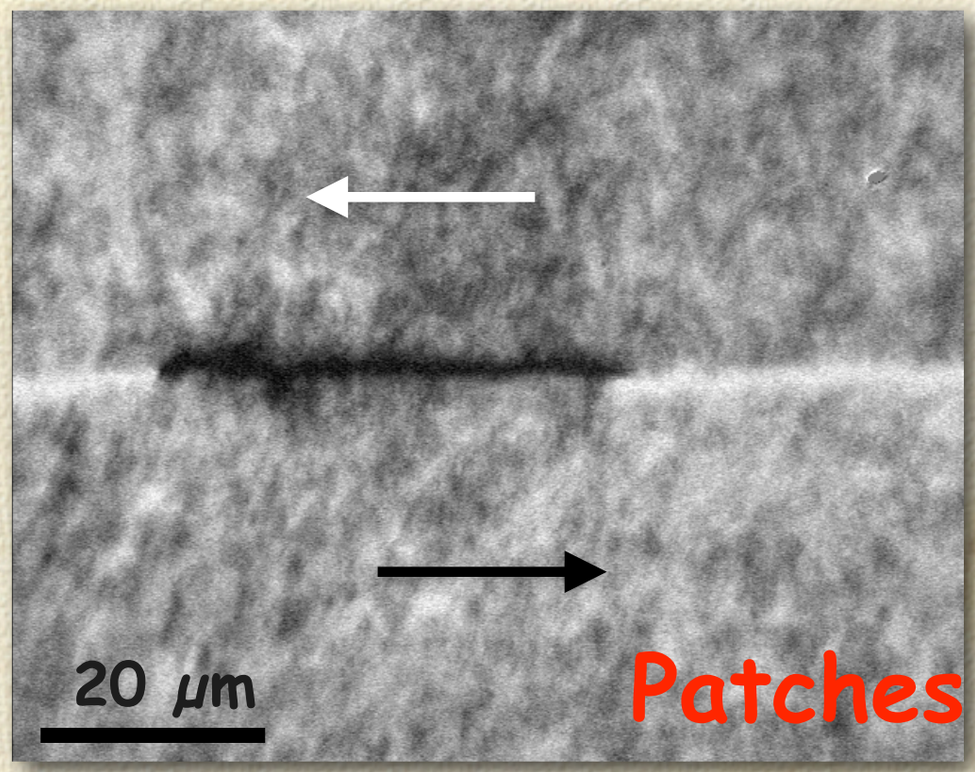

Sputtered Co film (60 nm thick)

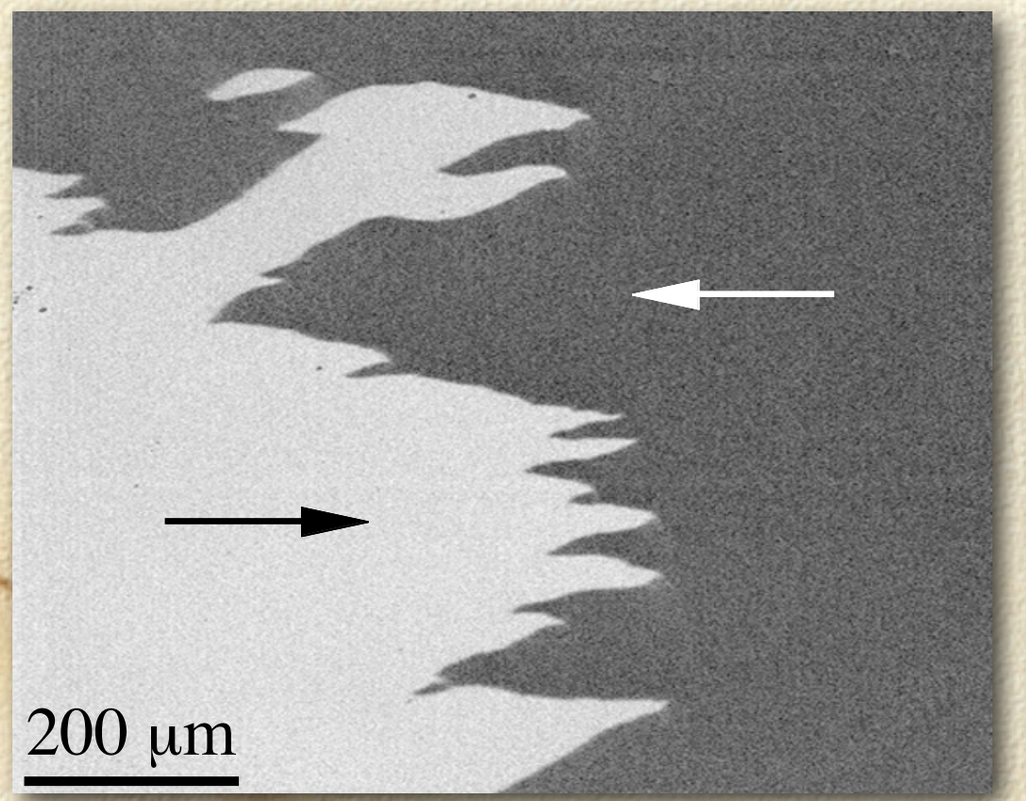

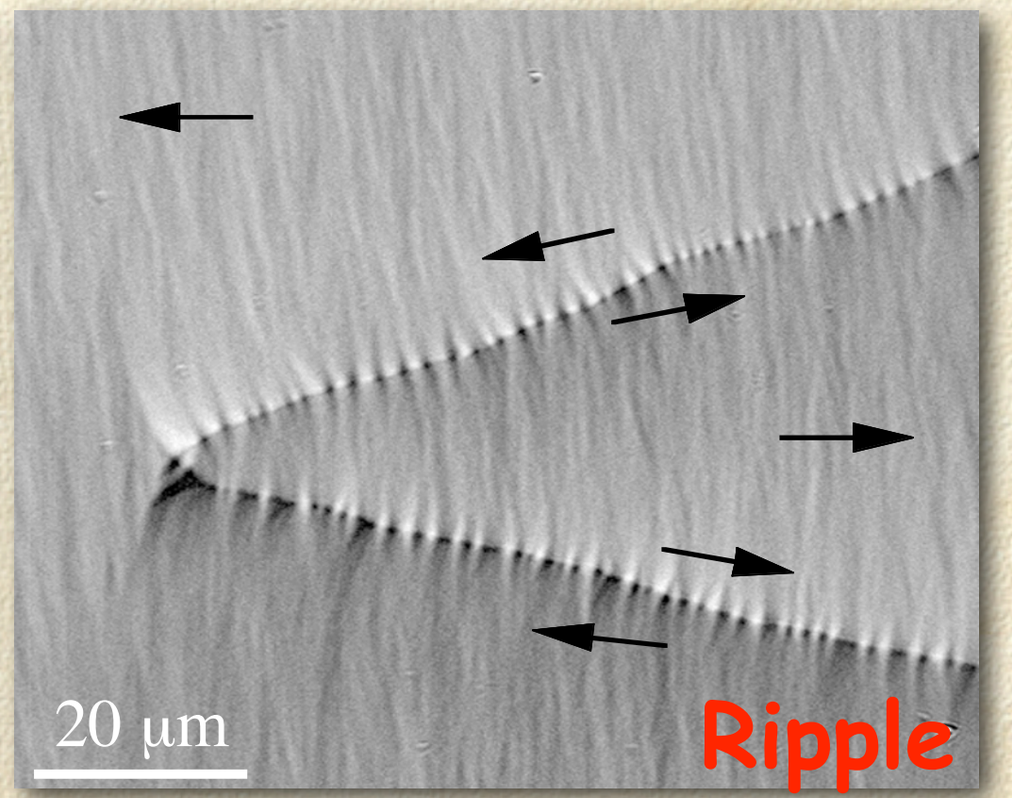

Nanocrystalline (Q<<1) materials

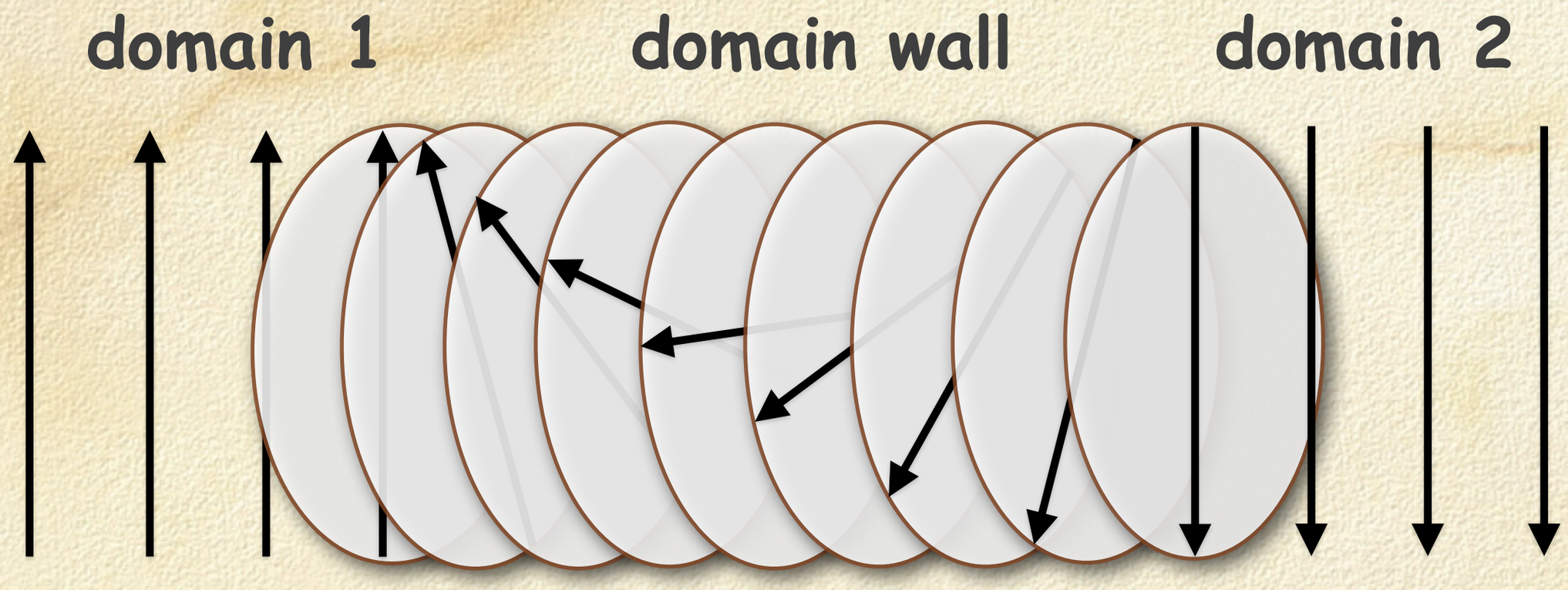

$$\pi\sqrt{A/K}$$

K: anisotropy constant
A: exchange constant

Nanocrystalline (Q<<1) materials

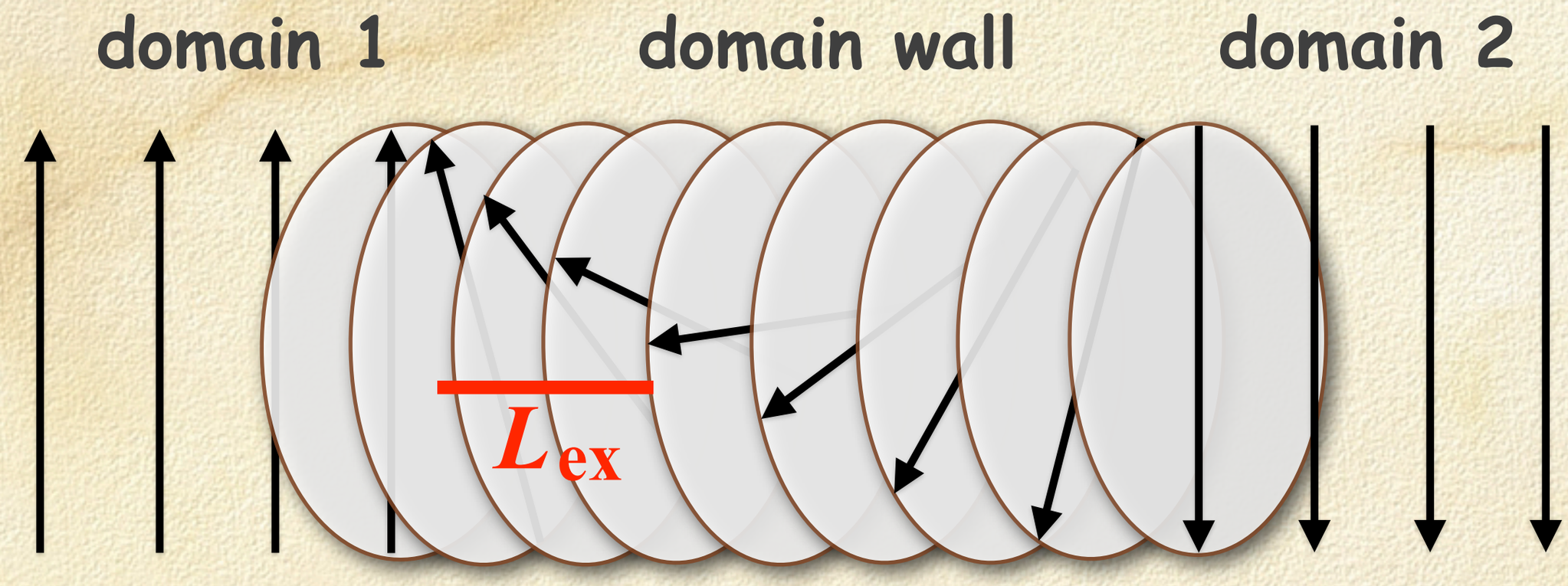

$$L_{ex} = \pi\sqrt{A/K}$$

K: anisotropy constant
A: exchange constant

ferromagnetic correlation length (exchange length):

minimum scale for appreciable variation of magnetization
(parallel moments for $L < L_{ex}$)

Nanocrystalline (Q<<1) materials

Random anisotropy model [Herzer 1989]:

Exchange interaction averages over anisotropy of grains

$$L_{ex} = \sqrt{A/K_{cryst}}$$

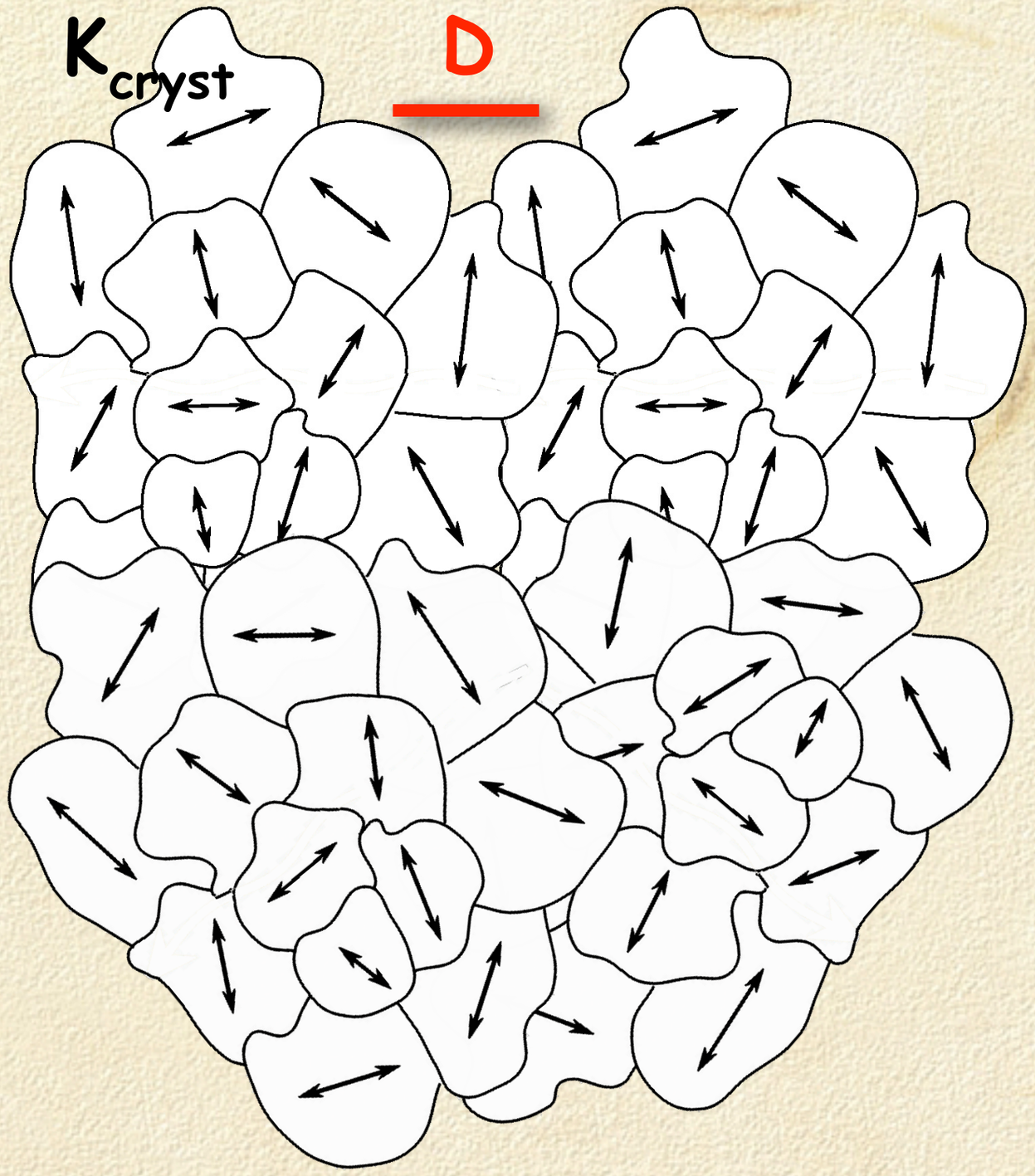

Nanocrystalline (Q<<1) materials

Random anisotropy model [Herzer 1989]:

Exchange interaction averages over anisotropy of grains

$$L_{ex} = \sqrt{A/K_{cryst}}$$

Nanocrystals: $D < L_{ex}$

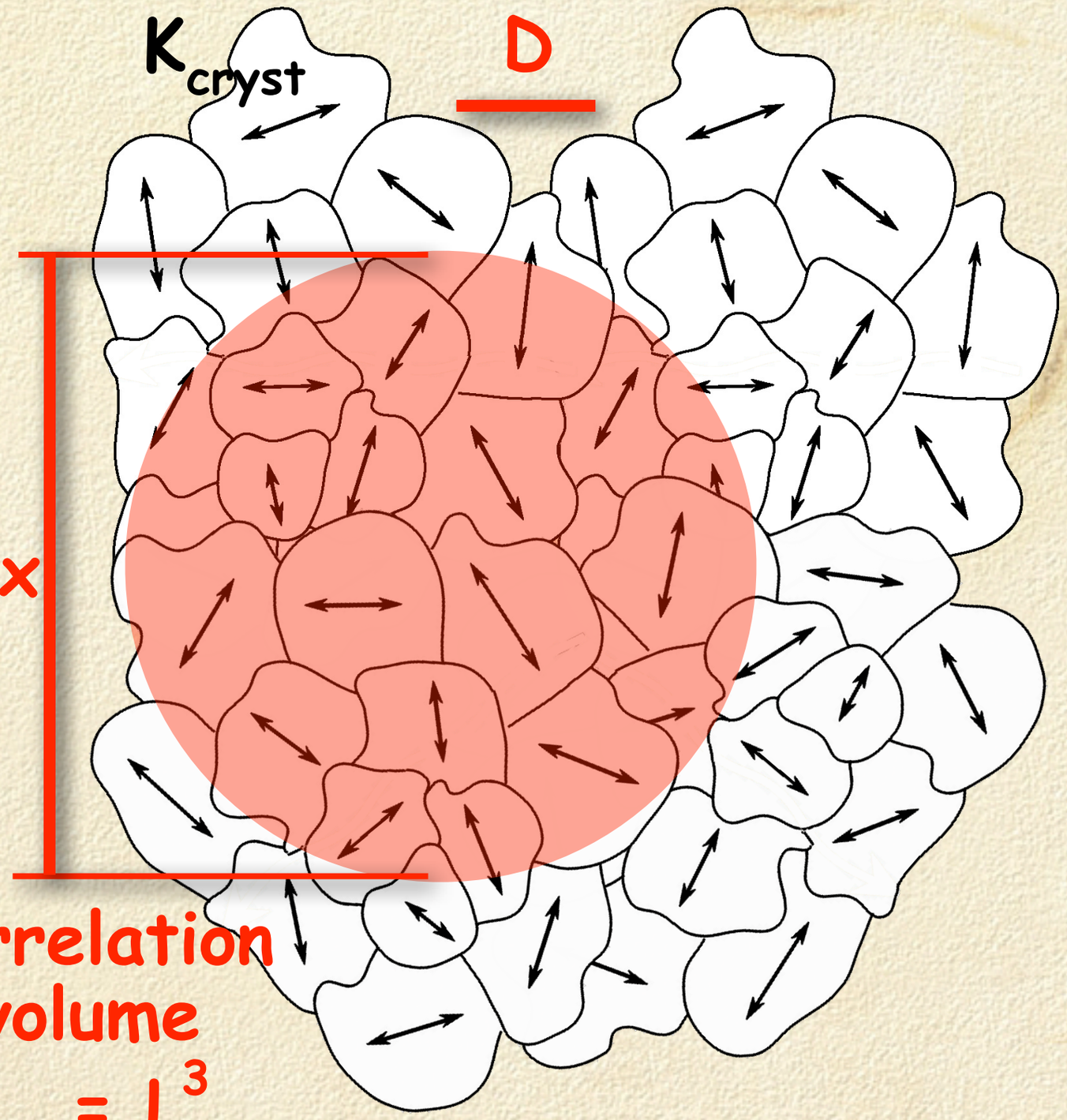

Nanocrystalline (Q<<1) materials

Random anisotropy model [Herzer 1989]:

Exchange interaction averages over anisotropy of grains

$$L_{ex} = \sqrt{A/K_{cryst}}$$

Nanocrystals: D < L_{ex}

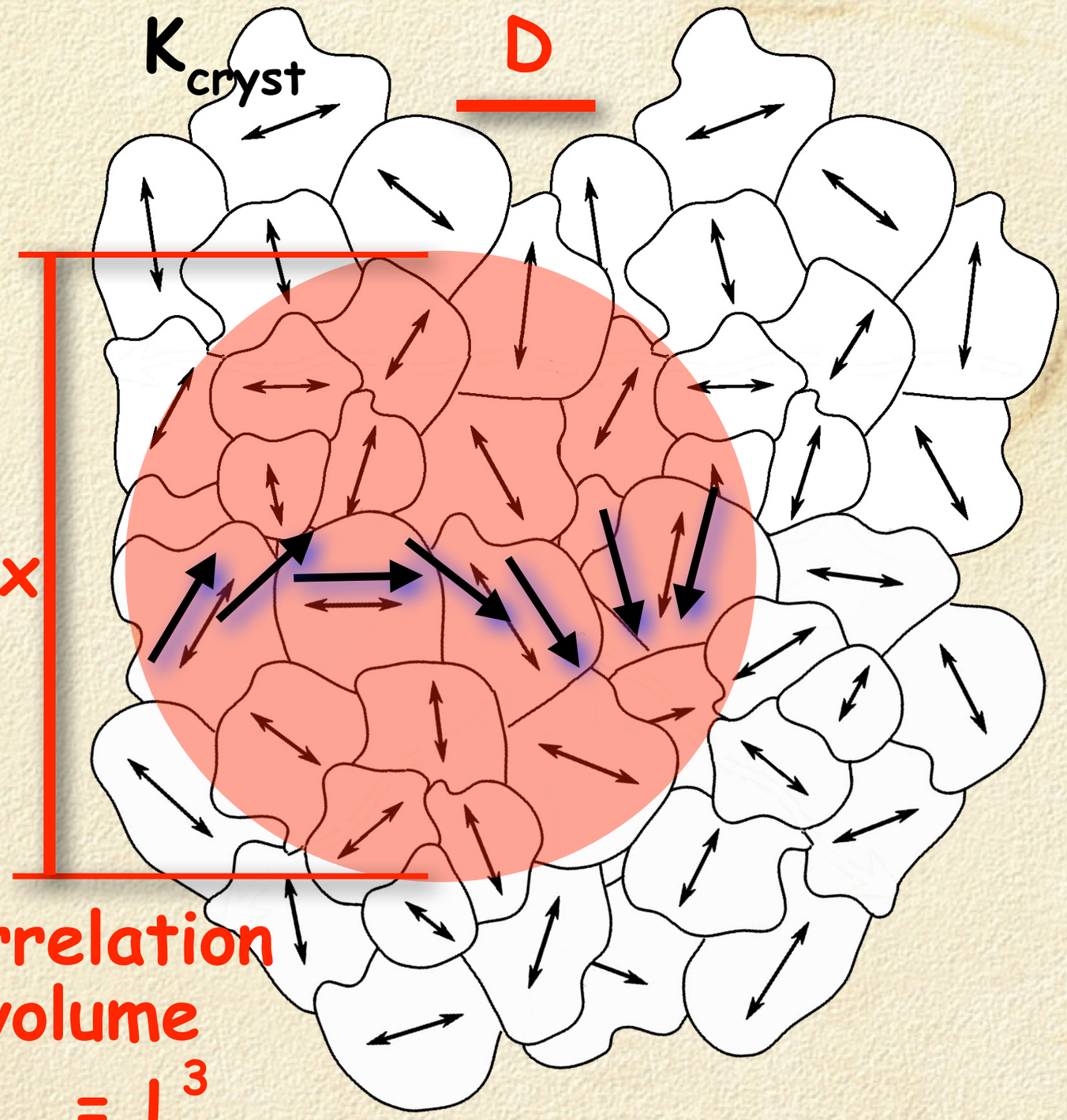

correlation volume

$V_{ex} = L_{ex}^3$

Nanocrystalline (Q<<1) materials

Random anisotropy model [Herzer 1989]:

Exchange interaction averages over anisotropy of grains

$$L_{ex} = \sqrt{A/K_{cryst}}$$

Nanocrystals: $D < L_{ex}$

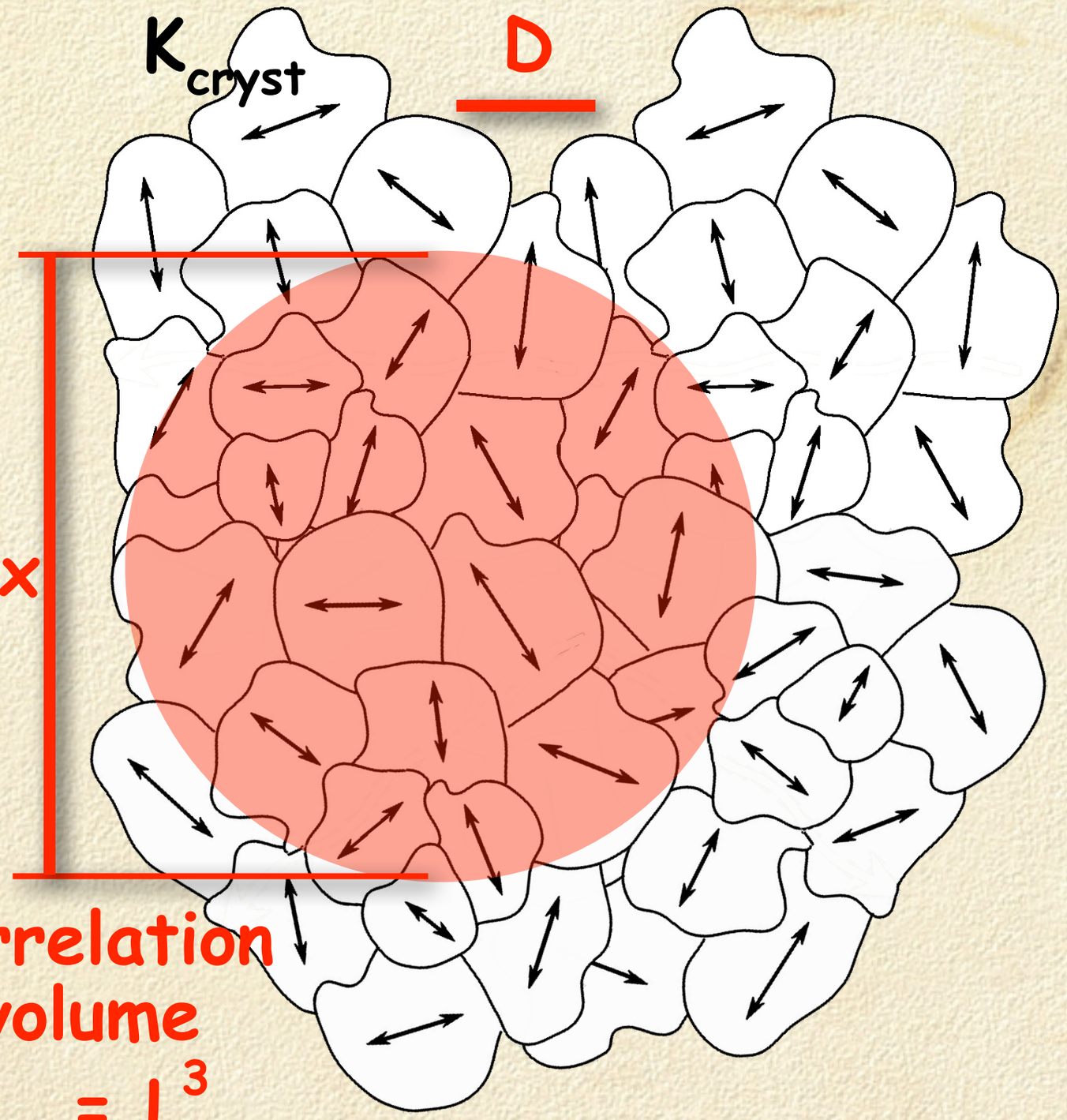

Nanocrystalline (Q<<1) materials

Random anisotropy model [Herzer 1989]:

Exchange interaction averages over anisotropy of grains

$$L_{ex} = \sqrt{A/K_{cryst}}$$

Nanocrystals: $D < L_{ex}$

→ $\langle K \rangle << K_{cryst}$

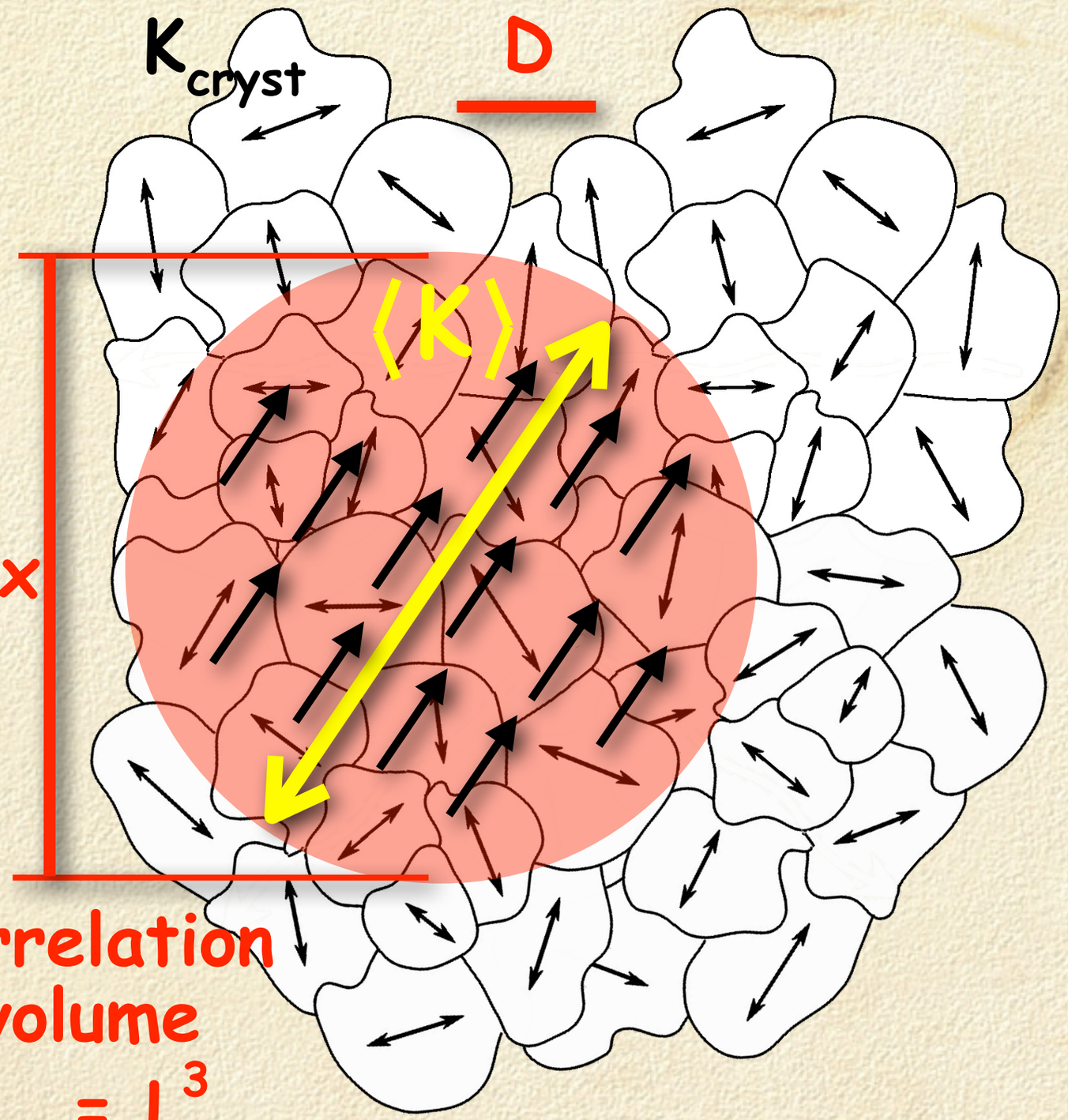

Nanocrystalline (Q<<1) materials

Random anisotropy model [Herzer 1989]:

Exchange interaction averages over anisotropy of grains

$$L_{ex} = \sqrt{A/K_{cryst}}$$

Nanocrystals: $D < L_{ex}$

$\rightarrow \langle K \rangle << K_{cryst}$

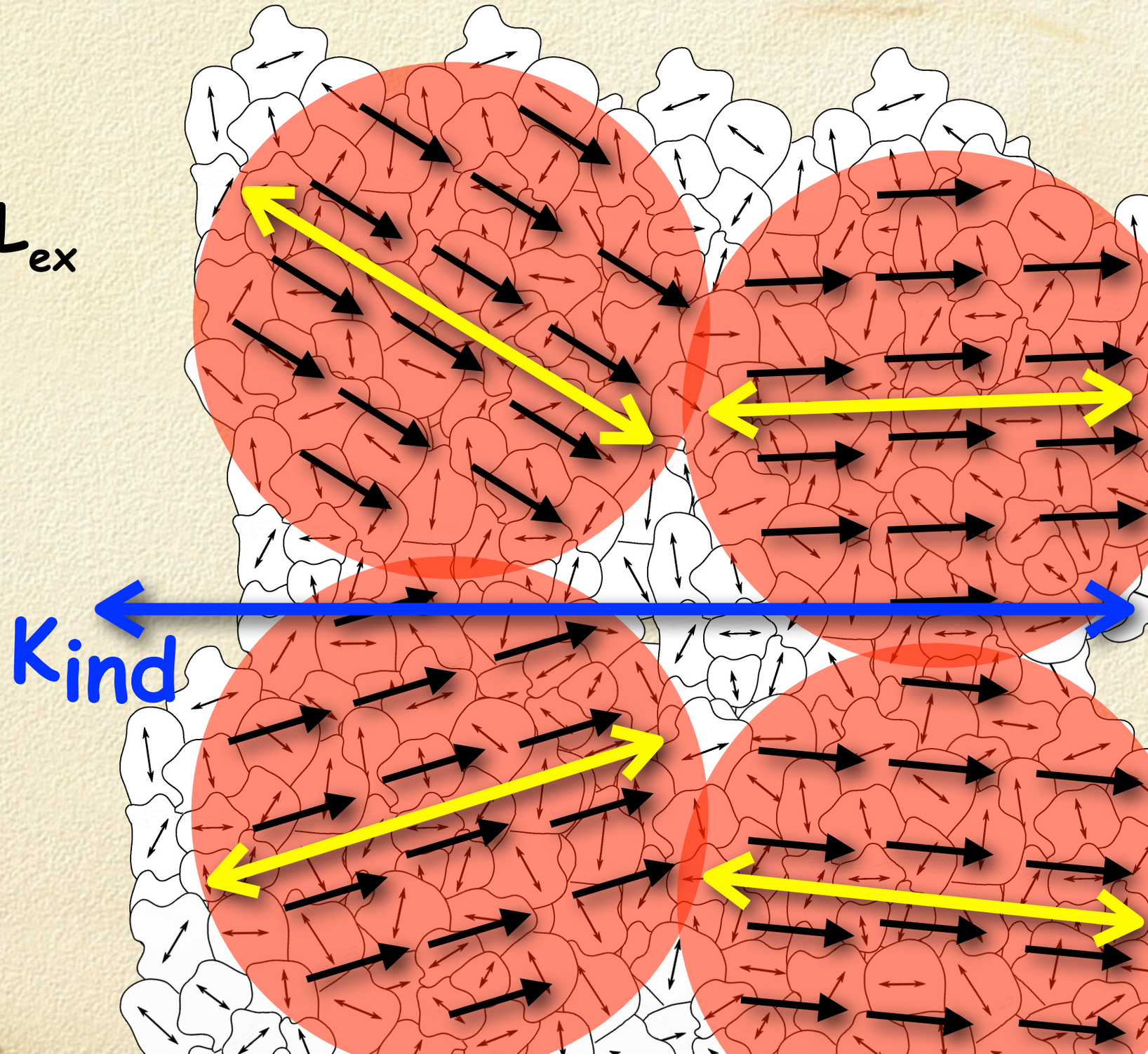

Exc ns

L_{ex}

No ex

→ $\langle K \rangle << K_{cryst}$

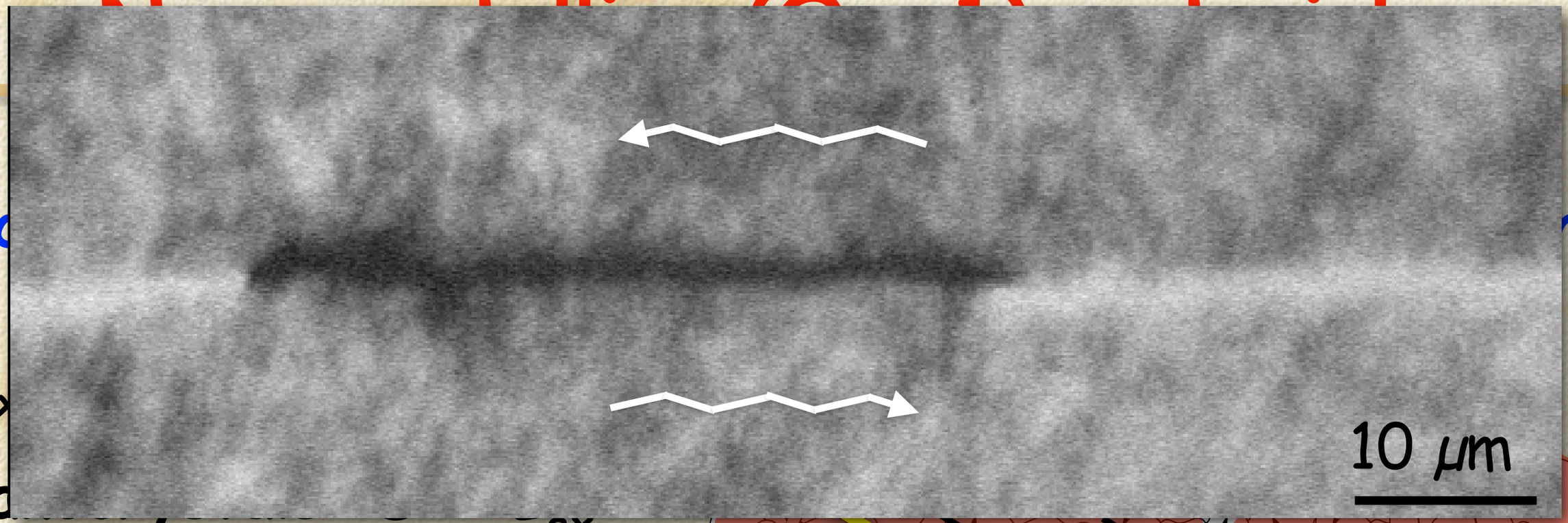

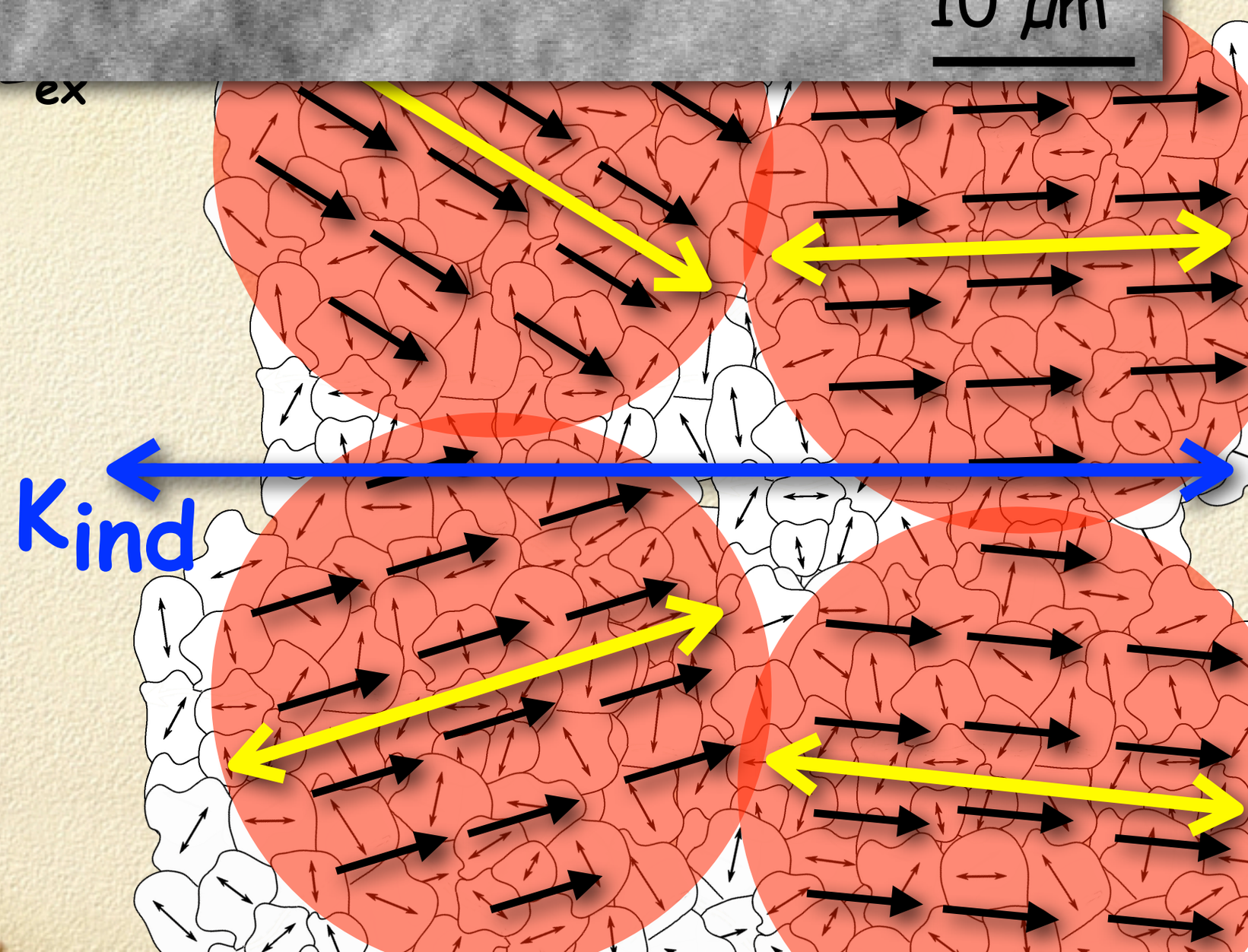

Nanocrystalline soft magnets

Interplay random/induced anisotropy

- Random anisotropy $\langle K \rangle$: modulated on scale of renormalized exchange length, $\langle K \rangle \approx 3$ J/m^3
- Induced anisotropy K_u: uniform on large scale, $K_u \approx 3 - 30$ J/m^3

  → interplay

S. Flohrer, R.S., Ch. Polak, G. Herzer,
Interplay of uniform and random anisotropy in nanocrystalline soft magnetic alloys.
Acta Mater. 53 (2005) 2937

G. Herzer, Anisotropies in soft magnetic nanocrystalline alloys.
J. Magn. Magn. Mat. 294 (2005) 99

Nanocrystalline soft magnets

Interplay random/induced anisotropy

- Random anisotropy $\langle K \rangle$: modulated on scale of renormalized exchange length, $\langle K \rangle \approx 3$ J/m^3
- Induced anisotropy K_u: uniform on large scale, $K_u \approx 3 - 30$ J/m^3

→ interplay

Low induced anisotropy

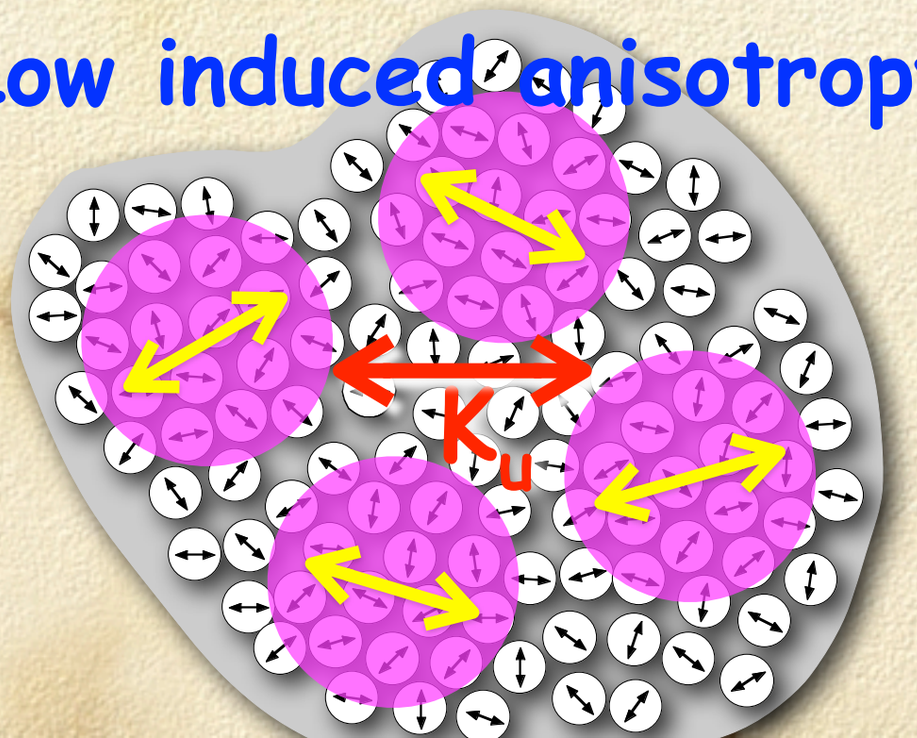

Strong induced anisotropy

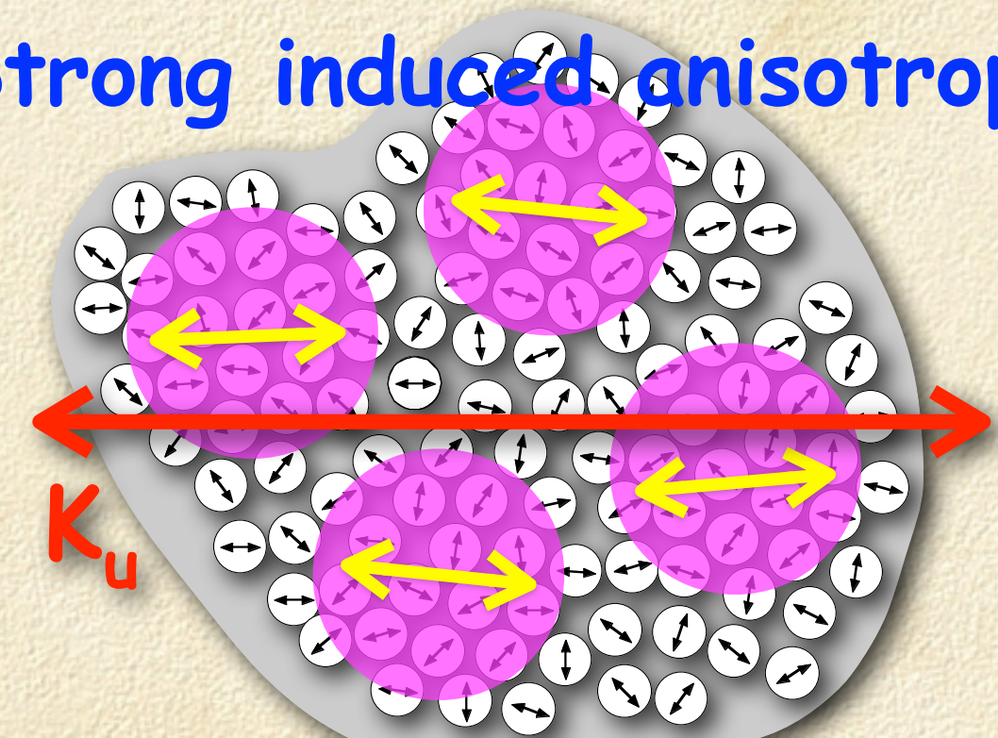

Nanocrystalline soft magnets

Interplay random/induced anisotropy

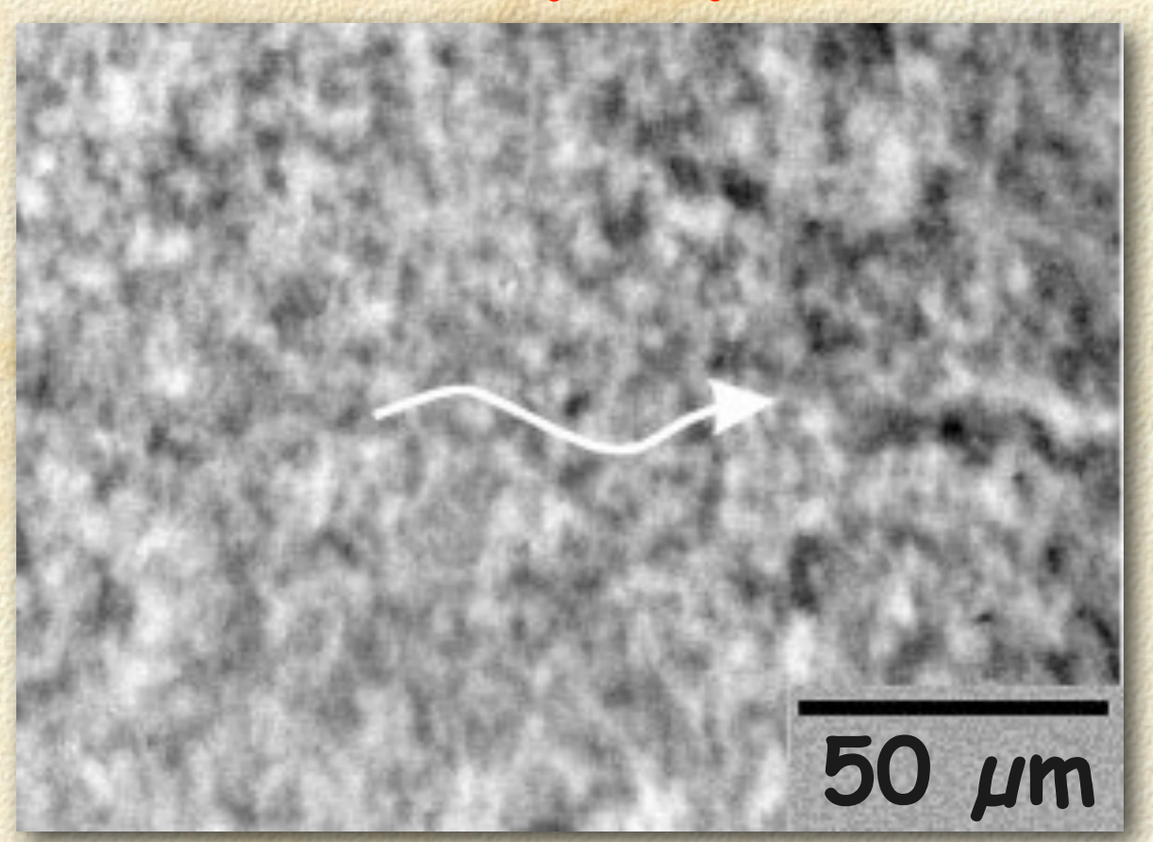

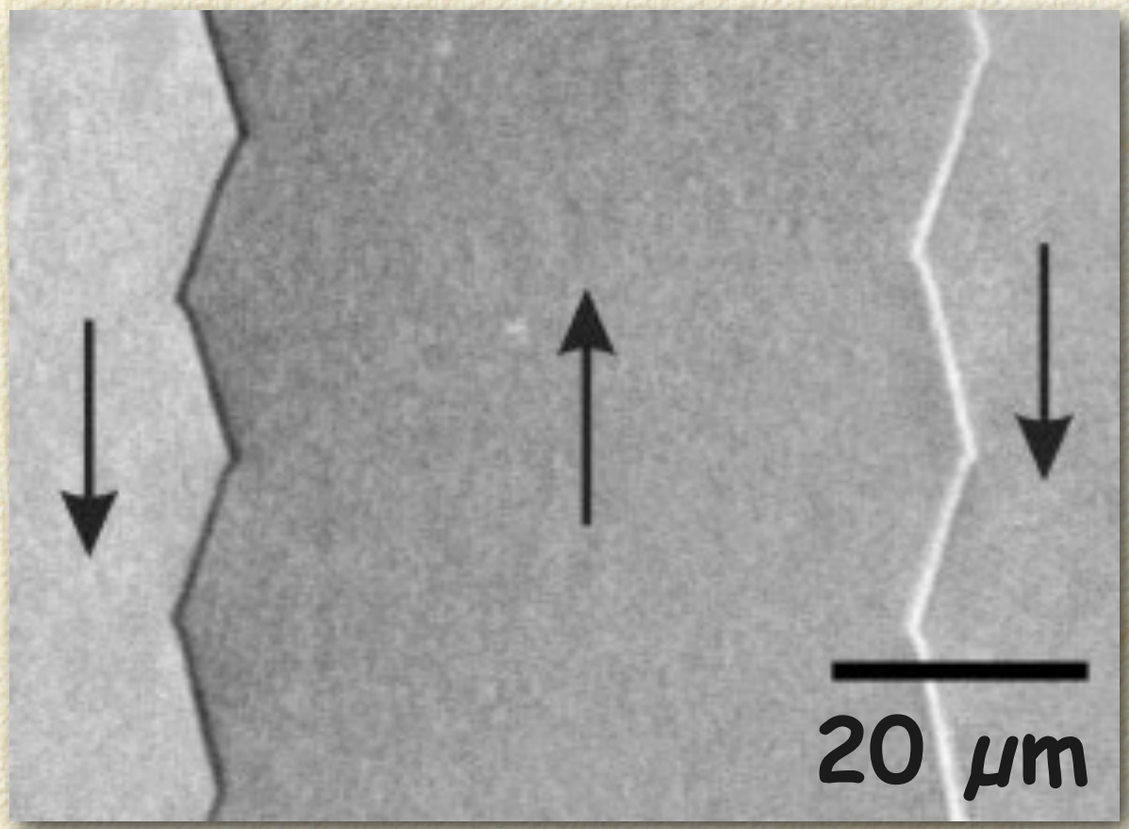

Low induced anisotropy

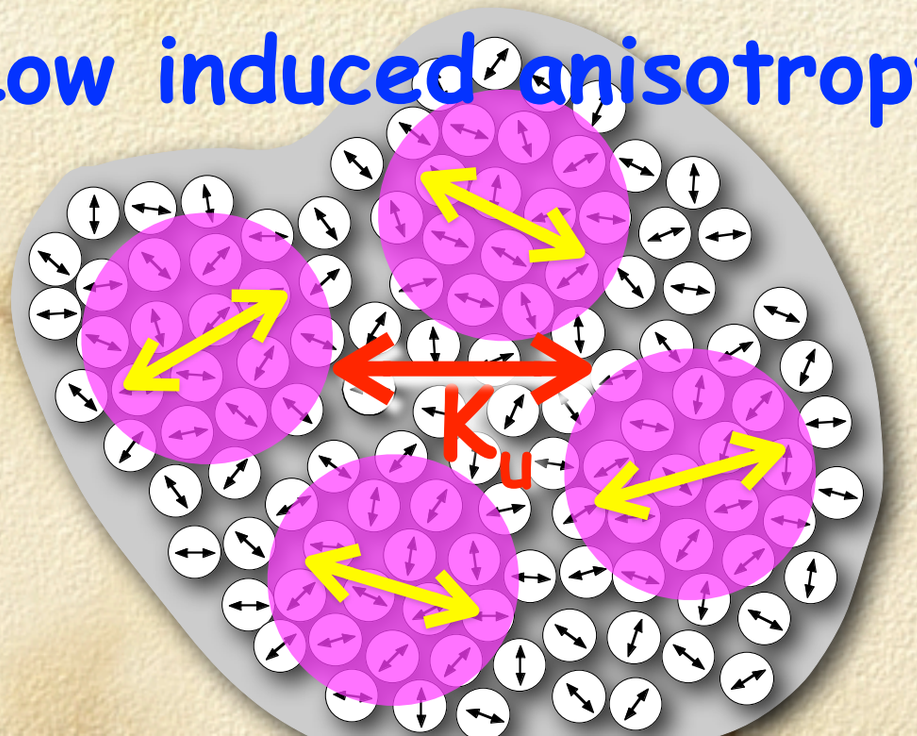

Strong induced anisotropy

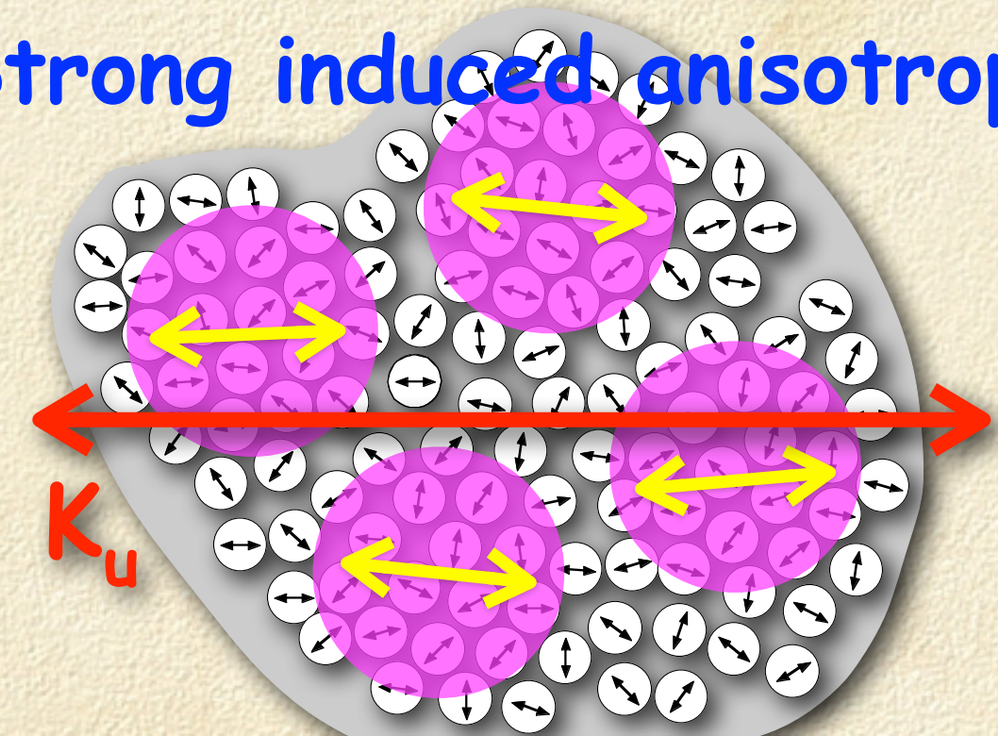

Nanocryst. core with transverse anis.

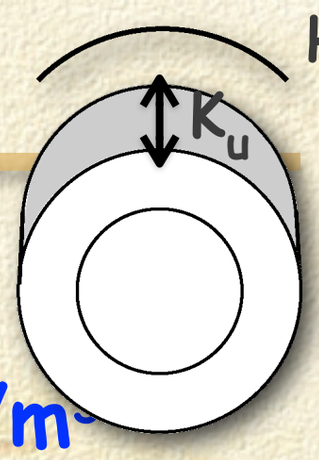

— decreasing induced transverse anisotropy ⟶

K_u = 33 J/m³	7.7 J/m³	2.3 J/m³	0.6 J/m³
μ_{15} = 22.000	86.200	274.500	559.900

demagnetized

H

H

100 μm

Nanocrystalline core with weak K_u

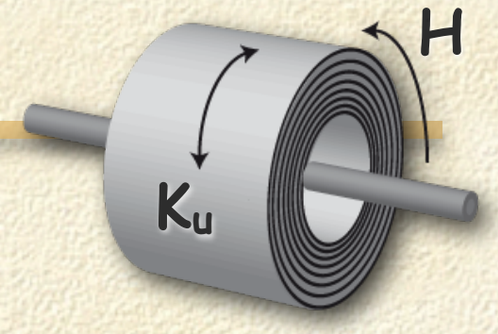

S. Flohrer et al., *Acta Mat.* 54 (2006)

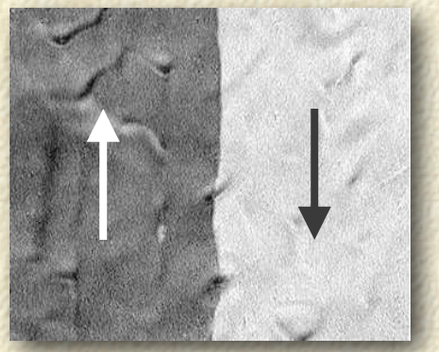

ground state

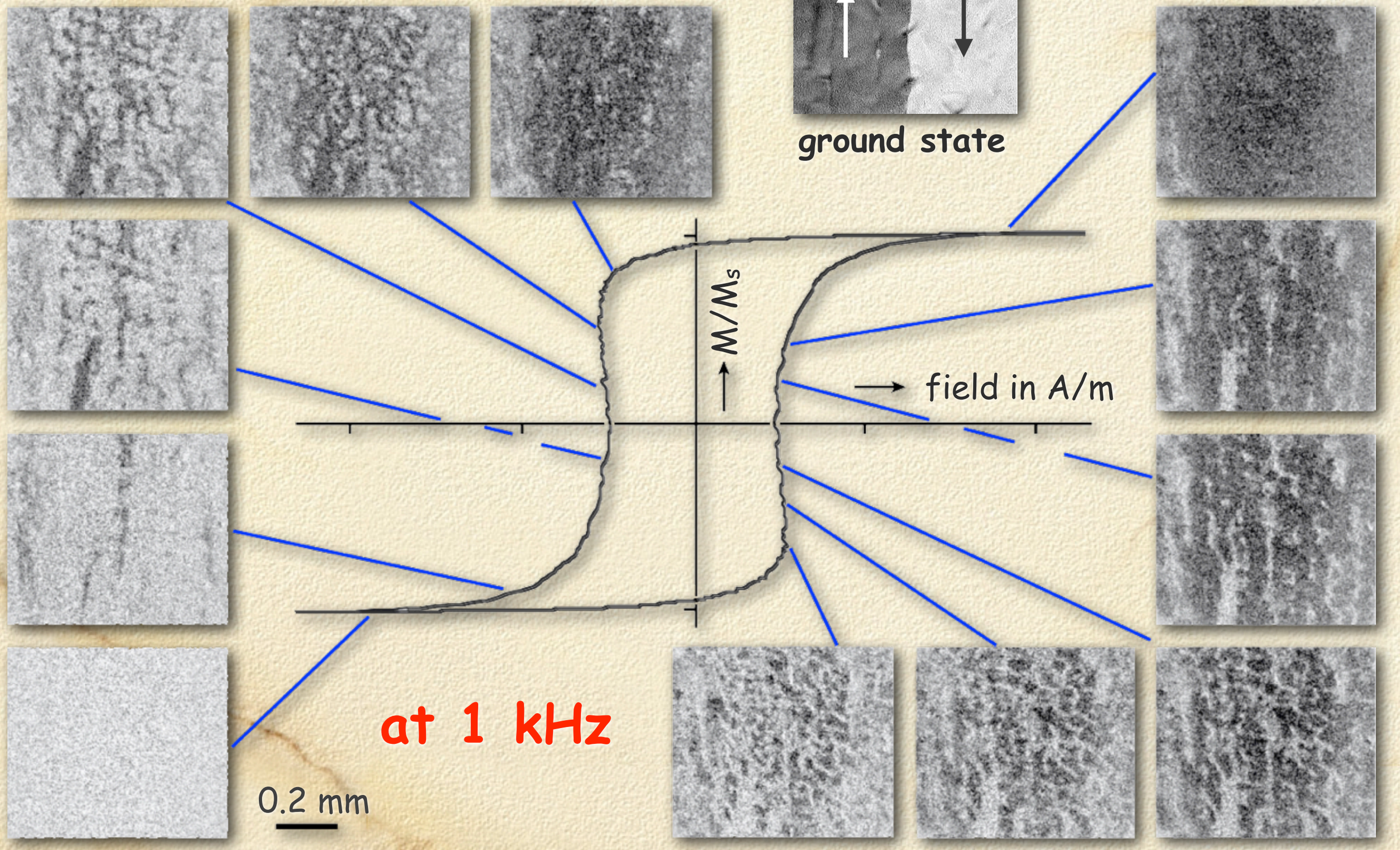

anisotropy

50 Hz | 1kHz | 5 kHz | 10 kHz

K_u = 29 J/m^3
strong

K_u = 10 J/m^3
moderate

K_u = 5 J/m^3
weak

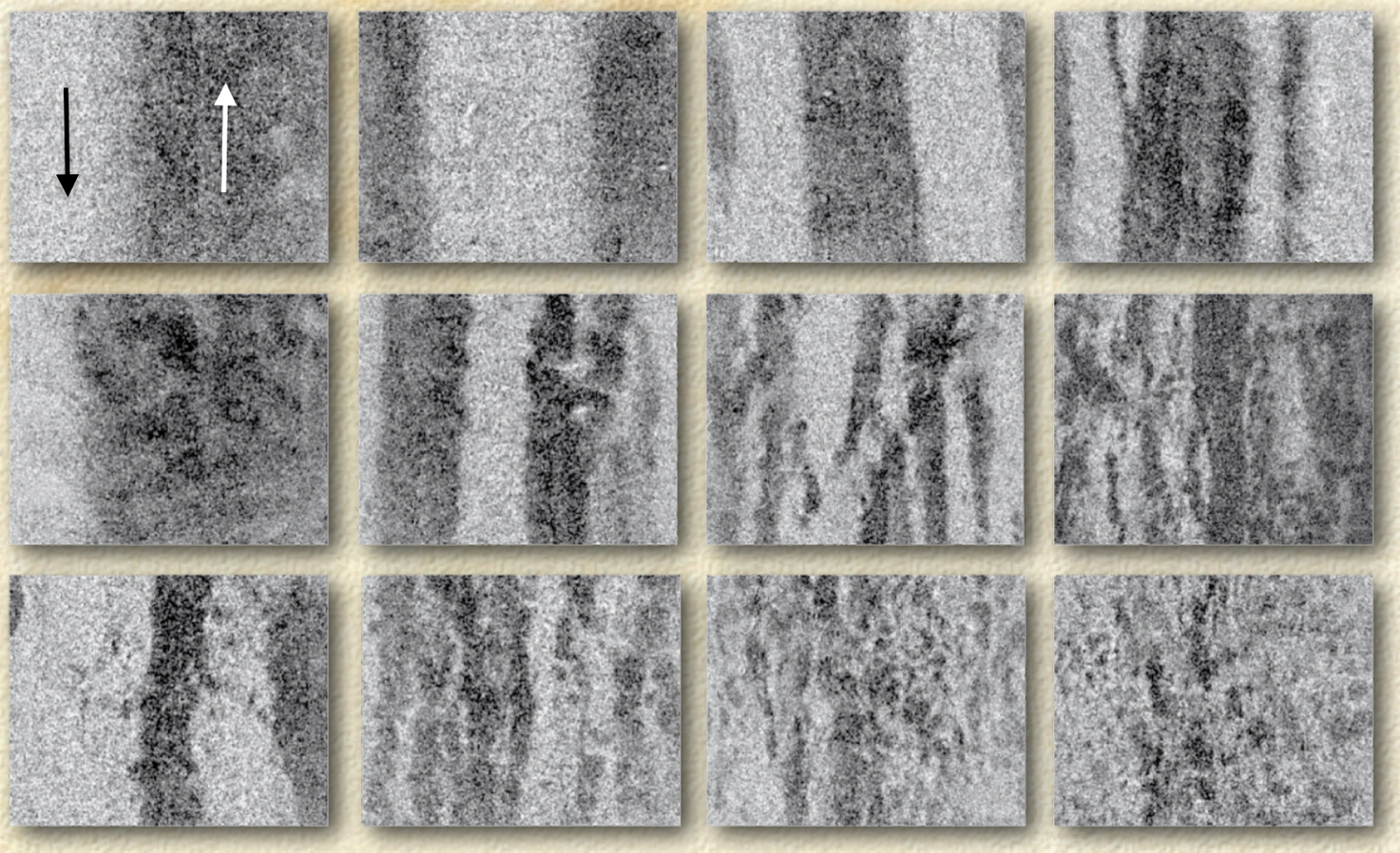

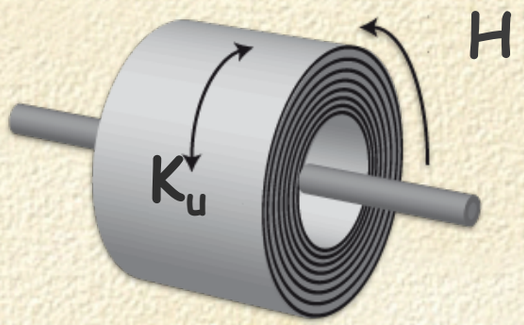

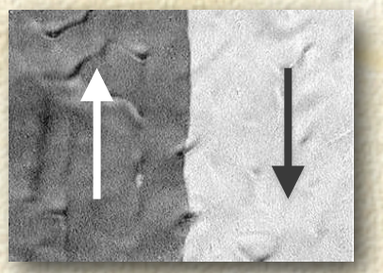

ground state

0.2 mm

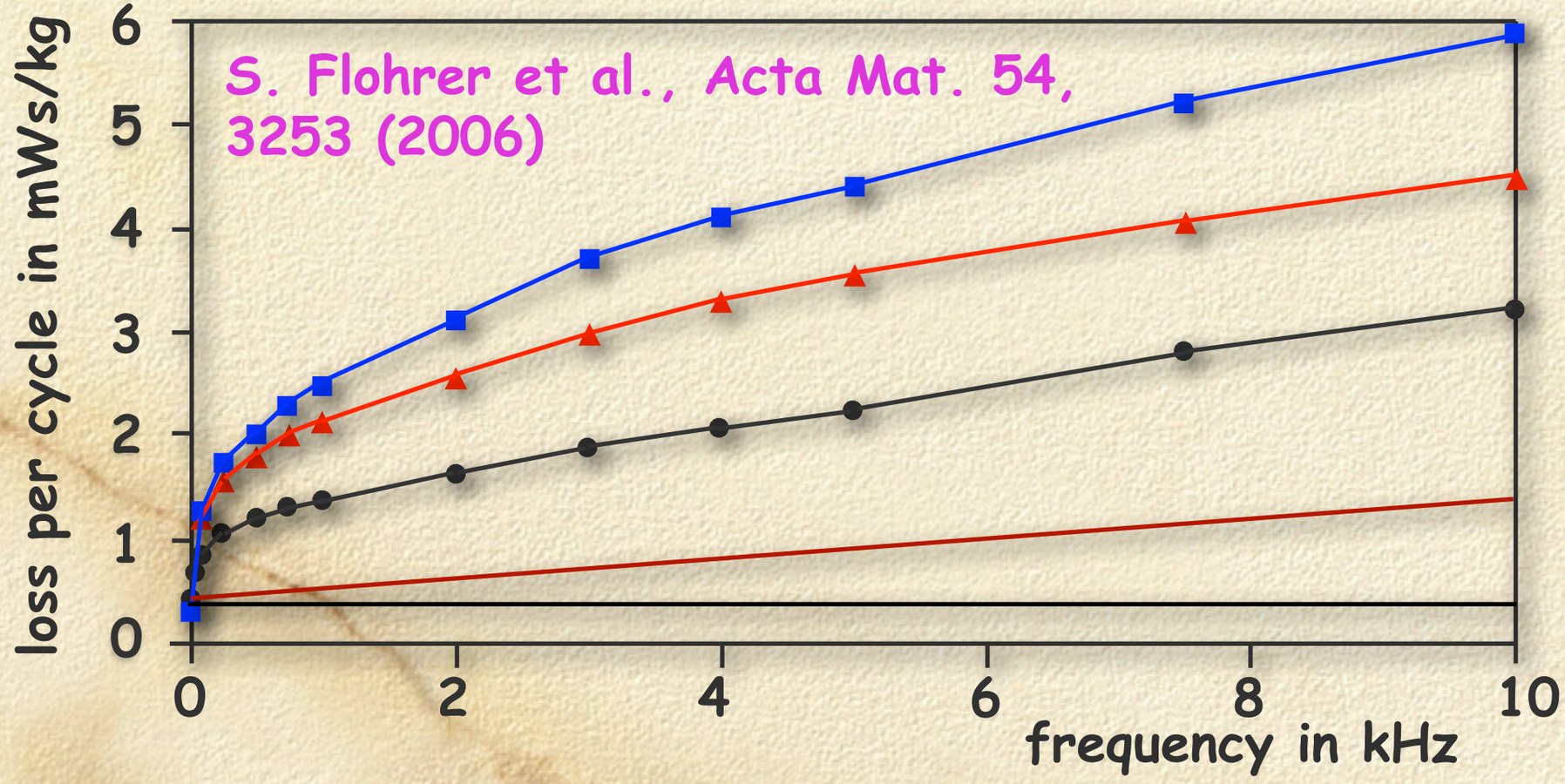

strong K_u

moderate K_u

weak K_u

classical eddy current loss

hysteresis loss

Nanocrystalline (Q<<1) materials

induced magnetic anisotropy

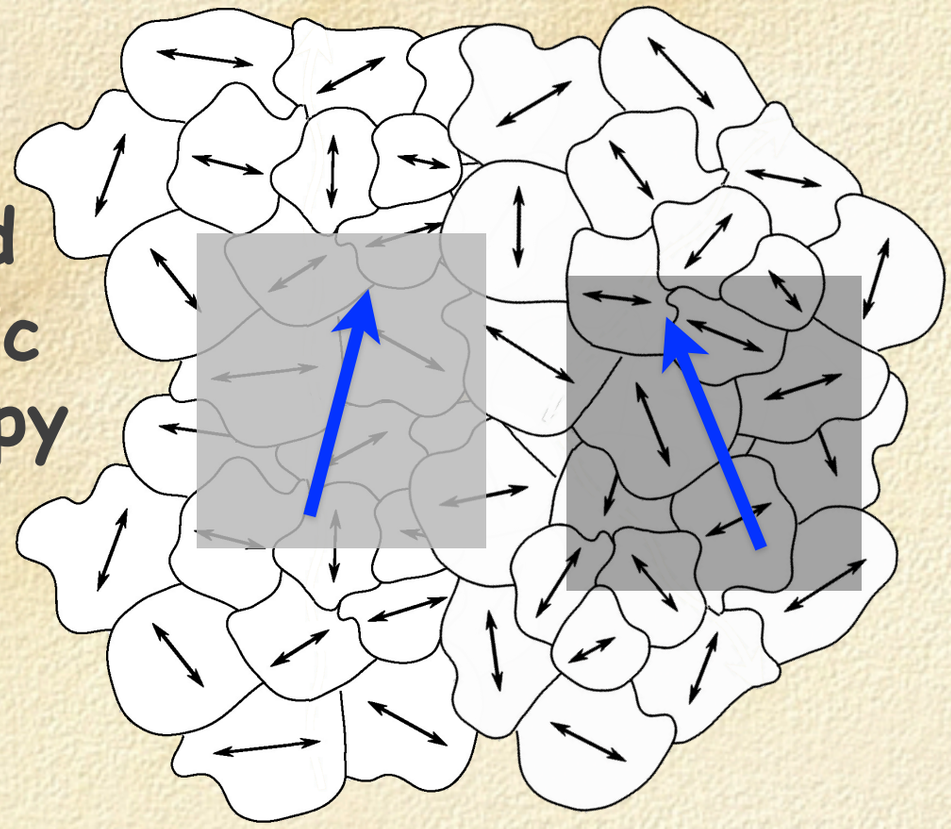

Ripple phenomenon in magnetic film

interface pole density
= $\sin\vartheta_1 - \sin\vartheta_2$

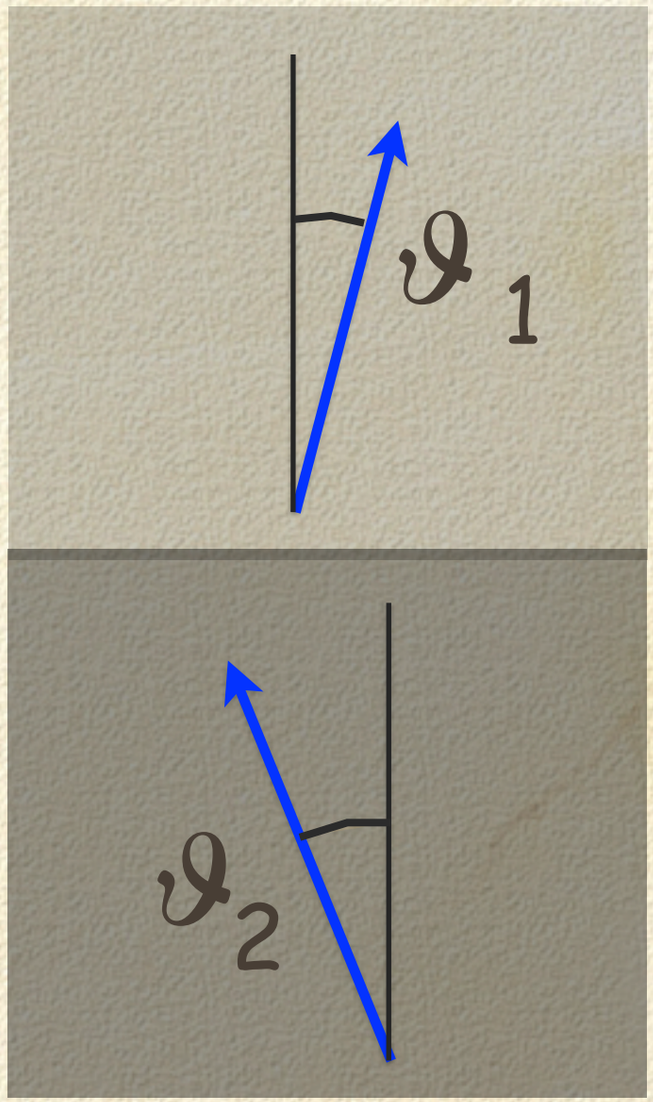

interface pole density
= $\cos\vartheta_1 - \cos\vartheta_2$

Nanocrystalline (Q<<1) materials

induced magnetic anisotropy

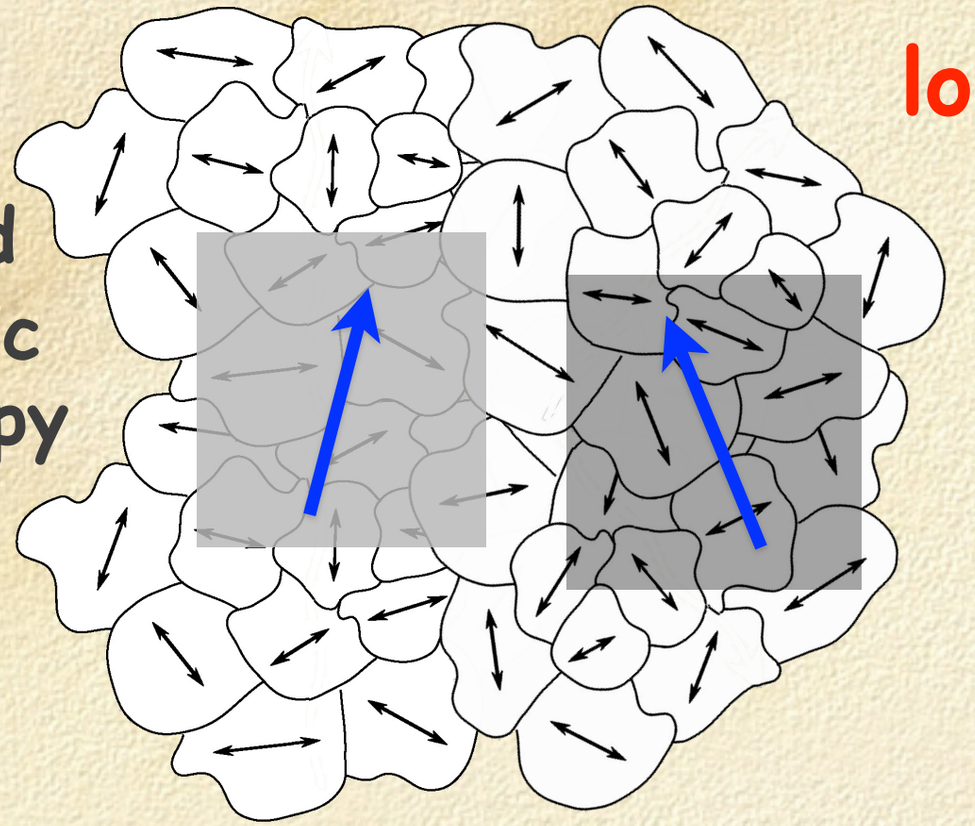

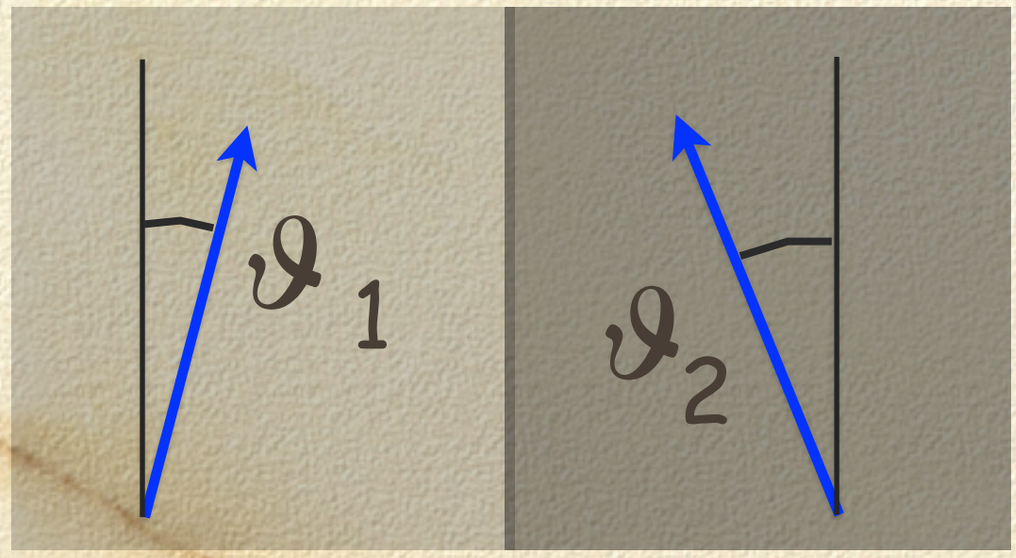

interface pole density
= $\sin\vartheta_1 - \sin\vartheta_2$

longitudinal variation prefered

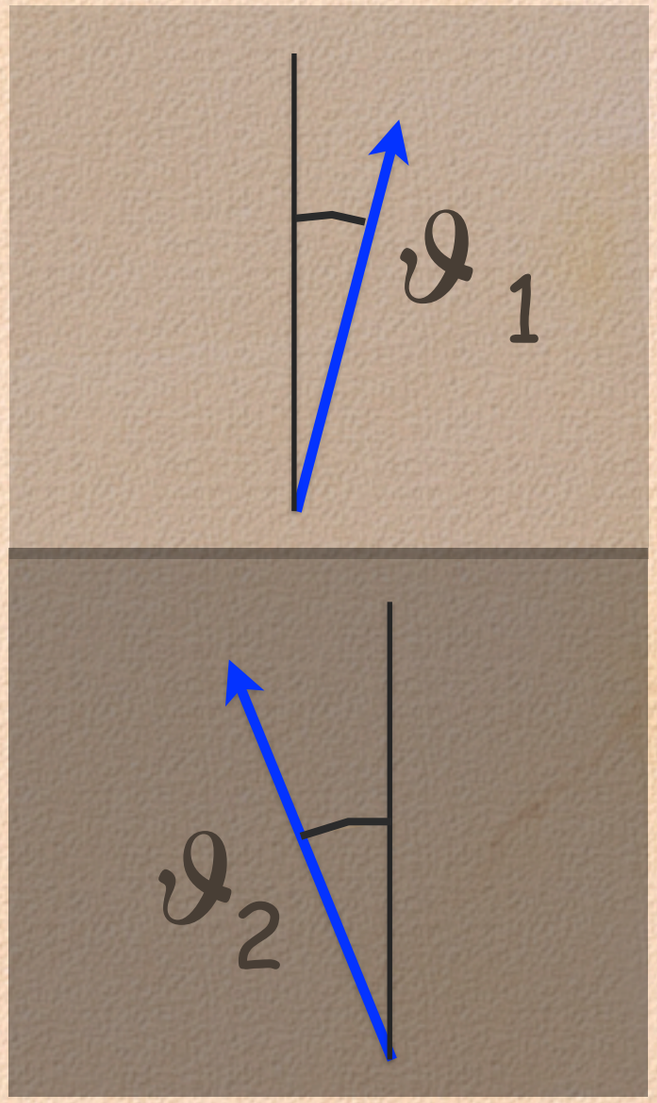

interface pole density
= $\cos\vartheta_1 - \cos\vartheta_2$

Nanocrystalline (Q<<1) materials

ripple in films

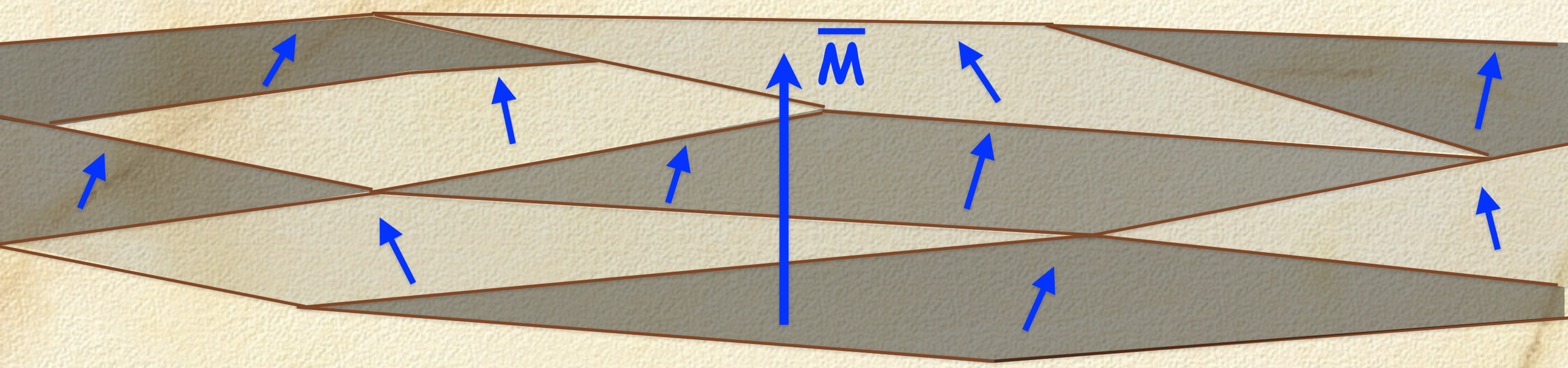

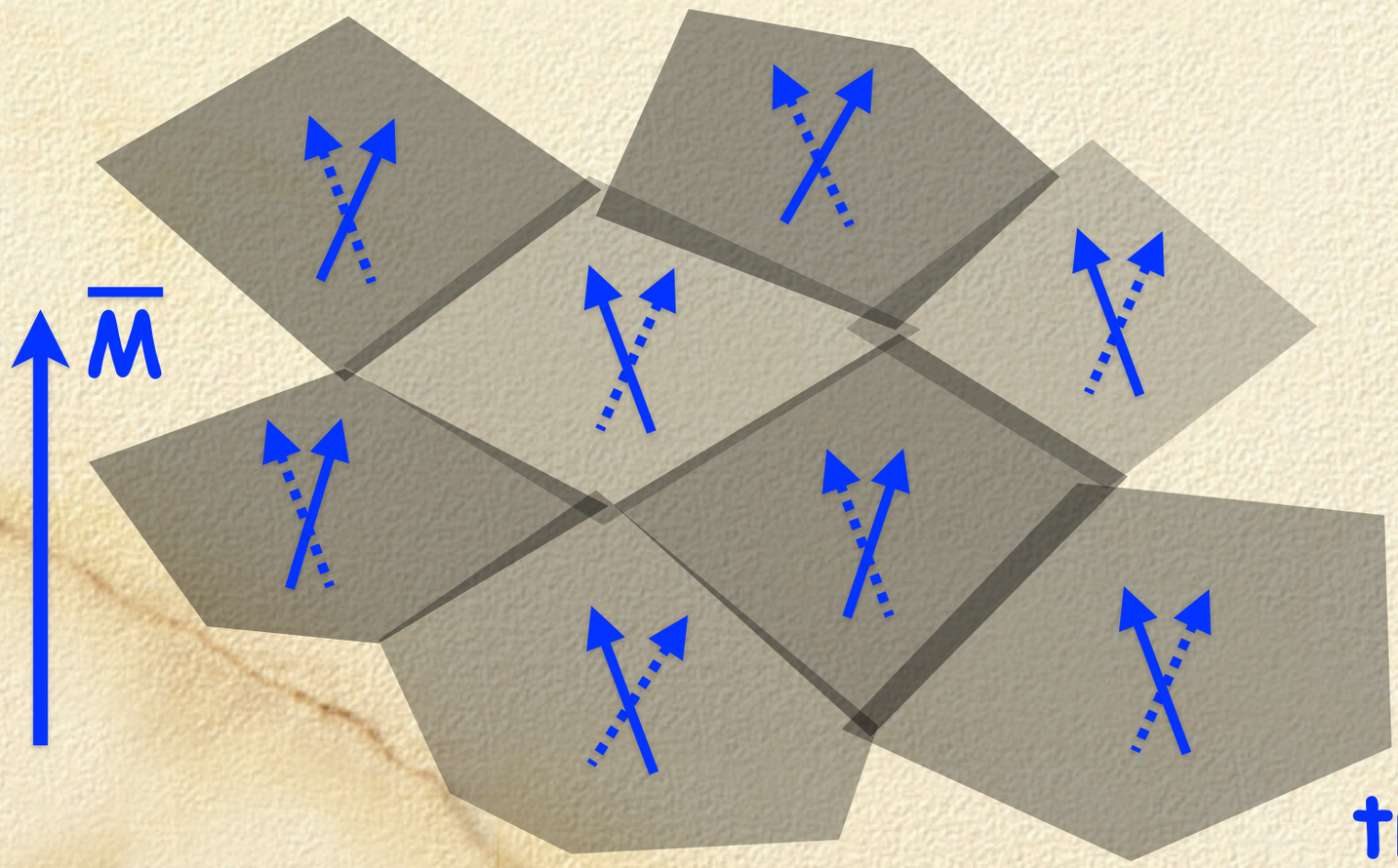

patches in
thick materials

Cancellation of
transverse component

Nanocrystalline (Q<<1) materials

Thinning of nanocrystalline ribbon

20 μm thick

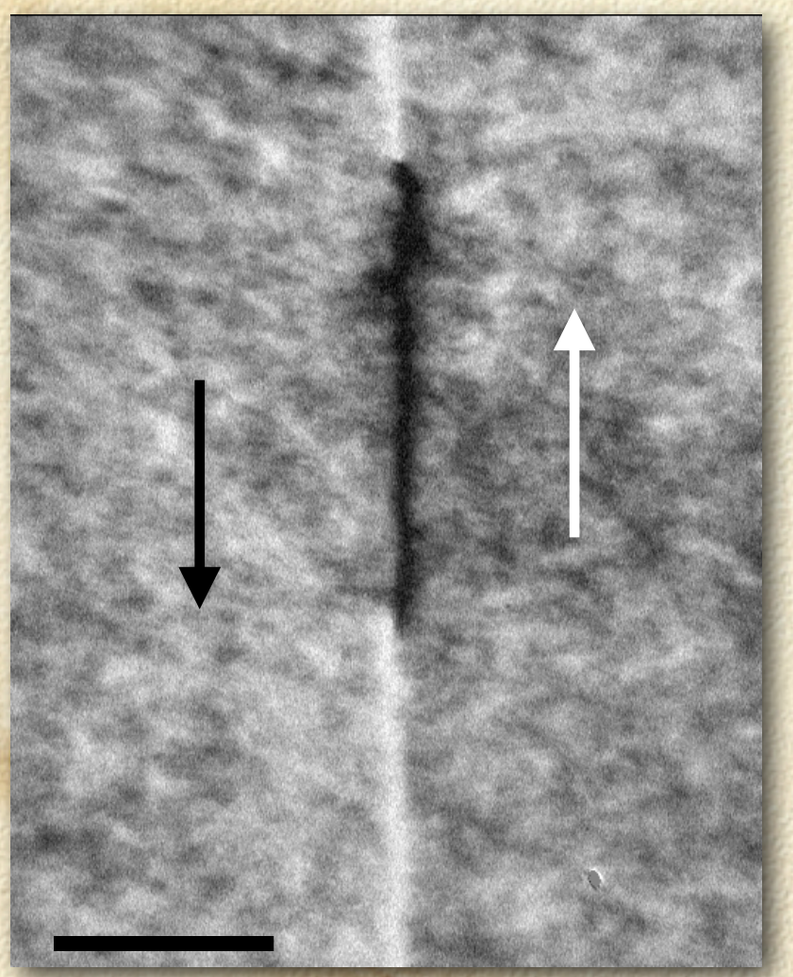

Patches

thinned to μm

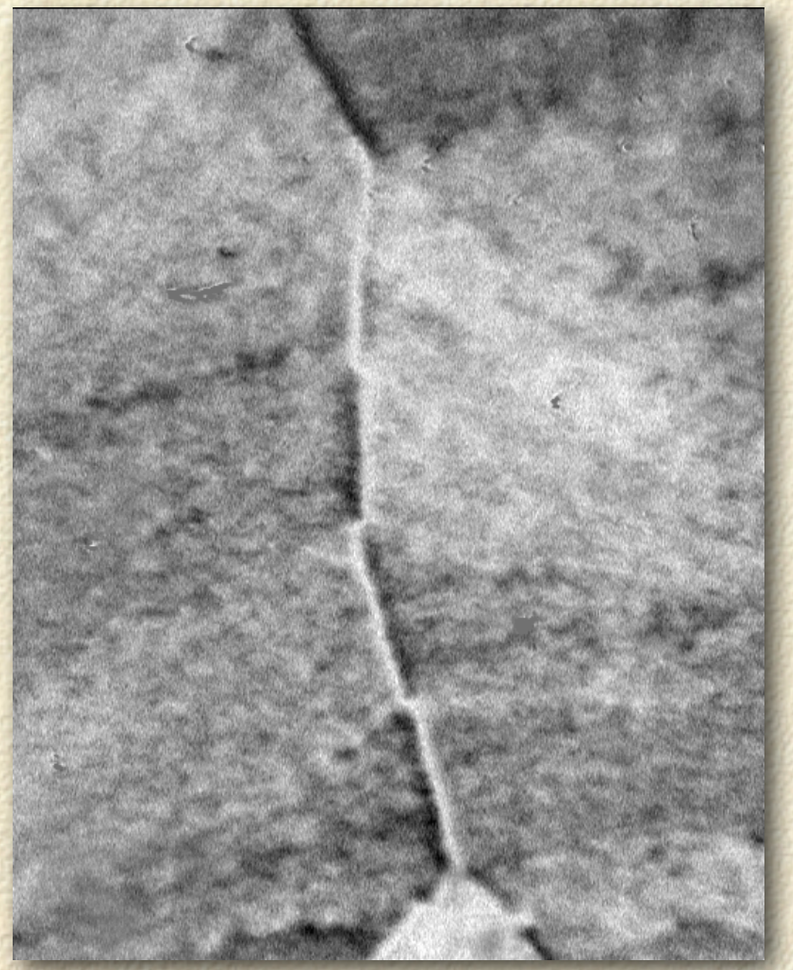

still thinner

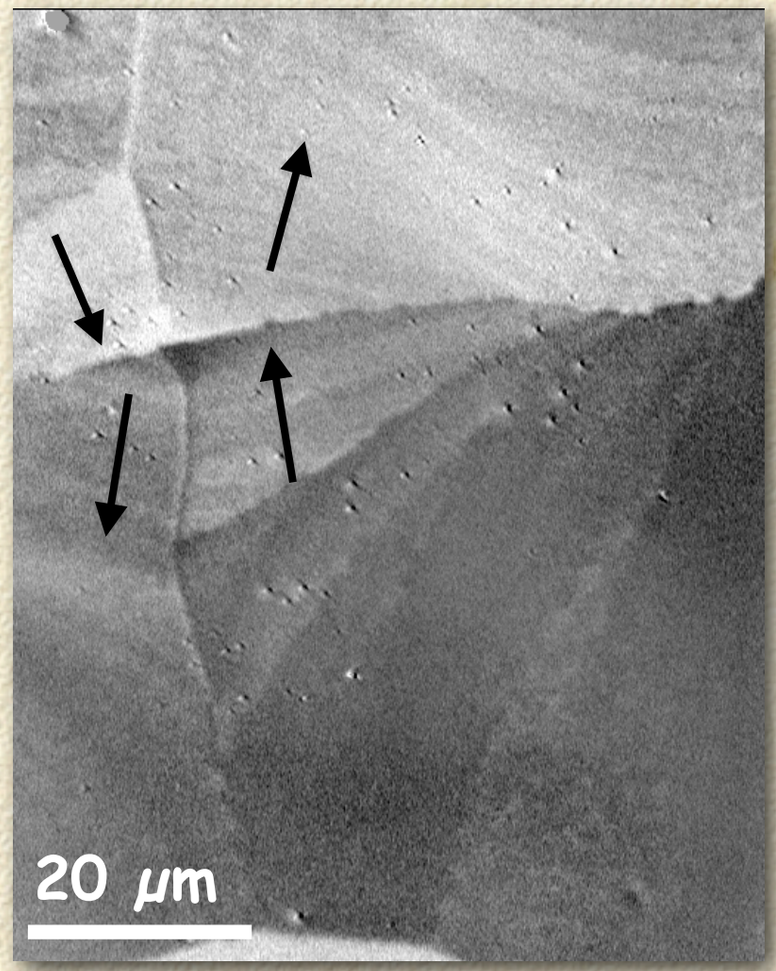

Ripple

Summary

- **Domains are formed to diminish stray field energy**
- Classification according to Q-factor
- Domains can be simple and complex, depending on many circumstances, especially surface orientation
- Bulk domains are usually wide and simple
- Domains must not be homogeneously magnetized areas

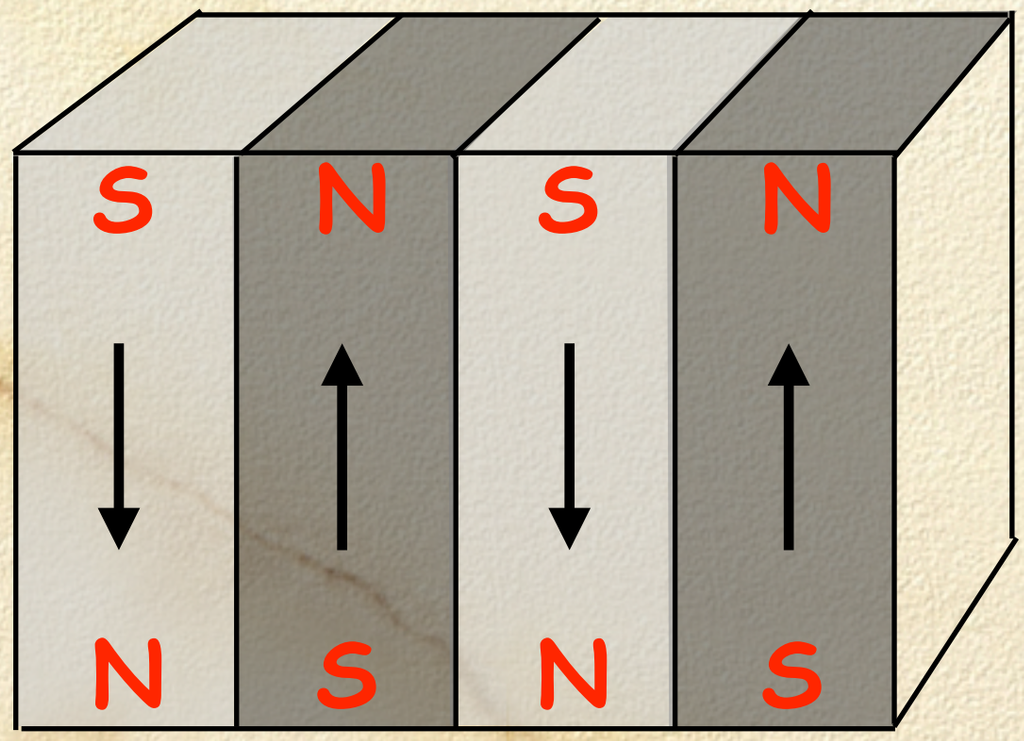

Summary

- Domains are formed to diminish stray field energy
- Classification according to Q-factor
- Domains can be simple and complex, depending on many circumstances, especially surface orientation
- Bulk domains are usually wide and simple
- Domains must not be homogeneously magnetized areas

High-Q material

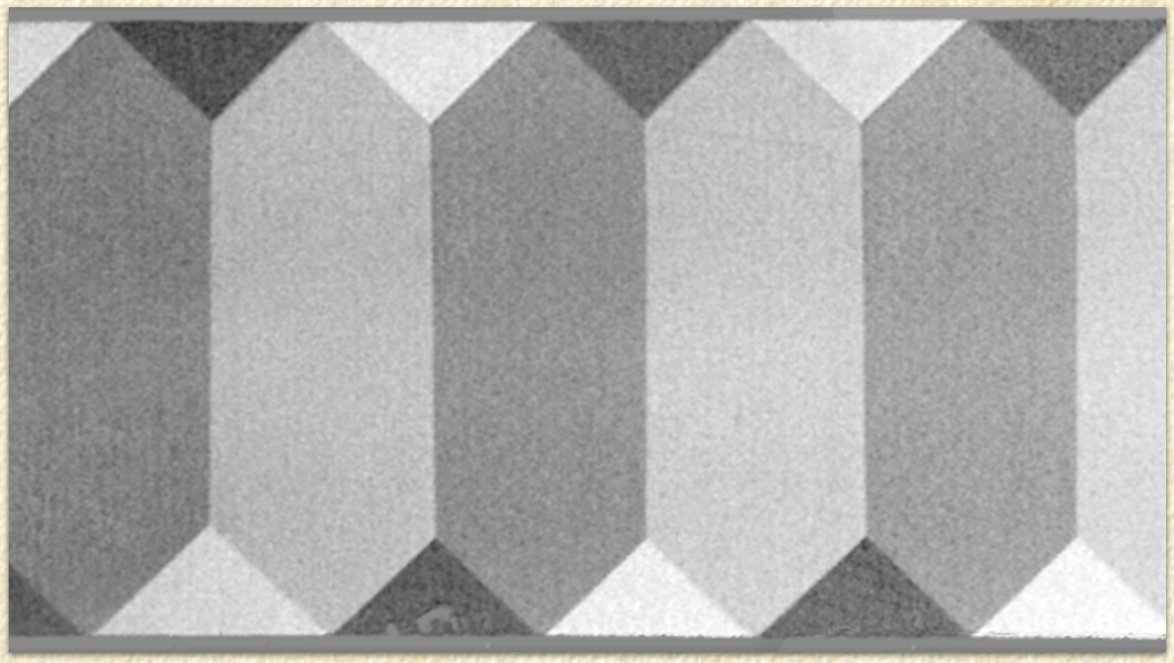

Low-Q material

Summary

- Domains are formed to diminish stray field energy
- Classification according to Q-factor
- Domains can be simple and complex, depending on many circumstances, especially surface orientation
- Bulk domains are usually wide and simple
- Domains must not be homogeneously magnetized areas

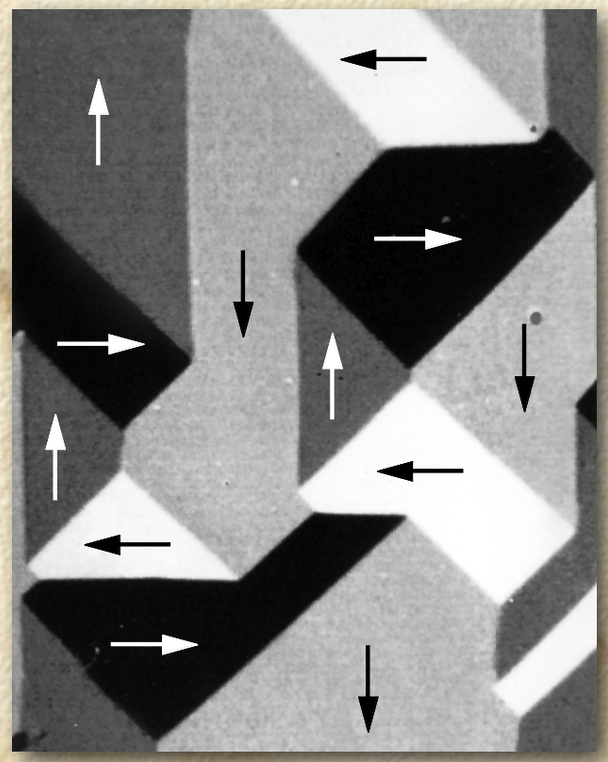

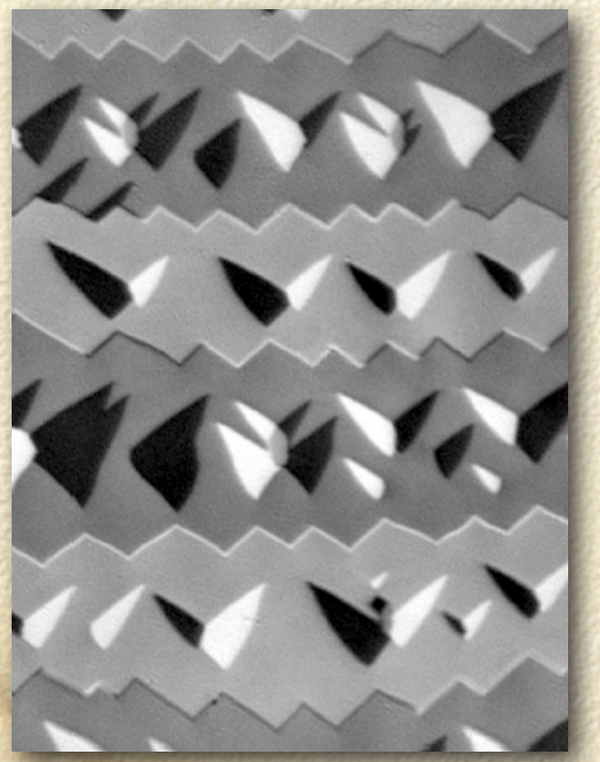

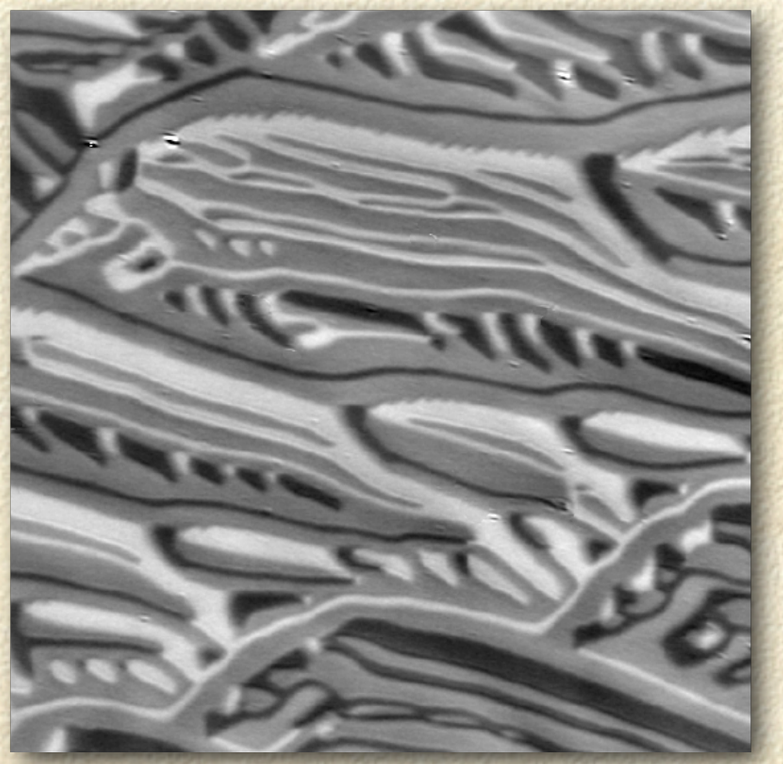

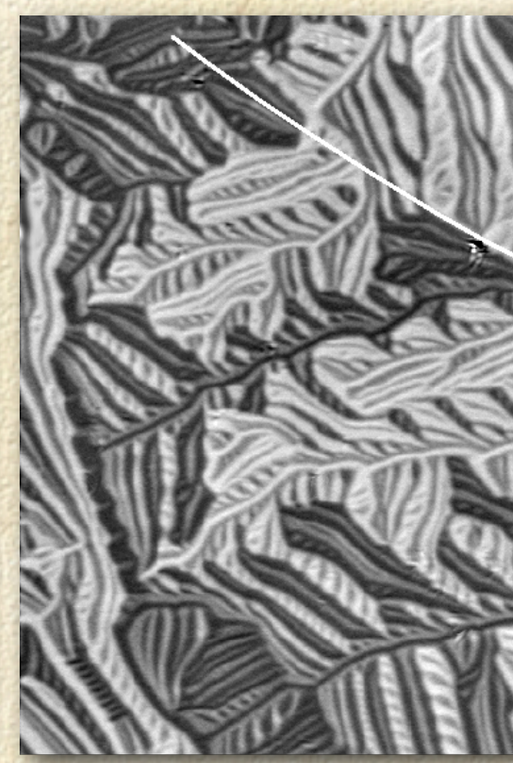

Summary

- Domains are formed to diminish stray field energy
- Classification according to Q-factor
- Domains can be simple and complex, depending on many circumstances, especially surface orientation
- Bulk domains are usually wide and simple
- Domains must not be homogeneously m areas

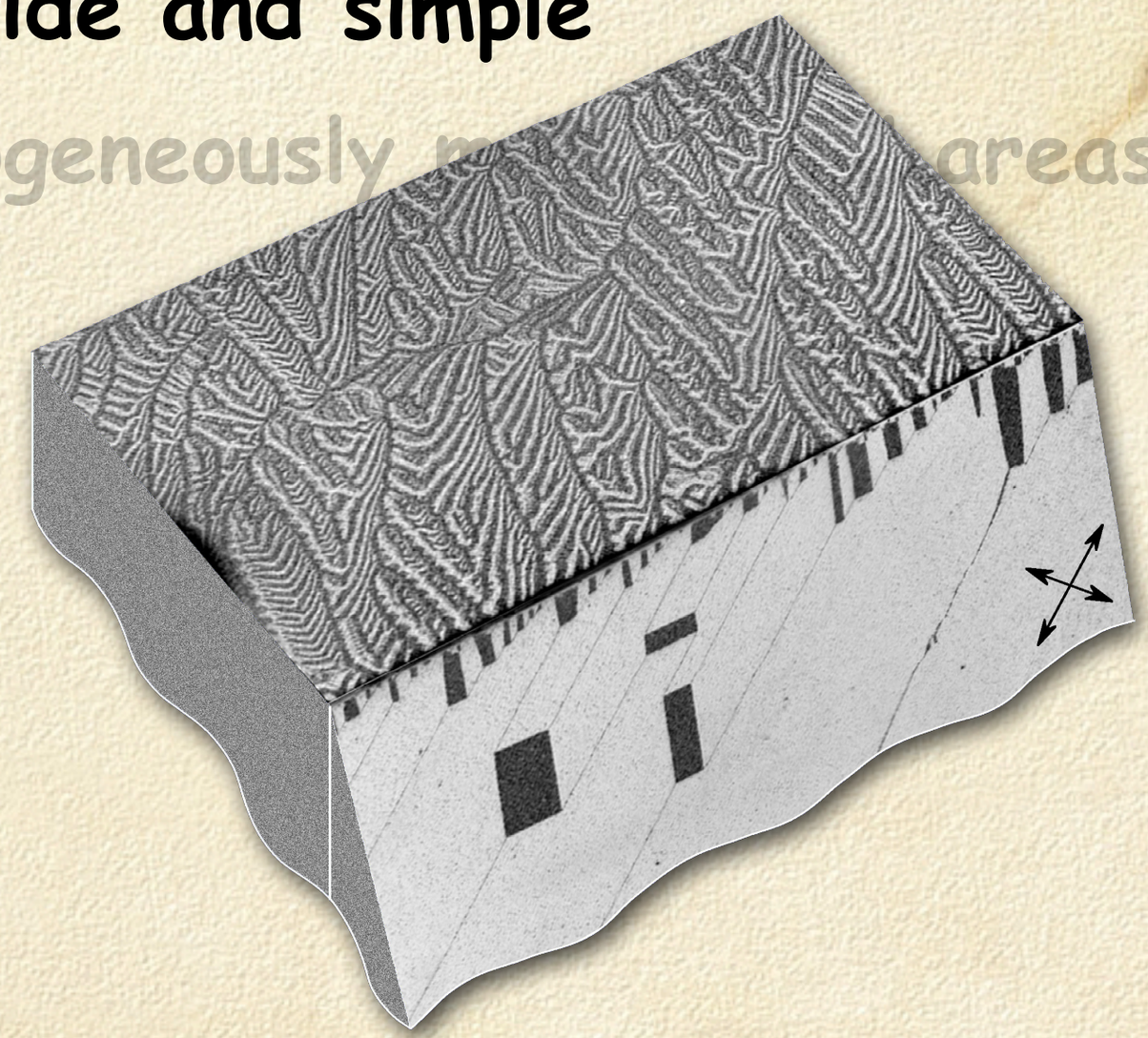

Summary

- Domains are formed to diminish stray field energy
- Classification according to Q-factor
- Domains can be simple and complex, depending on many circumstances, especially surface orientation
- Bulk domains are usually wide and simple
- Domains must not be homogeneously magnetized areas

Summary

- Domains are formed to diminish stray field energy
- Classification according to Q-factor
- Domains can be simple and complex, depending on many circumstances, especially surface orientation
- Bulk domains are usually wide and simple
- Domains must not be homogeneously magnetized areas

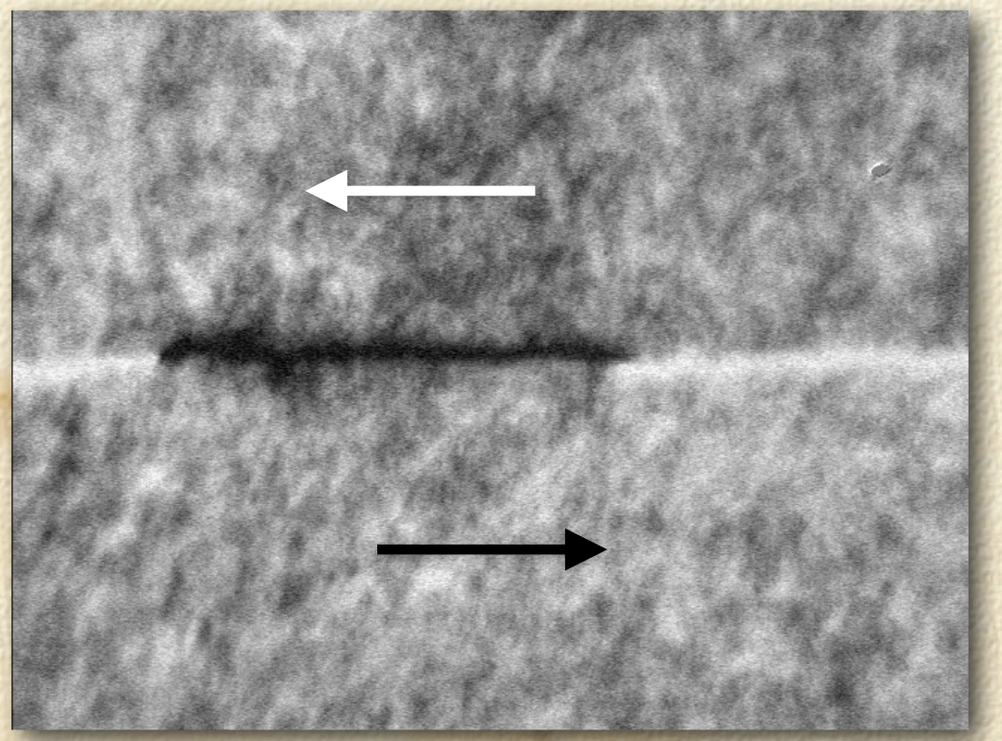

Patches in bulk nanocrystalline material

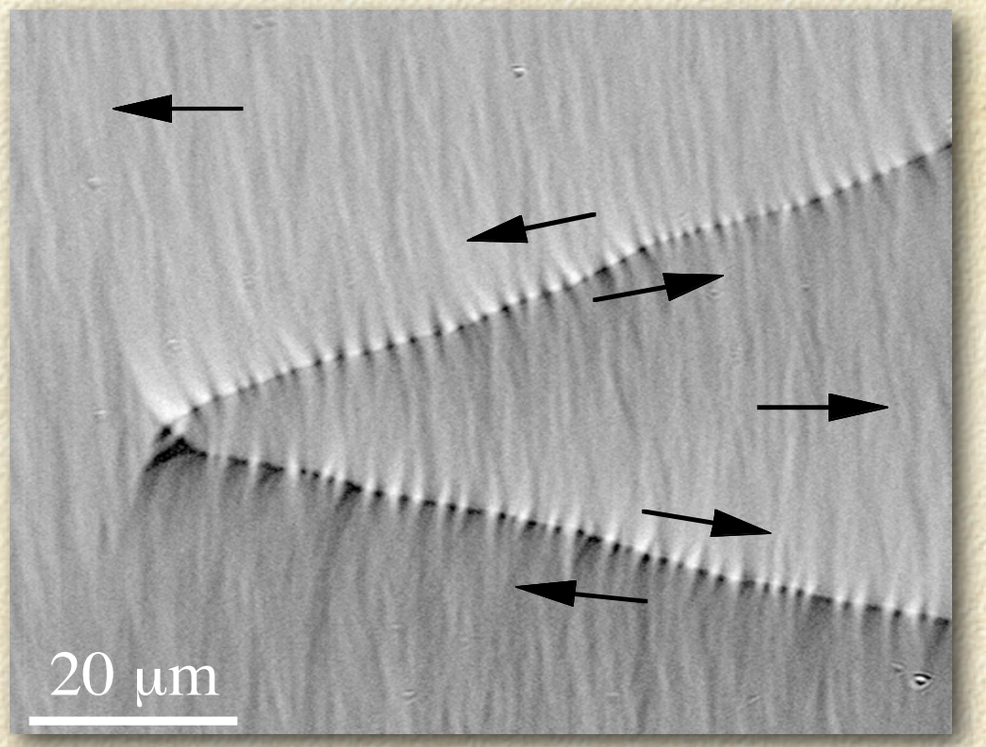

Ripple in nanocrystalline films

Summary

- Domains are formed to diminish stray field energy
- Classification according to Q-factor
- Domains can be simple and complex, depending on many circumstances, especially surface orientation
- Bulk domains are usually wide and simple
- Domains must not be homogeneously magnetized areas

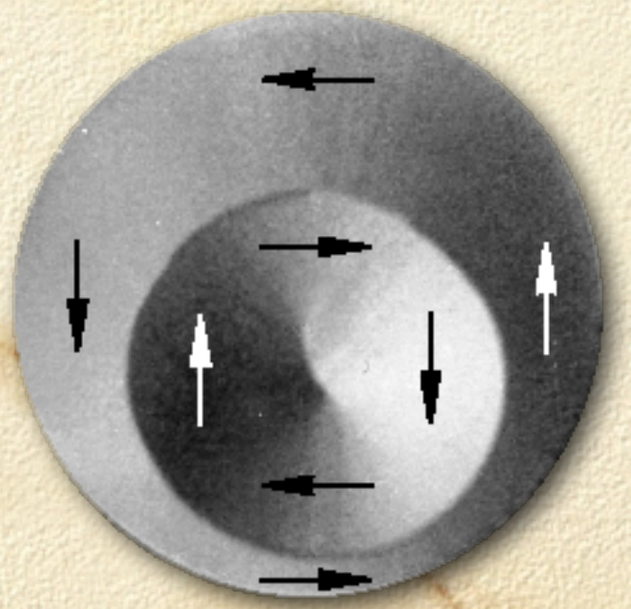

Shape-induced in
Q << 1 film elements

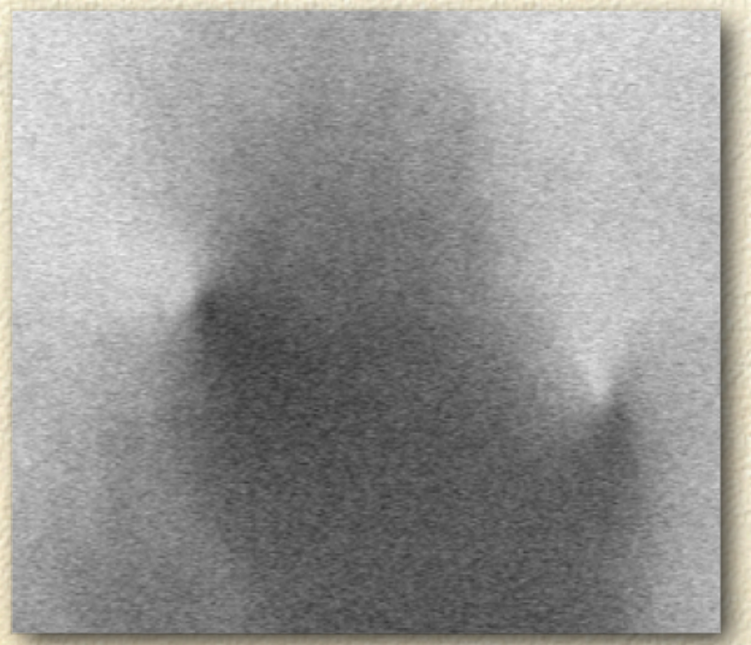

Q = 0 bulk material

Stripe domains in perpendicular
low-Q films

Summary

- Domains are formed to diminish stray field energy
- Classification according to Q-factor
- Domains can be simple and complex, depending on many circumstances, especially surface orientation
- Bulk domains are usually wide and simple
- Domains must not be homogeneously magnetized areas

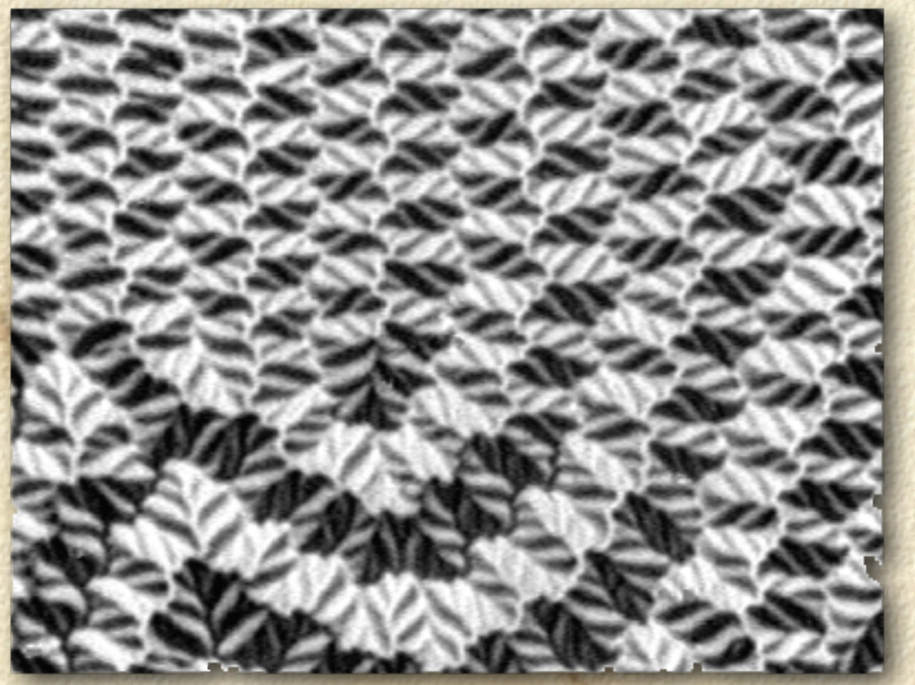

Branched closure domains in low-Q bulk material

Branched closure domains in medium-Q bulk material

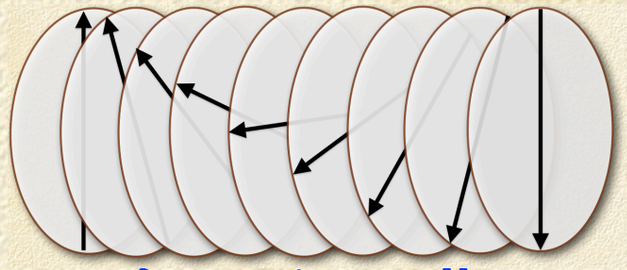

Domain walls

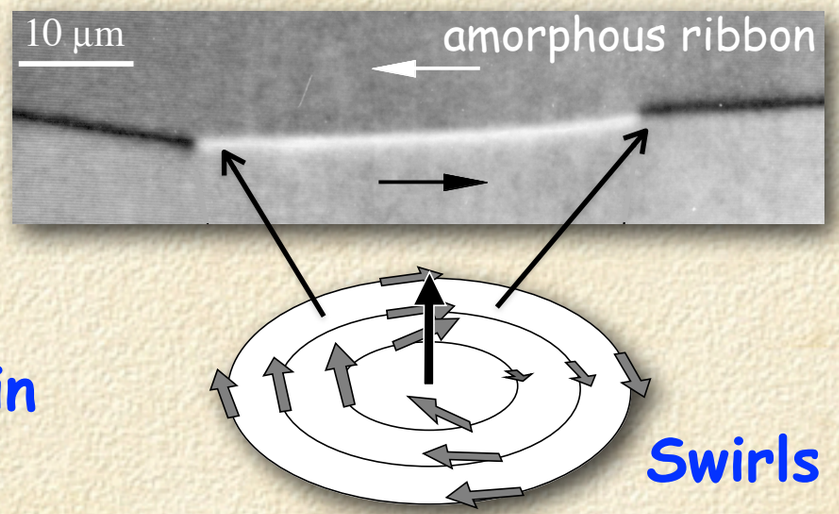

Swirls

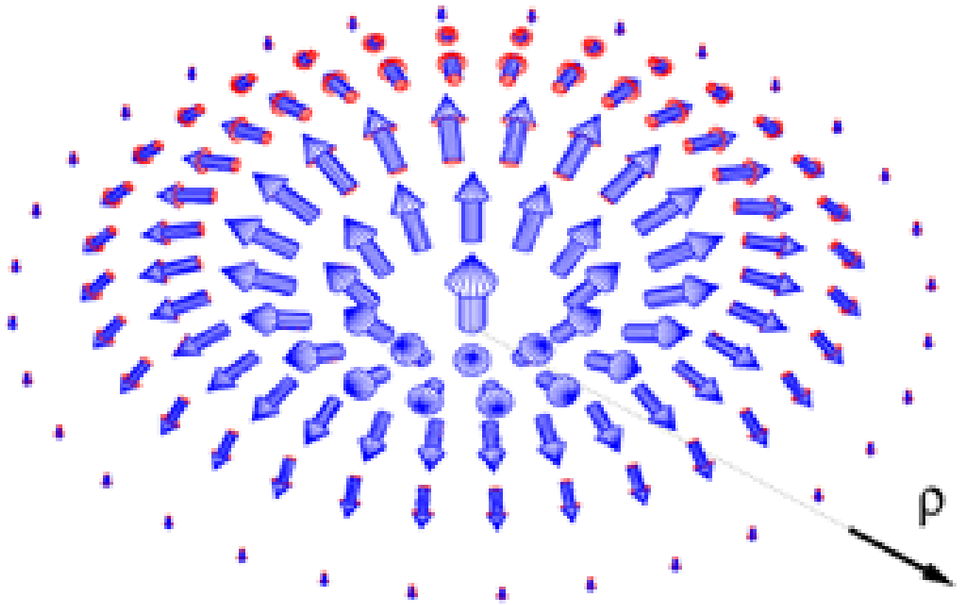

Skyrmions in non-centrosymmetric crystals with Dzyaloshinskii-Moriya coupling

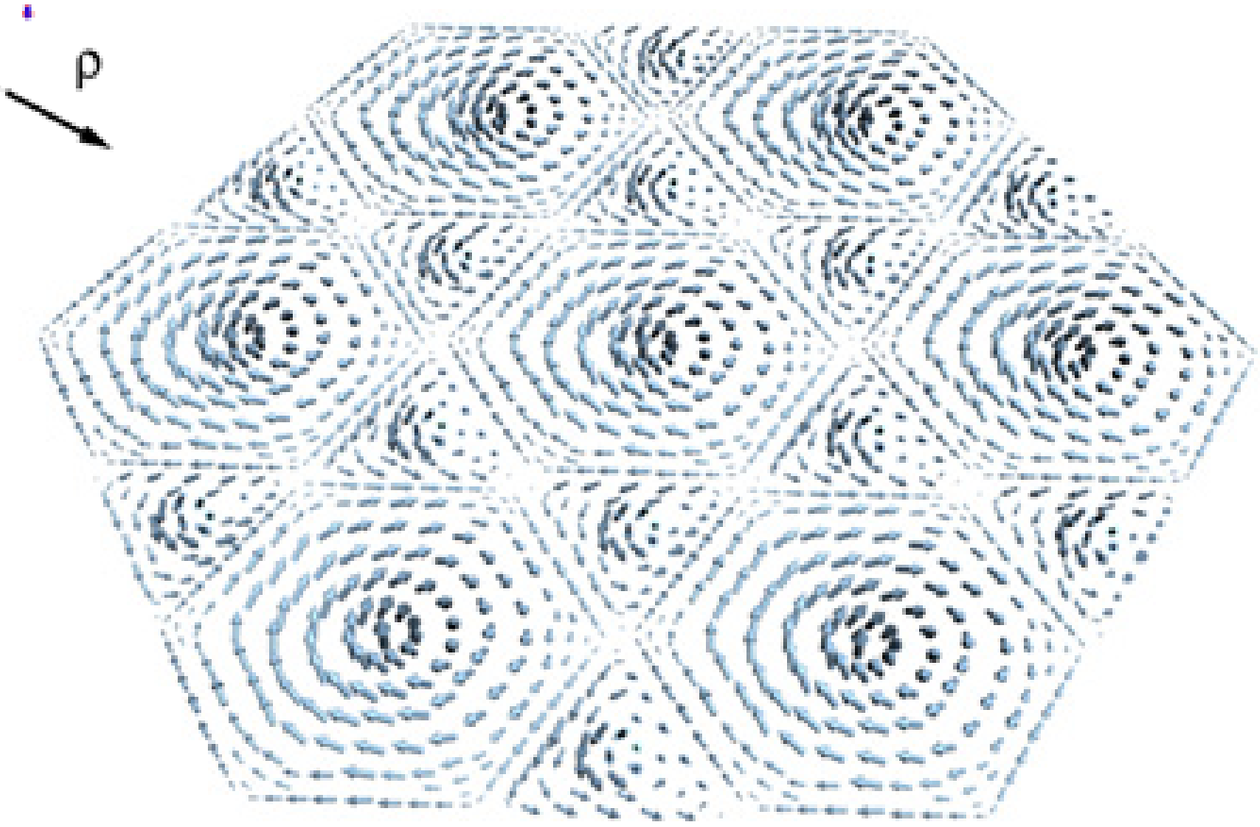

Courtesy
A. Bogdanov, U. Rössler
(IFW Dresden)

ergy

on

ation

d areas

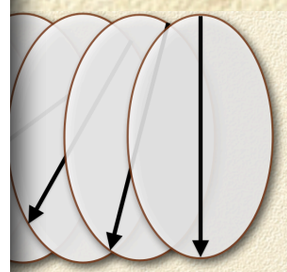

walls

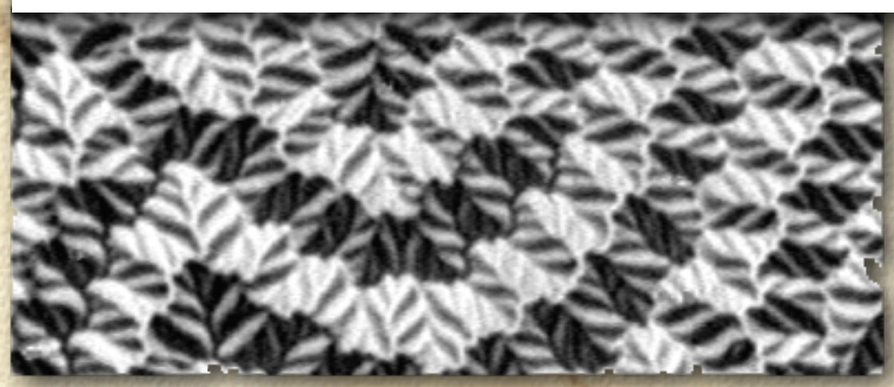

Branched closure domains in low-Q bulk material

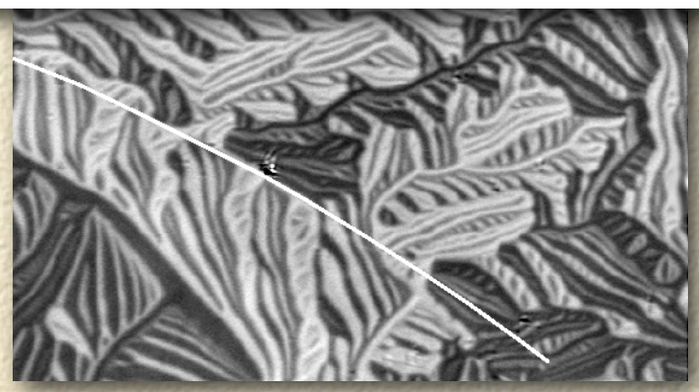

Branched closure domains in medium-Q bulk material

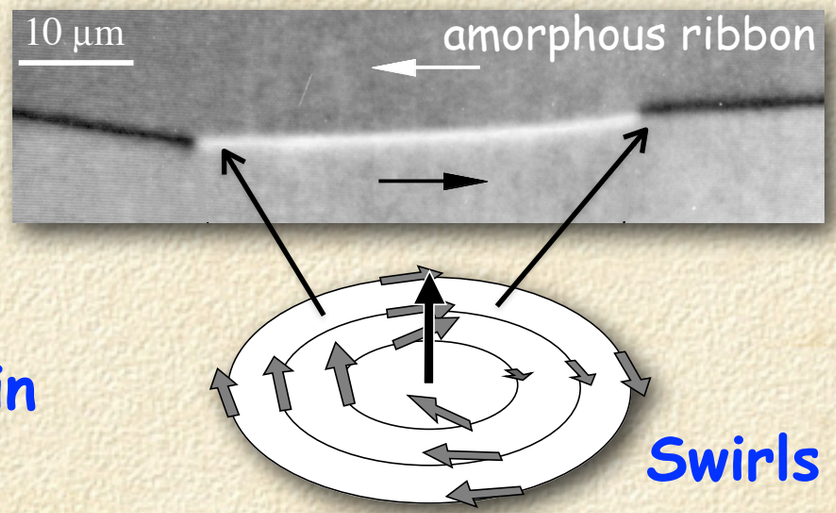

Swirls

Acknowledgement

Acknowledgement

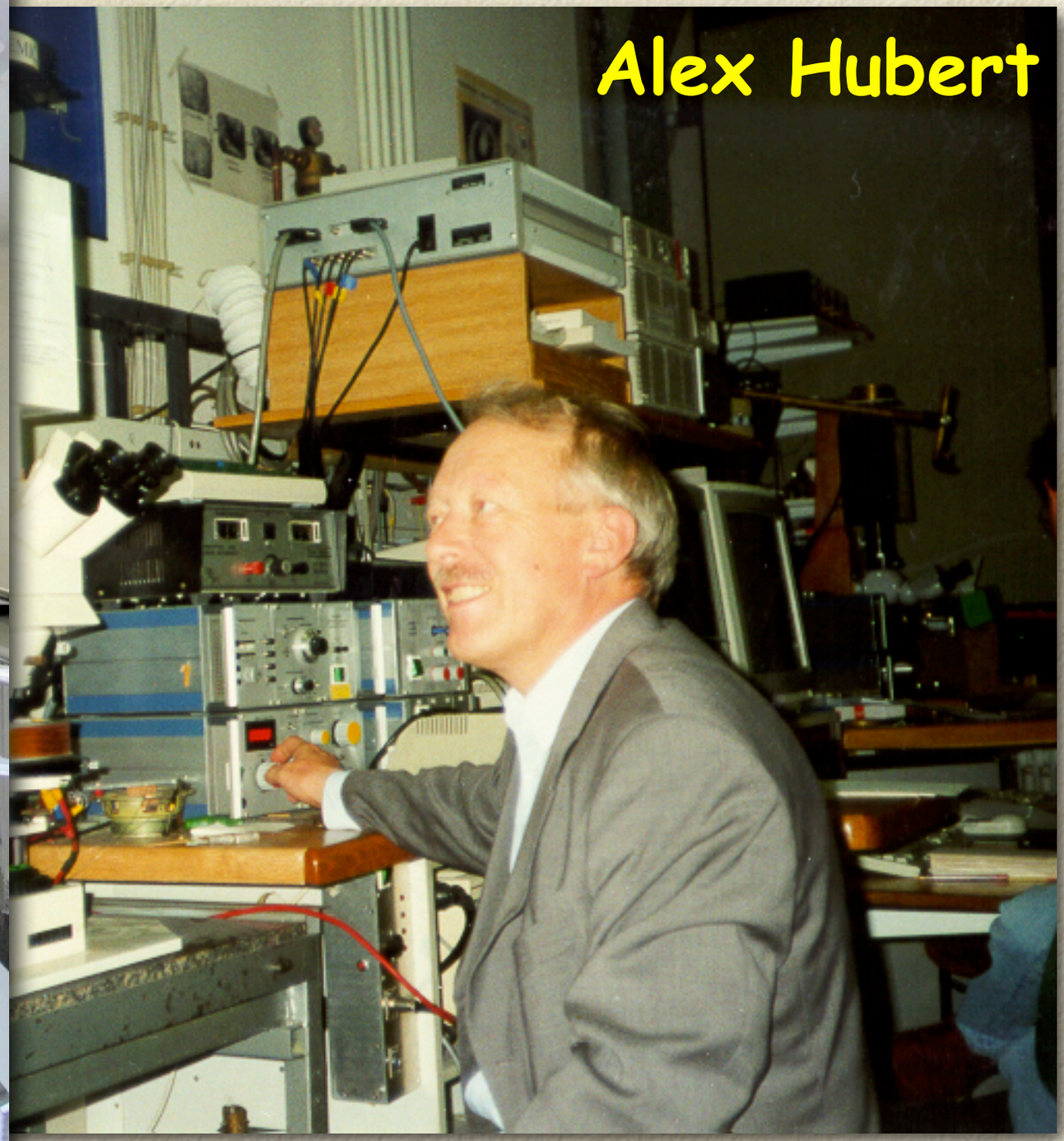

Acknowledgement

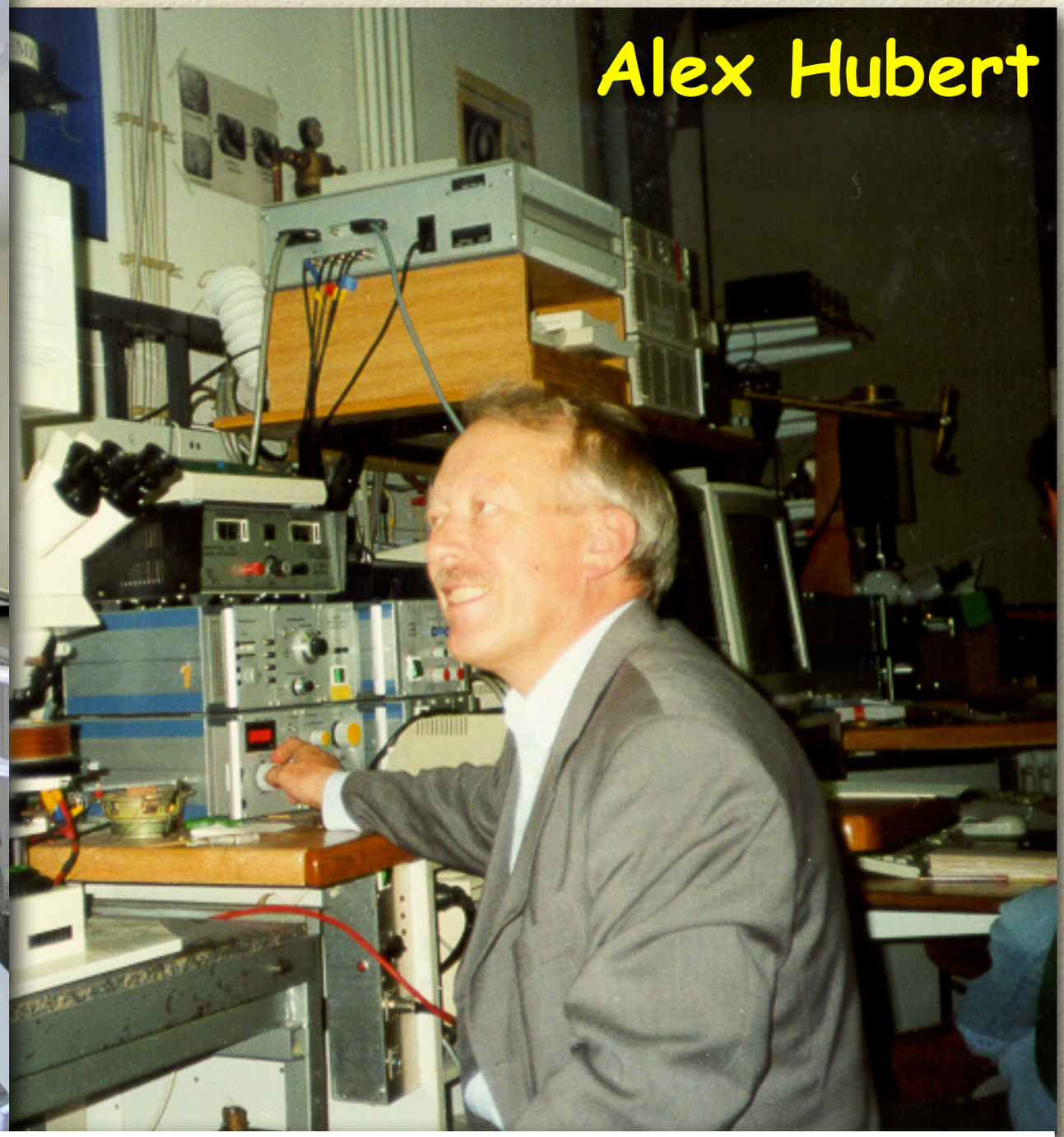

IEEE Magnetics Society

IEEE